Synthesis of Chiral BODIPYs through Point-to-Helical Chirality Control

By

Felicity Jane Frank

A thesis submitted in partial fulfilment of the requirements for the degree of

Doctor of Philosophy

August 2023

Acknowledgements

Firstly, I would like to thank both my PhD supervisors, Dr Michael Hall and Dr Julian Knight for all your help and support you have provided throughout my PhD, I cannot express my gratitude enough. I would also like to extend my thanks even further for Dr Hall who also guided me through summer projects and my MChem at Newcastle University, which ultimately inspired me to undertake this PhD. You have both taught me invaluable knowledge and helped me reach heights that I did not think possible. I am proud of the chemist I have become and that would not have been possible without your guidance.

I would also like to thank Dr Hanno Kossen, who not only was my secondary teaching supervisor but also a mentor and friend throughout my years at Newcastle University. Although you may be unaware of how much our ever more often catch-ups have helped me, I hope that you continue to inspire others the way you have me.

I also extend my gratitude to all past and present MJH group members, with a special thanks to Damon (Xin) Wen, who has shared this PhD journey with me, your true friendship has been invaluable to me. I am also thankful to other Johnston lab members including but by no means only Toni Pringle, Jay Tromans and Aminah Almarshad. The friendships forged throughout my years at Newcastle will be cherished, in many cases I know I have made friends for life, and for that I am so grateful.

To those who contributed to this thesis, I thank Dr Patrycja Brook for performing CPL spectroscopy and both Professor Wouter Herrebout and Jonathan Bogaerts for performing ECD spectroscopy. A wider thanks to Corrine Wills, Casey Dixon and the late Professor William McFarlane for your assistance and guidance with NMR spectroscopy as well as Dr Paul Waddell for his assistance in X-ray crystallography.

Finally, but by no means less, thank you to my partner Liam and his family, by showing me what unconditional love and support is.

Abstract

Molecules can exhibit helical chirality when their structures show a screw-shaped geometry and therefore can be either left- or right-handed. In the case of helically chiral fluorophores, they have the potential to emit circularly polarised luminescence (CPL). The 4,4-difluoro-4boron-3a,4a-diaza-s-indacene (BODIPY) fluorophores are a widely used class of molecules, which can exhibit helical structures which show CPL.

In this thesis, we have focused on the synthesis of helically chiral BODIPY architectures via point-to-helical chirality control. This was performed through the introduction of a point chiral group which induces helical chirality in another region of the molecule.

Herein we describe the synthesis of both 3,5-dichloro and -dibromo BODIPYs, as suitable intermediates enroute to *N,N,O,C* helically chiral BODIPYs. We have also developed a novel approach to 3,5-diiodo BODIPYs, which prove to be excellent substrates for both S_NAr and Pd cross-coupling reactions.

We also describe our development of novel synthetic routes to helically chiral BODIPYs, through the use of point-to-helical chirality control employing a range of naturally occurring α-amino acids to act similarly to chiral auxiliaries (note, these will be described as chiral directing groups throughout this thesis). Helicity can be introduced to the BODIPYs, with diastereomeric excesses (*de*) of up to 84%, showing excellent stereochemical control. Assignment of helical stereochemistry was performed via single crystal X-ray crystallography and electronic circular dichroism (ECD) spectra, demonstrating near mirror-image ECD spectra for the pairs of diastereomers.

The development of point-to-helical chirality routes to chiral BODIPYs opens up new strategies for the future synthesis of CPL emissive organic fluorophores.

Abbreviations

tetrakis	(triphenylphosphine)palladium(0)
$Pd[dppf]Cl_2$	[1,1′-Bis(diphenylphosphino)ferrocene]dichloropalladium(II)
Phen	1,10-phenanthroline
BINOL	1,1'-bi-2-naphthol
DDQ	2,3-Dichloro-5,6-dicyano-1,4-benoquinone
BODIPY	4,4-difluoro-4-bora-3a,4a-diaza-s-indacenes
DMAP	4-Dimethylaminopyridine
MeCN	acetonitrile
aq.	aqueous
ASAP	atmospheric solids analysis probe
BP	boiling point
PrCN	butyronitrile
CD	circular dichroism
CPL	circularly polarised luminescence
B_{CPL}	circularly polarised luminescence brightness
$Cu(OTf)_2$	copper(II) trifluoromethanesulfonate
CPL-SOM	CPL active small organic molecule
de	diastereomeric excess
DCM	dichloromethane
DMSO	dimethyl sulfoxide
DMF	dimethylformamide
ddd	double double doublet
dd	double doublet
dq	double quartet
d	doublet
ECD	electronic circular dichroism
S_EAr	electrophilic aromatic substitution
ES	electrospray
ESI	electrospray ionization
ee	enantiomeric excess

e.s	enantiomeric selectivity
eq.	equivalent
ETA	ethanolamine
HFIP	hexafluoro-2-propanol
HPLC	high performance liquid chromatography
h	hour
IR	infrared
LAH	lithium aluminium hydride
g_{lum}	luminescence dissymmetry factor
Mp	melting point
*m*CPBA	*meta*-chloroperoxybenzoic acid
MeOH	methanol
MIBK	methyl isobutyl ketone
MTBE	methyl tert-butyl ether
min	minute
M	molar
m	multiplet
DIPEA	*N,N*-diisopropylethylamine
nm	nanometre
NBS	*N*-bromosuccinimide
NCS	*N*-chlorosuccinimide
NIS	*N*-iodosuccinimide
NMR	nuclear magnetic resonance
S_NAr	nucleophilic aromatic substitution
ONSH	oxidative nucleophilic substitution of hydrogen
ppm	parts per million
pNSI	Pneumatically-assisted electrospray
EtCN	propionitrile
quant.	quantitative
q	quartet
RDS	rate determining step
R_f	retention factor

rt	room temperature
sat.	saturated
SET	single electron transfer
s	singlet
SD	standard deviation
TBAB	tetrabutylammonium chloride
TBAC	tetrabutylammonium chloride
p-chloranil	tetrachloro-1,4-benzoquinone
THF	tetrahydrofuran
TLC	thin layer chromatography
G3	third generation
TFA	trifluoroacetic acid
td	triple doublet
t	triplet
UV/Vis	ultraviolet / visible spectrophotometry

CHAPTER 1 INTRODUCTION 1

Chapter 1 Introduction

This thesis focuses on a strategy for the stereocontrolled synthesis of helically chiral fluorophores. More specifically, work will be focused on the synthesis of novel helically chiral 4,4-difluoro-4-bora-3a,4a-diaza-s-indacene (BODIPY) systems, demonstrating point-to-helical chirality control. These chiral BODIPYs will be accessed through their halogenated BODIPY counterparts, and therefore investigation into the synthesis of a range of new halogenated BODIPYs is also undertaken.

This chapter discusses relevant theory related to photophysical properties of compounds, specifically luminescence and circularly polarised luminescence. Further discussion of chirality, with specific focus on helical chirality is given alongside a general discussion of BODIPYs, including their typical reactivity and synthetic routes.

1.1 Introduction to Photophysics of Organic Fluorophores

In this section we will provide definitions of key concepts for photophysical properties displayed by fluorescent organic compounds. Many of these discussed properties will be seen in a number of our synthesised BODIPY compounds including our final helically chiral BODIPYs.

1.1.1 Luminescence

Luminescence is the emission of radiation from an electronically excited state of a compound. There are several different types of luminescence, which differ by virtue of the method of excitation, and which include photoluminescence (fluorescence and phosphorescence), chemiluminescence, crystalloluminescence and radioluminescence. Photoluminescence occurs upon the absorption of radiation, in the form of photons, exciting electrons of the compound from its ground state (S_0) to an excited state (typically S_1). Upon excitation, there are two types of photoluminescence that can occur, fluorescence and phosphorescence (Figure 1.1).

The first, fluorescence, occurs when the electrons relax back to the ground state immediately after excitation, emitting light in a timescale of 10^{-10} – 10^{-7} s. The

alternative, phosphorescence, occurs when the excited electrons invert their spin, resulting in intersystem crossing from an excited singlet (typically S_1) to triplet (typically T_1) state. This results in a delayed emission of light, from 10^{-6} to 10 s. The emission is delayed as relaxation back to the ground state (S_0) from the excited triplet state is formally forbidden due to a required change in spin state.

Vibrational relaxation can occur when photons excite electrons to a higher vibrational enery level of the same excited state. This excited electron gives some of its vibrational energy to another electron in the form of kinetic energy. This loss of energy from the excited electron results in relaxation to the energy minimum of the corresponding excited state.[1]

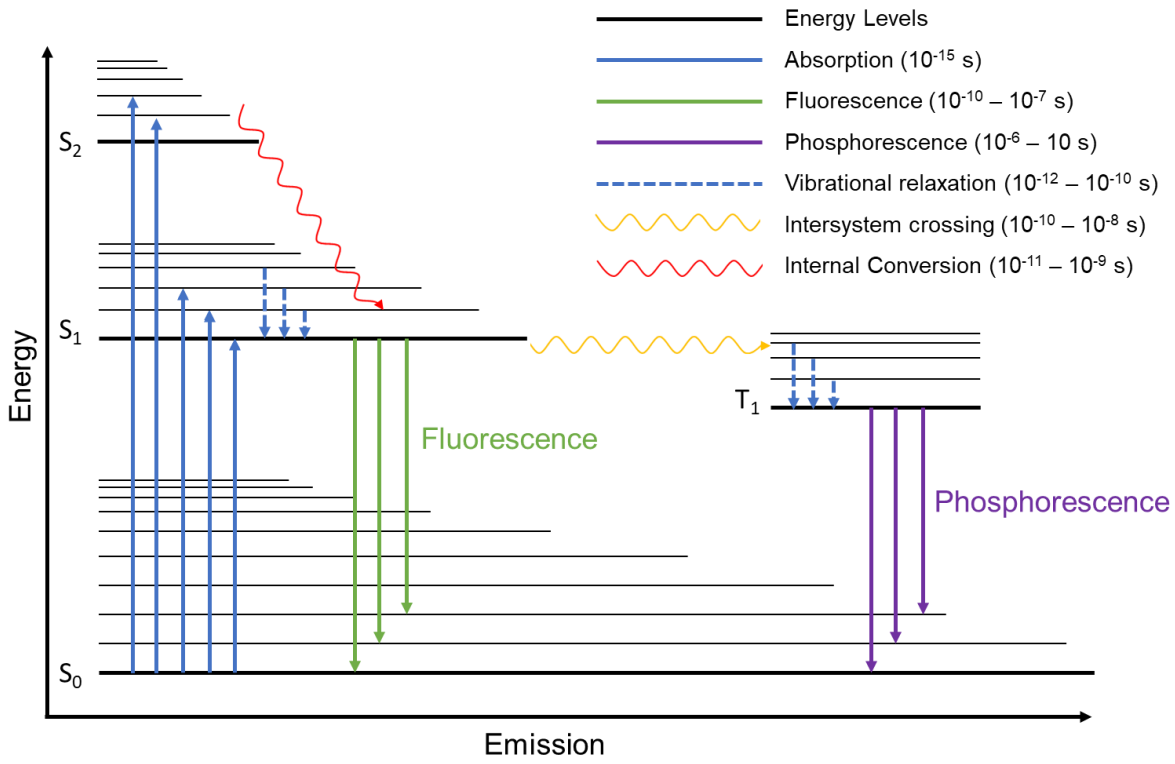

Figure 1.1. Jablonski diagram illustrating photoluminescence through the absorption and emission of photons. The ground state (S_0) is the lowest bold black line, with the excited singlet and triplet states labels on all other bold horizonal lines. All other horizonal lines represent vibrational energy levels within each excited state.

1.1.2 Molar Extinction Coefficient (ε)

The molar extinction coefficient is the measurement of the strength of absorption of a compound at a specific wavelength. It is related to the probability of the associated electronic transition. Molar extinction coefficient is directly related to absorption as shown in the Beer Lambert law below:

$$A = \varepsilon c l$$

In which A = absorption, ε = molar extinction coefficient, c = molar concentration and *l* = path length.

1.1.3 Fluorescence Quantum Yield (ϕ_F)

Fluorescence quantum yield is the efficiency at which a compound emits photons in fluorescence.[2] It is measured by the ratio between the number of photons absorbed vs the number emitted by a compound, giving a value between 0 and 1. Although the fluorescence quantum yield can be measured directly, it is more typically measured by the equation below, in which the fluorescence of the compound of interest is compared to that of a known standard compound:

$$QY = QY_{ref} \frac{\eta^2}{\eta^2{}_{ref}} \frac{I}{A} \frac{A_{ref}}{I_{ref}}$$

Where QY = quantum yield, η = refractive index of solvent, I = area under emission spectra and A = absorbance at excitation wavelength.

1.1.4 Stokes shift

Stokes shift is named after the physicist George Gabriel Stokes and represents the difference in wavelength between the maxima of the absorption and emission spectra of a compound.[3] The wavelength associated with a transition is inversely proportional to the energy which is either absorbed or emitted from the compound:

$$E = h\nu$$

In which E = energy, h = Planck's constant and ν is the frequency of light. Therefore, if the energy absorbed by a molecule to promote electrons to an excited state is

identical to the energy emitted upon relaxation of the electrons, the Stokes shift will be 0. However, there are two main ways in which the energy can be lost after excitation resulting in a Stokes shift, either as vibrational relaxation (as discussed previously), or dissipation and solvent reorganisation. Dissipation and solvent reorganisation occurs when a solvated fluorophore (which is a dipole) is excited, resulting in a change in dipole. For most species the excited state is much more polar than the ground state. The polar solvent molecules can reorientate their dipoles to stabilise the energy of the excited state faster than the in the ground state. This can result in a smaller energy difference between the excited and the ground state, resulting in a Stokes shift.

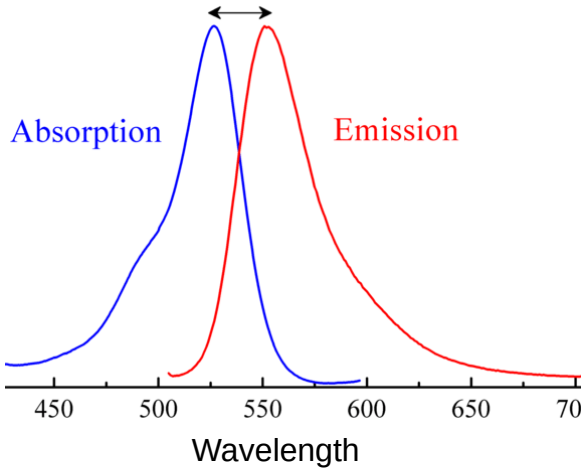

Figure 1.2. Normalised absorption and emission spectra of rhodamine 6G, with Stokes shift indicated.

1.1.5 Circular polarisation

In this section we will discuss both linear and circular polarisation of electromagnetic radiation.[4] Electromagnetic radiation consists of electromagnetic waves which are synchronised oscillating magnetic and electric fields. A photon is a particle representing a quantum of light or other electromagnetic radiation.

Polarisation of a photon (or ‘packet’ of photons) can be illustrated by showing the electric field of the photon as made up of two components, which are perpendicular sine waves. If the sine waves are in phase with each other then the resultant wave can be described as linearly polarised. In contrast, if the two perpendicular sine

waves are out of phase by 90 degrees (a quarter of a wavelength), the resulting wave is described as circularly polarised as the combined sine waves trace out a helical path as the photon propagates. Circularly polarised light can be described as either left- or right-handed, with left-handed circularly polarised light forming an anti-clockwise helix and right-handed circularly polarised light forming a clockwise helix. Circularly polarised light can be generated by initially converting unpolarised light into linearly polarised light through a linear polarizer. This is then further decomposed into left- or right-circularly polarised light through a quarter wave plate (Figure 1.3).

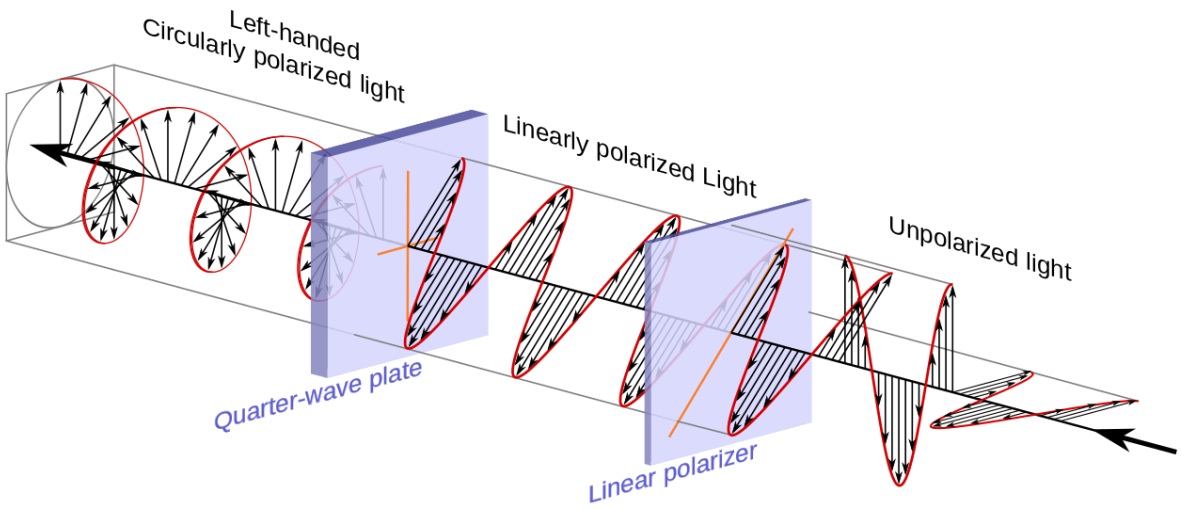

Figure 1.3. Generation of circularly polarised light. Unpolarised light passes through a Linear polariser and then a quarter-wave plate to generate either left- or right- circularly polarised light.

1.1.6 Circularly Polarized Luminescence (CPL)

Certain molecules are capable of emitting circularly polarised luminescence (CPL), which is the spontaneous emission of either right- or left-circularly polarised light. To be able to generate CPL a molecule in an excited state must undergo emission in a chiral field, which can be achieved through the use of a chiral fluorophore.[5] CPL generates optical signals which give information about the luminescence recorded as well as information on the chirality of the molecule.[6]

The difference in emission between right- and left-circularly polarised light is measured by CPL spectroscopy and is quantified by the luminescence dissymmetry factor (g_{lum}):

$$g_{lum} = \frac{(I_L - I_R)}{\frac{1}{2}(I_L + I_R)}$$

Where the intensity of emitted right- and left-handed polarised light is represented by I_R and I_L respectively. The value of g_{lum} can range from -2 to +2 for fully right- to fully left-handed polarised emission respectively. A value of 0 represents no CPL emitted. A theoretical equation to define g_{lum} is shown as:

$$g_{lum} = \frac{4(\boldsymbol{\mu} \cdot \boldsymbol{m} \cdot cos\tau)}{(\boldsymbol{\mu}^2 + \boldsymbol{m}^2)}$$

In which $\boldsymbol{\mu}$ and **m** are the magnetic and electric transition dipole moment vectors respectively and τ is the angle between them. Therefore, g_{lum} can be enhanced through considering these properties.

1.1.7 Circularly polarised luminescence brightness (B_{CPL})

In order to develop small molecule CPL emitters for future applications, it is important to develop parameters to allow direct comparison of different CPL-emitters from different chemical classes. Recently a new parameter was proposed to better represent overall CPL efficiency, named CPL brightness (B_{CPL}) which takes into account the absorption and emission efficiency of a species, by including quantum yield and extinction coefficient along with g_{lum}.[7, 8]

The measure of emission performance of a fluorophore is the fluorescence brightness (B), represented by the equation below:

$$B = \varepsilon_\lambda \times \phi_F$$

In which B is directly related to the molar extinction coefficient (ε) at the excitation wavelength (λ) and the quantum yield of fluorescence emission (ϕ_F). With this quantity, the brightness for CPL (B_{CPL}) can be calculated:

$$B_{CPL} = (\varepsilon_\lambda \times \phi_F) \times \frac{|g_{lum}|}{2} = B \times \frac{|g_{lum}|}{2}$$

1.1.8 Electronic Circular Dichroism (ECD)

Circular dichroism (CD) is the differential absorption of either left- or right-handed circularly polarised light.[9] When circularly polarised light is absorbed by an optically active chiral compound the extent of absorption may differ ($\varepsilon_L \neq \varepsilon_R$). CD of a molecule is the difference in molar extinction coefficients for right- and left-circularly polarised light:

$$\Delta_\varepsilon = \varepsilon_L - \varepsilon_R$$

Where ε_L and ε_R are the molar extinction coefficients for left- and right-circularly polarised light respectively. Because Δ_ε is a function of wavelength, the CD value (Δ_ε) must specify the wavelength at which it is valid.

Analogous to the use of g_{lum} in CPL, circular dichroism (CD) is quantified by the Kuhn dissymmetry ratio (g_{abs}):

$$g_{abs} = \frac{(\varepsilon_L - \varepsilon_R)}{\frac{1}{2}(\varepsilon_L + \varepsilon_R)}$$

Electronic circular dichroism (ECD) is a type of involved circular dichroism in which the wavelength of the circularly polarised light matches the electronic absorption bands in the visible spectra.

1.2 Molecules capable of CPL

In this section we will discuss a number of compounds which exhibit CPL, including chiral lanthanide complexes, small organic molecules capable of circularly polarised luminescence (CPL-SOMs) including chiral BODIPY compounds.

1.2.1 Chiral lanthanide complexes as CPL emitters

Chiral lanthanide complexes have played a crucial role in a number of fields including organic and optical sensing technologies, with a large number of reports of

their use in chiral sensing of biomolecules.[10-12] Chiral lanthanide complexes can be formed through the introduction of complex organic ligands, which upon coordination results in a chiral lanthanide environment. Chiral lanthanide complexes emit CPL through f → f transitions, which resulting in high luminescence dissymmetry factors (g_{lum}).[13] However, they typically have low ϕ_F, giving rise to low overall CPL emission and low B_{CPL}.

An example of a chiral lanthanide which emits CPL was published by Parker *et al.* in 2012. In this they showed that a Eu^{3+} could be made chiral through the introduction of a 9-coordinate ligand architecture, forming a C_3 symmetric complex **1**. The two enantiomers were formed in a racemic mixture which were separated by chiral HPLC (Figure 1.4).[14, 15]

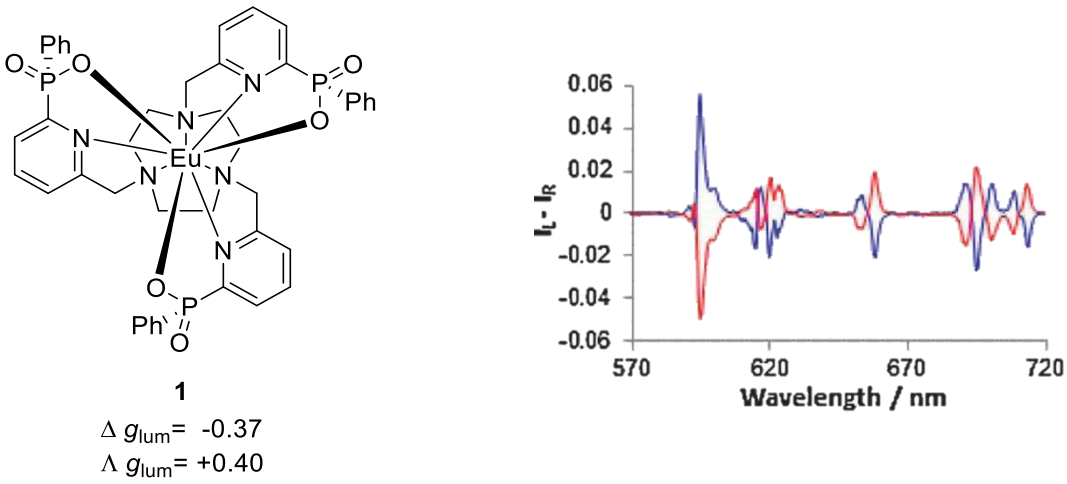

1

Δ g_{lum}= -0.37

Λ g_{lum}= +0.40

Figure 1.4. A) Λ Eu lanthanide complex **1** B) CPL spectra, Δ-(blue) and Λ-(red) enantiomers

Despite the advances in the development of chiral lanthanide complexes, they typically show low ϕ_F and therefore low B_{CPL}, limiting their usefulness in CPL applications.

1.2.2 Small organic molecules capable of emitting circularly polarised luminescence (CPL-SOMs)

CPL-SOMs have been investigated as alternatives to chiral lanthanide complexes due to a number of advantages, including ease of synthesis, solubility in common organic solvents, and the absence of potentially toxic lanthanide metals.[16]

The first reported examples of CPL-SOMs were a series of chiral ketones reported in 1967 by Emeis and Oosterhoff.[17] The chromophore in these molecules is a planar 'achiral' carbonyl group, however the overall molecule is chiral resulting in a chiral field and therefore CPL. Oosterhoff described the optical properties of (+)-trans-β-hydridanone **1.1**, showing it to be CPL active, with a g_{lum} value of +0.035 (Figure 1.5).

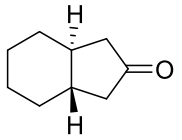

1.1

g_{lum} = 0.035

Figure 1.5. (+)-Trans-β-hydridanone **1.1.**

Since the work of Emeis and Oosterhoff there have been many new alternative classes of CPL-SOMs published in the literature,[16] which typically show extended conjugation and emit at long wavelengths.[18-20] Helicenes have a helical structure controlled by fused orthogonal rings. Their optical and chiroptical properties can be fine-tuned, leading to high g_{lum} values, such as helicene **1.2** (Figure 1.6, A).[21, 22] '#-Shaped' tetramers of azapentacenes **1.3** also demonstrate CPL through their extended biaryl skeleton (Figure 1.6, B).[23] Axial chiral binaphthyl, e.g. (*S*)-chiral binaphthyl **1.4** does not possess a mirror plane, resulting in it exhibiting CPL (Figure 1.6, C).[24]

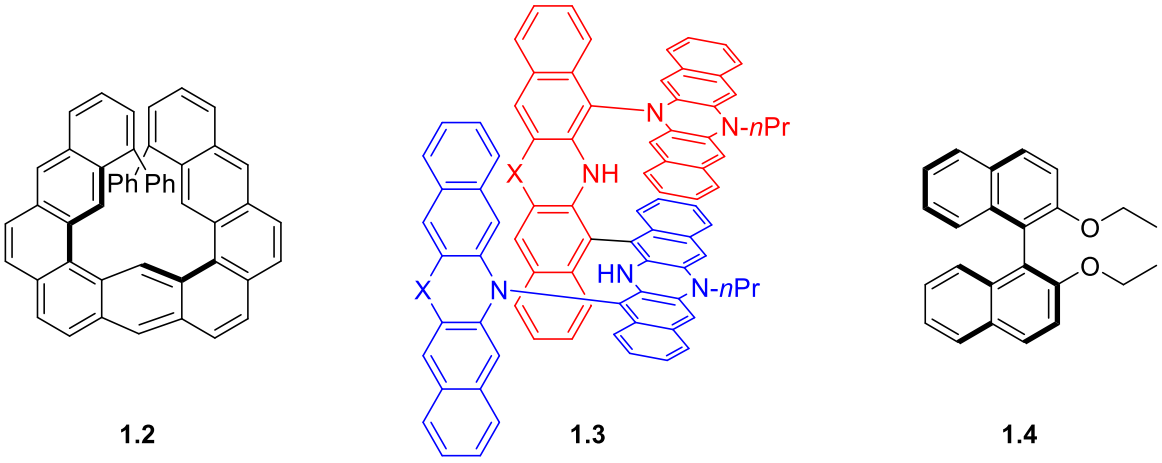

1.2 **1.3** **1.4**

g_{lum}= 0.013 g_{lum}= 0.0025 g_{lum}= 0.001

Figure 1.6. CPL-SOMs. A) Helicene B) '#-shaped' tetramer C) Chiral binaphthyl

In the examples given above, it is seen that helicene **1.2** shows a much larger g_{lum} value compared to the other examples. In the paper, authors explain this high g_{lum} through DFT calculations, showing the angle between the electric and magnetic transition dipole vectors to be 180º. Having anti parallel vectors maximises the observed g_{lum} seen for helicene **1.2** (Figure 1.6. CPL-SOMs. A) Helicene B) '#-shaped' tetramer C) Chiral binaphthylFigure 1.6).

In addition a number of chiral BODIPYs have been studied based around helical, planar, and axial chirality which will be discussed later.[25]

1.3 Introduction to the BODIPY dyes

Since this thesis is focussed on the synthesis of CPL-SOM BODIPYs, we will direct this section towards the discussion of typical characteristics of BODIPYs alongside common synthetic strategies.

4,4-Difluoro-4-bora-3a,4a-diaza-s-indacenes (BODIPYs) consist of a dipyrromethene group with a BF_2 moiety chelated through each nitrogen atom. After their initial discovery, the interest in BODIPYs over recent years has grown considerably due to their ease of preparation and optimal photophysical properties. BODIPYs commonly show sharp emission spectra with large Stokes shifts and high molar extinction coefficients (60000-80000 M^{-1} cm^{-1}).[26] They often present with high florescence quantum yields (0.6-1.0) which can be attributed to their low probability of

intersystem crossing from the singlet to triplet state as well as their relatively rigid structures which together help minimise pathways for non-radiative energy loss.[27, 28] BODIPYs have also been shown to have high photostability and low sensitivity to solvent polarity and pH. BODIPYs have been demonstrated to have a large variety of applications due to these optimal properties, showing huge potential in biomedical applications.[29, 30, 31] BODIPYs have been widely applied to this field, being used for biolabeling, photodynamic cancer therapy and bioimaging.[31, 32] BODIPYs have also shown potential for use in optoelectronic applications.[33] Due to ease in fine tuning their photophysical properties they have also been used as solid-state active materials in solar cells.[34]

The BODIPY core structure and the corresponding dipyrromethene precursor has two numbering systems - either the common or the IUPAC numbering system (Figure 1.7).

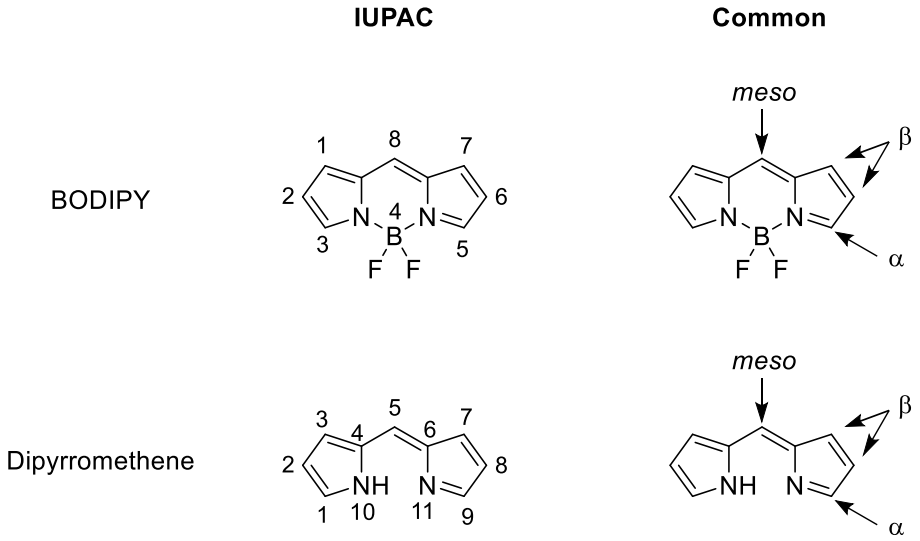

Figure 1.7. Structure of the BODIPY core and dipyrromethene precursor, showing both the IUPAC (left hand side) and common (right hand side) number system.

BODIPYs are commonly substituted at the *meso* position for two reasons, firstly ease of synthesis and secondly, change at this position typically shows minimal effects on the BODIPYs overall photophysical properties. Often an aryl moiety is present at the *meso* position as this can allow covalent tethering to receptors in biological tissue, enabling tagging of molecules.[35] BODIPYs can be also tuned to enhance their photophysical properties through the attachment of substituents,

particularly at the α and β positions.

1.3.1 Synthesis of BODIPY fluorophores through condensation chemistry

BODIPYs were initially synthesised serendipitously in 1968 by Treibs and Kreuzer attempting to acylate 2,4-dimethyl pyrrole.[36] In this one pot synthesis, 2,4-dimethyl pyrrole **1.5** was reacted with acetic anhydride **1.6** and $BF_3.OEt_2$ as a Lewis acid catalyst, forming the first BODIPY **1.9**. This BODIPY was formed through sequential acid catalysed condensations between 2,4-dimethyl pyrrole **1.5** and acetic anhydride **1.6** to form the dipyrromethene **1.8** followed by a subsequent *in-situ* boron chelation of a BF_2 moiety (Scheme 1.1).

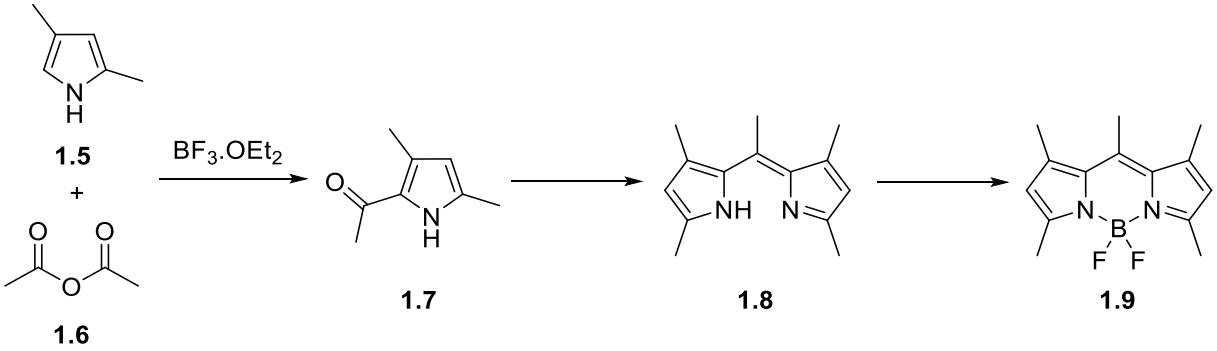

Scheme 1.1. First reported one-pot synthesis of BODIPYs by Treibs and Kreuzer.

Since this initial work there have been two main routes developed in which BODIPYs are synthesised, the first of which consists of the condensation of pyrrole **1.10** with an acylium equivalent **1.11** (Scheme 1.2). The corresponding acylpyrrole **1.12** is normally not isolated as it will react with another pyrrole to form the corresponding dipyrrin **1.13**. However, if a 1 to 1 equivalent of the pyrrole and acylium are reacted, the corresponding acylpyrrole can be combined with an alternative pyrrole moiety, synthesising asymmetric dipyrrins, which can be subsequently reacted with $BF_3.OEt_2$ to form an overall asymmetric BODIPY **1.14**.[37]

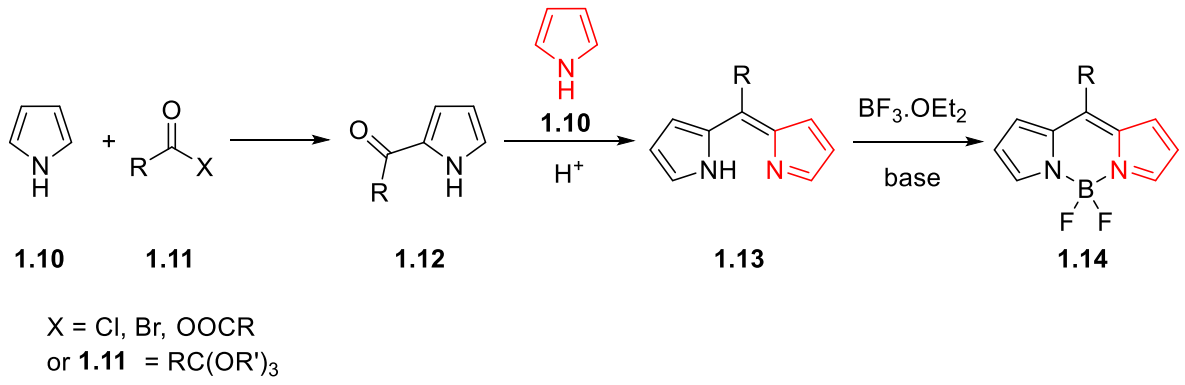

Scheme 1.2. Synthesis of BODIPYs via condensation of pyrrole with an acylium equivalent. This route can be utilised to synthesise asymmetric BODIPYs if the second added pyrrole (red) contains alternative moieties.

The second common approach is following the work of Lindsey *et al.*,[38] which involves a three-step synthesis which is initiated through an acid catalysed condensation reaction between pyrrole **1.10** and an aryl aldehyde **1.15** to form a dipyrromethane **1.16**. Dipyrromethane **1.16** is subsequently oxidised to the corresponding dipyrromethene (dipyrrin) **1.17**, either with DDQ or *p*-chloranil. The resulting dipyrromethene **1.17** is then treated with $BF_3.OEt_2$ to afford the final BODIPY **1.18** (Scheme 1.3).

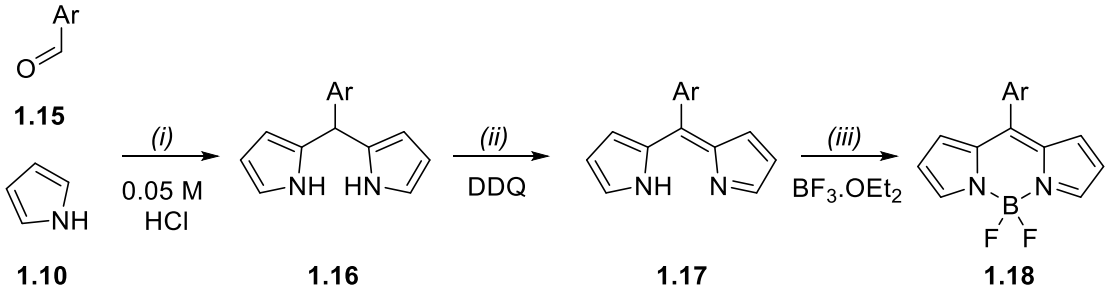

Scheme 1.3. General 3 step procedure towards BODIPYs, (i) = condensation, (ii) = oxidation, (iii) = chelation.

1.4 Functionalisation of BODIPYs

Following the synthesis of the core structure, functionalisation can be used to extend the BODIPYs architecture. Modification of the BODIPY is commonly used to fine tune the photophysical properties, often through the extension of the π-system. Numerous published methodologies exist for introducing various functionalities to the BODIPY core which are summarised below (Figure 1.8).[39, 40]

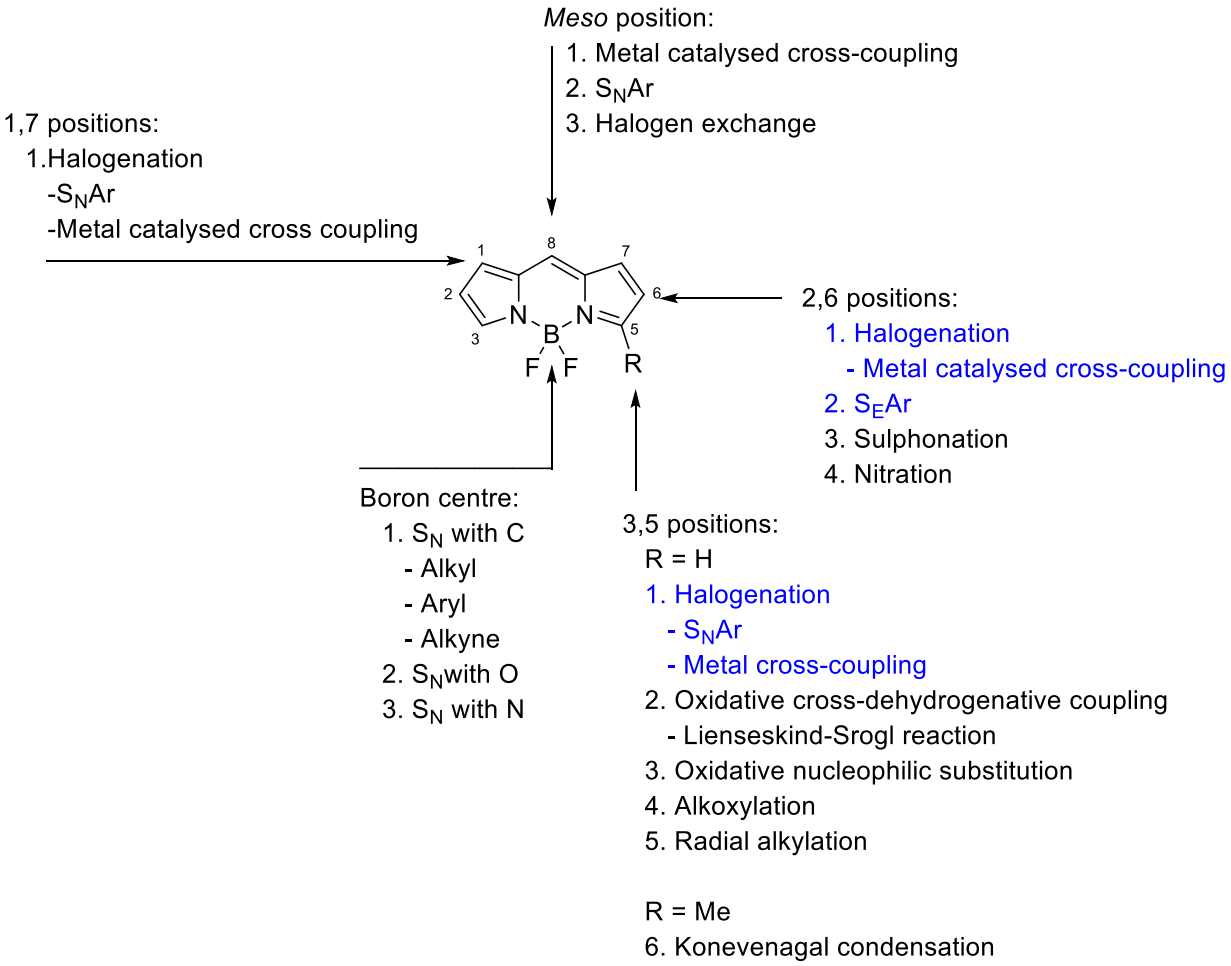

Figure 1.8. Functionalisation of BODIPYs, reactions highlighted blue discussed herein.

We will next focus on key BODIPY functionalisation chemistry that is used in this thesis, including electrophilic and nucleophilic aromatic substitution, single electron transfer and cross-coupling reactions.

1.4.1 Electrophilic Aromatic Substitution (S_EAr) of BODIPYs and dipyrromethanes

Electrophilic Aromatic Substitution (S_EAr) is commonly used to halogenate the BODIPY structure. S_EAr is most likely to occur at the 2,6 positions of the BODIPY as these sites have the least positive charge in the resonance structures.

Typically, the synthesis of brominated BODIPYs is accomplished with an electrophilic source of bromine such as Br_2 or *N*-bromosuccinimide (NBS). The BODIPY **1.19** can attack the Br_2, resulting in initial addition across the 2,6-positions to BODIPY **1.20** and then BODIPY **1.21**. It is seen that subsequent bromination can

occur at the 3,5-positions to BODIPY **1.22** and then eventually followed by the 1,7-positions to BODIPY **1.23**, which are least susceptible to electrophilic substitution (Scheme 1.4).[41]

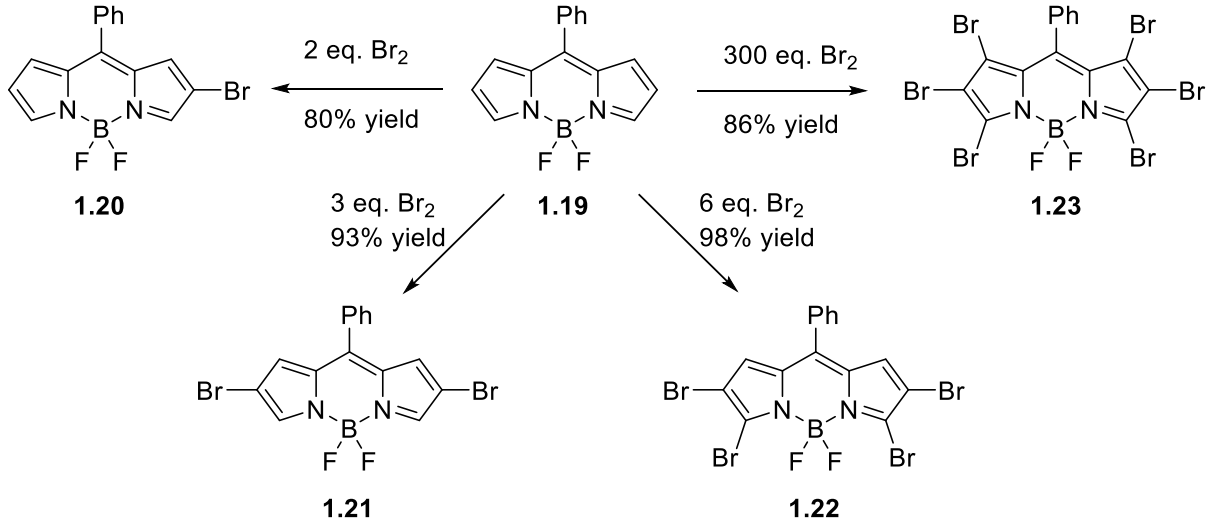

Scheme 1.4. Electrophilic aromatic substitution of BODIPY **1.19** with bromine, showing preferential 2,6 addition.

Due to the preferential S_EAr substitution at the 2,6 positions, synthesis of otherwise unsubstituted 3,5-dihalo BODIPYs via this methodology would not be possible. Therefore, to achieve preferential substitution at the 3,5 positions of the BODIPY, S_EAr is performed on the dipyrromethane precursor. The α position of a dipyrromethane species is most susceptible to electrophilic substitution. This was demonstrated by Ravikanth *et al*. in 2010, showing the successful synthesis of 3,5-dibromo BODIPY **1.25** through S_EAr upon the corresponding dipyrromethane species **1.24**.[42] The electrophilic brominating agent NBS substitutes at the α positions as this leads to the most stable carbocation upon electrophilic attack (Scheme 1.5). Note, that in contrast, after oxidation and chelation, the 2,6 positions become the most reactive towards electrophiles.

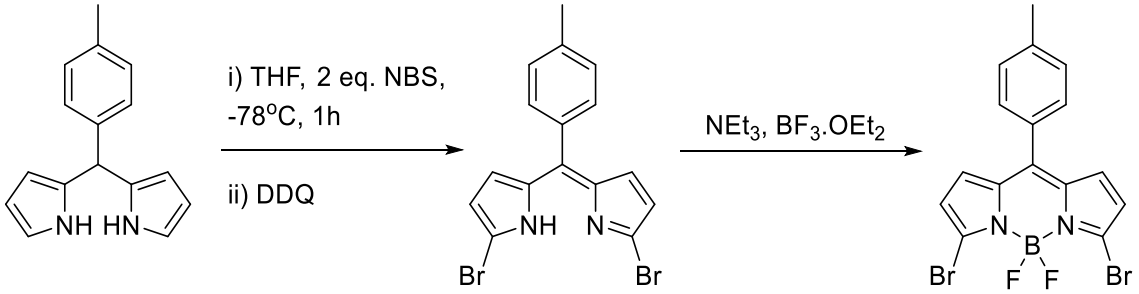

1.24 **1.25**

Scheme 1.5. Synthesis of 3,5-dibromo BODIPY **1.25** through electrophilic bromination prior to oxidation.

Synthesis of chlorinated BODIPYs through S_EAr chemistry shows the same preferential reactivity towards the 2,6 positions of the BODIPY, whilst 3,5-dichloro BODIPYs can be accessed similarly via S_EAr chlorination of the corresponding α positions of the dipyrromethane, followed by oxidation and chelation.[40, 43]

S_EAr chemistry can also be used to prepare 2,6-diiodo BODIPYs, however accessing otherwise unsubstituted 3,5-diiodo BODIPYs via S_EAr of dipyrromethanes has not been reported.[43, 44]

1.4.2 Single electron transfer (SET) reactions to synthesis 3,5-dichloro BODIPYs

An alternative approach towards 3,5-dichloro BODIPYs was published by Jaio *et al*. demonstrating the successful α-chlorination of BODIPYs.[45] Jiao reported that the use of $CuCl_2.H_2O$ as a chloride source results in the substitution of chlorine at the 3,5 positions of the BODIPY. This is postulated to occur through a series of single electron transfer (SET) steps. In the case of BODIPY **1.26**, this SET process from one pyrrole to $CuCl_2$ forms ClCu(I) and a radical cation **1.27** on the BODIPY core at the α position. This is subsequently followed by nucleophilic attack of a chloride anion to give the radical **1.28**. The final step involves an additional SET with a second Cu(II) followed by loss of H^+, forming the α-chloroBODIPY species **1.29** (Scheme 1.6).

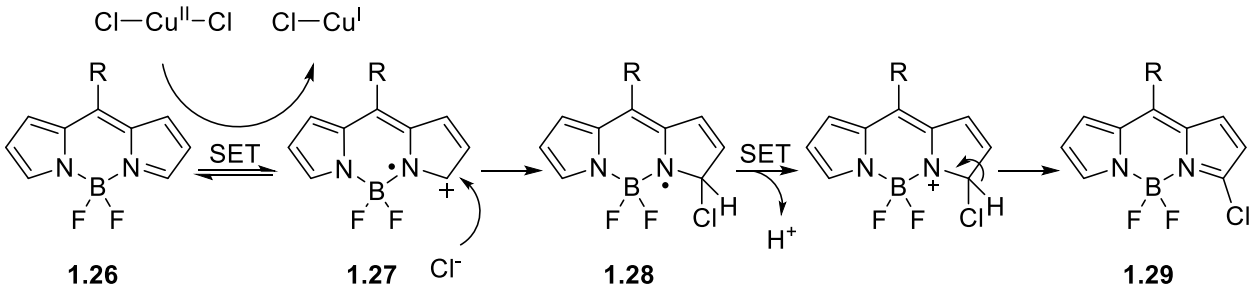

Scheme 1.6. α-chlorination via SET to Cu(I) from BODIPY **1.26**, nucleophilic addition followed by an additional SET to form mono chlorinated BODIPY **1.29**.

There has been a single report of 3,5-dichloro BODIPYs synthesised through this methodology, with no other 3,5-dihalo BODIPYs synthesised by this route.[45]

1.4.3 Nucleophilic Aromatic Substitution (S_NAr) of halogenated BODIPYs

3,5 and 2,6 halogenated BODIPYs show excellent reactivity towards nucleophilic aromatic substitution (S_NAr), which allows for easy functional elaboration. Typically, reported S_NAr reactions on BODIPYs have taken place at the 3,5-positions.[46-49] S_NAr has been attempted with a range of different nucleophiles, including O^-, S^-, N^-, Se^- and Te^- showing moderate to excellent yields.[50]

Dehaen and Boens demonstrated successful S_NAr of a range of nucleophiles upon 3,5-dichloro BODIPY **1.30**.[51] In this work they showed that reacting BODIPY **1.30** with a suitable nucleophile (2 eq.) at room temperature resulted in mono substitution. However, upon repetition of the reaction with more forcible conditions, using 4 eq. of the nucleophile and reflux, substitution at both the 3 and 5 positions of the BODIPY occurred (Table 1.1).

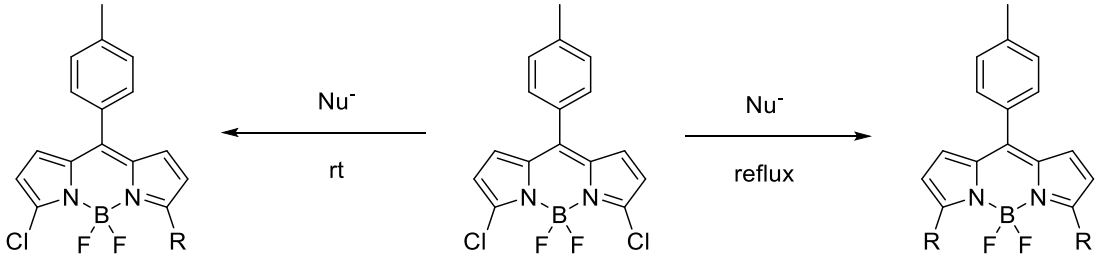

1.30

Nucleophile	**Solvent**	**Mono Yield**	**Di yield**
OMe	Methanol	65	66
OCH_2CH_2OH	MeCN	68	Excess decomposition
Piperidine	MeCN	74	64
NHPh	MeCN	69	64
SCH_2COOEt	MeCN	65	70
$CH(COOEt)_2$	MeCN	67	71

Table 1.1. Mono and di-substitution of BODIPY **1.30** by S_NAr.

1.4.4 Finkelstein/Halex reaction

An approach that we will employ in the synthesis of halogenated BODIPYs, is the Finkelstein or Halex reaction. A Finkelstein reaction was first reported by Hans Finkelstein, in which they showed the conversion of alkyl chlorides and alkyl bromides to alkyl iodides through an S_N2 reaction with sodium iodide in acetone (Scheme 1.7).[52]

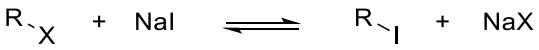

Scheme 1.7. Finkelstein precipitation driven reaction. X = Cl or Br

The Finkelstein reaction is typically a precipitation driven reaction, sodium iodide is readily soluble in acetone however the chloride or bromide counterpart is poorly soluble, with the precipitation of sodium chloride or bromide providing a driving force for the reaction.[53]

A Halex reaction is the general term for S_NAr halogen exchange reactions. The Halex reaction was initially used to form aromatic fluorides from aromatic chlorides, however it has been shown to have a broader reaction scope, including other

halogens and even non-aromatic substrates (Scheme 1.8).[54]

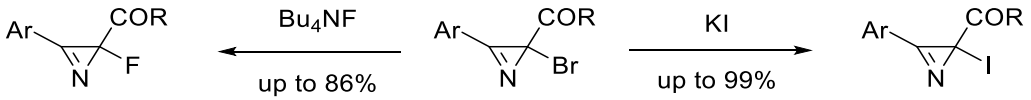

Scheme 1.8. Halex reaction demonstrating halogen exchange from Br to I or F.

1.4.5 Metal catalysed cross-couplings upon halogenated BODIPYs

To extend the BODIPY architecture, metal catalysed cross-couplings can be achieved on halogenated BODIPYs. In particular palladium catalysed cross-coupling reactions, in which the formation of a C-C bond is achieved from a C-Halo bond, have become ubiquitous in synthetic organic chemistry, and halo-BODIPYs have been shown to be excellent coupling partners.

In this section we will discuss a range of Pd catalysed cross-coupling reactions as applied to BODIPYs, including the Suzuki-Miyaura, Migita-Kosugi-Stille, Mizoroki-Heck and Sonogashira. In the case of dihalo BODIPYs, many of these cross-couplings have been shown to result in both mono and disubstitution, depending on the reaction conditions.

In 2009 Ziessel *et al*. showed a Suzuki-Miyaura cross-coupling upon a 3,5-dichloro BODIPY **1.31** containing a *meso*-aryl group with a reactive bromine subsitutent.[55] Suzuki-Miyaura coupling between the 3,5-dichloro *meso*-aryl BODIPY **1.31** and *p*-tolylboronic acid **1.32** was catalysed by tetrakis with potassium carbonate to give the trisubstituted BODIPY **1.33**, whilst with thienylboronic acid **1.34**, selective coupling at the 3,5 positions was observed, affording BODIPY **1.35** (Scheme 1.9).

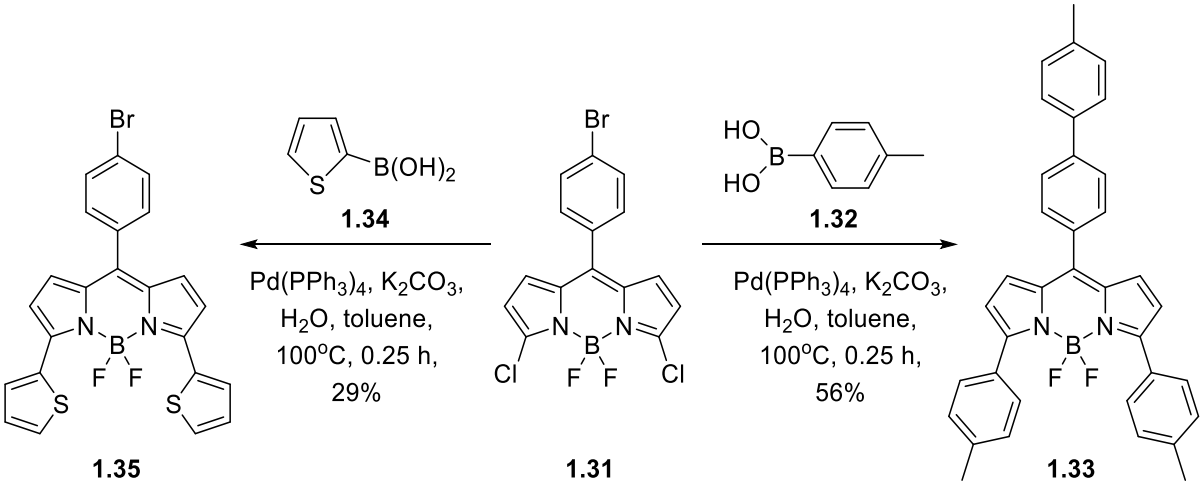

Scheme 1.9. Suzuki cross-coupling of 3,5-dichloro *meso*-aryl BODIPY **1.31**. Selective reactivity at the 3,5 positions when reacting with thienylboronic acid **1.34** with additional reactivity at the *meso* bromine substituent when reacted with *p*-tolylboronic acid **1.32**.

In 2011 Jiao *et al*. reported Suzuki-Miyaura cross-coupling upon 2,3,5,6-tetrabromo BODIPY **1.36**, showing the possibility of introducing multiple aryl groups in the 2,3,5,6-positions simultaneously to form tetraphenyl BODIPY **1.37** (Scheme 1.10).[41]

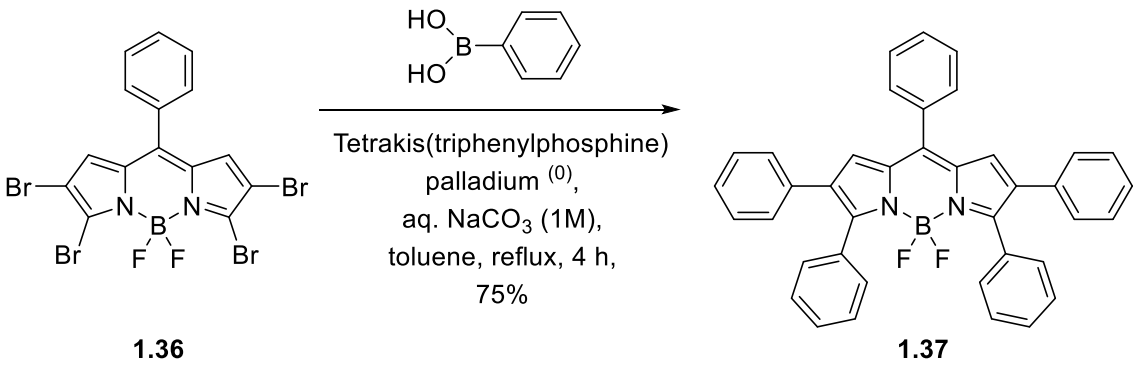

Scheme 1.10. Suzuki cross-coupling on 2,3,5,6-tetrabromo BODIPY **1.36**, introducing aryl groups simultaneously, synthesising 2,3,5,7-tetraphenyl BODIPY **1.37**.

In 2006 Dehaen *et al*. published a paper investigating a range of Palladium catalysed cross-couplings involving a 3,5-dichloro BODIPY.[56] Dehaen demonstrated the potential of Suzuki-Miyaura, Migita-Kosugi-Stille, Mizoroki-Heck and Sonogashira as suitable cross-coupling reactions upon 3,5-dichloro BODIPY **1.38** (Scheme 1.11). For both Migita-Kosugi-Stille and Suzuki-Miyaura cross-coupling reactions, the addition of a range of aryl groups at the 3,5 positions used $Pd(PPh_3)_4$ as the catalyst.

It was found that for each cross-coupling reaction a mixture of both the mono and di substituted products were observed.

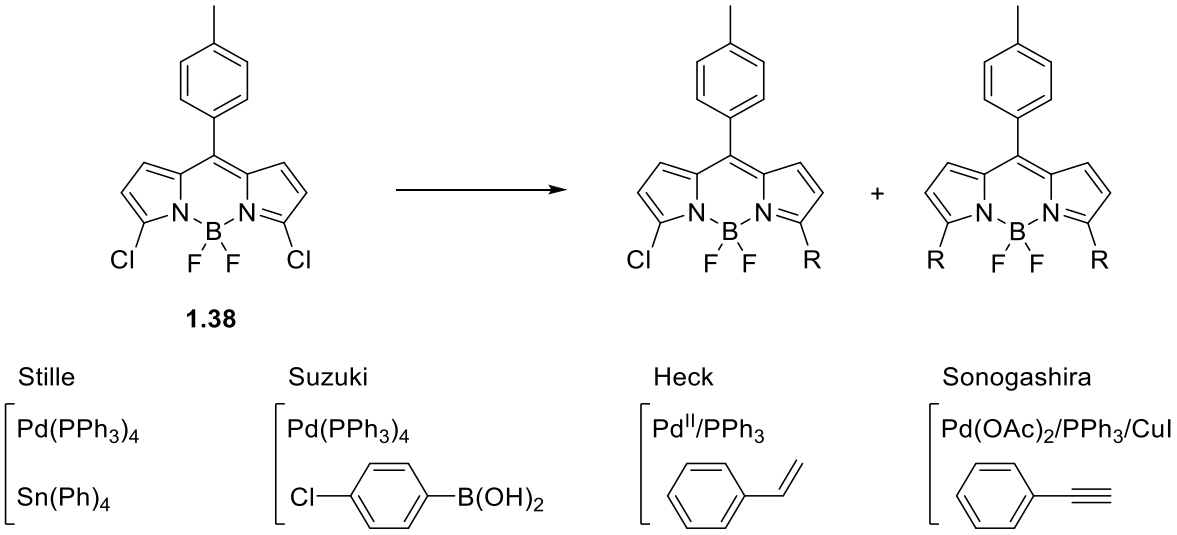

Scheme 1.11. Suzuki-Miyaura, Migita-Kosugi-Stille, Mizoroki-Heck and Sonogashira cross-coupling upon 3,5-dichloro BODIPY **1.38**, reported by Dehaen and coworkers.

In 2016 Jiao *et al*. published another comparative Suzuki-Miyaura, Mizoroki-Heck, Migita-Kosugi-Stille and Sonogashira paper, this time focusing on brominated BODIPYs.[57] A range of comparative reactions were carried out on 2,3,5,6 tetrabromo BODIPY **1.39**, showing cross-coupling at the 2,3,5,6 positions. In every case, preferential coupling was initially observed to occur at the 3,5 positions, with the 2,6 positions reacting subsequently (Scheme 1.12).

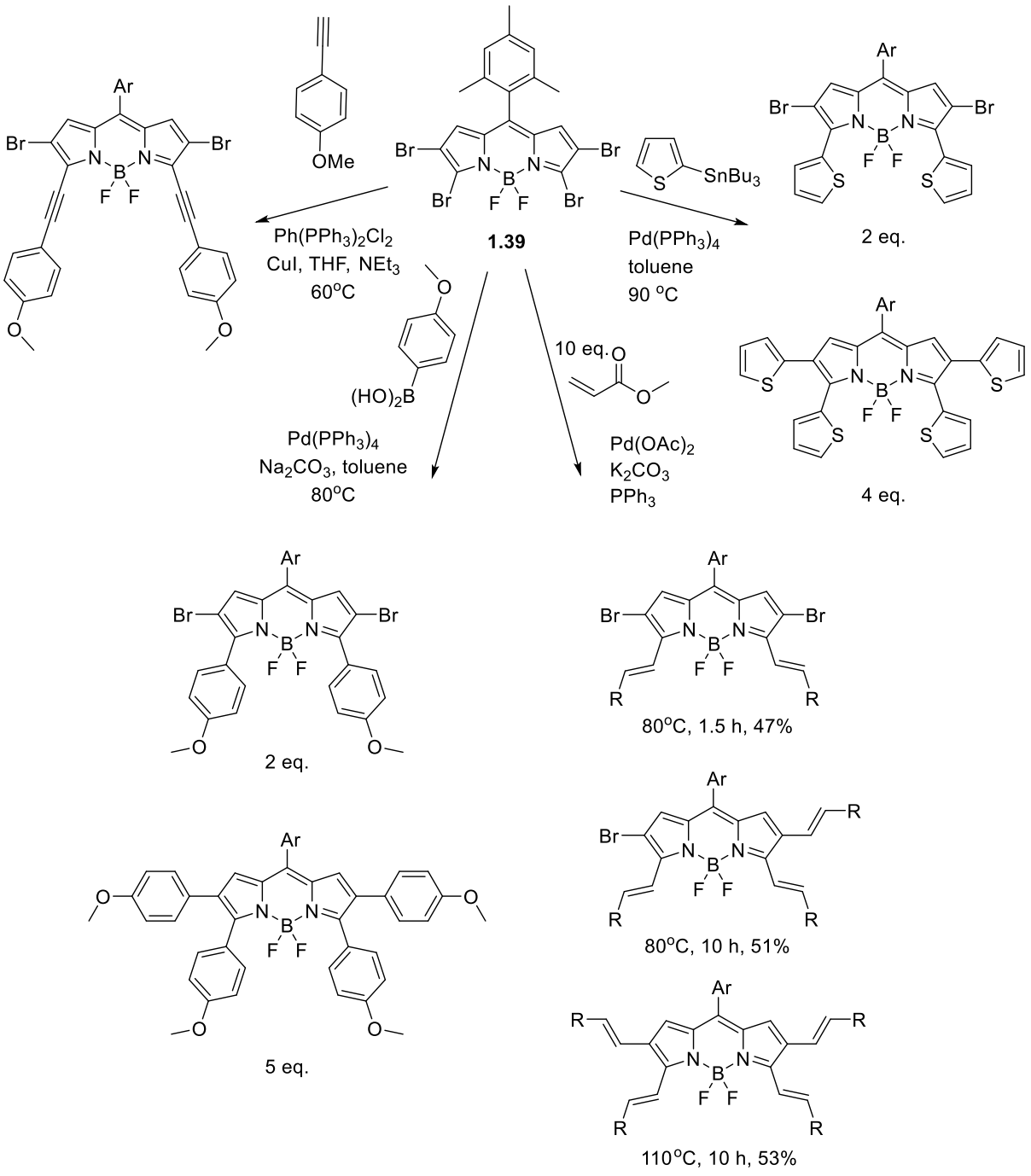

Scheme 1.12. Migita-Kosugi-Stille, Mizoroki-Heck, Sonogashira and Suzuki-Miyaura cross-couplings upon 2,3,5,6 tetrabromo BODIPY **1.39** reported by Jiao *et al*. Note preferential coupling for the 3,5 positions of the BODIPY core.

1.5 Chirality within BODIPYs

Typically, BODIPYs are achiral due to having a planar core structure. For a molecule to display CPL it must be intrinsically chiral in its excited state and therefore the achiral BODIPY must be chirally perturbed. There have been a number of different types of chirality observed in BODIPY systems.

1.5.1 Axial Chirality within BODIPY systems

Axial chirality has been exhibited within BODIPYs in a number of cases.[58] An example of a BODIPY showing axial chirality was shown by Akkaya *et al*. in 2014, showing the synthesis of a dissymmetric substituted orthogonal dimer, which is absent of a mirror plane.[59] This dimer was synthesised in a racemic mixture and therefore was separated by HPLC. ECD spectra was obtained, demonstrating the successful isolation of BODIPY **1.40** (

Figure 1.9).

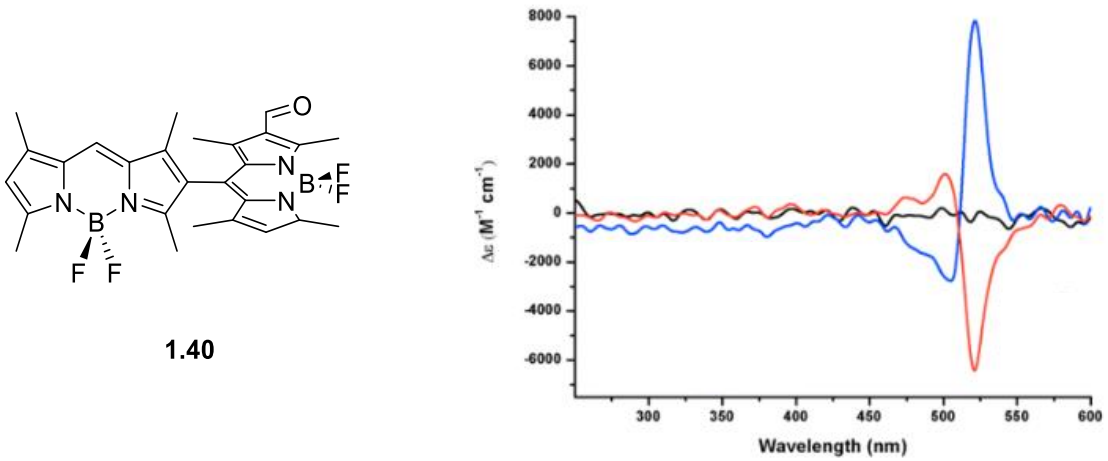

Figure 1.9. A) Orthogonal dimer BODIPY **1.40** exhibiting axial chirality. B) ECD spectra of each enantiomer in red and blue, with arbitrary assignment.

1.5.2 Helically Chiral BODIPYs

There are a small number of helically chiral BODIPYs published. Typically, reported cases of helically chiral BODIPYs are synthesised through direct desymmetrization upon O chelation on the boron centre. We will initially discuss the formation of cyclic

N,N,O,O BODIPYs containing a C_2 rotational axis with a further discussion of 'confused' *N,N,O,C* BODIPYs. We will also discuss the introduction of an external source of chirality into the BODIPY, resulting in overall helical chirality of the molecule.

1.5.2.1 Helically Chiral *N,N,O,O* BODIPYs containing a C_2 rotational axis

A simple, 'monomeric' helically chiral BODIPY, such as the *N,N,O,O*-chelated BODIPY **1.41**, was published by Hall *et al*. showing desymmetrisation through O chelation of the boron by its *ortho*-phenolic substituents. This induces helical chirality in the BODIPY, showing either a right- or left-handed helical structure throughout the molecule (Figure 1.10).[60] The two enantiomers, **(*M*)-1.41** and **(*P*)-1.41** were synthesised as a racemic mixture and separated by chiral HPLC.

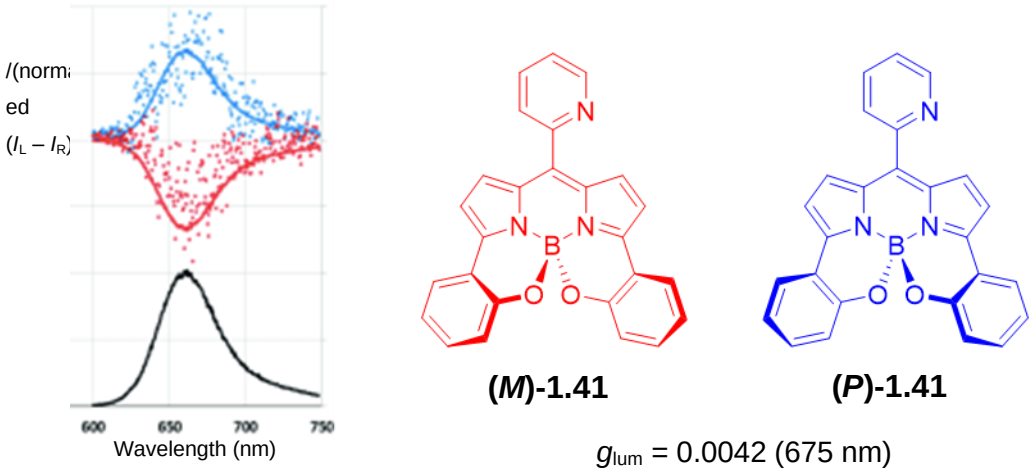

Figure 1.10. CPL spectrum of BODIPYs **(*M*)-1.41** and **(*P*)-1.41**, showing the emitted luminescence of both enantiomers (*P* = blue and *M* = red) The blue graph represents one enantiomer emitting an excess of left- circularly polarised light and the red graph represents the other enantiomer emitting an excess of right- circularly polarised light.

Another example of a helically chiral BODIPY, again possessing a C_2 rotational axis is *N,N,O,O*-chelated BODIPY dimer **1.42**. This molecule possesses a twist, in this case forming a figure-of-eight helix.[61] This BODIPY is formed in a racemic mixture of the *P,P*-isomer and *M,M*-isomer, separated by chiral HPLC (Figure 1.11). This twisted BODIPY **1.42** dimer is one of the most efficient CPL fluorophores reported to date (g_{lum} = 9 x 10^{-3}, ϕ_F = 0.58).

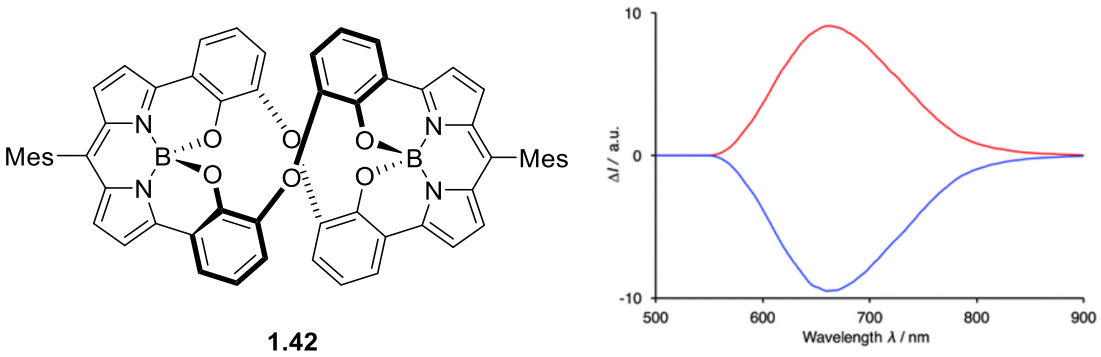

1.42

Figure 1.11. A) *N,N,O,O* BODIPY dimer **1.42**. B) CPL spectra of both enantiomers.

1.5.2.2 Helically chiral 'confused' *N,N,O,C* BODIPYs

An alternative approach to helically chiral BODIPYs was demonstrated by Hall *et al*. in 2017. This showed the synthesis of helically chiral BODIPYs via Suzuki cross-couplings of 3,5-dihalo BODIPYs.[8] Two types of helically chiral BODIPYs were formed, an *N,N,O,O*-boron chelated BODIPY (such as **(*P*)-1.44**) and a new structural class – *N,N,O,C*-boron chelated BODIPY (e.g. **(+)-1.43**). Both classes of helically chiral BODIPY were formed as the racemic mixture and required separation by chiral HPLC. The two enantiomers of the new *N,N,O,C*-BODIPY **(+)-1.43** displayed mirror image ECD and CPL spectra, as expected (Figure 1.12).

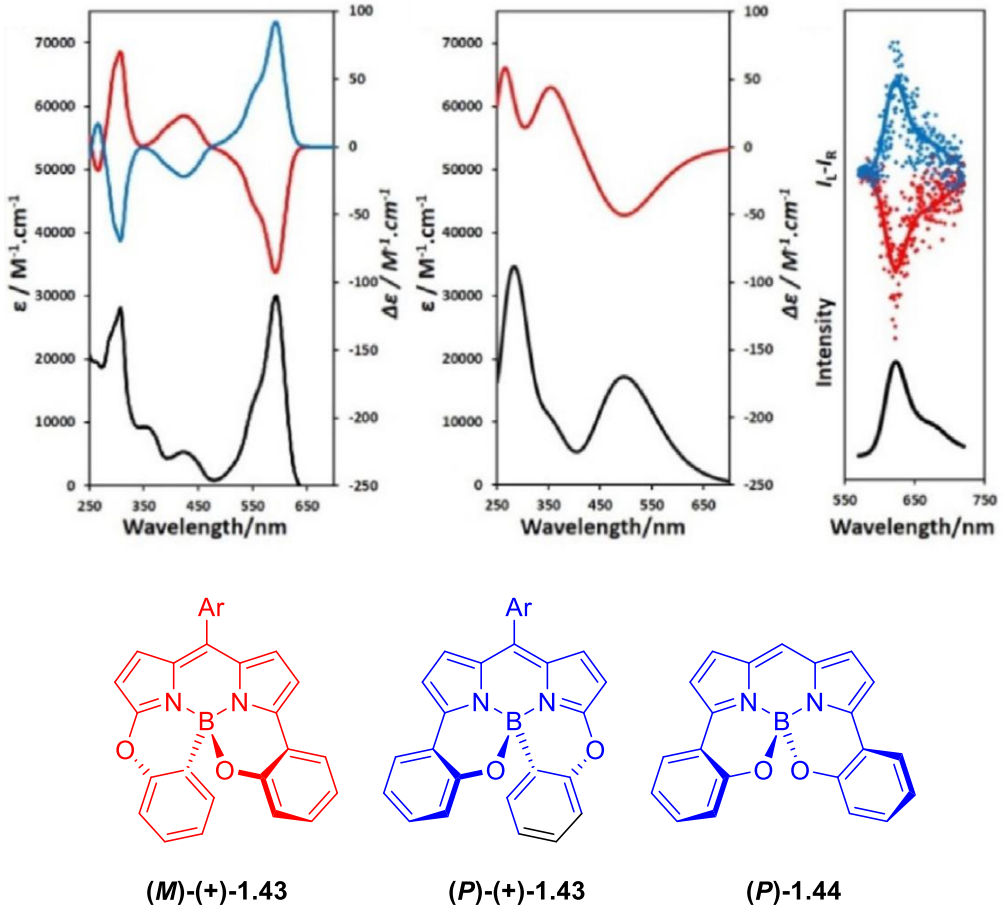

Figure 1.12. Helically chiral BODIPYs *N,N,O,O*- **1.44** and *N,N,O,C*- **1.43** synthesised by Hall *et al*. (a) Experimental ECD spectra [blue = (-)-**1.43** and red = (+)-**1.43**] and UV/Vis absorption spectrum [black = (*rac*)-**1.43**]. (b) Calculated Bolzmann weighted spectra: ECD [red = postulated (*M*)-**1.43**] c) Normalised experimental CPL spectra [blue = (-)-**1.43** and red = (+)-**1.43**] and fluorescence spectrum [black = (*rac*)-**1.43**].

1.5.2.3 Helically chiral BODIPYs through an external chiral source

An alternative example of helically chiral BODIPYs was reported by de la Moya *et al*. showing desymmeterisation of an achiral BODIPY by boron chelation with either (*S*) or (*R*)-BINOL through S_NAr chemsitry.[62] This gave rise to a C_2 rotational axis perpendicular to the chiral axis of the binaphthyl unit, giving a spiroBODIPY **1.45** (Figure 1.13). Each enantiomer was synthesised enantiomerically pure due to the use of either (*S*) and (*R*) BINOL starting materials thus avoiding the need for resolution by chiral HPLC.

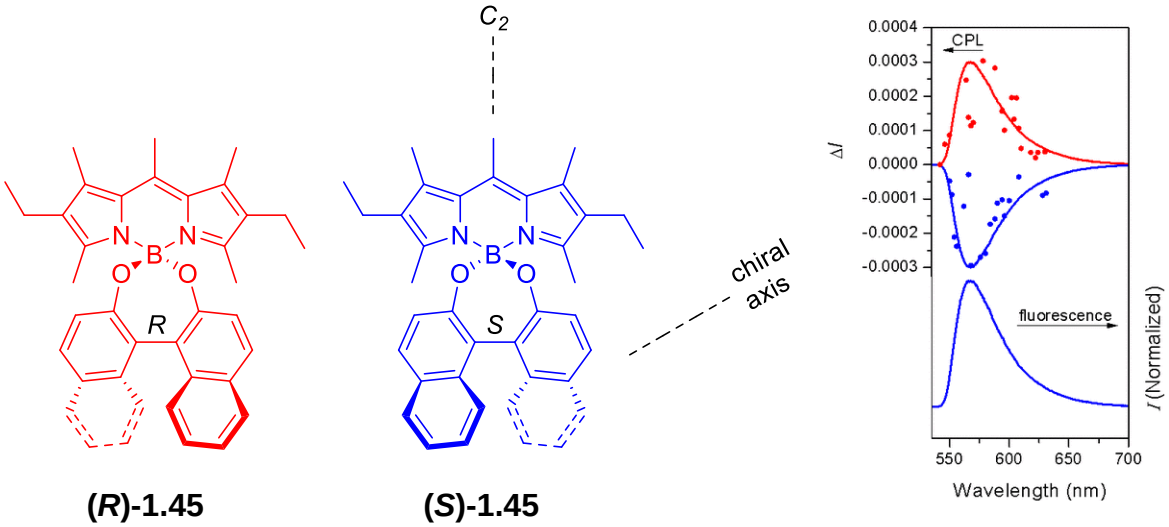

(*R*)-1.45 **(*S*)-1.45**

Figure 1.13. A) Chiral spiroBODIPYs. B) CPL data (upper) [red = **(R)-1.45** and blue = **(S)-1.45**] and total luminescence (lower).

One major problem in the synthesis of chiral BODIPYs is that typically they are synthesised in a racemic mixture due to the BODIPY core itself being planar and therefore achiral. Isolation of single enantiomers from the racemic mixture is essential for the measurement of CPL, and most often involves challenging separation using HPLC in the chiral stationary phase.[59] This is a very costly process, with the yield of the desired product limited.

1.6 Chiral induction

As a means to overcome issues surrounding the formation of racemic mixtures upon the synthesis of chiral compounds as discussed above, we will discuss alternative methods that lead to stereocontrol within a reaction.

1.6.1 Chiral Auxiliaries

One method to have stereocontrol in a reaction is to introduce a chiral auxiliary. A chiral auxiliary is a chiral group that is temporarily incorporated into a molecule with the purpose of controlling the stereochemical outcome of the synthesis. Because of this, chiral auxiliaries are widely used in the synthesis of enantiomerically and diastereomerically pure compounds. Typically, chiral auxiliaries are derived from natural products such as amino acids and terpenes due to the availability of these species in enantiomerically pure form.[63]

A common example of a chiral auxiliary is the Evans stereoselective aldol reaction through the use of chiral oxazolidinones.[64] The chiral oxazolidinone **1.46** is acylated and then undergoes an enolization with Lewis acid to form a (Z) enolate.[65] This enolate can undergo a diastereoselective aldol reaction with an aldehyde to form the desired β-hydroxy-carbonyl product **1.47** (Scheme 1.13).

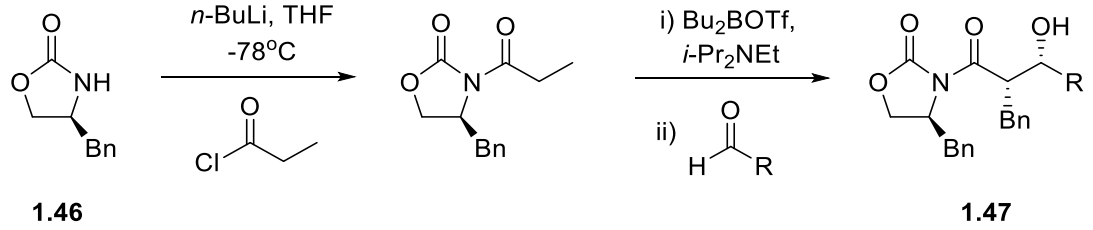

Scheme 1.13. Evans stereoselective aldol reaction utilising a chiral oxazolidinone as a chiral auxiliary.

The oxazolidinone can then be removed under a range of conditions depending on the desired functional group (Scheme 1.14).[65, 66]

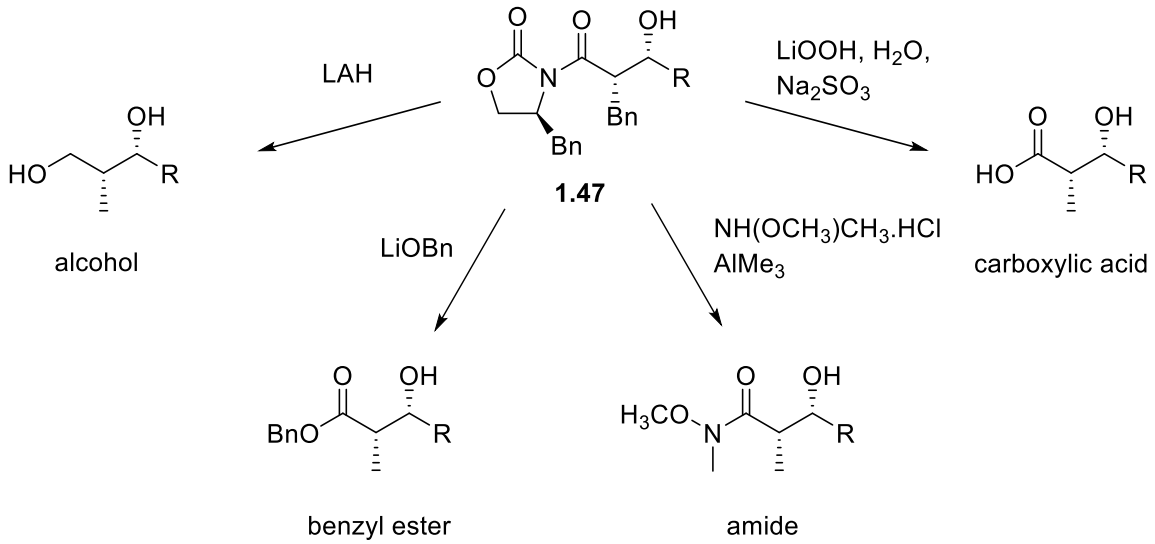

Scheme 1.14. Several different reaction conditions for the removal of oxazolidinones depending on desired functional group.

Through the introduction of a chiral auxiliary into an organic compound, stereocontrol is achieved, forming enantio- and diastereomerically pure compounds. This removes the need to separate racemic mixtures through costly chiral HPLC.

1.6.2 Chirality Transfer

An alternative method to stereocontrol is chirality transfer. This typically arises when stereochemical information is transmitted from one reaction component to the product.[67]

1.6.2.1 Point-to-axial chirality transfer

Point-to-axial chirality transfer has been demonstrated by Aggarwal *et al.* in the preparation of allenes. They showed near complete stereospecificity in the synthesis of either the *P* or *M* allene, from a single isomer of a point-chiral precursor. When the point chiral precursor **1.48** is subjected to oxidative conditions of *m*CPBA, *syn* elimination is achieved, synthesising allene **1.49** in complete stereoselectivity. However, when the precursor is subjected to alkylative conditions of MeOTf with a suitable base, *anti* elimination is achieved, synthesising allene **1.50** with an *e.s* of 83 – 98% (Scheme 1.15).[68]

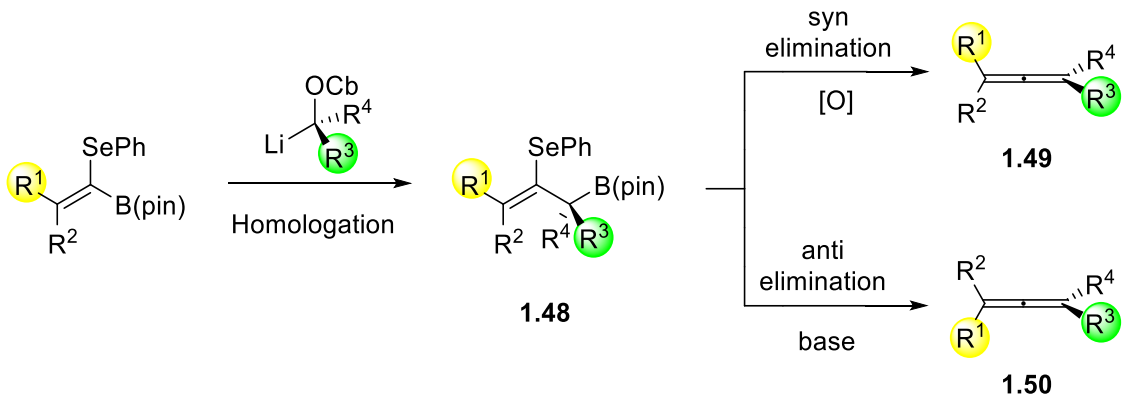

Scheme 1.15. Point-to-axial chirality transfer in allenes.

1.6.2.2 Point-to-helical chirality transfer

Carbery *et al*. demonstrated point-to-helical chirality transfer when synthesising a DMAP organocatalyst **1.52**. A point-chiral pyridyl triyne **1.51** undergoes a Rh-catalysed [2+2+2] cycloisomerization to form DMAP **1.52**, using the existing stereocentre to control the formed helicity showing high diastereoselectivity (Scheme 1.17).[69]

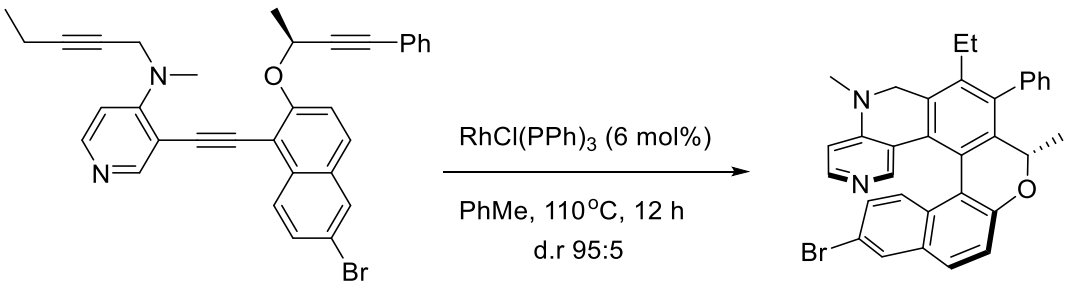

1.51 **1.52**

Scheme 1.16. Point-to-helical chirality transfer in the synthesis of DMAP organocatalyst **1.52**.

1.7 Project aim

The overall aim for this thesis was to explore point-to-helical chirality control within BODIPY systems as a means to synthesis helically chiral BODIPY compounds with diastereomeric control.

This proposed approach involves the synthesis of a range of 3,5-dihalo BODIPYs **1.53** which can undergo mono S_NAr with an enantiomerically pure chiral directing group followed by the subsequent introduction of a 2-hydroxyphenyl substituent via palladium catalysed Suzuki cross-coupling at the remaining halogenated position.

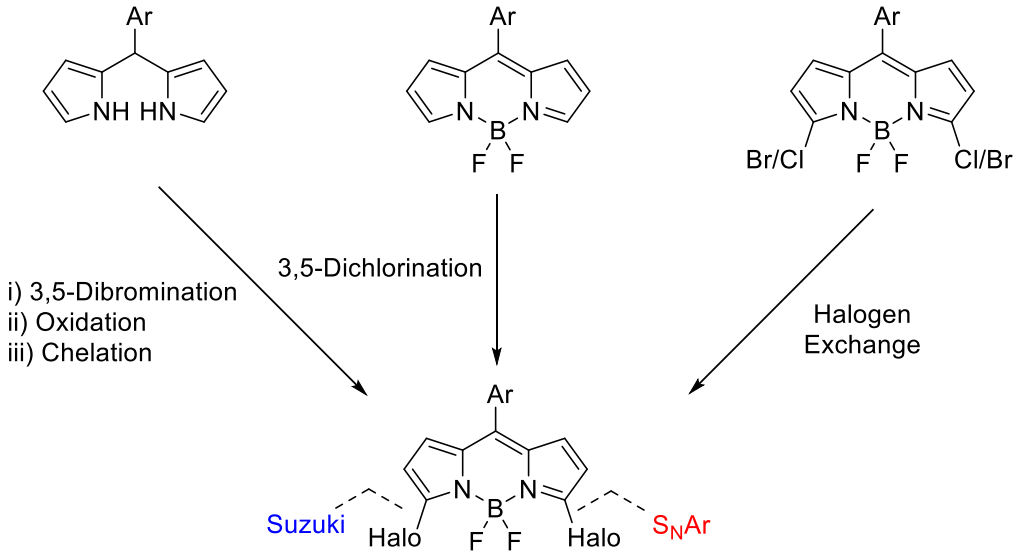

1.53

Scheme 1.17. Proposed synthesis of helically range of 3,5-dihalo BODIPY **1.53** precursors.

Multiple routes to helically chiral BODIPYs are explored. One route relies on *in-situ* ring closure upon coupling of an *ortho*-phenyl group, to form helically chiral diastereoisomers **1.54a** and **1.54b.** An alternative route of dechelation/rechelation of the boron centre will also be explored, incorporating a new boron moiety to form diastereoisomers **1.55a** and **1.55b**. Both of these synthetic routes to helically chiral diastereoisomers BODIPYs, are expected to show transfer of chirality from the point chiral group to the final helically chiral structure (Scheme 1.18).

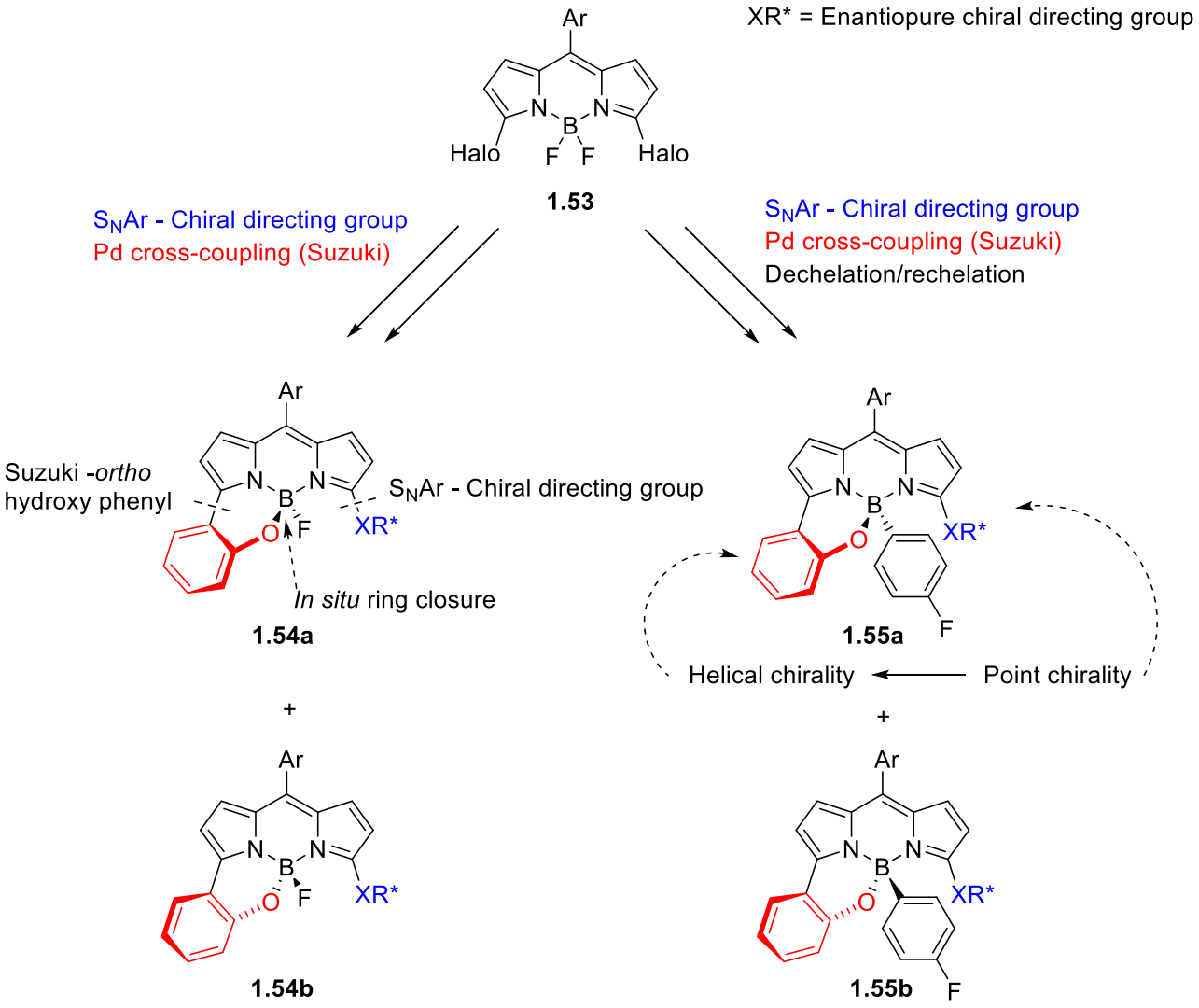

Scheme 1.18. Two alternative synthetic routes to helically chiral BODIPYs demonstrating point-to-helical chirality control.

After the synthesis and isolation of novel helically chiral BODIPYs, exploration of the chiroptical properties is imperative in the development of these new chiral SOMs.

In chapter 2 we will initially discuss the synthesis of 3,5-dichloro BODIPYs. Investigation into 3,5-dichloro BODIPY methodology optimisation is discussed, focusing on improvement of synthetic yields. Further study into 3,5-dibromo BODIPYs is also undertaken following the work of the Hall group. It is hoped that both these 3,5-dichloro and 3,5-dibromo BODIPYs will be suitable intermediates for S_NAr and Pd cross-coupling investigation.

In chapter 3 we discuss our attempt to synthesis novel 3,5-diiodo BODIPYs. Investigation into halogen exchange from both its 3,5-dichloro and 3,5-dibromo counterparts is carried out. It is hoped that 3,5-diiodo BODIPYs will show higher yields for subsequent Pd cross-coupling reactions compared to its dichloro and dibromo BODIPY counterparts.

In chapter 4 we report our investigation into S_NAr and Pd cross-coupling upon all previously synthesised 3,5-dihalo BODIPYs. We hoped to thus find the most suitable 3,5-dihalo BODIPY intermediate for the synthesis of our final helically chiral BODIPY. Furthermore, in chapter 4 we discuss the total synthesis of helically chiral BODIPYs demonstrating point-to-helical chirality control. In this we will investigate diastereomeric control through a range of chiral directing groups. In this chapter we will also discuss the characterisation and photophysical properties of each helically chiral BODIPY diastereoisomer.

Chapter 2 Synthesis of 3,5-Dichloro and 3,5-Dibromo-BODIPYs

2.1 Introduction

2.1.1. Aims

In this chapter we will discuss the synthetic approach to 3,5-dichloro and 3,5-dibromo BODIPYs. We wished to target 3,5-dihalo BODIPYs **1.53** as they can be used in S_NAr and Pd cross-coupling reactions to further develop the BODIPY structure. This is the synthetic approach that we intend to use in our overall route to helically chiral BODIPYs (Scheme 2.1).

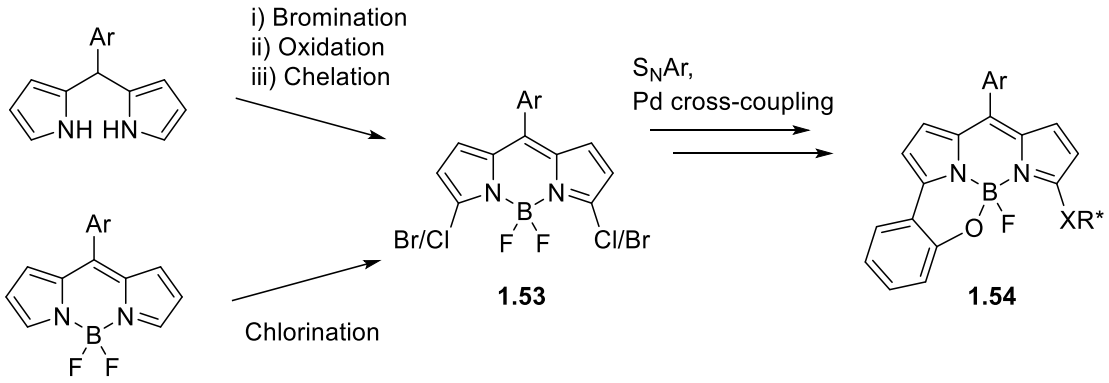

Scheme 2.1. General approach for the synthesis of 3,5-dichloro and 3,5-dibromo BODIPY **1.53** enroute to 3,5-functionalised BODIPYs **1.54**. XR* = enantiopure chiral directing group.

The synthesis of both 3,5-dichloro and 3,5-dibromo BODIPYs has been previously reported in literature, therefore we planned to adapt known synthetic routes as a means to access our target compounds.

2.1.2. 3,5-Dihalogenation strategies for the BODIPYs

As discussed in Chapter 1, S_EAr halogenation of an unsubstituted BODIPY occurs preferentially at the 2,6 positions. Therefore, obtaining 3,5-dihalo BODIPYs by direct S_EAr halogenation is synthetically challenging and alternative synthetic approaches are required for both 3,5-dichlorination and 3,5-dibromination.

There are two main literature routes towards otherwise unsubstituted 3,5-dichloro BODIPYs. The most commonly used of which is the S_EAr of a dipyrromethane with an electrophilic source of Cl, such as NCS. S_EAr of dipyrromethanes preferentially

occurs at the α-positions, which following oxidation and BF_2 chelation gives rise to their corresponding 3,5-dichloro BODIPYs. This synthetic approach was first reported by Baruah *et al*. in 2005 (Scheme 2.2).[70]

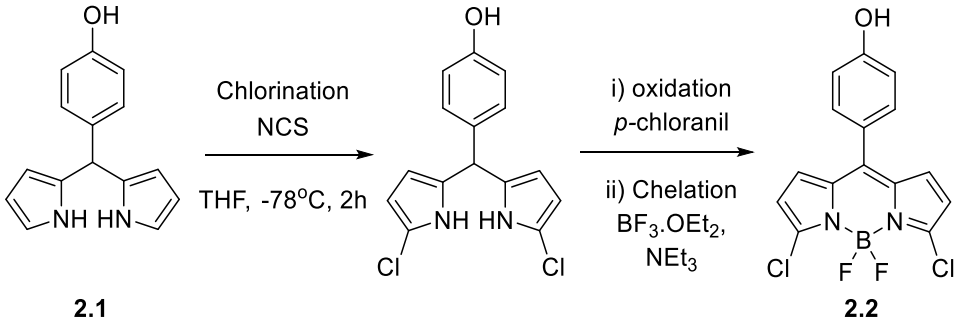

Scheme 2.2. Electrophilic chlorination at the α-positions of dipyrromethane **2.1** followed by oxidation and chelation to obtain 3,5-dichloro BODIPY **2.2**.

Selective bromination at the 3,5 positions of an unsubstituted BODIPY can be achieved through a very similar synthetic route as discussed above, which was previously discussed in Chapter 1.

The second main route towards 3,5-dichloro BODIPYs was reported by Jaio *et al*., demonstrating a copper mediated, oxidative nucleophilic substitution of hydrogen (ONSH) by chloride at the 3,5 positions. Jaio *et al*. demonstrated that either 3-chloro **2.3** or 3,5-dichloro BODIPYs **2.4** can be produced using this approach depending on the equivalents of $CuCl_2.H_2O$ used. This resulted in a range of 3,5-dichloro BODIPYs synthesised in good yields from 60 to 66% (Scheme 2.3).[45]

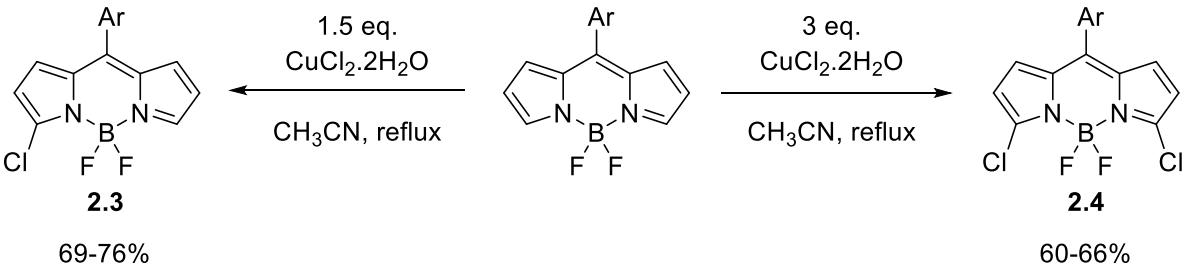

Scheme 2.3. ONSH by chloride to synthesis both 3-chloro and **2.3** 3,5-dichloro BODIPYs **2.4**.

As discussed in Chapter 1, Jiao *et al*. proposed that 3,5 dichlorination of BODIPYs proceeds through a number of SET steps.

2.2 Synthetic strategy towards 3,5-dichloro BODIPYs 2.11

In this section we discuss our synthetic efforts towards 3,5-dichloro BODIPYs, through evaluation of Jiao's copper mediated ONSH approach.

2.2.1 Synthesis of Dipyrromethane **2.7a** via Dehaen Condensation

In order to use the Jiao oxidative nucleophilic substitution of hydrogen (ONSH) by chloride approach to synthesise 3,5-dichloro BODIPYs, synthesis of starting material dipyrromethane **2.7** is required. Therefore our first synthetic target was dipyrromethane **2.7a**, which was planned to be synthesised via Dehaen's acid catalysed condensation chemistry of aryl aldehydes with 1*H*-pyrrole.[71]

Based on Dehaen's approach, the condensation of methyl 4-formylbenzoate **2.5a** with 2.2 equivalents 1*H*-pyrrole **2.6** in aqueous HCl (0.05 M) at rt was attempted on a 6.90 mmol scale. After 4 hours the product precipitated out of solution and was isolated by filtration to give the desired dipyrromethane **2.7a** in an excellent 99% yield. The structure of the desired dipyrromethane **2.7a** was confirmed through ^{1}H NMR, showing a distinctive one proton singlet at 5.53 ppm corresponding to the *meso* position (Scheme 2.4).

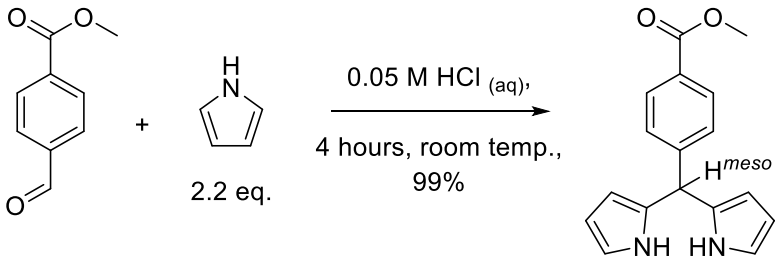

2.5a **2.6** **2.7a**

Scheme 2.4. Acid catalysed condensation between pyrrole **2.6** and methyl 4-formylbenzoate **2.5a** to form dipyrromethane **2.7a**.

The synthesis of dipyrromethane **2.7a** was performed 39 times over the course of the project as it is a key starting material for many subsequent reactions, including the synthesis both 3,5-dichloro and 3,5-dibromo BODIPYs. The condensation reaction was performed on a range of scales from 3.045- 24.36 mmol, giving an average yield of 89% and standard deviation of 10%.

A sample of dipyrromethane **2.7a** was purified by silica gel column chromatography for analytical purposes, however, it was found that the crude precipitate could simply be washed with water and petroleum ether to give the dipyrromethane **2.7a** at high enough purity to continue without the need for large scale silica gel column chromatography. Samples of dipyrromethane **2.7a** could be stored as solids at rt for up to 6 months, and despite minor colour changes remained clean by ^{1}H NMR.

2.2.2 Oxidation of dipyrromethane **2.7a** to dipyrromethene **2.8a**

The next step in our synthetic route is the oxidation of dipyrromethane **2.7a** using either *p*-chloranil or DDQ as the oxidising agent to give dipyrromethene **2.8a**. Following previously published procedures by Hall *et al*., the oxidation of dipyrromethane **2.7a** was subsequently investigated using both DDQ and *p*-chloranil.[8]

Oxidation of dipyrromethane **2.7a** was initially attempted with 1.1 equivalents of DDQ, on a 7.13 mmol scale at rt temp in THF for 4 hours. Upon ^{1}H NMR analysis of the crude reaction mixture, a complex mixture of compounds was seen, showing no presence of the desired dipyrromethene **2.8a**.

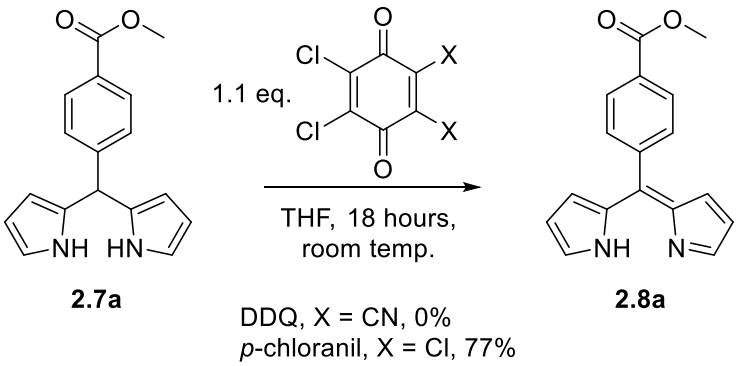

Scheme 2.5. Oxidation of dipyrromethane **2.7a** to dipyrromethene **2.8a** using either DDQ or *p*-chloranil.

Oxidation of dipyrromethane **2.7a** was further attempted using an alternative oxidising agent, *p*-chloranil, under otherwise identical reaction conditions. This proved much more successful, and after an aqueous work-up the desired dipyrromethene **2.8a** was obtained in a high crude yield of 77% (Scheme 2.5). Purification through silica gel column chromatography proved difficult due to the low

solubility of dipyrromethene **2.8a** in suitable chromatography solvents, resulting in poor separation on silica gel. This resulted in a lower isolated yield of 49%. Therefore, in subsequent reactions dipyrromethene **2.8a** was carried forward without purification, with the intent to undertake more rigorous purification following the next step.

The structure of dipyrromethene **2.8a** was confirmed through ^{1}H NMR. This showed the disappearance of the *meso* hydrogen atom at 5.53 ppm and a shift in the pyrrolic protons doublets from 6.88 (J = 8.5 Hz) and 6.56 ppm (J = 8.5 Hz) to 6.55 (J = 4.2 Hz) and 6.42 ppm (J = 4.3 Hz), indicating oxidation had occurred.

Dipyrromethene **2.8a** is a common starting material for a number of reactions and therefore was repeated 50 times throughout the project. This was repeated upon a number of scales (1.78 up to 17.6 mmol), maintaining high yields of 75% with a standard deviation of 5%.

2.2.3 Chelation of dipyrromethene **2.8a** to form BODIPY **2.11a**

The final step to BODIPY **2.11a** was a boron chelation of the dipyrromethene **2.8a** following the procedure reported by Lindsey *et al.* in which he demonstrates treating dipyrromethene **2.9** with $BF_3.OEt_2$ in the presence of Hünig's base to obtain BODIPY **2.10**.[72]

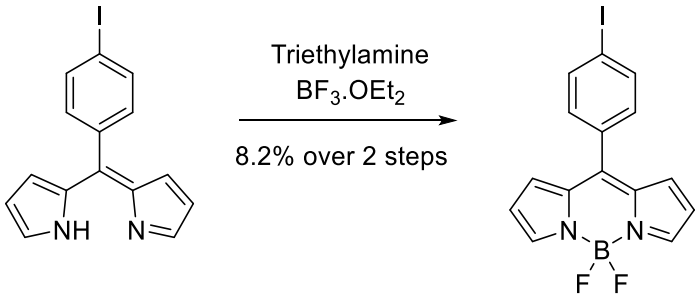

2.9 **2.10**

Scheme 2.6. Lindsey's synthetic route to BODIPY **2.10** through the addition of $BF_3.OEt_2$ under basic conditions.

Therefore, following the work of Lindsey *et al.* dipyrromethene **2.8a** was reacted with 2.2 equivalents of $BF_3.OEt_2$ under basic conditions (2.8 equivalents DIPEA) in DCM. After one hour at room temperature TLC indicated the full consumption of starting

material. After an acid/base work-up, the product **2.11a** was isolated through silica gel column chromatography to give a reasonable yield of 37%, over two steps. The structure of the desired BODIPY **2.11a** was confirmed through analysis of both $^{19}F\{^{1}H\}$ NMR, which showed a quartet at -145.1 ppm (J = 28.6 Hz), and $^{11}B\{^{1}H\}$ NMR, which showed a triplet at 0.25 ppm (J = 28.8 Hz), corresponding to the newly introduced BF_2 moiety.

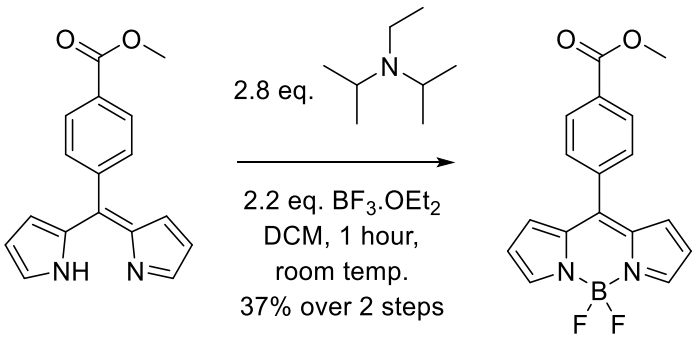

2.8a **2.11a**

Scheme 2.7. Chelation of a BF_2 moiety to dipyrromethene **2.8a** using $BF_3.OEt_2$ in the presence of Hünig's base.

To further confirm the molecular structure of BODIPY **2.11a**, crystals were grown by slow evaporation of the BODIPY **2.11a** in DCM. A suitable single crystal was then submitted for X-ray diffraction analysis. Examination of the X-ray diffraction data confirmed the expected structure of BODIPY **2.11a**, showing the *meso* aryl group to be out of plane with the core structure (Figure 2.1).

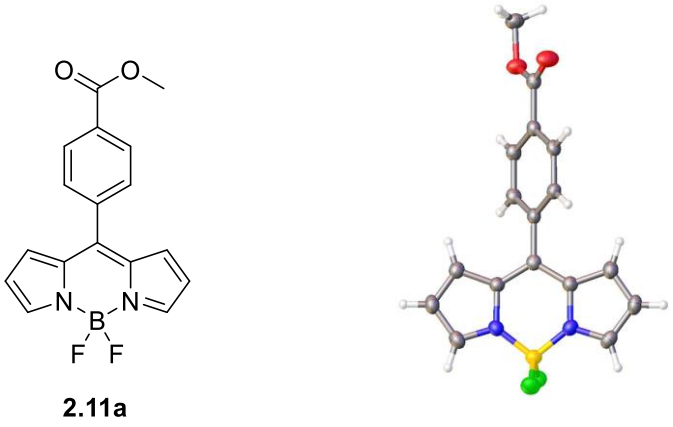

2.11a

Figure 2.1. Molecular structure of BODIPY **2.11a**.

In order to access large quantities of BODIPY **2.11a** for the investigation the subsequent ONSH by chloride step, this three-step condensation, oxidation and chelation was repeated 38 times, giving consistent yields of 26-49% with a standard deviation of 8%.

2.2.4 ONSH by chloride of BODIPY **2.11a**

Having synthesised BODIPY **2.11a**, subsequent copper mediated ONSH by chloride at the 3,5 positions towards 3,5-dichloro BODIPY **2.13a** was investigated, following Jiao's method, using $CuCl_2.2H_2O$ as both the oxidising agent and the Cl^- source (Scheme 2.8).[45]

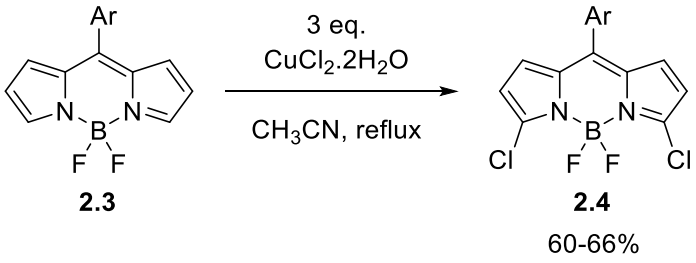

Scheme 2.8. Jiao's conditions for the copper mediated oxidation of BODIPY **2.3**, to obtain the desired 3,5-dichloro BODIPY **2.4**.

Therefore, BODIPY **2.11a** was refluxed with 3 equivalents of $CuCl_2.2H_2O$ in acetonitrile for 6 hours. Unfortunately following an aqueous work-up and column chromatography, the desired 3,5-dichloro **2.13a** product was not observed, instead monosubstituted 3-chloro BODIPY **2.12** was isolated in a 62% yield (Table 2.1, entry 1).

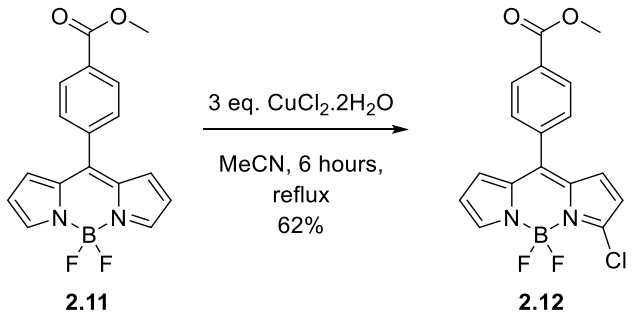

Scheme 2.9. Attempted chlorination of BODIPY **2.11a** based off Jiao's synthetic route.

As the isolation of the desired 3,5-dichloro BODIPY **2.13a** was not achieved using Jiaos conditions, further investigation into the ONSH with chloride of BODIPY **2.11a** was undertaken. A range of alternative solvents, oxidising agents, chloride sources and ligands were examined (Table 2.1).

A series of screening reactions were undertaken, all of which were completed on a 0.15 mmol scale in MeCN under reflux. The initial screening reaction increased the stoichiometry of $CuCl_2.2H_2O$ from 3 to 10 equivalents. After 1 hour the reaction was stopped, and the crude reaction mixture was purified by silica gel column chromatography, resulting in the isolation of the desired 3,5-dichloro BODIPY **2.13a** in a low yield of 29% (Table 2.1, entry 2). Upon inspection of the reaction mixture, solids could be seen, therefore it was postulated that the consistent low yields could be due to the poor solubility of $CuCl_2.2H_2O$ in MeCN. We attempted to overcome this solubility problem through the introduction of common copper chelating ligands.[73]

Another attempt at chlorination was undertaken, with the addition of 2 equivalents of 1,10-phenanthroline as a means to aid in solvation of $CuCl_2.2H_2O$. Therefore, BODIPY **2.11a** was reacted with 10 equivalents of $CuCl_2.2H_2O$, with the addition of 2 equivalents of 1,10-phenanthroline as suitable solvating ligand. After 1.5 hours, none of the desired 3,5-dichloro BODIPY **2.13a** was observed, indicating the addition of 1,10-phenanthroline resulted in inhibition of the desired chemistry, even with the extended reaction times of 90 mins (Table 2.1, entry 3).

Next, an alternative copper chelating ligand, ethanolamine (ETA), was investigated. The reaction was refluxed with 10 equivalents of $CuCl_2.2H_2O$ with the addition of 1 equivalent of ETA for 1 hour. After purification by silica gel column chromatography, a significant increase in yield to 57% of the 3,5-dichloro BODIPY **2.13a** was seen. (Table 2.1, entry 4). As a means to further increase the yield, chlorination upon BODIPY **2.11a** was repeated, with an increased equivalent of ETA (2 equivalents). This showed further enhancement of the yield to 67% after 1 hour (Table 2.1, entry 5). An additional attempt was carried out in which the reaction time was increased from 60 to 90 minutes, however this showed only a small increase in yield to 69% (Table 2.1, entry 6).

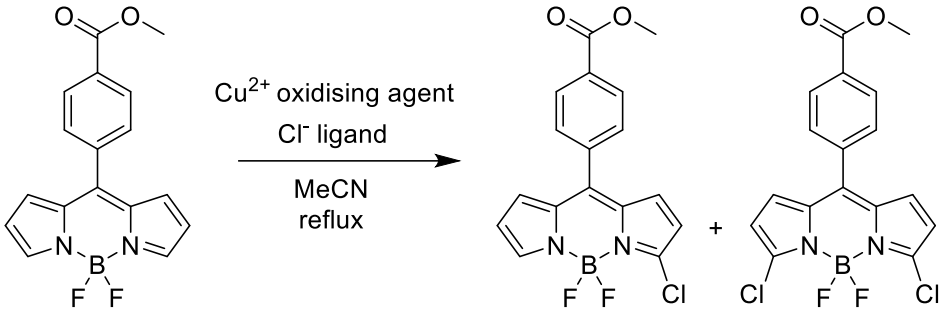

2.11a **2.12** **2.13a**

Entry	Copper Source	Additives	Ligand	Time/min	Dichloro BODIPY **2.13** yield/%
1	3 eq. $CuCl_2 \cdot 2H_2O$	-	0	360	-[a]
2	10 eq. $CuCl_2 \cdot 2H_2O$	-	0	60	29
3	10 eq. $CuCl_2 \cdot 2H_2O$	-	2 eq. Phen	90	-
4	10 eq. $CuCl_2 \cdot 2H_2O$	-	1 eq. ETA	60	57
5	10 eq. $CuCl_2 \cdot 2H_2O$	-	2 eq. ETA	60	67
6	10 eq. $CuCl_2 \cdot 2H_2O$	-	2 eq. ETA	90	69
7	5 eq. $CuCl_2 \cdot 2H_2O$ /5eq. $Cu(OTf)_2$	-	2 eq. ETA	90	63
8	5 eq. $CuCl_2 \cdot 2H_2O$ /5eq. $Cu(OTf)_2$	-	2 eq. ETA	110	99
9	10 eq. $Cu(OTf)_2$	5 eq. TBAC	2 eq. ETA	110	96
10	4.2 eq. $Cu(OTf)_2$	5 eq. TBAC	2 eq. ETA	110	0
11	10 eq. $Cu(OTf)_2$	5 eq. TBAC	2 eq. ETA	110	85[b]
12	10 eq. $Cu(OTf)_2$	5 eq. TBAC	0	110	38
13	10 eq. $Cu(OTf)_2$	5 eq. TBAC	2 eq. ETA	110	65[c]
14	10 eq. $Cu(OTf)_2$	5 eq. TBAC	2 eq. ETA	110	51[c, d]
15	10 eq. $Cu(OTf)_2$	5 eq. TBAC	2 eq. ETA	110	95[d]

Table 2.1. Synthesis of 3,5-dichloro BODIPY **2.13a**. Reactions carried out on a 0.15 mmol scale in MeCN (6 mL) under reflux; a) 3-chloro BODIPY **2.12** isolated with a yield of 62%; b) Reaction scaled up to 1.4 mmol; c) Reaction carried out under an atmosphere of nitrogen; d) Ambient light excluded. Phen = 1,10-phenanthroline, ETA = ethanolamine, TBAC = tetrabutylammonium chloride.

As a means to increase the yield further, alternative Cu^{2+} oxidising agents were investigated. The ONSH by chloride chemistry was attempted using a combination of 5 equivalents $CuCl_2.2H_2O$ and 5 equivalents of copper(II) trifluoromethanesulfonate ($Cu(OTf)_2$), with 2 equivalents of ETA for 1 hour. After purification a slightly lower yield of 63% was observed compared to using 10 equivalents of $CuCl_2.2H_2O$ (Table 2.1, entry 7). It was seen upon repetition of the reaction under identical conditions, a longer reaction time of 110 mins showed a huge improvement in yield of the desired 3,5-dichloro BODIPY **2.13a** to 99% after purification by silica gel column chromatography (Table 2.1, entry 8).

The complete replacement of $CuCl_2.2H_2O$ with $Cu(OTf)_2$ was examined as a means of separating the oxidising agent from the chloride source. It is hoped that upon successful separation, the scope of this reaction will be broadened, allowing the use of alternative nucleophiles, including alternative halide sources. The chlorination of BODIPY **2.11a** was attempted using 10 equivalents of $Cu(OTf)_2$ as the sole copper source with the addition of 5 equivalents of tetrabutylammonium chloride (TBAC) as the chloride source. The reaction was run in MeCN with the 2 equivalents of ETA for 1 hour. After an aqueous work-up and purification through silica gel column chromatography, 3,5-dichloro BODIPY **2.13a** was produced in a near quantitative yield of 96% (Table 2.1, entry 9). In an attempt to improve the efficiency of the reaction, chlorination was attempted again, reducing the equivalents of $Cu(OTf)_2$ from 10 to 4.2. This was unsuccessful, resulting in no conversion to the desired 3,5-dichloro BODIPY **2.13a** (Table 2.1, entry 10).

After successfully optimising the chlorination of BODIPY **2.11a** to 3,5-dichloro BODIPY **2.13a**, showing excellent yields of 96%, scale up under identical conditions was attempted to investigate the reproducibility of this reaction on a larger scale. Therefore, 1.4 mmol of BODIPY **2.11a** was treated with 10 equivalents of $Cu(OTf)_2$, 5 equivalents of TBAC and 2 equivalents of ETA for 1 hour, giving an excellent yield of 85% after purification (Table 2.1, entry 11).

A number of control experiments were carried out to gain further insight into the optimal conditions for the formation of 3,5-dichloro BODIPY **2.13a** (Table 2.1, entry 12-15). The first of which was the omission of ETA from the reaction, which resulted in a decreased yield to 38%, indicating that ETA does in fact play an important role

within this reaction (Table 2.1, entry 12). Completion of the reaction under nitrogen again showed a decrease in yield, suggesting atmospheric oxygen plays a role in the reaction, perhaps via oxidative recycling of the copper (Table 2.1, entry 13, 14). There was no indication of photochemical reactions, as there was no significant change in yield when the reaction was carried out in the dark (Table 2.1, entry 15).

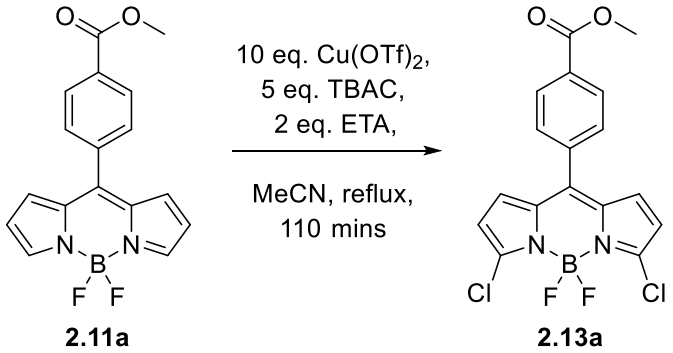

2.11a **2.13a**

Scheme 2.10. Optimised copper mediated oxidative C-H substitution to give 3,5-dichloro BODIPY **2.13a**.

3,5-dichloro BODIPY **2.13a** was further confirmed via HRMS, showing a mass of 395.0332, which is consistent for the $[M+H]^+$ of a molecule with formula of for $C_{17}H_{11}N_2O_2BF_2Cl_2^{35}$. Due to 3,5-dichloro BODIPY **2.13a** containing two chlorines, the mass spectrum should result in an isotopic ratio of 10:6:1. This expected isotopic ratio was overserved, further validating the successful addition two chlorines to BODIPY **2.11a**. The structure was corroborated by the disappearance of a singlet at 7.97 ppm in the ^1H NMR, which is consistent with the successful substitution at the 3,5 positions.

To further validate the structure of 3,5-dichloro BODIPY **2.13a**, crystals were obtained through slow evaporation of a DCM solution Therefore, a suitable single crystal was selected for X-ray diffraction analysis, confirming that chlorine was indeed incorporated at the 3,5 positions (Figure 2.2).

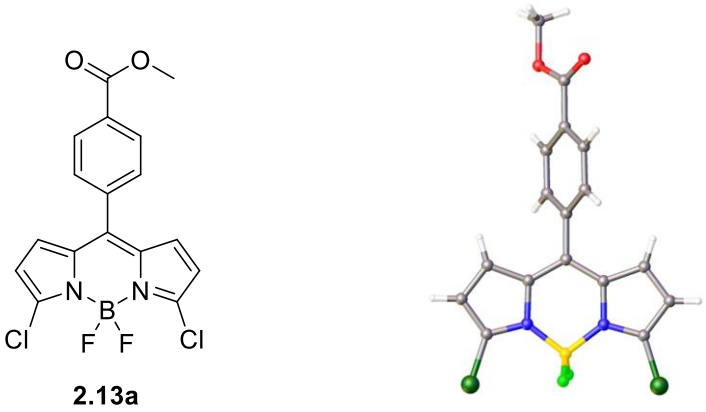

2.13a

Figure 2.2. Single crystal X-ray structure of 3,5-dichloroBODIPY **2.13a**.

2.2.5 Synthesis of alternative 3,5-dichloro BODIPYs **2.13b-f**

To test the reproducibility of our newly optimised synthetic route for the synthesis of 3,5-dichloro BODIPY **2.13a**, the methodology was applied to a range of *meso*-aryl substituted BODIPYs which were synthesised following standard procedures (Table 2.2).

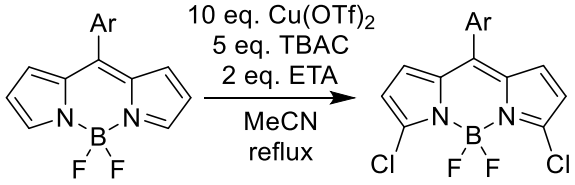

2.11a-f **2.13a-f**

Entry	Ar	Reaction Time/min	Product	Yield (%)
1	*para*-methylbenzoate **2.11a**	110	**2.13a**	96[a]
2	*para*-nitrophenyl **2.11e**	110	**2.13e**	92
3	*meta*-nitrophenyl **2.11b**	110	**2.13b**	99
4	*ortho*-tolyl **2.11f**	110	**2.13f**	31
5	*para*-methoxyphenyl **2.11c**	110	**2.13c**	66
6	*meta*-methoxyphenyl **2.11d**	110	**2.13d**	56
7	*meta*-methoxyphenyl **2.11d**	150	**2.13d**	70

Table 2.2. Synthesis of a range of meso-aryl 3,5-dichloro BODIPYs **2.13a-f** with new optimised conditions. All reactions carried out on a 0.14-0.25 mmol scale in MeCN (5-6 mL).

A range of electron deficient and electron rich aryl groups were chosen, with each reaction run on a 0.14-0.25 mmol scale in MeCN with 10 equivalents of $Cu(OTf)_2$, 5 equivalents TBAC and 2 equivalents of ETA. Initially electron deficient *meso*-aryl groups were explored, investigating both *para*- and *meta*-nitrophenyl BODIPYs **2.11e** and **2.11b**. Chlorination upon each nitrophenyl BODIPY **2.11e** and **2.11b** was run for 110 mins, showing excellent yields of the corresponding 3,5-dichloro BODIPYs **2.13e** and **2.13b** of 92 and 99% yield respectively (Table 2.2, entries 2 and 3). An alternative electron withdrawing *meso*-BODIPY, *ortho*-tolyl BODIPY **2.11f**, was subjected to chlorination reaction conditions. After refluxing BODIPY **2.11f** for 110 mins and an aqueous work-up, the crude reaction mixture was analysed by ^{1}H NMR, showing a complex mixture of products. The product was purified by column chromatography, giving a low yield of 31% for the corresponding 3,5-dichloro BODIPY **2.13f** (Table 2.2, entry 4).

Next, electron rich *meso*-methoxyphenyl BODIPYs were screened under identical chlorination conditions. Both *para*- and *meta*-methoxyphenyl BODIPY **2.11c** and **2.11d** were refluxed for 110 mins, showing moderate yields of the corresponding 3,5-chloro BODIPYs **2.13c** and **2.13d** of 56 and 66% respectively after purification through silica gel column chromatography. (Table 2.2, entries 5 and 6). In an attempt to increase the yield of both the *para* and *meta*-methoxyphenyl 3,5-dichloro BODIPYs, chlorination upon each methoxyphenyl BODIPY starting material was repeated with longer reaction times of 150 mins. In the case of *para*-methyoxyphenyl BODIPY **2.11c** there was no observed increase in yield however the *meta*-methoxyphenyl BODIPY **2.11d** showed an improved yield from 56 to 70% (Table 2.2, entry 7).

Chlorination at the 3,5 positions of the BODIPY appears to proceed faster for electron deficient *meso*-aryl groups. *Meso*-aryl groups are not co-planer with the BODIPY core structure therefore any electronic effects resulting from substitution at the *meso* position are likely to be inductive effects. Therefore, the electron deficient *meso* groups could result in electron deficiency at the core of the BODIPY, making the α-positions more susceptible to nucleophilic attack. Alternatively, electron rich *meso*-aryl groups, are expected to increase electron density in the core structure, reducing susceptibility to nucleophilic attack.

As discussed earlier, Jiao *et al*. proposed that chlorination under this methodology proceeds via a series of single electron transfer (SET) reactions. This a multistep mechanism which proceeds via an initial oxidative SET resulting in a cationic radical BODIPY species which is subsequently attacked by a chloride. As discussed above, both ester and nitro groups are electron withdrawing and have shown to result in high yields of their corresponding 3,5-dichloro BODIPYs whereas tolyl and methoxy aryl groups are electron donating and have shown low yields of their corresponding 3,5-dichloro BODIPYs. These observed yields can only be consistent with the proposed mechanism if the rate determining step is the attack of chloride upon the cationic radical intermediate as the electronics of the *meso* aryl groups would play a role in the ease of attack from the nucleophilic chloride ion.

In conclusion, an optimised copper mediated synthesis of 3,5-dichloro BODIPYs **2.13a-f** was achieved through a series of screening reactions, showing reaction conditions of 5 equivalents TBAC, 10 equivalents of $Cu(OTf)_2$ and 2 equivalents of ethanolamine, in MeCN under reflux (Scheme 2.10). This has resulted in a robust, high yielding route, up to 99%, which has shown to be successful on a range of aryl groups. These 3,5-dichloro BODIPYs **2.13a-f** are highly useful synthetic intermediates for subsequent cross-coupling and S_NAr reactions enroute to more complex BODIPY architectures. This optimised synthetic route towards 3,5-dichloro BODIPYs **2.13a-f** was published in Tetrahedron in 2020.[74]

2.3 Synthesis of 3,5-dibromo BODIPYs 2.14

The synthesis of alternative 3,5-dihalo BODIPYs in the form of 3,5-dibromo BODIPYs **2.14** was investigated as they were thought to be suitable alternative intermediates for future Pd catalysed cross-coupling reactions in the planned synthesis of chiral BODIPYs (Scheme 2.1). Following the successful synthesis of 3,5-dibromo BODIPY **2.14a**, this compound will be subjected to a range of S_NAr and coupling conditions alongside 3,5-dichloro BODIPY **2.13a** to determine the most suitable intermediate towards the final helically chiral BODIPYs.

2.3.1 Synthesis of 3,5-dibromo BODIPY **2.14a** adapted from optimised chlorination methodology

After the successful 3,5-dichlorination of a range of BODIPYs through the use of a copper oxidising agent in the presence of a source of chloride, it was thought that a similar methodology maybe possible for the synthesis of 3,5-dibromo BODIPYs. If the source of chloride can be substituted with a suitable bromide source, we postulate that this should result in the desired 3,5-dibromo BODIPY **2.14a**. Therefore, BODIPY **2.11a** was subjected to ONHS reaction chemistry using $Cu(OTf)_2$ as an oxidant and tetrabutylammonium bromide (TBAB) as a source of bromide in an attempt to synthesise 3,5-dibromo BODIPY **2.14a** (Scheme 2.11).

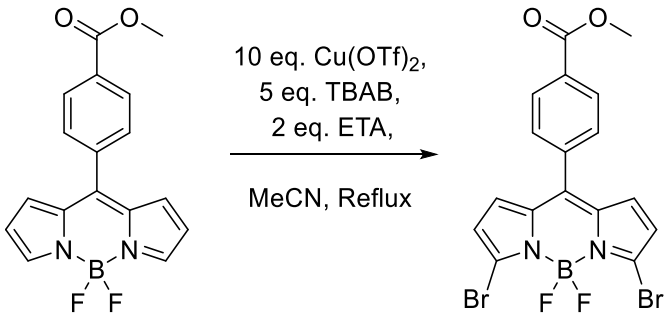

Scheme 2.11. Proposed copper mediated bromination of BODIPY **2.11a**, enroute to 3,5-dibromo BODIPY **2.14a**.

BODIPY **2.11a** was reacted with 5 equivalents of TBAB, 10 equivalents of $Cu(OTf)_2$ and 2 equivalents of ETA, under similar conditions to the previously optimised 3,5-dichloro BODIPY **2.13a** synthesis (Table 2.3, Entry 1). Unfortunately, analysis of the crude ^{1}H NMR showed the formation of an alternative major product, 2,3,5,6-tetrabromo BODIPY **2.15** due to over-bromination, with only traces of other brominated BODIPYs observable. The 2,3,5,6-tetrabromo BODIPY **2.15** was isolated by silica gel chromatography in a reasonable isolated yield of 41% (Scheme 2.12).

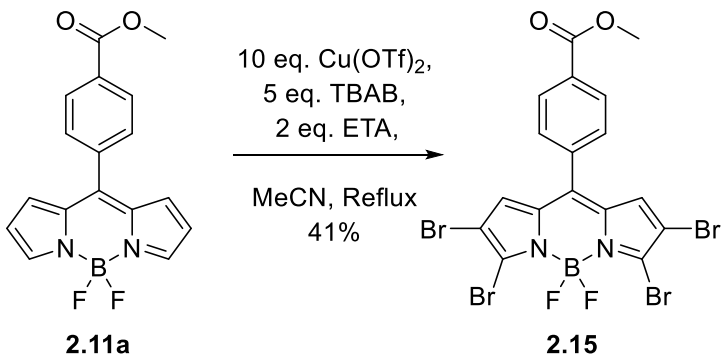

Scheme 2.12. Synthetic route for the synthesis of 2,3,5,6-tetrabromo BODIPY **2.15**.

The structure of 2,3,5,6-tetrabromo **2.15** was corroborated through ^{1}H NMR analysis, showing two, 2-proton doublets at 7.56 and 8.21 ppm (*J*= 8.5 Hz and 8.9 Hz respectively), corresponding to the *meso* aryl ring along with one other aromatic 2-proton singlet at 6.85 ppm, corresponding to the 1,7 positions of BODIPY **2.15**. Further confirmation of the formation of 2,3,5,6-tetrabromo BODIPY **2.15** was obtained through HRMS, in which the observed peak at m/z = 622.7449 is consistent with that calculated for $C_{17}H_9BBr_2{}^{79}Br_2{}^{81}F_2N_2O_2$ $[M\text{-}F]^+$ (622.7438). An isotopic ratio of 1:4:6:4:1 was observed at 618.7, 620.7, 622.7, 624.7 and 626.7, which is expected for a compound containing 4 bromines, further validating the structure of 2,3,5,6-tetrabromo BODIPY **2.15**.

Due to the observed over bromination of BODIPY **2.11a**, further investigation into this reaction was carried out. It was thought that a reduction in the equivalents of TBAB would reduce over bromination in the reaction. Therefore, BODIPY **2.11a** was reacted with 2 equivalents of TBAB, 10 equivalents of $Cu(OTf)_2$ and 2 equivalents of ETA in MeCN. The reaction was refluxed for 90 mins and after aqueous work-up, the crude reaction mixture was analysed by ^{1}H NMR, showing a 37% yield by NMR integration of the 2,3,5,6-tetrabromo BODIPY **2.15** along with 33% of a suspected tri substituted BODIPY **2.16** and traces of other brominated products. Attempts to purify both 2,3,5,6-tetrabromo BODIPY **2.15** and tri substituted BODIPY **2.16** by column chromatography were unsuccessful due to their very similar retention factors, resulting a single mixed fraction containing a 1 : 1.1 ratio of 2,3,5,6-tetrabromo BODIPY **2.15** and tri substituted BODIPY **2.16** (Table 2.3, Entry 2).

The reaction was then repeated with the same equivalents of both TBAB and $Cu(OTf)_2$ as the above reaction, at reduced temperature of 0°C. After 90 mins and an aqueous work-up, the crude reaction was analysed by ^1H NMR. Again, this indicated the presence of 2,3,5,6-tetrabromo BODIPY **2.15** in an estimated yield of 6% (calculated through NMR integration) alongside reasonable quantities of alternative brominated BODIPYs, and no evidence of starting material (Table 2.3, entry 3).

As a means to try and obtain a single brominated product, the bromination of BODIPY **2.11a** was repeated again using 2 equivalents of TBAB and a reduced 4 equivalents of $Cu(OTf)_2$. The reaction was stirred at 0 °C for 5 mins before being quenched with water. Upon analysis of the crude reaction mixture after work-up, ^1H NMR showed a complex mixture of brominated products, with no observable 2,3,5,6-tetrabromo BODIPY **2.15** or starting material present (Table 2.3, entry 4).

A final attempt was made in which BODIPY **2.11a** was reacted with 1 equivalent of TBAB and 4 equivalents $Cu(OTf)_2$ at 0 °C for 5 mins. Analysis of ^1H NMR following work-up unfortunately showed the formation of a large number of unidentified brominated BODIPY products and no remaining starting material (Table 2.3, entry 5).

Attempts to isolate the brominated BODIPY compounds, which were expected to be mono-, di-, and tri-brominated BODIPYs, were unsuccessful by silica gel column chromatography due to the similarities in polarity of each compound.

Entry	**Equivalents TBAB/$Cu(OTf)_2$**	**Temperature/°C**	**Time/mins**	**Tetrabromo 2.15 Yield/%**
1	5/10	Reflux	90	41% [a]
2	2/10	Reflux	90	37% [b,c]
3	2/10	0	90	6% [b,d]
4	2/4	0	5	0% [b,d]
5	1/4	0	5	0% [b,d]

Table 2.3. Bromination of BODIPY **2.11a**. a) Isolated yield, b) Yield calculated through ^1H NMR integration. C) Also contains tri-bromo BODIPYs, seen by ^1H NMR. D) Also contains a number of brominated BODIPY species.

Examination into the brominated products formed from BODIPY **2.11a** was undertaken through X-ray crystallography. Single crystals were obtained through

slow evaporation of a DCM solution from the purified 2,3,5,6-tetrabromo BODIPY **2.15** (Table 3, entry 1) and were examined by X-ray diffraction analysis. 2,3,5,6-Tetrabromo BODIPY **2.15** formed monoclinic crystals in the $P2_1/c$ space group, containing 4 molecules in the unit cell (Z = 4) with a unit cell volume of 1885.93(12) $Å^3$ (Figure 2.3A).

In addition, crystals were also obtained by slow evaporation from a DCM solution containing the 1.1 : 1 mixture of the tri/tetra brominated BODIPY obtained previously (Table 3, entry 2). Interestingly, X-ray diffraction analysis showed that a crystal had been obtained which contained both 2,3,5,6-tetrabromo BODIPY **2.15** and 2,3,6-tribromo BODIPY **2.16**. This new crystal structure was the same as that observed for pure 2,3,5,6-tetrabromo BODIPY **2.15**, also being monoclinic $P2_1/c$, with Z = 4 and a unit cell volume of 1865.6(2) $Å^3$. However, the mixed crystal exhibited occupational disorder, with molecules from both 2,3,5,6-tetrabromo BODIPY **2.15** and 2,3,6-tribromo BODIPY **2.16** distributed randomly throughout the crystal. This can be seen by examining the 3,5-positions of the BODIPYs, which show an average % occupation of 69 and 88% respectively, which translates into the crystal containing 43% of 2,3,6-tribromo BODIPY **2.16** and 57% of 2,3,5,6-tetrabromo BODIPY **2.15** (ratio of 1 : 1.4) (Figure 2.3B). This crystal structure was however very useful at it allowed assignment of the previously observed tri-brominated BODIPY product to be 2,3,6-tribromo BODIPY **2.16**.

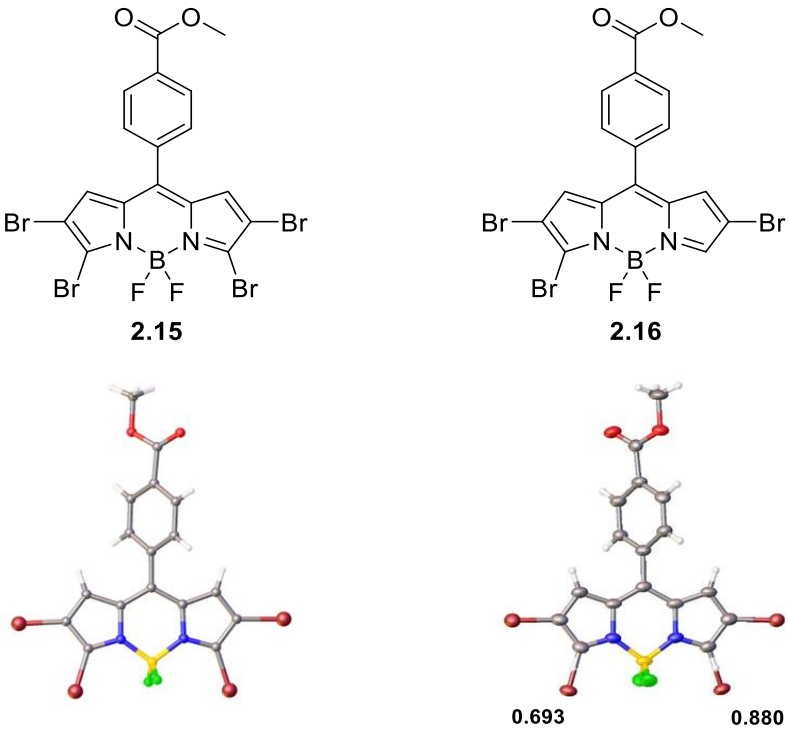

Figure 2.3. LHS = Crystal structure of 2,3,5,6-tetrabromo BODIPY **2.15**. RHS = Crystal structure comprised of a mixture of 2,3,5,6-tetrabromo BODIPY **2.15** and 2,5,6-tribromo BODIPY **2.16**, showing % occupation of 69 and 88% at the 3,5 positions.

With the assignment of the tribrominated BODIPY as 2,5,6-tribromo BODIPY **2.16**, we can postulate that the bromination reactions occurs at the 2,6 positions first, followed by bromination at the 3,5-positions. This is contrary to order of reactivity previously observed in the ONSH by chlorine chemistry using TBAC and $Cu(OTf)_2$.[74] Therefore, it is postulated that the bromination of BODIPY **2.11a** with TBAB and $Cu(OTf)_2$ proceeds not via an ONSH by bromine mechanism, but via classical S_EAr chemistry. We proposed that the in the bromination reaction, the bromide anions from TBAB are oxidised to Br_2 by $Cu(OTf)_2$, resulting in an electrophilic source of bromine which can subsequently engage in an S_EAr reaction with BODIPY **2.11a**, which has Hao *et al*. demonstrated on similar BODIPY structures (Scheme 2.13).[41]

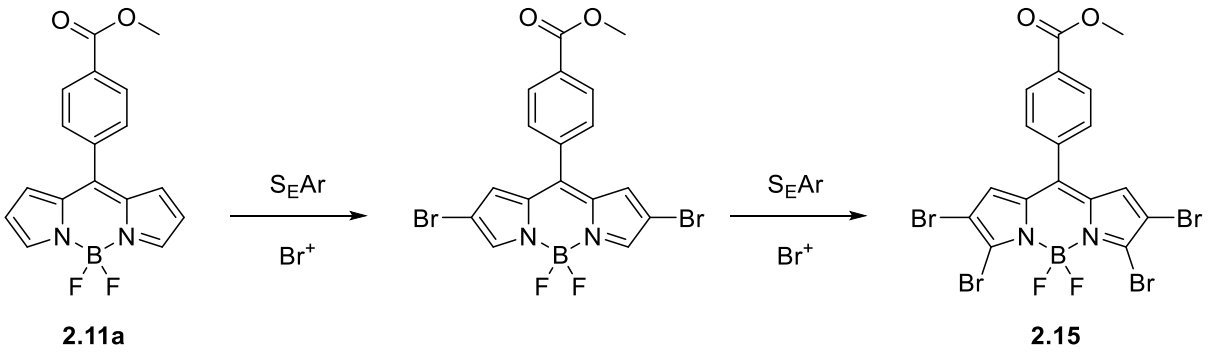

Scheme 2.13. Proposed S_EAr mechanism for the synthesis of 2,3,5,6-tetra bromo BODIPY **2.15a** with TBAB and $Cu(OTf)_2$.

Due to the failure to synthesis 3,5-dibromo BODIPY **2.14a** via an ONSH synthetic route, as seen for 3,5-dichloro BODIPY **2.13a**, an alternative route towards 3,5-dibromo BODIPY **2.14a** was investigated.

2.3.2 3,5-Dibromo BODIPY **2.14a** synthesis via α bromination of its corresponding dipyrromethane **2.7a**

As seen in chapter 1, the α position of dipyrromethanes are susceptible to S_EAr reaction chemistry, including bromination chemistry at these positions. Therefore, a new route was investigated based on the dibromination of the α positions of a corresponding dipyrromethane **2.7**. The thus produced α,α–dibrominated dipyrromethane **2.17** can be subsequently oxidised to the dipyrromethene **2.18** and then chelated with a BF_2 moiety to produce the desired 3,5-dibromo BODIPY **2.14** (Scheme 2.14).

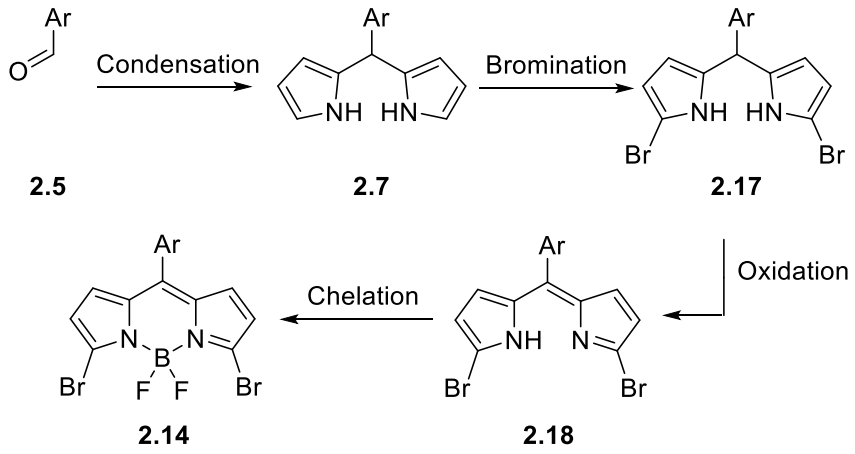

Scheme 2.14. Proposed 4-step synthetic route to 3,5-dibromo BODIPYs **2.19** initiated via S_EAr of bromine at the α positions of dipyrromethane **2.7** followed by oxidation and chelation.

2.3.2.1 Electrophilic bromination and subsequent oxidation of dipyrromethane **2.7a**

Hall *et al.* have reported the α,α-dibromination of dipyrromethane **2.7a** followed by oxidation to synthesize the corresponding α,α-dibromo dipyrromethene **2.18a**, and this method was chosen for the planned synthesis of 3,5-dibromo BODIPY **2.14a**.[8]

Following Hall's method, a series of bromination reactions were undertaken upon dipyrromethane **2.7a**, followed by oxidation with DDQ to the corresponding α,α-dibromo-dipyrromethene **2.18a**. In the first attempt, a THF solution of dipyrromethane **2.7a** was cooled to -78 ^oC for 30 mins, before the addition of 2 equivalents of NBS. The reaction mixture was then stirred at -78 ^oC for 1 hour, followed by the portion wise addition of 1 equivalent of solid DDQ over 10 mins. The reaction mixture was left to warm to room temperature for 30 mins before quenching with Na_2SO_3. The crude reaction mixture was then purified by silica gel column chromatography, resulting in a good yield of 78% of the desired α,α-dibromo dipyrromethene **2.18a** (Table 2.4, entry 1).

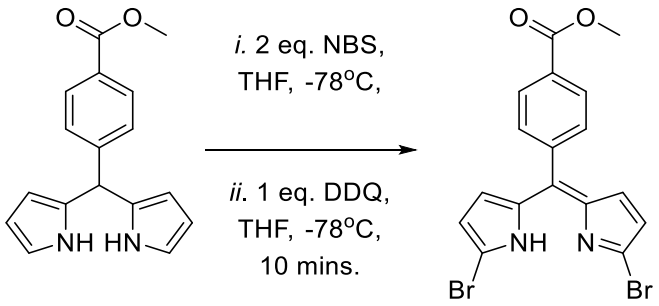

2.7a **2.18a**

Entry	Cooling time/mins	Scale/mmol	Time left to warm to rt/mins	Yield/%[a]
1	30	7.13	30	78[a]
2	30	7.13	60	0[b]
3	40	3.57	60	64[b]
4	45	3.57	120	60[b]
5	40	7.13	30	92[a]
6	30	10.70	30	40[b]
7	60	23.01	30	80[a]

Table 2.4. Synthesis of α,α-dibromo dipyrromethene **2.18a** from BODIPY **2.7a**. a) Isolated yields, b) Yields calculated by ^{1}H NMR integration.

As a means to further examine the bromination of dipyrromethane **2.7a**, the reaction upon BODIPY **2.7a** was repeated on an identical scale of 7.13 mmol. After the addition of DDQ the crude reaction mixture was left to warm to room temperature for a longer time of 1 hours before being quenched with Na_2SO_3. The crude reaction mixture was then subjected to an aqueous work-up and solvent was removed under reduced pressure. Surprisingly, upon inspection of the ^{1}α,α-dibromo dipyrromethene **2.18a** was observed, instead a complex mixture of products could be seen, none of which were isolated (Table 2.4, entry 2).

Therefore, bromination of dipyrromethane **2.7a** was further investigated. A series of reactions were undertaken exploring a number of reaction variables, including both the time over which the THF solution of dipyrromethane **2.7a** was cooled at the beginning of the reaction, and the time over which the crude reaction mixture was left to warm to room temperature before quenching, following the addition of DDQ.

It was seen that longer cooling of the THF solution of dipyrromethane **2.7a** positively affected the yield, however longer warming times after the addition of DDQ, prior to quenching, negatively affected the yield (Table 2.4, entries 3-6). The best yield was observed when dipyrromethane **2.7a** was stirred in THF at -78 ^{o}C for 40 mins before the addition of NBS and was left for 30 mins to warm to room temperature after the addition of DDQ prior to quenching. This showed a yield 92% after purification by silica gel column chromatography (Table 2.4, entry 5).

The structure of the α,α-dibromo dipyrromethene **2.7a** was corroborated through ^{1}H NMR analysis, showing two 2-proton doublets at 6.40 and 6.33 ppm corresponding to the 1,2,6,7 positions on the BODIPY.

Scale up of the bromination reaction was attempted, using 23.01 mmol of dipyrromethane **2.7a** starting material. Due to the larger volume of THF, the starting material was cooled for 1 hour before the addition of NBS. The reaction was stirred for 1 hour and then DDQ was added. The crude reaction mixture was left to warm to room temperature for 30 mins. A good yield of 80% was retained after purification by silica gel column chromatography (Table 2.4, entry 7).

α,α-Dibromo dipyrromethene **2.18a** can be purified by silica gel column chromatography, however it is poorly soluble in common lab solvents such as DCM. This results in highly dilute solutions of α,α-dibromo dipyrromethene whilst undertaking column chromatography, meaning that large amounts chromatography grade silica and solvents are required for purification of even small masses of product.

The optimised synthesis of α,α-dibromo dipyrromethene **2.18a** was repeated 21 times, on scales ranging from 3.57 to 23.01 mmol with average yields of 66% (SD = 10%). Due previously mentioned difficulties in purification by silica gel column chromatography, these repeat reactions were carried forward to the next steps, after only a simple aqueous work-up.

2.3.2.2 Chelation of BF_2 moiety into dipyrromethene **2.18a** to form 3,5-dibromo BODIPY **2.14a**

The final synthetic step towards 3,5-dibromo BODIPY **2.14a** is the chelation of a BF_2 moiety by the pyrrolic nitrogen atoms of α,α-dibromo dipyrromethene **2.18a**. This reaction has been reported by Hall *et al*. for the formation 3,5-dibromo BODIPY **2.14a**.[8]

Following this method, purified α,α-dibromo dipyrromethene **2.18a** was reacted with 2 equivalents of $BF_3.OEt_2$ and 2.5 equivalents of DIPEA in DCM for 1 hour. The crude reaction mixture was washed with water and purified by silica gel column chromatography to give 3,5-dibromo BODIPY **2.14a** in an excellent yield of 91% Scheme 2.15).

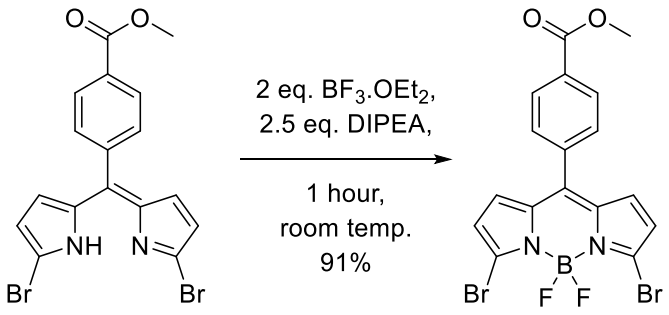

Scheme 2.15. Synthesis of 3,5-dibromo BODIPY **2.14a**.

Successful incorporation of the BF_2 moiety to form 3,5-dibromo BODIPY **2.14a** was confirmed by the presence of a triplet at 0.63 ppm (J = 28.0 Hz) in the $^{11}B\{^1H\}$ NMR spectrum and a quartet at -146.76 ppm (J = 28.0 Hz) in the $^{19}F\{^1H\}$ NMR spectrum.

The chelation of α,α-dibromo dipyrromethene **2.18a** was repeated 19 times over the course of this project as it is a key intermediate for further synthesis. However, as mentioned earlier, purification of dipyrromethene **2.18a** proved difficult due to solubility issues and therefore only two other chelation reactions were undertaken with purified starting material, showing an 89 and 99% yield.

Therefore, due to the purification of the corresponding α,α-dibromo dipyrromethene **2.18a** being impractical, all other chelation reactions were undertaken using crude α,α-dibromo dipyrromethene. Each reaction was purified by silica gel column chromatography, with each yield calculated over 4 steps (condensation, bromination, oxidation and chelation), showing an average yield of 25% (SD = 18%).

2.3.3 Synthesis of *meso*-aryl substituted 3,5-dibromo BODIPYs **2.14(b-d)**

After the successful synthesis of 3,5-dibromo BODIPY **2.14a** with a *para* ester-substituted aryl ring at the *meso* position, alternative *meso*-aryl groups were investigated in this reaction chemistry, with an aim to prepare a range of alternative 3,5-dibromo BODIPYs **2.14(b-d)** for future investigation.

Therefore, the synthesis of the corresponding dipyrromethane starting materials was undertaken, through the condensation of pyrrole with differently substituted arylaldehydes.

Following the previously described reaction procedure, *meta*-nitrobenzaldehyde was reacted with pyrrole in a 0.05 M HCl solution, and after 4 hours a yellow precipitate was formed. To provide a consistent isolation protocol for subsequent dipyrromethane synthesise, the crude reaction was diluted with DCM and subjected to a standard aqueous work-up. The ^{1}H NMR spectra of the crude reaction mixture showed the formation of *meta*-nitrophenyl dipyrromethane **2.7b**, alongside trace amounts of other material, giving a crude yield of 97% (Table 2.5, Entry 1).

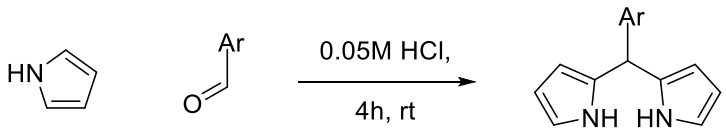

Entry	Benzaldehyde	Crude Yield/%[a]
1	*Meta*-nitro **2.7b**	97
2	*Para*-methoxy **2.7c**	53
3	*Meta*-methoxy **2.7d**	35

Table 2.5. Condensation of benzaldehydes with pyrrole to form dipyrromethanes **2.7b-d**. a) major component by ^{1}H NMR with crude yield calculated from recovered mass

In parallel, *meta*-methoxybenzaldehyde **2.7c** and *para*-methoxybenzaldehyde **2.7d** were also reacted with pyrrole in 0.05 M HCl solution on the same scale for 4 hours. In this case, no precipitate was observed and an oily residue was formed, which caused problems with reaction stirring. Both crude reactions were diluted with DCM and subjected to a standard aqueous work-up. Inspection of both the ^{1}H NMR spectra of the crude reaction mixtures showed for the formation of both *meta*-

methoxyphenyl and *para*-methoxyphenyl dipyrromethane **2.7c** and **2.7d**, albeit in lower purity than for *meta*-nitrophenyl dipyrromethane **2.7b** ((Table 2.5, Entries 2 and 3).

Due to previous issues in purifying *para*-methylbenzoate dipyrromethane **2.7a** due to lack of solubility, all newly synthesised dipyrromethanes **2.7(b-d)** were carried forward without further purification.

Following the successful synthesis of each corresponding dipyrromethane, in the next step dipyrromethanes **2.7(b-d)** were subjected to bromination, oxidation and chelation reactions, following the previously discussed optimised procedures (Table 2.4, entry 7 and Scheme 2.15).

For ease of calculation, the recovered mass of each dipyrromethene **2.7(b-d)** was used as yield to calculate equivalents in the following synthetic step, as ^{1}H NMR showed each dipyrromethane to be the major component. Therefore, each dipyrromethane **2.7(b-d)** was cooled to -78 ^{o}C in THF for 1 hour, followed by the addition of 2 equivalents of NBS and stirring for one hour. This was followed by a subsequent addition of DDQ before being warmed to room temperature for 30 mins and quenched with Na_2SO_3. After aqueous work-up and solvent removal under reduced pressure, each α,α-dibrominated dipyrromethene **2.18(b-d)** was redissolved in DCM chelated with 2 equivalents of BF_3OEt_2 and 2.5 equivalents of DIPEA for 1 hour. Following aqueous work-up, each crude reaction mixture was purified by silica gel column chromatography to obtain the corresponding 3,5-dibromo BODIPYs **2.14(b-d)** (Table 2.6, entries 2-4).

All three additionally synthesised 3,5-dibromo BODIPYs **2.14(b-d)** showed low overall yields, starting from pyrrole (Table 2.6, entries 2-4). However, since yields are calculated over multiple synthetic steps, including condensation, bromination, oxidation and chelation reactions it is difficult to determine the source of the low overall yield.

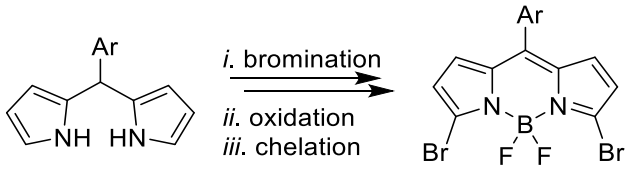

2.7(a-d) **2.14(a-d)**

Entry	Aryl	Product	Isolated Yield over three steps (%)
1	*para*-methylbenzoate (2.7a)	**2.14a**	53[a]
2	*meta*-nitrophenyl (2.7b)	**2.14b**	6
3	*para*-methoxyphenyl (2.7c)	**2.14c**	12
4	*meta*-methoxyphenyl (2.7d)	**2.14d**	8

Table 2.6. Synthesis of *meso*-aryl substituted 3,5 dibromo BODIPYs **2.14(a-d)** via bromination, oxidation and chelation reactions. a: synthesis previously discussed Table 2.4 and Scheme 2.15.

Despite the low overall yields, this synthetic route was suitable for the synthesis of sufficient quantities of *meso*-aryl substituted 3,5-dibromo BODIPYs **2.14(a-d)** to allow further investigation, as discussed in Chapter 3.

2.4 Conclusion

The aim of this chapter was to develop routes for the synthesis of both the 3,5-dichloro BODIPYs **2.13a-f** and 3,5-dibromo BODIPYs **2.14a-d**.

In this chapter a novel route to 3,5-dichloro BODIPYs has been developed. Following previously published methodology BODIPY **2.11** was synthesised over 3 steps, the investigation focussed on the development of a 3,5-dichlorination of BODIPY **2.11** using an ONSH by chloride reaction. Previous methodology by Jiao *et al*. for similar 3,5-dichlorination chemistry proved low yielding and unreliable, therefore the use of $Cu(OTf)_2$ as the oxidising agent, with TBAC as the chloride source and ethanolamine as a ligand was developed. This new methodology was shown to give excellent yields (up to 99%) in the ONSH by chloride 3,5-dichlorination of range of *meso*-aryl substituted BODIPYs (Scheme 2.16).[74]

Unfortunately, ONSH by bromide proved unsuccessful in the synthesis of the corresponding 3,5-dibromo BODIPYs. Therefore 3,5-dibromo BODIPY **2.14a** was

successfully synthesised via an alternative route based on the literature, involving the α,α-dibromination of the corresponding dipyrromethane, oxidation to the dipyrromethene and finally BF_2 chelation to give the desired product in 24% yield over 4 steps. This approach was also shown to be successful for a small range of *meso*-aryl substituted 3,5-dibromo BODIPYs **2.14(b-d)** (Scheme 2.16).

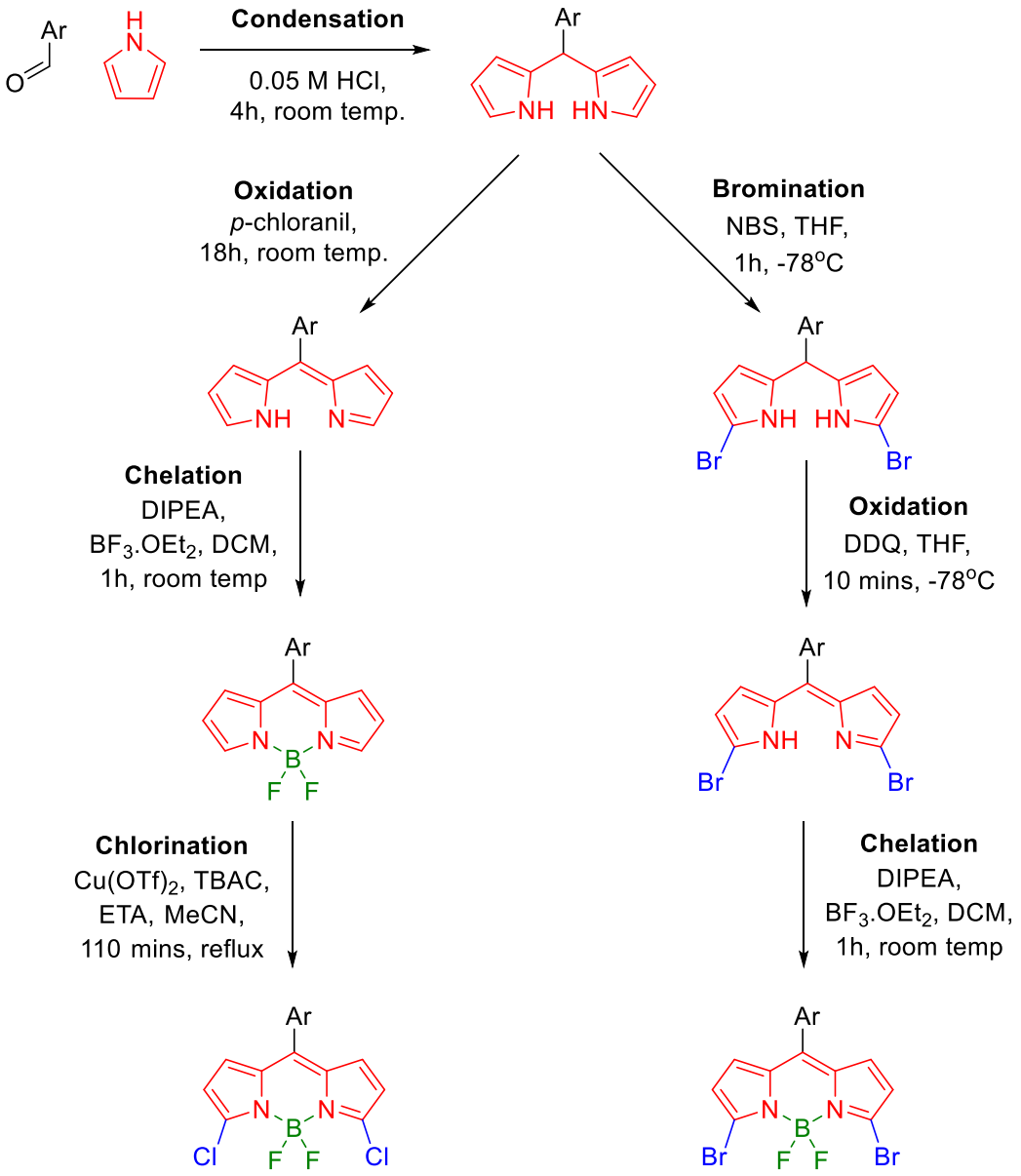

Scheme 2.16. Synthetic routes for the synthesis of 3,5-dichloro **2.13(a-d)** and 3,5-dibromo **2.14(a-d)** BODIPYs.

With a route for both the 3,5-dibromo **2.14(a-d)** and 3,5-dichloro BODIPYs **2.13(a-d)** in hand, exploration of their reactivity will be undertaken in subsequent chapters enroute to helically chiral BODIPYs.

Chapter 3 Synthesis of 3,5-diiodo BODIPYs

3.1 Introduction

In the previous chapter, we demonstrated the successful synthesis of both 3,5-dichloro and 3,5-dibromo BODIPYs.

Our overall aim of this thesis is the synthesis of helically chiral BODIPYs which are accessed through S_NAr and Pd catalysed cross-coupling reactions. 3,5-dihalo BODIPYs are suitable intermediates for this synthetic route, however it is thought that 3,5-diiodo BODIPYs may be a better candidate compared to there 3,5-dichloro and 3,5-dibromo BODIPY counterparts. As a consequence, the aim of this chapter is to successfully synthesis a range of 3,5-diiodo BODIPY compounds as novel key intermediates, being good candidates for subsequent cross-coupling reactions.

3.1.1. Existing iodinated BODIPYs reported in literature

There are only 12 published *meso* substituted BODIPYs containing iodine in both the 3 and 5 positions, disclosed in 6 different publications.[75-80] These publications demonstrate two routes towards 3,5-diiodo BODIPYs. The first of which is post functionalisation of the BODIPY through S_EAr chemistry and the second being iodination of the BODIPYs corresponding dipyrromethane species, which contains a carboxylic acid in the α positions.

3.1.1.1 Reported cases of 2,3,5,6-tetraodonation of BODIPYs through S_EAr chemistry

The first reported BODIPY showing iodination and chlorination at the 3 and 5 positions was published by Ortiz *et al*. in 2012. In this they used iodine monochloride as an electrophilic source of both iodine and chlorine in S_EAr reactions (Scheme 3.1).[75]

This synthetic iodination route demonstrates that S_EAr reactions with iodine monochloride occur preferentially at the 2,6 positions of BODIPY **3.1**. Ortiz's group also showed that 3,5 iodination of a BODIPY is possible, however this only occurs

subsequent to the initial 2,6-subsitution. They also demonstrated that longer reaction times and higher equivalents of ICl resulted in increased yields of the 3,5 substitution products.

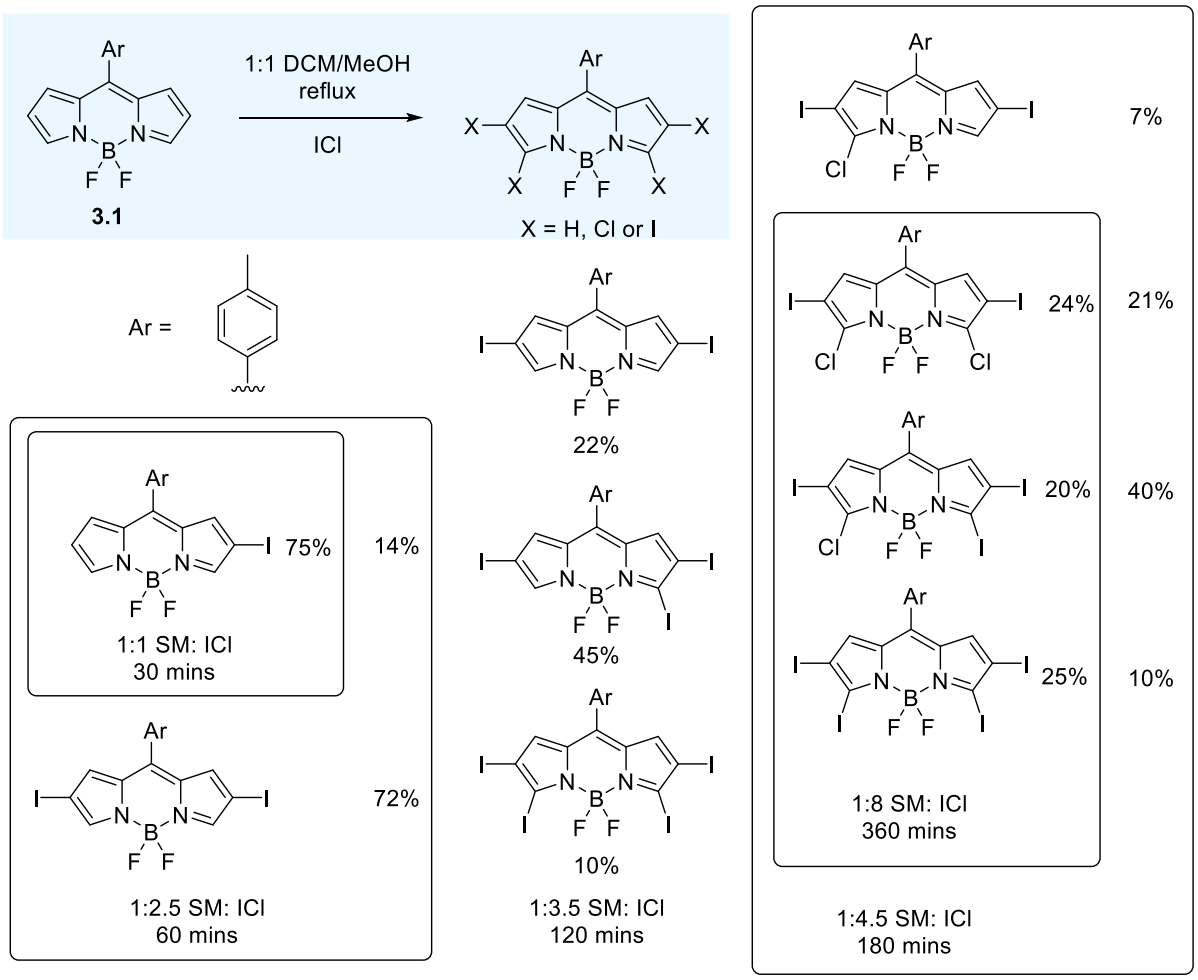

Scheme 3.1. Iodination of BODIPYs by Ortiz *et al*. using ICl as an electrophilic source of both iodine and chlorine.

In 2018 a patent was published by the University of Guangdong Technology, showing iodination of BODIPY **3.2** using I_2 as an electrophilic source of iodine. Again, initial substitution with iodine occurs preferentially at the 2,6 positions of the BODIPY.[76] This patent demonstrates that with an increase of temperature and equivalents of iodine, the likely hood of substituted increases, from mono iodo **3.3** to diiodo **3.4** and then tetraiodo BODIPY **3.5** (Scheme 3.2).

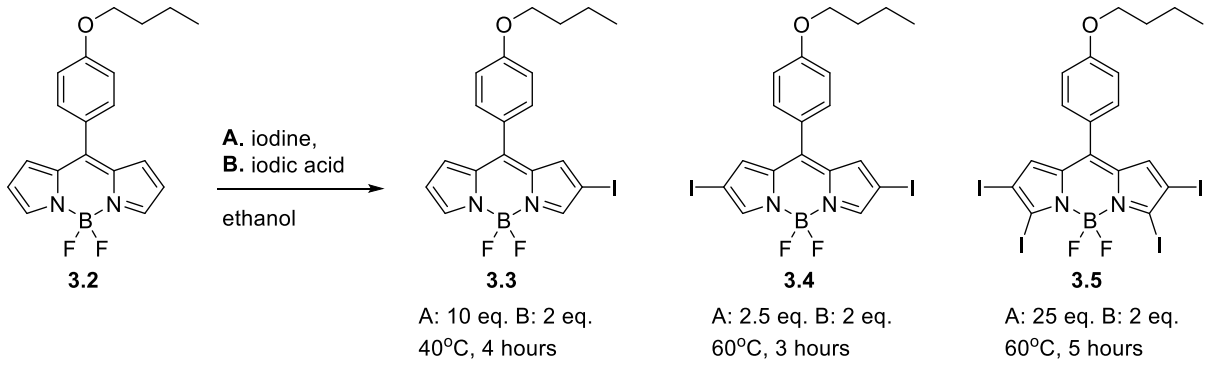

Scheme 3.2. Electrophilic addition of iodine to BODIPY **3.2**.

An alternative report of the synthesis of 2,3,5,6-tetraiodo BODIPYs was published by Hao *et al.* in 2018.[80] This study utilised a combination of both iodine and iodic acid. When the iodic acid is dissolved in EtOH, both $EtOH_2^+$ and IO_3^- are produced which facilitates the oxidation of I_2 to produce electrophilic I^+. This results in the tetra iodination of BODIPY **2.11a** to produce 2,3,5,6-tetraiodo BODIPY **3.4** (Scheme 3.3).

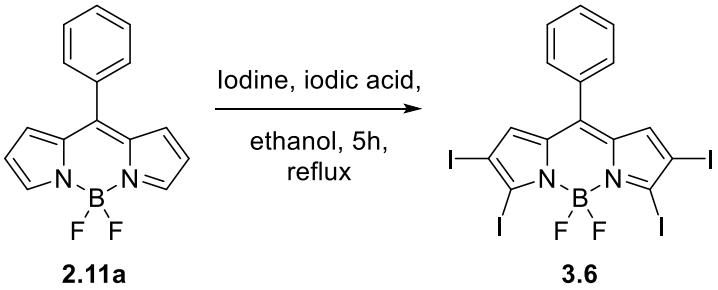

Scheme 3.3. S_EAr with iodine/iodic acid to form 2,3,5,6-tetraiodo BODIPY **3.6**.

All examples discussed above show preferential S_EAr at the 2,6 positions of the BODIPY, only showing substitution at the 3,5 positions once the 2,6 positions have reacted. Therefore, it was deemed that these synthetic routes would not be feasible for the synthesis of our target 3,5-diiodo BODIPYs, which are unsubstituted at the 2,6 positions.

There was one other published synthesis of 2,3,5,6-tetraiodo BODIPY **3.8**, reported in a 2018 by Huajun *et al.* in a patent from Hubei Grand Life Science and Tech Company. [77] In this patent the synthesis of not only 2,3,5,6-tetraiodo BODIPY **3.8** is reported but also the synthesis of 3,5-diiodo BODIPY **3.17a**. 3,5-diiodo BODIPY **3.17a** is reported to be synthesised in near quantitative yields through direct

iodination of BODIPY **3.7** with 2 equivalents of *N*-iodosuccinamide (NIS) (Scheme 3.4).

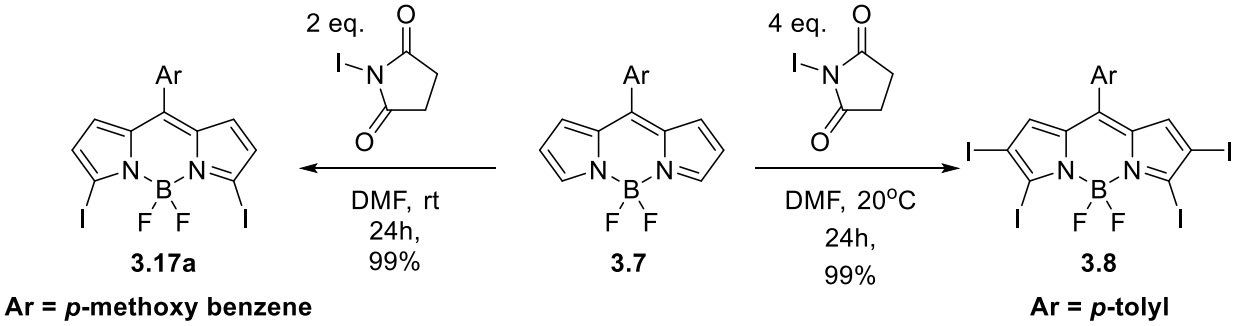

Scheme 3.4. Reported 3,5 diiodination and 2,3,5,6 tetraiodination of BODIPY **3.7**.

The reported synthesis of 3,5-diiodo BODIPY **3.17a** via this synthetic route is surprising as all other published iodination chemistry proceeds via an S_EAr mechanism, which should result in preferential substitution at the 2,6-positions. In addition, as discussed in Chapter 1, typically the treatment of BODIPYs with NBS leads to electrophilic substitution with bromine at the 2,6 positions preferentially.[41]

The ^{1}H NMR data provided in the report of Huajun *et al.* for their proposed 3,5-diiodo BODIPY **3.17a** was reported as "^{1}H NMR (400MHz, $CDCl_3$):δ = 3.83 (s, 3H), 5.39(d, *J* = 4.0 Hz, 1H), 6.33 (d, *J* = 4.0 Hz, 1H), 6.46 (s, 1H), 6.94 (d , *J* =4.0 Hz, 2H), 6.99 (s, 1H), 7.24 (d, *J* = 8.0 Hz, 2H) ppm". This does not appear to correlate with our ^{1}H NMR data of 3,5-diiodo BODIPY **3.17a** "^{1}H NMR (300 MHz, Chloroform-*d*) δ 7.44 (d, *J* = 8.8 Hz, 2H), 7.02 (d, *J* = 8.8 Hz, 2H), 6.71 – 6.70 (m, 4H), 3.90 (s, 3H)", the preparation of which is described later in this chapter.

We propose that data provided by Huajun *et al.* is a more likely to correlate with the related 2,3,6-triiodo BODIPY suggesting that this reaction did indeed follow the predicted S_EAr mechanism for iodination.

3.1.1.2 Synthesis of 3,5-diiodo BODIPYs from their corresponding dipyrromethanes

Examples from the remaining 2 publications which disclose the synthesis of 3,5-diiodo BODIPYs are shown below and are synthesized from their corresponding

dipyrromethane species, which contain a carboxylic acid in the α positions. All of the 3,5-diiodo BODIPYs contain steric blockage in the 2,6 positions.

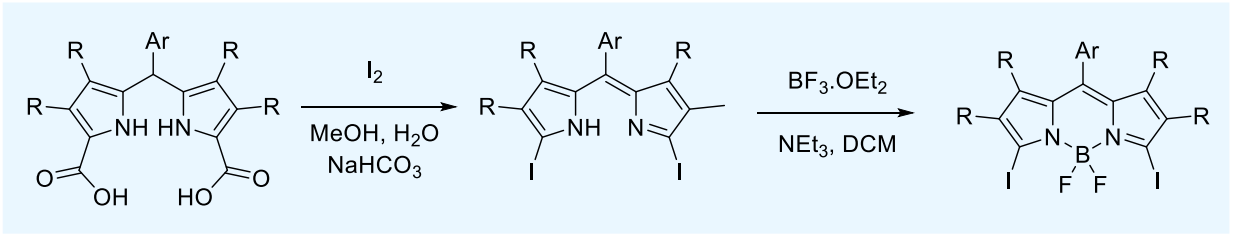

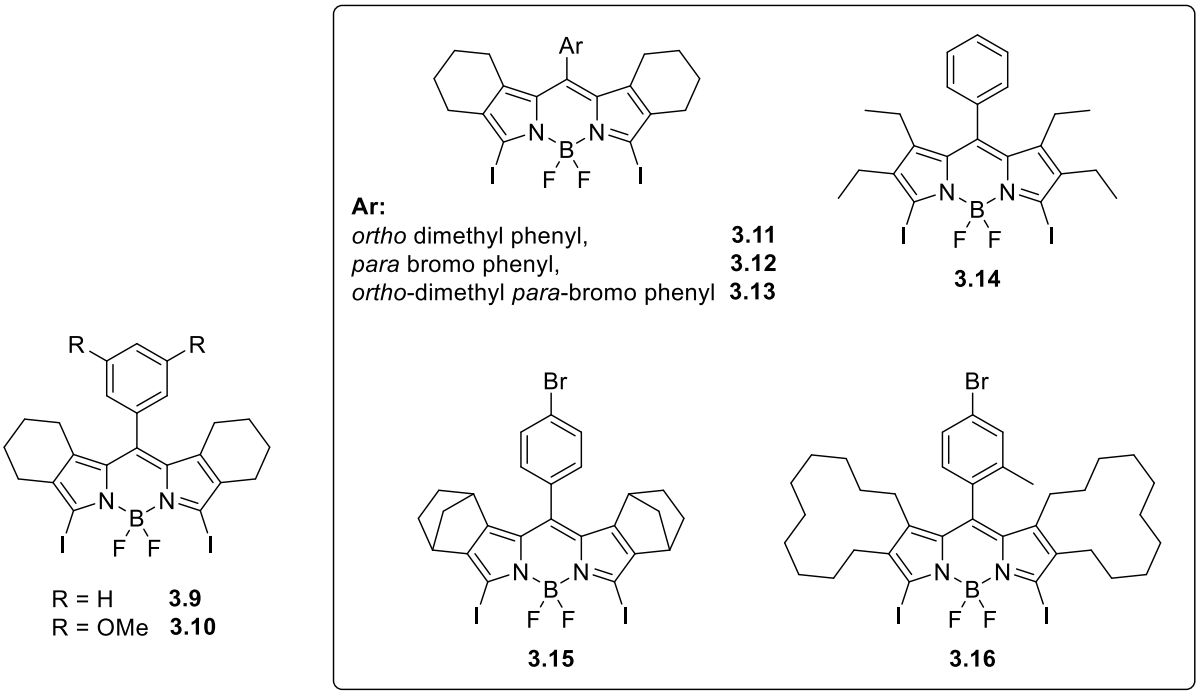

Vincente *et al*. 2016

Patent: Nitto Denko Corporation 2021

Figure 3.1. 3,5 Diiodo BODIPYs **3.9-3.16** synthesised via S_EAr with 2,6 steric blocking.

Vincente *et al*. in 2016 and a patent in 2021 by Nitto Denko Corporation reported a total of 8 novel 3,5-diiodo BODIPYs **3.9-3.16**.[79, 81] Each corresponding dipyrromethane species contained carboxylic acid groups in the α positions and were iodinated through S_EAr chemistry, forming α,α-diiodo dipyrromethenes. The dipyrromethenes are then chelated with a BF_2 moiety to form the desired 3,5-diiodo BODIPYs. (Figure 3.1). Each of these BODIPYs show steric blockage in the 2,6 positions, with no reported synthesis of otherwise unsubstituted 3,5-diiodo BODIPYs through this method.

Through this synthetic route has led to 3,5-diiodo BODIPYs **3.9-3.16**, all published results show steric blockage in the 2,6-positions, indicating that this route would not be possible for the synthesis of 2,6-unsubstituted 3,5-diiodo BODIPYs.

3.2 Results and discussion

In this section we will discuss the synthesis of otherwise unsubstituted 3,5-diiodo BODIPYs. As discussed above, there are very few reported syntheses of 3,5-diiodo BODIPYs. S_EAr iodination of BODIPYs allows access to 2,6-diiodo BODIPYs but is unlikely to be usable in the synthesis of simple 3,5-diiodo BODIPYs. Therefore, investigation into alternative routes towards 3,5-diiodo BODIPYs is explored herein.

3.2.1 Treatment of BODIPY **2.11a** with NIS enroute to diiodo BODIPY **3.17a**.

As discussed above, Hubei Grand Life Science and Technology Company reportedly achieved a selective 3,5 iodination of BODIPYs using 2 equivalents of NIS. The first challenge in this chapter was to validate this result as a route to 3,5 diiodo BODIPY **3.17a**.

Therefore, BODIPY **2.11a** was treated with 2 equivalents of NIS in DMF and stirred at room temperature for 24 hours. After a simple aqueous work-up, the crude reaction mixture was examined by ^{1}H NMR, which showed the presence of only unreacted starting material (Scheme 3.5).

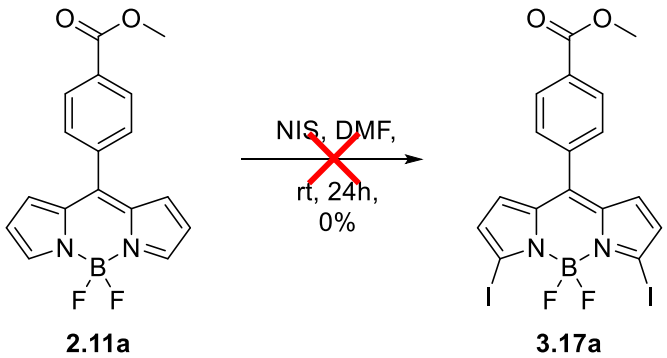

2.11a **3.17a**

Scheme 3.5. Attempted synthesis of 3,5 diiodo BODIPY **3.17a**.

Since this reaction had failed whilst following the literature procedure, and the original spectroscopic data for the proposed product was ambiguous, it was decided that examination this route would not be undertaken.

3.2.2 Synthesis of 3,5 diiodo BODIPY **3.17a-d** via an aromatic Finkelstein

After investigating the small number of published routes to 3,5 diiodo-BODIPYs, it was decided that none of the existing routes would be suitable for the synthesis of our target 3,5 diiodo-BODIPYs **3.17a-d**. Therefore, alternative synthetic routes had to be created.

We have successfully synthesised 3,5-dichloro and 3,5-dibromo BODIPYs therefore it was thought that a halogen exchange to the corresponding 3,5-diiodo BODIPYs could be possible. Finkelstein reactions are well reported in literature, which are precipitation driven halogen exchange reactions of either chloride or a bromide with iodide.[82] They were originally reported on alkyl halide species however more recently aromatic chemistry has been developed, showing halogen exchange via S_NAr chemistry.[54]

Although halogen exchange reactions have not be reported on BODIPYs, there are a large number of reported S_NAr reactions performed on 3,5-dihalo BODIPYs. Therefore, we postulated that halogen exchange via S_NAr reaction chemistry on BODIPYs may be possible.

Therefore, our planned route to synthesis 3,5-diiodo BODIPYs was based on aromatic Finkelstein chemistry. Note that Finkelstein-like reactions on aromatics are also known as Halex reactions (halogen exchange), in this thesis all reactions of this type will be referred to as aromatic Finkelstein reactions.

In a typical Finkelstein reaction, an alkyl halide is reacted with NaI in acetone, where the NaI acetone solution is at the saturation limit. NaI is more highly soluble in acetone compared to either sodium chloride or sodium bromide. This allows the substitution reaction to proceed to give the less thermodynamically favourable alkyl

iodide product, driven by the precipitation of either sodium chloride or sodium bromide.

Therefore, we propose to examine an aromatic Finkelstein reaction, to allow the substitution of chloride and bromide on 3,5-dihalo BODIPYs with NaI, to give a route to 3,5 diiodo-BODIPYs (Scheme 3.6).

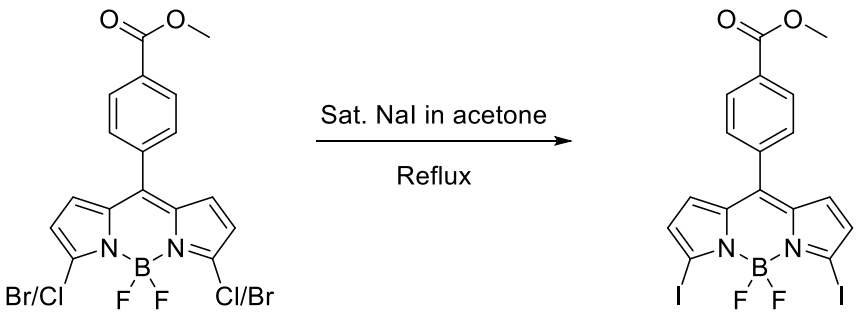

Scheme 3.6. Proposed synthesis of diiodo BODIPY **3.17a** via an aromatic Fickelstein reaction.

Typically, S_NAr reactions proceed via a two-step mechanism. The first of which being the rate determining reaction with the incoming nucleophile to form a Meisenheimer intermediate, followed by loss of the leaving group (Scheme 3.7).[77]

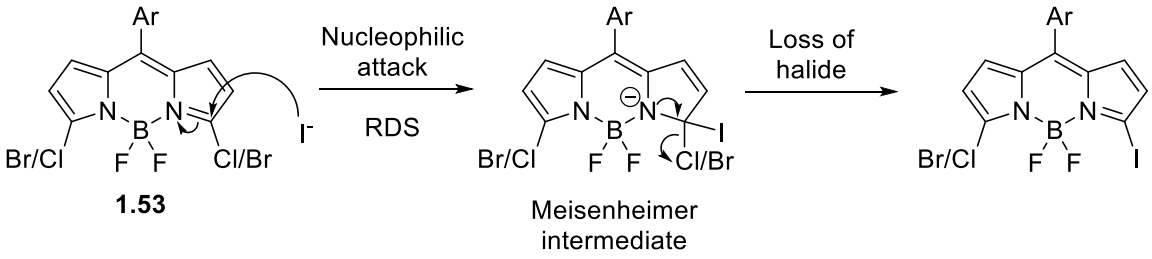

Scheme 3.7. Proposed S_NAr mechanism for aromatic Finkelstein reactions of 3,5-dihaloBODIPYs **1.53**.

According to the two-step S_NAr mechanism, the reactivity of the 3,5-dichloro BODIPY **2.13a** was expected to be higher than that of the 3,5-dibromo BODIPY **2.14a**.

In this mechanism the initial step is the rate determining step, having a more electronegative element at the 3/5 positions will result in a lower energy barrier for the nucleophilic attack by I^-. Because chlorine is more electronegative than bromine it will stabilise the build-up of negative charge in the transition state as it is able to attract electrons towards itself more strongly.

Therefore, the first reaction carried out utilised 3,5-dichloro BODIPY **2.13a** as the starting material. 3,5-Dichloro BODIPY **2.13a** was heated to reflux in a saturated solution of NaI in acetone for 48 hours. Following an aqueous work-up, the desired 3,5-diiodo BODIPY **3.17a** was obtained in a low yield of 13% (calculated from ^{19}F NMR integration of the crude reaction mixture) alongside 46% of monoiodonated BODIPY **3.18** and 32% of 3,5-dichloro starting material **2.13a**.

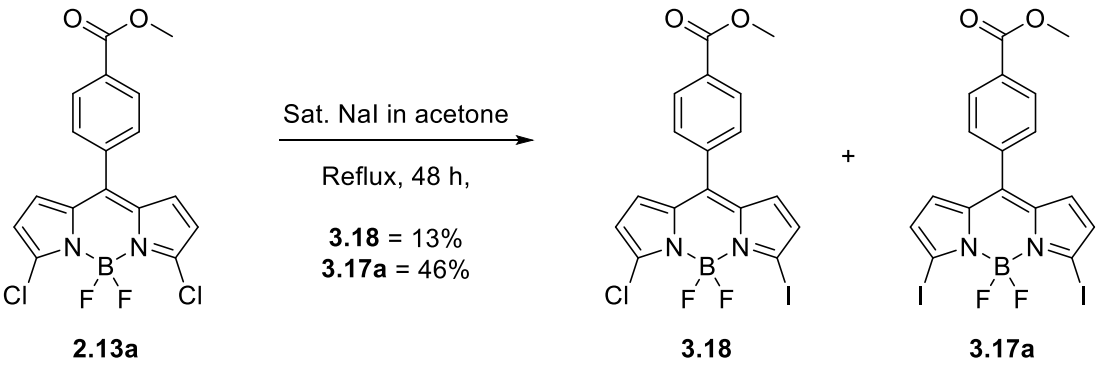

Scheme 3.8. Chlorine to iodine halogen exchange, synthesising both 3-chloro-5-iodo and 3,5-diiodo BODIPY **3.18** and **3.17a**.

Due to very similar R_f values of the starting material, 3-chloro-5-diodo and 3,5-diiodo BODIPY **3.17a**, separation of the desired product was unachievable by column chromatography.

Therefore, iodination of 3,5-dichloro BODIPY **2.13a** was repeated under identical conditions but with extended reaction time to try and push the reaction to completion. The 3,5-dichloro starting material **2.13a** was refluxed in a sat. NaI in acetone and monitored periodically by ^{19}F NMR (Figure 3.2).

Through monitoring the aromatic Finkelstein reaction of BODIPY **2.13a** using $^{19}F\{^1H\}$-NMR, it was seen that there was a steady increase in the formation of 3,5-diiodo BODIPY **3.17a**, along with the consumption of 3,5-dichloro BODIPY **2.13a**,

which was seen to be fully consumed after 215 hours. The formation of 3-chloro-5-iodo BODIPY **3.18** was also monitored, showing to reach its maximum yield of 57% at 64 hours, with a slow decrease over time after this point (Figure 3.2).

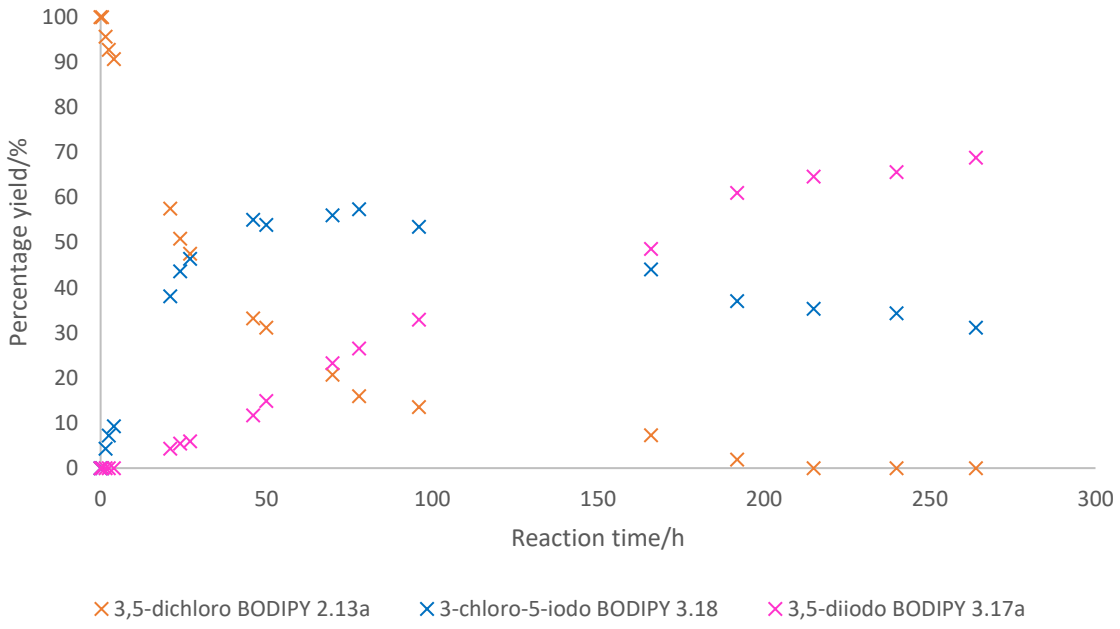

Figure 3.2. The progression of the aromatic Finkelstein reaction from 3,5-dichloro BODIPY **2.13a** to 3,5-diiodo BODIPY **3.17a**, monitored by $^{19}F\{^{1}H\}$ NMR. Reaction performed with 0.13 mmol of 3,5-dichloro BODIPY **2.13a** in a saturated solution of NaI (2 mL) under reflux.

After 264 hours the reaction was stopped, and after an aqueous work-up a mixture of 3-chloro-5-iodo BODIPY **3.18** and 3,5-diiodo BODIPY **3.17a** was obtained in a ratio of 31:69 (calculated by $^{19}F\{^{1}H\}$ NMR, Figure 3.3). This corresponds to an estimated yield of 69% of the 3,5-diiodo BODIPY **3.17a**, as no other species could be seen in the ^{1}H NMR. As discussed previously, separation of these two products was not possible due to similarities in R_f. Although the reaction of 3,5-dichloro BODIPY **2.13a** with a saturated solution of NaI showed the successful synthesis of 3,5-diiodo BODIPY **3.17a**, this methodology was not practical for synthetic use due to a requirement of reaction times over 200 h.

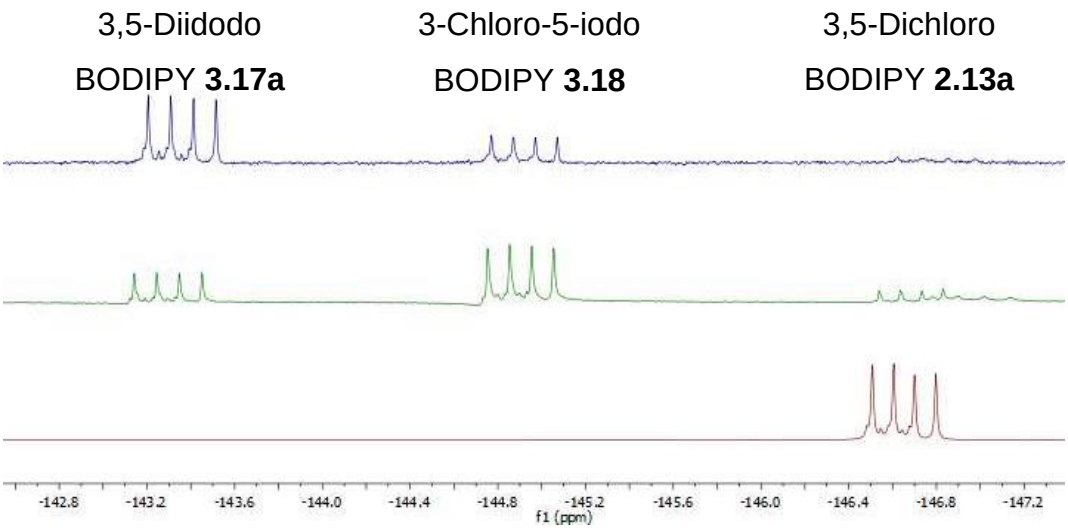

Figure 3.3. $^{19}F\{^{1}H\}$-NMR (282 MHz,acetone-h_6) monitored aromatic Finkelstein reaction at A = 0 h, B = 78 h, C = 240 h.

Due to the very long reaction time when converting 3,5-dichloro BODIPY **2.13a** into 3,5-diiodo BODIPY **3.17a** using acetone as a solvent, investigation into alternative, polar, higher boiling solvents was undertaken as a means to reduce the reaction time by increasing the reaction temperature (Table 3.1).

Therefore, aromatic Finkelstein reactions were carried out with high boiling polar solvents, starting with DMSO and DMF. Thus, 3,5-dichloro BODIPY **2.13a** was refluxed in both saturated solutions of NaI in DMSO and NaI in DMF. Each reaction was stirred for 24 hours, and each crude reaction was examined by ^{19}F NMR, showing the complete consumption of starting material in both cases. Unfortunately, none of the desired product was observed, as the expected quartet at -143 ppm was not seen. The crude reaction mixtures of both reactions were subjected to an aqueous work-up and was further inspected by ^{1}H NMR, showing the formation of a complex mixture of compounds which proved to be inseparable by silica gel column chromatography. (Table 3.1, Entry 2 and 3). It was postulated that the high reaction temperatures resulted in the degradation of the 3,5-dichloro BODIPY starting material **2.13a** in both reactions.

A further reaction was carried out in a saturated solution of NaI in DMSO, in which 3,5-dichloro BODIPY **2.13a** was stirred at a lower temperature of 110 ^{o}C for 24 h in an attempt to reduce degradation. Unfortunately, this again showed the loss of the 3,5-dichloro BODIPY **2.13a** starting material, resulting in a complex mixture of

products obtained with no observable formation of 3,5-diiodo BODIPY **3.17a** in the ^{19}F NMR (Table 3.1, entry 4).

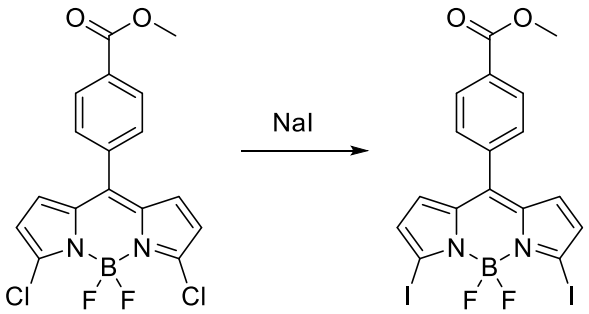

2.13a **3.17a**

Entry	solvent	temp./^{o}C	time/h	Yield/%
1	acetone	reflux (65)	264	69[a]
2	DMSO	reflux (189)	24	0[e]
3	DMF	110	24	0[e]
4	DMSO	110	24	0[e]
5	MeCN	reflux (82)	36	84[a,b]
6	MeCN	reflux (82)	72	100
7	EtCN	reflux (97)	24	95, 83[c]
8	^{n}PrCN	reflux (117)	24	21[a]

Table 3.1. Aromatic Finkestein on 3,5-dichloro BODIPY **2.13**. Typical reaction: 0.1-0.13 mmol substrate in 3 mL saturated NaI solution under air. a) Conversion by ^{19}F NMR. b) 5% yield of corresponding 3-chloro-5-iodo-BODIPY **3.18**. c) Reaction scale 3.35 mmol. d) Under N_2. e) complex mixture of products obtained.

After the unsuccessful formation of 3,5-diiodo BODIPY **3.17a** using both DMSO and DMF an alternative set of nitrile solvents were investigated. MeCN is a known solvent for aromatic Finkelstein (or Halex) reactions, with a higher boiling point than acetone and high polarity (dielectric constant of 38).[83]

Therefore, 3,5-dichloro BODIPY **2.13a** was stirred in a saturated solution of NaI in MeCN at reflux. The reaction was monitored by TLC, showing the disappearance of starting material after 36 hours. The crude reaction mixture was analysed by ^{19}F NMR, showing only trace amounts of starting material along with 84% of 3,5-diiodo BODIPY **3.17a** and 5% of the corresponding 3-chloro-5-iodo BODIPY **3.18** (Table

3.1, entry 5). This reaction was repeated, in which 3,5-dichloro BODIPY **2.13** was stirred for a longer time of 72 h in a refluxing solution of NaI in MeCN. After an aqueous work-up, full conversion to the desired 3,5-diiodo BODIPY **3.17a** was seen by ^{19}F NMR and this was purified by silica gel column chromatography to give an excellent yield of 100% (Table 3.1, entry 6).

The analysis of ^{1}H NMR spectra gave us confidence that the 3,5-diiodo BODIPY **3.17a** had formed, showing a distinctive shift in both the pyrrolic doublets from 6.79 ppm (J = 4.5 Hz) and 6.45 ppm (J = 4.4 Hz) to 6.72 ppm (J = 4.2 Hz) and 6.61 ppm (J = 4.2 Hz) (Figure 3.4).

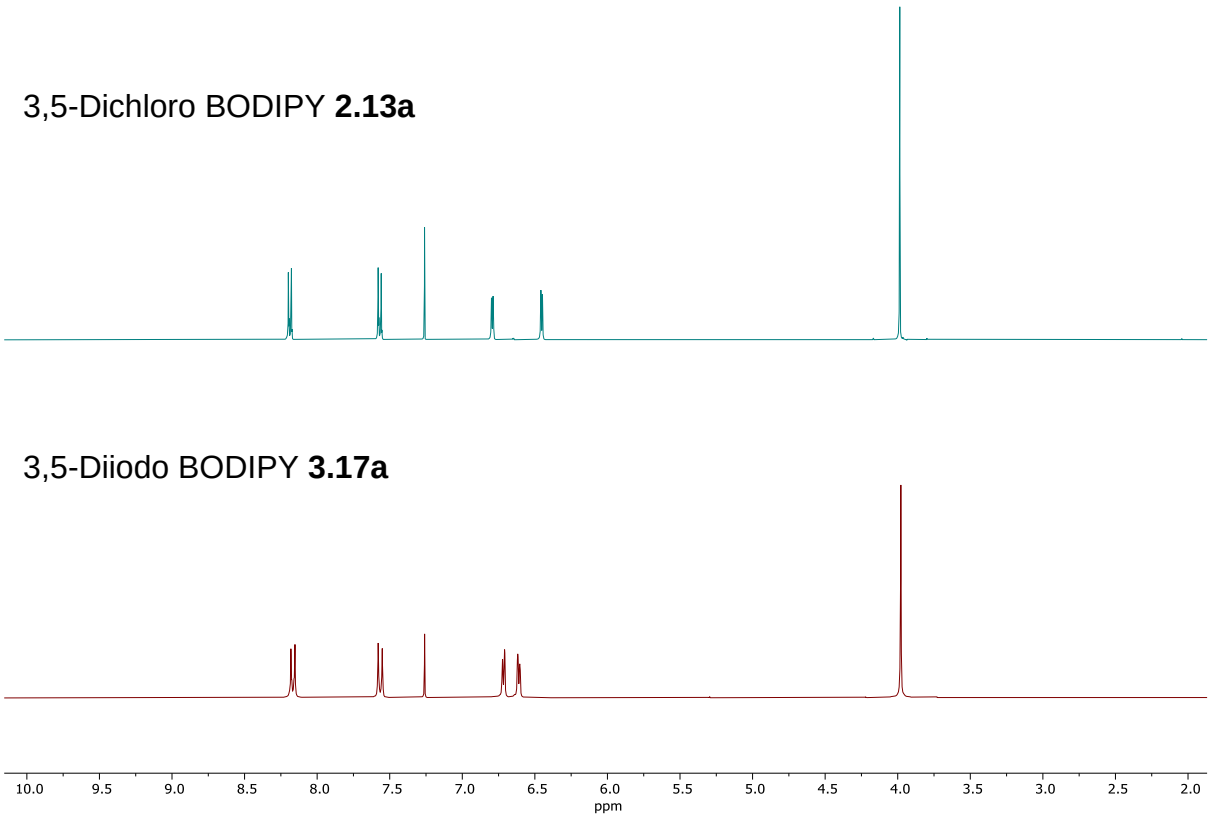

Figure 3.4. Comparison of the ^{1}H NMR spectra of 3,5-dichloro and 3,5-diiodo BODIPY **2.13** and **3.17a**.

Due to the success of using MeCN as an aprotic polar solvent, investigation into related alkyl nitriles as solvent was carried out. As the alkane length chain increases, the boiling point increases, allowing access to potentially shortened reaction times (Figure 3.5).

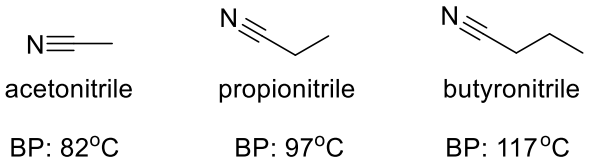

Figure 3.5. Alkyl nitrile solvents to be examined.

Therefore, the reaction using 3,5-dichloro BODIPY **2.13** was repeated under reflux in a saturated solution of NaI in propionitrile. The reaction was monitored by TLC, showing the disappearance of starting material after 24 hours. After an aqueous work-up the formation of 3,5-diiodo BODIPY **3.17a** was confirmed through ^{1}H NMR spectroscopy, showing an excellent 95% yield after purification by silica gel column chromatography (Table 3.1, entry 7).

Interestingly, upon repetition of this iodination reaction using an alternative higher boiling solvent of butyronitrile, after stirring 3,5-dichloro BODIPY **2.13** for 24 hours a reduction in yield of the desired product to 21% was observed by direct ^{19}F NMR analysis of the reaction mixture, along with the presence of a considerable amount of starting material (Table 3.1, entry 8).

This drop in yield was suspected to arise due to the low solubility of NaI in butyronitrile compared to propionitrile. As a means to test this hypothesis, the solubility of NaI was measured in acetonitrile, propionitrile and butyronitrile. This was performed by stirring 10 mL of each solvent with an excess of solid NaI for 24 hours. After which the solutions were filtered to remove undissolved material, and 5 mL of each solution was evaporated under reduced pressure and the residue weighed (Table 3.2).

Solvent	**mg/mL of NaI**
Acetonitrile	109.5
Propionitrile	54.1
Butyronitrile	23.4

Table 3.2. Measured solubility of NaI in acetonitrile, propionitrile and butyronitrile.

It was observed that there is a steady decrease in the solubility of NaI in the chosen solvents, decreasing from acetonitrile to butyronitrile (Table 3.2). This fits with our

hypothesis that NaI is poorly soluble in butyronitrile, which could result in lower yields.

After testing various reaction conditions which are discussed above, it was determined that reacting 3,5-dichloro BODIPY **2.13a** with NaI saturated in propionitrile produced the best results. Thus, the aromatic Finkelstein reaction of 3,5-dichloro BODIPY **2.13a** with NaI was repeated an additional 8 times throughout the project. The reaction was shown to be robust to scale up, retaining high yields of 83% when performed on a 3.35 mmol scale (Table 3.1, entry 7), and giving an average yield of 92% (SD = 5%)

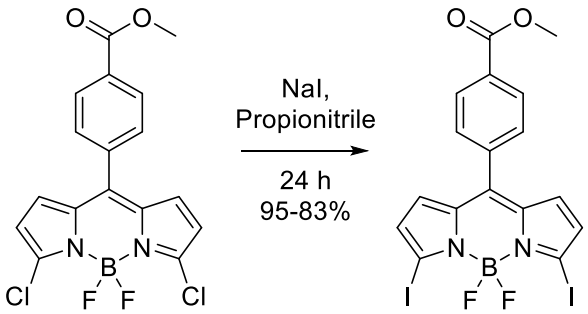

Scheme 3.9. Optimised aromatic Finkelstein iodination of 3,5-dichloro BODIPY **2.13a**.

Following the successful synthesis of 3,5-diiodo BODIPY **3.17a** through aromatic Finkelstein iodination, the substrate scope was expanded to encompass a range of *meso*-aryl substituted 3,5-dichloro BODIPYs **2.13b-d**, investigating both electron withdrawing and donating substituents (Table 3.3, entries 1-3).

Initially, aromatic Finkelstein was attempted with 3,5-dichloro BODIPY **2.13b** containing a strongly electron withdrawing 3-nitrophenyl group in the *meso* position, in which it was stirred in a refluxing saturated solution of NaI in EtCN. The reaction was monitored by TLC, showing complete consumption of the starting material within 6 hours. The product was purified by silica gel column chromatography, giving 93% of the corresponding 3,5-diiodo-BODIPY **3.17b** (Table 3.3, Entry 1). The structure of BODIPY **3.17b** was confirmed via HRMS, showing a mass of 565.8842, which is consistent for the $[M+H]^+$ of a molecule with formula of $C_{15}H_8{}^{11}BI_2F_2N_3O_2$.

Conversely, we saw that upon reacting electron donating *para*- and *meta*-methoxyphenyl containing 3,5-dichloro BODIPYs **2.13c** and **2.13d**, the aromatic Finkelstein reaction proved to be slower. Each reaction was refluxed in a saturated solution of NaI and monitored by TLC, however 72 h was required for full conversion to the desired 3,5-diiodo products for both the *para*- and *meta*-methoxyphenyl BODIPYs. Both products were purified by silica gel column chromatography, resulting in yields of 51% and 91% for the *para*- and *meta*-methoxyphenyl 3,5-diiodo BODIPYs **3.17c** and **3.17d** respectively (Table 3.3, entry 2 and 3).

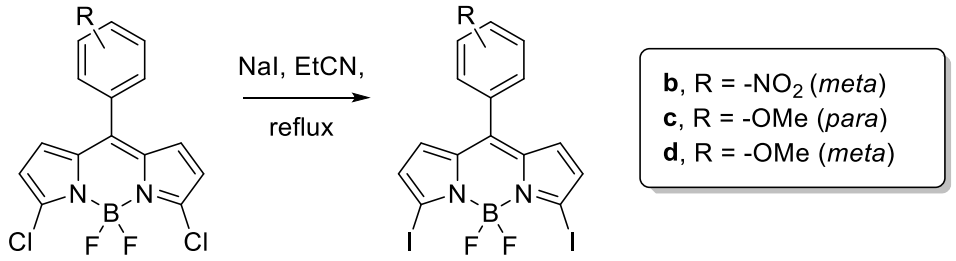

Entry	Aryl	Time/h	Yield/%
1	*meta*-nitrophenyl	6	93 (**3.17b**)
2	*para*-methoxyphenyl	72	51 (**3.17c**)
3	*meta*-methoxyphenyl	72	91 (**3.17d**)

Table 3.3. Aromatic Finkelstein reactions from 3,5-dichloro to 3,5-diiodo BODIPYs **3.1b-d**. Each reaction was run in EtCN under reflux (97^{o}C).

It is observed that a strongly electron withdrawing group, nitrophenyl resulted in a greatly reduced reaction time and an electron donating group methoxyphenyl resulting in a much longer reaction time compared to methyl benzoate 3,5-dichloro BODIPY **3.17a**. This can be attributed to electron withdrawing *meso* groups withdrawing electron density at the 3/5 positions of the BODIPY, helping to stabilise the build-up of negative charge in the transition state, lowering its energy.

It is important to note that the observed yields and reaction times correlate well with the Hammett constants associated with these *meso*-aryl groups substituents (**2.13b** σ(*m*-NO_2) = 0.71; **2.13a**, σ(*p*-CO_2Me) = 0.45; **2.13d**, σ (*m*-OMe) = 0.12; **2.13c**, σ (*p*-OMe) = -0.27), supporting a stepwise S_NAr mechanism.

3.2.3 Synthesis of 3,5-diiodo BODIPYs **3.17a-d** from 3,5-dibromo BODIPYs **2.14a-d**

As discussed earlier, due to S_NAr reactions typically going through a stepwise mechanism, the 3,5-dichloro BODIPY **2.13a** starting material was initially selected over its bromo counterpart as it was expected to react faster. After the successful aromatic Finkelstein reaction to form 3,5-diiodo BODIPY **3.17a** from its 3,5-dichloro **2.13a** counterpart, further investigation into halogen exchange from 3,5-dibromo BODIPY **2.14a** was undertaken as a means to test this hypothesis.

Therefore, we subjected 3,5-dibromo BODIPY **2.14a** to the optimised aromatic Finkelstein reaction conditions, in which the substrate was stirred in a saturated solution of NaI in propionitrile at reflux. The reaction was monitored by TLC, showing full conversion to the desired 3,5 diiodo BODIPY **3.17a** within 1.5 hours, which was isolated using silica gel column chromatography to give a quantitative yield (Scheme 3.10).

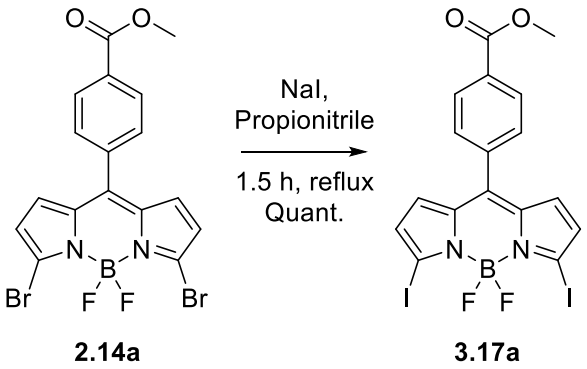

2.14a **3.17a**

Scheme 3.10. 3,5-Dibromo to 3,5-diiodo-BODIPY **3.17a** aromatic Finkelstein reaction via optimised reaction conditions, refluxing saturated NaI in propionitrile.

Surprisingly, the aromatic Finkelstein reaction with 3,5-dibromo BODIPY **2.14a** was faster than that with the corresponding 3,5-dichloro analogue **2.13a**, which appears to be inconsistent with a traditional stepwise S_NAr mechanism. It is therefore postulated that the aromatic Finkelstein reaction with 3,5-dibromo BODIPY **2.14a** and NaI occurs via a concerted S_NAr mechanism. This would be consistent with the observed relative rates, as the rate of a concerted S_NAr reaction depends on the bond strength of the C-Halo bond, as this bond is broken during the rate determining step.[84] Therefore, for a concerted S_NAr reaction, the rate of reaction is expected to be higher for the 3,5-dibromo BODIPY **2.14a** compared to the 3,5-dichloro species **2.13a** due to the lower bond strength (C-Cl bond dissociation energy in 1-

chlorobenzene = 95.5 kcal/mol, C-Br bond dissociation energy in 1-bromobenzene = 80.4 kcal/mol) (Figure 3.6).[85]

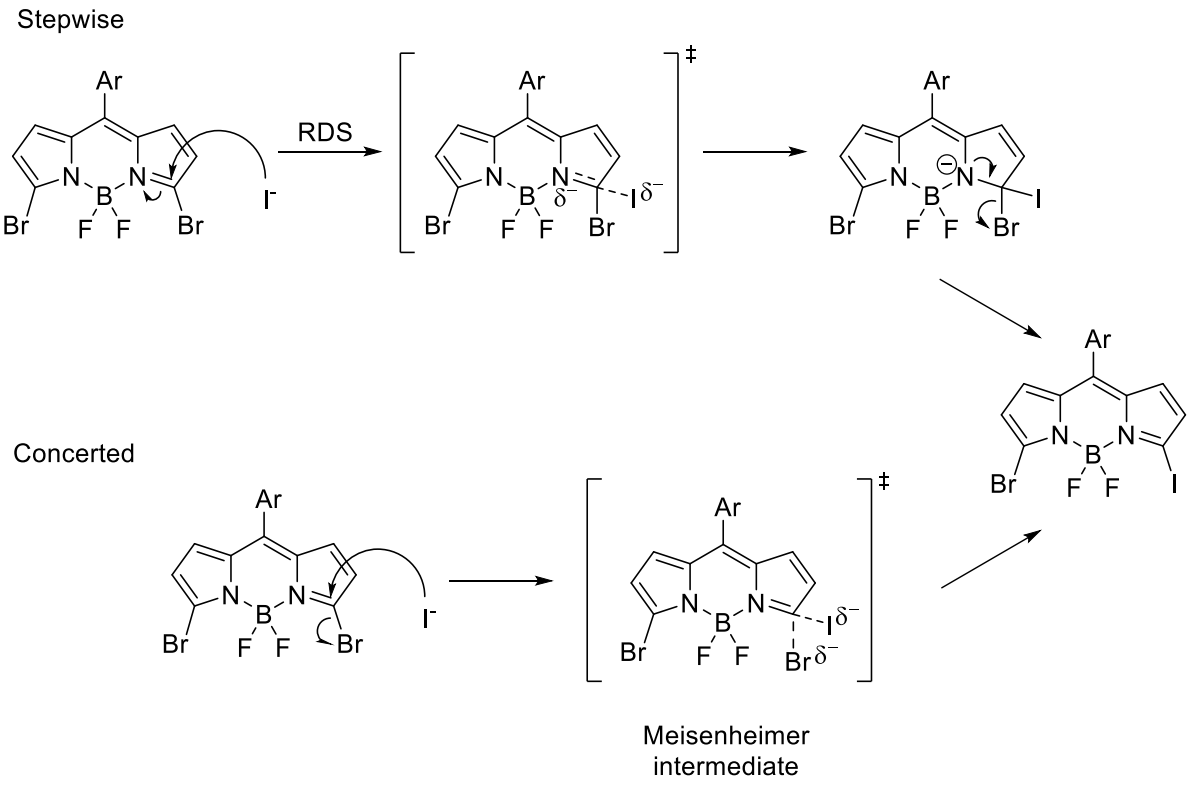

Figure 3.6. Stepwise vs concerted S_NAr reaction mechanism on BODIPY systems.

Further investigation into the aromatic Finkelstein reaction was undertaken, looking at a range of electron withdrawing and electron donating aryl-substituted 3,5-dibromo BODIPY **2.14b-d** starting materials. To make direct comparisons with the aromatic Finkelstein reactions described earlier using 3,5-dichloro BODIPYs **2.13b-d**, we used 3,5-dibromo BODIPYs with identical *meso* aryl groups **2.14b-d** (for synthesis, see Chapter 2).

Each aryl-substituted 3,5-dibromo BODIPY **2.14b-d** was exposed to the optimised reaction conditions. Thus, *meta*-nitrophenyl 3,5-dibromo BODIPY **2.14b**, containing an electron withdrawing aryl group, was reacted with a saturated solution of NaI in propionitrile at reflux, showing full conversion to its 3,5-diiodo BODIPY **3.17b** counterpart after 0.5 hours. The crude reaction mixture was purified by silica gel column chromatography to give *meta*-nitro 3,5-diiodo BODIPY **3.17b** in a 98% yield (Table 3.4, entry 2).

Meta- and *para*-methoxy 3,5-dibromo BODIPYs **2.14c** and **2.14d**, containing electron donating aryl groups, were both reacted with a saturated solution of NaI in propionitrile at reflux, showing full consumption of starting material by TLC after 2 hours. After purification by silica gel column chromatography, *meta*- and *para*-methoxy 3,5-diiodo BODIPYs **3.17c** and **3.17d** were isolated in a 62% and 88% yield respectively (Table 3.4, entries 3 and 4).

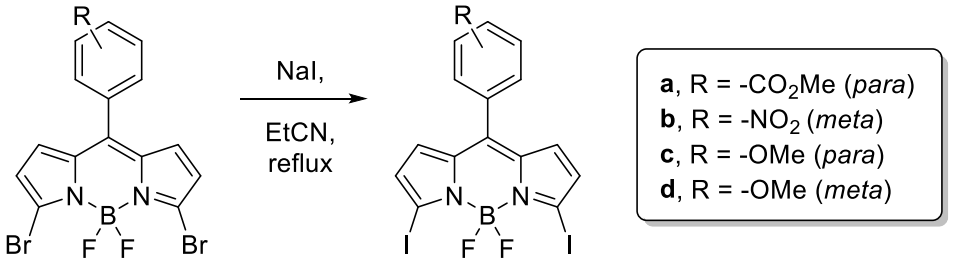

2.14a-d **3.17a-d**

.Entry	Starting Material	Time/h	Yield/%
1	**2.14a**	1.5	90, 100 (**3.17a**)
2	**2.14b**	0.5	98 (**3.17b**)
3	**2.14c**	2	62 (**3.17c**)
4	**2.14d**	2	88 (**3.17d**)
5	**2.14a**	1.5	99[a] (**3.17a**)
6	**2.14a**	1.5	97[b] (**3.17a**)
7	**2.14a**	1.5	90[c] (**3.17a**)

Table 3.4. Aromatic Finkelstein reactions of 3,5-dibromo BODIPYs **2.14a-d** to give 3,5-diiodo BODIPYs **3.17a-d**. Each reaction was run in EtCN under reflux (97°C). a) Under a nitrogen atmosphere. b) Absence of light. c) Both an absence of light and under a nitrogen atmosphere.

It was observed that all of the aromatic Finkelstein reactions on the 3,5-dibromo BODIPYs **2.14a-d** to give the corresponding 3,5-diiodo BODIPYs **3.17a-d**, had a faster rate of reaction compared to those with the 3,5-dichloro BODIPYs **2.13a-d**. These observed faster rates for 3,5-dibromo BODIPYs are consistent with a concerted S_NAr mechanism for these substrates, with the weaker C-Br bond resulting in a change to a concerted S_NAr mechanism.

The observed reaction times of the 3,5-dibromo BODIPYs **2.13a-d** also correlated with the Hammett constants associated with the *meso*-aryl group substituents, those with electron withdrawing groups reacting faster. However, the difference in reaction rate between systems with different *meso*-aryl group substituents was considerably less pronounced than with the corresponding 3,5-dichloro BODIPYs **2.12a-d**. This less pronounced influence of the *meso*-aryl group substituents also fits with a more concerted S_NAr mechanism.

Li *et al*. have recently reported a photo-induced aromatic Finkelstein reaction for the conversion of aryl-bromides to aryl-iodides, via a UV light induced radical mechanism.[86] All of the previous halogen exchange reactions (Table 3.3 and Table 3.4) were typically carried out in ambient conditions (open to air and light), therefore we carried out a range of control experiments, in which 3,5-dibromo BODIPY **3.14a-d** was reacted with NaI in the absence of air and/or light, to rule out a possible photo-induced mechanism. No significant change in yield or reaction time in any of the control experiments was seen, indicating this is not a photoinduced radical mechanism (Table 3.4, entries 5-7).

In conclusion, the novel synthesis of 3,5-diiodo BODIPY **3.17a-d** was achieve through an aromatic Finkelstein type reaction. This reaction has been shown to be a robust, high yielding reaction, across a range of substrates. This novel route to 3,5-diidodo BODIPY **3.17a-d** was published in Organic Letters in 2021, along with a comparision of the reactivity of the 3,5-dichloro- **2.13a,** 3,5-dibromo- **2.14a** and 3,5-diiodo BODIPY **3.17a** in a range of Pd catalyzed cross-coupling reactions, which will be discussed next.[87]

3.2.4 Palladium cross-coupling on 3,5-dihalo BODIPYs

After the successful, rapid and high yielding synthesis of 3,5-diiodo BODIPYs **3.17a-d**, attention was directed into exploring their performance in further reactions, compared to their corresponding 3,5-dichloro and 3,5-dibromo counterparts.

Therefore, in the second part of this chapter we will discuss a range of Pd cross-coupling reactions: Sonogashira; Migita-Kosugi-Stille; Mizoroki-Heck and Suzuki-Miyaura, as applied to 3,5-dichloro-, 3,5-dibromo- and 3,5-diiodo BODIPYs. Such cross-coupling reactions are commonly used for the further functionalisation of

BODIPYs at the 3,5-positions, as the introduction of substituents at the 3,5 positions is known to have a significant impact on the photophysical properties (e.g. absorption and emission maxima) of BODIPYs.[88]

3.2.4.1 Migita-Kosugi-Stille cross-coupling on 3,5-dihalo BODIPYs

Initially, a double Migita-Kosugi-Stille was investigated as a means to add an aryl group to the 3,5 positions of the BODIPY, allowing comparison of the reactivity of the different halogenated BODIPYs.

In the literature, Migita-Kosugi-Stille reactions are most commonly undertaken using $Pd(PPh_3)_4$ as a catalyst in toluene with $PhSnBu_3$ as the organostannane aryl source. A typical example of this was demonstrated by Quintard *et al.*, in which they showed the coupling of a range of aryl halides **3.19** with a polymer-immobilised alkyl tin species **3.20** (Scheme 3.11). This reaction was performed with 5 mol% of $Pd(PPh_3)_4$ in toluene at 110°C, showing successful addition of an aryl group across the C-Cl, C-Br and C-I bonds.[89] Immobilisation of the organotin reagent facilitates removal of the tin-containing by products at the end of the reaction, which is often a significant challenge.

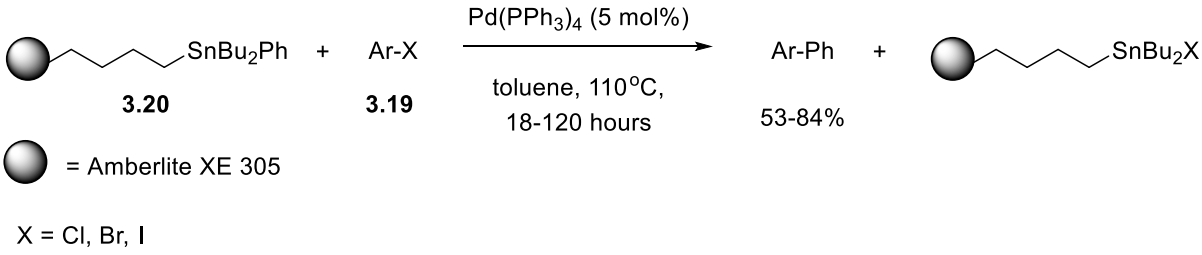

Scheme 3.11. Migita-Kosugi-Stille cross-coupling demonstrating the addition of a phenyl ring across a range of aryl-halide species **3.19**.

We planned to undertake Migita-Kosugi-Stille cross-coupling reactions on 3,5-dihalo BODIPYs **2.13a, 2.14a** and **3.17a** with $PhSnBu_3$ (Scheme 3.12).

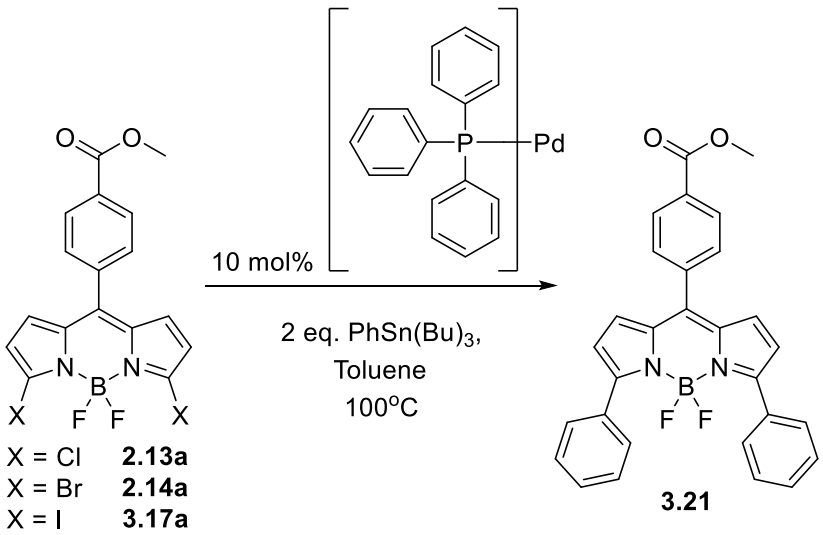

Scheme 3.12. Proposed Migita-Kosugi-Stille cross-coupling for the synthesis of 3,5-diaryl BODIPY **3.21**. X = Cl, Br, I.

Therefore, a Migita-Kosugi-Stille cross-coupling reaction first attempted with 3,5-dichloro BODIPY **2.13a**, using 10 mol% of $Pd(PPh_3)_4$ and 2 equivalents of $PhSnBu_3$ in toluene at 100°C. The reaction was monitored by TLC and after 16 hours two new products were observed. Following aqueous work-up and silica gel column chromatography, two products were isolated, the desired 3,5-diphenyl BODIPY **3.21** in a moderate yield of 35% and a by-product in a yield of 24% (Table 3.5, entry 1).

The structure of 3,5-diphenyl BODIPY **3.21** was confirmed by ^{1}H-NMR, showing the appearance of a 4H multiplet at 7.99-7.81 ppm and 6H multiplet at 7.54-7.37 ppm corresponding to the protons on the newly added phenyl rings.

Analysis of the ^{1}H NMR spectrum of the by-product showed the loss of molecular symmetry due to the presence of four, 1H doublets at 6.76 (*J* = 4.3 Hz), 6.74 (*J* = 4.1 Hz), 6.59 (*J* = 4.1 Hz) and 6.41 ppm (*J* = 4.3 Hz) corresponding to four different pyrrolic proton environments.

In addition there were 4 new signals in the alkyl region, a 2H triplet at 3.03 ppm (*J* = 7.8 Hz), a 2H pentet at 1.71 ppm (*J* = 7.7 Hz), a 2-proton heptet at 1.43 ppm (*J* = 7.4 Hz) and a 3H triplet at 0.94 ppm (*J* = 7.3 Hz), indicated the presence of an n-butyl group (Figure 3.7). Therefore, we assigned the by-product to be 3-butyl-5-phenyl BODIPY **3.22**. It is thought that this alternative compound arises from a competing

cross coupling in which a butyl group from the $PhSn(Bu)_3$ species is coupled instead of the Ph group under the Migita-Kosugi-Stille conditions.[90-92]

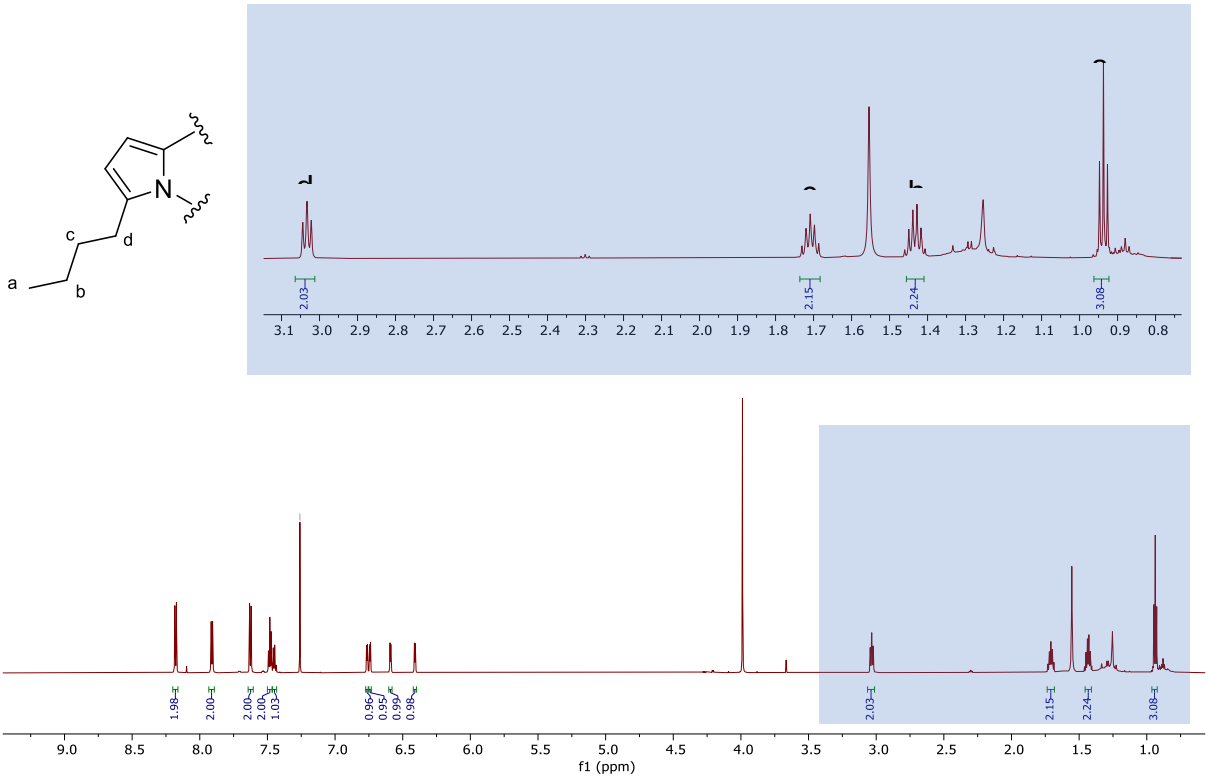

Figure 3.7. ^1H NMR spectra of 3-butyl-5-phenyl BODIPY **3.22**, showing the presence of an n-butyl group.

For the purposes of comparison, the Migita-Kosogi-Stille reaction was then repeated using the 3,5-dibromo and 3,5-diiodo BODIPY starting materials **2.14a** and **3.17a** under the reaction conditions as discussed above.

3,5-Dibromo BODIPY **2.14a** was reacted with 2 equivalents of $PhSnBu_3$ and 10 mol% of $Pd(PPh_3)_4$ in toluene at 100°C. After 16 hours and purification by silica gel column chromatography two products were again isolated. The desired 3,5-diphenyl BODIPY **3.21** was isolated in a good yield of 77% alongside a 3-butyl-5-phenyl BODIPY **3.22** by-product in a yield of 8% (Table 3.5, entry 2).

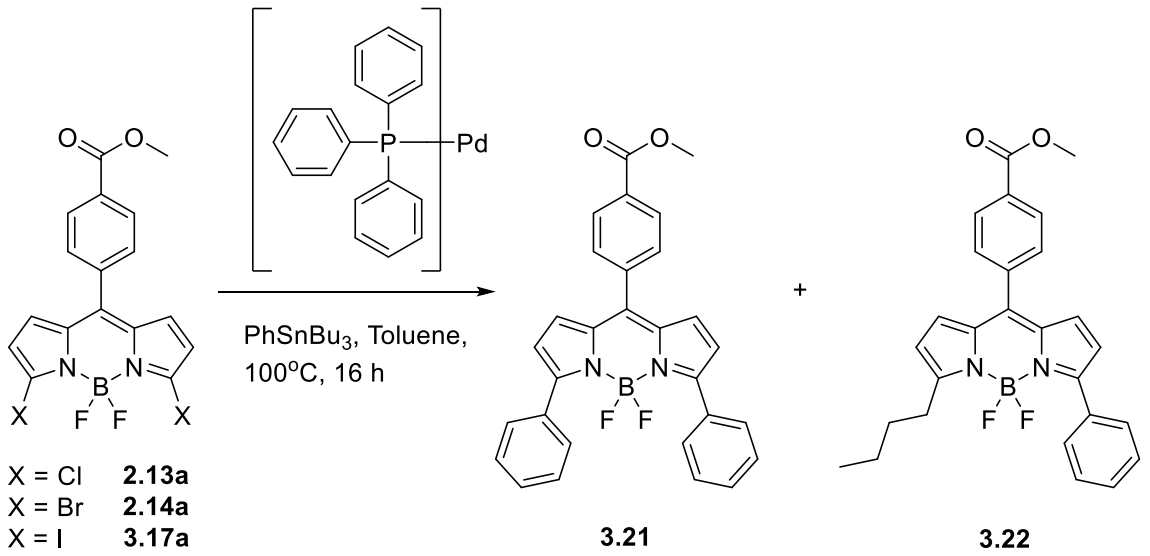

Entry	Starting Material	Yields/%
1	X = Cl	35 (**3.21**), 24 (**3.22**)
2	X = Br	77 (**3.21**), 8 (**3.22**)
3	X = I	51 (**3.21**), 17 (**3.22**)

Table 3.5. Migita-Kosugi-Stille reaction at the 3,5-positions of BODIPY starting material. X = Cl, Br or I

Upon repetition of the reaction using 3,5-diiodo BODIPY **3.17a** as the starting material, following the same reaction conditions and purification protocols, the desired 3,5-diphenyl BODIPY **3.21** was isolated in a yield of 51% together with a 17% yield of the 3-butyl-5-phenyl BODIPY **3.22** (Table 3.5, entry 3).

Thus, the comparison of the three different 3,5-dihalo BOIPDYs under these Migita-Kosugi-Stille cross-coupling conditions showed that, although the 3,5-diiodo BODIPY **3.17a** proved to be superior compared to the corresponding 3,5-dichloro BODIPY **2.13a**, the 3,5-dibromo BODIPY **2.14a** gives the highest yield of diphenyl BODIPY **3.21** and the lowest yield of the n-butyl containing by-product **3.22**. Under these reaction conditions there is a possibility for proton dehalogenation to occur. Typically, the better the leaving group, the more likely for proton dehalogenation to occur. Iodine is the best leaving group compared to both bromine and chlorine, therefore the observed lower yield for this Kosugi-Stille cross-coupling when utilising 3,5-diiodo

BODIPY **3.17a** compared to 3,5-dibromo BODIPY **3.14a** could be due to a competing side reaction of proton dehalogenation.

3.2.4.2. Mizoroki-Heck cross-coupling on 3,5-dihalo BODIPYs

Next, the introduction of an alkene moiety in the form of styrene was investigated via a Mizoroki-Heck reaction at the 3,5 positions of the BODIPY, allowing comparison of the reactivity of the different halogenated BODIPYs.

Typically, published literature procedures of Mizoroki-Heck cross-coupling reactions involve $Pd(OAc)_2$ as the Pd catalyst with a PPh_3 ligand and NEt_3 base. These reaction conditions have also been reported specifically on halogenated BODIPY substrates.[93, 94] For example, Shen *et al*. reported the introduction of styrene at the 2,6 positions of BODIPY **3.23**, using $Pd(Oac)_2$ and NEt_3 in DMF, resulting in a 41% yield of BODIPY **3.24** (Scheme 3.13).[95]

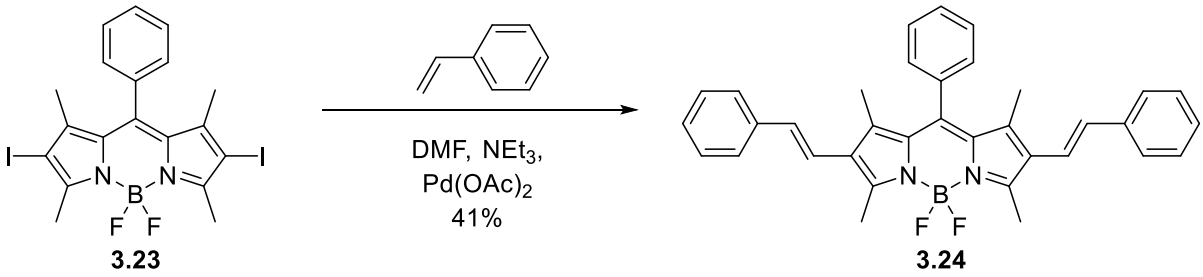

3.23 **3.24**

Scheme 3.13. Heck reaction on 2,6-diiodo BODIPY **3.23**.

Therefore, we adapted this literature procedure for the introduction of styrene at the 3,5 positions of BODIPY **2.13a**, **2.14a** and **3.17a** (Table 3.6. Mizoroki-Heck reactions on dichloro- dibromo- and diiodoBODIPY **2.13a, 2.14a** and **3.17a** starting materials to form the desired 3,5-distyryl BODIPY **3.25.**

Mizoroki-Heck cross-coupling was initially attempted on 3,5-dichloro BODIPY **2.13a**, in which the starting material was treated with 5 equivalents of $PhCHCH_2$, 3 mol% of $Pd(OAc)_2$, 7 mol% PPh_3 and 3 equivalents of NEt_3 and stirred for 8 hours at room temperature in DMF. This proved to be unsuccessful, after an aqueous work-up the crude reaction mixture was analysed by ^1H NMR, showing a complex mixture of compounds, none of which being desired product (Table 3.6, entry 1).

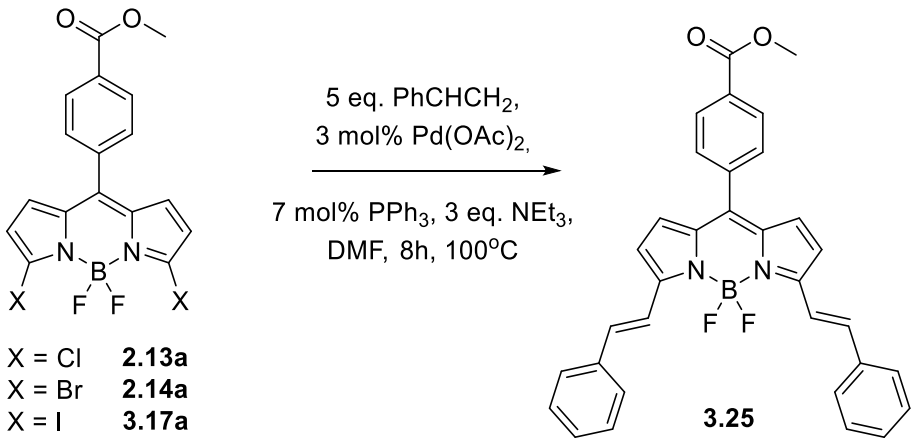

Entry	Starting Material	Yield/%
1	X = Cl	0
2	X = Br	3
3	X = I	30

Table 3.6. Mizoroki-Heck reactions on dichloro- dibromo- and diiodoBODIPY **2.13a**, **2.14a** and **3.17a** starting materials to form the desired 3,5-distyryl BODIPY **3.25**.

Next, 3,5-dibromo BODIPY **2.14a** with was treated with 5 equivalents of $PhCHCH_2$, 3 mol% $Pd(OAc)_2$, 7 mol% PPh_3, 3 equivalents of NEt_3 and stirred at 100°C for 8 hours in DMF. The crude reaction mixture was subjected to an aqueous work-up and was purified by silica gel column chromatography, giving 3% yield of the desired 3,5-distyryl BODIPY **3.25**. The structure 3,5-distyryl BODIPY **3.25** was confirmed through ^{1}H NMR, showing two distinctive 1H doublets corresponding to alkene protons at 7.36 and 7.80 ppm, with a coupling constant of 16.4 Hz, indicative of a *trans* double bond (Table 3.6, entry 2).

Finally, Mizoroki-Heck cross-coupling was repeated upon the 3,5-diiodo BODIPY **3.17a** under the same reaction conditions and purification protocols, and the desired 3,5-distyryl BODIPY **3.25** was isolated in a good yield of 30% (Table 3.6, entry 3).

3,5-Distyryl BODIPY **3.25** was successfully crystallised through slow evaporation of a DCM solution. A suitable single crystal was submitted for single X-ray analysis, confirming the molecular structure (Figure 3.8). 3,5-Distyryl BODIPY **3.25** formed monoclinic crystals in the $P2_{1/n}$ space group, containing 4 molecules in the unit cell ($Z = 4$).

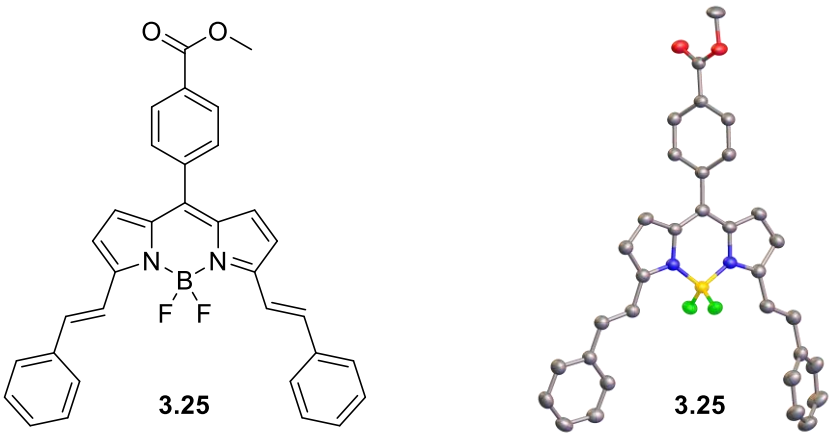

Figure 3.8. Single crystal X-ray structure of 3,5-distyryl BODIPY **3.25**.

3,5-Diiodo BODIPY **3.17a** showed to be the best 3,5-dihalo BODIPY starting material for our tested Mizoroki-Heck reaction conditions, resulting a higher yield of the desired 3,5-distyryl BODIPY **3.25** compared to its 3,5-dibromo and 3,5-dichloro **2.13a** and **2.14a** counterparts. Mizoroki-Heck reactions are typically challenging for 3,5-dihalo BODIPYs, therefore, the 30% yield for the double coupling with 3,5-diiodo BODIPY **3.17a** is still an excellent result, equating to a 55% yield per styrene coupling.[57, 96]

3.2.4.3. Sonogashira cross-coupling on 3,5-dihalo BODIPYs

Further examination of Pd cross-coupling reactions lead us to investigate Sonogashira cross-couplings with different of 3,5-dihalo BODIPY, as a means to introduce an alternative alkyne moiety at the 3,5-positions of a the BODIPY system.

Commonly in literature, Sonogashira reactions that are carried out on BODIPYs utilise catalytic quantities $PdCl_2(PPh_3)_2$ with CuI in THF with a non-nucleophilic base, such as NEt_3. For example Van Lier *et al*. demonstrated the coupling of 2-iodo-BODIPY **3.26** with the alkyne containing steroid ethinylestradiol **3.27**, under these conditions (Scheme 3.14).[97]

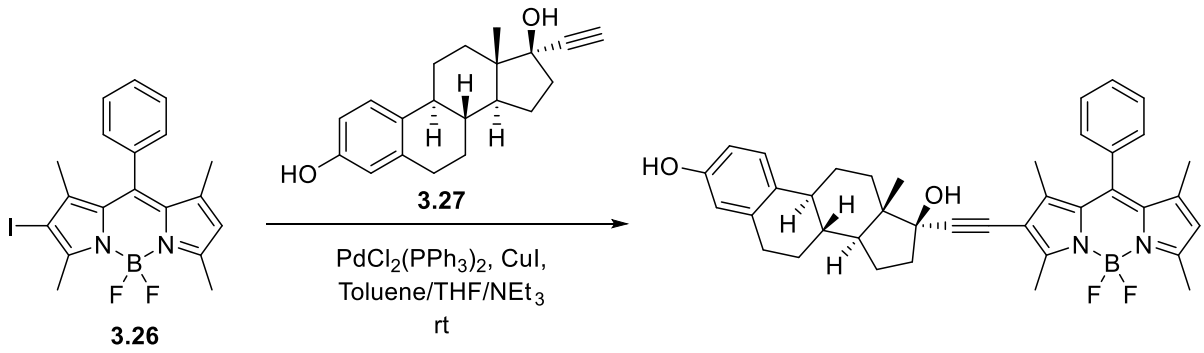

Scheme 3.14. Sonogashira cross-coupling upon 2-iodo BODIPY **3.26**.

Therefore, following the work of Van Lier's group, the above procedure was adapted as a means to synthesis the desired 3,5-di(phenylethynyl) BODIPY **3.28**.

Sonogashira cross-coupling was initially attempted on 3,5-dichloro BODIPY **2.13a** in which it was reacted with 5 equivalents of phenylacetylene, $PdCl_2(PPh_3)_2$ (5 mol%), CuI (5 mol%) and 11 equivalents Et_3N in THF. After 40 hours at room temperature the crude reaction was subjected to an aqueous work-up and purification by column chromatography. Both the desired 3,5-di(phenylethynyl) BODIPY **3.28** and singly reacted 3-phenylethynyl-5-chloro BODIPY **3.29** was isolated in a yield of 24% and 21% respectively (Table 3.7, entry 1).

The structure of the 3,5-di(phenylethynyl) BODIPY **3.28** was validated by ^{1}H-NMR, showing a distinctive 4H multiplet at 7.77-7.67 ppm and 6H multiplet at 7.48-7.35 ppm corresponding to the newly added aromatic rings in the α position. The structure of monophenylacetylene BODIPY **3.29** was also determined through ^{1}H NMR, showing asymmetry in the BODIPY core through four distinct 1H pyrrolic doublets at 6.81ppm (J = 4.4 Hz), 6.79 ppm (J = 4.3 Hz), 6.73 ppm (J = 4.4 Hz) and 6.45 ppm (J = 4.4 Hz) in conjunction with a 2H multiplet at 7.68 ppm and a 3H multiplet at 7.40 ppm validating the addition of a single phenylethynyl group.

This Sonogashira reaction was repeated with both the 3,5-dibromo and 3,5-diiodo BODIPY **2.14a** and **3.17a** starting materials. Therefore, 3,5-dibromo and 3,5-diiodo BODIPY **2.14a** and **3.17a** were each treated with 5 equivalents of phenylacetylene, $PdCl_2(PPh_3)_2$ (5 mol%), CuI (5 mol%) and 11 equivalents Et_3N in THF. Each reaction was stirred at room temperature for 40 hours, subjected to an aqueous work-up and silica gel column chromatography.

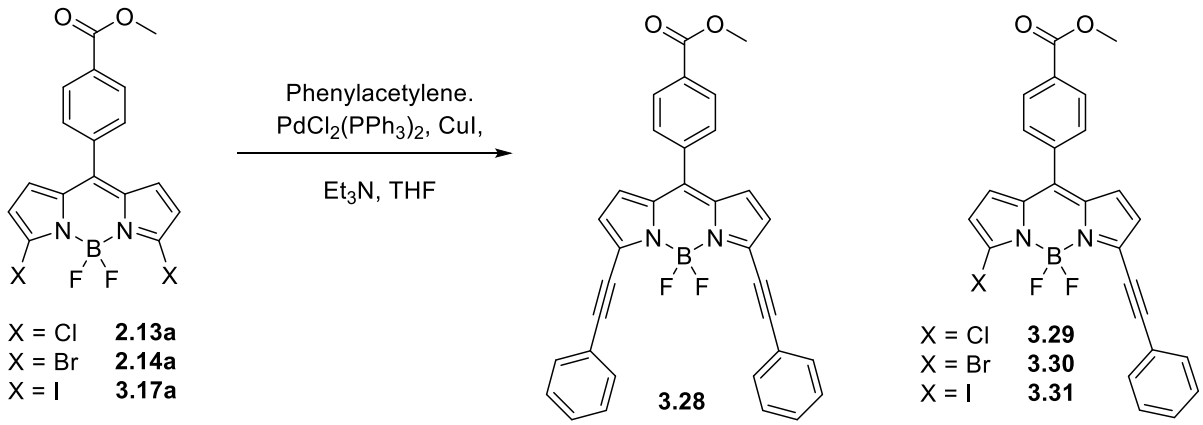

Entry	Starting Material	Yield/%
1	**2.13a**	24 (**3.28**), 21 (**3.29**)
2	**2.14a**	30 (**3.28**), 18 (**3.30**)
3	**3.17a**	37 (**3.28**), 51 (**3.31**)

Table 3.7. Sonogashira cross-coupling on 3,5-dichloro-, 3,5-dibromo- and 3,5-diiodoBODIPY starting materials **2.13a**, **2.14a** and **3.17a**.

The desired 3,5-di(phenylethynyl) BODIPY **3.28** was formed in a yield of 30% and 37% alongside 18% and 57% of the partially reacted 3-bromo-5-phenylethynyl BODIPY **3.30** and 3-bromo-5-phenylethynyl BODIPY **3.31** (Table 3.7, entry 2).

The identity of 3-bromo-5-phenylethynyl BODIPY **3.30** and 3-iodo-5-phenylethynyl BODIPY **3.31** were each confirmed by [1]3-bromo-5-phenylethynyl BODIPY **3.30** the pyrrolic peaks were shown by a 1H doublet at 6.82 ppm (J = 4.3 Hz), a 2H triplet at 6.73 ppm (J = 3.9 Hz) and a 1H doublet at 6.54 ppm (J = 4.3 Hz). Very similar pyrrolic peaks were seen for the 3-iodo-5-phenylethynyl BODIPY **3.31** with a 1H doublet at 6.81 ppm (J = 4.3 Hz), a 2H multiplet at 6.73 ppm and a 1H doublet at 6.62 ppm (J = 4.2 Hz).

Sonongashira cross-coupling on 3,5-dichloro, 3,5-dibromo and 3,5-diiodo BODIPY showed both the formation of 3-halo-5-phenylethynyl BODIPYs **3.29, 3.30** and **3.31** and 3,5-di(phenylethynyl) BODIPY **3.28**, however the yields of the desired 3,5-di(phenylethynyl) BODIPY **3.28** were low for all 3,5-dihalo BODIPY starting materials. In the case of 3,5-diiodo BODIPY **3.17a** the highest yield of 37% was seen, but improvements to this reaction were required.

3.2.4.3.1. Sonogashira cross-coupling on 3,5-dihalo BODIPYs via optimised reaction Knight group conditions

Due to low obtained yields of the desired 3,5-di(phenylethynyl) BODIPY **3.28** via the Sonogashira cross-coupling chemistry reported above, alternative reaction conditions were explored.

Previous work in the Knight group had found that the obtained yields from Sonogashira cross-couplings could be improved by utilizing Pd[dppf]Cl_2 as the catalyst with *N*,*N*-diisopropylamine as the base.[98] Therefore, we planned to test the coupling of 3,5-dihalo BODIPYs with phenylacetylene under these optimised Sonogashira conditions (Scheme 3.15).

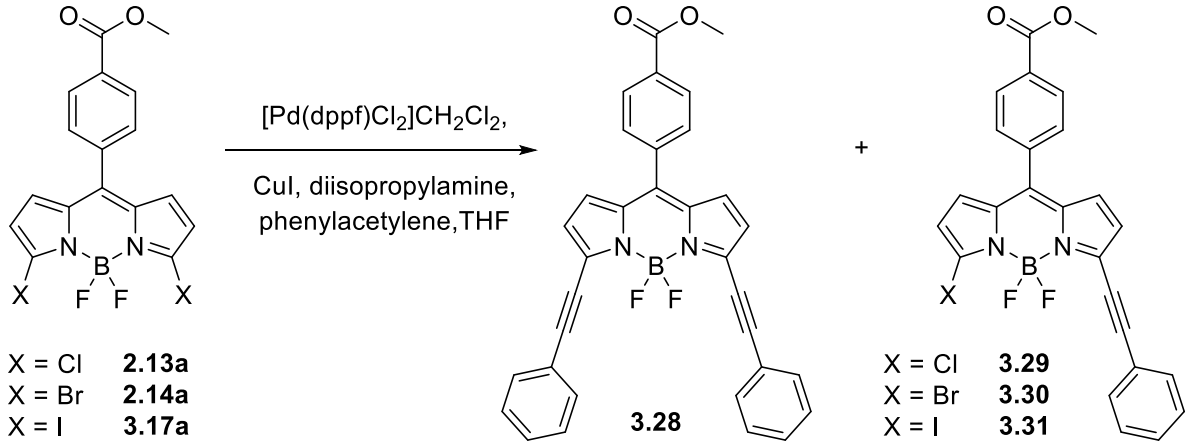

Scheme 3.15. Proposed new Sonogashira reactions utilising Pd[dppf]Cl_2. X = Cl, Br or I

Under these alternative Sonogashira conditions, each 3,5-dihalo BODIPY **2.13a**, **2.14a** and **3.17a** was reacted with 5 equivalents of phenylacetylene, [Pd(dppf)Cl_2]CH_2Cl_2 (5 mol%), CuI (5 mol%) and 110 equivalents of diisopropylamine in THF. Each reaction was stirred at room temperature of 48 hours, before an aqueous work-up and purification by silica gel column chromatography.

3,5-Dichloro BODIPY **2.13a** gave an isolated yield of 10% of the desired 3,5-diphenylethynyl BODIPY **3.28**, along with 22% of recovered starting material and 29% of a previously unobserved by-product (Table 3.8, entry 1). The ^{1}H NMR of the new by-product showed a 1H heptet-doublet at 3.85 ppm (J = 6.5 Hz) and a 6H doublet at 1.39 ppm (J = 6.5 Hz). COSY showed correlation from both signals discussed to a broad 1H doublet at 6.31 ppm (J = 8.6 Hz).

Therefore, we suggest that this by-product is 3-phenylethynyl-5-isopropylamino BODIPY **3.32** arising from S_NAr with diisopropylamine. It is surprising to see that this S_NAr reaction resulted in the substitution of a single isopropylamino group instead of a diisopropylamino group as the nucleophile in question is diisopropylamine. This indicates the additional isopropyl group had been omitted in this S_NAr reaction, allowing for the substitution of only a mono-isopropylamino group. Therefore, we postulate that an S_N1 reaction resulting in the loss of an isopropyl group has occurred in conjunction with the S_NAr reaction (Figure 3.9. ^{1H} NMR (700 MHz, Chloroform-d) spectrum of 3-chloro-5-phenylethynyl BODIPY **3.29** and 3-phenylethynyl-5-propan-2-amine BODIPY **3.32.** Light blue box = expanded 1H heptet-doublet. Light pink box = expanded 6H doublet.). Similar reactions have been observed on halogenated BODIPYs by other members of the Halls group, resulting in the substitution of an isopropylamino group at the 3 position (Aminah Almarshad, PhD).

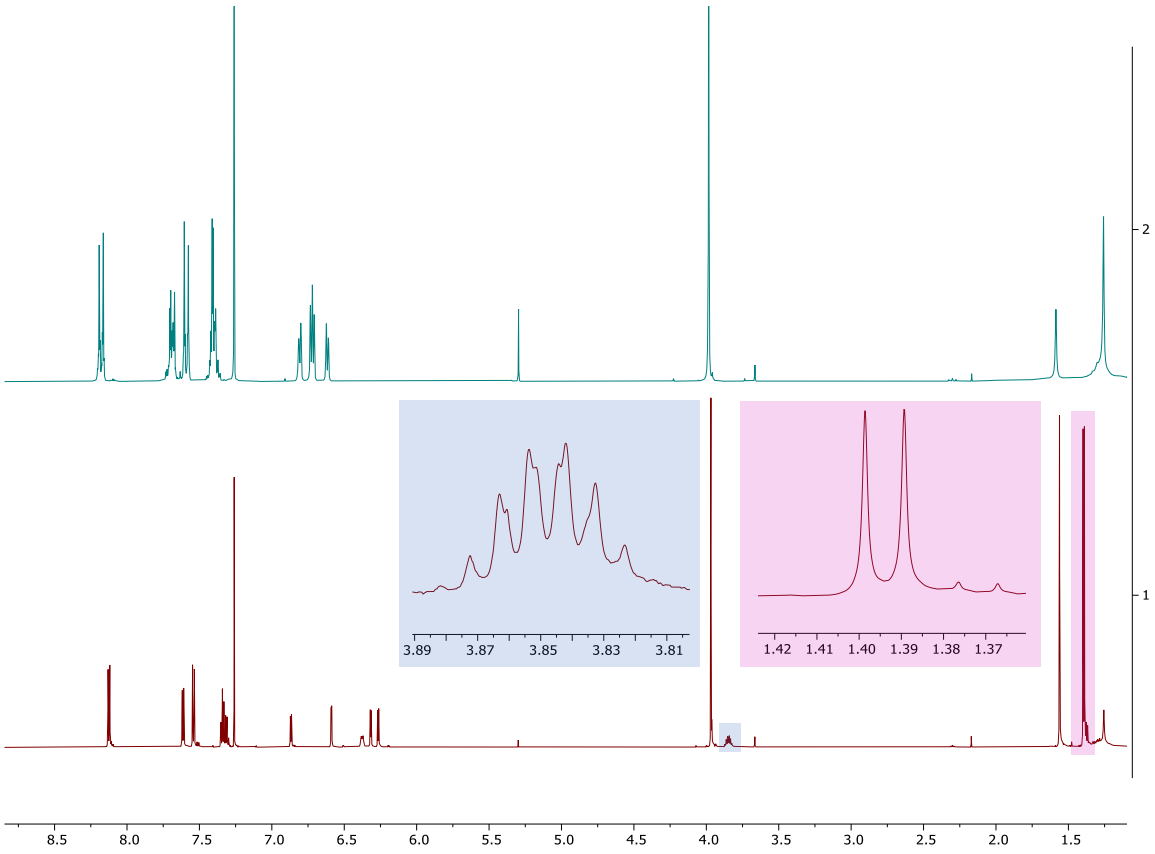

Figure 3.9. ^{1}H NMR (700 MHz, Chloroform-*d*) spectrum of 3-chloro-5-phenylethynyl BODIPY **3.29** and 3-phenylethynyl-5-propan-2-amine BODIPY **3.32**. Light blue box = expanded 1H heptet-doublet. Light pink box = expanded 6H doublet.

In contrast, when the 3,5-dibromo and 3,5-diiodo BODIPYs **2.14a** and **3.17a** were exposed to the optimised Sonogashira reaction conditions, yields of 49% and 61% were observed for the desired di(phenylethynyl) BODIPY **3.28** respectively (Table 3.8, entries 2 and 3). Additionally, none of the 3-phenylethynyl-5-propan-2-amine BODIPY **3.32** by-product was observed in either reaction using 3,5-dibromo or 3,5-diiodo BODIPYs **2.14a** and **3.17a** as starting materials.

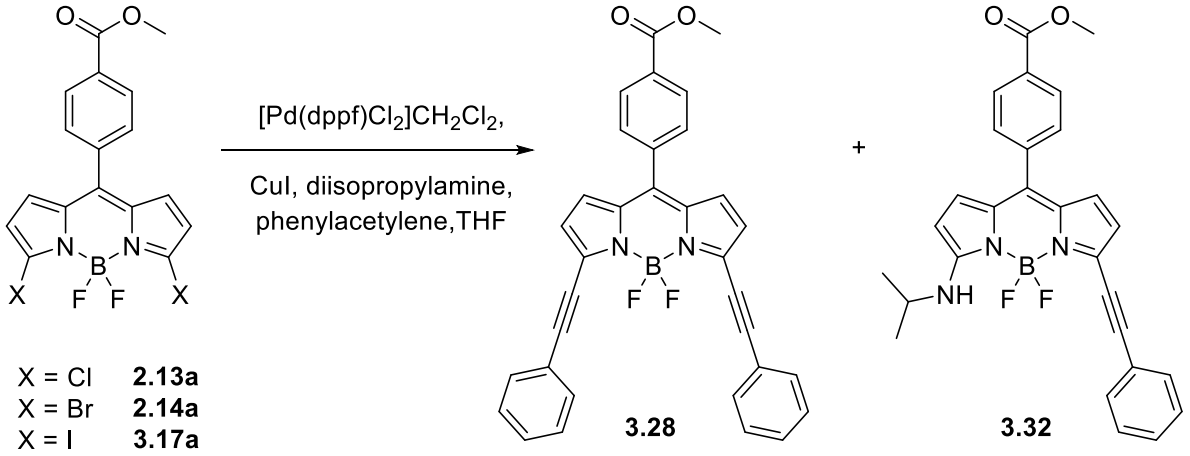

Entry	Starting Material	Yield/%
1	**2.13a**	10 (**3.28**), 29 (**3.32**)[a]
2	**2.14a**	49 (**3.28**)
3	**3.17a**	61 (**3.28**)

Table 3.8. Sonogashira cross-coupling under optimised conditions, utilising Pd[dppf]Cl_2 catalyst. Competing S_NAr is demonstrated when starting with 3,5-dichloro BODIPY **2.13a**. X = Cl,Br or I. a) 22% Recovered starting material.

The use of optimised Sonogahira reactions conditions showed a large increase in yield from 37 to 61% for the desired diphenylethynyl BODIPY **3.28** when using 3,5-diiodo BODIPY **3.17a** as the starting material, the 3,5-diiodo BODIPY **3.17a** proving to be a superior substrate for Sonogahira reactions catalysed by Pd[dppf]Cl_2 in comparison to the 3,5-dichloro and 3,5-dibromo BODIPYs **2.13a** and **3.14a**.

3.2.4.4 Suzuki-Miyuara cross-coupling on 3,5-dihalo BODIPYs

Finally, the last Pd cross-coupling comparison investigated on 3,5-dihalo BODIPYs **2.13a**, **2.14a** and **3.17a** was a double Suzuki-Miyaura reaction. Although the

majority of reported Suzuki-Miyuara cross-couplings utilise $Pd(PPh_3)_4$ as the catalyst, previous work carried out in the Knight group has shown that XPhos Pd G3 precatalyst **3.37** gives superior yields in Suzuki reactions with BODIPYs.[98] Therefore our investigation into Suzuki-Miyaura reaction focussed on using this precatalyst.

3.2.4.4.1. Synthesis of XPhos G3 Precatalyst **3.37**

Before Suzuki-Miyaura cross-coupling could be attempted, synthesis of the XPhos G3 precatalyst was undertaken. XPhos Pd G3 precatalyst **3.37** was synthesised via the 3-step reaction sequence reported by Buchwald *et al.* in 2013.[99]

The initial mesylate addition was undertaken through the slow addition of methanesulphonic acid in diethyl ether to 2-aminobiphenyl **3.33**. This afforded a 2-ammoniumbiphenyl mesylate **3.34** as a white solid which was collected by vacuum filtration, giving an excellent yield of 96%. The 2-ammoniumbiphenyl mesylate **3.34** was exposed to a nitrogen atmosphere, dissolved in anhydrous toluene and reacted with 2 equivalents of $Pd(OAc)_2$ at 50^{o}C for 45 mins. The cyclometalated palladium intermediate **3.35** was then collected and dried under vacuum, giving a good yield of 88%.

Finally, the organopalladium intermediate **3.35** was treated with XPhos **3.36** at room temperature for 30 mins. The desired precatalyst was triturated with pentane from the crude reaction mixture and the solvent removed under reduced pressure to afford the final XPhos Pd G3 precatalyst **3.37** in a 79% yield (Scheme 3.16).

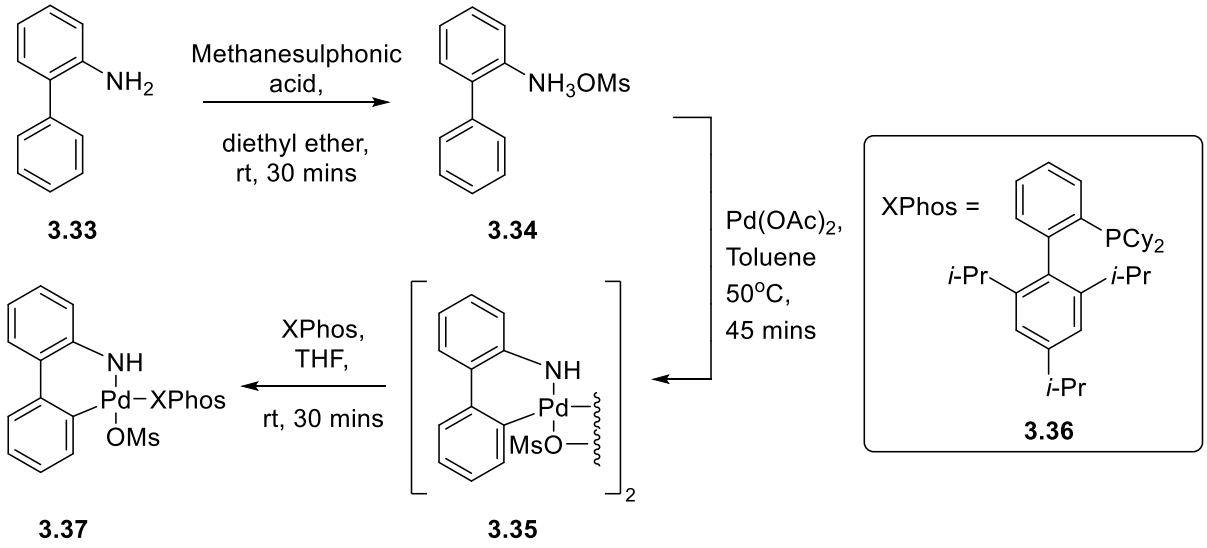

Scheme 3.16. 3-Step synthesis to afford the XPhos Pd G3 precatalyst **3.37**.

The formation of XPhos Pd G3 precatalyst **3.37** was confirmed using ^{31}P NMR, which revealed a distinct peak at 35.64 ppm, consistent with the literature (

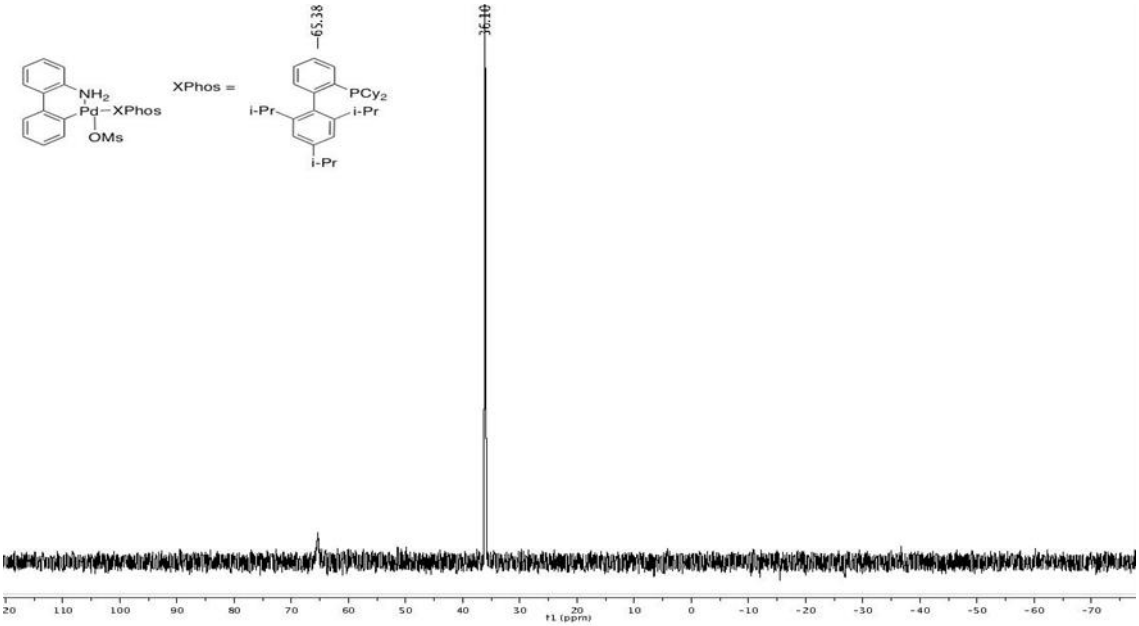

Figure 3.10). ^{1}H NMR of the precatalyst showed it to be sufficiently pure for use in reactions without requiring any further purification steps.

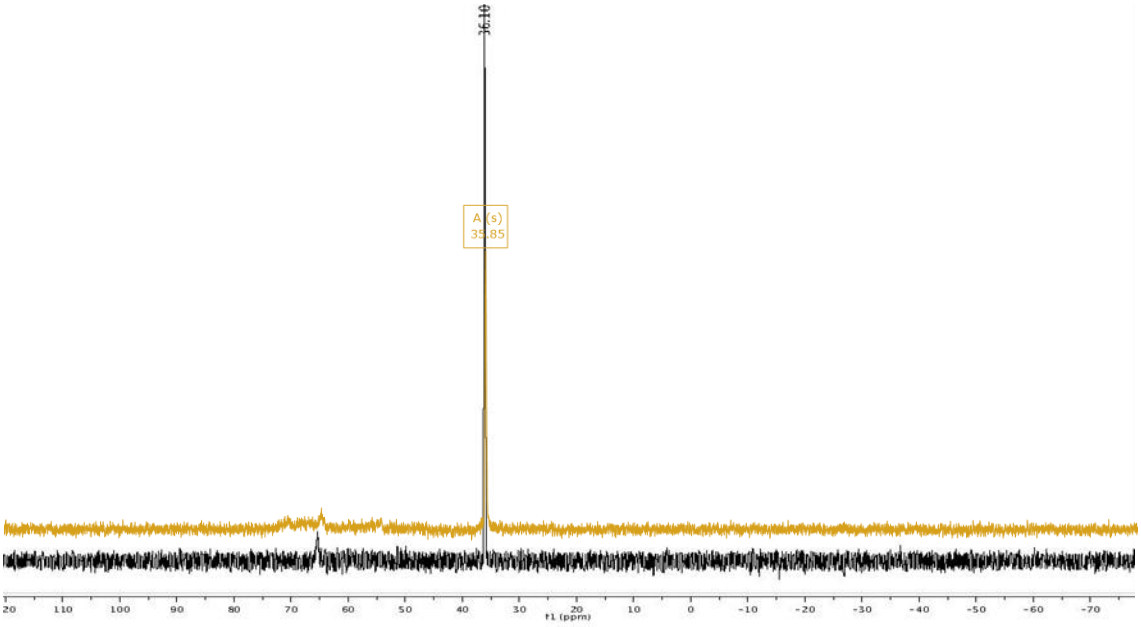

Figure 3.10. ^{31}P NMR (121 MHz, Chloroform-*d*) comparing literature (black) and synthesised (yellow) XPhos pd G3 precatalyst **3.37**.

3.2.4.4.2. Suzuki Miyaura cross-coupling attempts

After the successful synthesis of XPhos Pd G3 precatalyst **3.37**, Suzuki-Miyaura cross-coupling reactions were carried out on the 3,5-dihalo BODIPYs **2.13a**, **2.14a** and **3.17a**. Following the optimised Suzuki-Miyaura reaction conditions developed by Knight's group, each of the 3,5-dihalo BODIPYs **2.13a**, **2.14a** and **3.17a** was reacted with XPhos Pd G3 (8 mol%), 4 equivalents of $K_3PO_4.H_2O$ and 4 equivalents of phenyl boronic acid in dry THF:water (20:3) at 75 ^oC for 16 hours (Table 3.9). Each crude reaction mixture was subjected to an aqueous work-up and purified by silica gel column chromatography.

Reaction of 3,5-dichloro BODIPY **2.13a** resulted in the isolation of the desired 3,5-diphenyl BODIPY **3.21** in a yield of 6% along with a by-product, 3-chloro-5-phenyl BODIPY **3.38** in a 4% yield (Table 3.9, entry 1).

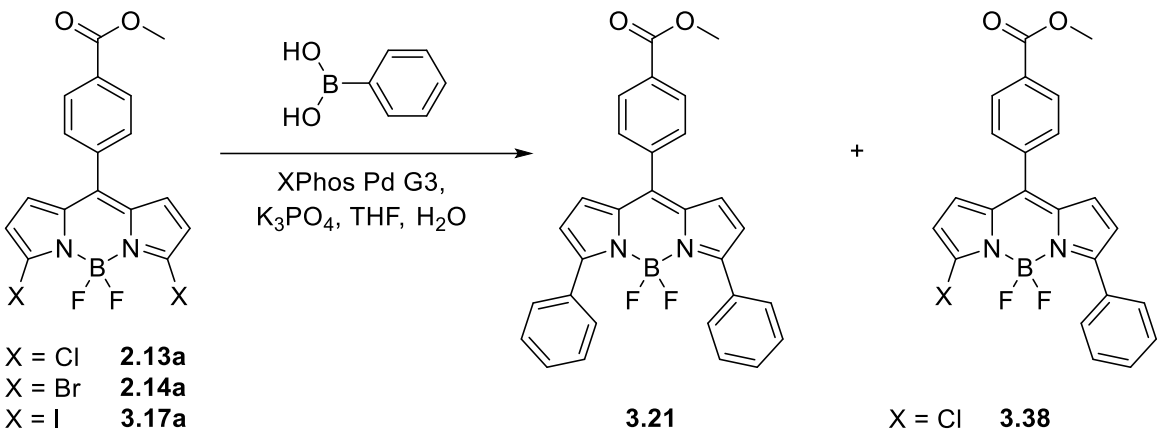

Entry	Starting Material	Yield/%
1	**2.13a**	6 (**3.21**), 4 (**3.38**)
2	**2.14a**	5 (**3.21**)
3	**3.17a**	90 (**3.21**)

Table 3.9. Suzuki-Miyaura cross-coupling reactions of 3,5-dihalo BODIPYs, utilising XPhos Pd G3 precatalyst for double arylation with $PhB(OH)_2$.

The structure of 3,5-diphenyl BODIPY **3.21** was confirmed through ^1H NMR, showing comparable spectra as seen in the Migita-Kosugi-Stille cross-coupling previous. In addition, the structure of 3-chloro-5-phenyl BODIPY **3.38** was confirmed by HRMS showing 437.1036 m/z which is consistent for the $[M+H]^+$ of a molecule with the formula of $C_{23}H_{16}{}^{11}B^{35}ClF_2N_2O_2$, whilst the mass spectra showed the expected 3:1 ratio of chlorine isotopes (m/z = 437.1, 439.1).

Both 3,5-dibromo BODIPY **2.14a** and 3,5-diiodo BODIPY **3.17a** were subjected to the Suzuki-Miyaura cross-coupling conditions discussed above, resulting in isolation of the desired 3,5-diphenyl BODIPY **3.21** in a 51 and 90% yield respectively (Table 3.9, entries 2 and 3).

3,5-Diphenyl BODIPY **3.21** was successfully crystallised through slow evaporation of a DCM solution. A suitable single crystal was submitted for single X-ray analysis, showing the successful addition of phenyl groups across the 3,5 positions to form 3,5-diphenyl BODIPY **3.21**. This confirmed the molecular structure and validated that a successful double Suzuki-Miyaura reaction had occurred. (Figure 3.11). 3,5-

Diphenyl BODIPY **3.21** formed triclinic crystals in the P-1 space group, containing 2 molecules in the unit cell (Z = 2).

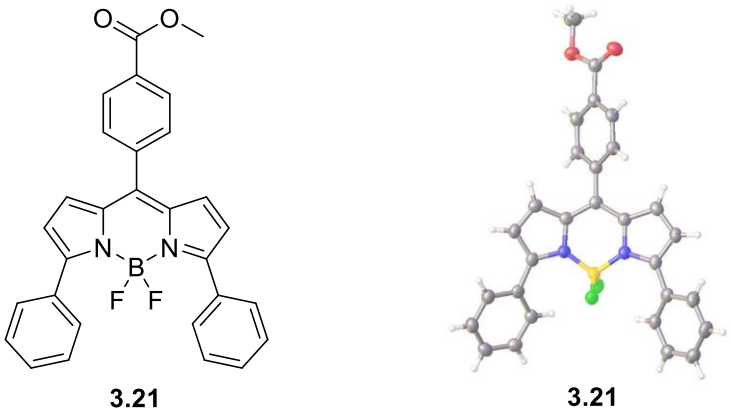

Figure 3.11. Single crystal X-ray structure of 3,5-diphenyl BODIPY **3.21**.

Comparison of the reactions of the three different 3,5-dihalo BODIPYs under these Suzuki-Miyaura cross-coupling conditions showed that 3,5-diiodo BODIPY **3.17a** was a superior starting material, compared to its 3,5-dichloro **2.13a** and 3,5-dibromo BODIPY **2.14a** counterparts, giving an excellent yield of 90% of the desired 3,5-diphenyl BODIPY **3.21**.

In this section a successful examination of a range of palladium-catalysed cross-coupling reactions with 3,5-dihalo BODIPYs was completed, demonstrating the introduction of aryl, alkenyl and alkynyl substituents into the 3,5-positions of BODIPYs. All of the cross-coupling reactions examined, apart from the Migita-Kosugi-Stille, showed superior yields when using 3,5-diiodo BODIPY **3.17a** as the starting material.

3.3 Conclusion

In conclusion we successfully demonstrated the first reported case of aromatic Finkelstein reactions on both 3,5-dichloro and 3,5-dibromo BODIPY **2.13a** and **2.14a**. Through this optimised aromatic Finkelstein reaction, a range of novel 3,5-diiodo BODIPYs **3.17a-d** were synthesized with high yields. This chemistry has resulted in the publication of four new 3,5-diiodo BODIPYs, an 25% increase in total number of published examples of 3,5-diiodo BODIPYs.

Interestingly, we found that aromatic Finkelstein reactions were faster with the 3,5-dibromo BODIPYs **2.14a-d** in comparison to the corresponding 3,5-dichloro BODIPYs **2.13a-d**. This suggests that the reaction proceeds via a concerted S_NAr mechanism in the case of the 3,5-dibromo BODIPYs **2.14a**.

The performance of the novel 3,5-diiodo BODIPY **3.17a** was compared against its 3,5-dichloro **2.14a** and 3,5-dibromo **2.14a** counterparts in a range of palladium catalysed cross-couplings, including Mizoroki-Heck, Sonogashira, Migita-Kosugi-Stille and Suzuki-Miyaura. The newly synthesised 3,5-diiodo BODIPY **3.17a** showed to be an excellent cross-coupling partner, showing the best yields to the desired products in all investigated cross-couplings, apart from the Migita-Kosugi-Stille.

Through the synthesis and evaluation of 3,5-diiodo BODIPYs **3.17a-d**, we have shown that these molecules are extremely useful starting materials for the synthesis of 3,5-substituted BODIPYs. Given the successful development of a new synthetic route to produce 3,5-diiodo BODIPYs **3.17a-d**, in the next chapter their potential use in S_NAr chemistry will be examined, in comparison to their 3,5-dichloro and 3,5-dibromo counterparts. In addition, the use of 3,5-diiodo BODIPYs **3.17a** as key starting materials in the synthesis of helically chiral compounds will be investigated.

Chapter 4 Synthesis of Helically Chiral BODIPYs Demonstrating Point-to-Helical Chirality Control

4.1 Introduction

4.1.1 Aims

In this chapter we aim to explore point-to-helical chirality control within BODIPY systems as a means to synthesize helically chiral BODIPYs. It is proposed that through the introduction of a point chiral group to the 3 or 5 position of a BODIPY, this group can act similarly to a chiral auxiliary and direct the formation of helical chirality through an *in-situ* ring closure of an *ortho*-hydroxyphenyl substituent onto the boron atom of the BODIPY **4.1** to form an *M* or *P* helix (Scheme 4.1).

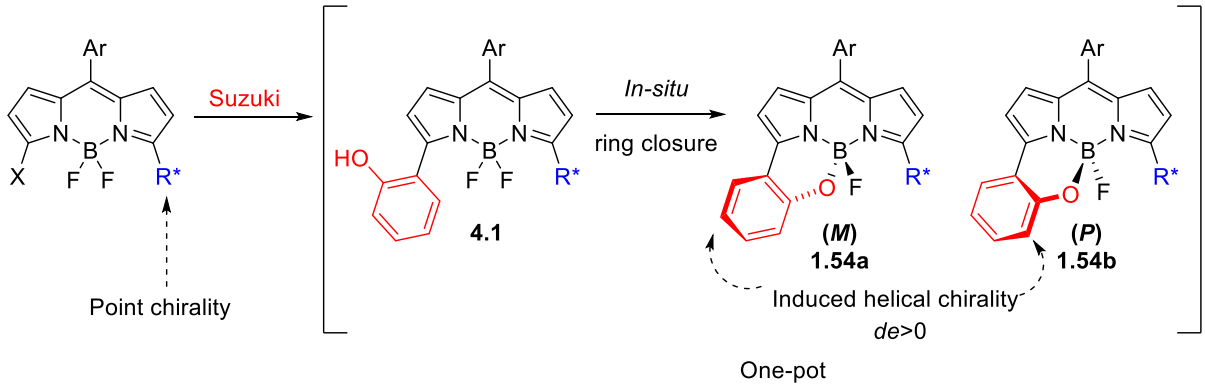

Scheme 4.1. Point-to-helical chirality control in BODIPY systems. R* = chiral directing group.

Therefore, our planned synthetic route utilizes S_NAr chemistry at the 3 position of 3,5-dihalo BODIPYs **2.13a**, **2.14a** and **3.17a** to introduce an enantiopure chiral directing group in the form of an amino acid derivative. After the introduction of the chiral directing group, Suzuki cross-coupling at the remaining 5 position with *ortho*-hydroxyphenyl boronic acid will be attempted. We expect the hydroxyl group of the newly attached phenyl group to undergo an *in-situ* reaction at the boron centre as seen in work by Hall *et al*. which will be discussed further in this chapter. It is hoped that this will ring closure will displace a fluorine atom, resulting in two diastereoisomeric helically chiral BODIPYs. It is proposed that the enantiopure chiral directing group will show a preference for the formation of one of the diastereomeric helically chiral BODIPYs (Scheme 4.2).

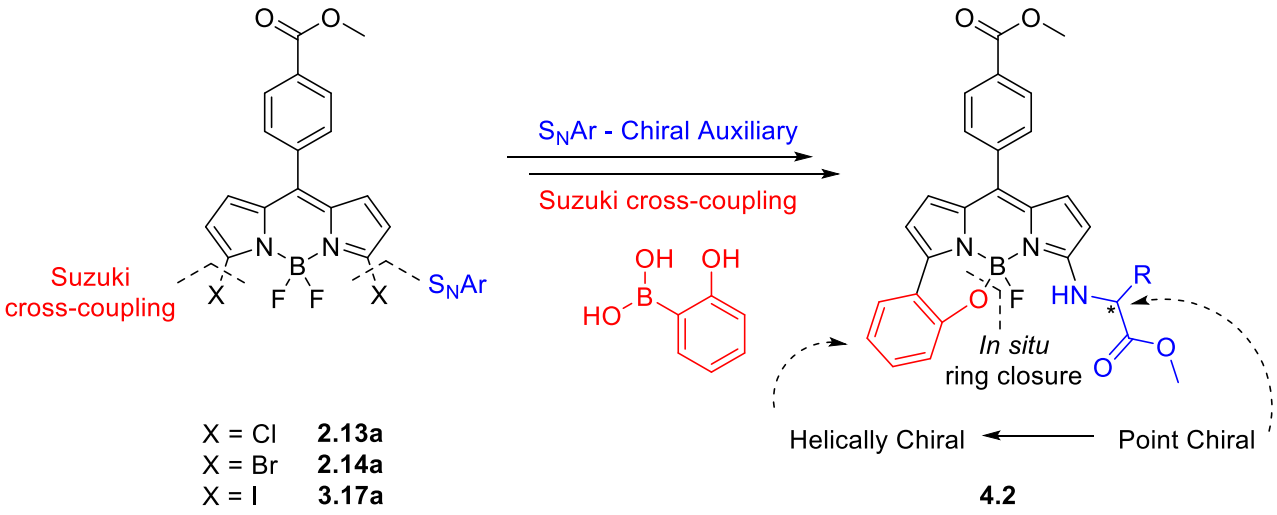

Scheme 4.2. Proposed diastereoselective route to helically chiral BODIPY **4.2** through the introduction of chiral directing groups via S_NAr chemistry followed by Suzuki cross-coupling and *in-situ* ring closure. X = Cl, Br or I.

Pd cross-couplings are well known with 3,5-dihalo BODIPYs as discussed in Chapter 3. Therefore, the first objective was to examine our newly synthesised 3,5-dihalo BODIPYs **2.13a**, **2.14a** and **3.17a** (see Chapter 3) in S_NAr chemistry to determine the most suitable 3,5-dihalo BODIPY to be used for both the required Pd cross-couplings and S_NAr reactions.

4.2 Results and discussion

4.2.1 Planned route to helically chiral BODIPYs via *in-situ* ring closure

Following the planned synthetic route above, investigation into the introduction of a chiral directing group through S_NAr followed by Suzuki cross-coupling and *in-situ* ring closure to form helically chiral diastereoisomers will be discussed.

4.2.1.1 S_NAr reactions of (*S*)-valine methyl ester **4.3** with 3,5-dihalo BODIPYs **2.13a**, **2.14a** and **3.17a**.

The first step in our synthetic route towards helically chiral BODIPYs is an S_NAr reaction with 3,5-dihalogenated BODIPYs. Therefore, S_NAr reactions on 3,5-dihalo BODIPY **2.13a** and **3.17a** were investigated, using a nitrogen containing amino acid derivative as an enantiopure chiral directing group. Amino acid esters were chosen as chiral directing groups, as they are readily accessible "chiral pool" molecules, in which both the *R* and *S* enantiomers are commonly available, and which display a large variety of different side chains. We propose that the steric bulk of the amino acid ester side chains will have an impact on the diastereoselectivity in the *in-situ* ring closure step required to form helically chiral diastereoisomers. As a result, L-valine methyl ester **4.3** was chosen as a suitable chiral directing group to investigate, due to containing a large, isopropyl group. Note that L-valine methyl ester is in the *S* configuration and will be named as (*S*)-valine methyl ester **4.3** from this point.

S_NAr reactions on 3,5-dichloro BODIPYs were previously published by Dehaen *et al*. and have been discussed earlier (see Chapter 1). Dehaen has shown that 3,5-dichloro BODIPYs have a tendency for mono substitution across a range of nucleophiles at lower reaction temperatures, double substitution only being possible under more forcing conditions.[51]

Previously work has also been carried out in the Hall group, in which mono S_NAr has been attempted upon 3,5-dichloro BODIPY **2.13a** using 2 eq. of a nitrogen containing nucleophile and 2.2 eq. of NEt_3 at room temperature (Scheme 4.3).

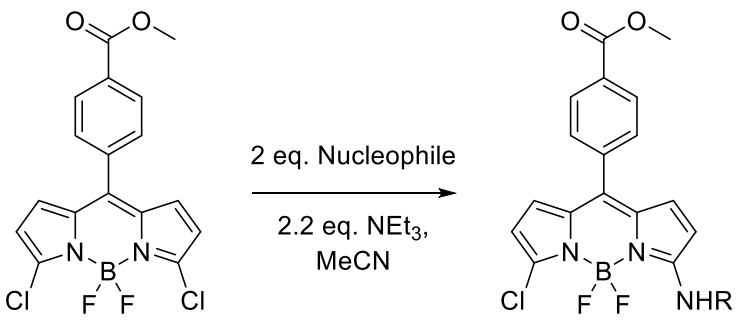

Scheme 4.3. Previous work carried out be Hall's group showing the mono substitution of a nucleophile at room temperature.

Therefore, based on the work of Hall and Dehaen *et al*. we attempted a mono S_NAr reaction on 3,5-dichloro BODIPY **2.13a**. Therefore 3,5-dichloro BODIPY **2.13a** was reacted with 2 equivalents of (*S*)-valine methyl ester **4.3** and 2.2 equivalents of NEt_3 at room temperature in MeCN. The reaction progression was monitored by TLC, showing the disappearance of the 3,5-dichloro BODIPY **2.13a** starting material after 2 hours. The crude reaction mixture was subjected to an aqueous work-up and was analysed by ^{1}H NMR, showing the clean formation of 3-chloro-5-(*S*)-valinyl methyl ester BODIPY **4.4** with no by-products observed. 3-Chloro-5-(*S*)-valinyl methyl ester BODIPY **4.4** was purified by silica gel column chromatography, resulting in a quantitative yield (Table 4.1, entry 1).

Analysis of the ^{1}H NMR spectra showed a 6H triplet at 1.06 ppm (J = 7.0 Hz), a 1H double doublet at 4.01 ppm (J = 9.4, 5.9 Hz) and a 1H heptet at 2.30 ppm (J = 6.4 Hz), which is indicative of the addition of the valinyl group. The structure of 3-chloro,5-(*S*)-valinyl methyl ester BODIPY **4.4** was further validated by HRMS, showing 490.1540 m/z which is consistent for the $[M+H]^+$ of a molecule with the formula of $C_{23}H_{23}{}^{11}B^{35}ClF_2N_3O_4$, with the mass spectra showing a 3:1 ratio of the chlorine isotopes (m/z = 490.2, 492.2).

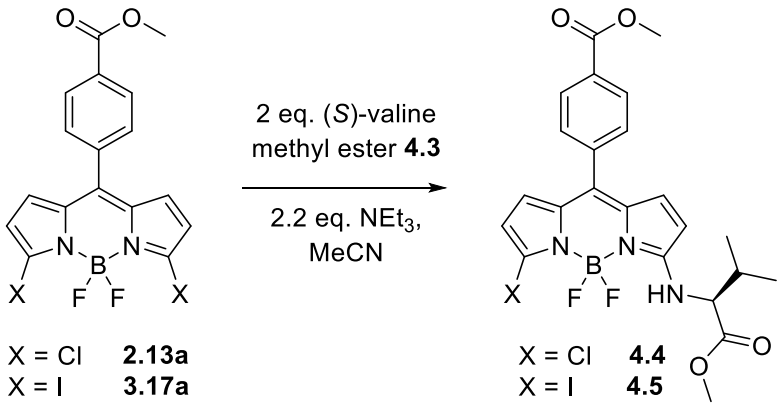

Entry	Starting Material	Temp/^{o}C	Time/h	Yield/%[a]
1	3,5-dichloro BODIPY **2.13a**	r.t (25)	2	Quant.
2	3,5-diiodo BODIPY **3.17a**	50	3	Quant.

Table 4.1. Base mediated S_NAr reaction of (*S*)-valine methyl ester with 3,5-dihalo BODIPYs **2.13a** and **3.17a**. X = Cl or I. a) quantitative = full conversion by ^{1}H NMR.

The S_NAr reaction with (*S*)-valine methyl ester **4.3** was further investigated with 3,5-diiodo BODIPY **3.17a** as an alternative starting material. Therefore 3,5-diiodo BODIPY **3.17a** was reacted with 2 equivalents of (*S*)-valine methyl ester **4.3** and 2.2 equivalents of NEt_3 in MeCN at 50^{o}C, and the reaction was monitored by TLC. Note the higher reaction temperature was determined based on additional S_NAr reactions carried out, as discussed in Section 4.2.3. After 3.5 hours, complete consumption of the starting material was observed. An aqueous work-up and purification via silica gel column chromatography was performed, in which 3-iodo-5-(*S*)-valinyl methyl ester BODIPY **4.5** was isolated in quantitative yields. (Table 4.1, entry 2).

The desymmetrisation of the BODIPY in the S_NAr reaction could be seen through ^{1}H NMR, showing 4 distinctive pyrrolic doublets at 6.83 (*J* = 5.0 Hz), 6.51 (*J* = 3.8 Hz), 6.22 (*J* = 3.9 Hz) and 6.18 ppm (*J* = 5.0 Hz). Introduction of a single valinyl group could also be seen via the appearance of two 3H doublets at 1.07 (*J* = 6.9 Hz) and 1.04 (*J* = 6.7 Hz), a 1H double doublet at 4.00 ppm (*J* = 9.5, 5.9 Hz) and a 1H heptet at 2.29 ppm (*J* = 6.7 Hz).

The mono S_NAr reactions of both 3,5-dichloro and 3,5-diiodo BODIPY **2.13a** and **3.17a** were successful with (*S*)-valine methyl ester **4.3**, showing high yields and providing sufficient material for further studies.

4.2.1.2 Suzuki cross-coupling on 3-halo,5-(*S*)-valinyl methyl ester BODIPYs **4.4** and **4.5**

After the successful synthesis of a 3-halo,5-(*S*)-valinyl methyl ester BODIPYs **4.4** and **4.5**, investigation into subsequent Suzuki cross-coupling was undertaken. After careful consideration, it was determined that Suzuki cross-coupling with *ortho*-hydroxyphenyl boronic acid would be used over its *ortho*-methoxy counterpart. It has been reported in literature by Hall *et al*. that spontaneous ring closure can occur between the oxygen on a *ortho*-hydroxyphenyl group and the boron centre to form *N,N,O,O* BODIPY **4.6** under Suzuki cross-coupling conditions (Scheme 4.4).[8]

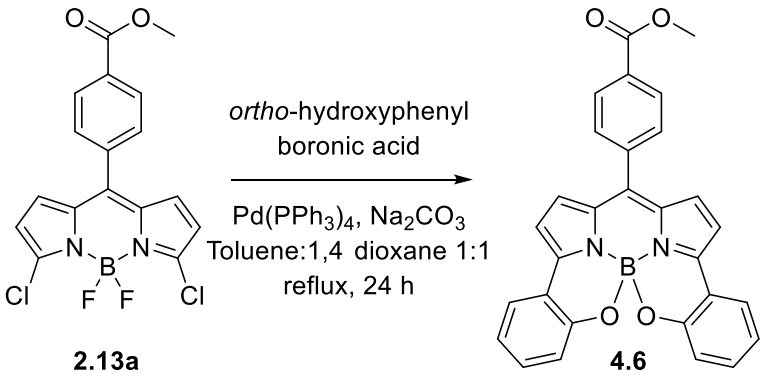

Scheme 4.4. Suzuki cross-coupling of 3,5-dichloro BODIPY **2.13a** with *ortho*-hydroxyphenyl boronic acid, showing spontaneous ring closure to form *N,N,O,O* BODIPY **4.6**.

Therefore, we planned to carry out a Suzuki cross-coupling reaction on both 3-chloro-5-(*S*)-valinyl methyl ester BODIPY **4.4** and 3-iodo-5-(*S*)-valinyl methyl ester BODIPY **4.5** with an *ortho*-hydroxyphenyl boronic acid. The conditions used for this Suzuki cross-coupling are those discussed in Chapter 3 as they proved to work well on BODIPY systems (Scheme 4.5).

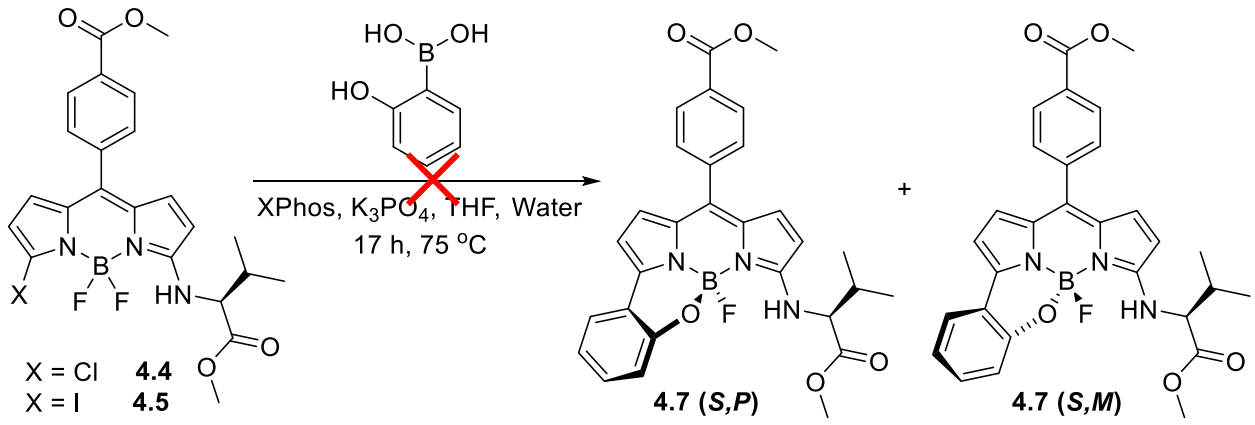

Scheme 4.5. Proposed Suzuki cross-coupling with *ortho*-hydroxyphenyl boronic acid demonstrating spontaneous ring closure to form both *N,N,O,F*-5-(*S,P*)-valinyl methyl ester BODIPY and *N,N,O,F*-5-(*S,M*)-valinyl methyl ester BODIPY **4.7**.

The first Suzuki cross-coupling was attempted on 3-chloro-5-(*S*)-valinyl methyl ester BODIPY **4.4** in which it was reacted with 1.5 equivalents of *ortho*-hydroxyphenyl boronic acid and XPhos G3 catalyst (7 mol%) in THF and water at 75°C for 17 h. The crude reaction mixture was subjected to an aqueous work-up and purified by silica gel column chromatography (2:1, petrol:ethyl acetate), obtaining a red solid.

The isolated Suzuki product was analysed by ^{1}H NMR, confirming the presence of the newly added phenolic ring by three new signals in the aromatic region, a 1H double doublet at 7.44 ppm (J = 7.1, 1.3 Hz), a 1H double double doublet at 7.27 ppm (J = 9.1, 7.3, 1.8 Hz) and a 2H multiplet at 6.96 ppm. However, upon ^{19}F and ^{11}B NMR analysis, a quartet at -144.43 ppm and a triplet at 1.21 ppm were observed respectively, indicating the presence of the BF_2 group (Figure 4.1).

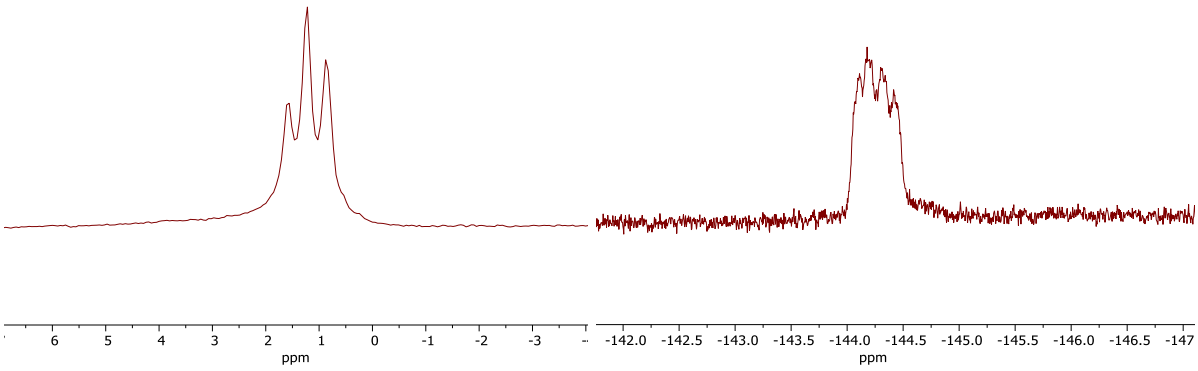

Figure 4.1. ^{11}B and ^{19}F NMR of BODIPY **4.8** showing a triplet and quartet respectively.

This suggests that the Suzuki cross-coupling reaction had successfully incorporated an *ortho*-hydroxyphenyl group at the 3 position, however ring closure between the oxygen of the phenyl ring and the boron centre had not taken place, giving a yield of 46% for 3-*ortho*-hydroxyphenyl-5-(*S*)-valinyl methyl ester BODIPY **4.8** (
Table 4.2, entry 1). As the yield was relatively low, all other fractions from the silica gel column were combined, in the hope of further understanding the reaction. Unfortunately, this showed a large number of unidentifiable side products by ^{1}.

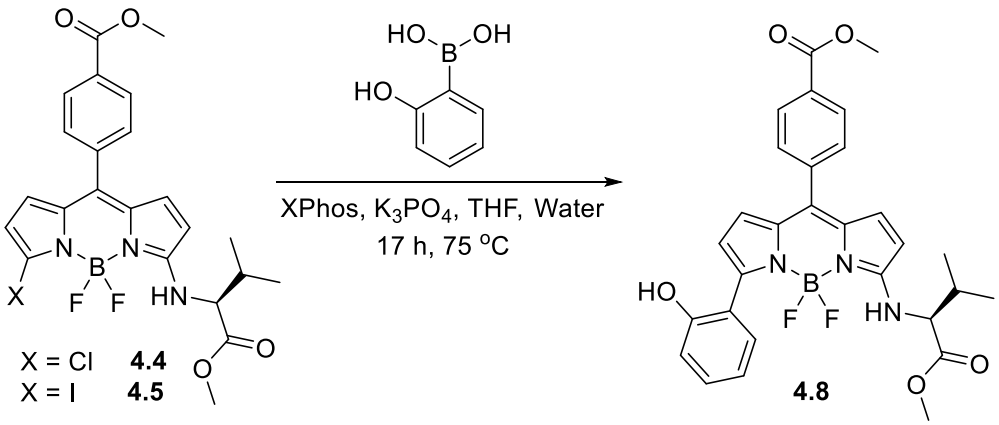

Entry	Starting Material	Yield of 4.7/%	Yield of 4.8/%
1	3-chloro,5-*S*-valinyl methyl ester BODIPY **4.4**	0	46
2	3-iodo,5-*S*-valinyl methyl ester BODIPY **4.5**	0	52

Table 4.2. Suzuki cross-coupling on 3-halo-5-(*S*)-valinyl methyl ester BODIPYs **4.4** and **4.5**, resulting in the addition of an *ortho*-hydroxyphenyl group at the 3 position.

3-Iodo-5-(*S*)-valinyl methyl ester BODIPY **4.5** was subjected to the same Suzuki cross-coupling reaction conditions as discussed above. After an aqueous work-up and purification via silica gel column chromatography, isolation of 3-*ortho*-hydroxyphenyl-5-(*S*)-valinyl methyl ester BODIPY **4.8** was achieved in a 52% yield. (
Table 4.2, entry 2). This again shows unsuccessful ring closure to the desired *N,N,O,F*-5-(*S,P*)-valinyl methyl ester BODIPY and *N,N,O,F*-5-(*S,M*)-valinyl methyl ester BODIPY **4.7**.

4.2.2 Ring closure of 3-*ortho*-hydroxyphenyl,5-(*S*)-valinyl methyl ester BODIPY **4.8**

Due to the unsuccessful synthesis *N,N,O,F*-5-(*S,P*)-valinyl methyl ester BODIPY and *N,N,O,F*-5-(*S,M*)-valinyl methyl ester BODIPY **4.7**, alternative means to achieve the ring closure of 3-*ortho*-hydroxyphenyl-5-(*S*)-valinyl methyl ester BODIPY **4.8** was investigated.

4.2.2.1 $BF_3.OEt_2$ mediated ring closure

A newly planned route to synthesize synthesis *N,N,O,F*-5-(*S,P*)-valinyl methyl ester BODIPY and *N,N,O,F*-5-(*S,M*)-valinyl methyl ester BODIPY **4.7** was investigated, using $BF_3.OEt_2$ as a Lewis acid as a means to coordinate the oxygen of the *ortho*-hydroxyphenyl group to boron. Similar such ring closures using $BF_3.OEt_2$ have been demonstrated by Halls group.[100]

Therefore, the same conditions as discussed in Chapter 2, in which dipyrromethane **2.8a** is chelated with a BF_2 moiety (Scheme 2.7), were investigated as a means to achieve ring closure using $BF_3.OEt_2$. 3-*Ortho*-hydroxyphenyl-5-(*S*)-valinyl methyl ester BODIPY **4.7** was treated with 2.2 equivalents of $BF_3.OEt_2$ and 2.8 equivalents of DIPEA in DCM and stirred for 1 hour. After an aqueous work-up, the solvent was removed under reduced pressure and analysed by ^{1}H NMR. The reaction however was unsuccessful, showing no formation of either of the desired *N,N,O,F*-5-(*S,P*)-valinyl methyl ester BODIPY or *N,N,O,F*-5-(*S,M*)-valinyl methyl ester BODIPY **4.7**, with full recovery of the starting material **4.7** (Scheme 4.6).This prompted investigation of alternative Lewis acids for this step.

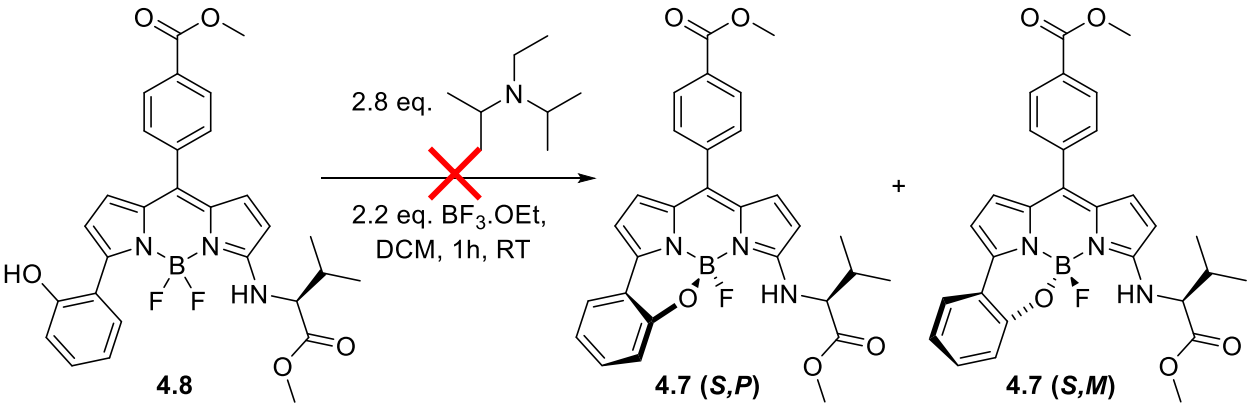

Scheme 4.6. Proposed Lewis acid mediated ring closure of 3-*ortho*-hydroxyphenyl-5-(*S*)-valinyl methyl ester BODIPY **4.8** using $BF_3.OEt_2$.

4.2.2.2 $SnCl_4$ for Lewis acid mediated ring closure

Due to unsuccessful ring closure of 3-*ortho*-hydroxyphenyl-5-(*S*)-valinyl methyl ester BODIPY **4.8** using $BF_3.OEt_2$, $SnCl_4$ was investigated as an alternative Lewis acid. This was based off the work of Harriman *et al*. in which they demonstrated ring closure of an *ortho*-hydroxyphenyl group through the formation of a new B-O bond to form BODIPY **4.9** (Scheme 4.7).[101]

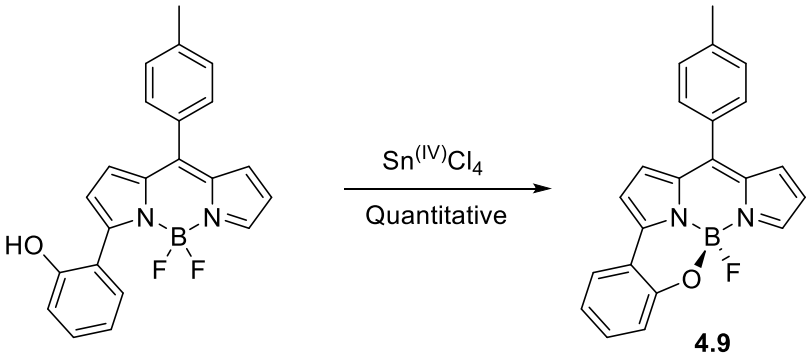

Scheme 4.7. B-O bond formation, mediated by the addition of $SnCl_4$, resulting in ring closure to form BODIPY **4.9**.

Therefore, 3-*ortho*-hydroxyphenyl-5-(*S*)-valinyl methyl ester BODIPY **4.8** was dissolved in deuterated chloroform and was treated with a minimal amount of $SnCl_4$ in an NMR tube. The resulting reaction mixture was analysed by ^1H NMR immediately, showing full conversion of the 3-*ortho*-hydroxyphenyl-5-(*S*)-valinyl methyl ester BODIPY **4.8** to the desired helically chiral *N,N,O,F*-5-(*S*)-valinyl methyl ester BODIPYs **4.7a** (major) and **4.7b** (minor). (Scheme 4.8).

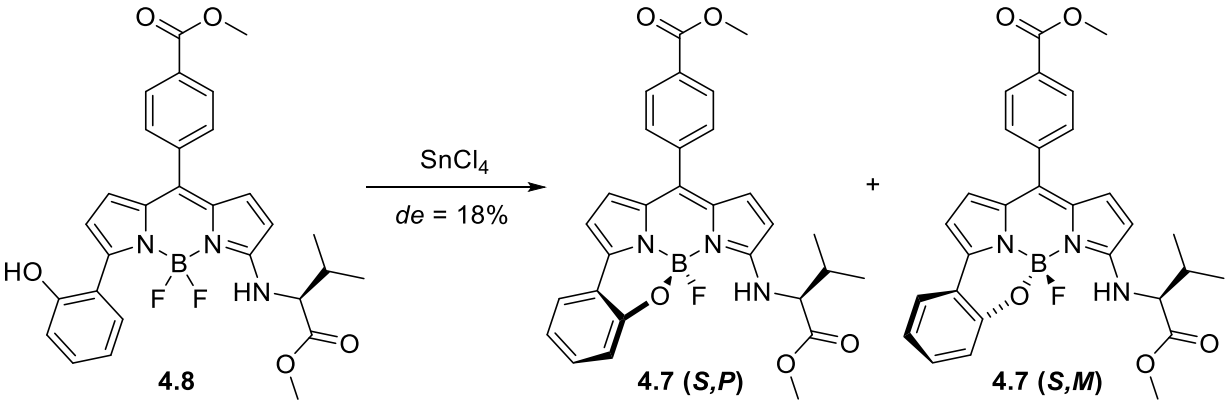

Scheme 4.8. Ring closure of 3-*ortho*-hydroxyphenyl-5-(*S*)-valinyl methyl ester BODIPY **4.8** using minimal $SnCl_4$ (one drop).

Inspection of the $^{11}B\{^{1}H\}$-NMR spectrum of helically chiral *N,N,O,F*-5-(*S*)-valinyl methyl ester BODIPYs **4.7a** and **4.7b** showed one doublet at δ = 0.2 ppm (*J* = 49.6 Hz), corresponding to boron coupling to one fluorine atom, supporting a ring closed product.

Interestingly, in the $^{19}F\{^{1}H\}$-NMR two quartets were observed at δ = -142.94 ppm (*J* = 44.46 Hz) and -141.96 (*J* = 45.48 Hz) corresponding to the formation of the two diastereomers **4.7a** and **4.7b**. Through the integration of the $^{19}F\{^{1}H\}$-NMR quartet peaks, it was shown that the two diastereomers had been formed in unequal amounts with a diastereomeric excess (*de*) of 18%. It is postulated that the observed diastereocontrol is caused by the (*S*)-valinyl methyl ester group influencing the helical chirality upon ring closure (Figure 4.2). Although this was a promising result, the relaxation delay of 0.1 seconds that was used in this $^{19}F\{^{1}H\}$-NMR spectra was too short to ensure complete relaxation of the fluorines, making comparison of the peaks by integration difficult. Therefore, all future ^{19}F NMR spectra run to measure *de* used a longer relaxation time of 30 seconds.

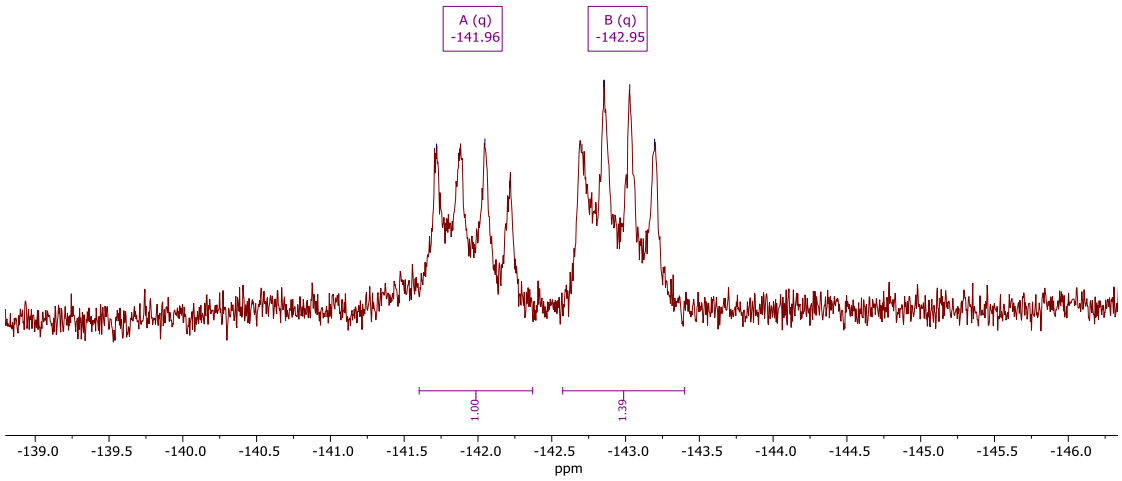

Figure 4.2. ^{19}F NMR of helically *N,N,O,F*-5-(*S*)-valinyl methyl ester BODIPYs **4.7a** and **4.7b**, showing two quartets, indicating the formation of 2 diastereoisomers.

Although the synthesise of *N,N,O,F*-5-(*S*)-valinyl methyl ester BODIPYs **4.7a** and **4.7b** seemed successful, it was found upon long exposure to $SnCl_4$ (>20 mins), decomposition of the sample material occurred and, as a result, isolation of each diastereoisomer was not possible. This synthetic approach therefore successfully

showed proof-of-principle point-to-helical chirality transfer, however due to degradation of the *N,N,O,F*-5-(*S*)-valinyl methyl ester BODIPYs **4.7a** and **4.7b**, further investigation into this route was not feasible. As a result, exploration into alternative synthetic routes to helically chiral BODIPYs were undertaken in which $SnCl_4$ would not be utilised.

4.2.3 Alternative amino ester acid derivatives as chiral directing groups

Although the above synthetic route towards helically chiral BODIPYs resulted in a successful proof-of-principle point-to-helical chirality transfer *de* of 18%, the observed diastereoselectivity was not high. Therefore, before alternative synthetic routes to helically chiral BODIPYs were explored, further study into alternative chiral directing groups was undertaken as a means to potentially increase the aimed for point-to-helical chirality transfer *de*.

Therefore, a series of S_NAr reactions were carried out on 3,5-dihalo BODIPYs **2.13a** and **3.17a**, investigating a set of amino acid esters containing different R groups with a range of steric size and functional groups. Each S_NAr reaction was run in MeCN with 2 equivalents of the amino acid ester derivative and 2.2 equivalents of NEt_3. Note that for clarity, each amino acid ester derivative has been named from its *R* or *S* configuration.

The first S_NAr reaction carried out utilised (*S*)-serine ethyl ester as the chiral directing group. The reaction was stirred at rt with 3,5-dichloro BODIPY **2.13a** and the progress of the reaction was monitored by TLC. Full consumption of the starting material was seen after 2 hours. The crude reaction mixture was subjected to an aqueous work-up and analysed by ^1H NMR, showing the formation of the desired 3-chloro-5-(*S*)-serinyl ethyl ester BODIPY **4.10** in 86% yield. ^1H NMR analysis of samples of 3-chloro-5-(*S*)-serinyl ethyl ester BODIPY **4.10** showed that the material was not stable in $CDCl_3$, with significant degradation occurring after 16 hours. Further analysis of the samples stored as solids also showed degradation, albeit slower, thus this molecule was not taken forward for further reactions (Table 4.3, entry 1).

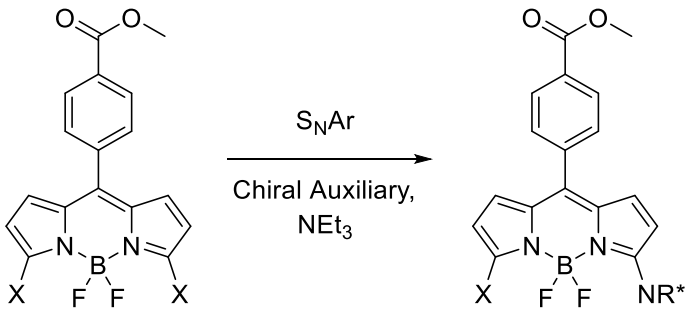

X = Cl **2.13a**
X = I **3.17a**

X = Cl **4.10**
X = I **4.11-4.17**

NR* =

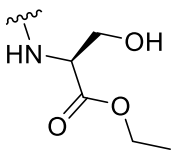
(*S*)-serine ethyl ester **4.10**

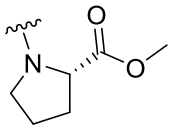
(*S*)-proline methyl ester **4.11**

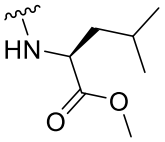
(*S*)-leucine methyl ester **4.12**

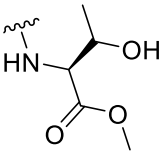
(*S*)-threonine methyl ester **4.13**

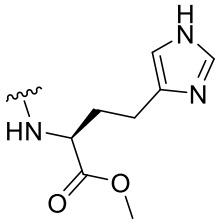
(*S*)-histidine methyl ester **4.14**

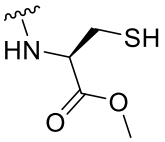
(*R*)-cysteine methyl ester **4.15**

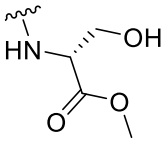
(*R*)-serine methyl ester **4.16**

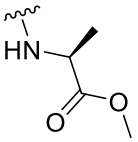
(*S*)-alanine methyl ester **4.17**

Entry	Starting Material	Chiral Aux.[c]	Temp./°C	Time/h	Compd. number	Yield /%[d]
1	3,5-dichloro BODIPY **2.13a**	(*S*)-serine ethyl ester	r.t	2	**4.10**	86[a]
2	3,5-diiodo BODIPY **3.17a**	(*S*)-proline methyl ester	r.t	2	**4.11**	67
3	3,5-diiodo BODIPY **3.17a**	(*S*)-proline methyl ester	50	2	**4.11**	78
4	3.5-diiodo BODIPY **3.17a**	(*S*)-proline methyl ester	50	3	**4.11**	Quant.
5	3,5-diiodo BODIPY **3.17a**	(*S*)-leucine methyl ester	50	3	**4.12**	90

6	3,5-diiodo **3.17a**	BODIPY	*(S)*-threonine methyl ester	50	4.3	**4.13**	87
7	3,5-diiodo **3.17a**	BODIPY	(*S*)-threonine methyl ester	50	16	**4.13**	77
8	3,5-diiodo **3.17a**	BODIPY	(*S*)-histidine methyl ester	50	3.5	**4.14**	Complex mixture
9	3,5-diiodo **3.17a**	BODIPY	(*R*)-cysteine methyl ester	50	1.5	**4.15**	67% [b]
10	3,5-diiodo **3.17a**	BODIPY	(*R*)-serine methyl ester	50	3.5	**4.16**	quant
11	3,5-diiodo **3.17a**	BODIPY	(*S*)-alanine methyl ester	50	3.5	**4.17**	92

Table 4.3. Series of S_NAr chiral directing group reactions on 3,5-dihalo BODIPYs **2.13a** and **3.17a**. a) Decomposed after 16 hours. b) Calculated by crude ^{1}H NMR, degradation upon purification. c) All chiral directing groups used are in the hydrochloride form. NR* = nitrogen containing chiral directing group. d) quantitative = full conversion by ^{1}H NMR.

The next amino acid ester derivative investigated was (*S*)-proline methyl ester. (*S*)-proline methyl ester was reacted with 3,5-diiodo BODIPY **3.17a** and after 2 hours at room temperature the crude reaction mixture was subjected to an aqueous work-up and analysed by ^{1}H NMR, showing the desired 3-iodo-5-(*S*)-prolinyl methyl ester BODIPY **4.11** in a yield of 67% through NMR integration (Table 4.3, entry 2).

The above S_NAr reaction utilizing (*S*)-proline methyl ester as the chiral directing group was repeated at an increased temperature of 50^{o}C in an attempt to improve reaction yield. The reaction mixture was stirred for 2 hours before being subjected to an aqueous work-up and purified via silica gel column chromatography. The desired 3-iodo-5-(*S*)-prolinyl methyl ester BODIPY **4.11** was isolated in an improved yield of 78% (Table 4.3, entry 3). This S_NAr reaction with (*S*)-proline methyl ester was repeated an additional time in an attempt to further increase the yield of the desired 3-iodo-5-(*S*)-prolinyl methyl ester BODIPY **4.11**. Therefore, 3,5-diiodo BODIPY **3.17a** and (*S*)-proline methyl ester were reacted at 50^{o}C and the progression of the reaction was monitored by TLC. After 3 hours, full consumption of the diiodo BODIPY starting material **3.17a** was observed and following an aqueous work-up and purification through silica gel chromatography, quantitative yields of 3-iodo-5-

(*S*)-prolinyl methyl ester BODIPY **4.11** were observed. (Table 4.3, entry 4). The structure of 3-iodo-5-(*S*)-prolinyl methyl ester BODIPY **4.11** was verified by ^{1}H NMR, showing a de-symmetrised BODIPY structure with three 2H multiplets in the aliphatic region at 4.24 – 3.97 ppm, 2.45 – 2.20 ppm and 2.16 – 2.00 ppm, corresponding to the newly attached substituted pyrrolidine ring found in (*S*)-proline methyl ester.

This S_NAr reaction using (*S*)-proline methyl ester showed that quantitative yields of the corresponding mono substituted BODIPYs could be obtained with slightly harsher reaction conditions when using 3,5-diiodo BODIPY **3.17a** as a starting material, compared to S_NAr reactions with 3,5-dichloro BODIPY **2.13a**. Therefore, since our synthetic route to helically chiral BODIPYs requiring both S_NAr and Pd cross-coupling reactions, further S_NAr reactions in this section were carried out on 3,5-diiodo BODIPY **3.17a** only, as the anticipated mono-iodo BODIPY products would be better substrates for subsequent Pd cross-coupling reactions (see Chapter 3).

The next S_NAr reaction undertaken reacted 3,5-diiodo BODIPY **3.17** with (*S*)-leucine methyl ester at 50^{o}C with the reaction progression monitored by TLC. The full consumption of the 3,5-diiodo BODIPY starting material **3.17** was seen after 3 hours, resulting in a 90% yield of 3-iodo-5-(*S*)-leucinyl methyl ester BODIPY **4.12** after an aqueous work-up and purification via silica gel column chromatography (Table 4.3, entry 5). The structure of 3-iodo-5-(*S*)-leucinyl methyl ester BODIPY **4.12** was verified by ^{1}H NMR, showing two new signals in the aliphatic reaction, a 3H multiplet at 1.88-1.75 ppm and a 6H double doublet at 0.97 (J = 15.4, 6.3 Hz), which is indicative of the isopentenyl group in the leucine substituent.

The next chiral directing group investigated was (*S*)-threonine methyl ester, which underwent an S_NAr reaction with 3,5-diiodo BODIPY **3.17a**. After 4.3 hours, 3,5-diiodo BODIPY **3.17a** was still present in the reaction mixture by TLC, however the reaction was quenched with water, subjected to an aqueous work-up and purified by silica gel column chromatography, resulting in a good yield of 87% of the desired 3-iodo-5-(*S*)-threoninyl methyl ester BODIPY **4.13** (Table 4.3, entry 6). The structure of 3-iodo-5-(*S*)-threoninyl methyl ester BODIPY **4.13** was confirmed by ^{1}H NMR, showing the addition of two 3H singlets at 3.82 ppm and 1.34 ppm, corresponding to two new methyl groups as well as a broad singlet at 2.75 ppm corresponding to the

OH group. In an attempt to increase the yield of the desired 3-iodo-5-(*S*)-threoninyl methyl ester BODIPY **4.13**, the S_NAr reaction was repeated at 50°C and was left overnight. Inspection of the reaction mixture by TLC indicated full consumption of the 3,5-diiodo BODIPY starting material **3.17a**. However, after aqueous work-up and silica gel chromatography a slight drop in yield to 77% was observed, which could indicate that a longer reaction time of 16 hours resulted in some degradation of the 3-iodo-5-(*S*)-threoninyl methyl ester BODIPY **4.13** product (Table 4.3, entry 7).

The synthesis of 3-iodo-5-(*S*)-histidinyl methyl ester BODIPY **4.14** was attempted from 3,5-diiodo BODIPY **3.17a** and (*S*)-histidine methyl ester. The reaction was stirred at 50°C for 3.5 hours, showing the full consumption of starting material by TLC. The crude reaction mixture was subjected to an aqueous work-up and silica gel column chromatography, resulting in a fraction containing three different molecules with very similar retention factors. $^{19}F\{^1H\}$ NMR confirmed the presence of three peaks, showing the presence of more than one compound, whilst the desired 3-iodo-5-(*S*)-histidinyl methyl ester BODIPY **4.14** was not observed (Table 4.3, entry 8). Due to difficulties in the formation and isolation of the desired product, amino ester was no longer investigated.

Next, an S_NAr reaction using (*R*)-cysteine methyl ester was attempted with 3,5-diiodo BODIPY **3.17a** at 50°C. Full consumption of the 3,5-diiodo BODIPY starting material **3.17a** was shown after 1.5 hours by TLC and following aqueous work-up a crude yield of 67% of the desired 3-iodo-5-(*R*)-cysteinyl methyl ester BODIPY **4.15** was obtained. Preliminary ^1H NMR analysis showed the presence of 3-iodo-5-(*R*)-cysteinyl methyl ester BODIPY **4.15** with reasonable purity, however attempted purification by silica gel column chromatography resulted in degradation, showing a complex mixture of compounds via ^1H NMR after purification (Table 4.3, entry 9).

(*R*)-Serine methyl ester was the next chiral directing group to be investigated. Therefore (*R*)-serine methyl ester was reacted with 3,5-diido BODIPY **3.17a** at 50°C. After 3.5 hours the crude reaction was subjected to an aqueous work-up and silica gel column chromatography purification, giving quantitative yields of 3-iodo-5-(*R*)-serinyl methyl ester BODIPY **4.16** (Table 4.3, entry 10). The structure of 3-iodo-5-(*R*)-serinyl methyl ester BODIPY **4.16** was confirmed through ^1H NMR, showing a distinctive 2 proton multiplet at 4.17 – 4.01 ppm and 1 proton double triplet at 4.37

ppm (J = 8.7, 4.3 Hz) indicative of the aliphatic CH_2 and CH groups in serine. The structure of 3-iodo-5-(*R*)-serinyl methyl ester BODIPY **4.16** was further validated by HRMS showing 492.1295 m/z which is consistent for the $[M+H]^+$ of a molecule with the formula of $C_{22}H_{22}{}^{11}B^{35}ClF_2N_3O_5$.

Finally, (*S*)-alanine methyl ester was reacted with 3,5-diiodo BODIPY **3.17a** at 50^{o}C and monitored by TLC. After 3.5 hours, full consumption of 3,5-diiodo BODIPY **3.17a** was observed. The crude reaction was subjected to an aqueous work and purification via silica gel column chromatography to give an excellent yield of 92% of the desired 3-iodo-5-(*S*)-alaninyl methyl ester BODIPY **4.17** (Table 4.3, entry 11). The structure was confirmed by ^{1}H NMR, showing a 3H doublet 1.62 ppm (J = 7.1 Hz) and a 3H singlet at 3.80 ppm, indicative of the newly added alaninyl methyl ester group.

After testing the S_NAr reactions of 3,5-diiodo BODIPY **3.17a** with various enantiopure amino acid esters, several showed promising results. We then evaluated which of these compounds would be the most appropriate in synthesizing helically chiral BODIPYs via a point-to-helical chirality transfer with high diastereocontrol.

In parallel to the investigation of the S_NAr chemistry, other members of the Hall group undertook preliminary work in evaluating several point-to-helical chirality transfer reactions for helically chiral BODIPYs, resulting in a wide range of reaction *de* measurements on the final products.[102] Several amino acid esters as chiral directing groups were investigated, in which the helically chiral BODIPYs were synthesised via an acid mediated de-chelation/re-chelation synthetic route, as discussed in Section 4.2.5. This investigation showed drastically higher *de* in helically chiral BODIPY diastereoisomers synthesised when using a serinyl structured chiral directing group, as compared to alaninyl, valinyl, leucinyl, prolinyl and threoninyl groups (Table 4.4). Therefore, it was decided that (*S*)-serine methyl ester would be the chosen amino acid ester to investigate further, enroute to our helically chiral BODIPYs.

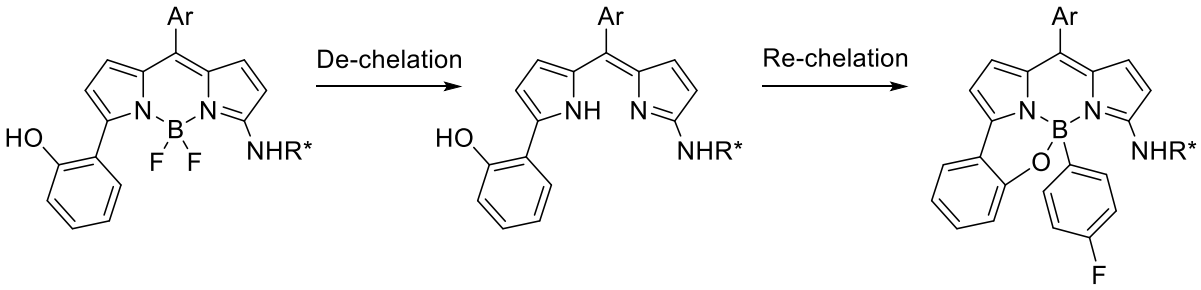

Chiral directing group	L-ala-OMe	L-val-OMe	L-leu-OMe	L-pro-OMe	L-ser-OMe	L-ser-OEt	L-thr-OMe
***de*/%**	3	8	9	47	**61**	**65**	2

Table 4.4. Observed *de* through ^{19}F NMR integration of the synthesised helically chiral BODIPYs, serinyl chiral directing groups in bold.

Reasons as to why (*S*)-serine methyl ester results in a drastically high *de* compared to alternative chiral directing groups is unclear. It is postulated that a 7-membered intermediate **4.18** is formed, involving chelation of the serine side chain, during the formation of a helically chiral BODIPY **4.19** and this intermediate is responsible for efficient transfer of chirality (Scheme 4.9).

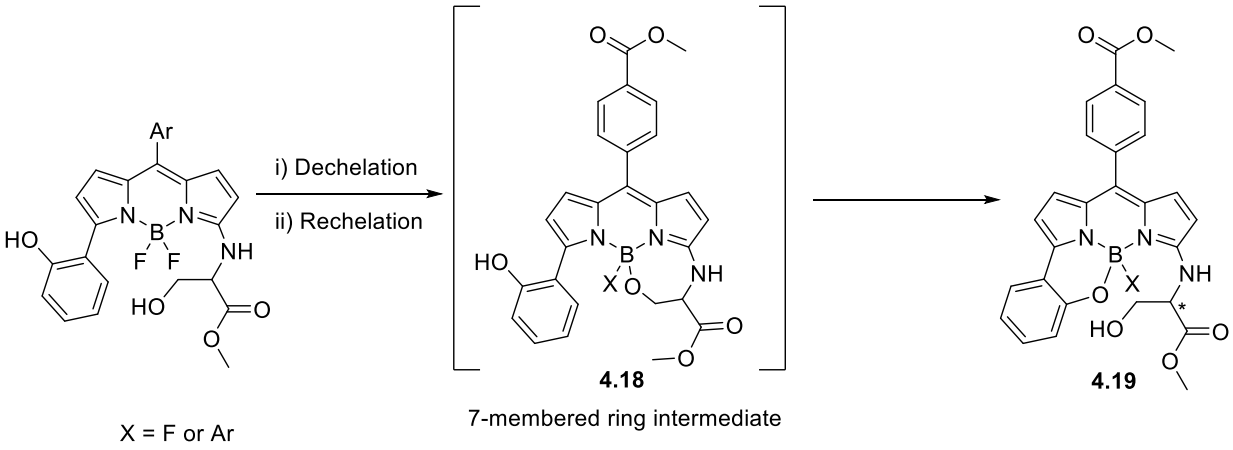

Scheme 4.9. Proposed 7-membered ring intermediate **4.18** when using serine methyl ester as a chiral directing group.

Thus, we next focussed on S_NAr reactions using of both (*R*) and (*S*) serine methyl ester as suitable chiral directing groups with both 3,5-dibromo and 3,5-diiodo BODIPY **2.14a** and **3.17a** using reaction conditions discussed above.

As discussed previously, 3,5-diiodo BODIPY **3.17a** reacts with (*R*)-serine methyl ester in 3.5 hours at 50°C to give quantitative yields of the desired 3-iodo-5-(*R*)-serinyl methyl ester BODIPY **4.16** (Table 4.5, entry 1).

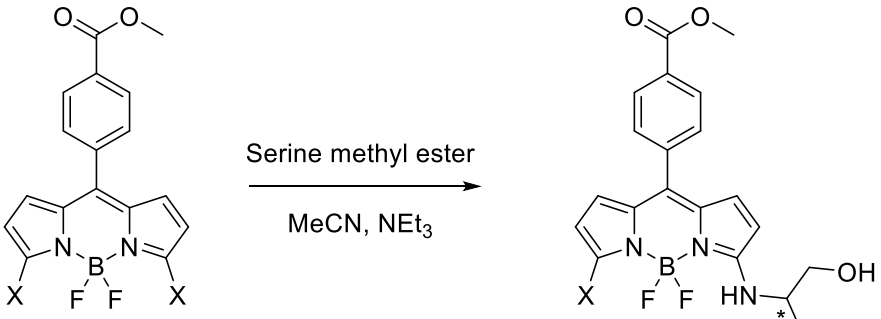

Entry	Starting material	Chiral Directing group	Temp/°C	Time/h	Yield/%[c]
1	3,5-diiodo BODIPY **3.17a**	(*R*)-serine methyl ester	50	3.5	**4.16** quant[a]
2	3,5-diiodo BODIPY **3.17a**	(*R*)-serine methyl ester	r.t	16	**4.16** quant
3	3,5-dibromo BODIPY **2.14a**	(*R*)-serine methyl ester	40	2	**4.20** quant
4	3,5-diiodo BODIPY **3.17a**	(*S*)-serine methyl ester	r.t.	16	**4.21** quant
5	3,5-diiodo BODIPY **3.17a**	(*S*)-serine methyl ester	50	3.5	**4.21** quant[b]

Table 4.5. Reaction conditions for the mono S_NAr of 3,5-dihalo BODIPYs **2.14a** and **3.17a** with both (*R*)- and (*S*)-serine methyl ester. All reactions were carried out on an 0.087 mmol scale. a) Synthesis previously discussed, Table 4.3. b) Scaled up to 2.8 mmol. c) quantitative = full conversion by ^1H NMR.

Following on from this result, further investigation into S_NAr reactions with 3,5-diiodo BODIPY **3.17a** were undertaken at a lower temperature. Thus, 3,5-diiodo BODIPY

3.17a was stirred a room temperature (25^{o}C) overnight with 2 equivalents of (*R*)-serine methyl ester and NEt_3 in DCM, showing complete consumption of starting material after 16 hours by TLC. The crude reaction was purified by silica gel column chromatography, to give quantitative yields of the desired 3-iodo-5-(*R*)-serinyl methyl ester BODIPY **4.16** (Table 4.5, entry 2).

To obtain comparative data for S_NAr reactions with all three 3,5-dihalo BODIPY species **2.13a**, **2.14a** and **7.13a**, an S_NAr reaction with (*R*)-serine methyl ester was also performed with 3,5-dibromo BODIPY **2.14a** at 40^{o}C with monitoring by TLC. After 2 hours complete consumption of the starting material was observed, showing quantitative yields of the desired 3-bromo-5-(*R*)-serinyl methyl ester BODIPY **4.20** after purification via silica gel column chromatography (Table 4.5, entry 3).

Interestingly comparison of the results of the S_NAr reactions for (*R*)-serine methyl ester with all three of the 3,5-dihalo BODIPYs shows a clear trend in reactivity. The fastest rate of reaction is seen for 3,5-dichloro **2.13a** (r.t. 2 hours), followed by the 3,5-dibromo **2.14a** (40^{o}C, 2 hours) and then finally the 3,5-diiodo BODIPY **3.17a** (50^{o}C, 3.5 hours). A more rapid reaction of 3,5-dichloro BODIPY **2.13a** indicates that these reactions are likely to be occurring via a classical stepwise S_NAr mechanism. Therefore, the same conditions as discussed in Chapter 2, in which dipyrromethane **2.8a** is chelated with a BF_2 moiety (Scheme 2.7), were investigated as a means to achieve ring closure using $BF_3.OEt_2$. 3-*Ortho*-hydroxyphenyl-5-(*S*)-valinyl methyl ester BODIPY **4.7** was treated with 2.2 equivalents of $BF_3.OEt_2$ and 2.8 equivalents of DIPEA in DCM and stirred for 1 hour

Additional S_NAr reactions were investigated in which (*S*)-serine methyl ester was reacted with 3,5-diiodo BODIPY **3.17a**, to allow access to the enantiomeric product 3-iodo-5-(*S*)-serinyl methyl ester BODIPY **4.21**. The rationale for synthesizing both 3-iodo-5-(*R*)- and 3-iodo-5-(*S*)-serinyl methyl ester BODIPY enantiomers **4.16** and **4.21,** is to allow access to both enantiomers of the final helically chiral diastereoisomers, facilitating later enantiomeric excess (*ee*) measurement of the final products by chiral HPLC.

(*S*)-Serine methyl ester and 3,5-diiodo BODIPY **3.17a** were reacted together, firstly at room temperature for 16 hours and secondly at 50^{o}C for 3.5 hours. Both reactions were subjected to an aqueous work-up and purification via silica gel column

chromatography, giving quantitative yields of 3-iodo-5-(*S*)-serinyl methyl ester BODIPY **4.21** in both cases (Table 4.5, entry 4 and 5). As expected, 3-iodo-5-(*S*)-serinyl methyl ester BODIPY **4.21** showed comparable NMR to its (*R*)-serinyl methyl ester BODIPY **4.16** counterpart. After the successful synthesis of a range of 3-iodo-5-amino acid ester BODIPYs **4.11-4.17** and **4.21**, with an emphasis on serine methyl ester based substituents, next 3-iodo-5-(*R*)-serinyl methyl ester BODIPY **4.16** was further investigated as a key starting material for the synthesis of helically chiral BODIPY diastereoisomers **4.23a** and **4.23b** through Suzuki functionalisation of the 3-position.

4.2.4 Suzuki cross-coupling of 3-iodo-5-(*R*)-serinyl methyl ester BODIPY **4.16** with *ortho*-hydroxy phenylboronic acid

In Chapter 3, the Suzuki cross-coupling of 3,5-diiodo BODIPYs was discussed, with the use of a Pd XPhos gen 3 catalyst. Therefore, 3-iodo-5-(*R*)-serinyl methyl ester BODIPY **4.16** was stirred with 2 equivalents of *ortho*-hydroxyphenyl boronic acid and XPhos Pd G3 precatalyst (7 mol%) at 75^{o}C in THF:Water (8:1). After 17 hours the reaction mixture was subjected to an aqueous work-up, giving an excellent 82% crude yield (>90% purity by ^{1}H NMR) of the desired 3-*ortho*-hydroxyphenyl-5-(*R*)-serinyl methyl ester BODIPY **4.22** (Scheme 4.10).

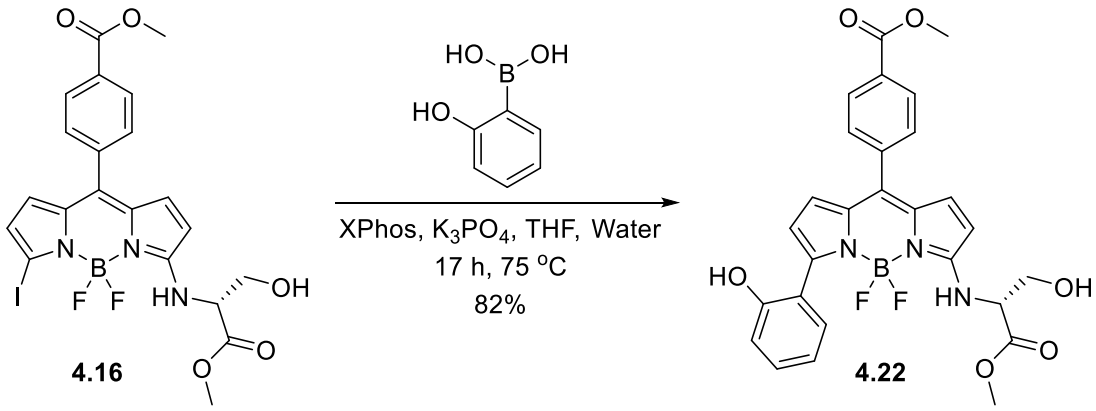

Scheme 4.10. Suzuki cross-coupling of *ortho*-hydroxyphenyl boronic acid to form 3-*ortho*-hydroxyphenyl-5-(*R*)-serinyl methyl ester BODIPY **4.22**.

Unfortunately, upon attempted purification by silica gel chromatography, 3-*ortho*-hydroxyphenyl-5-(*R*)-serinyl methyl ester BODIPY **4.22** degraded, resulting in the ^{1}H NMR of collected fractions containing multiple unidentifiable side products alongside **4.22** as a minor component. Therefore, this reaction was repeated under identical

conditions and the crude 3-*ortho*-hydroxyphenyl-5-(*R*)-serine methyl ester BODIPY **4.22** was carried forward without additional purification.

Analysis of the ^{1}H NMR of 3-*ortho*-hydroxyphenyl-5-(*R*)-serinyl methyl ester BODIPY **4.22** showed that the reaction had occurred cleanly with minimal by-product formation, the structure being confirmed through the appearance of three new aromatic signals, a double doublet at 7.49 ppm (*J* = 7.6, 1.6 Hz), a double double doublet at 7.32 ppm (*J* = 8.1, 7.1, 1.7 Hz) and a 2H multiplet 7.04 – 6.95 ppm alongside a broad singlet at 5.71 ppm, corresponding to the newly added aromatic protons and OH phenol ring (Figure 4.3).

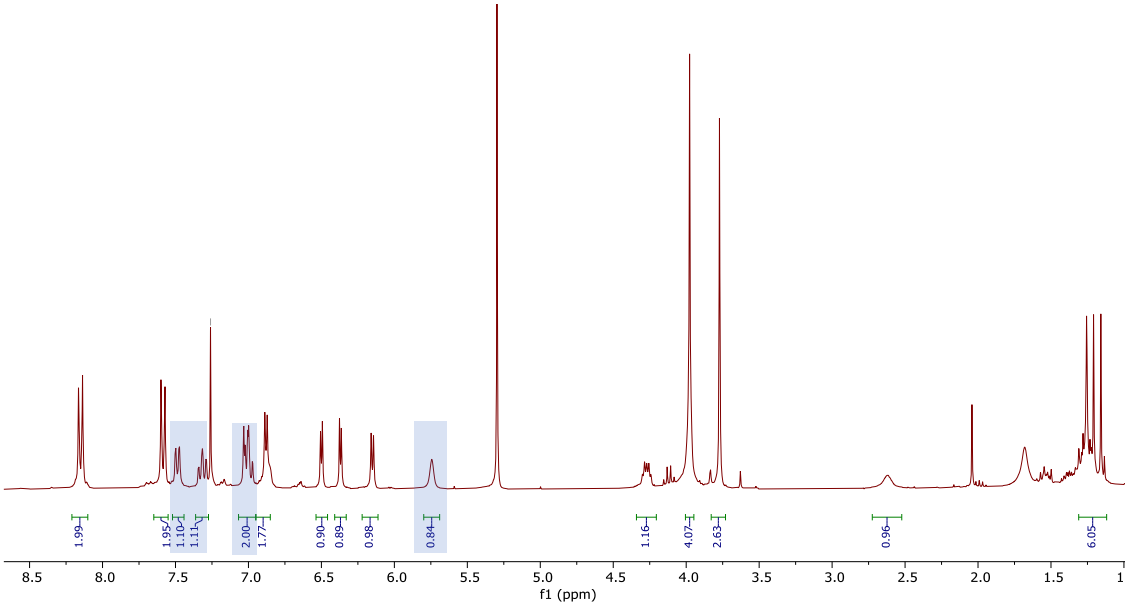

Figure 4.3. Crude ^{1}H NMR of 3-*ortho*-hydroxyphenyl-5-(*R*)-serinyl methyl ester BODIPY **4.22**, light blue highlighting newly added *ortho*-hydroxyphenyl moiety.

4.2.5 Synthesis of *N,N,O,C* 5-(*R*)-serinyl methyl ester BODIPY diastereoisomers **4.23a** and **4.23b** via de-chelation/re-chelation

The use of $SnCl_4$ as a suitable reagent for the ring closure 3-*ortho*-hydroxyphenyl-5-(*S*)-valinyl methyl ester BODIPY **4.8** was discussed earlier in this chapter. This method resulted in degradation of the desired synthesised helically chiral BODIPYs **4.7** after a short period of time (< 20 mins). Due to this observed product degradation upon ring closure of 3-*ortho*-hydroxyphenyl-5-(*S*)-valinyl methyl ester BODIPY **4.8** using $SnCl_4$, an alternative approach was investigated to form the target helically chiral BODIPYs.

Therefore, it was proposed that de-chelation of the boron centre of 3-*ortho*-hydroxyphenyl-5-(*R*)-serinyl methyl ester BODIPY **4.22**, would result in the formation of the corresponding dipyrromethene. Re-chelation of the dipyrromethene with a boronic acid which would chelate with both the nitrogen atoms of the dipyrromethene and the oxygen atom of the 3-*ortho*-hydroxyphenyl- group. This would create a new boron centre and in that step two helically chiral BODIPY diastereoisomers should be formed.

Para-fluoro phenylboronic acid was the chosen as a suitable chelating reagent, capable of forming bonds to the N, N and O atoms of the dipyrromethene. The introduction of a *para*-fluoro phenyl group also adds a suitable ^{19}F NMR tag as a means to calculate *de* through NMR integration (Scheme 4.11).

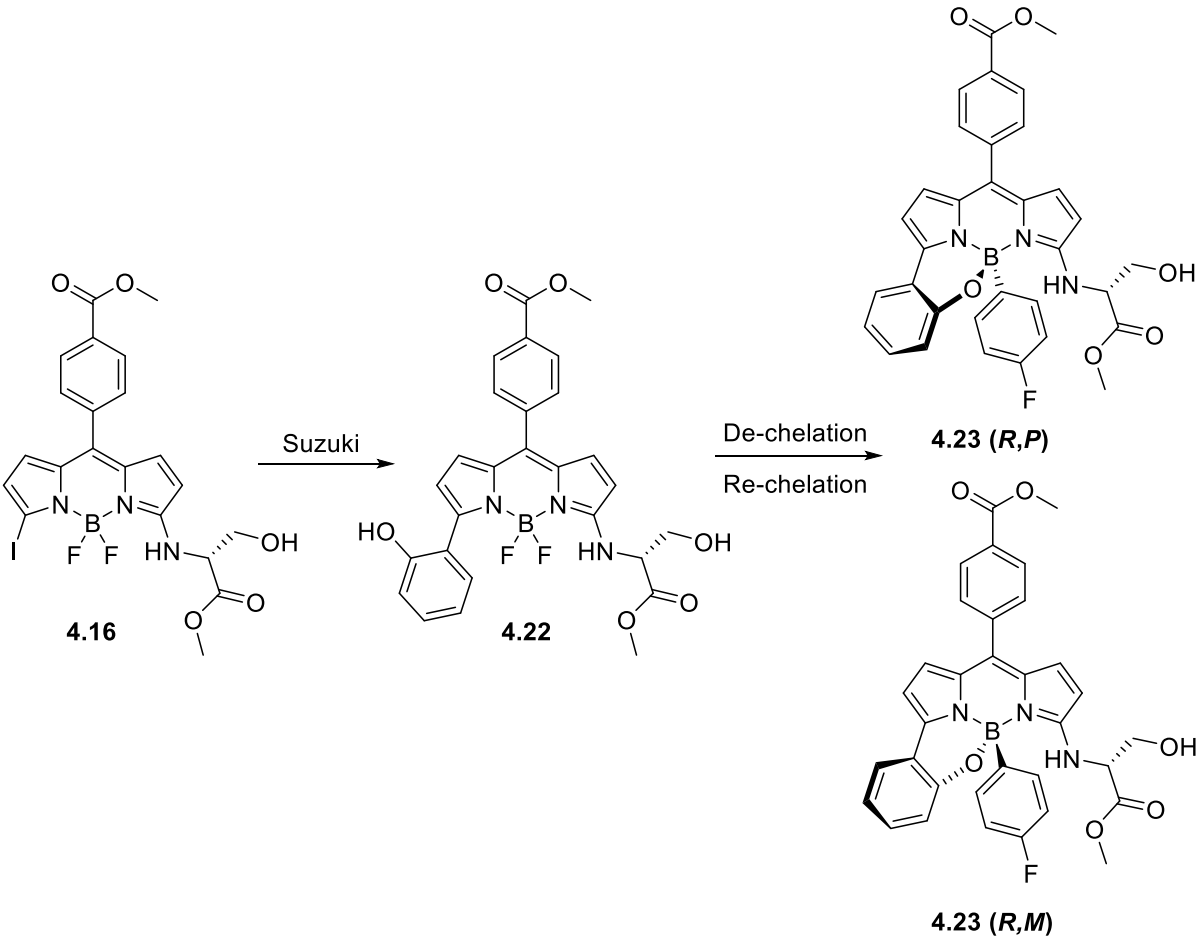

Scheme 4.11. Newly devised route towards helically chiral *N,N,O,C*-5-(*R,P*)-serinyl methyl ester BODIPY and *N,N,O,C*-5-(*R,M*)-serinyl methyl ester BODIPY **4.23** via de-chelation/re-chelation chemistry.

4.2.5.1 De-chelation-re-chelation of 3-*ortho*-hydroxyphenyl-5-(*R*)-serinyl methyl ester BODIPY **4.22**

After the successful formation of the Suzuki coupled 3-*ortho*-hydroxyphenyl-5-(*R*)-serinyl methyl ester BODIPY **4.22** a de-chelation/re-chelation reaction to afford *N,N,O,C*-5-(*R,P*)-serinyl methyl ester BODIPY and *N,N,O,C*-5-(*R,M*)-serinyl methyl ester BODIPY **4.23** was attempted.

The de-chelation step followed the work of Rutledge *et al*. in which they showed the removal of the boron centre of BODIPY **4.24** under acidic conditions of TFA to form dipyrromethene **4.25** (Scheme 4.12).[103]

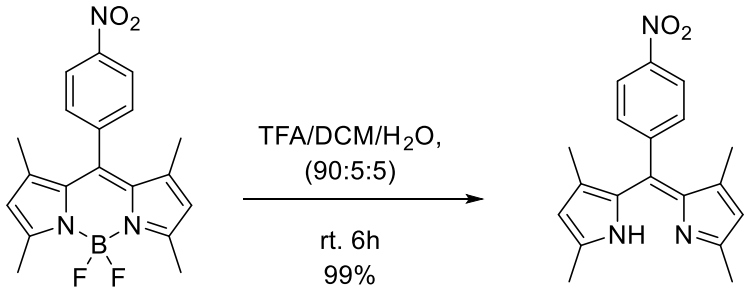

4.24 **4.25**

Scheme 4.12. De-chelation of a BF_2 moiety from BODIPY **4.24** under TFA acidic conditions to form dipyrromethene **4.25**.

3-*Ortho*-hydroxyphenyl-5-(*R*)-serinyl methyl ester BODIPY **4.22** contains an ester moiety which could be hydrolysed if reacted with water, therefore the above procedure was adapted in which the water was exchanged with MeOH.

Therefore, this two-step de-chelation/re-chelation was initiated by an acidic de-chelation in which 3-*ortho*-hydroxyphenyl-5-(*R*)-serinyl methyl ester BODIPY **4.22** was stirred in a 90:5:5 ratio of TFA:DCM:MeOH for 50 mins. This was followed by the removal of solvent under reduced pressure followed by the crude reaction mixture being diluted with DCM and subjected to an aqueous work-up.

Subsequently, the presumed de-chelated α-*ortho*-hydroxyphenyl-α-(*R*)-serinyl methyl ester dipyrromethene **4.26** was dissolved in DCM and cooled to 0^{o}C before being reacted with *para*-fluoro phenylboronic acid and stirred for 3.5 hours to form the desired helically chiral *N,N,O,C*-5-(*R*)-serinyl methyl ester BODIPYs **4.23a** (predominantly major) and **4.23b** (predominately minor) (Table 4.6).

Upon analysis of the ^{19}F NMR spectra of the crude reaction mixture of *N,N,O,C*-5-(*R*)-serinyl methyl ester BODIPYs **4.23a** and **4.23b** , two singlets at -116.41 and -115.58 ppm were present respectively, indicating the formation of two diastereoisomers. Each singlet in the ^{19}F NMR was integrated, showing a *de* of 33%. The crude reaction mixture was purified by silica gel column chromatography, showing an isolated yield of 28 and 14% and for each *N,N,O,C*-5-(*R*)-serinyl methyl ester BODIPY diastereoisomer **4.23a** and **4.23b** respectively. The *de* observed after purification was comparable to that measured via ^{19}F NMR integration, indicating that the *de* was retained (Table 4.6, entry 1).

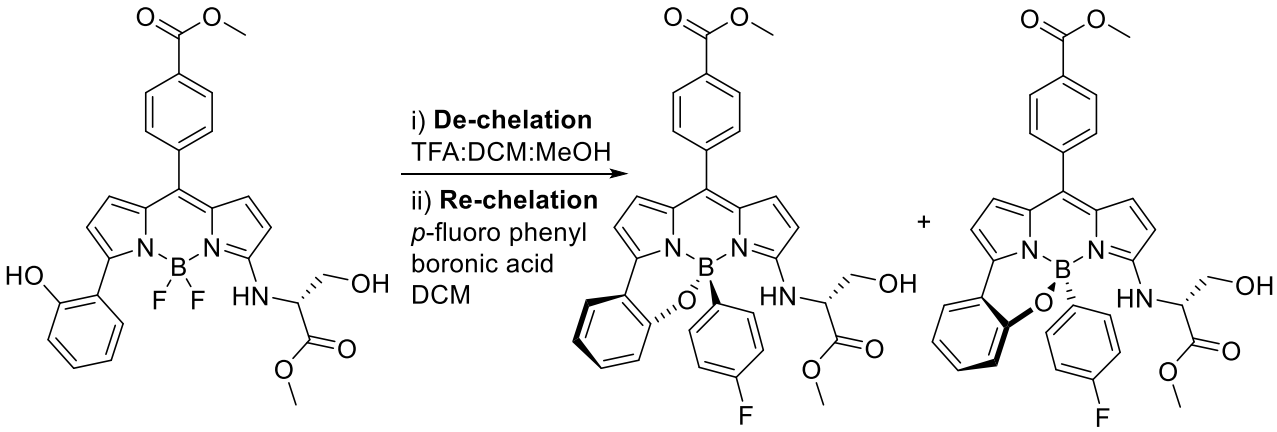

Entry	Time/min	Temp/^{0}C	*de*/%	Yield/%
1	210	0	33	28 (**4.23a**), 14 (**4.23b**)
2	30	r.t (25)	50	36 (**4.23a**), 12 (**4.23b**)
3	5	35	77	29 (**4.23a**), 4 (**4.23b**)
4	2	45	68	75 (**4.23a**), 14 (**4.23b**)
5	2	55	10	19 (**4.23a**), 23 (**4.23b**)

Table 4.6. One-pot de-chelation/re-chelation to form helically chiral chiral *N,N,O,C*-5-(*R*)-serinyl methyl ester BODIPYs **4.23a** and **4.23b**. All reactions attempted on a 0.1 mmol scale. Each *de* was calculated after purification by silica gel column chromatography.

The structure of *N,N,O,C*-5-(*R*)-serinyl methyl ester BODIPYs **4.23a** and **4.23b** were both verified by HRMS. The two diastereomers showed 592.2052 and 592.2057 m/z values, both of which are consistent with $C_{33}H_{27}{}^{11}BFN_3O_6$ $[M+H]^+$.

To further explore the diastereomeric control of this re-chelation reaction, a series of reactions with *para*-fluorophenyl boronic acid were undertaken at different temperatures. Each re-chelation reaction was run in chloroform with the disappearance of starting material monitored by TLC. Each reaction was subjected to an aqueous work-up and purified via silica gel column chromatography to isolate each diastereoisomer **4.23a** and **4.23b**.

Therefore α-*ortho*-hydroxyphenyl-α-(*R*)-serinyl methyl ester dipyrromethene **4.26** was reacted with *para*-fluorophenyl boronic acid at 25ºC with TLC being run after 30 mins, showing complete consumption of starting material. This resulted in the isolation of the two diastereoisomers **4.23a** and **4.23b** in a yield of 36 and 12% respectively, resulting in a *de* of 50% (Table 4.6, entry 2).

The next chelation reaction of α-*ortho*-hydroxyphenyl-α-(*R*)-serinyl methyl ester dipyrromethene **4.26** with *para*-fluorophenyl boronic acid was run at 35ºC. TLC was run after 5 mins, showing the complete consumption dipyrromethene starting material **4.26**. This reaction showed a *de* of 77%, however a drop in overall yield of both diastereoisomers **4.23a** and **4.23b** to 29 and 4% was observed respectively (Table 4.6, entry 3).

The temperature was increased by another ten degrees to 45ºC, with the chelation of α-*ortho*-hydroxyphenyl-α-(*R*)-serinyl methyl ester dipyrromethene **4.26** with *para*-fluorophenyl boronic acid being run at 45ºC for 2 mins. Excellent yields of 74 and 14% were observed for each diastereoisomer **4.23a** and **4.23b** respectively, giving a *de* of 68% (Table 4.6, entry 4).

A final chelation reaction of α-*ortho*-hydroxyphenyl-α-(*R*)-serinyl methyl ester dipyrromethene **4.26** with *para*-fluorophenyl boronic acid was run at 55ºC for 2 mins. This reaction gave a low *de* of 10% with yields of 19 and 29% of each of the diastereomers **4.23a** and **4.23b** respectively, interestingly in this case the diastereoselectivity has inverted (Table 4.6, entry 5).

Through de-chelation/re-chelation chemistry, in which the re-chelation was run over a range of different temperatures (0 – 55ºC), the observed *de* was shown to be temperature dependent. It was observed that at lower temperature the reaction is less diastereoselective, and as temperature increases, the *de* increases. An increase

in *de* of 33 to 77% was observed from 0 to 35°C, with 35°C giving the highest *de* of 77%. This trend is unusual, as a typical diastereoselective reaction should show higher *de* at lower temperatures. However, when the temperature is increased further, the diastereoselectivity decreases, with the re-chelation reaction at 55°C even showing an inversion of diastereoselectivity. Not only did the *de* vary greatly with temperature, but there was also a significant difference in yields at different temperatures. Thus, suggesting a complex mechanism or mechanisms are occurring in the reaction.

Upon inspection of *para*-fluorophenyl boronic acid starting material by ^{19}F NMR, it was seen that there were a number of species present. This is common for boronic acids as they are often seen to undergo dehydration reactions to form cyclic trimers and polymeric systems, which can equilibrate with the free boronic acid.[104, 105] It is postulated that when re-chelation reactions are run at lower temperatures, the boronic acids may not be able to equilibrate to form the needed reactive species, impacting on the reaction.

It should be noted that due to difficulties in purification, the key starting material for the re-chelation chemistry, the de-chelated α-*ortho*-hydroxyphenyl-α-(*R*)-serinyl methyl ester dipyrromethene **4.26** had not been columned and neither had the precursor 3-*ortho*-hydroxyphenyl-5-(*R*)-serinyl methyl ester BODIPY **4.22**. Therefore, it is possible that batches of starting material may contain variable levels of impurities, which could impact on the re-chelation reactions.

4.2.5.2 Synthesis of α-*ortho*-hydroxyphenyl-α-(*R*)-serinyl methyl ester dipyrromethene **4.26**

In order to facilitate investigation into the re-chelation reactions, it was important to ensure that α-*ortho*-hydroxyphenyl-α-(*R*)-serinyl methyl ester dipyrromethene **4.26** starting material was pure. Therefore, purification was attempted after de-chelation of 3-*ortho*-hydroxyphenyl-5-(*R*)-serinyl methyl ester BODIPY **4.22**.

Thus, 3-*ortho*-hydroxyphenyl-5-(*R*)-serinyl methyl ester BODIPY **4.22** was treated with a 90:5:5 ratio of TFA:DCM:MeOH at room temperature. The reaction was stirred for 30 mins and then the solvent was removed under reduced pressure followed by purification via silica gel chromatography.

Purification of the crude reaction mixture by silica gel column chromatography resulted in the isolation of a single compound. Analysis of the isolated compound by ^{1}H NMR spectra, showed that a new compound had been synthesised. However, upon studying its ^{11}B and ^{19}F NMR a singlet and triplet was observed respectively. This indicates that this isolated compound still contained a boron centre and therefore cannot be the desired α-*ortho*-hydroxyphenyl-α-(*R*)-serinyl methyl ester dipyrromethene **4.26** (Scheme 4.13).

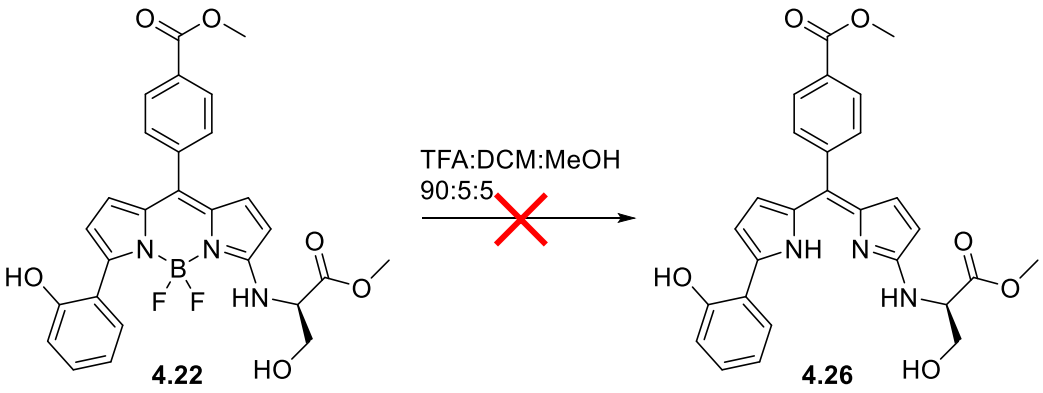

Scheme 4.13. De-chelation of boron centre of 3-*ortho*-hydroxyphenyl-5-(*R*)-serinyl methyl ester BODIPY **4.22** under acidic conditions.

This was a surprising result as above it was shown that this dipyrromethene **4.26** must form enroute to synthesis BODIPY **4.23** (Table 4.6. One-pot de-chelation/re-chelation to form helically chiral chiral *N,N,O,C-5*-(*R*)-serinyl methyl ester BODIPYs **4.23a** and **4.23b.** All reactions attempted on a 0.1 mmol scale. Each *de* was calculated after purification by silica gel column chromatography. Therefore, It is unclear why purification of α-*ortho*-hydroxyphenyl-α-(*R*)-serinyl methyl ester dipyrromethene **4.26** was unsuccessful. However, it could be postulated that dipyrromethene **4.26** contained still contained residual TFA after removal of solvent under reduced pressure and during purification via silica gel column chromatography, these strongly acidic conditions caused degradation of the desired product.

4.2.5.3 De-chelation of 3-iodo-5-(*R*)-serinyl methyl ester BODIPY **4.16**

Due to the unsuccessful isolation of α-*ortho*-hydroxyphenyl-α-(*R*)-serinyl methyl ester dipyrromethene **4.26** an alternative synthetic route was investigated in which de-chelation under acidic conditions could be attempted earlier in the synthetic route.

Therefore, the synthetic route order was changed, in which de-chelation of 3-iodo-5-(*R*)-serine methyl ester BODIPY **4.16** was attempted before Suzuki cross-coupling. It was hoped that the de-chelated α-iodo-α-(*R*)-serinyl methyl ester dipyrromethene **4.27** would be more robust to purification than the previous α-*ortho*-hydroxyphenyl-α-(*R*)-serinyl methyl ester dipyrromethene **4.26** and therefore could be taken forward in the synthesis of helically chiral *N,N,O,C*-5-(*R*)-serinyl methyl ester BODIPY diastereoisomers **4.23a** and **4.23b** (Scheme 4.14).

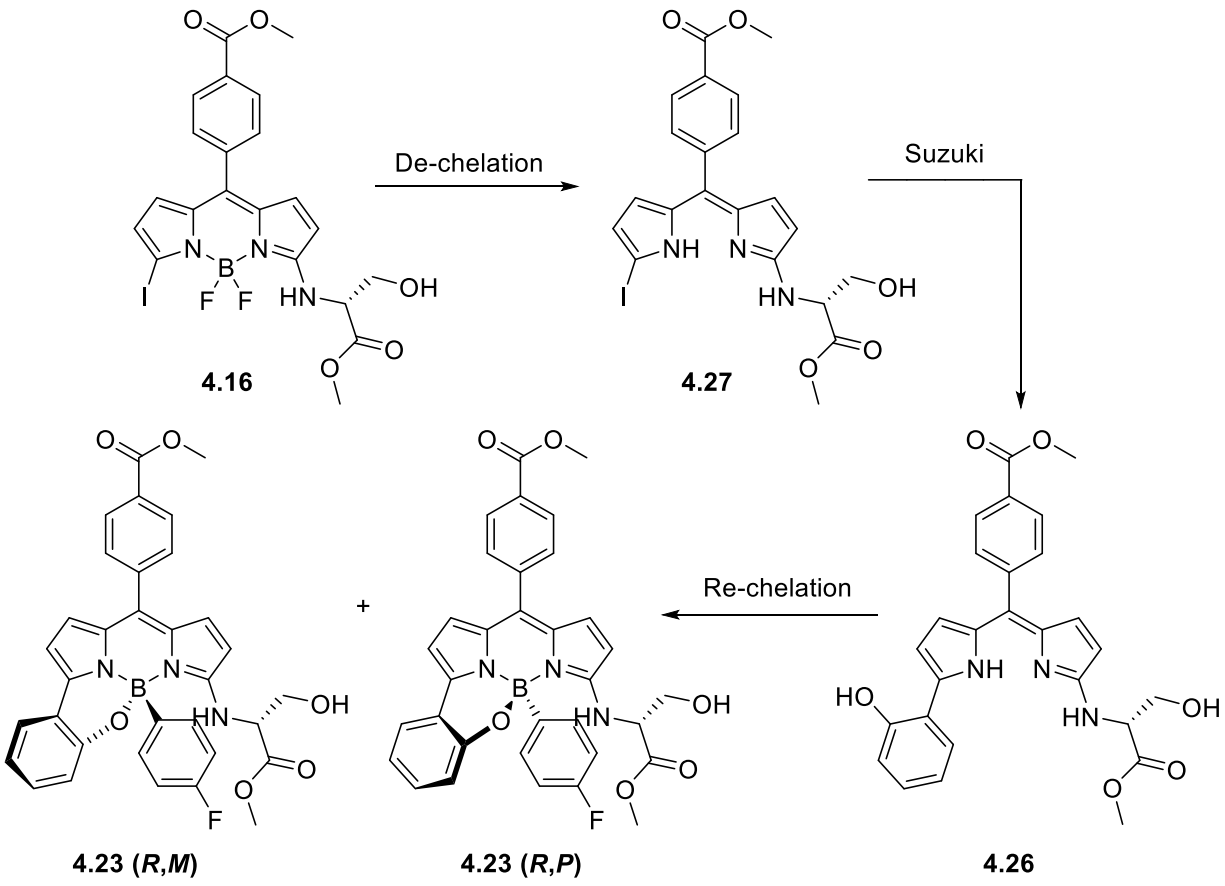

Scheme 4.14. New proposed synthetic route to form final helically chiral *N,N,O,C*-5-(*R,P*)-serinyl methyl ester BODIPY and *N,N,O,C*-5-(*R,M*)-serinyl methyl ester BODIPY **4.23**.

Before attempting the de-chelation of 3-iodo-5-(*R*)-serine methyl ester BODIPY **4.16**, a simpler compound, 3,5-dibromo BODIPY **2.14a** was subjected to the same de-chelation reaction conditions discussed earlier as a means to further understand and optimise this synthesis.

Therefore, 3,5-dibromo BODIPY **2.14a** was mixed with a 90:5:5 ratio of TFA:DCM:MeOH and was stirred for 50 mins at room temperature before being

subjected to an aqueous work-up and analysed by ^{1}H NMR. Unfortunately, upon ^{1}H analysis, no conversion to the desired α,α-dibromo dipyrromethene **2.18a** was observed, showing only 3,5-dibromo BODIPY **2.14a** starting material (Table 4.7, entry 1).

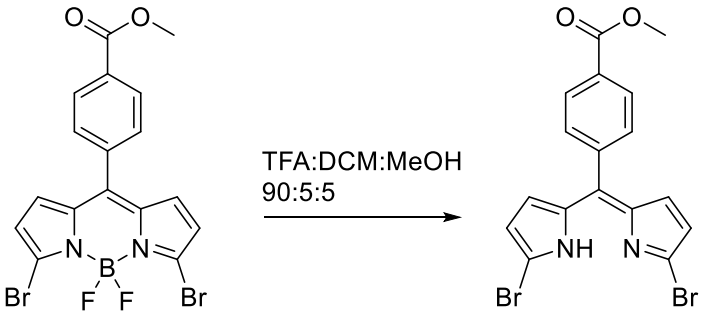

2.14a **2.18a**

Entry	**Time/h**	**Yield/%[a]**
1	50 mins	0
2	24	88

Table 4.7. Acidic de-chelation of 3,5-dibromo BODIPY **2.14a**. a = yield calculated via ^{1}H NMR integration.

Therefore, the de-chelation reaction of 3,5-dibromo BODIPY **2.14a** was repeated under identical conditions with the progression of the reaction being monitored by TLC. After 24 hours full consumption of the 3,5-dibromo BODIPY starting material **2.14a** was observed. Therefore, the crude reaction mixture was subjected to an aqueous work-up and analysed by ^{1} showing 88% conversion to the desired α,α-dibromo dipyrromethene **2.18a** (calculated by ^{1}H NMR integration) (Table 4.7, entry 2, Figure 4.4).

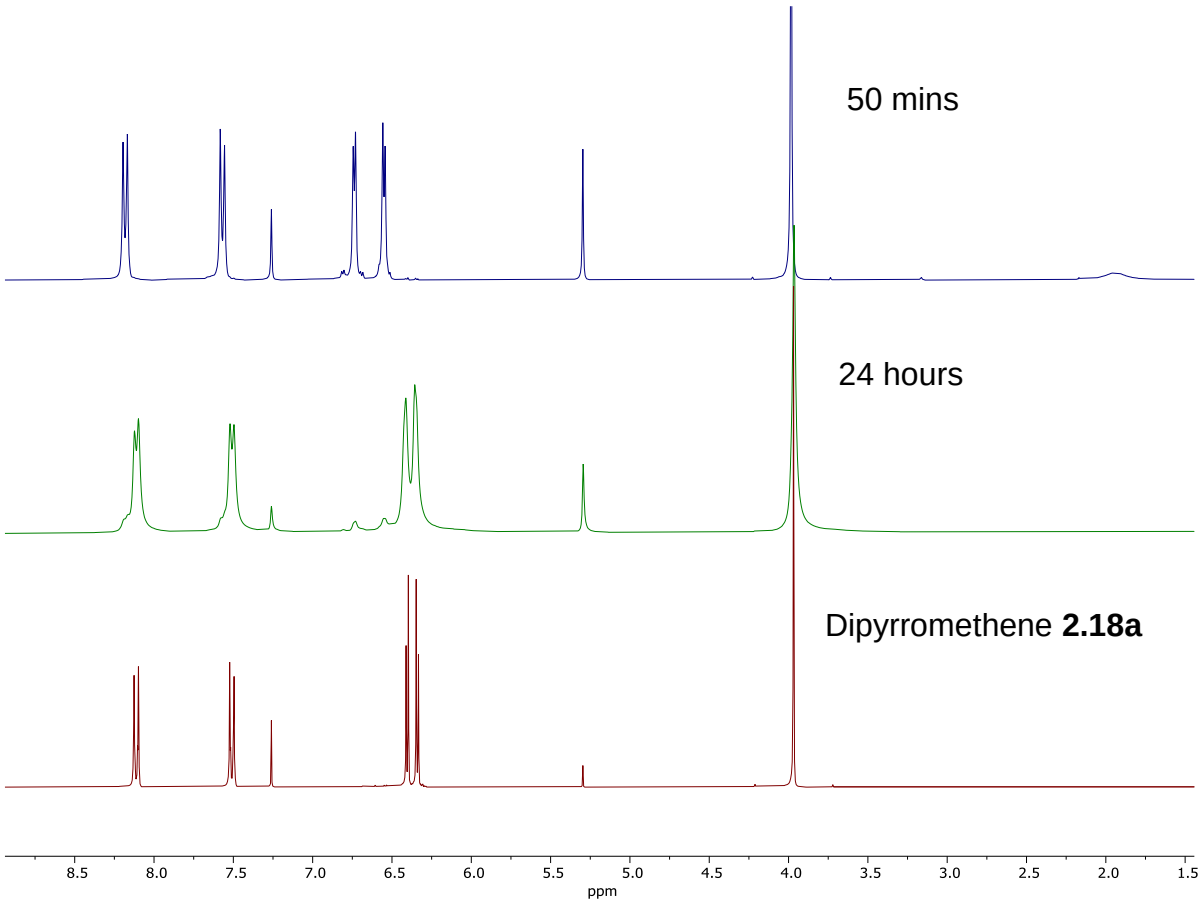

Figure 4.4. ^{1}H NMR of a) 3,5-dibromo BODIPY **2.14a** b) de-chelation of 3,5-dibromo BODIPY **2.14a** after 50 mins c) de-chelation of 3,5-dibromo BODIPY **2.14a** after 24 hours.

Due to the successful de-chelation of 3,5-dibromo BODIPY **2.14a** after 24 hours, it was decided that de-chelation of 3-iodo-5-(*R*)-serine methyl ester BODIPY **4.16** would be possible using similar reaction times.

Therefore, 3-iodo-5-(*R*)-serine methyl ester BODIPY **4.16** was stirred at room temperature in a TFA:DCM:MeOH mixture for 24 hours in an attempt to afford α-iodo-α-(*R*)-serinyl methyl ester dipyrromethene **4.27**. After 24 hours and an aqueous work-up the crude reaction mixture was analysed by ^{1}H, ^{11}B and ^{19}F NMR. ^{1}H NMR showed the complete disappearance of 3-iodo-5-(*R*)-serine methyl ester BODIPY **4.16** with the appearance of a new major compound, however the ^{11}B and ^{19}F NMR spectra showed a triplet and a multiplet respectively, indicating the presence of fluorine and boron atoms. This indicated that the desired, dechelated α-iodo-α-(*R*)-serinyl methyl ester dipyrromethene **4.27** had not formed (Scheme 4.15).

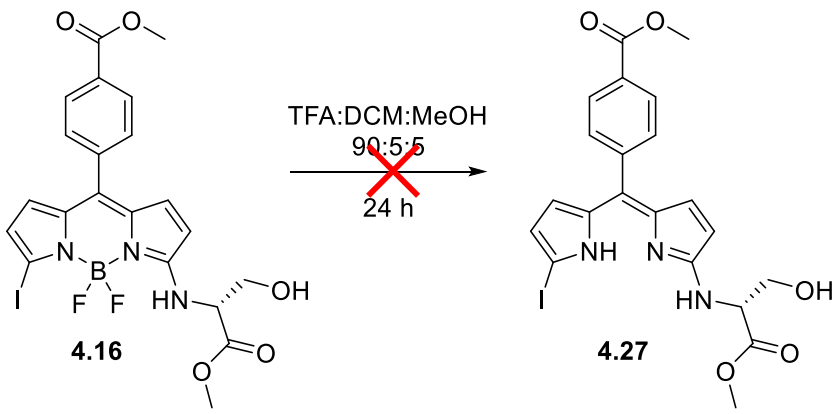

Scheme 4.15. Acidic de-chelation of 3-iodo-5-(*R*)-serine methyl ester BODIPY **4.16**.

The crude reaction mixture was purified via silica gel column chromatography in an attempt to isolate any α-iodo-α-(*R*)-serinyl methyl ester dipyrromethene **4.27** present, however degradation on silica appeared to occur preventing isolation of any of the desired product. Due to the no observed α-iodo-α-(*R*)-serinyl methyl ester dipyrromethene **4.27** being formed via TFA mediated dechelation, this synthetic route was not investigated further.

4.2.6 Synthesis of *N,N,O,C*-5-(*R*)-serinyl methyl ester BODIPY diastereoisomers **4.23a** and **4.23b** using α,α-dibromo dipyrromethene **2.18a** as starting material

Due to the failure to isolate both α-*ortho*-hydroxyphenyl-α-(*R*)-serinyl methyl ester dipyrromethene **4.26** and α-iodo-α-(*R*)-serinyl methyl ester dipyrromethene **4.27** from acidic de-chelation reactions, a new route was devised in which these strongly acidic conditions were avoided.

A new route was proposed utilising a α,α-dibromo dipyrromethene **2.18a** as an alternative starting material. It was hoped that α,α-dibromo dipyrromethene **2.18a** could undergo sequential halogen exchange, S_NAr and Suzuki cross-coupling reactions to form α-*ortho*-hydroxyphenyl–α-(*R*)-serinyl methyl ester dipyrromethene **4.26**. α-*Ortho*-hydroxyphenyl–α-(*R*)-serinyl methyl ester dipyrromethene **4,26** could then be chelated with *para*-fluoro phenyl boronic acid to form *N,N,O,C*-5-(*R*)-serinyl methyl ester BODIPY diastereoisomers **4.23a** and **4.23b**, avoiding the need for any acidic de-chelation step (Scheme 4.16).

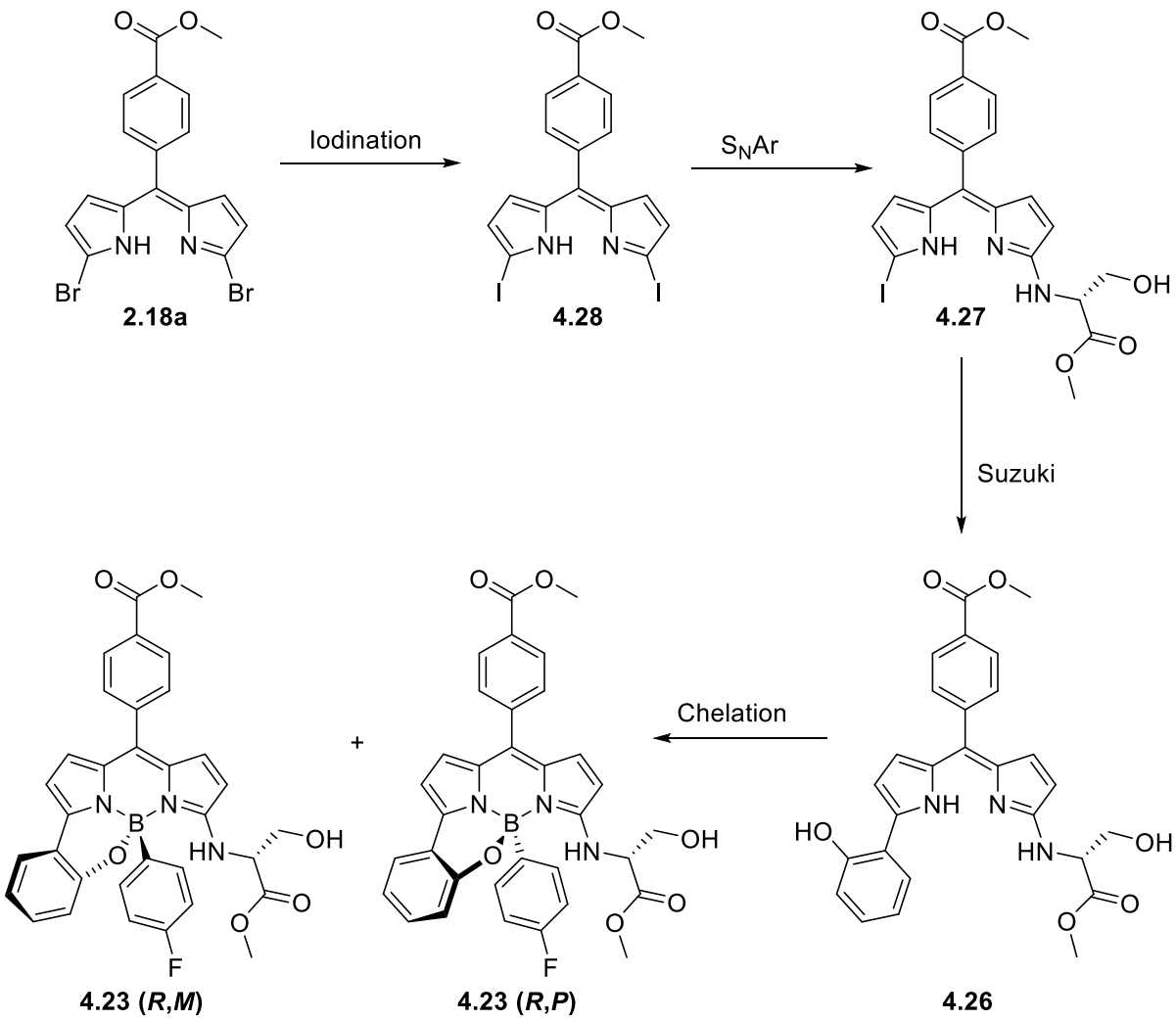

Scheme 4.16. New proposed synthetic route to helically *N,N,O,C*-5-(*R,P*)-serinyl methyl ester BODIPY and *N,N,O,C*-5-(*R,M*)-serinyl methyl ester BODIPY **4.23**, avoiding a de-chelation step.

4.2.6.1 Aromatic Finkelstein reaction on α,α-dibromo dipyrromethene

This new synthetic route was initiated by an aromatic Finkelstein reaction on α,α-dibromo dipyrromethene **2.18a** to convert it to its α,α-diiodo dipyrromethene **4.28** counterpart, using optimised conditions previously discussed in Chapter 3.

Therefore, α,α-dibromo dipyrromethene **2.18a** (for synthesis see Chapter 2) was reacted with a saturated solution of NaI in propionitrile at reflux (Scheme 4.17). This aromatic Finkelstein reaction was monitored by TLC, showing complete consumption of the starting material after 24 hours. After an aqueous work-up, the crude product

was purified by silica gel column chromatography to give α,α–diiodo dipyrromethene **4.28** in an excellent yield of 92%.

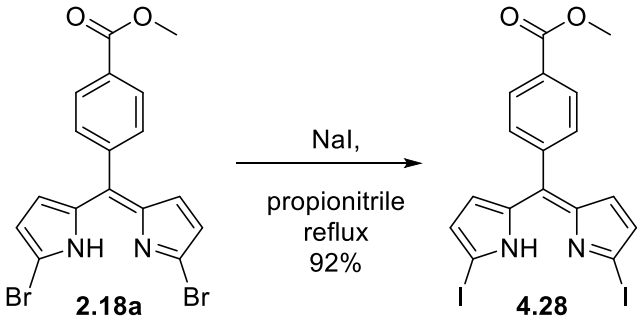

Scheme 4.17. Aromatic Finkelstein reaction to form α,α-diiodo dipyrromethene **4.28**.

The structure of α,α–diiodo dipyrromethene **4.28** was confirmed by ^{1}H NMR, showing a shift in the pyrrolic peaks of two 2H doublets at 6.39 (*J* = 4.2 Hz) and 6.32 ppm (*J* = 4.2 Hz) in α,α–dibromo dipyrromethene **2.18a** to 6.49 (*J* = 4.2 Hz) and 6.29 ppm (*J* = 4.2 Hz) in the newly formed α,α–diiodo dipyrromethene **4.28** (Figure 4.5).

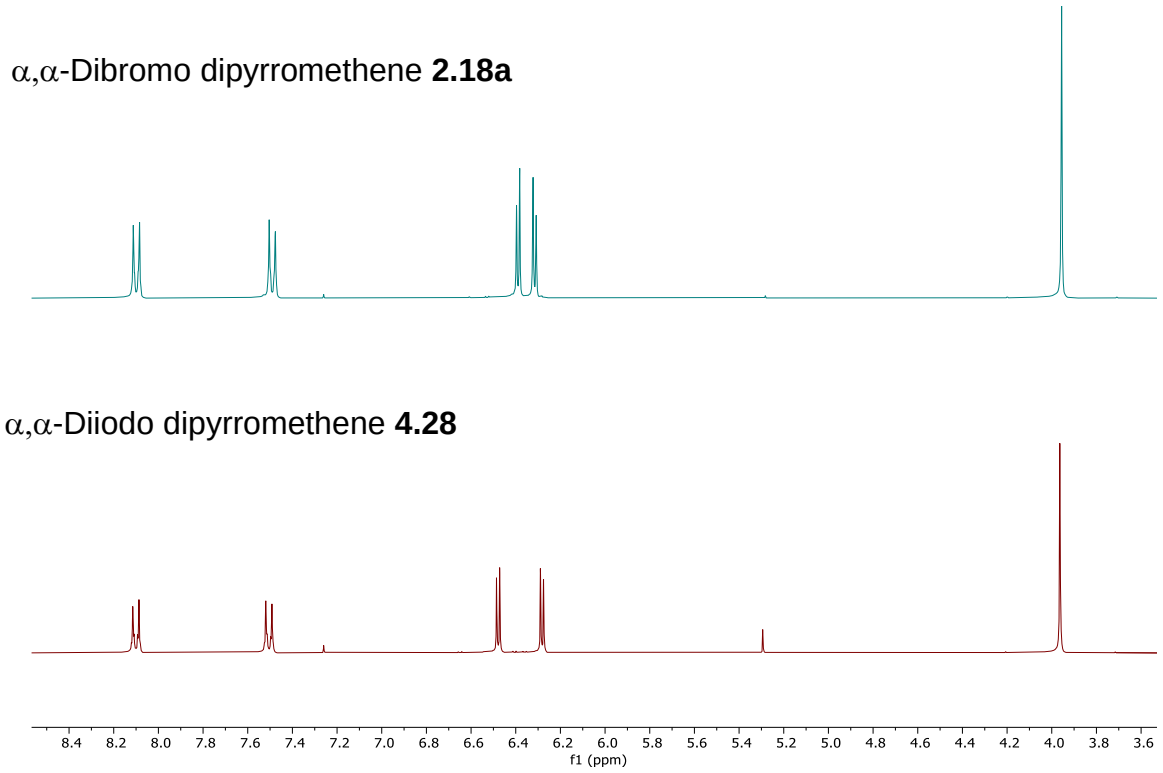

Figure 4.5. Comparison of the ^{1}H NMR spectra of α,α-dibromo dipyrromethene **2.18a** with α,α-diiodo dipyrromethene **4.28**.

The structure of α, α-diiodo dipyrromethene **4.28** was further confirmed by X-ray crystallography. α, α-Diiodo dipyrromethene **4.28** was successfully crystallised through slow evaporation of a DCM solution. A suitable single crystal was submitted for single X-ray analysis, confirming the structure (Figure 4.6). α,α–Diiodo-dipyrromethene **4.28** formed triclinic crystals in the P-1 space group, containing 2 molecules in the unit cell.

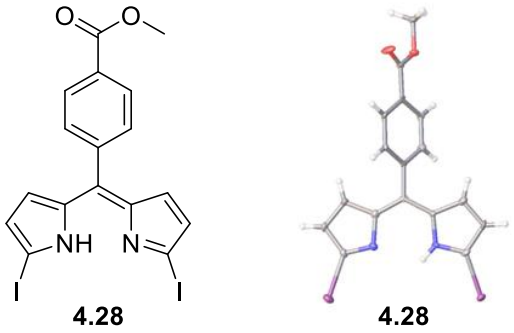

Figure 4.6. Single crystal X-ray structure of α,α-diiodo dipyrromethene **4.28**.

After the successful synthesis of α,α-diiodo dipyrromethene **4.28**, S_NAr reactions at the α position could be examined.

4.2.6.2 S_NAr reactions of (*R*)-serine methyl ester with α,α–dihalo dipyrromethenes **2.18a** and **4.28**

After the successful synthesis of α,α-diiodo dipyrromethene **4.28**, investigation of a base catalysed S_NAr at the 3-position was attempted, using previously discussed conditions.

Therefore, α,α-diiodo dipyrromethene **4.28** was reacted with 2 equivalents of (*R*)-serine methyl ester and 2.2 equivalents of NEt_3 in MeCN at reflux. The reaction was monitored by TLC, showing the presence of α,α-diiodo dipyrromethene **4.28** starting material after 24 hours. Subsequently, the reaction mixture was stirred for an additional 26 hours before being subjected to an aqueous work-up. Upon inspection of the ^1H NMR spectra of the crude reaction mixture, a large number of unidentifiable products had been formed. Purification of the crude mixture by column chromatography was attempted, however the desired dipyrromethene **4.29** was not isolated (Scheme 4.18).

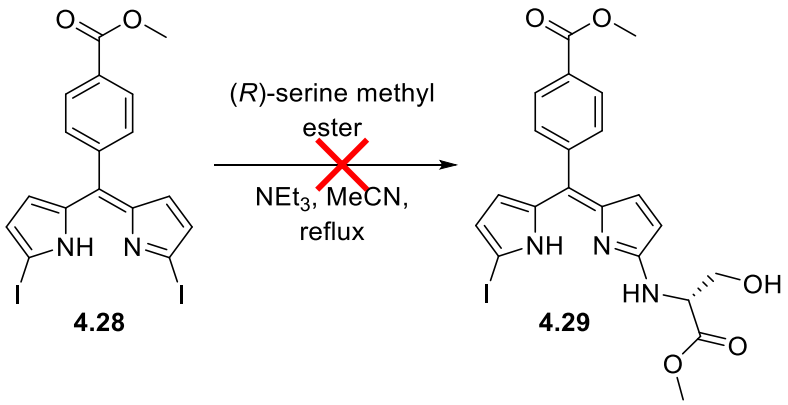

Scheme 4.18. S_NAr upon α,α-diiodo dipyrromethene **4.28**.

Due to the failure to synthesis α-iodo-α-(*R*)-serinyl methyl ester dipyrromethene **4.29** from α,α-diiodo dipyrromethene **4.28**, alternative reactions were investigated. It was decided that attempting S_NAr with an alternative dipyrromethene in the form of α,α-dibromo dipyrromethene **2.18a** may result in successful substitution as the α positions of α,α-dibromo dipyrromethene **2.18a** should be more susceptible to nucleophilic attack.

Therefore, α,α-dibromo dipyrromethene **2.18a** was subjected to S_NAr conditions, in which it was stirred in MeCN with 2 equivalents of (*R*)-serine methyl ester and 2.2 equivalents of NEt_3 at reflux. The reaction was monitored by TLC and showed the disappearance of α,α-dibromo starting material **2.18a** after 24 hours (Scheme 4.19).

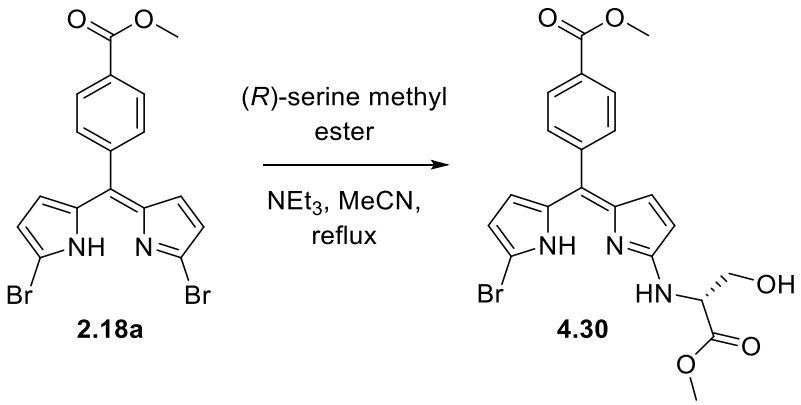

Scheme 4.19. S_NAr of α,α-dibromo dipyrromethene **2.18a** with (*R*)-serine methyl ester.

The crude reaction was purified by silica gel column chromatography and analysed by ^1H NMR. Oddly, there seemed to be discrepancies between the TLC and NMR, with TLC showing a single compound and ^1H NMR showing two compounds.

The ^{1}H NMR showed the appearance of more than 4 environments in the pyrrolic region, however only showing two other signals in the aromatic region, two 2H doublets at 7.97 (*J* = 8.3 Hz) and 7.38 ppm (*J* = 8.3 Hz), together corresponding to the *para*-methyl benzoate group in the *meso* position of the dipyrromethene. Integration of all pyrrolic peaks, showed that they totalled 4 protons when compared against the 3H singlet at 3.87 ppm, corresponding to the *para*-methyl group in the *meso* position. Therefore, it was postulated that α-bromo-α-(*R*)-serinyl methyl ester dipyrromethene **4.30** existed as two rotamers in solution, observable by ^{1}H NMR, potentially due to restricted rotation around the dipyrromethene (Figure 4.7).

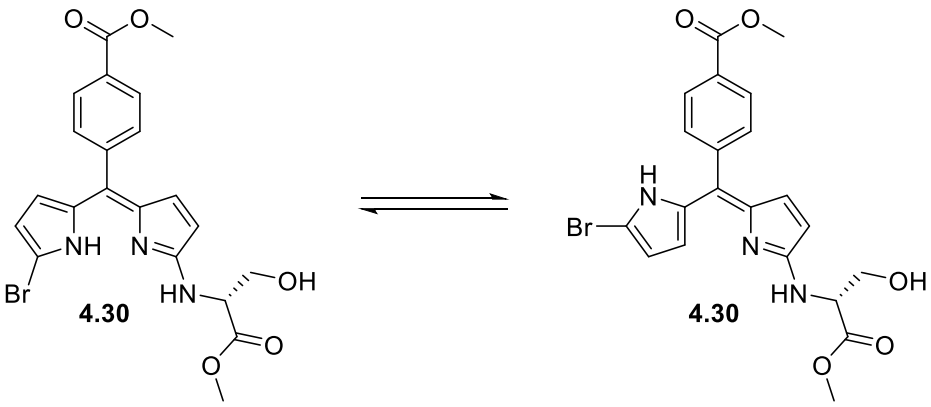

Figure 4.7. Rotamers of α-bromo-α-(*R*)-serinyl methyl ester dipyrromethene **4.30**.

Upon closer examination of the ^{1}H NMR, integration of the pyrrolic peaks shows two sets of 4 pyrrolic environments, in a roughly 2:1 ratio, indicating this is the ratio of the two rotamers. This was shown through doublets at 6.11 and 6.01 ppm with an integration of 0.66 and 0.33 respectively. Both signals at 5.94 and 6.12 show the overlapping of two environments, each integrating to one, again indicating the presence of rotamers. The final pyrrolic peak at 6.14 ppm is a doublet however it could be possible that the two pyrrolic environments had identical ppm, resulting in two overlapping peaks appearing as a doublet (Figure 4.8).

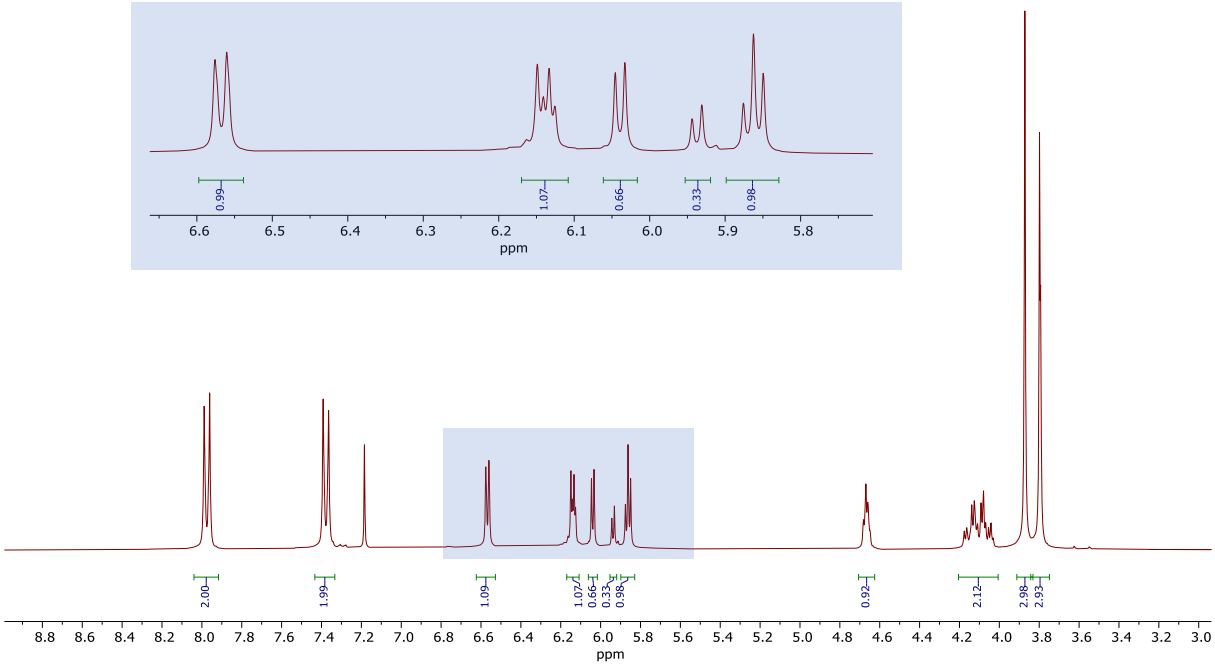

Figure 4.8. ^{1}H NMR of α-bromo-α-(*R*)-serinyl methyl ester dipyrromethene **4.30**. Blue showing expanded pyrrolic region.

α-Bromo-α-(*R*)-serinyl methyl ester dipyrromethene **4.30** was then carried forward to the next steps in which it was subjected to an aromatic Finkelstein reaction as a means to change bromide for an iodide to aid in later Suzuki cross-couplings.

Therefore, α-bromo-α-(*R*)-serinyl methyl ester dipyrromethene **4.30** was subjected to optimised aromatic Finkelstein reaction conditions, as discussed in Chapter 3, in which it was refluxed in a saturated solution of NaI in propionitrile. The reaction mixture was stirred for 24 hours before being subjected to an aqueous work-up. Unfortunately, upon inspection of the ^{1}H NMR of the reaction mixtures, none of the desired α-iodo-α-(*R*)-serinyl methyl ester dipyrromethene **4.29** was observed, only showing unreacted α-bromo-α-(*R*)-serinyl methyl ester dipyrromethene **4.30** starting material (Scheme 4.20).

Although BODIPYs have been shown to undergo aromatic Finkelstein reactions, the dipyrromethenes are more electron rich, resulting in the α positions less susceptible to nucleophilic attack, making them unreactive under these conditions.

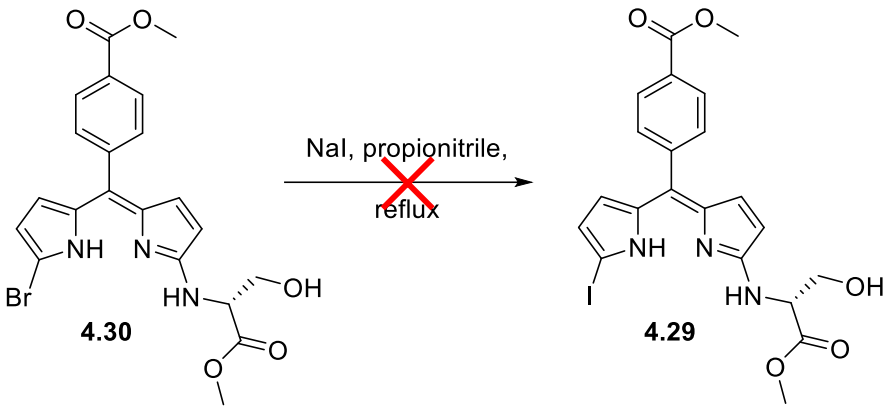

Scheme 4.20. Attempted aromatic Finkelstein of reaction on α-bromo-α-(*R*)-serinyl methyl ester dipyrromethene **4.30** using a saturated solution of NaI in propionitrile.

After multiple failures of aromatic Finkelstein and S_NAr reactions on dipyrromethenes, it was deemed that this approach was not feasible. As a result, alternative routes to *N,N,O,C*-5-(*R*)-serinyl methyl ester BODIPY diastereoisomers **4.23a** and **4.23b** were explored.

4.2.7 Synthesis of helically chiral *N,N,O-C*-(*S*)-serinyl methyl ester BODIPY BODIPYs **4.27a** and **4.27b** via alternative de-chelation/re-chelation conditions.

Due to the low reactivity of dipyrromethenes compared to their BODIPY counterparts in S_NAr reactions, as demonstrated above, alternative de-chelation methods were investigated, avoiding the use of TFA.

In 2014 Ravikanth *et al*. reported the use of a range of different Lewis acids to facilitate the removal of a BF_2 moiety from BODIPY **4.31** to its corresponding dipyrromethene **4.32**.[106] Ravikanth demonstrated that a number of different of Lewis acids were excellent candidates for facilitating de-chelation of BODIPY **4.31** (Table 4.8).

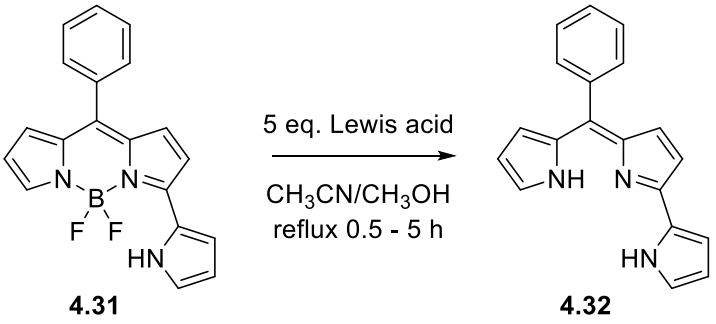

Reagent	Time/h	Product/%
$TiCl_4$	1	90
$ZrCl_4$	0.5	96
$FeCl_3$	2	dec.[a]
$AlCl_3$	1	86
$SnCl_4$	5	60
$Sc(OTf)_3$	0.5	94

Table 4.8. De-chelation of BODIPY **4.31** to its corresponding dipyrromethene **4.32** with Lewis acids. a) Decomposition of starting material.

Based off the work of Ravikanth *et al*. the Lewis acid mediated de-chelation of 3-iodo-5-(*S*)-serinyl methyl ester BODIPY **4.21** was attempted using $AlCl_3$ (Scheme 4.21).

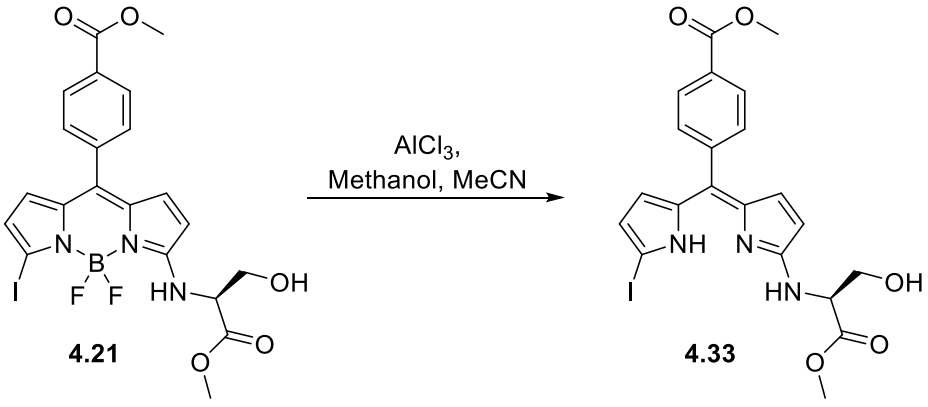

Scheme 4.21. Proposed de-chelation of 3-iodo-5-(*S*)-serinyl methyl ester BODIPY **4.21** using Lewis acid $AlCl_3$.

Therefore, 3-iodo-5-(*S*)-serinyl methyl ester BODIPY **4.21** was dissolved in MeCN and a solution of $AlCl_3$ in MeOH was added (5 equivalents $AlCl_3$ dissolved in MeOH).

The reaction was heated to reflux and stirred for 30 mins before undergoing an aqueous work-up. The crude reaction mixture was analysed by ^{11}B, ^{19}F and ^{1}H NMR. ^{1}H NMR showed the full consumption of 3-iodo-5-(*S*)-serine methyl ester BODIPY **4.21** starting material, with both ^{11}B and ^{19}F having no signals, indicating the successful de-chelation of the BF_2 group.

The crude compound was purified by silica gel column chromatography to give the product in a 64% yield. However, analysis of its ^{1}H NMR showed that an unexpected product had been formed in place of the desired de-chelated product. An extra pyrrolic proton peak was present in the ^{1}H NMR, shown as 1H double doublet at 7.04 ppm. Further analysis of the COSY NMR showed coupling between this newly observed signal at 7.04 and two pyrrolic peaks, suggesting a loss of the iodine during the reaction, resulting in the synthesis of α-(*S*)-serinyl methyl ester dipyrromethene **4.34** (Scheme 4.22).

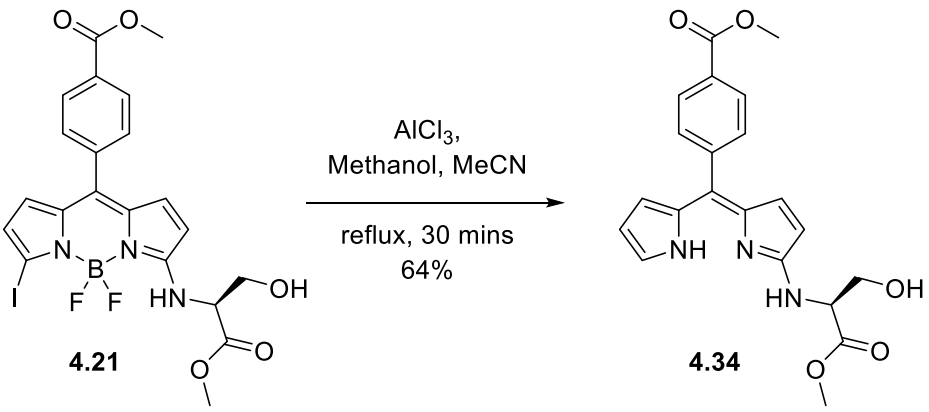

Scheme 4.22. De-chelation of 3-iodo-5-(*S*)-serinyl methyl ester BODIPY **4.21** using Lewis acid $AlCl_3$, resulting in the loss of iodine.

As a result, it was decided that de-chelation should instead be attempted on 3-*ortho*-hydroxyphenyl-5-(*S*)-serinyl methyl ester BODIPY **4.35** after Suzuki cross-coupling had been undertaken, to form α–*ortho*–hydroxyphenyl-α-(*S*)-serinyl methyl ester dipyrromethene **4.36**.

Therefore, 3-*ortho*-hydroxyphenyl-5-(*S*)-serinyl methyl ester BODIPY **4.35**, prepared under identical conditions discussed earlier for the synthesis of 3-*ortho*-hydroxyphenyl-5-(*R*)-serinyl methyl ester BODIPY **4.22**, was stirred in MeCN and a solution of $AlCl_3$ in MeOH was added (5 equivalents $AlCl_3$ dissolved in MeOH). The reaction was heated to reflux and stirred for 30 mins, followed by an aqueous work-

up and analysed by ^{11}B and ^{19}F NMR, indicating the removal of the BF_2 centre. The crude reaction was purified by silica gel column chromatography, successfully affording α–*ortho*–hydroxyphenyl-α-(*S*)-serinyl methyl ester dipyrromethenene **4.36** in a good yield of 50% as a red/brown solid (Scheme 4.23).

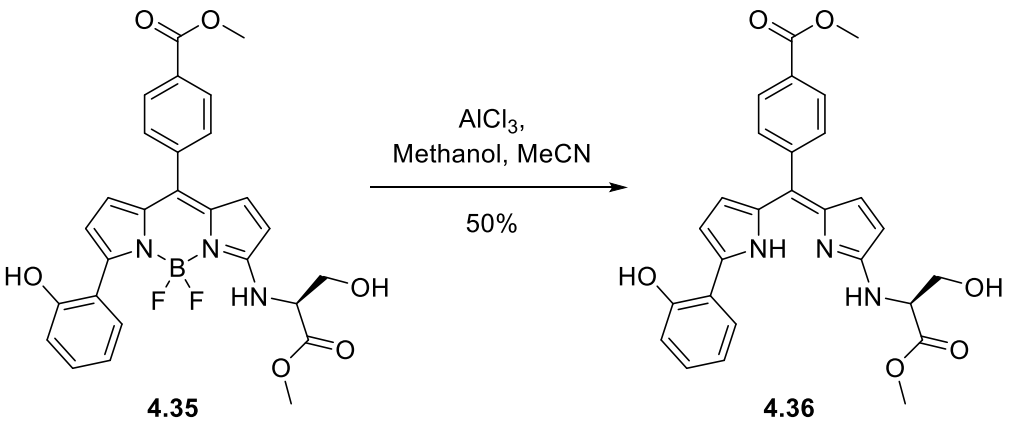

Scheme 4.23. De-chelation of 3-*ortho*-hydroxyphenyl-5-(*S*)-serinyl methyl ester BODIPY **4.35** using $AlCl_3$.

The structure of α–*ortho*–hydroxyphenyl-α-(*S*)-serinyl methyl ester dipyrromethene **4.36** was validated by HRMS, showing a peak at 488.1847 m/z which is consistent with the $[M+H]^+$ of a molecule with the formula of $C_{27}H_{25}N_3O_6$ (488.1816).

After isolating purified α–*ortho*–hydroxyphenyl-α-(*S*)-serinyl methyl ester dipyrromethene **4.36**, a more in-depth study into the re-chelation reaction with *para*-fluorophenyl boronic acid could be undertaken. Due to having purified α–*ortho*–hydroxyphenyl-α-(*S*)-serinyl methyl ester dipyrromethene **4.36**, the yield and *de* of the helically chiral *N,N,O,C*-5-(*S*)-serinyl methyl ester BODIPY diastereoisomers **4.37a** and **4.37b** formed through chelation reactions could more accurately measured.

Therefore, re-chelation reactions were attempted between α–*ortho*–hydroxyphenyl-α-(*S*)-serinyl methyl ester dipyrromethene **4.36** and *para*-fluorophenyl boronic acid using a number of different reaction temperatures to examine the impact of reaction temperature on the *de* of the *N,N,O,C*-5-(*S*)-serinyl methyl ester BODIPYs **4.37a** (major) and **4.37b** (minor) formed. Each reaction was run with 0.1 mmol of α–*ortho*–hydroxyphenyl-α-(*S*)-serinyl methyl ester dipyrromethene **4.36** in 20 mL of $CHCl_3$ under a nitrogen atmosphere, where the solvated starting material was

equilibrated at the desired temperature for 20 mins before the addition of *para*-fluorophenyl boronic acid (dissolved in $CHCl_3$), added dropwise over 5 mins. Each crude reaction mixture was then immediately quenched with water, before being subjected to an aqueous work-up and analysed. ^{1}H NMR each crude reaction mixture showed clean conversion to the desired diastereoisomers **4.27a** and **4.37b** in each reaction, and the *de* of each crude reaction was calculated by ^{19}F NMR integration.

Initially, chelation upon α–*ortho*–hydroxyphenyl-α-(*S*)-serinyl methyl ester dipyrromethene **4.36** was run at -41°C (acetone/acetonitrile bath), showing an excellent yield of 92%, with a *de* of 57% calculated from ^{19}F NMR (Table 4.9, entry 1).

Next the re-chelation of α–*ortho*–hydroxyphenyl-α-(*S*)-serinyl methyl ester dipyrromethene **4.36** was attempted at 0 and 25°C, with both reactions showing an increase in *de* to 70 and 84% respectively for the synthesised *N,N,O,C*-5-(*S*)-serinyl methyl ester BODIPYs **4.37a** and **4.37b** (Table 4.9, entry 2 and 3).

Three re-chelation reactions were attempted on α–*ortho*–hydroxyphenyl-α-(*S*)-serinyl methyl ester dipyrromethene **4.36** (35, 45 and 55°C). When re-chelation was run at 35°C a *de* of 83% was measured from ^{19}F NMR integration (Table 4.9, entry 4). Each subsequent reaction showed a decrease in *de* as temperature was increased, showing 82 and 77% for 45°C and 55°C reactions respectively (Table 4.9, entries 5 and 6). A final re-chelation of α–*ortho*–hydroxyphenyl-α-(*S*)-serinyl methyl ester dipyrromethene **4.36** was attempted at reflux (61°C), showing a decrease in *de* to 66% of the desired *N,N,O,C*-5-(*S*)-serinyl methyl ester BODIPYs **4.37a** and **4.37b** (Table 4.9, entry 7).

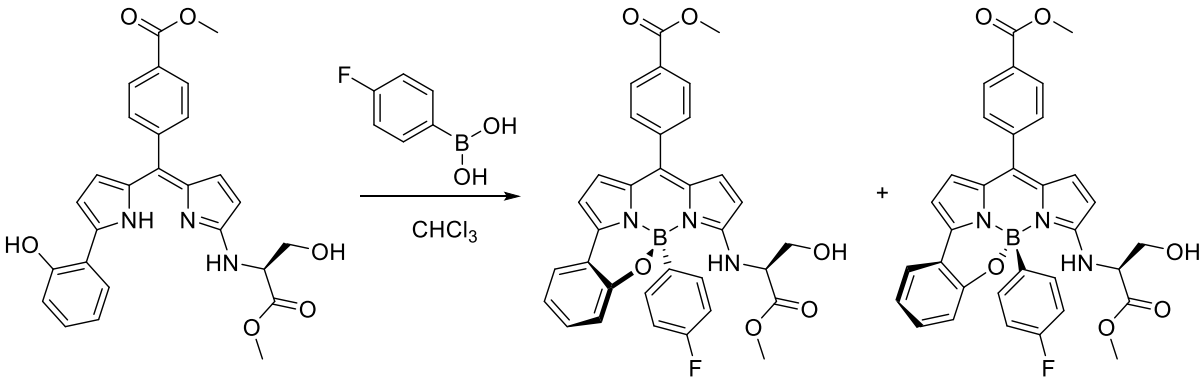

4.36 **4.37 (*S*,*P*)** **4.27 (*S*,*M*)**

Entry	Temperature/°C	Yield/%	*de* before column	*de* after purification
1	-41	92	57	49
2	0	87	70	55
3	RT (25)	75	84	81
4	35	73	83	84
5	45	78	82	77
6	55	72	77	69
7	reflux	79	66	57

Table 4.9. Chelation of α–*ortho*–hydroxyphenyl-α-(*S*)-serinyl methyl ester dipyrromethene **4.36** with *para*-fluoro phenylboronic acid to synthesis *N,N,O,C*-5-(*S,P*)-serinyl methyl ester BODIPY and *N,N,O,C*-5-(*S,M*)-serinyl methyl ester BODIPY **4.27.**

Each crude reaction mixture was purified via silica gel column chromatography, isolating each *N,N,O,C*-5-(*S*)-serinyl methyl ester BODIPY diastereoisomer **4.37a** and **4.37b**. Therefore, the *de* of each reaction was also measured after purification by silica gel column chromatography, which showed the same trend as the pre-columned reactions, with diastereoisomer **4.37a** continuing to be the major diastereoisomer and **4.37b** being the minor. There was a small general decrease in the *de* of each reaction after purification, this can be attributed to a small amount of compound being lost on the column, and therefore the *de* measured from ^{19}F NMR integration is a truer representation of diastereocontrol observed (Table 4.9, column 5).

As a means to further understand the reaction mechanism of this re-chelation step, *N,N,O,C*-5-(*S*)-serinyl methyl ester BODIPY diastereoisomer **4.37a** was re-exposed to the re-chelation reaction conditions to test for epimerisation.

Therefore, *N,N,O,C*-5-(*S*)-serinyl methyl ester BODIPY **4.37a** was dissolved in $CHCl_3$, stirred at room temperature for 20 mins and then a solution of *para*-fluorophenyl boronic acid was added dropwise over 5 mins. This was then immediately quenched with water and subjected to an aqueous work-up. After an aqueous work-up, the product was analysed by ^1H NMR, showing no interconversion to the other diastereoisomer **4.37b**, showing that no epimerisation occurred under these conditions.

4.2.7.1 Crystal structures of helically chiral *N,N,O,C*-5-(*S*)-serinyl methyl ester BODIPY **4.37a** and **4.37b** and *N,N,O,C*-5-(*R*)-serinyl methyl ester BODIPY **4.23a** and **4.23b**

The relative stereochemistry of each of the *N,N,O,C*-5-(*R*)-serinyl methyl ester BODIPY diastereoisomers **4.23a** and **4.23b** and *N,N,O,C*-5-(*S*)-serinyl methyl ester BODIPY diastereoisomers **4.37a** and **4.37b** could not be determined by NMR analysis. Therefore, as a means to determine the absolute and relative stereochemistry, single crystal growth for both the major and minor diastereomer from each of the *N,N,O,C*-5-(*R*)-serinyl methyl ester BODIPYs **4.23** and *N,N,O,C*-5-(*S*)-serinyl methyl ester BODIPYs **4.37** was attempted through slow evaporation in a range of solvents (DCM, $CHCl_3$, MeOH) for single crystal X-ray analysis. Unfortunately, all attempts at crystallisation through slow evaporation was unsuccessful therefore, alternative methods for crystallization were attempted.

Further attempts to crystallise each of the major and minor diastereomer from each of the *N,N,O,C*-5-(*R*)-serinyl methyl ester BODIPYs **4.23** and *N,N,O,C*-5-(*S*)-serinyl methyl ester BODIPYs **4.37** were undertaken via encapsulated nanodroplet crystallisation (ENaCt) by Elle Watson. ENaCt uses a SPTLabtech Mosquito liquid handling robot, using solutions of *N,N,O,C*-5-(*R*)-serinyl methyl ester BODIPYs **4.23a** and **4.23b** and *N,N,O,C*-5-(*S*)-serinyl methyl ester BODIPYs **4.37a** and **4.37b** in twelve different solvents, namely DMSO, DMF, MeOH, HFIP, toluene, DCE, ethyl acetate, MTBE, 2-MeTHF, MeCN, MIBK and nitromethane. 50 nL droplets of each

solution is transferred onto a 96 well plate, containing encapsulating oils, and samples allowed to crystallise over 14 days.[107]

The major diastereomer of *N,N,O,C-(R)*-5-Serinyl methyl ester BODIPY **4.23a** was successfully crystallised via encapsulated nanodroplet crystallisation in DMSO, forming single crystals suitable for X-ray diffraction. A suitable single crystal was submitted for single X-ray analysis, confirming the single crystal X-ray structure of *N,N,O,C*-5-serinyl methyl ester BODIPY (Figure 4.9).

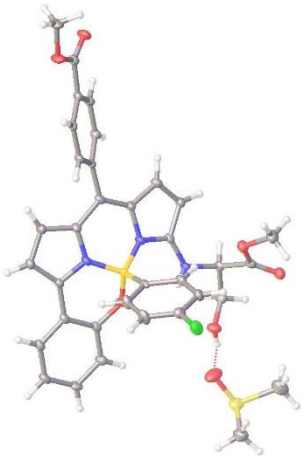

Figure 4.9. Single crystal X-ray structure of rac-*N,N,O,C*-5-(*R*,*M*)-serinyl methyl ester BODIPY and *N,N,O,C*-5-(*S*,*P*)-serinyl methyl ester BODIPY **4.23a** and **4.37a** respectively.

The crystal structure shows that *N,N,O,C-(R)*-5-serinyl methyl ester BODIPY **4.23a** crystallised as a solvate with DMSO. Further analysis of the crystal structure data showed the space group to be P-1, this indicates that the unit cell has an inversion centre. For an inversion centre to exist in the unit cell, an equal amount of each stereoisomer must be present in the crystal. Therefore, this means the unit cell contains a racemic mixture of *N,N,O,C*-5-(*R,M*)-serinyl methyl ester BODIPY **4.23a** and *N,N,O,C*-5-(*S,P*)-serinyl methyl ester BODIPY **4.37a**. It is postulated that this racemic mixture has occurred through racemisation of the chiral directing group, likely in the de-chelation step, and that the crystal has formed from the small quantities of *N,N,O,C*-5-(*S,P*)-serinyl methyl ester BODIPY **4.37a** preferentially crystallising with the major *N,N,O,C*-5-(*R,M*)-serinyl methyl ester component **4.23a**. Thus, although this crystal structure validates that we have successfully synthesised helically chiral compounds, this single crystal X-ray structure cannot be used to determine the absolute stereochemistry of *N,N,O,C-(R)*-5-serinyl methyl ester

BODIPY **4.23** crystallised in this case. However, the crystal structure does allow assignment of relative stereochemistry, the major isomers being *N,N,O,C*-5-(*R,M*)-serinyl methyl ester BODIPY **4.23a** and *N,N,O,C*-5-(*S,P*)-serinyl methyl ester BODIPY **4.37a**. Therefore, this allows the assignment of absolute stereochemistry as the R/S centres are known and by extrapolation the absolute stereochemistry of the minor diastereomers can be assigned (Table 4.10).

Helically chiral BODIPY	Absolute stereochemistry
4.23a (major)	*RM*
4.23b (minor)	*RP*
4.37a (major)	*SP*
4.37b (minor)	*RM*

Table 4.10. Absolute stereochemistry of each *N,N,O,C-(R)*-5-serinyl methyl ester BODIPYs **4.23a** and **4.23b** and *N,N,O,C-(S)*-5-serinyl methyl ester BODIPY **4.37a** and **4.37b**.

4.2.7.2 Measurements of enantiomeric excess of each synthesised *N,N,O,C*-5-serinyl methyl ester BODIPY **4.23a**, **4.23b**, **4.37a** and **4.37b**

Next the enantiopurity of each of the synthesised helically chiral *N,N,O,C*-5-(*R,M*)-serinyl methyl ester BODIPY **4.23a**, *N,N,O,C*-5-(*R,P*)-serinyl methyl ester BODIPY **4.23b**, *N,N,O,C*-5-(*SP*) serinyl methyl ester BODIPY **4.37a** and *N,N,O,C*-5-(*SR*)-serinyl methyl ester BODIPY **4.37b** were examined through chiral HPLC.

N,N,O,C-5-(*R,M*)-serinyl methyl ester BODIPY **4.23a** is an enantiomer of *N,N,O,C*-5-(*S,P*)-serinyl methyl ester BODIPY **4.37a** and *N,N,O,C*-5-(*R,P*)-serinyl methyl ester BODIPY **4.23b** is an enantiomer of *N,N,O,C*-5-(*S,M*)-serinyl methyl ester BODIPY **4.37b**. Therefore, because each set of diastereoisomers are enantiomers of each other, a comprehensive study into their enantiopurity could be undertaken. This was achieved by running chiral HPLC measurements of a 1:1 mixture of each set of enantiomers as well as each enantiomer singularly. Each single enantiomer spectra could then be integrated to calculate the relative amount of interconversion of the chiral centre had occurred (see section 6.4).

The enantiomeric excess (*ee*) of all 4 helically chiral *N,N,O,C*-5-serinyl methyl ester BODIPY compounds **4.23a**, **4.23b**, **4.37a** and **4.37b** were measured by submitting each of the diastereoisomers to chiral HPLC conditions (Table 4.11).

Helically Chiral BODIPY	***ee***
4.23a (*R,M*) major	97%
4.23b (*R,P*) minor	96%
4.37a (S,*P*) major	98%
4.37b (S,*M*) minor	99%

Table 4.11. *ee* of each isolated helically chiral *N,N,O,C*-5-serinyl methyl ester BODIPY compounds **4.23a**, **4.23b**, **4.37a** and **4.37b**.

Each diastereoisomer showed high *ee*, indicating retention of the point-chiral serinyl group. It is therefore interesting that *N,N,O,C*-5-(*R,M*)-serinyl methyl ester BODIPY **4.23a** crystallised as a racemic mixture of two enantiomers, even though the racemic component *N,N,O,C*-5-(*S,P*)-serinyl methyl ester BODIPY **4.37a** was only present in minimal amounts. However single crystal X-ray diffraction does not provide information on the bulk sample.

4.3 Chiroptical properties of helically chiral BODIPYs

Once chiral HPLC had confirmed that we had enantiopure samples of each pair of diastereoisomers, their chiroptical properties could be measured, namely their CPL and EDC spectra.

4.3.1 CPL spectroscopy of *N,N,O,C*-5-serinyl methyl ester BODIPYs **4.23a**, **4.23b**, **4.37a** and **4.37b**

Measurement of the CPL spectra of each helically chiral *N,N,O,C*-5-(*R,M*)- **4.23a**, *N,N,O,C*-5-(*R,P*)- **4.23b**, *N,N,O,C*-5-(*S,P*)- **4.37a** and *N,N,O,C*-5-(*S,M*)- methyl ester BODIPY **4.37b** was undertaken. CPL measurements were ran by Dr Patrycja Brook at Durham University. Unfortunately, no observed CPL signal was seen for any of the synthesised helically chiral BODIPY compounds, due to low emission intensities.

Typically, for compounds to produce a CPL output they must have a rigid structure. The synthesised helically chiral *N,N,O,C*-5-serinyl methyl ester BODIPYs **4.23a**, **4.23b**, **4.37a** and **4.37b** each contain a free rotating serinyl methyl ester group,

therefore we postulate that this substituent has resulted in a decrease fluorescence quantum yields and thus low CPL emission. Due to the lack of measurable CPL signals, calculations of *N,N,O,C*-5-serinyl methyl ester BODIPYs **4.23a**, **4.23b**, **4.37a** and **4.37b** g_{lum} values could not be achieved. This was an unsurprising result as the fluorescence quantum yields of each of the final helically chiral compounds were low (Table 4.12. ϕ_F of each isolated helically chiral N,N,O,C-5-serinyl methyl ester BODIPY compounds **4.23a, 4.23b, 4.37a** and **4.37b.**

Helically Chiral BODIPY	ϕ_F
4.23a	0.06
4.23b	0.04
4.37a	0.02
4.37b	0.03

Table 4.12. ϕ_F of each isolated helically chiral N,N,O,C-5-serinyl methyl ester BODIPY compounds **4.23a**, **4.23b**, **4.37a** and **4.37b**.

4.3.2 ECD spectroscopy of *N,N,O,C*-5-serinyl methyl ester BODIPYs **4.23a**, **4.23b**, **4.37a** and **4.37b**

Next ECD spectra of all 4 helically chiral *N,N,O,C*-5-serinyl methyl ester BODIPYs **4.23a**, **4.23b**, **4.37a** and **4.37b** were measured by Prof. Herrebout and Jonathan Bogaerts at the University of Antwerp. Each pair of enantiomeric helically chiral BODIPYs showed mirror image spectra (Figure 4.10).

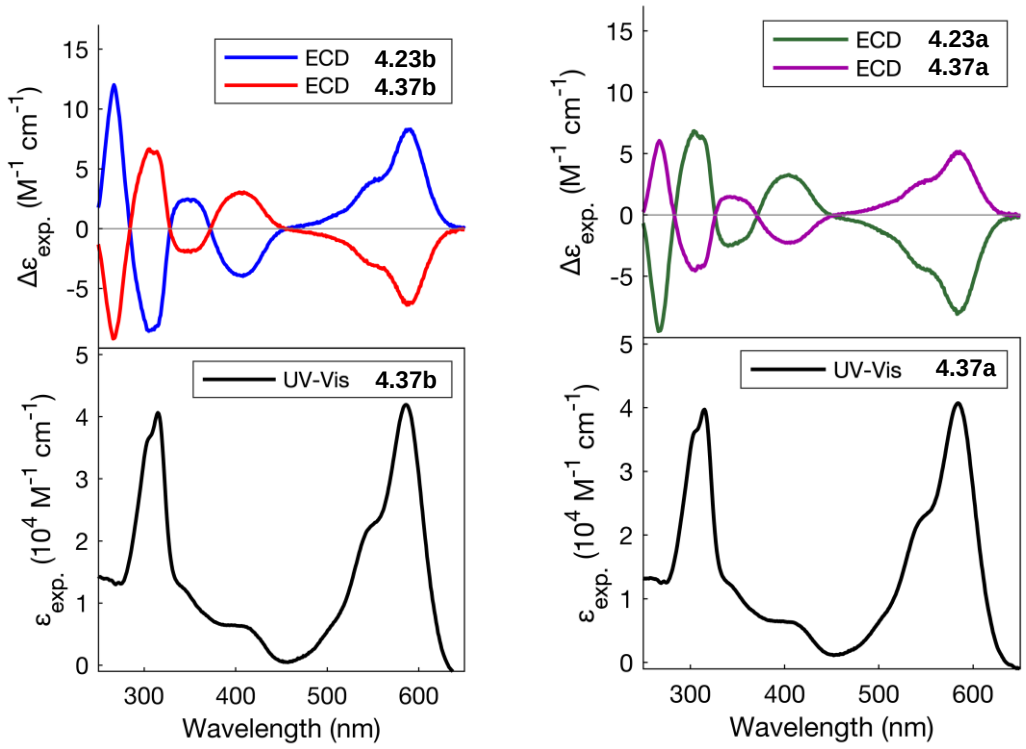

Figure 4.10. A) red and blue = ECD spectra of BODIPY **4.37b** and **4.23b** respectively, enantiomers of each other. Black = UV-Vis of BODIPY **4.37b**. B) purple and green = ECD spectra of BODIPY **4.37a** and **4.23a** respectively, enantiomers of each other. Black = UV-Vis of BODIPY **4.37a**.

The team of Prof Herrebout, also attempted to calculate the ECD spectra of each *N,N,O,C*-5-serinyl methyl ester BODIPY **4.23a**, **4.23b**, **4.37a** and **4.37b** via TD-DFT calculations. Through comparisons of the theoretical ECD spectrum and the experimental ECD spectrum, the absolute stereochemistry of each enantiomer of each diastereotopic helically chiral BODIPY **4.23a**, **4.23b**, **4.37a** and **4.37b** can be assigned in the future. We are currently awaiting results of these calculations, and then will be able to assign the absolute stereochemistry of each *N,N,O,C*-5-serinyl methyl ester BODIPY **4.23a**, **4.23b**, **4.37a** and **4.37b** via ECD measurements and confirm our crystallographic assignments.

4.4 Conclusion

In this chapter we have successfully synthesised novel helically chiral BODIPY compounds, being the first reported example of point-to-helical control within a BODIPY system. We have shown that the stereochemistry of the chiral directing group is retained throughout the reaction sequence. Furthermore point-to-helical control is demonstrated in the synthesis of helically chiral *N,N,O,C*-5-serinyl methyl ester BODIPY showing fantastic *de* of up to 84% (Figure 4.11).

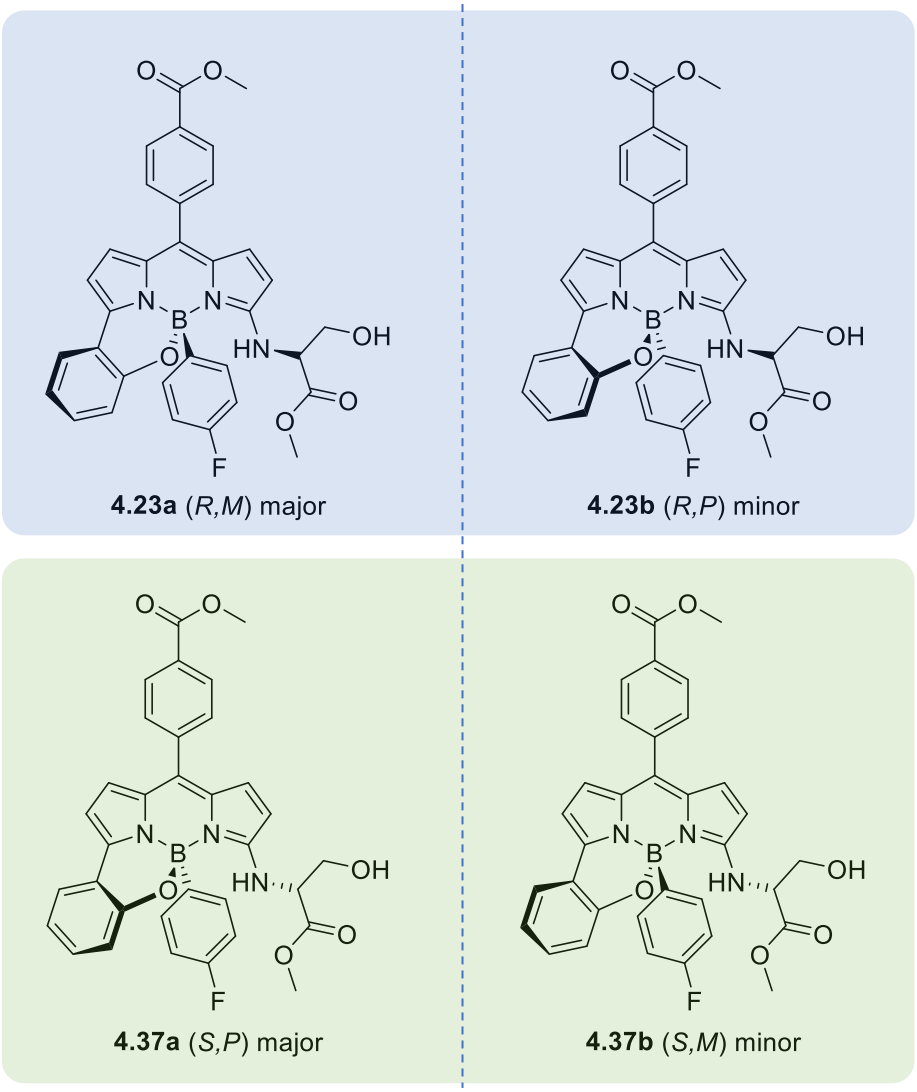

Figure 4.11. blue = two diastereoisomers *N,N,O,C*-5-(*R,M*)-serinyl methyl ester BODIPY **4.23a** and diastereoisomers *N,N,O,C*-5-(*R,P*)-serinyl methyl ester BODIPY **4.23b** synthesised from (*R*)-serine methyl ester point chiral group. Green = two diastereoisomers *N,N,O,C*-5-(*S,P*)-serinyl methyl ester BODIPY **4.37a** and *N,N,O,C*-5-(*S,M*)-serinyl methyl ester BODIPY **4.37b** synthesised from (*S*)-serine methyl ester point chiral group. Each column shows enantiomers of each other.

Mirror image ECD spectra were obtained for the pairs of enantiomers, and this will be used for future confirmation of absolute stereochemistry. We have shown a new point-to-helical control approach, which could be used in future designs of BODIPY systems. Although our synthesised helically chiral BODIPYs do not exhibit CPL, future systems can be designed with CPL emission as part of the design.

Chapter 5 Conclusions and Future Work

This thesis has resulted in the development of synthetic routes to a set of 3,5-dihalo BODIPYs, including the 3,5-chloro **2.13a-f**, 3,5-dibromo **2.14a-d** and 3,5-diiodo BODIPYs **3.17a-d**. We have shown a significant improvement in published routes to 3,5-dichloro BODIPYs, showing that optimisation of this ONSH with chloride reaction was possible through the addition of a copper chelating ligand and alternative copper sources, resulting in yields of up to 99%.[74] A novel synthesis of 3,5-diiodo BODIPYs **3.17a-d** was developed, providing access to previously unobtainable 3,5-diiodo BODIPY architectures. This involved conversion of the 3,5-dichloro **2.13a-d** and 3,5-dibromo **3.14a-d** counterparts via an aromatic Finkelstein reaction with NaI. This aromatic Finkelstein reaction allowed access to a wide range of novel 3,5-diiodo BODIPYs in up to quantitative yields, which were shown to be excellent coupling partners in Pd cross-coupling reactions.[87]

Finally using the newly synthesised 3,5-diiodo BODIPYs, we devised a synthetic route to helically chiral BODIPYs. This route involved the introduction of a chiral directing group in the form of serine methyl ester, a Suzuki cross-coupling of *ortho*-hydroxyphenyl boronic acid, then a final de-chelation/re-chelation of the boron centre, resulting in an *in-situ* ring closure between the boron and the oxygen on the *ortho*-hydroxyphenyl group. This formed two sets of diastereomeric helically chiral BODIPYs, firstly *N,N,O,C*-5-(*R,M*)-serinyl methyl ester BODIPY **4.23a** and *N,N,O,C*-5-(*S,P*)-serinyl methyl ester BODIPY **4.37a**, and secondly *N,N,O,C*-5-(*R,P*)-serinyl methyl ester BODIPY **4.23b** and *N,N,O,C*-5-(*S,M*)-serinyl methyl ester BODIPY **4.37b**. Due to the presence of the serine methyl ester group, the helicity formed in the final re-chelation step was diastereomerically controlled, showing *de* up to 84%. This was a fantastic result, being the first case of point-to-helical chirality control in BODIPY structures.

There are a number of future projects that could be explored based on this thesis. The first, simplest project would be the examination of alternative chiral directing groups as a means to enhance the observed *de* of the final helically chiral BODIPYs.

More interestingly, alternative helically chiral systems could be synthesised, with the focus directed towards more rigid structures through double ring formation at the

boron centre of the BODIPY. It is thought that the increased rigidity of such structures could result in higher fluorescence quantum yield and therefore CPL.

One proposed structure would be the synthesis of *N,N,O,O* BODIPY **5.1**, in which chelation at the boron is achieved not only through hydroxyphenyl ring but also through the serine chiral directing group. As discussed previous in our synthesis of helically chiral serine BODIPYs, we postulated that serine methyl ester goes through a 7-membered transition state, enhancing diastereomeric control. If this hypothesis is true, the synthesis of *N,N,O,O* BODIPY **5.1** should be possible (Figure 5.1).

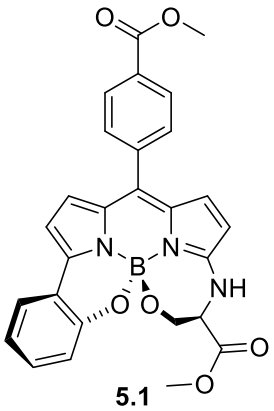

Figure 5.1. Proposed *N,N,O,O* BODIPY **5.1**, exhibiting double ring closure.

The synthesis of *N,N,O,O* BODIPY **5.1** could be achieved through the treatment of its α-*ortho*-hydroxyphenyl-α-(*R*)-serinyl methyl ester dipyrromethene **4.26** counterpart with $BF_3.OEt_2$. If the synthesis of *N,N,O,O* BODIPY **5.1** could be achieved, it is expected to be more emissive of CPL than our synthesised helically chiral *N,N,O,C-5*-serinyl methyl ester BODIPYs **4.23a**, **4.23b**, **4.37a** and **4.37b**.

If the synthesis of the above *N,N,O,O* BODIPY **5.1** proved successful, showing the formation of a 7-membered ring, further investigation into alternative BODIPY systems exhibiting this ring could be undertaken. Typically in literature, S_NAr reactions undertaken on 3,5-dihalo BODIPYs show a single substitution, however under more forcible conditions (higher temperature and longer reaction times), double addition has been reported. Therefore, the synthesis of 3,5-diserinyl methyl ester BODIPY **5.2** is possible. This doubly substituted BODIPY could undergo a de-chelation/re-chelation using methods discussed in this chapter, resulting in *N,N,O,O* BODIPY **5.3** (Figure 5.2).

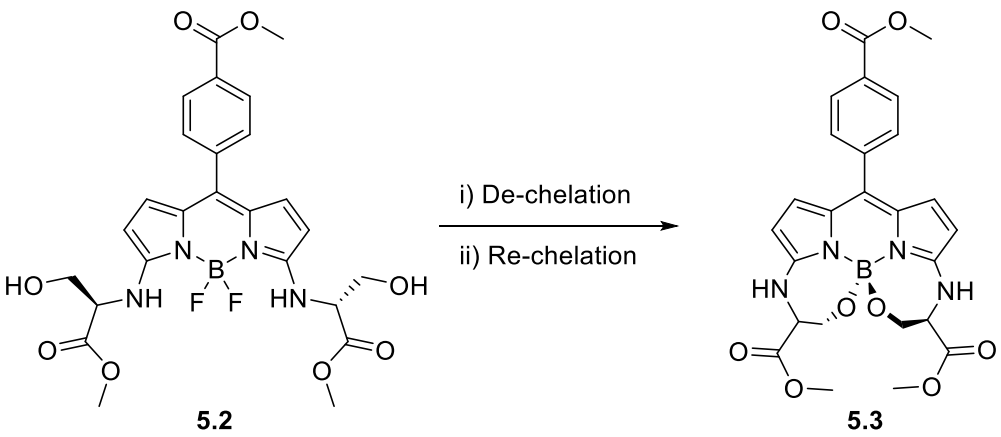

Figure 5.2. Proposed synthesis of *N,N,O,O* BODIPY **5.3**, synthesised via double S_NAr chemistry.

It is thought that the synthesis of *N,N,O,O* BODIPY **5.3** could be carried out with considerable levels of point-to-helical stereocontrol, through the use of enantiomerically pure *(R)*-serine methyl ester. This interesting chiral BODIPY architecture could then be investigated for CPL properties.

Chapter 6 Experimental Procedures and Characterisation

6.1 General experimental information

6.1.1 Analysis

^{1}H, ^{13}C, ^{11}B and ^{19}F NMR spectra were recorded directly with a Bruker Advance III HD 700 MHz, Jeol Lambda 500 MHz, Jeol ECS-400 MHz or Brucker Avance 300 MHz. HRMS data was provided by the EPSRC National Mass Spectrometry Service (University of Swansea). IR spectra were obtained as neat samples using a Varian 800 FT-IR Scimitar Series spectrometer scanning from 4000-600 cm^{-1}. UV-Vis spectra were obtained using a UV-1800 Shimadzu UV spectrophotometer scanning from 300 – 700 nm. Fluorescence quantum yield spectra were obtained using Shimadzu RF-6000 spectrofluorophotometer. Fluorescence quantum yield data was obtained against a standard reference of either Rhodamine 6G or Cresyl violet, 99% pure, laser grade.

6.1.2 Procedures

Standard Schlenk techniques were used for all air sensitive reactions, under a nitrogen atmosphere. Solvents were dried over activated molecular sieves and used directly. Manual column chromatography was performed using Geduran silicagel 60 (40-63 μm)

6.2 Experimental Procedures and Characterisation Data

6.2.1 Chapter 2

6.2.1.1 Methyl 4-(di(1*H*-pyrrol-2-yl)methyl)benzoate **2.7a** [69]

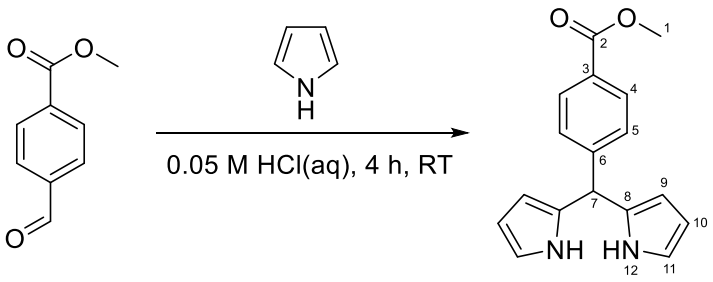

To a 250 mL round bottom flask was added an aqueous solution of HCl (0.05 M, 100 mL, 5 mmol), pyrrole (2.34 mL, 33 mmol) and methyl 4-formylbenoate (1.85 g, 11.3 mmol). The reaction was stirred, opened to air, for 4 hours at room temperature, forming a light pink precipitate over time. The light pink precipitate was filtered and the solid was washed with water (25 mL) and petroleum ether (50 mL). The crude product was purified through silica gel column chromatography (DCM) to give methyl 4-(di(1*H*-pyrrol-2-yl)methyl)benzoate (2.79 g, 9.95 mmol, 88%) as a pale yellow solid.

Rf: 0.56 (DCM). **Mp:** 162 – 164 ^{o}C [lit. 162.1 – 162.7 ^{o}C]. **IR** (neat): ν_{max}/cm^{-1} 3335 (N-H, w), 1703 (C=O, w). **HRMS:** (pNSI) calcd for $C_{17}H_{16}N_2O_2$ $[M+H]^+$: 281.1285, found 281.1288. **^{1}H NMR** (300 MHz, Chloroform-*d*) δ 7.98 (m*, *J* = 8.39 Hz, 4H, *H^4*, *H^{12}*), 7.29 (d, *J* = 8.04 Hz, 2H, *H^5*), 6.72 (d, *J* = 1.5 Hz, 2H, *H^{11}*), 6.17 (m, 2H, *H^{10}*), 5.89 (m, 2H, *H^9*), 5.53 (s, 1H, *H^7*), 3.91 (s, 3H, *H^1*). **^{13}C NMR** (75 MHz, Chloroform-*d*) δ 167.0 (*C^2*), 147.5 (*C^3*), 131.7 (*C^8*), 130.1 (*C^4*), 128.6 (*C^6*), 128.4 (*C^5*), 117.7 (*C^{11}*), 108.7 (*C^{10}*), 107.7 (*C^9*), 52.3 (*C^1*), 44.1 (*C^7*).

*doublet corresponding to *H^4* with multiplet underneath corresponding to *H^{12}*.

6.2.1.2 Methyl (Z)-4-((1*H*-pyrrol-2-yl)(2*H*-pyrrol-2-ylidene)methyl)benzoate **2.8a** [8]

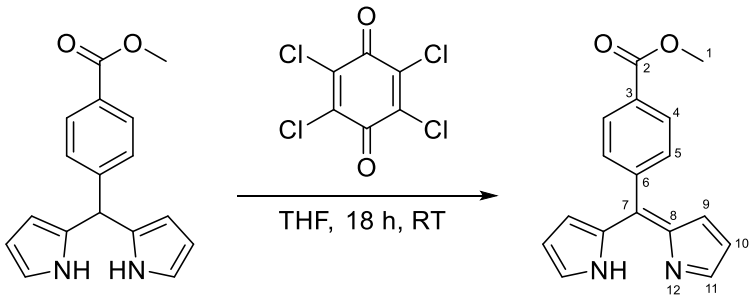

To a 250 mL round bottom flask under nitrogen, was added methyl 4-(di(1*H*-pyrrol-2-yl)methyl)benzoate (0.500 g, 1.78 mmol), THF (5 mL, 61.6 mmol) and *p*-chloranil (0.482 g, 1.96 mmol). The reaction was stirred overnight at room temperature, diluted with DCM (40 mL) and quenched with saturated $Na_2SO_{3\ (aq)}$. The organic layer was washed with brine (25 mL) and water (2 x 25 mL), dried over Na_2SO_4, filtered and the solvent was removed under reduced pressure to give a dark green solid. The crude product was purified through silica gel column chromatography (DCM) to give methyl (Z)-4-((1*H*-pyrrol-2-yl)(2*H*-pyrrol-2-ylidene)methyl)benzoate (0.383 g, 1.37 mmol, 77%) as a dark green solid.

Rf: 0.24 (DCM). **Mp:** 129 - 131 °C [lit. 130 – 130.1 °C]. **IR** (neat): ν_{max}/cm^{-1} 3356 (N-H, w), 1703 (C=O, m) 1571 (C=C, m). **HRMS:** (pNSI) calcd for $C_{17}H_{15}N_2O_2$ $[M+H]^+$: 279.1130, found 279.1128. **^{1}H NMR** (300 MHz, Chloroform-*d*) δ 8.12 (td, *J* = 8.4, 1.7 Hz, 2H, *H*^{4}), 7.71 (t, *J* = 1.3 Hz, 2H, *H*^{11}), 7.57 (td, *J* = 8.3, 1.6 Hz, 2H, *H*^{5}), 6.55 (dd, *J* = 4.2, 1.1 Hz, 2H, *H*^{9}), 6.42 (dd, *J* = 4.3, 1.5 Hz, 2H, *H*^{10}), 3.98 (s, 3H, *H*^{1}). **^{13}C NMR** (75 MHz, Chloroform- *d*) δ 166.4 (C^2), 143.8 (C^{11}), 141.5 (C^3) 140.7 (C^8), 139.5 (C^8), 130.5 (C^7), 130.4 (C^5), 128.8 (C^9), 128.6 (C^4), 117.7 (C^{10}), 52.1 (C^1).

6.2.1.3 Methyl 4-(5,5-difluoro-5*H*-4λ^4,5λ^4-dipyrrolo[1,2-c:2',1'-*f*][1,3,2] diazaborinin-10-yl)benzoate **2.11a** [8]

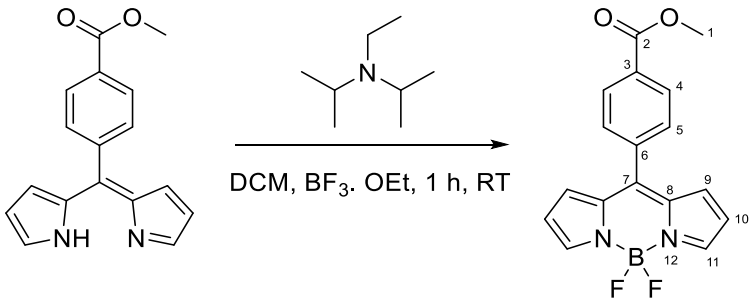

To a 100 mL round bottom flask, under nitrogen atmosphere, was added methyl (Z)-4-((1*H*-pyrrol-2-yl)(2*H*-pyrrol-2-ylidene)methyl)benzoate (0.5304 g, 1.91 mmol), DCM (10 mL), N,N-diisopropylethylamine (0.92 mL, 5.27 mmol) and $BF_3.OEt_2$ (0.52 mL, 4.23 mmol). The reaction was stirred for 1 hour at room temperature and diluted with DCM (50 mL). The organic layer was washed with 0.1 M NaOH $_{(aq)}$ (100 mL), 0.1 M HCl $_{(aq)}$ (100 mL) and water (100 mL), dried over Na_2SO_4, filtered and the solvent was removed under reduced pressure to give a dark red solid. The crude product was purified through silica gel column chromatography (DCM) to give methyl 4-(5,5-difluoro-5*H*-4λ^4,5λ^4-dipyrrolo[1,2-c:2',1'-*f*][1,3,2]diazaborinin-10-yl)benzoate (0.229 g, 0.707 mmol, 37%) as a red solid.

Rf: 0.49 (DCM). **Mp:** 102-104 ^oC [lit. 202 ^oC]. **IR** (neat): ν_{max}/cm^{-1} 1719 (C=O, m) 1507 (C=C, m) 1288. **HRMS:** (pNSI) calcd for $C_{17}H_{13}BF_2N_2O_2$ $[M+H]^+$: 307.1057, found 307.1059. **^{1}H NMR** (300 MHz, Chloroform-*d*) δ 8.20 (td, *J* = 8.6, 2.0 Hz, 2H, *H^4*), 7.97 (s, 2H, H*^{11}*), 7.65 (td, *J* = 8.6, 1.9 Hz, 2H, *H^5*), 6.89 (d, *J* = 4.3 Hz, 2H, *H^9*), 6.58 (d, *J* = 3.7 Hz, 2H, *H^{10}*), 3.99 (s, 3H, *H^1*).**^{13}C NMR** (75 MHz, Chloroform- *d*) δ 166.0 (C*^{2}*), 145.5 (C*^{11}*), 144.5 (C*^{3}*) 137.7 (C*^{8}*), 134.4 (C*^{8}*), 131.9 (C*^{7}*), 131.1 (C*^{5}*), 130.1 (C*^{9}*), 129.3 (C*^{4}*), 118.6 (C*^{10}*), 52.3 (C*^{1}*). **^{11}B NMR** (96 MHz, Chloroform-*d*) δ 0.25 (t, *J* = 28.8 Hz). **^{19}F NMR** (282 MHz, Chloroform-*d* δ -145.05 (q, *J* = 57.2, 28.6 Hz). **UV-Vis:** λ_{max} = 505 nm (DCM). **Molar extinction coefficient (ε)** = 51000 M^{-1} cm^{-1}

6.2.1.4 Methyl 4-(3,7-dichloro-5,5-difluoro-5*H*-4λ^4,5λ^4-dipyrrolo[1,2-*c*:2',1'-*f*][1,3,2]diazaborinin-10-yl)benzoate **2.13a** [72]

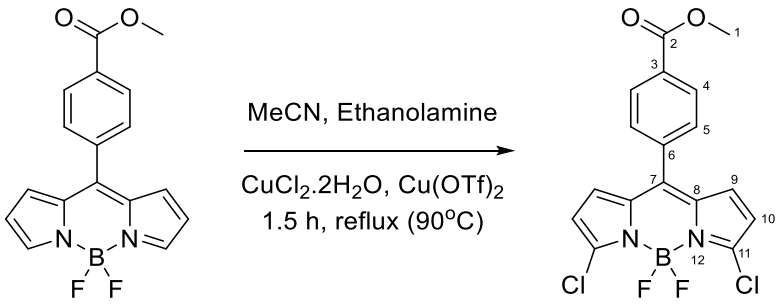

To a 100 mL round bottom flask was added methyl 4-(5,5-difluoro-5*H*-4λ^4,5λ^4-dipyrrolo[1,2-c:2',1'-*f*][1,3,2]diazaborinin-10-yl)benzoate (50 mg, 0.15 mmol), MeCN (4 mL), ethanolamine (18.75 µl, 0.31 mmol) and $Cu(OTF)_2$ (0.278 g, 0.77 mmol). The reaction mixture was heated to reflux (90 °C) and $CuCl_2.2H_2O$ was added (0.113 g, 0.77 mmol). The reaction was stirred for 1.8 hours, left to cool to room temperature (15 mins) and diluted with DCM (25 mL). The organic layer was washed with H_2O (3 x 10 mL), dried over Na_2SO_4, filtered and the solvent was removed under reduced pressure to give a dark red solid. The crude product was purified through silica gel column chromatography (4:1 petrol : ethyl acetate) to give methyl 4-(3,7-dichloro-5,5-difluoro-5*H*-4λ^4,5λ^4-dipyrrolo[1,2-*c*:2',1'-*f*][1,3,2]diazaborinin-10-yl)benzoate (60.2 mg, 0.15 mmol, 99%) as a red/pink solid.

Rf: 0.29 (Petrol:ethyl acetate 4:1). **Mp:** 221-222 °C. **IR (neat):** ν_{max}/cm^{-1} 1720 (C=O, m), 1534 (C=C, m). **HRMS:** (pNSI) calcd for $C_{17}H_{11}N_2O_2BF_2Cl_2$ $[M+H]^+$: 395.0332, found 395.0333. **^{1}H NMR** (400 MHz, Chloroform-*d*) δ 8.12 (td, *J* = 8.6, 1.9 Hz, 2H, *H*^{4}), 7.50 (td, *J* = 8.6, 2.0 Hz, 2H, *H*^{5}), 6.72 (dd, *J* = 4.4, 1.1 Hz, 2H, *H*^{9}), 6.38 (dd, *J* = 4.4, 0.9 Hz, 2H, *H*^{10}), 3.92 (s, 3H, *H*^{1}). **^{13}C NMR** (75 MHz, Chloroform-*d*) δ 165.9 (*C*^{2}), 145.6 (*C*^{11}), 142.1 (*C*^{6}), 136.4 (*C*^{3}), 133.4 (*C*^{8}), 132.2 (*C*^{7}), 131.2 (*C*^{9}), 130.2 (*C*^{5}), 129.5 (*C*^{4}), 119.1 (*C*^{10}), 52.4 (*C*^{1}). **^{11}B NMR** (96 MHz, Chloroform-*d*) δ 0.47 (t, *J* = 28.5 Hz).**^{19}F NMR** (282 MHz, Chloroform-*d*) δ -148.19 (q, *J* = 55.5, 27.7 Hz). **UV-Vis:** λ_{max} = 515 nm (DCM). **Molar extinction coefficient (ε)** = 39000 M^{-1} cm^{-1}. **ϕ_F:** 0.189 (DCM)

6.2.1.5 Methyl 4-(3,7-dichloro-5,5-difluoro-5*H*-4λ^4,5λ^4-dipyrrolo[1,2-*c*:2',1'-*f*][1,3,2]diazaborinin-10-yl)benzoate **2.13a** [72]

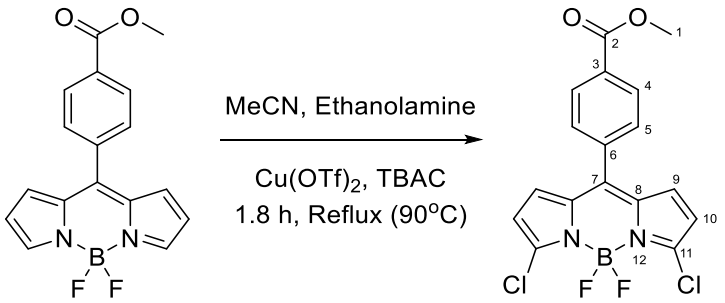

To a 100 mL round bottom flask was added methyl 4-(5,5-difluoro-5*H*-4λ^4,5λ^4-dipyrrolo[1,2-c:2',1'-*f*][1,3,2]diazaborinin-10-yl)benzoate (50 mg, 0.15 mmol), MeCN (4 mL), ethanolamine (18.75 μl, $Cu(OTf)_2$ (0.556 g, 1.53 mmol) and TBAC (0.213 g, 0.765 mmol). The reaction was heated to reflux (90°C) and stirred for 1h 50 mins, left to cool to room temperature (15 mins) and diluted with DCM (25 mL). The organic layer was washed with water (3 x 10 mL), was dried over Na_2SO_4, filtered and the solvent was removed under reduced pressure to give a dark red solid. The crude product was purified through silica gel column chromatography (4:1 petrol:ethyl acetate) to give methyl 4-(3,7-dichloro-5,5-difluoro-5*H*-4λ^4,5λ^4-dipyrrolo[1,2-*c*:2',1'-*f*][1,3,2]diazaborinin-10-yl)benzoate (58 mg, 0.15 mmol, 96%) as a red/pink solid.

Rf: 0.29 (Petrol:ethyl acetate 4:1). **Mp:** 221-222 °C. [lit. 219-220 °C]. **IR (neat):** ν_{max}/cm^{-1} 3120-2950 (C-H, w) 1717 (C=O, s). **HRMS:** (pNSI) calcd for $C_{17}H_{11}N_2O_2BF_2Cl_2$ $[M+H]^+$: 295.0332, found 295.0333. **^{1}H NMR** (400 MHz, Chloroform-*d*) δ 8.12 (td, *J* = 8.6, 1.9 Hz, 2H, *H*^{4}), 7.50 (td, *J* = 8.6, 2.0 Hz, 2H, *H*^{5}), 6.72 (dd, *J* = 4.4, 1.1 Hz, 2H, *H*^{9}), 6.38 (dd, *J* = 4.4, 0.9 Hz, 2H, *H*^{10}), 3.92 (s, 3H, *H*^{1}). **^{13}C NMR** (75 MHz, Chloroform-*d*) δ 165.9 (*C*^{2}), 145.6 (*C*^{11}), 142.1 (*C*^{6}), 136.4 (*C*^{3}), 133.4 (*C*^{8}), 132.2 (*C*^{7}), 131.2 (*C*^{9}), 130.2 (*C*^{5}), 129.5 (*C*^{4}), 119.1 (*C*^{10}), 52.4 (*C*^{1}). **^{19}F NMR** (282 MHz, Chloroform-*d*) δ -148.19 (q, *J* = 55.5, 27.7 Hz). **^{11}B NMR** (96 MHz, Chloroform-*d*) δ 0.47 (t, *J* = 28.5 Hz).**UV-Vis:** λ_{max} = 515 nm (DCM). **Molar extinction coefficient (ε)** = 87000 $M^{-1}\,cm^{-1}$. **ϕ_F:** 0.189 (DCM)

6.2.2 General procedures for the synthesis of BODIPYs **2.11a-f** [72]

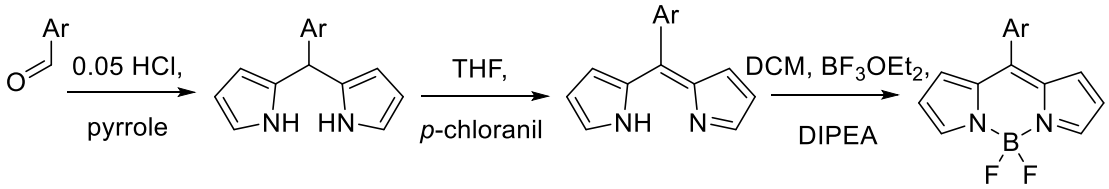

2.11(a-f)

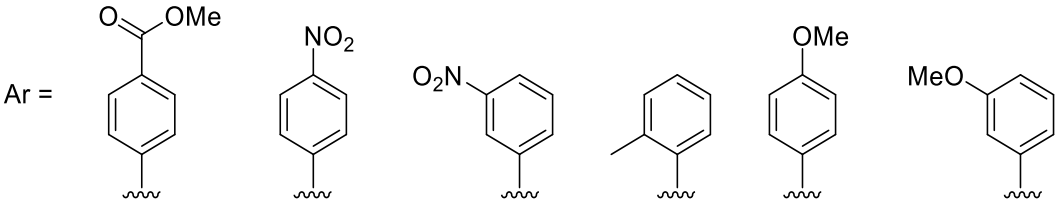

a **e** **b** **f** **c** **d**

To a 250 mL round bottom flask was added an aqueous solution of HCl (0.05 M, 50 mL per gram of aryl aldehyde), pyrrole (3 eq.) and then aryl aldehyde (**a-f**) (1 eq.) portion wise. The reaction mixture was stirred, open to air, for 4 hours at room temperature, resulting in the formation of a light yellow precipitate (**2.11a-b, 2.11e-f**) or a light yellow oil (**2.11c-d**). In the case of (**2.11a-b, 2.11e-f**), the precipitate was collected by filtration and washed with water (12.5 mL per gram of aryl aldehyde) and petroleum ether (25 mL per gram of aryl aldehyde). In the case of (**2.11a-b, 2.11e-f**), the reaction mixture was diluted with DCM (25 mL per gram of aryl aldehyde), washed with water (2 x 25 mL, per gram of aryl aldehyde), dried over solid Na_2SO_4, filtered and the solvent was removed under reduced pressure to give the crude dipyrromethanes as a yellow solid (**2.11a-b, 2.11e-f**) or yellow oil (**2.11c-d**). The crude dipyrromethanes were carried to the next step without further purification affording.

To a 250 mL round bottom flask under nitrogen, was added crude dipyrromethane (1 eq.), followed by THF (20 mL per gram of crude dipyrromethane) and then *p*-chloranil (1.1 eq.). The reaction mixture was stirred overnight at room temperature, diluted with DCM (40 mL per gram of crude dipyrromethane) and quenched with saturated $Na_2SO_{3\,(aq)}$. The organic layer was washed with brine (50 mL per gram of crude dipyrromethane) and water (2 x 25 mL per gram of crude dipyrromethane), dried over solid Na_2SO_4, filtered and the solvent was removed under reduced

pressure to give the crude dipyrromethenes as green solids. These were carried to the next step without further purification.

To a 100 mL round bottom flask, under nitrogen atmosphere, was added crude dipyrromethene (1 eq.), followed by DCM (10 mL per gram of crude dipyrromethene), *N,N*-diisopropylethylamine (2.8 eq.) and $BF_3.OEt_2$ (2.2 eq.). The reaction mixture was stirred for 1 hour at room temperature and then diluted with DCM (50 mL per gram of crude dipyrromethene). The organic layer was washed with 0.1 M $NaOH_{(aq)}$ (100 mL per gram of crude dipyrromethene), 0.1 M $HCl_{(aq)}$ (100 mL per gram of crude dipyrromethene) and water (100 mL per gram of crude dipyrromethene), dried over solid Na_2SO_4, filtered and the solvent was removed under reduced pressure to give the crude BODIPYs as dark red solids. These were purified by two silica gel column chromatography steps (1: DCM; 2: petroleum ether:ethyl acetate 4:1) to give BODIPYs **2.11a-f**.

6.2.2.1 Methyl 4-(5,5-difluoro-5*H*-4λ^4,5λ^4-dipyrrolo[1,2-c:2',1'-*f*][1,3,2]diazaborinin-10-yl)benzoate **2.11a**

Starting with methyl 4-formylbenzoate (2 g, 12.18 mmol) the desired product was obtained as a red solid (229 mg, 0.71 mmol, 25% over 3 steps).

Rf: 0.49 (DCM); **Mp:** 195-196 ^oC [lit. 202 ^oC][S1]; **IR** (neat): ν_{max}/cm^{-1} 3113 (C-H, w), 1712 (C=O, s); **HRMS:** (pNSI) calcd for $C_{17}H_{14}BF_2N_2O_2$ $[M+H]^+$: 307.1057, found 307.1059; **^{1}H NMR** (300 MHz, Chloroform-*d*) δ 8.19 (d, *J* = 8.5 Hz, 2H), 7.96 (s, 2H), 7.63 (d, *J* = 8.5 Hz, 2H), 6.88 (d, *J* = 4.2 Hz, 2H), 6.56 (d, *J* = 3.6 Hz, 2H), 3.98 (s, 3H); **^{13}C NMR** (75 MHz, Chloroform-*d*) δ 166.4, 145.0, 138.1, 134.9, 132.3, 131.6, 130.6, 129.7, 129.7, 119.1, 52.7; **^{11}B NMR** (96 MHz, Chloroform-*d*) δ 0.25 (t, *J* = 28.8 Hz); **^{19}F NMR** (282 MHz, Chloroform-*d*) δ -145.05 (q, *J* = 28.6 Hz).

6.2.2.2 5,5-Difluoro-10-(4-nitrophenyl)-5*H*-4λ^4,5λ^4-dipyrrolo[1,2-*c*:2',1'-*f*][1,3,2]diazaborinine **2.11e**

Starting with 4-nitrobenzaldehyde (2 g, 13.23 mmol) the desired product was obtained as a red solid (999 mg, 3.21 mmol, 24% over 3 steps).

Rf: 0.83 (DCM); **Mp:** 271-272 °C [lit. 277-278 °C][S3]; **IR** (neat): ν_{max}/cm^{-1} 3106 (C-H, m); **^{1}H NMR** (300 MHz, Chloroform-*d*) δ 8.41 (d, *J* = 8.7 Hz, 2H), 8.00 (s, 2H), 7.76 (d, *J* = 8.7 Hz, 2H), 6.85 (d, *J* = 4.2 Hz, 2H), 6.59 (d, *J* = 4.2 Hz, 2H); **^{13}C NMR** (75 MHz, Chloroform-*d*) δ 149.3, 145.7, 139.9, 134.7, 131.4, 131.3, 123.8, 119.6, 119.5; **^{11}B NMR** (96 MHz, Chloroform-*d*) δ 0.24 (t, *J* = 28.3 Hz); **^{19}F NMR** (282 MHz, Chloroform-*d*) δ -144.98 (q, *J* = 28.3 Hz).

6.2.2.3 5,5-Difluoro-10-(3-nitrophenyl)-5*H*-4λ^{4},5λ^{4}-dipyrrolo[1,2-*c*:2',1'-*f*][1,3,2]diazaborinine **2.11b**

Starting with 3-nitrobenzaldehyde (2 g, 13.23 mmol) the desired product was obtained as a red solid (111.8 mg, 0.36 mmol, 6% over 3 steps).

Rf: 0.43 (Petroleum ether:ethyl acetate 4:1); **Mp:** 146-147 °C; **IR** (neat): ν_{max}/cm^{-1} 3093 (C-H, m); **^{1}H NMR** (300 MHz, Chloroform-*d*) δ 8.52 – 8.36 (m, 2H), 8.00 (s, 2H), 7.90 (ddd, *J* = 7.7, 1.6, 1.2 Hz, 1H), 7.76 (td, *J* = 7.7, 1.0 Hz, 1H), 6.86 (d, *J* = 4.1 Hz, 2H), 6.59 (d, *J* = 4.1 Hz, 2H); **^{13}C NMR** (75 MHz, Chloroform-*d*) δ 145.7, 136.0, 135.3, 134.8, 134.8, 131.3, 129.9, 125.4, 125.1, 119.5, 119.5; **^{11}B NMR** (96 MHz, Chloroform-*d*) δ 0.25 (t, *J* = 28.4 Hz); **^{19}F NMR** (282 MHz, Chloroform-*d*) δ -144.91 (q, *J* = 28.4 Hz).

6.2.2.4 5,5-Difluoro-10-(*o*-tolyl)-5*H*-4λ^{4},5λ^{4}-dipyrrolo[1,2-*c*:2',1'-*f*][1,3,2]diazaborinine **2.11f**

Starting with 2-methylbenzaldehyde (1 g, 8.32 mmol) the desired product was obtained as an orange solid (118 mg, 0.42 mmol, 5% over 3 steps)

Rf: 0.11 (DCM); **Mp:** 181-182 °C; **IR** (neat): ν_{max}/cm^{-1} 2980 (C-H, m); **^{1}H NMR: (**300 MHz, Chloroform-*d*) δ 7.91 (s, 2H), 7.46 – 7.39 (m, 1H), 7.36 – 7.25 (m, 3H), 6.69 (d, *J* = 4.2 Hz, 2H), 6.48 (d, *J* = 4.2 Hz, 2H), 2.22 (s, 3H); **^{13}C NMR:** (75 MHz,

Chloroform-*d*) δ 146.7, 144.1, 136.1, 135.2, 132.7, 130.7, 130.2, 129.5, 129.4, 125.0, 118.3, 19.8; **^{11}B NMR** (96 MHz, Chloroform-*d*) δ 0.32 (t, *J* = 29.8 Hz); **^{19}F NMR** (282 MHz, Chloroform-*d*) δ -144.9 (dq, $J_{(F-F)}$ = 105.2 Hz, $J_{(B-F)}$ = 29.0 Hz), -145.7 (dq, $J_{(F-F)}$ = 105.2 Hz, $J_{(B-F)}$ = 29.0 Hz).

6.2.2.5 5,5-Difluoro-10-(4-methoxyphenyl)-5*H*-4λ^4,5λ^4-dipyrrolo[1,2-*c*:2',1'-*f*][1,3,2]diazaborinine **2.11c**

Starting with 4-methoxybenzaldehyde (2 g, 14.69 mmol) the desired product was obtained as an orange/red solid (237.6 mg, 0.80 mmol, 22% over 3 steps)

Rf: 0.19 (Petrol:ethyl acetate); **Mp:** 139-140 ^{o}C [lit. 137-138 ^{o}C][S5]; **IR** (neat): ν_{max} cm^{-1} 2982 (C-H, m); **^{1}H NMR** (300 MHz, Chloroform-*d*) δ 7.92 (s, 2H), 7.53 (d, *J* = 8.8 Hz, 2H), 7.04 (d, *J* = 8.8 Hz, 2H), 6.97 (d, *J* = 4.1 Hz, 2H), 6.54 (d, *J* = 4.1 Hz, 3H), 3.91 (s, 3H); **^{13}C NMR** (75 MHz, Chloroform- *d*) δ 161.8, 147.1, 143.1, 134.5, 132.1, 131.0, 126.0, 118.0, 113.8, 55.2; **^{11}B NMR** (96 MHz, Chloroform-*d*) δ 0.30 (t, *J* = 29.3 Hz); **^{19}F NMR** (282 MHz, Chloroform-*d*) δ -145.03 (q, *J* = 29.3 Hz).

6.2.2.6 5,5-Difluoro-10-(3-methoxyphenyl)-5*H*-4λ^4,5λ^4-dipyrrolo[1,2-*c*:2',1'-*f*][1,3,2]diazaborinine **2.11d**

Starting with 3-methoxybenzaldehyde (2 g, 14.69 mmol) the desired product was obtained as an orange/red solid (440 mg, 1.48 mmol, 10% over 3 steps)

Rf: 0.70 (DCM); **Mp:** 109-111^{o}C [lit. 125-126 ^{o}C][S4]; **IR** (neat): ν_{max}/cm^{-1} 3111 (C-H, m); **^{1}H NMR** (300 MHz, Chloroform-*d*) δ 7.93 (s, 2H), 7.47 – 7.40 (m, 1H), 7.19 – 7.05 (m, 3H), 6.96 (d, *J* = 4.2 Hz, 2H), 6.53 (d, *J* =4.2 Hz, 2H), 3.85 (s, 3H); **^{13}C NMR** (75 MHz, Chloroform- *d*) δ 159.1, 146.8, 143.9, 134.6, 134.6, 131.3, 129.2, 122.7, 118.2, 116.0, 115.8, 55.2; **^{11}B NMR** (96 MHz, Chloroform-*d*) δ 0.29 (t, *J* = 28.3 Hz); **^{19}F NMR** (282 MHz, Chloroform-*d*) δ -144.8 – -145.3 (m).

6.2.2.7 3,7-dichloro-5,5-difluoro-10-(3-nitrophenyl)-5H-4λ^4,5λ^4-dipyrrolo[1,2-*c*:2',1'-f][1,3,2]diazaborinine **2.13b** [72]

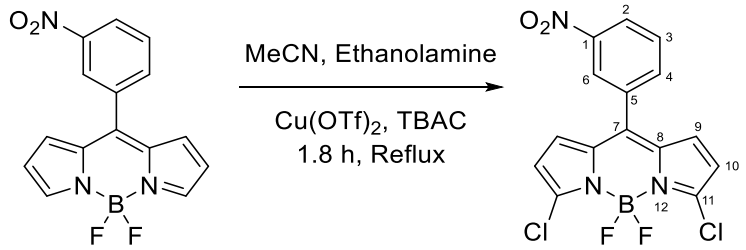

To a 100 mL round bottom flask was added 5,5-difluoro-10-(3-nitrophenyl)-5H-4λ^4,5λ^4-dipyrrolo[1,2-*c*:2',1'-f][1,3,2]diazaborinine (57.0 mg, 0.18 mmol), acetonitrile (5 mL), ethanolamine (22.0 μL, 0.36 mmol), $Cu(OTf)_2$ (657.2 mg, 1.82 mmol) and tetrabutylammonium chloride (252.5 mg, 0.91 mmol). The reaction was heated to reflux and stirred for 1h 50 mins, left to cool to room temperature (15 mins) and diluted with dichloromethane (25 mL). The organic layer was washed with water (3 x 10 mL), was dried over Na_2SO_4 (s), filtered and the solvent was removed under reduced pressure to give a dark red solid. The crude product was purified through silica gel column chromatography (4:1 petrol:ethyl acetate) to 3,7-dichloro-5,5-difluoro-10-(3-nitrophenyl)-5H-4λ^4,5λ^4-dipyrrolo[1,2-*c*:2',1'-f][1,3,2]diazaborinine (69.3 mg, 0.18 mmol, 99%) as a red/pink amorphous solid.

Rf: 0.20 (Petrol:ethyl acetate 4:1). **Mp:** 183-185 ^oC. **IR (neat):** ν_{max}/cm^{-1} 3133-2962 (C-H, w). **HRMS:** (ASAP+) calcd for $C_{15}H_8B^{11}Cl_2{}^{35}F_2N_3O_2$ $[M+H]^+$: 382.0136, found 382.0128. **^{1}H NMR** (300 MHz, Chloroform-*d*) δ 8.45 (d, *J* = 8.0 Hz, 1H, H^2), 8.36 (s, 1H, H^6), 7.72 - 7.82 (m, 2H, H^3, H^4), 6.77 (d, *J* = 4.4 Hz, 2H, H^{10}), 6.49 (d, *J* = 4.4 Hz, 2H, H^{10}). **^{13}C NMR** (75 MHz, Chloroform-*d*) δ 147.9 (C^{11}), 146.2 (C^1), 139.7 (C^5), 135.6 (C^4), 133.5 (C^7), 133.2 (C^3), 130.9 (C^8), 129.7 (C^9), 125.2 (C^2), 124.7 (C^6), 119.5 (C^{10}). **^{19}F NMR** (282 MHz, Chloroform-*d*) δ -147.95 (q, *J* = 27.7 Hz), -148.19 (q, *J* = 27.7 Hz). **^{11}B NMR** (96 MHz, Chloroform-*d*) δ 0.43 (t, *J* = 27.7 Hz). **UV-Vis:** λ_{max} = 519 nm (DCM). **Molar extinction coefficient (ε)** = 87000 M^{-1} cm^{-1}. **ϕ_F:** 0.37 (DCM)

6.2.2.8 3,7-dichloro-5,5-difluoro-10-(4-nitrophenyl)-5H-4λ^4,5λ^4-dipyrrolo[1,2-*c*:2',1'-*f*][1,3,2]diazaborinine **2.13e** [72]

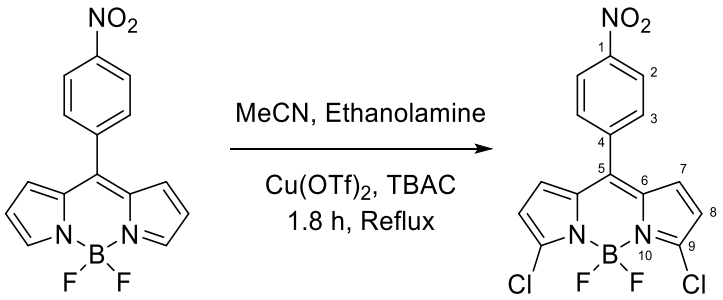

To a 100 mL round bottom flask was added 5,5-difluoro-10-(4-nitrophenyl)-5H-4λ^4,5λ^4-dipyrrolo[1,2-*c*:2',1'-*f*][1,3,2]diazaborinine (78.0 mg, 0.25 mmol), acetonitrile (6 mL), ethanolamine (30.1 μL, 0.50 mmol) $Cu(OTf)_2$ (361.7 mg, 2.49 mmol) and tetrabutylammonium chloride (346.3 mg, 1.25 mmol). The reaction was heated to reflux and stirred for 1h 50 mins, left to cool to room temperature (15 mins) and diluted with dichloromethane (25 mL). The organic layer was washed with water (3 x 10 mL), was dried over Na_2SO_4(s), filtered and the solvent was removed under reduced pressure to give a dark red solid. The crude product was purified through silica gel column chromatography (4:1 petrol:ethyl acetate) to give 3,7-dichloro-5,5-difluoro-10-(4-nitrophenyl)-5H-4λ^4,5λ^4-dipyrrolo[1,2-*c*:2',1'-*f*][1,3,2]diazaborinine (83.2 mg, 0.21 mmol, 92%) as a red/pink solid.

Rf: 0.65 (Petrol:ethyl acetate 4:1). **Mp:** 348-350 ^oC. **IR (neat):** ν_{max}/cm^{-1} 3142-2962 (C-H, m). **HRMS:** (ASAP+) calcd for $C_{15}H_8B^{11}Cl_2{}^{35}F_2N_3O_2$ $[M+H]^+$: 382.0136, found 382.0120. **^{1}H NMR:** (300 MHz, Chloroform-*d*) δ 8.40 (d, *J* = 8.8 Hz, 1H, H*^{2}*), 7.69 (d, *J* = 8.8 Hz, 1H, H*^{3}*), 6.76 (d, *J* = 4.4 Hz, 1H, H*^{7}*), 6.48 (d, *J* = 4.4 Hz, 1H, H*^{8}*). **^{13}C NMR** (126 MHz, Chloroform-*d*) δ 149.1 (C*^{9}*), 146.5 (C*^{4}*), 140.1 (C*^{1}*), 138.3 (C*^{5}*), 133.2 (C*^{6}*), 131.2 (C*^{3}*), 131.0 (C*^{7}*), 123.7 (C*^{2}*), 119.7 (C*^{8}*). **^{19}F NMR** (282 MHz, Chloroform-*d*) δ -148.10 (q, *J* = 27.5 Hz). **^{11}B NMR** (96 MHz, Chloroform-*d*) δ 0.46 (t, *J* = 27.5 Hz). **UV-Vis:** λ_{max} = 522 nm (DCM). **Molar extinction coefficient (ε)** = 67000 M^{-1} cm^{-1}. **ϕ_F:** 0.84 (DCM).

6.2.2.9 3,7-Dichloro-5,5-difluoro-10-(4-methoxyphenyl)-5H-4λ^4,5λ^4-dipyrrolo[1,2-*c*:2',1'-*f*][1,3,2]diazaborinine **2.11c** [72]

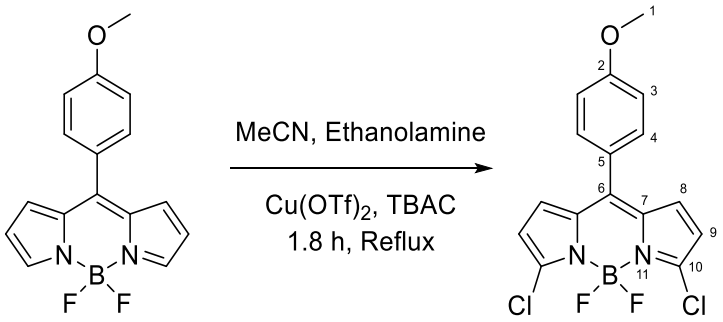

To a 100 mL round bottom flask was added 5,5-difluoro-10-(4-methoxyphenyl)-5H-4λ^4,5λ^4-dipyrrolo[1,2-*c*:2',1'-*f*][1,3,2]diazaborinine (40.7 mg, 0.14 mmol), acetonitrile (4 mL), ethanolamine (16.5 μL, 0.27 mmol) $Cu(OTf)_2$ (493.6 mg, 1.37 mmol) and tetrabutylammonium chloride (189.8 mg, 0.68 mmol). The reaction was heated to reflux and stirred for 1h 50 mins, left to cool to room temperature (15 mins) and diluted with dichloromethane (25 mL). The organic layer was washed with water (3 x 10 mL), was dried over Na_2SO_4(s), filtered and the solvent was removed under reduced pressure to give a dark red solid. The crude product was purified through silica gel column chromatography (4:1 petrol:ethyl acetate) to give 3,7-dichloro-5,5-difluoro-10-(4-methoxyphenyl)-5H-4λ^4,5λ^4-dipyrrolo[1,2-*c*:2',1'-*f*][1,3,2]diazaborinine (35.1 mg, 0.095 mmol, 70%) as a red/pink solid.

Rf: 0.35 (Petrol:ethyl acetate 4:1). **Mp:** 134-137 ^oC. **IR (neat):** ν_{max}/cm^{-1} 2922 (C-H, m). **HRMS:** (ASAP+) calcd for $C_{16}H_{11}B^{11}Cl_2{}^{35}F_2N_2O$ $[M+H]^+$: 366.0424, found 366.0391. **^{1}H NMR:** (300 MHz, Chloroform-*d*) δ 7.45 (d, *J* = 8.8 Hz, 1H, H*^{4}*), 7.04 (d, *J* = 8.8 Hz, 1H, H*^{3}*), 6.88 (d, *J* = 4.1 Hz, 2H, H*^{8}*), 6.44 (d, *J* = 4.2 Hz, 1H, H*^{9}*), 3.91 (s, 3H, H*^{1}*). **^{13}C NMR** (75 MHz, Chloroform-*d*) δ 161.8 (C*^{10}*), 143.9 (C*^{2}*), 133.4 (C*^{5}*), 132.0 (C*^{4}*), 131.1 (C*^{6}*), 124.5 (C*^{7}*), 118.4 (C*^{8}*), 118.3 (C*^{9}*), 113.9 (C*^{3}*), 55.3 (C*^{1}*). **^{19}F NMR** (282 MHz, Chloroform-*d*) δ -148.15 (q, *J* = 27.9 Hz). **^{11}B NMR** (96 MHz, Chloroform-*d*) δ 0.48 (t, *J* = 27.9 Hz). **UV-Vis:** λ_{max} = 512 nm (DCM**). Molar extinction coefficient (ε)** = 58000 $M^{-1}\,cm^{-1}$. **ϕ_F:** 0.63 (DCM)

6.2.2.10 3,7-dichloro-5,5-difluoro-10-(3-methoxyphenyl)-5H-4λ^4,5λ^4-dipyrrolo[1,2-*c*:2',1'-*f*][1,3,2]diazaborinine **2.13d** [72]

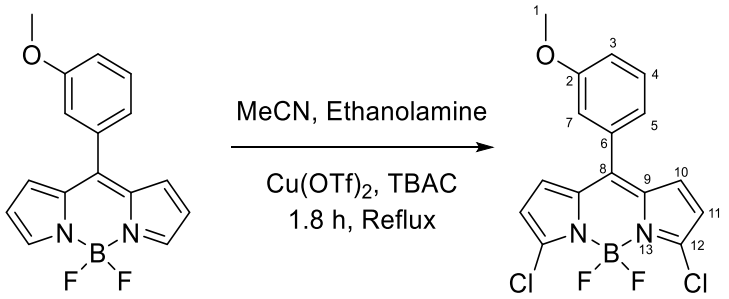

To a 100 mL round bottom flask was added 5,5-difluoro-10-(3-methoxyphenyl)-5H-4λ^4,5λ^4-dipyrrolo[1,2-*c*:2',1'-*f*][1,3,2]diazaborinine (75.5 mg, 0.25 mmol), acetonitrile (6 mL), ethanolamine (30.7 μL, 0.51 mmol) $Cu(OTf)_2$ (916.1 mg, 2.53 mmol) and tetrabutylammonium chloride (351.8 mg, 1.27 mmol). The reaction was heated to reflux and stirred for 1h 50 mins, left to cool to room temperature (15 mins) and diluted with dichloromethane (25 mL). The organic layer was washed with water (3 x 10 mL), was dried over Na_2SO_4(s), filtered and the solvent was removed under reduced pressure to give a dark red solid. The crude product was purified through silica gel column chromatography (4:1 petrol:ethyl acetate) to give 3,7-dichloro-5,5-difluoro-10-(3-methoxyphenyl)-5H-4λ^4,5λ^4-dipyrrolo[1,2-*c*:2',1'-*f*][1,3,2]diazaborinine (36.3 mg, 0.099 mmol, 56%) as a red/pink solid.

Rf: 0.30 (Petrol:ethyl acetate 4:1). **Mp:** 139-141 ^oC. **IR (neat):** ν_{max}/cm^{-1} 3127-2959 (C-H, w). **HRMS:** (ASAP+) calcd for $C_{16}H_{11}B^{11}Cl_2{}^{35}F_2N_2O$ $[M+H]^+$: 367.0391, found 367.0382. **^{1}H NMR** (500 MHz, Chloroform-*d*) δ 7.42 (t, *J* = 7.9, 1H, H*^{4}*), 7.11 (dd, *J* = 8.4, 2.5 Hz, 1H, H*^{5}*), 7.06 (d, *J* = 7.5 Hz, 1H, H*^{3}*), 7.02 (s, 1H, H*^{7}*), 6.89 (d, *J* = 4.1 Hz, 2H, H*^{10}*), 6.43 (d, *J* = 4.1, 2H, H*^{11}*), 3.86 (s, 3H, H*^{1}*). **^{13}C NMR** (126 MHz, Chloroform-*d*) δ 159.3 (C*^{12}*), 144.9 (C*^{2}*), 143.5 (C*^{6}*), 133.6 (C*^{8}*), 133.4 (C*^{4}*), 131.5 (C*^{9}*), 129.6 (C*^{5}*), 122.8 (C*^{10}*), 118.8 (C*^{3}*), 116.1 (C*^{7}*), 116.1 (C*^{11}*), 55.4 (C*^{1}*). **^{19}F NMR** (282 MHz, Chloroform-*d*) δ -148.23 (q, *J* = 27.8 Hz). **^{11}B NMR** (96 MHz, Chloroform-*d*) δ 0.48 (t, *J* = 27.8 Hz). **UV-Vis:** λ_{max} = 515 nm (DCM). **Molar extinction coefficient (ε)** = 49000 M^{-1} cm^{-1}. **ϕ_F:** 0.62 (DCM)

6.2.2.11 3,7-dichloro-5,5-difluoro-10-(o-tolyl)-5H-4λ^4,5λ^4-dipyrrolo[1,2-*c*:2',1'-*f*][1,3,2]diazaborinine **2.13f** [72]

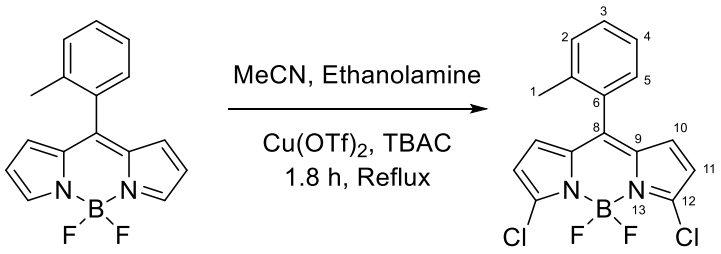

To a 100 mL round bottom flask was added 5,5-difluoro-10-(o-tolyl)-5H-4λ^4,5λ^4-dipyrrolo[1,2-*c*:2',1'-*f*][1,3,2]diazaborinine (54.2 mg, 0.21 mmol), acetonitrile (5 mL), ethanolamine (25.3 μL, 0.41 mmol) $Cu(OTf)_2$ (747.9 mg, 2.07 mmol) and tetrabutylammonium chloride (277.9 mg, 1.03 mmol). The reaction was heated to reflux and stirred for 1h 50 mins, left to cool to room temperature (15 mins) and diluted with dichloromethane (25 mL). The organic layer was washed with water (3 x 10 mL), was dried over Na_2SO_4(s), filtered and the solvent was removed under reduced pressure to give a dark red solid. The crude product was purified through silica gel column chromatography (4:1 petrol:ethyl acetate) to give 3,7-dichloro-5,5-difluoro-10-(*o*-tolyl)-5H-4λ^4,5λ^4-dipyrrolo[1,2-*c*:2',1'-*f*][1,3,2]diazaborinine (22.5 mg, 0.064 mmol, 31%) as a red/pink solid.

Rf: 0.55 (Petrol:ethyl acetate 4:1). **Mp:** 152-155°C. **IR (neat):** ν_{max}/cm^{-1} 3133-2924 (C-H, w). **HRMS:** (ASAP+) calcd for $C_{16}H_{11}B^{11}Cl_2{}^{35}F_2N_2$ $[M+H]^+$: 351.0442, found 351.0438. **^{1}H NMR** (300 MHz, Chloroform-*d*) δ 7.43 (t, *J* = 8.0 Hz, 1H, H*^{4}*), 7.35 – 7.27 (m, 2H, H*^{3}*, H*^{5}*), 7.24 – 7.19 (m, 1H, H*^{2}*), 6.62 (d, *J* = 4.2 Hz, 2H, H*^{11}*), 6.39 (d, *J* = 4.2 Hz, 2H, H*^{10}*), 2.22 (s, 3H, H*^{1}*). **^{13}C NMR** (126 MHz, Chloroform-*d*) δ 145.2 (C*^{12}*), 143.5 (C*^{6}*), 136.6 (C*^{8}*), 134.2 (C*^{7}*), 131.5 (C*^{5}*), 131.1 (C*^{4}*), 130.6 (C*^{3}*), 129.98 (C*$^{2/9}$*), 129.96 (C*$^{2/9}$*), 125.5 (C*^{10}*), 119.0 (C*^{11}*), 20.0 (C*^{1}*). **^{19}F NMR** (282 MHz, Chloroform-*d*) δ -148.44 (q, *J* = 27.8 Hz). **^{11}B NMR** (96 MHz, Chloroform-*d*) δ 0.50 (t, *J* = 27.8 Hz). **UV-Vis:** λ_{max} = 515 nm (DCM). **Molar extinction coefficient (ε)** = 87000 M^{-1} cm^{-1}. **ϕ_F:** 0.87 (DCM).

6.2.2.12 Methyl 4-(2,3,7,8-tetrabromo-5,5-difluoro-5*H*-4λ4,5λ4-dipyrrolo[1,2-*c*:2',1'-*f*][1,3,2]diazaborinin-10-yl)benzoate **2.15**

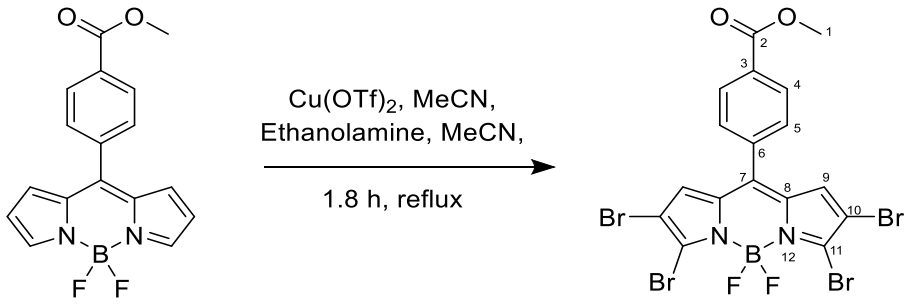

To a round bottom flask was added methyl 4-(5,5-difluoro-5*H*-4λ^4,5λ^4-dipyrrolo[1,2-c:2',1'-*f*][1,3,2]diazaborinin-10-yl)benzoate (50 mg, 0.153 mmol), MeCN (4 mL), ethanolamine (18.75 μl, 0.307 mmol), $Cu(OTf)_2$ (0.556 g, 1.53 mmol) and TBAB (0.246 g, 0.763 mmol). The reaction mixture was heated to reflux (90 ^oC) and was stirred for 1 hour 50 minutes, resulting in a dark purple mixture which was left to cool to room temperature. The resulting reaction mixture was diluted with DCM (30 mL) and washed with H_2O (3 x 10 mL). The organic layer was dried under Na_2SO_4, filtered and removed solvent under reduced pressure. The crude product was purified using column chromatography (4:1 petrol : ethyl acetate) to give a purple solid of methyl 4-(2,3,7,8-tetrabromo-5,5-difluoro-5*H*-4λ^4,5λ^4-dipyrrolo[1,2-*c*:2',1'-*f*][1,3,2]diazaborinin-10-yl)benzoate (40 mg, 0.0623 mmol, 41%).

Rf: 0.31 (Petrol:ethyl acetate 4:1). **Mp:** 254-256 ^oC. **IR** (neat): ν_{max}/cm^{-1} 1710 (C=O, m), 1528 (C=C, m). **HRMS:** (pNSI) calcd for C17H9BBr4F2N2O2 [M-F]-: 618.7478, found 618.7489. **^{1}H NMR** (400 MHz, Chloroform-*d*) δ 8.21 (d, *J* = 8.9 Hz, 2H, *H*^{4}), 7.56 (d, *J* = 8.5 Hz, 2H, *H*^{5}), 6.85 (s, 2H, *H*^{9}), 4.00 (s, 3H, *H*^{1}). **^{13}C NMR** (75 MHz, Chloroform-*d*) δ 165.9 (*C*^{2}), 145.6 (*C*^{11}), 142.1 (*C*^{6}), 136.4 (*C*^{7}), 133.4 (*C*^{3}), 132.2 (*C*^{8}), 131.2 (*C*^{5}), 130.2 (*C*^{4}), 129.5 (*C*^{9}), 119.1 (*C*^{10}), 52.4 (*C*^{1}). **^{19}F NMR** (282 MHz, Chloroform-*d*) δ -148.31 (q 27.4 Hz). **^{11}B NMR** (96 MHz, Chloroform-*d*) δ 0.27 (t, *J* = 28.3 Hz).

6.2.2.13 Methyl (Z)-4-((5-bromo-1*H*-pyrrol-2-yl)(5-bromo-2*H*-pyrrol-2-ylidene)methyl)benzoate **2.18a** [8]

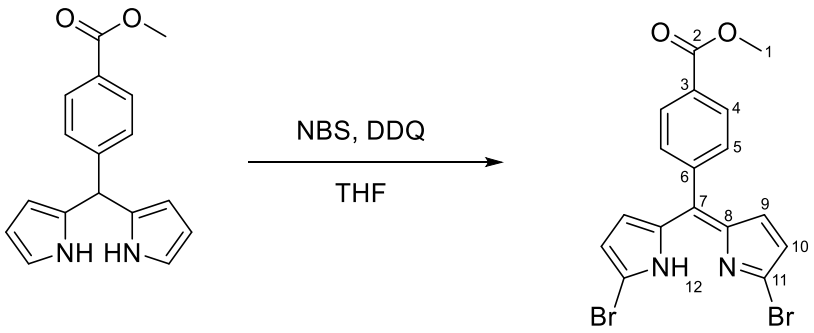

To a 250 mL round bottom flask, was added methyl 4-(di(1*H*-pyrrol-2-yl)methyl)benzoate (2g, 7.13 mmol), dry THF (100 mL), cooled to -78°C and stirred at this temp for 30 mins. To the cooled reaction mixture was added recrystallised NBS (2.54g, 14.27 mmol) in two portions, stirred at -78°C for 1 hour then added DDQ (1.62 g, 7.13 mmol) in portions over 10 mins. The crude reaction mixture was warmed to room temp for 30 mins and quenched with sat. sodium sulphite$_{(aq)}$ (50 mL) and diluted with DCM (100 mL). The reaction mixture was washed with water (3 x 250 mL), dried the organic layer over $MgSO_4$ and the solvent was removed under reduced pressure to give methyl (*Z*)-4-((5-bromo-1*H*-pyrrol-2-yl)(5-bromo-2*H*-pyrrol-2-ylidene)methyl)benzoate (3.055 g, 7.01 mmol, 92%). The crude product was of high enough purity to continue without purification.

R_f: 0.62 (DCM). **Mp:** 149-152 °C. **IR** (neat): ν_{max}/cm^{-1} 2981 (C-H, m), 1717 (C=O, s). **HRMS:** (ES+) calcd for $C_{17}H_{13}{}^{79}Br^{81}BrN_2O_2^+$ $[M+H]^+$: 436.9323, found 436.9339. **^{1}H NMR** (300 MHz, $CDCl_3$) δ 12.29 (s, 1H, H*^{12}*), 8.10 (d, *J* = 8.5 Hz, 2H, H*^{4}*), 7.49 (d, *J* = 8.6 Hz, 2H, H*^{5}*), 6.39 (d, *J* = 4.2 Hz, 2H, H*^{9}*), 6.32 (d, *J* = 4.2 Hz, 2H, H*^{10}*), 3.96 (s, 3H, H*^{1}*). **^{13}C NMR** (75 MHz, $CDCl_3$) δ 166.5 (C*^{2}*), 140.0 (C*$^{6/8}$*), 140.0 (C*$^{6/8}$*), 137.8 (C*^{7}*), 131.0 (C*^{3}*), 130.8 (C*^{5}*), 130.2 (C*^{11}*), 129.9 (C*^{9}*), 129.1 (C*^{4}*), 120.9 (C*^{10}*), 52.4 (C*^{1}*).

6.2.2.14 Methyl 4-(3,7-dibromo-5,5-difluoro-5*H*-4λ^4,5λ^4-dipyrrolo[1,2-c:2',1'-f][1,3,2]diazaborinin-10-yl)benzoate **2.14a** [8]

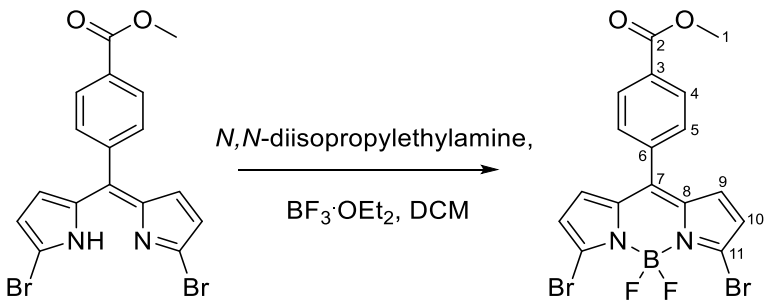

To a round bottom flask, under nitrogen atmosphere, was added methyl (*Z*)-4-((5-bromo-1*H*-pyrrol-2-yl)(5-bromo-2*H*-pyrrol-2-ylidene)methyl)benzoate (3.055 g, 7.00 mmol), DCM (15 mL), NN-diisopropylethylamine (3.05 mL, 17.51 mmol) and $BF_3.OEt_2$ (1.73 mL, 14.00 mmol). The reaction was stirred for 1 hour at room temperature and then the organic layer was washed with 0.1 M NaOH $_{(aq)}$ (100 mL), 0.1 M HCl $_{(aq)}$ (100 mL) and water (100 mL). The organic layer was dried over Na_2SO_4, filtered and the solvent was removed under reduced pressure to give a dark pink solid. The crude product was purified through silica gel column chromatography (DCM) to give methyl 4-(3,7-dibromo-5,5-difluoro-5*H*-4λ^4,5λ^4-dipyrrolo[1,2-*c*:2',1'-*f*][1,3,2]diazaborinin-10-yl)benzoate (1.64 g, 3.39 mmol, 48%, [53% over 3 steps]) as a pink solid.

Rf: 0.6 (DCM). **Mp:** >237-239 ^oC. **IR** (neat): ν_{max}/cm^{-1} 3092 (C-H, w), 1709 (C=O, w). **HRMS:** (ES+): calcd for $C_{17}H_{12}B^{79}Br^{81}BrF_2N_2O_2^+$[M+Na]$^+$: 504.9126, found 504.9143. **^{1}H NMR** (300 MHz, Chloroform-*d*) δ 8.18 (d, *J* = 8.6 Hz, 2H, H^{4}), 7.57 (d, *J* = 8.6 Hz, 2H, H^{5}), 6.74 (d, *J* = 4.3 Hz, 2H, H^{9}), 6.55 (d, *J* = 4.3 Hz, 2H, H^{10}), 3.98 (s, 3H, H^{1}). **^{13}C NMR** (75 MHz, Chloroform-*d*) δ 166.2 (C^{2}), 141.6 (C^{7}), 136.7 (C^{3}), 135.4 (C^{8}), 133.7 (C^{11}), 132.4 (C^{6}), 131.6 (C^{9}), 130.5 (C^{5}), 129.8 (C^{4}), 123.3 (C^{10}), 52.7 (C^{1}). **^{11}B NMR** (96 MHz, Chloroform-*d*) δ 0.63 (t, *J* = 28.0 Hz).**^{19}F NMR** (282 MHz, Chloroform-*d*) δ -146.76 (q, *J* = 28.0 Hz). **UV-Vis:** λ_{max} = 526 nm (DCM). Molar extinction coefficient (ε) = 91000 M^{-1} cm^{-1}. **ϕ_F:** 0.50 (DCM)

6.2.2.15 2,2'-((4-Methoxyphenyl)methylene)bis(1*H*-pyrrole) **2.7c** [72]

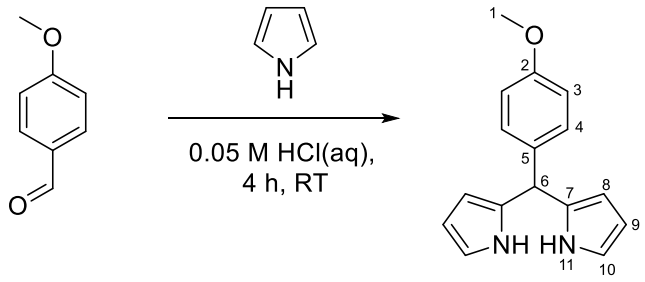

To a 250 mL round bottom flask was added an aqueous solution of HCl (0.05 M, 100 mL, 5 mmol), pyrrole (3.06 mL, 44.07 mmol) and 3-methoxybenzaldehyde (1.79 mL, 14.69 mmol). The reaction was stirred, opened to air, for 4 hours at room temperature, forming a creamy sticky oil over time. The crude product was extracted with DCM (2 x 50 mL) and then washed with water (2 x 50 mL). The organic layer was dried over $MgSO_4$, filtered and solvent was removed under reduced pressure to afford 2,2'-((3-methoxyphenyl)methylene)bis(1*H*-pyrrole) (1.9658 g, 7.80 mmol, 53%) as a grey/green oil. This crude product was of high enough purity to carry on to the next step without any purification necessary.

R_f: 0.6 (1:1 ethyl acetate:DCM). **HRMS:** (ESI+) calcd for $C_{16}H_{17}N_2O$ $[M+H]^+$: 253.1335, found 253.1234. **IR** (neat): ν_{max}/cm^{-1} 3382 (N-H, m), 3101-2906 (C-H, w), 1143 (C-O, s). **^{1}H NMR** (300 MHz, Chloroform-*d*) δ 8.00 (s, 1H, H^{11}), 7.27 (d, *J* = 7.7 Hz, 2H, H^3), 7.01 (d, *J* = 8.7 Hz, 2H, H^4), 6.78 – 6.68 (m, 2H, H^{10}), 6.34 (q, *J* = 2.8 Hz, 2H, H^9), 6.12 – 6.02 (m, 2H, H^8), 5.46 (s, 1H, H^6), 3.90 (s, 3H, H^1). **^{13}C NMR** (75 MHz, Chloroform-*d*) δ 157.9 (C^2), 134.1 (C^5), 132.7 (C^7), 129.0 (C^3), 116.9 (C^{10}), 113.5 (C^4) 107.8 (C^9), 106.8 (C^8), 54.8 (C^1), 42.6 (C^6).

6.2.2.16 (Z)-2-Bromo-5-((5-bromo-2*H*-pyrrol-2-ylidene)(4-methoxyphenyl)methyl)-1*H*-pyrrole **2.18c** [83]

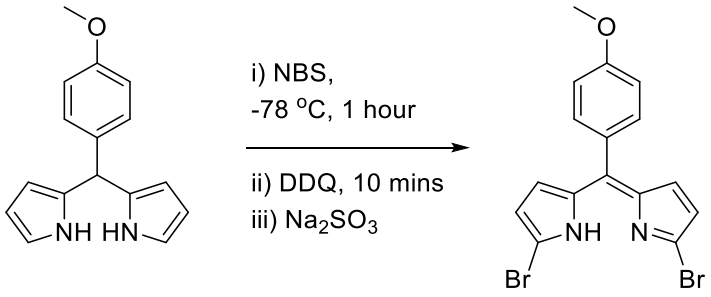

To a 500 mL round bottom flask was added, 2,2'-((4-methoxyphenyl)methylene)bis(1*H*-pyrrole) (1.9658 g, 7.79 mmol), dry THF (100 mL), cooled to -78ºC and stirred at this temp for 30 mins. To the cooled reaction mixture was added recrystallised NBS (2.77 g, 15.58 mmol) in two portions, stirred at -78ºC for 1 hour then added DDQ (2.16 g, 7.79 mmol) in portions over 10 mins. The crude reaction mixture was warmed to room temp and quenched with sat. sodium sulphite$_{(aq)}$ (50 mL) and diluted with DCM (100 mL). The reaction mixture was washed with water (3 x 250 mL), dried the organic layer over $MgSO_4$ and the solvent was removed under reduced pressure to give (*Z*)-2-bromo-5-((5-bromo-2*H*-pyrrol-2-ylidene)(4-methoxyphenyl)methyl)-1*H*-pyrrole (3.6752 g, 9 mmol, 116%). The crude product was of high enough purity to continue without purification.

6.2.2.17 3,7-Dibromo-5,5-difluoro-10-(4-methoxyphenyl)-5*H*-4λ^4,5λ^4-dipyrrolo[1,2-*c*:2',1'-*f*][1,3,2]diazaborinine **2.14c** [83]

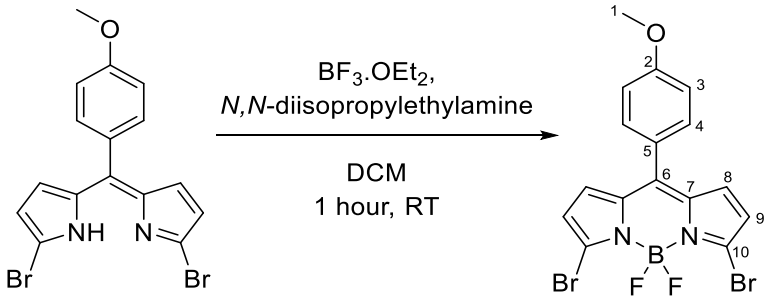

To a round bottom flask, under nitrogen atmosphere, was added (*Z*)-2-bromo-5-((5-bromo-2*H*-pyrrol-2-ylidene)(4-methoxyphenyl)methyl)-1*H*-pyrrole (3.6752 g, 9.00 mmol), DCM (15 mL), *N,N*-diisopropylethylamine (3.92 mL, 22.51 mmol), $BF_3{\cdot}OEt_2$ (2.22 mL, 18.01 mmol). The reaction was stirred for 1 hour at room temp and then the organic layer was washer with 0.1 M $NaOH_{(aq)}$ (100 mL), 0.1 M $HCl_{(aq)}$ (100 mL) and water (100 mL). The organic layer was dried over $MgSO_4$, filtered and the solvent was removed under reduced pressure to give a dark pink solid. The crude product was purified through silica gel column chromatography (DCM) to give 3,7-dibromo-5,5-difluoro-10-(4-methoxyphenyl)-5*H*-4λ^4,5λ^4-dipyrrolo[1,2-*c*:2',1'-*f*][1,3,2]diazaborinine (825.5 mg, 1.81 mmol, 20% [12% over 3 steps]) as a pink solid.

R_f: 0.875 (DCM). **IR** (neat): ν_{max}/cm^{-1} 3121-2846 (C-H, w). **^{1}H NMR** (300 MHz, Chloroform-*d*) δ 7.44 (d, *J* = 8.7 Hz, 2H, H*^{3}*), 7.03 (d, *J* = 8.8 Hz, 2H, H*^{4}*), 6.82 (d, *J* = 4.3 Hz, 2H, H*^{8}*), 6.53 (d, *J* = 3.9 Hz, 2H, H*^{9}*), 3.90 (s, 3H, H*^{1}*). **^{13}C NMR** (75 MHz, Chloroform-*d*) δ 162.3 (C*^{2}*), 143.5 (C*^{6}*), 135.5 (C*^{7}*), 132.4 (C*^{3}*), 131.9 (C*^{10}*), 131.7 (C*^{8}*), 124.9 (C*^{5}*), 122.6 (d, *J* = 3.6 Hz, C*^{9}*), 114.3 (C*^{4}*), 55.7 (C*^{1}*). **^{19}F NMR** (282 MHz, Chloroform-*d*) δ -146.62 (dd, *J* = 57.1, 28.5 Hz). **^{11}B NMR** (96 MHz, Chloroform-*d*) δ 0.63 (t, *J* = 28.3 Hz). **UV-Vis:** λ_{max} = 519 nm (DCM). Molar extinction coefficient (ε) = 95000 M^{-1} cm^{-1}. **ϕ_F:** 0.15

6.2.2.18 2,2'-((3-methoxyphenyl)methylene)bis(1*H*-pyrrole) **2.7d** [72]

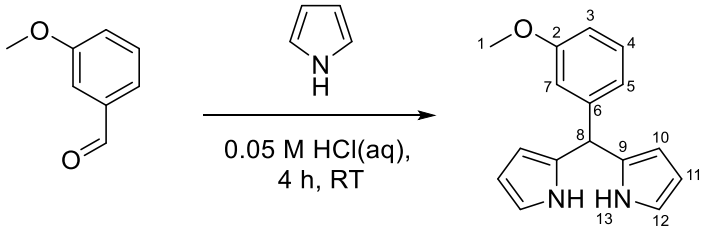

To a 250 mL round bottom flask was added an aqueous solution of HCl (0.05 M, 100 mL, 5 mmol), pyrrole (3.06 mL, 44.07 mmol) and 3-methoxybenzaldehyde (1.79 mL, 14.69 mmol). The reaction was stirred, opened to air, for 4 hours at room temperature, forming a creamy sticky oil over time. The crude product was extracted with DCM (2 x 50 mL) and then washed with water (2 x 50 mL). The organic layer was dried over $MgSO_4$, filtered and solvent was removed under reduced pressure to afford 2,2'-((3-methoxyphenyl)methylene)bis(1*H*-pyrrole) (1.2849 g, 5.09 mmol, 35%) as a grey/green oil. This crude product was of high enough purity to carry on to the next step without any purification necessary.

R_f: 0.55 (1:1 ethyl acetate:DCM). **HRMS:** (ESI+) calcd for $C_{16}H_{17}N_2O$ $[M+H]^+$: 253.1335, found 253.1232. **IR** (neat): ν_{max}/cm^{-1} 3382 (N-H, m), 3101 2836 (C-H, w), 1143 (C-O, s). **^{1}H NMR** (300 MHz, $CDCl_3$) δ 7.94 (s, 2H, H^{13}), 7.40 – 7.31 (m, 1H, $H^{3/4/7}$), 6.96 – 6.86 (m, 1H, $H^{3/4/7}$), 6.86 – 6.81 (m, 1H, $H^{3/4/7}$), 6.71 (td, *J* = 2.7, 1.6 Hz, 2H,H^{12}), 6.37 (q, *J* = 2.2 Hz, , H^5), 6.27 (dt, *J* = 3.4, 2.7 Hz, 2H, H^{11}), 6.03 (ddq, *J* = 2.6, 1.7, 0.7 Hz, 2H, H^{10}), 5.46 (s, 1H,H^8), 3.83 (s, 3H, H^1). **^{13}C NMR** (75 MHz, $CDCl_3$) δ 159.6 (C^2), 132.4 (C^6), 129.5 (C^9), 120.8 ($C^{3/4/7}$), 117.7 ($C^{3/4/7}$), 117.3 (C^{12}), 114.3 ($C^{3/4/7}$), 112.04 ($C^{3/4/7}$), 107.9 (C^{11}), 107.1 (C^{10}), 55.0 (C^1), 43.8 (C^8).

6.2.2.19 (*Z*)-2-bromo-5-((5-bromo-2*H*-pyrrol-2-ylidene)(3-methoxyphenyl)methyl)-1*H*-pyrrole **2.18d** [83]

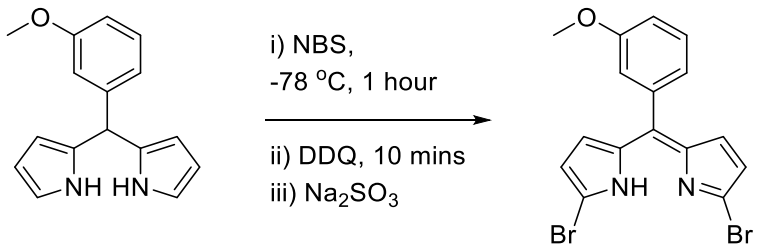

To a 500 mL round bottom flask was added, 2,2'-((3-methoxyphenyl)methylene)bis(1*H*-pyrrole) (1.2849 g, 5.09 mmol), dry THF (90 mL), cooled to -78ºC and stirred at this temp for 30 mins. To the cooled reaction mixture was added recrystallised NBS (1.81 g, 10.18 mmol) in two portions, stirred at -78ºC for 1 hour then added DDQ (1.16 g, 5.09 mmol) in portions over 10 mins. The crude reaction mixture was warmed to room temp and quenched with sat. sodium sulphite$_{(aq)}$ (50 mL) and diluted with DCM (100 mL). The reaction mixture was washed with water (3 x 250 mL), dried the organic layer over $MgSO_4$ and the solvent was removed under reduced pressure to give (*Z*)-2-bromo-5-((5-bromo-2*H*-pyrrol-2-ylidene)(3-methoxyphenyl)methyl)-1*H*-pyrrole (3.0702 g, 7.52 mmol, 148%). The crude product was of high enough purity to continue without purification.

6.2.2.20 3,7-Dibromo-5,5-difluoro-10-(3-methoxyphenyl)-5*H*-4λ^4,5λ^4-dipyrrolo[1,2-*c*:2',1'-*f*][1,3,2]diazaborinine **2.14d** [83]

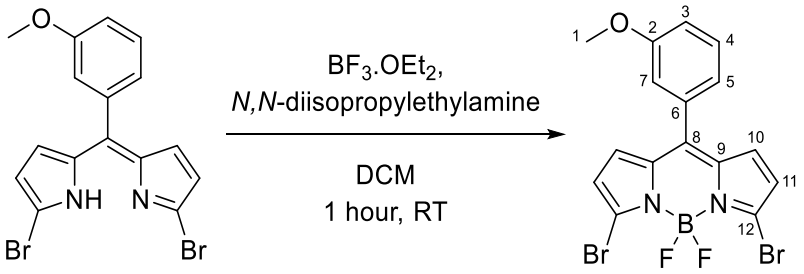

To a round bottom flask, under nitrogen atmosphere, was added (*Z*)-2-bromo-5-((5-bromo-2*H*-pyrrol-2-ylidene)(3-methoxyphenyl)methyl)-1*H*-pyrrole (3.0702 g, 7.52 mmol), DCM (15 mL), *N,N*-diisopropylethylamine (3.28 mL, 18.81 mmol), $BF_3{\cdot}OEt_2$ (1.89 mL, 15.05 mmol). The reaction was stirred for 1 hour at room temp and then the organic layer was washer with 0.1 M $NaOH_{(aq)}$ (100 mL), 0.1 M $HCl_{(aq)}$ (100 mL) and water (100 mL). The organic layer was dried over $MgSO_4$, filtered and the solvent was removed under reduced pressure to give a dark pink solid. The crude product was purified through silica gel column chromatography (DCM) to give 3,7-dibromo-5,5-difluoro-10-(3-methoxyphenyl)-5*H*-4λ^4,5λ^4-dipyrrolo[1,2-*c*:2',1'-*f*][1,3,2]diazaborinine (561.1 mg, 1.23 mmol, 16% [8% over 3 steps]) as a pink solid.

R_f: 0.85 (DCM). **^{1}H NMR** (300 MHz, Chloroform-*d*) δ 7.41 (d, 1H, H^4), 7.11 (ddd, *J* = 8.4, 2.6, 1.0 Hz, 1H, H^3), 7.05 (ddd, *J* = 7.5, 1.7, 1.0 Hz, 1H, H^5), 7.01 (dd, *J* = 2.6, 1.6 Hz, 1H, H^7), 6.83 (d, *J* = 3.9 Hz, 2H, H^{10}), 6.53 (d, *J* = 4.2 Hz, 2H, H^{11}), 3.85 (s, 3H, H^1). **^{13}C NMR** (75 MHz, Chloroform-*d*) δ 159.5 (C^2), 143.0 (C^8), 135.6 (C^9), 133.7 (C^6), 132.8 (C^{12}), 131.8 (C^{10}), 129.8 (C^4), 122.9 (C^5), 122.9 (C^{11}), 116.3 (C^3), 116.2 (C^7), 55.6 (C^1). **^{19}F NMR** (282 MHz, Chloroform-*d*) δ -146.75 (q, *J* = 28.6 Hz). **^{11}B NMR** (96 MHz, Chloroform-*d*) δ 0.62 (t, *J* = 28.2 Hz)

6.2.2.21 2,2'-((3-Nitrophenyl)methylene)bis(1*H*-pyrrole) **2.7b** [72]

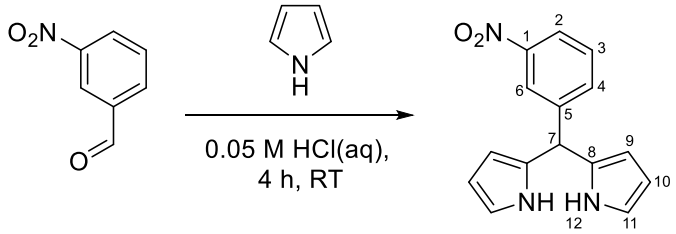

To a 250 mL round bottom flask was added an aqueous solution of HCl (0.05 M, 100 mL, 5 mmol), pyrrole (2.74 mL, 39.7 mmol) and 3-nitrobenzaldehyde (2 g, 13.23 mmol). The reaction was stirred, opened to air, for 4 hours at room temperature, forming a creamy precipitate over time. The creamy precipitate was filtered and the solid was washed with water (25 mL) and petroleum ether (50 mL) to afford 2,2'-((3-nitrophenyl)methylene)bis(1*H*-pyrrole) (3.43 g, 97%). This crude product was of high enough purity to carry on to the next step without any purification necessary.

IR: 3387 (N-H, m), 3345 (N-H, m), 3100 (C-H, w), 2981 (C-H, w), 1511 (N-O, s), 1351 (N-C, s). **Mp:** 139-144°C. **HRMS:** (ESI+) calcd for $C_{15}H_{14}N_3O_2$ $[M+H]^+$: 268.1081, found 268.0991. **^{1}H NMR** (300 MHz, $CDCl_3$) δ 8.20 – 7.98 (m, 4H, $H^{2,6,12}$), 7.55 (ddd, *J* = 7.8, 1.6, 1.6 Hz, 1H, H^4), 7.48 (ddd, *J* = 7.7, 7.7, 0.8 Hz, 1H, H^3), 6.75 (td, *J* = 2.7, 1.5 Hz, 2H, H^{10}), 6.17 (dd, *J* = 4.3, 1.8 Hz, 2H, H^9), 5.87 (dddd, *J* = 3.4, 2.5, 1.5, 0.9 Hz, 2H, H^{11}), 5.58 (s, 1H, H^7). **^{13}C NMR** (75 MHz, $CDCl_3$) δ 148.6 (C^1), 144.6 (C^5), 134.7 (C^4), 131.2 (C^8), 129.6 (C^3), 123.4 ($C^{2/6}$), 122.2 ($C^{2/6}$), 118.2 (C^{10}), 108.9 (C^9), 107.9 (C^{11}), 43.8 (C^7).

6.2.2.22 (*Z*)-2-Bromo-5-((5-bromo-2*H*-pyrrol-2-ylidene)(3-nitrophenyl)methyl)-1*H*-pyrrole **2.18b** [83]

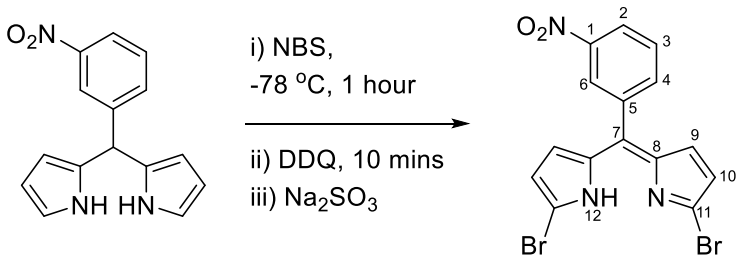

To a 500 mL round bottom flask was added, 2,2'-((3-nitrophenyl)methylene)bis(1*H*-pyrrole) (4.4320 g, 16.58 mmol), dry THF (200 mL), cooled to -78°C and stirred at this temp for 30 mins. To the cooled reaction mixture was added recrystallised NBS (5.9 g, 33.16 mmol) in two portions, stirred at -78°C for 1 hour then added DDQ (4.59 g, 16.58 mmol) in portions over 10 mins. The crude reaction mixture was warmed to room temp and quenched with sat. sodium sulphite$_{(aq)}$ (100 mL) and diluted with DCM (200 mL). The reaction mixture was washed with water (3 x 500 mL), dried the organic layer over $MgSO_4$ and the solvent was removed under reduced pressure to give (*Z*)-2-bromo-5-((5-bromo-2*H*-pyrrol-2-ylidene)(3-nitrophenyl)methyl)-1*H*-pyrrole (7.9511 g, 18.79 mmol, 113%). The crude product was of high enough purity to continue without purification.

IR (neat): ν_{max}/cm^{-1} 3231 (N-H, m, broad), 2955-2808 (C-H, m), 1526 (N-O, s). **HRMS:** (ESI+) calcd for $C_{15}H_{10}N_3O_2$ $[M+H]^+$: 421.9134, found 421.9125. **^{1}H NMR** (300 MHz, $CDCl_3$) δ 8.36 (ddd, *J* = 8.1, 2.4, 1.2 Hz, 1H, H*^{2}*), 8.32 – 8.28 (m, 1H, H*^{6}*), 7.80 – 7.74 (m, 1H, H*^{4}*), 7.66 (ddd, *J* = 8.2, 7.6, 0.6 Hz, 1H, H*^{3}*), 6.36 (s, 4H, H*^{9,10}*). **^{13}C NMR** (75 MHz, $CDCl_3$) δ 147.9 (C*^{1}*), 140.0 (C*^{8}*), 137.2 (C*^{5}*), 136.5 (C*^{4}*), 135.7 (C*^{7}*) 131.0 (C*^{11}*), 129.7 (C*$^{9/10}$*), 129.2 (C*^{3}*), 125.4 (C*^{6}*), 124.3 (C*^{2}*), 121.4 (C*$^{9/10}$*).

6.2.2.23 3,7-Dibromo-5,5-difluoro-10-(3-nitrophenyl)-5*H*-4λ^4,5λ^4-dipyrrolo[1,2-*c*:2',1'-*f*][1,3,2]diazaborinine **2.14b** [83]

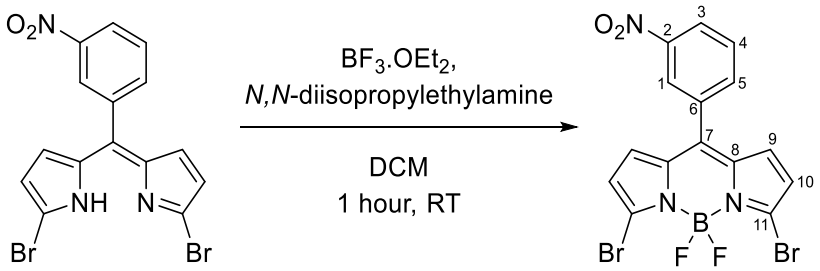

To a round bottom flask, under nitrogen atmosphere, was added (*Z*)-2-bromo-5-((5-bromo-2*H*-pyrrol-2-ylidene)(3-nitrophenyl)methyl)-1*H*-pyrrole (7.9511 g, 18.79 mmol), DCM (40 mL), *N,N*-diisopropylethylamine (8.18 mL, 46.99 mmol) and $BF_3.OEt_2$ (4.64 mL, 37.59 mmol). The reaction was stirred for 1 hour at room temperature and then the organic layer was washed with 0.1 M NaOH $_{(aq)}$ (200 mL), 0.1 M HCl $_{(aq)}$ (200 mL) and water (200 mL). The organic layer was dried over Na_2SO_4, filtered and the solvent was removed under reduced pressure to give a dark pink solid. The crude product was purified through silica gel column chromatography (DCM) to give 3,7-dibromo-5,5-difluoro-10-(3-nitrophenyl)-5*H*-4λ^4,5λ^4-dipyrrolo[1,2-*c*:2',1'-*f*][1,3,2]diazaborinine (358.7 mg, 0.76 mmol, 4% [6% over 3 steps]) as a pink solid.

IR (neat): ν_{max}/cm^{-1} 2919 (C-H, m). **R**$_f$: 0.85 (DCM). **^{1}H NMR** (300 MHz, Chloroform-*d*) δ 8.46 (ddd, *J* = 8.1, 2.4, 1.1 Hz, 1H, H*^{3}*), 8.41 – 8.34 (m, 1H, H*^{1}*), 7.83 (dt, *J* = 7.7, 1.4 Hz, 1H,H*^{5}*), 7.75 (d,d, *J* = 8.1, 7.6 Hz, 1H, H*^{4}*), 6.71 (d, *J* = 4.4 Hz, 2H, H*^{9}*), 6.59 (d, *J* = 4.4 Hz, 2H, H*^{10}*). **^{13}C NMR** (75 MHz, Chloroform-*d*) δ 148.4 (C*^{2}*), 139.3 (C*^{7}*), 135.9 (C*^{5}*), 135.4 (C*^{8}*), 134.7 (C*^{11}*), 134.1 (C*^{6}*), 131.3 (C*^{9}*), 130.1 (C*^{4}*), 125.6 (C*^{3}*), 125.0 (C*^{1}*), 123.8 (C*^{10}*). **^{19}F NMR** (282 MHz, Chloroform-*d*) δ -146.74 (ddd, *J* = 55.6, 27.9, 18.9 Hz). **^{11}B NMR** (96 MHz, Chloroform-*d*) δ 0.59 (t, *J* = 28.2 Hz).

6.2.3 Chapter 3

6.2.3.1 Methyl 4-(5,5-difluoro-3,7-diiodo-5*H*-4λ^4,5λ^4-dipyrrolo[1,2-*c*:2',1'-*f*][1,3,2]diazaborinin-10-yl)benzoate **3.17a** [83]

Method A:

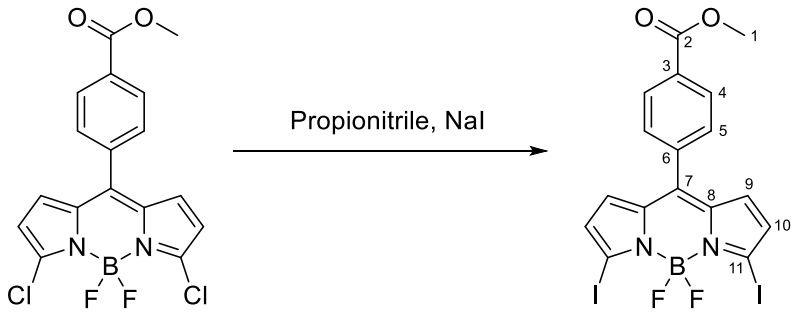

To a 25mL round bottom flask was added methyl 4-(3,7-dichloro-5,5-difluoro-5*H*-4λ^4,5λ^4-dipyrrolo[1,2-*c*:2',1'-*f*][1,3,2]diazaborinin-10-yl)benzoate (50 mg, 0.13 mmol) and saturated NaI solution (0.8 mL). The reaction mixture was refluxed for 24 hours then diluted with DCM (10 mL). The organic layer was washed with H_2O (2 x 10 mL), dried over Na_2SO_4, filtered and the solvent was removed under reduced pressure to give a dark purple solid. The crude product was purified through silica gel column chromatography (1:2 Petrol : DCM) to give methyl 4-(3,7-diiodo-5,5-difluoro-5*H*-4λ^4,5λ^4-dipyrrolo[1,2-*c*:2',1'-*f*][1,3,2]diazaborinin-10-yl)benzoate (66 mg, 0.12 mmol, 95%) as a purple solid.

Method B:

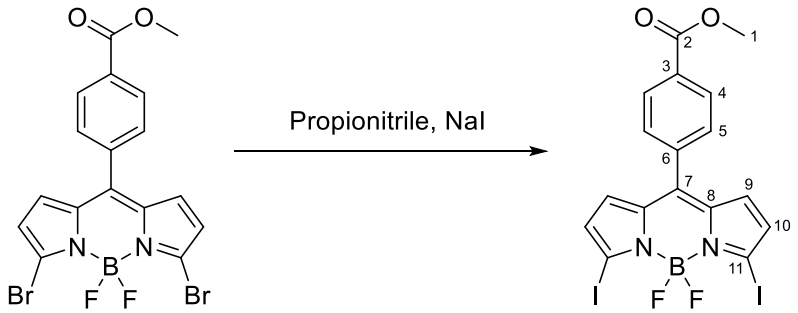

To a 25 mL round bottom flask was added methyl methyl 4-(3,7-dibromo-5,5-difluoro-5*H*-4λ^4,5λ^4-dipyrrolo[1,2-*c*:2',1'-*f*][1,3,2]diazaborinin-10-yl)benzoate (1.0 g,

2.07 mmol) and saturated NaI solution (30 mL). The reaction mixture was refluxed for 1.5 hours then diluted with DCM (100 mL). The organic layer was washed with H_2O (2 x 100 mL), dried over Na_2SO_4, filtered and the solvent was removed under reduced pressure to give a purple solid. The crude product was purified through silica gel column chromatography (DCM) to give methyl 4-(5,5-difluoro-3,7-diiodo-5*H*-4λ^4,5λ^4-dipyrrolo[1,2-*c*:2',1'-*f*][1,3,2]diazaborinin-10-yl)benzoate (1.07 g, 1.85 mmol, 90%) as a purple solid.

Methyl 4-(5,5-difluoro-3,7-diiodo-5*H*-4λ^4,5λ^4-dipyrrolo[1,2-*c*:2',1'-*f*][1,3,2]diazaborinin-10-yl)benzoate **3.17a**

R_f: 0.85 (DCM). **Mp**: 156-157 ^oC. **^{1}H NMR** (300 MHz, $CDCl_3$) δ 8.17 (d, *J* = 8.4 Hz, 2H, H*4*), 7.57 (d, *J* = 8.4 Hz, 2H, H*5*), 6.72 (d, *J* = 4.2 Hz, 2H, H*9*), 6.61 (d, *J* = 4.2 Hz, 2H, H*10*), 3.98 (s, 3H, H*1*). **^{13}C NMR** (75 MHz, Chloroform-*d*) δ 166.2 (C*2*), 139.7 (C*7*), 137.8 (C*8*), 136.9 (C*3*), 132.3 (C*6*), 131.6 (C*10*), 130.6 – 130.4 (m, C*9*), 130.4 (C*5*), 129.8 (C*4*), 104.0 (C*11*), 52.7 (C*1*). **^{19}F NMR** (282 MHz, Chloroform-*d*) δ -144.75 (q, *J* = 29.5 Hz). **^{11}B NMR** (96 MHz, Chloroform-*d*) δ 0.72 (t, *J* = 30.1 Hz). **IR** (neat): ν_{max}/cm^{-1} 3107 (C-H, w), 1707 (C=O, w). **HRMS:** (ASAP+) calcd for $C_{17}H_{11}BI_2F_2N_2O_2$ $[M-F]^+$: 558.8990, found 558.8995. **UV-Vis:** λ_{max} = 545 nm (DCM**). Molar extinction coefficient (ε)** = 63,000 $M^{-1}\,cm^{-1}$. **ϕ_F:** 0.13

6.2.3.2 5,5-Difluoro-3,7-diiodo-10-(3-nitrophenyl)-5*H*-4λ^4,5λ^4-dipyrrolo[1,2-*c*:2',1'-*f*][1,3,2]diazaborinine **3.17b** [83]

Method A:

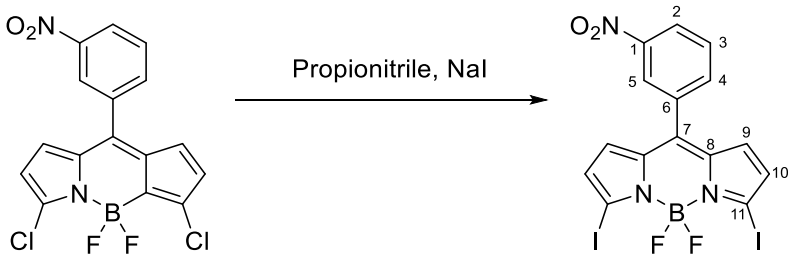

To a 25 ml round bottom flask was added methyl 3,7-dichloro-5,5-difluoro-10-(3-nitrophenyl)-5*H*-4λ^4,5λ^4-dipyrrolo[1,2-c:2',1'-*f*][1,3,2]diazaborinine (43 mg, 0.13 mmol) and saturated NaI solution (2 ml). The reaction mixture was refluxed for 6 hours then odiluted with DCM (10 ml). The organic layer was washed with H_2O (2 x 40 ml), dried over Na_2SO_4, filtered and the solvent was removed under reduced pressure to give a purple solid. The crude product was purified through silica gel column chromatography (1:1 Petrol:ethyl acetate) to give 5,5-difluoro-3,7-diiodo-10-(3-nitrophenyl)-5*H*-4λ^4,5λ^4-dipyrrolo[1,2-c:2',1'-*f*][1,3,2]diazaborinine (59.2 mg, 0.10 mmol 93%) as a pink solid.

Method B:

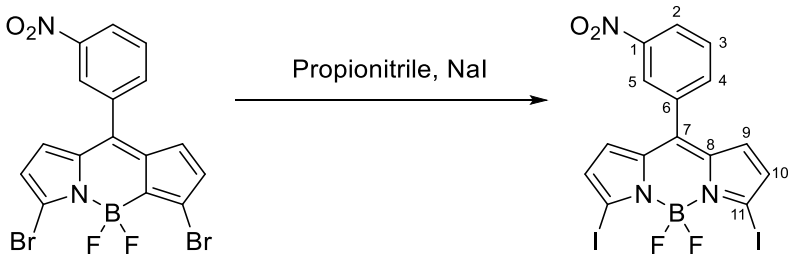

To a 25 mL round bottom flask was added methyl 3,7-dibromo-5,5-difluoro-10-(3-nitrophenyl)-5*H*-4λ^4,5λ^4-dipyrrolo[1,2-c:2',1'-*f*][1,3,2]diazaborinine (63.2 mg, 0.13 mmol) and saturated NaI solution (2 mL). The reaction mixture was refluxed for 30 mins then diluted with DCM (10 mL). The organic layer was washed with H_2O (2 x 40 mL), dried over Na_2SO_4, filtered and the solvent was removed under reduced

pressure to give a purple solid. The crude product was purified through silica gel column chromatography (DCM) to give 5,5-difluoro-3,7-diiodo-10-(3-nitrophenyl)-5*H*-4λ^4,5λ^4-dipyrrolo[1,2-c:2',1'-*f*][1,3,2]diazaborinine (74.1 mg, 0.13 mmol, 98%) as a purple solid.

5,5-Difluoro-3,7-diiodo-10-(3-nitrophenyl)-5*H*-4λ^4,5λ^4-dipyrrolo[1,2-*c*:2',1'-*f*][1,3,2]diazaborinine **3.17b**

R_f: 0.73 (DCM). **Mp:** 115-116 ^{o}C. **^{1}H NMR** (300 MHz, Chloroform-*d*) δ 8.44 (ddd, *J* = 8.1, 2.2, 1.2 Hz, 1H, H^{2}), 8.36 (t, *J* = 1.8 Hz, 1H, H^{5}), 7.83 (dt, J = 7.6, 1.3 Hz, 1H, H^{4}), 7.74 (t, *J* = 7.9 Hz, 1H, H^{3}), 6.74 (d, *J* = 4.3 Hz, 2H, H^{9}), 6.59 (d, *J* = 4.2 Hz, 2H, H^{10}). **^{13}C NMR** (75 MHz, Chloroform-*d*) δ 148.3 (C^{1}), 137.7 (C^{8}), 137.4 (C^{5}), 135.9 (C^{4}), 134.2 (C^{7}), 131.3 (C^{10}), 131.0 – 130.8 (m, C^{9}), 130.1 (C^{3}), 125.5 (C^{2}), 124.9 (C^{6}), 105.1 (C^{11}). **^{19}F NMR** (282 MHz, Chloroform-*d*) δ -144.72 (dq, *J* = 29.3, 10.4 Hz). **^{11}B NMR** (96 MHz, Chloroform-*d*) δ 0.73 (t, *J* = 29.0 Hz). **IR** (neat): ν_{max}/cm^{-1} 2920 (C-H, w), 1527 (N-O, s). **HRMS:** (ASAP+) calcd for $C_{15}H_8BI_2F_2N_3O_2$ $[M+H]^+$: 565.8848, found 565.8842. **UV-Vis:** λ_{max} = 548 nm (DCM). **Molar extinction coefficient (ε)** = 73,000 M^{-1} cm^{-1}. ϕ_F: 0.35

6.2.3.3 5,5-Difluoro-3,7-diiodo-10-(4-methoxyphenyl)-5*H*-4λ^4,5λ^4-dipyrrolo[1,2-*c*:2',1'-*f*][1,3,2]diazaborinine **3.17c** [83]

Method A:

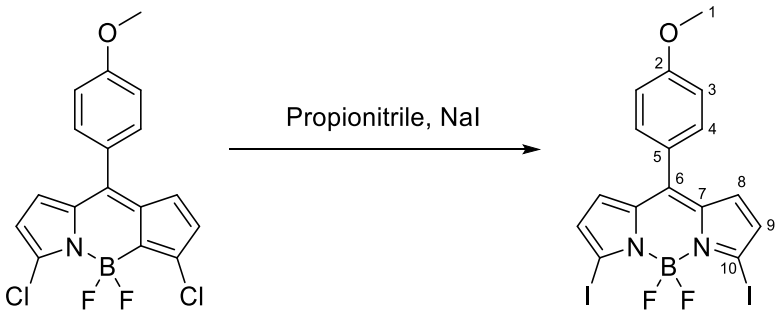

To a 25 mL round bottom flask was added methyl 3,7-dichloro-5,5-difluoro-10-(4-methoxyphenyl)-5*H*-4λ^4,5λ^4-dipyrrolo[1,2-c:2',1'-*f*][1,3,2]diazaborinine (34.5 mg, 0.09 mmol) and saturated NaI solution (2 mL). The reaction mixture was refluxed for 144 hours then diluted with DCM (10 mL). The organic layer was washed with H_2O (2 x 40 mL), dried over Na_2SO_4, filtered and the solvent was removed under reduced pressure to give a purple solid. The crude product was purified through silica gel column chromatography (3:1 Petrol:ethyl acetate) to give 5,5-difluoro-3,7-diiodo-10-(4-methoxyphenyl)- 5*H*-4λ^4,5λ^4-dipyrrolo[1,2-c:2',1'-*f*][1,3,2]diazaborinine (26.3 mg, 0.05 mmol 51%) as a purple solid.

Method B:

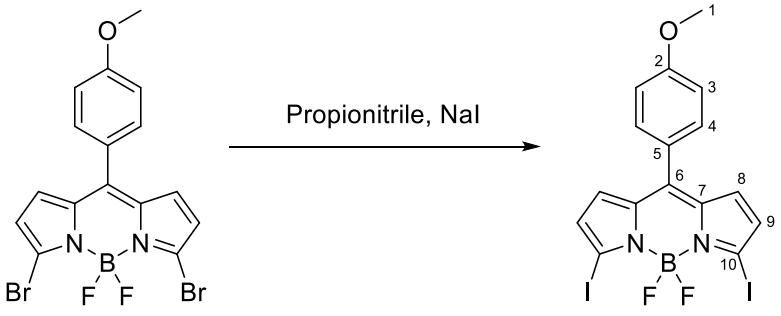

To a 25 mL round bottom flask was added methyl 3,7-dibromo-5,5-difluoro-10-(4-methoxyphenyl)-5*H*-4λ^4,5λ^4-dipyrrolo[1,2-c:2',1'-*f*][1,3,2]diazaborinine (308.8 mg, 0.68 mmol) and saturated NaI solution (6 mL). The reaction mixture was refluxed for

2.5 hours then diluted with DCM (50 mL). The organic layer was washed with H_2O (2 x 100 mL), dried over Na_2SO_4, filtered and the solvent was removed under reduced pressure to give a purple solid. The crude product was purified through silica gel column chromatography (DCM) to give 5,5-difluoro-3,7-diiodo-10-(4-methoxyphenyl)-5*H*-4λ^4,5λ^4-dipyrrolo[1,2-c:2',1'-*f*][1,3,2]diazaborinine (231.7 mg, 0.42 mmol, 62%) as a purple solid.

5,5-Difluoro-3,7-diiodo-10-(4-methoxyphenyl)-5*H*-4λ^4,5λ^4-dipyrrolo[1,2-*c*:2',1'-*f*][1,3,2]diazaborinine **3.17c**

R_f: 0.83 (DCM). **Mp:** 180-183 ^oC. **^{1}H NMR** (300 MHz, Chloroform-*d*) δ 7.44 (d, *J* = 8.8 Hz, 2H, H*^{3}*), 7.02 (d, *J* = 8.8 Hz, 2H, H*^{4}*), 6.71 – 6.70 (m, 4H, H*^{8,9}*), 3.90 (s, 3H, H*^{1}*). **^{13}C NMR** (75 MHz, Chloroform-*d*) δ 162.2 (C*^{2}*), 141.7 (C*^{5}*), 138.0 (C*^{6}*), 132.3 (C*^{3}*), 131.8 (C*^{8}*), 130.0 – 129.8 (m, C*^{9}*), 125.1 (C*^{7}*), 114.3 (C*^{4}*), 102.0 (C*^{10}*), 55.7 (C*^{1}*). **^{19}F NMR** (282 MHz, Chloroform-*d*) δ -144.47 (d, *J* = 29.7 Hz). **^{11}B NMR** (96 MHz, Chloroform-*d*) δ 0.69 (t, *J* = 29.3 Hz). **IR** (neat): ν_{max}/cm^{-1} 2985 (C-H, w). **HRMS:** (ASAP+) calcd for $C_{16}H_{11}BF_2I_2N_2O$ $[M+H]^+$: 550.9103, found 550.9101. **UV-Vis:** λ_{max} = 537 nm (DCM). **Molar extinction coefficient (ε)** = 66000 M^{-1} cm^{-1}. **ϕ_F:** 0.14

6.2.3.4 5,5-Difluoro-3,7-diiodo-10-(3-methoxyphenyl)-5*H*-4λ^4,5λ^4-dipyrrolo[1,2-*c*:2',1'-*f*][1,3,2]diazaborinine **3.17d** [83]

Method A:

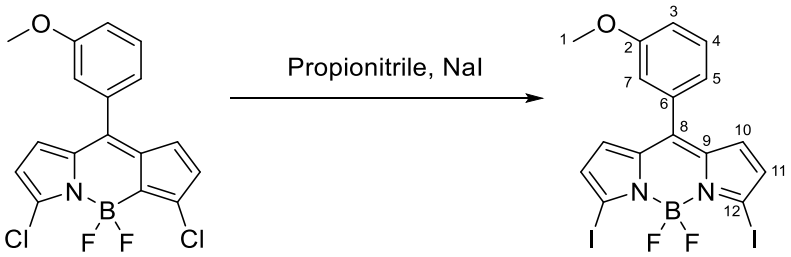

To a 25 mL round bottom flask was added methyl 3,7-dichloro-5,5-difluoro-10-(3-methoxyphenyl)-5*H*-4λ^4,5λ^4-dipyrrolo[1,2-c:2',1'-*f*][1,3,2]diazaborinine (38.5 mg, 0.11 mmol) and saturated NaI solution (2 mL). The reaction mixture was refluxed for 72 hours then diluted with DCM (10 mL). The organic layer was washed with H_2O (2 x 100 mL), dried over Na_2SO_4, filtered and the solvent was removed under reduced pressure to give a purple solid. The crude product was purified through silica gel column chromatography (DCM) to give 5,5-difluoro-3,7-diiodo-10-(3-methoxyphenyl)-5*H*-4λ^4,5λ^4-dipyrrolo[1,2-c:2',1'-*f*][1,3,2]diazaborinine (52.6 mg, 0.096 mmol, 91%) as a purple solid.

Method B:

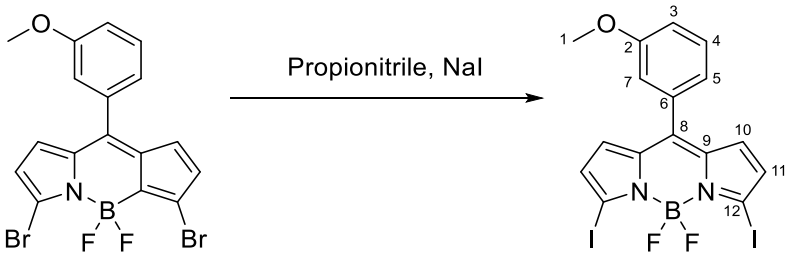

To a 25 mL round bottom flask was added methyl 3,7-dibromo-5,5-difluoro-10-(3-methoxyphenyl)-5*H*-4λ^4,5λ^4-dipyrrolo[1,2-c:2',1'-*f*][1,3,2]diazaborinine (342.4 mg, 0.75 mmol) and saturated NaI solution (6 mL). The reaction mixture was refluxed for 2.5 hours then diluted with DCM (50 mL). The organic layer was washed with H_2O (2 x 100 mL), dried over Na_2SO_4, filtered and the solvent was removed under reduced

pressure to give a purple solid. The crude product was purified through silica gel column chromatography (DCM) to give 5,5-difluoro-3,7-diiodo-10-(3-methoxyphenyl)-5*H*-4λ^4,5λ^4-dipyrrolo[1,2-c:2',1'-*f*][1,3,2]diazaborinine (278 mg, 0.51 mmol, 88%) as a purple solid.

5,5-Difluoro-3,7-diiodo-10-(3-methoxyphenyl)-5*H*-4λ^4,5λ^4-dipyrrolo[1,2-*c*:2',1'-*f*][1,3,2]diazaborinine **3.17d**

R_f: 0.80 (DCM). **Mp:** 210-211 ^{o}C. **^{1}H NMR** (300 MHz, Chloroform-*d*) δ 7.40 (dd, *J* = 8.1, 7.5 Hz, 1H, H^{4}), 7.11 (ddd, *J* = 8.4, 2.6, 1.0 Hz, 1H, H^{5}), 7.06 (ddd, *J* = 7.5, 1.6, 1.0 Hz, 1H, H^{3}), 7.02 (dd, *J* = 2.6, 1.6 Hz, 1H, H^{7}), 6.73 – 6.68 (m, 4H, H^{10,11}), 3.85 (s, 3H, H^{1}). **^{13}C NMR** (75 MHz, Chloroform-*d*) δ 159.5 (C^{2}), 141.2 (C^{6}), 138.0 (C^{9}), 133.9 (C^{8}), 131.9 (C^{10}), 130.2 – 130.0 (m, C^{11}), 129.8 (C^{4}), 122.9 (C^{3}), 116.3 (C^{5}), 116.1 (C^{7}), 103.1 (C^{12}), 55.6 (C^{1}). **^{19}F NMR** (300 MHz, Chloroform-*d*) δ -144.69 (q, *J* = 29.4 MHz). **^{11}B NMR** (96 MHz, Chloroform-*d*) δ 0.71 (t, *J* = 30.2 Hz). **IR** (neat): ν_{max}/cm^{-1} 3156 (C-H, w) 2958-2902 (C-H, w). **HRMS:** (ASAP+) calcd for $C_{16}H_{11}BF_2I_2N_2O$ $[M+H]^+$: 550.9103, found 550.9102. **UV-Vis:** λ_{max} = 541 nm (DCM). **Molar extinction coefficient (ε)** = 76000 M^{-1} cm^{-1}. **ϕ_F:** 0.12.

6.2.3.5 Methyl 4-(5,5-difluoro-3,7-diphenyl-5*H*-4λ^4,5λ^4-dipyrrolo[1,2-*c*:2',1'-*f*][1,3,2]diazaborinin-10-yl)benzoate **3.21** and methyl 4-(3-butyl-5,5-difluoro-7-phenyl-5*H*-5λ4,6λ4-dipyrrolo[1,2-*c*:2',1'-*f*][1,3,2]diazaborinin-10-yl)benzoate **3.22** [83]

Method A:

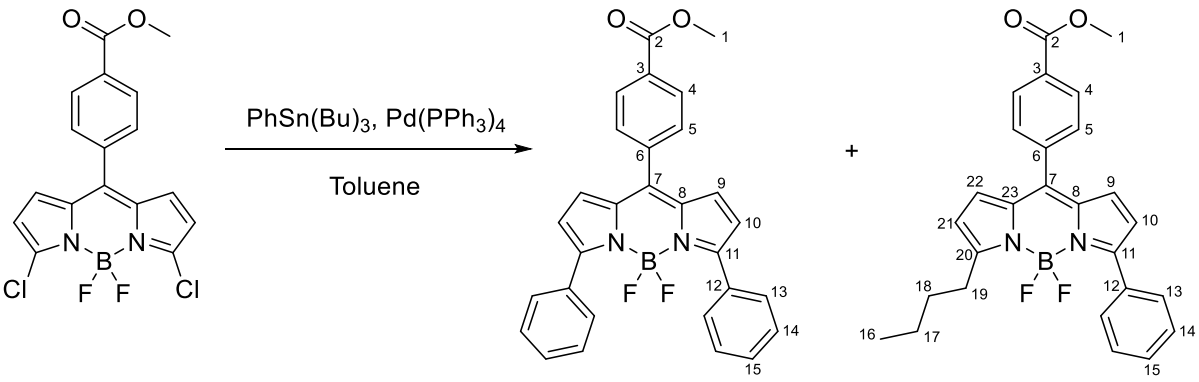

To a 50 mL Schlenk flask, under nitrogen atmosphere, was added methyl 4-(3,7-dichloro-5,5-difluoro-5*H*-4λ^4,5λ^4-dipyrrolo[1,2-*c*:2',1'-*f*][1,3,2]diazaborinin-10-yl)benzoate (39.5 mg, 0.1 mmol), $PhSn(Bu)_3$ (73.4 mg, 0.2 mmol), $Pd(PPh_3)_4$ (11 mg, 10 mol%, 0.01 mmol), dry toluene (6 mL) and was degassed using freeze thaw method (x3). The reaction mixture was heated to 100^{o}C, stirred for 16 hours then left to cool to room temp (10 mins). To the crude reaction mixture was added water (10 mL) and the product was extracted with DCM (3 x 30 mL). The organic layer was dried over $MgSO_4$, filtered and the solvent was removed under reduced pressure to give a dark purple solid. The crude product was purified by silica gel column chromatography (1:1 petrol:DCM) to give methyl 4-(5,5-difluoro-3,7-diphenyl-5H-4λ^4,5λ^4-dipyrrolo[1,2-*c*:2',1'-*f*][1,3,2]diazaborinin-10-yl)benzoate (16.7 mg, 0.035 mmol, 35%) as a purple solid and methyl 4-(3-butyl-5,5-difluoro-7-phenyl-5*H*-5λ4,6λ4-dipyrrolo[1,2-*c*:2',1'-*f*][1,3,2]diazaborinin-10-yl)benzoate (10.4 mg, 0.024 mmol, 24%) as a purple solid.

Method B:

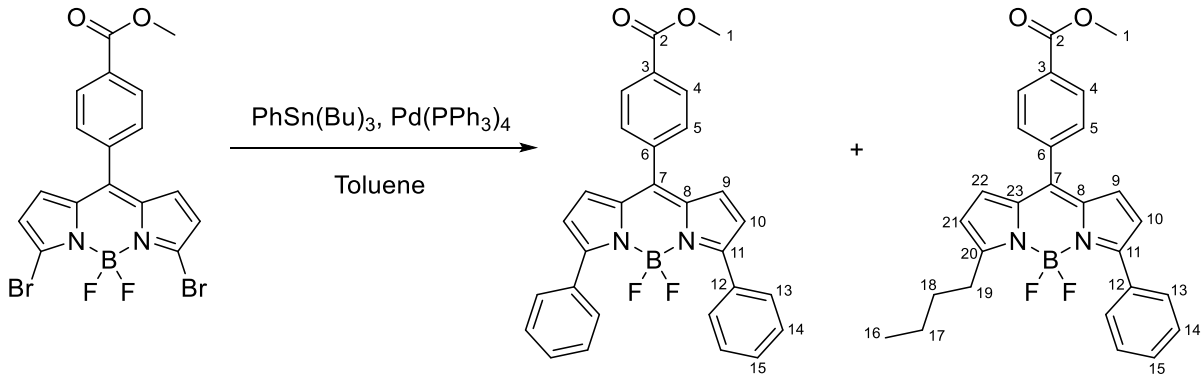

To a 50 mL Schlenk flask, under nitrogen atmosphere, was added methyl 4-(3,7-dibromo-5,5-difluoro-5*H*-4λ^4,5λ^4-dipyrrolo[1,2-*c*:2',1'-*f*][1,3,2]diazaborinin-10-yl)benzoate (48.2 mg, 0.1 mmol), $PhSn(Bu)_3$ (73.4 mg, 0.2 mmol), $Pd(PPh_3)_4$ (11 mg, 10 mol%, 0.01 mmol), dry toluene (6 mL) and was degassed using freeze thaw method (x3). The reaction mixture was heated to 100^{o}C, stirred for 16 hours then left to cool to room temp (10 mins). To the crude reaction mixture was added water (10 mL) and the product was extracted with DCM (3 x 30 mL). The organic layer was dried over $MgSO_4$, filtered and the solvent was removed under reduced pressure to give a dark purple solid. The crude product was purified by silica gel column chromatography (1:1 petrol:DCM) to give methyl 4-(5,5-difluoro-3,7-diphenyl-5H-4λ^4,5λ^4-dipyrrolo[1,2-*c*:2',1'-*f*][1,3,2]diazaborinin-10-yl)benzoate (36.6 mg, 0.077 mmol, 77%) as a purple solid and methyl 4-(3-butyl-5,5-difluoro-7-phenyl-5*H*-5λ4,6λ4-dipyrrolo[1,2-*c*:2',1'-*f*][1,3,2]diazaborinin-10-yl)benzoate (4.0 mg, 0.008 mmol, 8%) as a purple solid.

Method C:

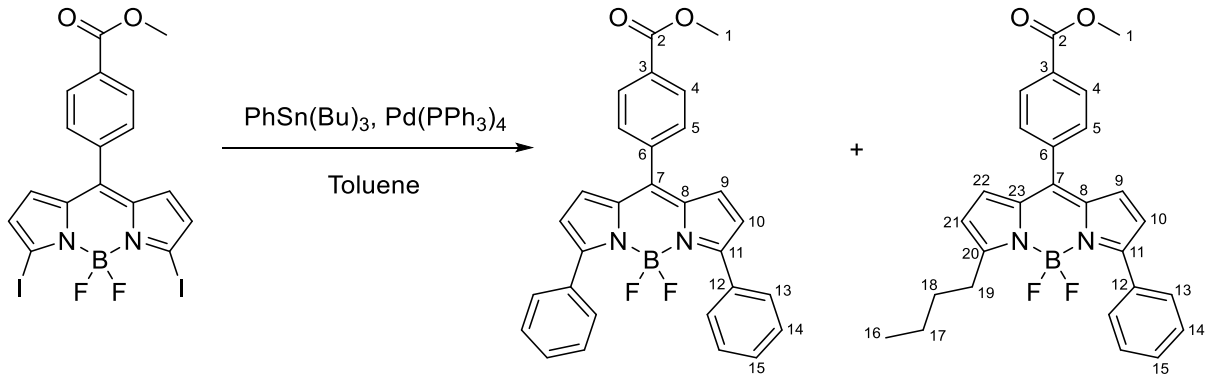

To a 50 mL Schlenk flask, under nitrogen atmosphere, was added methyl 4-(3,7-diiodo-5,5-difluoro-5*H*-4λ^4,5λ^4-dipyrrolo[1,2-*c*:2',1'-*f*][1,3,2]diazaborinin-10-yl)benzoate (57.8 mg, 0.1 mmol), $PhSn(Bu)_3$ (73.4 mg, 0.2 mmol), $Pd(PPh_3)_4$ (11 mg, 10 mol%, 0.01 mmol), dry toluene (6 mL) and was degassed using freeze thaw method (x3). The reaction mixture was heated to 100^{o}C, stirred for 16 hours then left to cool to room temp (10 mins). To the crude reaction mixture was added water (10 mL) and the product was extracted with DCM (3 x 30 mL). The organic layer was dried over $MgSO_4$, filtered and the solvent was removed under reduced pressure to give a dark purple solid. The crude product was purified by silica gel column chromatography (1:1 petrol:DCM) to give methyl 4-(5,5-difluoro-3,7-diphenyl-5H-4λ^4,5λ^4-dipyrrolo[1,2-*c*:2',1'-*f*][1,3,2]diazaborinin-10-yl)benzoate (24.2 mg, 0.051 mmol, 51%) as a purple solid and methyl 4-(3-butyl-5,5-difluoro-7-phenyl-5*H*-5λ4,6λ4-dipyrrolo[1,2-*c*:2',1'-*f*][1,3,2]diazaborinin-10-yl)benzoate (8.8 mg, 0.017 mmol, 17%) as a purple solid.

Methyl 4-(5,5-difluoro-3,7-diphenyl-5*H*-4λ^4,5λ^4-dipyrrolo[1,2-*c*:2',1'-*f*][1,3,2]diazaborinin-10-yl)benzoate **3.21** [83]

R_f: 0.18 (1:1 40/60 petroleum ether : DCM). **Mp:** 104-105 ^{o}C. **^{1}H NMR** (300 MHz, Chloroform-*d*) δ 8.22 (d, *J* = 8.5 Hz, 2H, H^4), 7.99 – 7.81 (m, 4H, H^{13}), 7.68 (d, *J* = 8.5 Hz, 2H, H^5), 7.54 – 7.37 (m, 6H, H^{14,15}), 6.84 (d, *J* = 4.3 Hz, 2H, H^9), 6.64 (d, *J* = 4.1 Hz, 2H, H^{10}), 4.00 (s, 3H, H^1). **^{13}C NMR** (75 MHz, Chloroform-*d*) δ 166.5 (C^2), 159.6 (C^{11}), 142.5 (C^7), 138.9 (C^3), 136.2 (C^8), 132.6 (C^{12}), 131.8 (C^6), 130.7 (C^{5,9}), 129.8 (C^{15}), 129.6 (C^{13}), 129.6 (C^4), 128.4 (C^{14}), 121.4 (C^{10}), 52.6 (C^1). **^{19}F NMR**

(282 MHz, Chloroform-*d*) δ -132.47 (q, *J* = 31.8 Hz). **^{11}B NMR** (96 MHz, Chloroform-*d*) δ 1.43 (t, *J* = 31.2 Hz). **IR** (neat): ν_{max}/cm^{-1} 2973 (C-H, m), 1876 (C=O, w). **HRMS:** (ASAP+) calcd for $C_{29}H_{21}BF_2N_2O_2$ $[M+H]^+$: 479.1747, found 479.1745. **UV-Vis:** λ_{max} = 557 nm (DCM). **Molar extinction coefficient (ε)** = 58000 M^{-1} cm^{-1}. **ϕ_F:** 0.03.

Methyl 4-(3-butyl-5,5-difluoro-7-phenyl-5*H*-5λ4,6λ4-dipyrrolo[1,2-*c*:2',1'-*f*][1,3,2]diazaborinin-10-yl)benzoate **3.22**

R_f: 0.38 (1:1 40/60 petroleum ether : DCM). **Mp:** 169-170 °C. **^{1}H NMR** (300 MHz, Chloroform-*d*) δ 8.18 (d, *J* = 8.1 Hz, 2H, H*^{4}*), 7.95 – 7.86 (m, 2H, H*^{13}*), 7.63 (d, *J* = 8.1 Hz, 2H, H*^{5}*), 7.57 – 7.38 (m, 3H, H*^{14,15}*), 6.76 (d, *J* = 4.3 Hz, 1H, H*^{22}*), 6.74 (d, *J* = 4.1 Hz, 1H, H*^{9}*), 6.59 (d, *J* = 4.1 Hz, 1H, H*^{10}*), 6.41 (d, *J* = 4.3 Hz, 1H, H*^{21}*), 3.99 (s, 3H, H*^{1}*), 3.03 (t, *J* = 7.8 Hz, 2H, H*^{19}*), 1.71 (p, *J* = 7.7 Hz, 2H, H*^{18}*), 1.43 (h, *J* = 7.4 Hz, 2H, H*^{17}*), 0.94 (t, *J* = 7.3 Hz, 3H, H*^{16}*). **^{13}C NMR** (176 MHz, Chloroform-*d*) δ 166.6 (C*^{2}*), 165.5 (C*^{20}*), 157.7 (C*^{11}*), 141.7 (C*^{7}*), 138.8 (C*^{3}*), 135.7 (C*^{8}*), 134.6 (C*^{23}*), 132.9 (C*^{12}*), 131.7 (C*^{6}*), 131.2 (C*^{22}*), 130.6 (C*^{5}*), 129.7 (C*^{9}*), 129.6 (C*^{4}*), 129.5 (C*^{15}*), 129.5 (C*^{13}*), 128.4 (C*^{14}*), 120.1 (C*^{10}*), 119.7 (C*^{21}*), 52.6 (C*^{1}*), 30.7 (C*^{18}*), 28.9 (C*^{19}*), 22.8 (C*^{17}*), 14.1 (C*^{16}*). **^{19}F NMR** (282 MHz, Chloroform-*d*) δ -138.27 (q, *J* = 32.1 Hz). **^{11}B NMR** (96 MHz, Chloroform-*d*) δ 1.21 (t, *J* = 33.3 Hz). **IR** (neat): ν_{max}/cm^{-1} 3001 (C-H, s), 2994 (C-H, m), 1710 (C=O, m). **HRMS:** (ASAP+) calcd for $C_{27}H_{25}BF_2N_2O_2$ $[M+H]^+$: 459.2050, found 459.2052. **UV-Vis:** λ_{max} = 538 nm (DCM). **Molar extinction coefficient (ε)** = 67000 M^{-1} cm^{-1}. **ϕ_F:** 0.04

6.2.3.6 Methyl 4-(5,5-difluoro-3,7-di((*E*)-styryl)-5H-4λ^4,5λ^4-dipyrrolo[1,2-*c*:2',1'-*f*][1,3,2]diazaborinin-10-yl)benzoate **3.25** [83]

Method A:

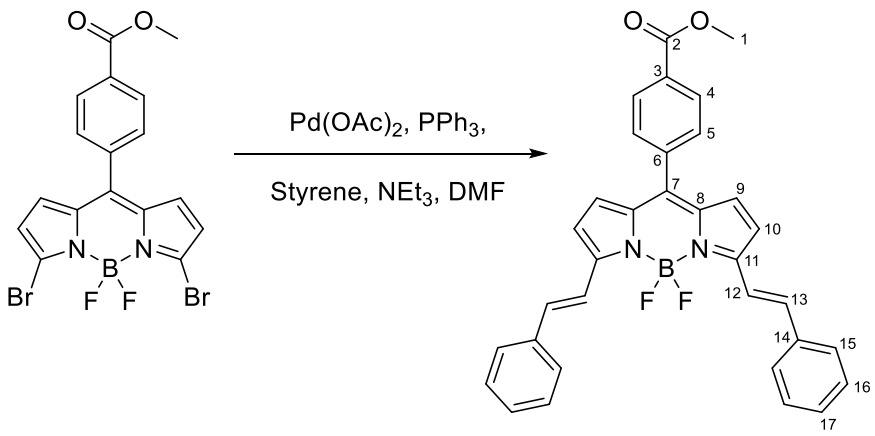

To a 50 mL Schlenck flask, under nitrogen atmosphere, was added methyl 4-(3,7-dibromo-5,5-difluoro-5*H*-4λ^4,5λ^4-dipyrrolo[1,2-*c*:2',1'-*f*][1,3,2]diazaborinin-10-yl)benzoate (48.2 mg, 0.1 mmol), $Pd(OAc)_2$ (0.7 mg, 0.003 mmol, 3 mol%), PPh_3 (2 mg, 0.007 mmol, 7 mol%) and was stirred for 10 mins. To the reaction mixture was added styrene (28.7 μL, 0.25 mmol), NEt_3 (41.8 μL, 0.3 mmol), dry DMF (0.5 mL), degassed (x3) and heated to 100^{o}C. The reaction mixture was stirred for 8 hours, quenched with water (20 mL) and the organic layer was extracted with DCM (3 x 20 mL). The organic layer was dried over $MgSO_4$, filtered and the solvent was removed under reduced pressure to give a purple solid. The crude product was purified by silica gel column chromatography (1:2 petrol:DCM) to give methyl 4-(5,5-difluoro-3,7-di((*E*)-styryl)-5H-4λ^4,5λ^4-dipyrrolo[1,2-*c*:2',1'-*f*][1,3,2]diazaborinin-10-yl)benzoate (1.4 mg, 0.003 mmol, 3%) as a blue solid.

Method B:

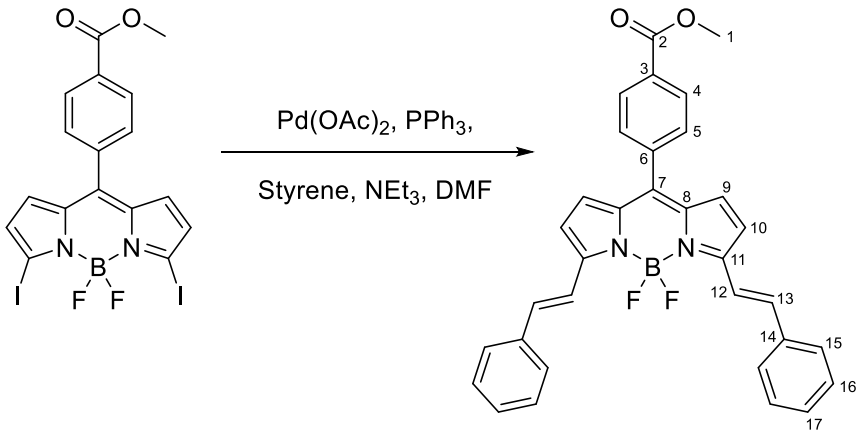

To a 50 mL Schlenck flask, under nitrogen atmosphere, was added methyl 4-(3,7-diiodo-5,5-difluoro-5*H*-4λ^4,5λ^4-dipyrrolo[1,2-*c*:2',1'-*f*][1,3,2]diazaborinin-10-yl)benzoate (57.8 mg, 0.1 mmol), $Pd(OAc)_2$ (0.7 mg, 0.003 mmol, 3 mol%), PPh_3 (2 mg, 0.007 mmol, 7 mol%) and was stirred for 10 mins. To the reaction mixture was added styrene (28.7 μL, 0.25 mmol), NEt_3 (41.8 μL, 0.3 mmol), dry DMF (0.5 mL), degassed (x3) and heated to 100^{o}C. The reaction mixture was stirred for 8 hours, quenched with water (20 mL) and the organic layer was extracted with DCM (3 x 20 mL). The organic layer was dried over $MgSO_4$, filtered and the solvent was removed under reduced pressure to give a purple solid. The crude product was purified by silica gel column chromatography (1:2 petrol:DCM) to give methyl 4-(5,5-difluoro-3,7-di((*E*)-styryl)-5H-4λ^4,5λ^4-dipyrrolo[1,2-*c*:2',1'-*f*][1,3,2]diazaborinin-10-yl)benzoate (16 mg, 0.030 mmol, 30%) as a blue solid.

Methyl 4-(5,5-difluoro-3,7-di((*E*)-styryl)-5H-4λ^4,5λ^4-dipyrrolo[1,2-*c*:2',1'-*f*][1,3,2]diazaborinin-10-yl)benzoate **3.25**

R_f: 0.40 (1:2 40/60 petroleum ether : DCM). **Mp:** 263-264 ^{o}C. **^{1}H NMR** (300 MHz, Chloroform-*d*) δ 8.17 (d, *J* = 8.5 Hz, 2H, H^{4}), 7.80 (d, *J* = 16.4 Hz, 2H, H^{12}), 7.67 (d, *J* = 7.1 Hz, 4H, H^{15}), 7.60 (d, *J* = 8.5 Hz, 2H, H^{5}), 7.48 – 7.36 (m, 6H, H^{16,17}), 7.36 (d, *J* = 16.4 Hz, 1H, H^{13}), 6.95 (d, *J* = 4.5 Hz, 2H, H^{10}), 6.76 (d, *J* = 4.5 Hz, 2H, H^{9}), 3.99 (s, 3H, H^{1}). **^{13}C NMR** (75 MHz, Chloroform-*d*) δ 166.6 (C^{2}), 155.4 (C^{11}), 138.9 (C^{3}), 137.9 (C^{7}), 137.3 (C^{13}), 136.5 (C^{14}), 136.1 (C^{8}), 131.5 (C^{6}), 130.6 (C^{5}), 129.6 (C^{4}), 129.5 (C^{9}), 129.4 (C^{17}), 129.0 (C^{16}), 127.8 (C^{15}), 119.4 (C^{12}), 116.8 (C^{10}), 52.6 (C^{1}). **^{19}F NMR** (282 MHz, Chloroform-*d*) δ -139.54 (q, *J* = 32.9 Hz). **^{11}B NMR** (96 MHz,

Chloroform-*d*) δ 1.32 (t, *J* = 32.9 Hz). **IR** (neat): ν_{max}/cm^{-1} 2921 (C-H, s) 2852 (C-H, m) 1722 (C=O, m). **HRMS:** (ASAP+) calcd for $C_{33}H_{25}BF_2N_2O_2$ $[M+H]^+$: 531.2061, found 531.2063. **UV-Vis:** λ_{max} = 619 nm (DCM). **Molar extinction coefficient (ε)** = 96000 M^{-1} cm^{-1}. **ϕ_F:** 0.03

6.2.3.7 Methyl 4-(5,5-difluoro-3,7-bis(phenylethynyl)-5*H*-4λ^4,5λ^4-dipyrrolo[1,2-*c*:2',1'-*f*][1,3,2]diazaborinin-10-yl)benzoate **3.28** and methyl 4-(3-chloro-5,5-difluoro-7-(phenylethynyl)-5*H*-4λ4,5λ4-dipyrrolo[1,2-*c*:2',1'-*f*][1,3,2]diazaborinin-10-yl)benzoate **3.29** [83]

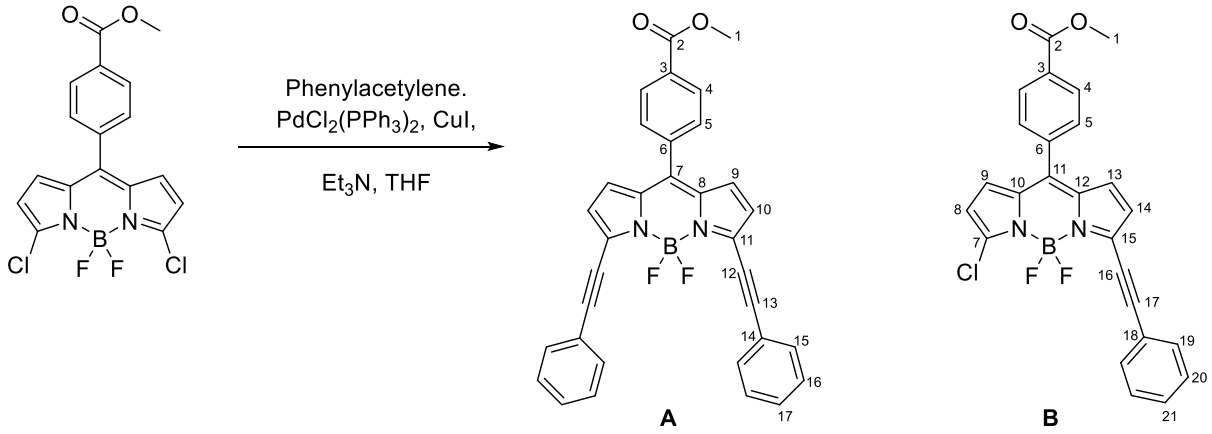

To a Schlenk flask was added methyl 4-(3,7-dichloro-5,5-difluoro-5*H*-4λ^4,5λ^4-dipyrrolo[1,2-*c*:2',1'-*f*][1,3,2]diazaborinin-10-yl)benzoate (39.4 mg, 0.1 mmol), $PdCl_2(PPh_3)_2$ (3.5 mg, 0.005 mmol, 5 mol%), CuI (1.0 mg, 0.005 mmol, 5 mol%) and dry THF (2 mL) and was subsequently degassed (x3). To the reaction mixture was added phenylacetylene (27 μL, 0.5 mmol), Et_3N (153.3 μL, 1.1 mmol) and was degassed (x3). The resulting reaction mixture was stirred, under a nitrogen atmosphere, at room temperature for 40 hours. The reaction mixture was diluted with DCM (10 mL), the organic layer was washed with H_2O (3 x 15 mL), dried over $MgSO_4$, filtered and the solvent was removed under reduced pressure to give a dark blue solid. The crude product was purified through silica gel column chromatography (DCM) to give methyl 4-(5,5-difluoro-3,7-bis(phenylethynyl)-5*H*-4λ^4,5λ^4-dipyrrolo[1,2-*c*:2',1'-*f*][1,3,2]diazaborinin-10-yl)benzoate (12.8 mg, 0.024 mmol, 24%) as a blue solid and methyl 4-(3-chloro-5,5-difluoro-7-(phenylethynyl)-5*H*-4λ4,5λ4-dipyrrolo[1,2-*c*:2',1'-*f*][1,3,2]diazaborinin-10-yl)benzoate (9.7 mg, 0.021 mmol, 21%) as a pink solid.

Methyl 4-(5,5-difluoro-3,7-bis(phenylethynyl)-5*H*-4λ^4,5λ^4-dipyrrolo[1,2-*c*:2',1'-*f*][1,3,2]diazaborinin-10-yl)benzoate **3.28**

R_f: 0.91 (DCM). **Mp:** 204-205 °C. **^{1}H NMR** (300 MHz, Chloroform-*d*) δ 8.19 (d, *J* = 8.5 Hz, 2H, H*[4]*), 7.77 – 7.67 (m, 4H, H*[15]*), 7.62 (d, *J* = 8.5 Hz, 2H, H*[5]*), 7.48 – 7.35 (m, 6H, H*[16,17]*), 6.81 (d, *J* = 4.1 Hz, 2H, H*[9]*), 6.73 (d, *J* = 4.3 Hz, 2H, H*[10]*), 3.98 (s, 3H, H*[1]*). **^{13}C NMR** (75 MHz, Chloroform-*d*) δ 166.4 (C*[2]*), 140.3 (C*[7]*), 138.7 (C*[11]*), 138.3 (C*[3]*), 136.5 (C*[8]*), 132.6 (C*[15]*), 132.0 (C*[6]*), 130.7 (C*[5]*), 130.2 (C*[9]*), 129.8 (C*[17]*), 129.7 (C*[4]*), 128.6 (C*[16]*), 124.2 (C*[10]*), 122.4 (C*[18]*), 103.6 (C*[13]*), 83.5 (C*[12]*), 52.6 (C*[1]*). **^{19}F NMR** (282 MHz, Chloroform-*d*) δ -146.86 (q, *J* = 27.6 Hz). **^{11}B NMR** (96 MHz, Chloroform-*d*) δ 0.73 (t, *J* = 27.9 Hz). **IR** (neat): ν_{max}/cm^{-1} 2937 (C-H, s), 2190 (C≡C, m), 1718 (C=O, m). **HRMS:** (ASAP+) calcd for $C_{33}H_{21}BF_2N_2O_2$ $[M+H]^+$: 527.1748, found 527.1751. **UV-Vis:** λ_{max} = 619 nm (DCM). Molar extinction coefficient (ε) = 85000 M^{-1} cm^{-1}. **ϕ_F:** 0.78.

Methyl 4-(3-chloro-5,5-difluoro-7-(phenylethynyl)-5*H*-4λ4,5λ4-dipyrrolo[1,2-*c*:2',1'-*f*][1,3,2]diazaborinin-10-yl)benzoate **3.29**

R_f: 0.74 (DCM). **Mp:** 216-217 °C. **^{1}H NMR** (700 MHz, Chloroform-*d*) δ 8.19 (d, *J* = 8.5 Hz, 2H, H*[4]*), 7.70 – 7.66 (m, 2H, H*[19]*), 7.59 (d, *J* = 8.5 Hz, 2H, H*[5]*), 7.43 – 7.37 (m, 3H, H*[20,21]*), 6.81 (d, *J* = 4.4 Hz, 1H, H*[13]*), 6.79 (d, *J* = 4.3 Hz, 1H, H*[9]*), 6.73 (d, *J* = 4.4 Hz, 1H, H*[14]*), 6.45 (d, *J* = 4.4 Hz, 1H, H*[8]*), 3.99 (s, 3H, H*[1]*). **^{13}C NMR** (176 MHz, Chloroform-*d*) δ 166.3 (C*[2]*), 145.6 (C*[7]*), 141.4 (C*[11]*), 139.0 (C*[15]*), 137.5 (C*[3]*), 135.7 (C*[12]*), 134.4 (C*[10]*), 132.6 (C*[19]*), 132.2 (C*[6]*), 131.0 (C*[9]*), 130.7 (C*[13]*), 130.6 (C*[5]*), 130.0 (C*[21]*), 129.8 (C*[4]*), 128.6 (C*[20]*), 124.4 (C*[14]*), 122.0 (C*[18]*), 119.2 (C*[8]*), 103.5 (C*[17]*), 82.8 (C*[16]*), 52.7 (C*[1]*). **^{19}F NMR** (282 MHz, Chloroform-*d*) δ -147.53 (d, *J* = 27.6 Hz). **^{11}B NMR** (96 MHz, Chloroform-*d*) δ 0.59 (t, *J* = 28.0 Hz). **IR** (neat): ν_{max}/cm^{-1} 3054 (C-H, w), 1717 (C=O, m). **HRMS:** (ASAP+) calcd for $C_{25}H_{16}BClF_2N_2O_2$ $[M+H]^+$: 461.1044, found 461.1037. **UV-Vis:** λ_{max} = 567 nm (DCM). **Molar extinction coefficient (ε)** = 60000 M^{-1} cm^{-1}. **ϕ_F:** 0.60.

6.2.3.8 Methyl 4-(5,5-difluoro-3,7-bis(phenylethynyl)-5*H*-4λ^4,5λ^4-dipyrrolo[1,2-*c*:2',1'-*f*][1,3,2]diazaborinin-10-yl)benzoate **3.28** and methyl 4-(3-bromo-5,5-difluoro-7-(phenylethynyl)-5*H*-4λ4,5λ4-dipyrrolo[1,2-*c*:2',1'-*f*][1,3,2]diazaborinin-10-yl)benzoate **3.30** [83]

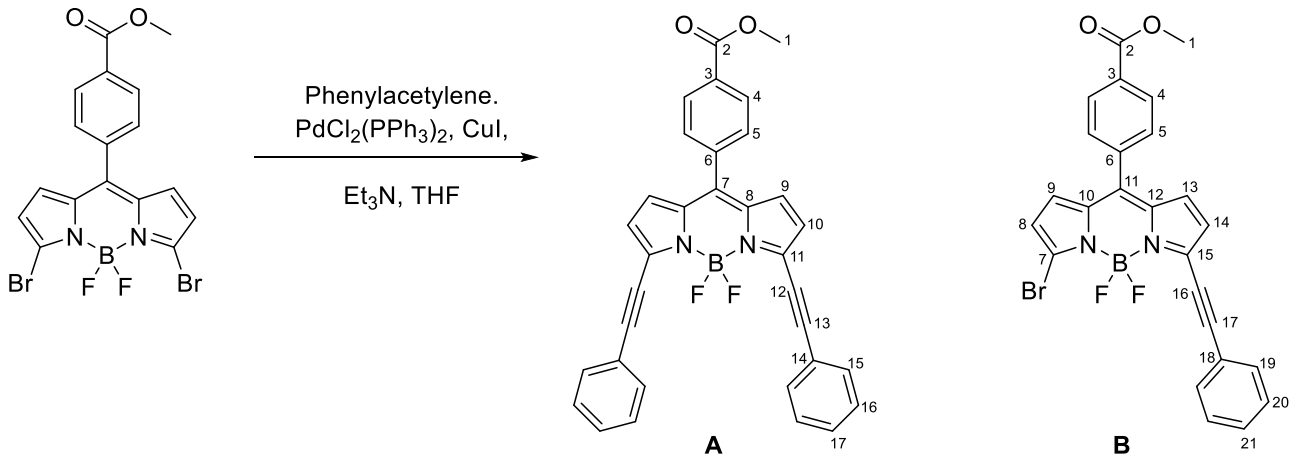

To a Schlenk flask was added methyl 4-(3,7-dibromo-5,5-difluoro-5*H*-4λ^4,5λ^4-dipyrrolo[1,2-*c*:2',1'-*f*][1,3,2]diazaborinin-10-yl)benzoate (48.2 mg, 0.1 mmol), $PdCl_2(PPh_3)_2$ (3.5 mg, 0.005 mmol, 5 mol%), CuI (1.0 mg, 0.005 mmol, 5 mol%) and dry THF (2 mL) and was subsequently degassed (x3). To the reaction mixture was added phenylacetylene (27 μL, 0.5 mmol), Et_3N (153.3 μL, 1.1 mmol) and was degassed (x3). The resulting reaction mixture was stirred, under a nitrogen atmosphere, at room temperature for 40 hours. The reaction mixture was diluted with DCM (10 mL), the organic layer was washed with H_2O (3 x 15 mL), dried over $MgSO_4$, filtered and the solvent was removed under reduced pressure to give a dark blue solid. The crude product was purified through silica gel column chromatography (DCM) to give methyl 4-(5,5-difluoro-3,7-bis(phenylethynyl)-5*H*-4λ^4,5λ^4-dipyrrolo[1,2-*c*:2',1'-*f*][1,3,2]diazaborinin-10-yl)benzoate (15.8 mg, 0.030 mmol, 30%) as a blue solid and methyl 4-(3-bromo-5,5-difluoro-7-(phenylethynyl)-5*H*-4λ4,5λ4-dipyrrolo[1,2-*c*:2',1'-*f*][1,3,2]diazaborinin-10-yl)benzoate (9.3 mg, 0.018 mmol, 18%) as a pink solid.

Methyl 4-(5,5-difluoro-3,7-bis(phenylethynyl)-5*H*-4λ^4,5λ^4-dipyrrolo[1,2-*c*:2',1'-*f*][1,3,2]diazaborinin-10-yl)benzoate **3.28**

Analytical data as reported above.

Methyl 4-(3-bromo-5,5-difluoro-7-(phenylethynyl)-5*H*-4λ4,5λ4-dipyrrolo[1,2-*c*:2',1'-*f*][1,3,2]diazaborinin-10-yl)benzoate **3.30**

Rf: 0.88 (DCM). **IR** (neat): ν_{max}/cm^{-1} , 2924 (C-H, m), 2195 (C≡C, m), 1718 (C=O, s). **^{1}H NMR** (700 MHz, Chloroform-*d*) δ 8.19 (d, *J* = 8.4 Hz, 2H, H^{4}), 7.70 – 7.67 (m, 2H, H^{19}), 7.60 (d, *J* = 8.4 Hz, 2H, H^{5}), 7.43 – 7.38 (m, 3H, H^{20,21}), 6.82 (d, *J* = 4.3 Hz, 1H, H^{9}), 6.73 (t, *J* = 3.9 Hz, 2H, H^{8,13}), 6.54 (d, *J* = 4.3 Hz, 1H, H^{14}), 3.99 (s, 3H, H^{1}). **^{13}C NMR** (176 MHz, Chloroform-*d*) δ 166.32 (C^{2}), 140.97 (C^{11}), 139.24 (C^{10}), 137.56 (C^{3}), 136.08 (C^{12}), 135.78 (C^{7}), 133.11 (C^{15}), 132.58 (C^{19}), 132.22 (C^{6}), 130.92 (C^{13}), 130.84 (C^{9}), 130.59 (C^{5}), 130.00 (C^{21}), 129.79 (C^{4}), 128.60 (C^{20}), 124.65 (C^{8}), 122.90 (C^{14}), 122.05 (C^{18}), 103.74 (C^{17}), 82.89 (C^{16}), 52.70 (C^{1}). **^{19}F NMR** (282 MHz, Chloroform-*d*) δ -146.93 (q, *J* = 27.8 Hz). **^{11}B NMR** (96 MHz, Chloroform-*d*) δ 0.67 (t, *J* = 27.9 Hz).

6.2.3.9 Methyl 4-(5,5-difluoro-3,7-bis(phenylethynyl)-5*H*-4λ^4,5λ^4-dipyrrolo[1,2-*c*:2',1'-*f*][1,3,2]diazaborinin-10-yl)benzoate **3.28** and methyl 4-(3-iodo-5,5-difluoro-7-(phenylethynyl)-5*H*-4λ4,5λ4-dipyrrolo[1,2-*c*:2',1'-*f*][1,3,2]diazaborinin-10-yl)benzoate **3.31** [83]

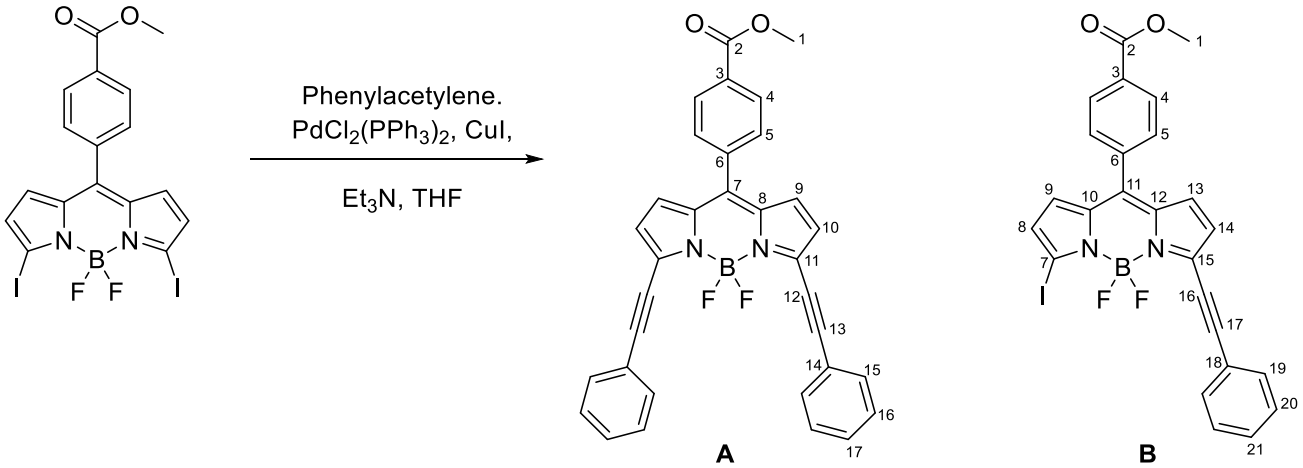

To a Schlenk flask was added methyl 4-(3,7-diiodo-5,5-difluoro-5*H*-4λ^4,5λ^4-dipyrrolo[1,2-*c*:2',1'-*f*][1,3,2]diazaborinin-10-yl)benzoate (57.8 mg, 0.1 mmol), $PdCl_2(PPh_3)_2$ (3.5 mg, 0.005 mmol, 5 mol%), CuI (1.0 mg, 0.005 mmol, 5 mol%) and dry THF (2 mL) and was subsequently degassed (x3). To the reaction mixture was added phenylacetylene (27 μL, 0.5 mmol), Et_3N (153.3 μL, 1.1 mmol) and was degassed (x3). The resulting reaction mixture was stirred, under a nitrogen atmosphere, at room temperature for 40 hours. The reaction mixture was diluted with DCM (10 mL), the organic layer was washed with H_2O (3 x 15 mL), dried over $MgSO_4$, filtered and the solvent was removed under reduced pressure to give a dark blue solid. The crude product was purified through silica gel column chromatography (DCM) to give methyl 4-(5,5-difluoro-3,7-bis(phenylethynyl)-5*H*-4λ^4,5λ^4-dipyrrolo[1,2-*c*:2',1'-*f*][1,3,2]diazaborinin-10-yl)benzoate (19.6 mg, 0.037 mmol, 37%) as a blue solid and methyl 4-(3-iodo-5,5-difluoro-7-(phenylethynyl)-5*H*-4λ4,5λ4-dipyrrolo[1,2-*c*:2',1'-*f*][1,3,2]diazaborinin-10-yl)benzoate (28.0 mg, 0.051 mmol, 51%) as a purple solid.

Methyl 4-(5,5-difluoro-3,7-bis(phenylethynyl)-5*H*-4λ^4,5λ^4-dipyrrolo[1,2-*c*:2',1'-*f*][1,3,2]diazaborinin-10-yl)benzoate **3.28**

Analytical data as reported above.

Methyl 4-(3-iodo-5,5-difluoro-7-(phenylethynyl)-5*H*-4λ4,5λ4-dipyrrolo[1,2-*c*:2',1'-*f*][1,3,2]diazaborinin-10-yl)benzoate **3.31**

^{13}C NMR (176 MHz, Chloroform-*d*) δ 166.34 (C^{2}), 140.03 (C^{11}), 139.41 (C^{12}), 138.35 (C^{7}), 137.67 (C^{3}), 135.94 (C^{15}), 132.59 (C^{19}), 132.18 (C^{6}), 130.97 (C^{9}), 130.85 (C^{14}), 130.55 (C^{5}), 130.07 (C^{8}), 129.99 (C^{21}), 129.78 (C^{4}), 128.59 (C^{20}), 124.75 (C^{13}), 122.10 (C^{18}), 103.88 (C^{17}), 103.17 (C^{10}), 82.98 (C^{16}), 52.70 (C^{1}). **^{1}H NMR** (300 MHz, Chloroform-*d*) δ 8.18 (d, *J* = 8.5 Hz, 2H, H^{4}), 7.75 – 7.66 (m, 2H, H^{19}), 7.59 (d, *J* = 8.5 Hz, 2H, H^{5}), 7.45 – 7.35 (m, 3H, H^{20,21}), 6.81 (d, *J* = 4.3 Hz, 1H, H^{14}), 6.75 – 6.70 (m, 2H, H^{8,13}), 6.62 (d, *J* = 4.2 Hz, 1H, H^{9}), 3.98 (s, 3H, H^{1}). **^{11}B NMR** (96 MHz, Chloroform-*d*) δ 0.69 (t, *J* = 28.4 Hz). **^{19}F NMR** (282 MHz, Chloroform-*d*) δ -145.93 (q, *J* = 28.5 Hz).

6.2.3.10 Methyl 4-(5,5-difluoro-3,7-bis(phenylethynyl)-5*H*-4λ^4,5λ^4-dipyrrolo[1,2-*c*:2',1'-*f*][1,3,2]diazaborinin-10-yl)benzoate **3.28** and methyl 4-(5,5-difluoro-3,7-bis(phenylethynyl)-5*H*-4λ^4,5λ^4-dipyrrolo[1,2-*c*:2',1'-*f*][1,3,2]diazaborinin-10-yl)benzoate **3.32** [83]

Method A

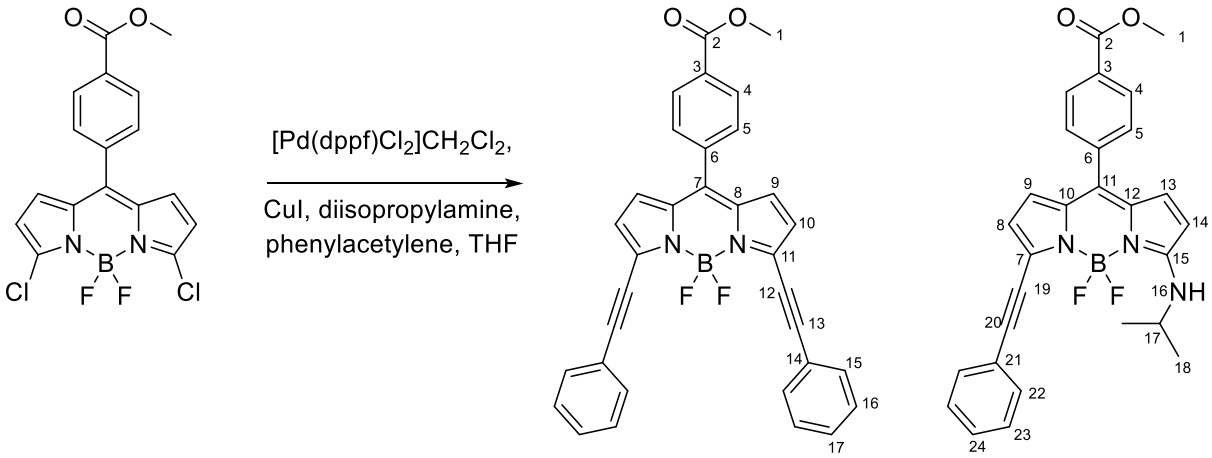

To a round bottom flask was added methyl 4-(3,7-dichloro-5,5-difluoro-5*H*-4λ^4,5λ^4-dipyrrolo[1,2-*c*:2',1'-*f*][1,3,2]diazaborinin-10-yl)benzoate (48.2 mg, 0.1 mmol), [Pd(dppf)Cl$_2$]CH$_2$Cl$_2$ (4.1 mg, 0.005 mmol, 5 mol%), CuI (1.0 mg, 0.005 mmol, 5 mol%), dry THF (3 mL), diisopropylamine (1.9 mL, 11.0 mmol) and phenylacetylene (89 μL, 0.81 mmol). The resulting reaction mixture was stirred at room temp for 48 hours and subsequently poured into cold distilled water (20 mL) then extracted with DCM (3 x 10 mL). The combined extracted reaction mixture was washed with water (3 x 15 mL), dried over MgSO$_4$, filtered and the solvent was removed under reduced pressure to give a dark purple solid. The crude product was purified through silica gel column chromatography (1:1 petrol: diethyl ether) to give methyl 4-(5,5-difluoro-3,7-bis(phenylethynyl)-5*H*-4λ^4,5λ^4-dipyrrolo[1,2-*c*:2',1'-*f*][1,3,2]diazaborinin-10-yl)benzoate (5.3 mg, 0.01 mmol, 10%) as a blue solid and methyl 4-(5,5-difluoro-3,7-bis(phenylethynyl)-5*H*-4λ^4,5λ^4-dipyrrolo[1,2-*c*:2',1'-*f*][1,3,2]diazaborinin-10-yl)benzoate (13.5 mg, 0.026 mmol, 29%) as a pink solid.

Method B

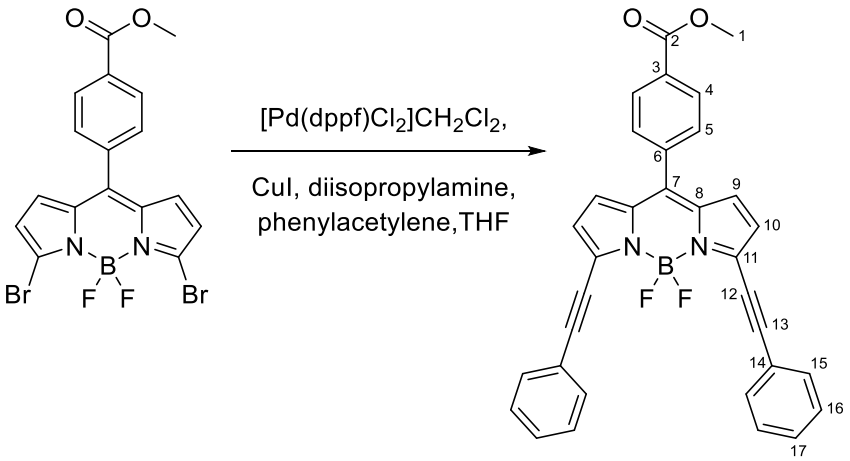

To a round bottom flask was added methyl 4-(3,7-dibromo-5,5-difluoro-5*H*-4λ^4,5λ^4-dipyrrolo[1,2-*c*:2',1'-*f*][1,3,2]diazaborinin-10-yl)benzoate (48.2 mg, 0.1 mmol), [Pd(dppf)Cl_2]CH_2Cl_2 (4.1 mg, 0.005 mmol, 5 mol%), CuI (1.0 mg, 0.005 mmol, 5 mol%), dry THF (3 mL), diisopropylamine (1.9 mL, 11.0 mmol) and phenylacetylene (89 μL, 0.81 mmol). The resulting reaction mixture was stirred at room temp for 48 hours and subsequently poured into cold distilled water (20 mL) then extracted with DCM (3 x 10 mL). The combined extracted reaction mixture was washed with water (3 x 15 mL), dried over $MgSO_4$, filtered and the solvent was removed under reduced pressure to give a dark purple solid. The crude product was purified through silica gel column chromatography (1:1 petrol: diethyl ether) to give methyl 4-(5,5-difluoro-3,7-bis(phenylethynyl)-5*H*-4λ^4,5λ^4-dipyrrolo[1,2-*c*:2',1'-*f*][1,3,2]diazaborinin-10-yl)benzoate (25.4 mg, 0.049 mmol, 49%) as a blue solid.

Method C

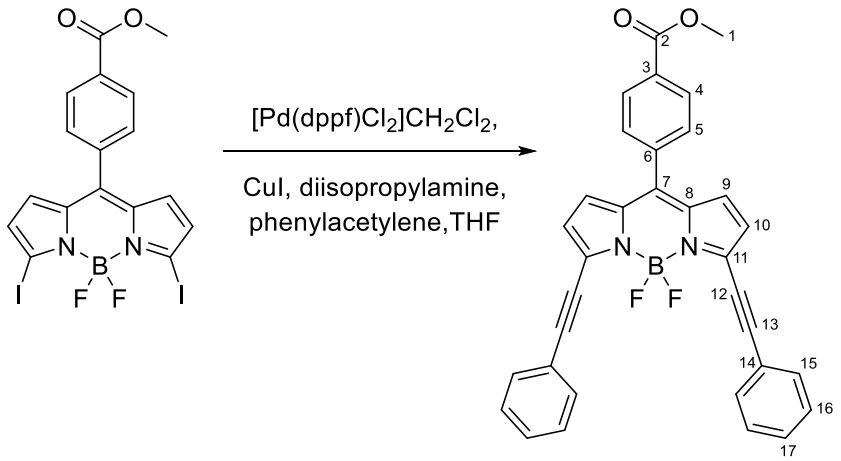

To a round bottom flask was added methyl 4-(3,7-diiodo-5,5-difluoro-5*H*-4λ^4,5λ^4-dipyrrolo[1,2-*c*:2',1'-*f*][1,3,2]diazaborinin-10-yl)benzoate (57.8 mg, 0.1 mmol), [Pd(dppf)Cl_2]CH_2Cl_2 (4.1 mg, 0.005 mmol, 5 mol%), CuI (1.0 mg, 0.005 mmol, 5 mol%), dry THF (3 mL), diisopropylamine (1.9 mL, 11.0 mmol) and phenylacetylene (89 μL, 0.81 mmol). The resulting reaction mixture was stirred at room temp for 48 hours and subsequently poured into cold distilled water (20 mL) then CC, extracted with DCM (3 x 10 mL). The combined extracted reaction mixture was washed with water (3 x 15 mL), dried over $MgSO_4$, filtered and the solvent was removed under reduced pressure to give a dark purple solid. The crude product was purified through silica gel column chromatography (1:1 petrol: diethyl ether) to give methyl 4-(5,5-difluoro-3,7-bis(phenylethynyl)-5*H*-4λ^4,5λ^4-dipyrrolo[1,2-*c*:2',1'-*f*][1,3,2]diazaborinin-10-yl)benzoate (32.1 mg, 0.061 mmol, 61%) as a blue solid.

Methyl 4-(5,5-difluoro-3,7-bis(phenylethynyl)-5*H*-4λ^4,5λ^4-dipyrrolo[1,2-*c*:2',1'-*f*][1,3,2]diazaborinin-10-yl)benzoate **3.28**

Analytical data as reported above.

Methyl 4-(5,5-difluoro-3,7-bis(phenylethynyl)-5*H*-4λ^4,5λ^4-dipyrrolo[1,2-*c*:2',1'-*f*][1,3,2]diazaborinin-10-yl)benzoate **3.32**

Rf: 0.71 (DCM). **Mp:** 187-189 ^oC**. IR** (neat): ν_{max}/cm^{-1} 3658 (N-H, m), 2980-2889 (C-H, s), 1724 (C=O, w). **^{1}H NMR** (700 MHz, Chloroform-*d*) δ 8.12 (d, *J* = 8.5 Hz, 2H, H*^{4}*), 7.66 – 7.58 (m, 2H, H*^{22}*), 7.54 (d, *J* = 8.5 Hz, 2H, H*^{5}*), 7.40 – 7.28 (m, 3H, H*^{23,24}*),

6.87 (d, *J* = 5.0 Hz, 1H, H^{13}), 6.59 (d, *J* = 3.9 Hz, 1H, H^{9}), 6.38 (d, *J* = 8.3 Hz, 1H, H^{16}), 6.32 (d, *J* = 3.9 Hz, 1H, H^{8}), 6.27 (d, *J* = 5.0 Hz, 1H, H^{14}), 3.97 (s, 3H, H^{1}), 3.85 (heptd, *J* = 6.5, 1.6 Hz, 1H, H^{17}), 1.39 (d, *J* = 6.5 Hz, 6H, H^{18}). **^{13}C NMR** (176 MHz, Chloroform-*d*) δ 166.73 (C^{2}), 161.51 (C^{15}), 139.23 (C^{3}), 135.63 (C^{13}), 134.40 (C^{12}), 133.62 (C^{10}), 131.83 (C^{22}), 130.86 (C^{6}), 130.56 (C^{5}), 129.62 (C^{4}), 129.50 (C^{11}), 128.34 (C^{23}), 128.29 (C^{24}), 125.61 (C^{7}), 123.56 (C^{21}), 120.26 (C^{9}), 119.54 (C^{8}), 112.03 (C^{14}), 95.16 (C^{20}), 83.43 (C^{19}), 52.51 (C^{1}), 47.55 (C^{17}), 23.62 (C^{18}). **^{19}F NMR** (282 MHz, Chloroform-*d*) δ -148.21 (q, *J* = 32.1 Hz). **^{11}B NMR** (96 MHz, Chloroform-*d*) δ 1.09 (t, *J* = 33.5 Hz).

6.2.3.11 XPhos G3 Precatalyst **3.37** [95]

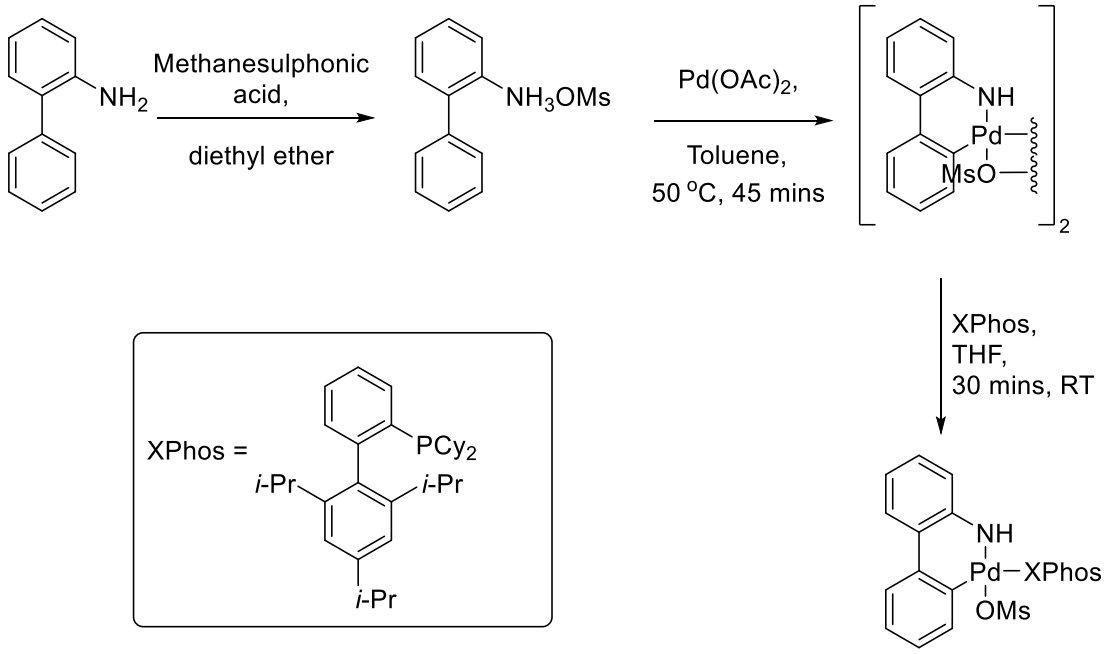

To a 250 mL round bottom flask, was added 2-aminobiphenyl (5 g, 29.5 mmol) and diethyl ether (100 mL). Methanesulfonic acid (1.92 mL) was mixed with diethyl ether (15 mL) and added slowly to the round bottom flask. The reaction mixture was stirred at room temp for 30 mins then the precipitate was filtered and washed with diethyl ether (3 x 15 mL). The precipitate was dried under vacuum overnight to give [1,1'-biphenyl]-2-yl-λ^5-azaneyl methanesulfonate (7.4835 g, 28.2 mmol, 96%) as an off-white solid. This crude product was of high enough purity to continue to the next step without any further purification required.

To a 50 mL round bottom flask, under a nitrogen atmosphere, was added [1,1'-biphenyl]-2-yl-λ^5-azaneyl methanesulfonate (0.95 g, 3.58 mmol), palladium acetate (0.7997 g, 3.58 mmol) and toluene (13 mL). The reaction mixture was heated to 50^{o}C and was stirred for 45 mins, forming a milky precipitate, then cooled to room temp. The suspension was filtered and the precipitate was washed with toluene (25 mL) and diethyl ether (3 x 25 mL) and then dried under vacuum overnight to afford the organopalladium intermediate (1.166 g, 1.58 mmol, 88%) as a creamy grey solid.

To a 100 mL round bottom flask was added the organopalladium intermediate (1.1656 g, 1.58 mmol), XPhos (1.5 g, 3.15 mmol), THF (30 mL) and was stirred at room temp for 30 mins. 90% of the solvent was subsequently removed under reduced pressure and then the product was triturated from pentane (x3). The solvent was removed under reduced pressure to afford XPhos Pd G3 (1.0593 g, 1.25 mmol, 79%) as a grey/brown solid. The crude mixture was at high purity, resulting in no further purification required.

IR (neat): ν_{max}/cm^{-1} 2962-2931 (C-H, m). **^{31}P NMR** (121 MHz, Chloroform-*d*) δ 35.64.

Analytical data is consistent with literature.

6.2.3.12 Methyl 4-(5,5-difluoro-3,7-diphenyl-5*H*-4λ^4,5λ^4-dipyrrolo[1,2-*c*:2',1'-*f*][1,3,2]diazaborinin-10-yl)benzoate **3.21** and methyl 4-(3-chloro-5,5-difluoro-7-phenyl-5*H*-5λ^4,6λ^4-dipyrrolo[1,2-*c*:2',1'-*f*][1,3,2]diazaborinin-10-yl)benzoate **2.38** [83]

Method A:

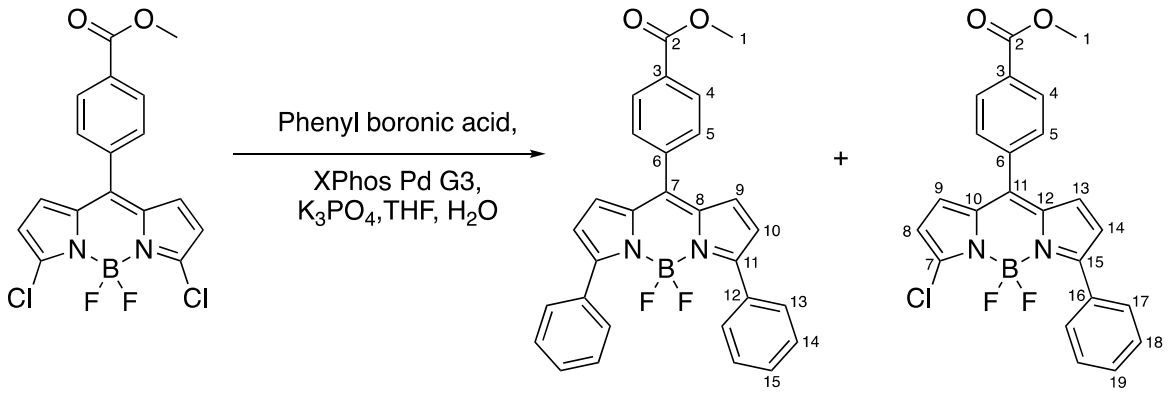

To a 50 mL Schlenk flask, under nitrogen atmosphere, was added methyl 4-(3,7-dichloro-5,5-difluoro-5*H*-4λ^4,5λ^4-dipyrrolo[1,2-*c*:2',1'-*f*][1,3,2]diazaborinin-10-yl)benzoate (39.5 mg, 0.1 mmol), phenyl boronic acid (48.8 mg, 0.4 mmol), XPhos Pd G3 (6.8 mg, 0.008 mmol, 8 mol%), K_3PO_4 (92.1 mg, 0.4 mmol), dry THF (8 mL), water (1.2 mL) and degassed (x3). The reaction mixture was heated to 75^{o}C, stirred for 16 hours then diluted with DCM (50 mL). The reaction mixture was wased with water (3 x 50mL), the organic layer was dried over $MgSO_4$, filtered and the solvent was removed under reduced pressure to give a purple solid. The crude product was purified by silica gel column chromatography (DCM) to give methyl 4-(5,5-difluoro-3,7-diphenyl-5*H*-4λ^4,5λ^4-dipyrrolo[1,2-*c*:2',1'-*f*][1,3,2]diazaborinin-10-yl)benzoate (3.1 mg, 0.006 mmol, 6%) as a purple solid and methyl 4-(3-chloro-5,5-difluoro-7-phenyl-5*H*-5λ^4,6λ^4-dipyrrolo[1,2-*c*:2',1'-*f*][1,3,2]diazaborinin-10-yl)benzoate (1.7 mg, 0.004 mmol, 4%) as a pink solid.

Method B:

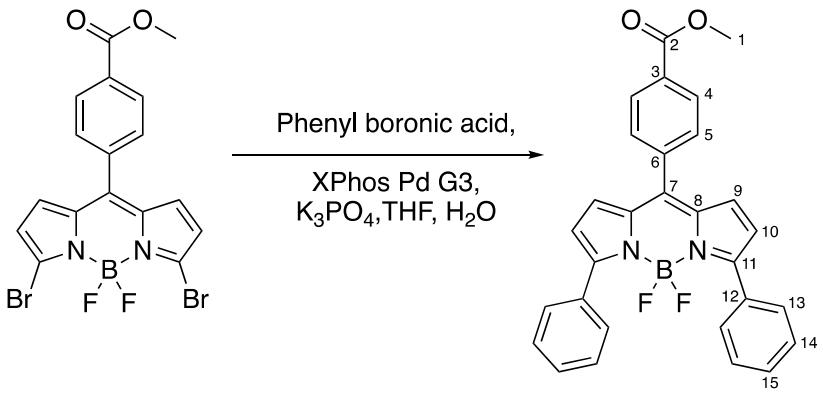

To a 50 mL Schlenk flask, under nitrogen atmosphere, was added methyl 4-(3,7-dibromo-5,5-difluoro-5*H*-4λ^4,5λ^4-dipyrrolo[1,2-*c*:2',1'-*f*][1,3,2]diazaborinin-10-yl)benzoate (48.2 mg, 0.1 mmol), phenyl boronic acid (48.8 mg, 0.4 mmol), XPhos Pd G3 (6.8 mg, 0.008 mmol, 8 mol%), K_3PO_4 (92.1 mg, 0.4 mmol), dry THF (8 mL), water (1.2 mL) and degassed (x3). The reaction mixture was stirred at room temp for 17 hours, diluted with DCM (50 mL) and washed with water (3 x 50mL). The organic layer was dried over $MgSO_4$, filtered and the solvent was removed under reduced pressure to give a purple solid. The crude product was purified by silica gel column chromatography (DCM) to give methyl 4-(5,5-difluoro-3,7-diphenyl-5*H*-4λ^4,5λ^4-dipyrrolo[1,2-*c*:2',1'-*f*][1,3,2]diazaborinin-10-yl)benzoate (38.7 mg, 0.081 mmol, 81%) as a purple solid.

Method C:

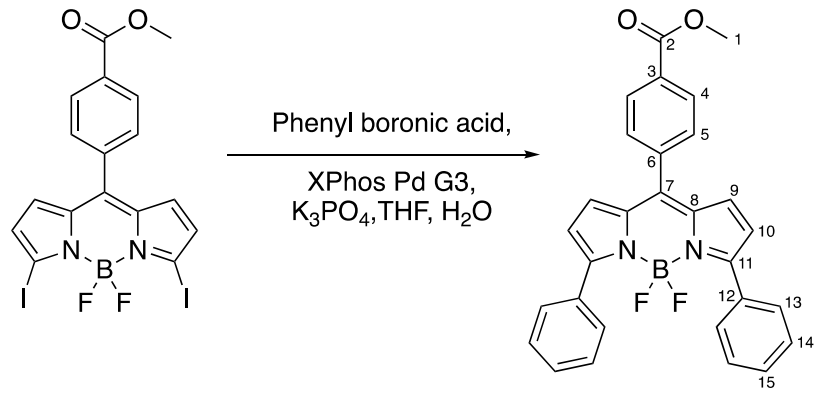

To a 50 mL Schlenk flask, under nitrogen atmosphere, was added methyl 4-(3,7-diiodo-5,5-difluoro-5*H*-4λ^4,5λ^4-dipyrrolo[1,2-*c*:2',1'-*f*][1,3,2]diazaborinin-10-yl)benzoate (57.8 mg, 0.1 mmol), phenyl boronic acid (48.8 mg, 0.4 mmol), XPhos Pd G3 (6.8 mg, 0.008 mmol, 8 mol%), K_3PO_4 (92.1 mg, 0.4 mmol), dry THF (8 mL), water (1.2 mL) and degassed (x3). The reaction mixture was stirred at room temp for 17 hours, diluted with DCM (50 mL) and washed with water (3 x 50mL). The organic layer was dried over $MgSO_4$, filtered and the solvent was removed under reduced pressure to give a purple solid. The crude product was purified by silica gel column chromatography (DCM) to give methyl 4-(5,5-difluoro-3,7-diphenyl-5*H*-4λ^4,5λ^4-dipyrrolo[1,2-*c*:2',1'-*f*][1,3,2]diazaborinin-10-yl)benzoate (41.8 mg, 0.087 mmol, 87%) as a purple solid.

Methyl 4-(5,5-difluoro-3,7-diphenyl-5*H*-4λ^4,5λ^4-dipyrrolo[1,2-*c*:2',1'-*f*][1,3,2]diazaborinin-10-yl)benzoate **3.21**

Analytical data as reported above.

Methyl 4-(3-chloro-5,5-difluoro-7-phenyl-5*H*-5λ^4,6λ^4-dipyrrolo[1,2-*c*:2',1'-*f*][1,3,2]diazaborinin-10-yl)benzoate **2.33**

R_f: 0.78 (DCM). **Mp:** 169-170 ^oC. **^{1}H NMR** (300 MHz, Chloroform-*d*) δ 8.20 (d, *J* = 8.3 Hz, 2H, H^{4}), 7.99 – 7.89 (m, 2H, H^{17}), 7.62 (d, *J* = 8.3 Hz, 2H, H^{5}), 7.55 – 7.45 (m, 3H, H^{18,19}), 6.88 (d, *J* = 4.3 Hz, 1H, H^{13}), 6.76 – 6.69 (m, 2H, H^{9,14}), 6.40 (d, *J* = 4.2 Hz, 1H, H^{8}), 3.99 (s, 3H, H^{1}). **^{13}C NMR** (75 MHz, Chloroform-*d*) δ 166.4 (C^{2}), 161.7 (C^{15}), 143.2 (C^{7}), 142.3 (C^{11}), 137.8 (C^{3}), 136.8 (C^{12}), 133.1 (C^{10}), 132.4 (C^{13}), 132.1 (C^{6}), 132.0 (C^{16}), 130.6 (C^{5}), 130.4 (C^{19}), 129.7 (C^{4}), 129.6 (C^{17}), 129.6 (C^{9}), 128.6 (C^{18}), 122.2 (C^{14}), 118.5 (C^{8}), 52.7 (C^{1}). **^{19}F NMR** (282 MHz, Chloroform-*d*) δ -140.06 (q, *J* = 29.8 Hz). **^{11}B NMR** (96 MHz, Chloroform-*d*) δ 0.96 (t, *J* = 30.2 Hz). **IR** (neat): ν_{max}/cm^{-1} 3055, 2997 (C-H, w), 1724 (C=O, m). **HRMS:** (ASAP+) calcd for $C_{23}H_{16}BClF_2N_2O_2$ $[M+H]^+$: 437.1044, found 437.1036. **UV-Vis:** λ_{max} = 537 nm (DCM). **Molar extinction coefficient (ε)** = 67000 M^{-1} cm^{-1} **ϕ_F:** 0.03**.**

6.2.4 Chapter 4

6.2.4.1 Methyl (*S*)-4-(3-chloro-7-((1-ethoxy-3-hydroxy-1-oxopropan-2-yl)amino)-5,5-difluoro-5*H*-5λ^4,6λ^4-dipyrrolo[1,2-*c*:2',1'-*f*][1,3,2]diazaborinin-10-yl)benzoate **4.4**

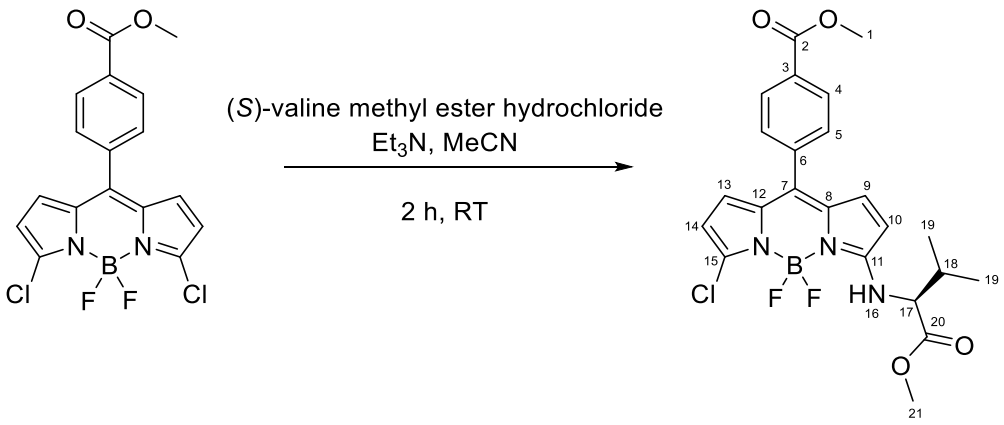

To a round bottom flask under nitrogen was added methyl 4-(3,7-dichloro-5,5-difluoro-5*H*-4λ^4,5λ^4-dipyrrolo[1,2-*c*:2',1'-*f*][1,3,2]diazaborinin-10-yl)benzoate (50 mg, 0.127 mmol), (*S*)-valine methyl ester hydrochloride (41.5 mg, 0.254 mmol), Et_3N (38.7 μl, 0.279 mmol) and MeCN (7 mL). The reaction was stirred at room temperature for two hours and then quenched with water. The aqueous layer was extracted with DCM (2 x 30 mL) and washed the organic layer with brine (50 mL) and water (50 mL). The organic layer was dried under Na_2SO_4, filtered and removed solvent under reduced pressure. The crude product was purified using column chromatography (1:1 petrol : ethyl acetate) to give an orange product of (*S*)-4-(3-chloro-7-((1-ethoxy-3-hydroxy-1-oxopropan-2-yl)amino)-5,5-difluoro-5*H*-5λ^4,6λ^4-dipyrrolo[1,2-*c*:2',1'-*f*][1,3,2]diazaborinin-10-yl)benzoate (60.9 mg, 0.124 mmol, 98%)

Rf: 0.63 (Petrol:ethyl acetate 1:1). **Mp:** 111-113 ^oC. **IR** (neat): ν_{max}/cm^{-1} 3378.3 (N-H, w), 2960 (C-H, w), 1720 (C=O, m), 1602 (C=C m), 1070 (C-O, m). **HRMS:** (pNSI) calcd for $C_{23}H_{23}B^{11}Cl^{35}F_2N_3O_4$ $[M+H]^+$: 490.1521, found 490.1540. **^{1}H NMR** (400 MHz, Chloroform-*d*) δ 8.12 (d, *J* = 8.0 Hz, 2H, *H^4*), 7.52 (d, *J* = 8.6 Hz, 2H, *H^5*), 6.84 (d, *J* = 4.5 Hz, 1H, H*^{14}*), 6.76 (d, *J* = 9.4 Hz, 1H, H*^{16}*), 6.32 (d, *J* = 3.9 Hz, 1H, H*^{10}*), 6.21 (d, *J* = 4.0 Hz, 1H, H*^{9}*), 6.16 (d, *J* = 5.0 Hz, 1H, H*^{13}*), 4.01 (dd, *J* = 9.4, 5.9 Hz, 1H, H*^{17}*), 3.97 (s, 3H, H*^{21}*), 3.81 (s, 3H, H*^{1}*), 2.30 (hept, *J* = 6.4 Hz, 1H, H*^{18}*), 1.06 (t, *J* = 7.0 Hz, 6H, H*^{19}*). **^{13}C NMR** (75 MHz, Chloroform-*d*) δ 170.0 (C*^{20}*), 166.4 (C*^{2}*),

161.2 (C^{11}), 138.2 (C^{6}), 135.5 (C^{15}), 132.9 (C^{8}), 131.4 (C^{9}), 131.3 (C^{7}), 131.1 (C^{4}), 130.9 (C^{3}), 130.2 (C^{5}), 129.4 (C^{10}), 120. 8 (C^{12}), 113.2 (C^{13}), 110.8 (C^{14}), 63.3 (C^{17}), 52.8 (C^{21}), 52.4 (C^{1}), 32.2 (C^{18}), 18.9 (C^{19}), 17.8 (C^{19}). **^{19}F NMR** (282 MHz, Chloroform-*d*) δ -148.24 (q, *J* = 31.4 Hz). **^{11}B NMR** (96 MHz, Chloroform-*d*) δ 0.93 (t, *J* = 30.2 Hz). **UV-Vis:** λ_{max} = 506 nm (DCM). **Molar extinction coefficient (ε)** = 39000 M^{-1} cm^{-1}.

6.2.4.2 Methyl (*S*)-4-(5,5-difluoro-3-iodo-7-((1-methoxy-3-methyl-1-oxobutan-2-yl)amino)-5*H*-5λ^4,6λ^4-dipyrrolo[1,2-c:2',1'-f][1,3,2]diazaborinin-10-yl)benzoate **4.5**

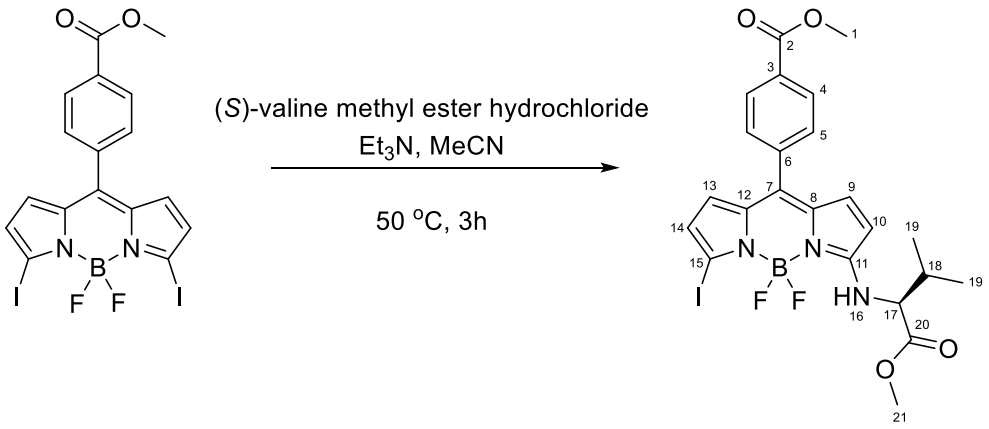

To a round bottom flask under nitrogen was added methyl 4-(5,5-difluoro-3,7-diiodo-5*H*-4λ^4,5λ^4-dipyrrolo[1,2-*c*:2',1'-*f*][1,3,2]diazaborinin-10-yl)benzoate (50 mg, 0.087 mmol), (*S*)-valine methyl ester hydrochloride (29.0 mg, 0.173 mmol), NEt_3 (26.5 μL, 0.19 mmol) and MeCN (7 mL). The reaction was heated to 50°C, stirred for 3 hours, then allowed to cool to room temp. The reaction was diluted with DCM (20 mL) and was washed with water (3 x 20 mL). The organic layer was dried over $MgSO_4$, filtered and solvent removed under reduced pressure. This afforded methyl (*S*)-4-(5,5-difluoro-3-iodo-7-((1-methoxy-3-methyl-1-oxobutan-2-yl)amino)-5*H*-5λ^4,6λ^4-dipyrrolo[1,2-c:2',1'-f][1,3,2]diazaborinin-10-yl)benzoate (50.5 mg, 0.087 mmol, 100%) as an orange solid.

^{1}H NMR (300 MHz, Chloroform-*d*) δ 8.11 (d, *J* = 8.3 Hz, 2H, H^{4}), 7.50 (d, *J* = 8.2 Hz, 2H, H^{5}), 6.83 (d, *J* = 5.0 Hz, 1H, H^{10}), 6.77 (d, *J* = 9.7 Hz, 1H, H^{16}), 6.51 (d, *J* = 3.8 Hz, 1H, H^{14}), 6.22 (d, *J* = 3.9 Hz, 1H, H^{13}), 6.18 (d, *J* = 5.0 Hz, 1H, H^{9}), 4.00 (dd, *J* = 9.5, 6.0 Hz, 1H, H^{17}), 3.95 (s, 3H, H^{1}), 3.80 (s, 3H, H^{19}), 2.29 (dq, *J* = 13.4, 6.7 Hz, 1H, H^{20}), 1.07 (d, *J* = 6.9 Hz, 3H, H$^{21/22}$), 1.04 (d, *J* = 6.7 Hz, 3H, H$^{21/22}$). **^{13}C NMR** (75 MHz, Chloroform-*d*) δ 170.3 (C^{18}), 166.6 (C^{2}), 161.6 (C^{8}), 138.5 (C^{3}), 135.8 (C^{10}), 133.5 (C^{11,12}), 131.11 (C^{6}), 130.6 (C^{7}), 130.4 (C^{5}), 129.6 (C^{4}), 125.1 (C^{14}), 122.1 (C^{13}), 111.4 (C^{9}), 83.3 (C^{15}), 63.5 (C^{17}), 52.9 (C^{19}), 52.5 (C^{1}), 32.3 (C^{20}), 19.1 (C$^{21/22}$), 18.1 (C$^{21/22}$). **^{11}B NMR** (96 MHz, Chloroform-*d*) δ 0.97 (t, *J* = 33.2 Hz). **^{19}F NMR** (282 MHz, Chloroform-*d*) δ -144.83 – -146.98 (m).

6.2.4.3 Methyl (*S*)-4-(5,5-difluoro-3-(2-hydroxyphenyl)-7-((1-methoxy-3-methyl-1-oxobutan-2-yl)amino)-5*H*-5λ^4,6λ^4-dipyrrolo[1,2-c:2',1'-f][1,3,2]diazaborinin-10-yl)benzoate **4.8**

Method A:

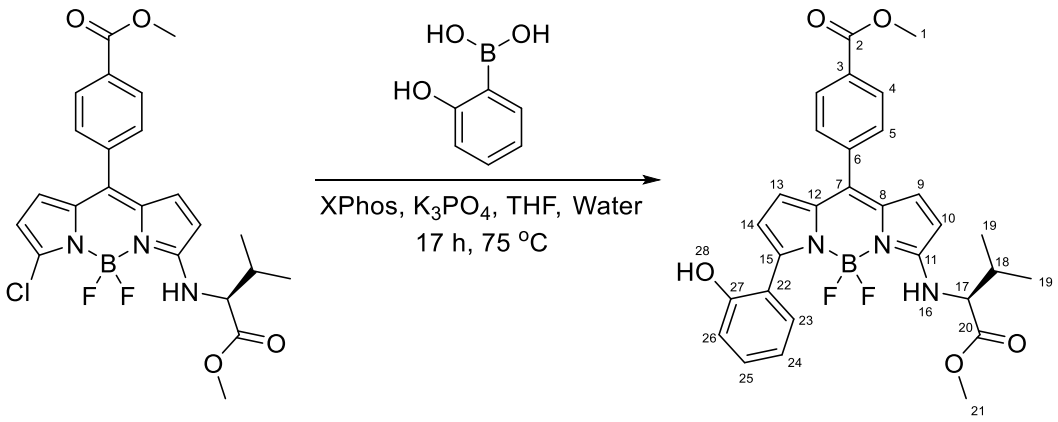

To a 50 mL Schlenk flask was added methyl (*S*)-4-(3-chloro-7-((1-ethoxy-3-hydroxy-1-oxopropan-2-yl)amino)-5,5-difluoro-5*H*-5λ^4,6λ^4-dipyrrolo[1,2-*c*:2',1'-*f*][1,3,2]diazaborinin-10-yl)benzoate (88 mg, 0.180 mmol), 2-hydroxyphenyl boronic acid (37 mg, 0.27 mmol), XPhos (10.7 mg, 7% mol) and K_3PO_3 (82 mg, 0.36 mmol). The Schlenk flask was degassed three times, added dry THF (10 mL) and water (1.5 mL) and then degassed again three times. The reaction was stirred for 17 hours at 75 °C and dilute with DCM (25 mL). The organic layer was washed with H_2O (3 x 10 mL), dried over Na_2SO_4, filtered and the solvent was removed under reduced pressure to give a purple solid. The crude product was purified through silica gel column chromatography (1:1 petrol:ethyl acetate) to give methyl (*S*)-4-(5,5-difluoro-3-(2-hydroxyphenyl)-7-((1-methoxy-3-methyl-1-oxobutan-2-yl)amino)-5*H*-5λ^4,6λ^4-dipyrrolo[1,2-c:2',1'-f][1,3,2]diazaborinin-10-yl)benzoate (45.6 mg, 0.083 mmol, 46%) as a red solid.

Rf: 0.52 (Petrol:ethyl acetate 1:1). **Mp:** 126-127 °C. **IR** (neat): ν_{max}/cm^{-1} 3380 (O-H, br, w), 2917 (C-H, w), 1719 (C=O, m), 1603 (C=C m), 1101 (C-O, m). **^{1}H NMR** (400 MHz, Chloroform-*d*) δ 8.08 (d, *J* = 8.5 Hz, 2H, H*^{4}*), 7.52 (d, *J* = 8.4 Hz, 2H, H*^{5}*), 7.44 (dd, *J* = 7.8, 1.3 Hz, 1H, H*^{26}*), 7.27 (ddd, *J* = 9.1, 7.3, 1.8 Hz, 1H, H*^{25}*), 6.96 (m, 2H, H*^{24}*, H*^{23}*), 6.81 (d, *J* = 4.8 Hz, 1H, H*^{13}*), 6.55 (d, *J* = 3.7 Hz, 1H H*^{10}*), 6.29 (d, *J* = 4.0

Hz, 1H, H^{9}), 6.09 (d, *J* = 5.1 Hz, 1H, H^{14}), 5.71 (t, *J* = 3.9 Hz, 1H, H^{28}), 3.91 (s, 3H, H^{1}), 3.87 (dd, *J* = 9.8, 6.7 Hz, 1H, H^{17}), 3.68 (s, 3H, H^{21}), 2.13 (hept, *J* = 6.6 Hz, 1H, H^{18}), 5.07 (dd, *J* = 6.9, 3.4 Hz, 6H, H^{19}). **^{13}C NMR** (75 MHz, Chloroform-*d*) δ 170.0 (C^{20}), 166.3 (C^{2}), 161.0 (C^{27}) 153.5 (C^{11}), 141.4 (C^{6}), 138.6 (C^{8}), 135.3 (C^{9}), 133.6 (C^{7}), 133.0 (C^{23}), 132.0 (C^{15}), 131.2 (C^{25}), 130.7 (C^{4}), 130.1 (C^{3}), 129.9 (C^{5}), 129.2 (C^{24}), 121.1 (C^{22}), 120.6 (C^{10}), 119.8 (C^{26}), 115.9 (C^{12}), 115.2 (C^{14}), 110.7 (C^{13}), 63.2 (C^{17}), 52.4 (C^{21}), 52.1 (C^{1}), 31.7 (C^{18}), 18.6 (C^{19}), 17.8 (C^{19}). **^{19}F NMR** (282 MHz, Chloroform-*d*) δ -144.43 (q, *J* = 33.0 Hz). **^{11}B NMR** (96 MHz, Chloroform-*d*) δ 1.21 (t, *J* = 35.9 Hz). **UV-Vis:** λ_{max} = 509 nm (DCM). Molar extinction coefficient (ε) = 13000 M^{-1} cm^{-1}.

Method B:

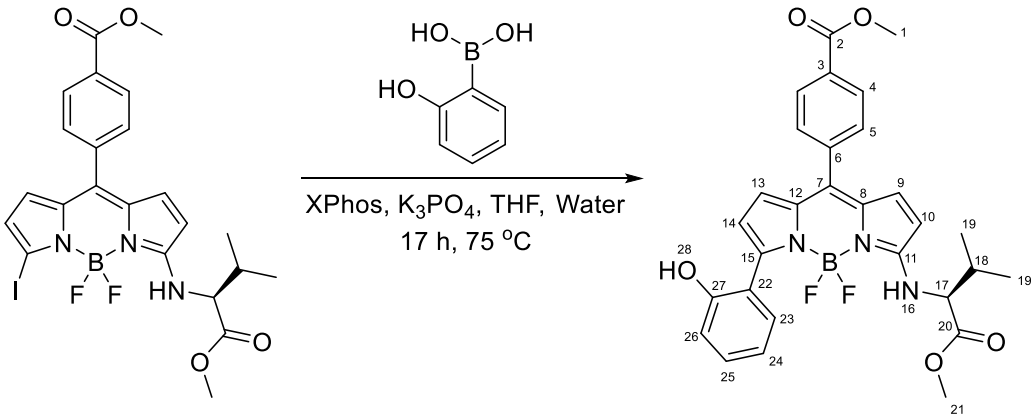

To a 50 mL Schlenk flask was added methyl (*S*)-4-(5,5-difluoro-3-iodo-7-((1-methoxy-3-methyl-1-oxobutan-2-yl)amino)-5*H*-5λ^4,6λ^4-dipyrrolo[1,2-c:2',1'-f][1,3,2]diazaborinin-10-yl)benzoate (54 mg, 0.093 mmol), 2-hydroxyphenyl boronic acid (25.7 mg, 0.186 mmol), XPhos (4.7 mg, 0.0056 mmol, 5 mol%) and K_3PO_4 (42.8 mg, 0.186 mmol). The Schlenk flask was degassed three times, added dry THF (6.6 mL) and water (1 mL) and then degassed again three times. The reaction was heated to 75 °C and stirred overnight, then diluted with DCM (25 mL). The organic layer was washed with H_2O (3 x 20 mL), dried over Na_2SO_4, filtered and the solvent was removed under reduced pressure to give a purple solid. The crude product was purified through silica gel column chromatography (2:1 petrol:ethyl acetate) to give methyl (*S*)-4-(5,5-difluoro-3-(2-hydroxyphenyl)-7-((1-methoxy-3-methyl-1-oxobutan-2-yl)amino)-5*H*-5λ^4,6λ^4-dipyrrolo[1,2-c:2',1'-f][1,3,2]diazaborinin-10-yl)benzoate (26.2 mg, 0.048 mmol, 52%) as a red solid.

Methyl (*S*)-4-(5,5-difluoro-3-iodo-7-((1-methoxy-3-methyl-1-oxobutan-2-yl)amino)-5*H*-5λ^4,6λ^4-dipyrrolo[1,2-c:2',1'-f][1,3,2]diazaborinin-10-yl)benzoate **4.5**

Analytical data reported as above

6.2.4.4 Methyl (S)-4-(10b-fluoro-10-((1-methoxy-3-methyl-1-oxobutan-2-yl)amino)-10b*H*-11-oxa-4b1,10aλ^4-diaza-10bλ^4-boracyclopenta[e]aceanthrylen-7-yl)benzoate **4.7**

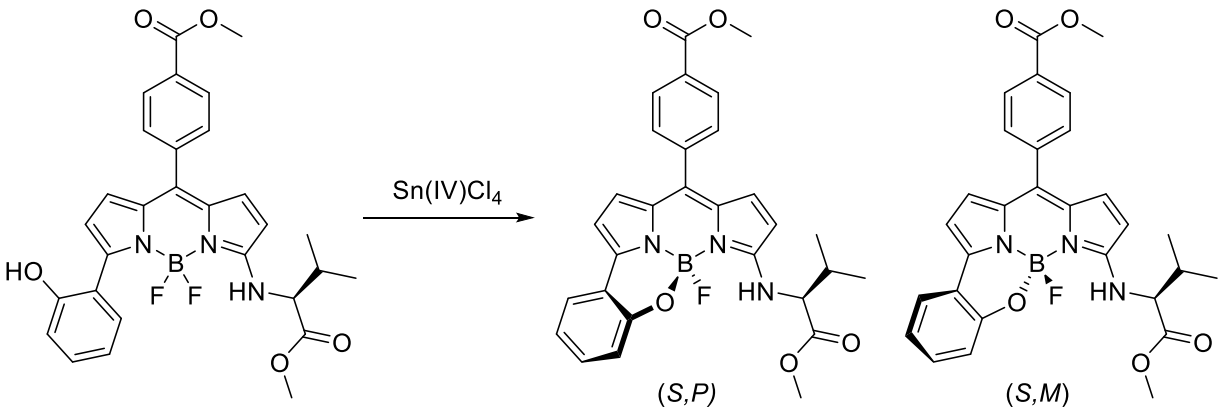

To an NMR tube was added methyl (*S*)-4-(5,5-difluoro-3-(2-hydroxyphenyl)-7-((1-methoxy-3-methyl-1-oxobutan-2-yl)amino)-5*H*-5λ^4,6λ^4-dipyrrolo[1,2-c:2',1'-f][1,3,2]diazaborinin-10-yl)benzoat (14.4 mg, 0.03 mmol), DCM (1 mL) and $Sn^{(IV)}Cl_4$ (1 drop). The reaction mixture was stirred at room temperature for 10 minutes and then ^{19}F NMR ran. The crude reaction mixture was then diluted with DCM (5 mL). The organic layer was washed with H_2O (2 x 10 mL), dried over Na_2SO_4, filter and the solvent was removed under reduced pressure to give a mixture of two diastereoisomers of methyl (S)-4-(10b-fluoro-10-((1-methoxy-3-methyl-1-oxobutan-2-yl)amino)-10b*H*-11-oxa-4b1,10aλ^4-diaza-10bλ^4-boracyclopenta[e]aceanthrylen-7-yl)benzoate (13.5 mg, 0.03 mmol, 99%) as a purple solid.

Mp: 132-134 ^oC. **R_f:** 0.19, 0.20 (4:2 petrol:ethyl acetate). **IR** (neat): ν_{max}/cm^{-1} 3401 (N-H, w), 2915 (C-H, w), 1723 (C=O, m), 1613 (C=C m). **^{19}F NMR** (282 MHz, Chloroform-*d*) δ -144.96 (q, *J* = 45.48 Hz), -142.94 (q, *J* = 44.46). **^{11}B NMR** (96 MHz, Chloroform-*d*) δ 0.2 (d, *J* = 49.6 Hz)

6.2.4.5 Methyl (*S*)-4-(3-chloro-7-((1-ethoxy-3-hydroxy-1-oxopropan-2-yl)amino)-5,5-difluoro-5*H*-5λ4,6λ4-dipyrrolo[1,2-*c*:2',1'-*f*][1,3,2]diazaborinin-10-yl)benzoate **4.10**

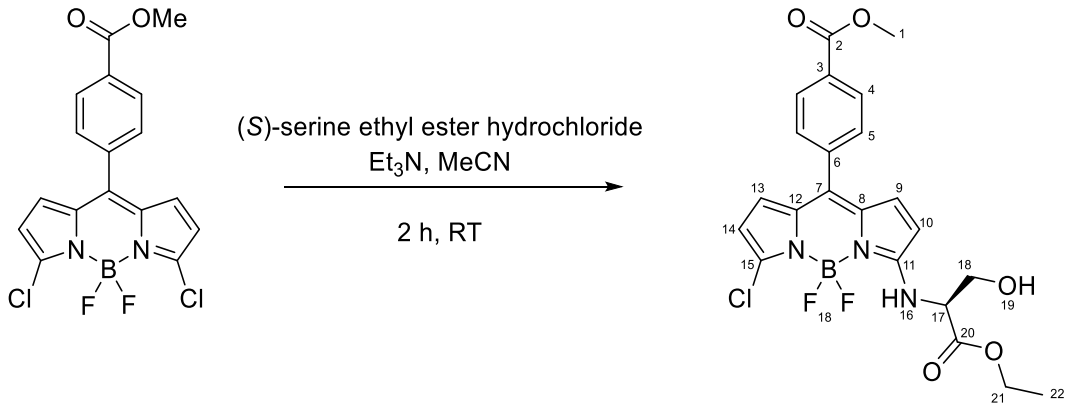

To a round bottom flask under nitrogen was added methyl 4-(3,7-dichloro-5,5-difluoro-5*H*-4λ^4,5λ^4-dipyrrolo[1,2-*c*:2',1'-*f*][1,3,2]diazaborinin-10-yl)benzoate (50 mg, 0.127 mmol), (*S*)-serine ethyl ester hydrochloride (43 mg, 0.254 mmol), Et_3N (38.7 μl, 0.279 mmol) and MeCN (7 mL). The reaction was stirred at room temperature for two hours and then quenched with water. The aqueous layer was extracted with DCM (2 x 30 mL) and washed the organic layer with brine (50 mL) and water (50 mL). the organic layer was dried under Na_2SO_4, filtered and removed solvent under reduced pressure. The crude product was purified using column chromatography (1:1 petrol : ethyl acetate) to give an orange product of methyl (*S*)-4-(3-chloro-7-((1-ethoxy-3-hydroxy-1-oxopropan-2-yl)amino)-5,5-difluoro-5*H*-5λ4,6λ4-dipyrrolo[1,2-*c*:2',1'-*f*][1,3,2]diazaborinin-10-yl)benzoate (56.7 mg, 0.110 mmol, 86%)

Rf: 0.48 (Petrol:ethyl acetate 1:1). **Mp:** 126-127 ^oC. **IR** (neat): ν_{max}/cm^{-1} 3380 (O-H, br, w), 2960 (C-H, w), 1720 (C=O, m), 1602 (C=C m), 1070 (C-O, m). **HRMS:** (ESI+) calcd for $C_{22}H_{22}BClF_2N_3O_5$ $[M+H]^+$: 492.1304, found 492.1283. **^{1}H NMR** (400 MHz, Chloroform-*d*) δ 8.09 (d, *J* = 9.0 Hz, 2H, *H*^{4}), 7.51 (d, *J* = 8.5 Hz, 2H, *H*^{5}), 7.08 (d, *J* = 7.3 Hz, 1H, H^{16}), 6.85 (d, *J* = 5.0 Hz, 1 H, H^{14}), 6.32 (d, *J* = 4.21 Hz, 1H, H^{10}), 6.22 (d, *J* = 5.0 Hz, 1H, H^{13}), 6.20 (d, *J* = 3.9 Hz, 1H, H^9), 4.36 (dt, *J* = 8.4, 4.5 Hz, 1 H, H^{17}), 4.31 (q, *J* = 3.4 Hz, 2H, H^{21}), 4.09 (dd, *J* = 8.0, 4.3 Hz, 1H, H^{18}), 3.98 (s, 3H, H^1), 2.19 (s, 1H, H^{19}), 1.3 (t, *J* = 7.0 Hz, 1H, H^{22}). **^{13}C NMR** (75 MHz, Chloroform-*d*) δ 168.7 (C^{20}),166.4 (C^2),161.3 (C^{11}), 130.0 (C^6), 135.4 (C^{15}), 133.0 (C^8), 131.4 (C^9), 131.2 (C^7), 130.9 (C^4), 130.8 (C^3), 130.2 (C^2), 129.4 (C^{10}), 120.8 (C^{12}), 113.1 (C^{13}), 111.4 (C^{14}), 62.9 (C^{18}), 62.5 (C^{21}), 59.0 (C^{19}), 52.3 (C^1), 14.0 (C^{22}). **^{19}F NMR** (282

MHz, Chloroform-*d*) δ -148.36 (q, *J* = 35.2 Hz). **^{11}B NMR** (96 MHz, Chloroform-*d*) δ 0.88 (t, *J* = 33.2 Hz). **UV-Vis:** λ_{max} = 507 nm (DCM). Molar extinction coefficient (ε) = 80000 M^{-1} cm^{-1}.

6.2.4.6 Methyl (5,5-difluoro-7-iodo-10-(4-(methoxycarbonyl)phenyl)-5*H*-4λ^4,5λ^4-dipyrrolo[1,2-*c*:2',1'-*f*][1,3,2]diazaborinin-3-yl)-L-prolinate **59.3**

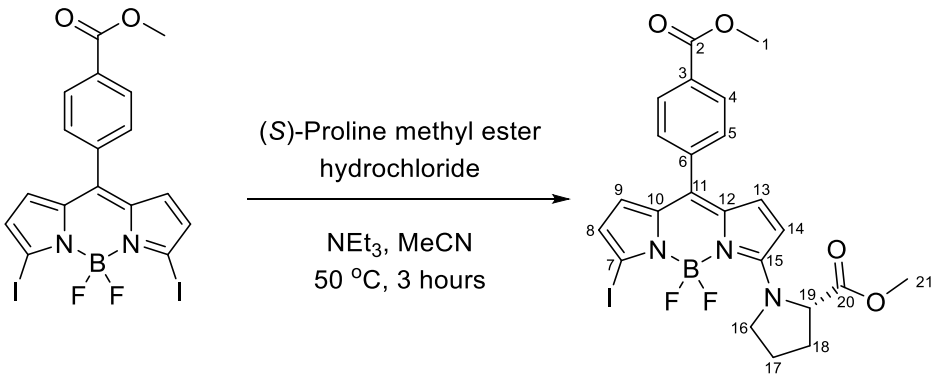

To a round bottom flask under nitrogen was added methyl 4-(5,5-difluoro-3,7-diiodo-5*H*-4λ^4,5λ^4-dipyrrolo[1,2-*c*:2',1'-*f*][1,3,2]diazaborinin-10-yl)benzoate (50 mg, 0.087 mmol), (*S*)-proline methyl ester hydrochloride (27.3 mg, 0.174 mmol), NEt_3 (26.5 μL, 0.191 mmol) and MeCN (7 mL). The reaction was heated to 50°C, stirred for 3 hours, then allowed to cool to room temp. The reaction was diluted with DCM (20 mL) and was washed with water (3 x 20 mL). The organic layer was dried over $MgSO_4$, filtered and solvent removed under reduced pressure. The crude product was purified by silica gel column chromatography (DCM) to afford methyl (5,5-difluoro-7-iodo-10-(4-(methoxycarbonyl)phenyl)-5*H*-4λ^4,5λ^4-dipyrrolo[1,2-*c*:2',1'-*f*][1,3,2]diazaborinin-3-yl)-L-prolinate (39 mg, 0.067 mmol, 78%) as an orange solid.

R_f: 0.78 (DCM). **Mp:** 176-178 °C. **IR** (neat): ν_{max}/cm^{-1} 2924 (C-H, m), 1823 (C=O, w). **^{1}H NMR** (300 MHz, Chloroform-*d*) δ 8.07 (d, *J* = 8.4 Hz, 2H, H*^{4}*), 7.45 (d, *J* = 8.2 Hz, 2H, H*^{5}*), 6.74 (d, *J* = 5.1 Hz, 1H, H*^{8}*), 6.48 (d, *J* = 3.7 Hz, 1H, H*^{14}*), 6.32 – 6.02 (m, 2H, H*^{9,13}*), 5.16 (s, 1H, H*^{19}*), 4.24 – 3.97 (m, 2H, H*^{16}*), 3.93 (s, 3H, H*^{21}*), 3.75 (s, 3H, H*^{1}*), 2.45 – 2.20 (m, 2H, H*^{18}*), 2.16 – 2.00 (m, 2H, H*^{17}*). **^{13}C NMR** (75 MHz, Chloroform-*d*) δ 171.8 (C*^{20}*), 166.5 (C*^{2}*), 160.9 (C*^{7}*), 139.0 (C*^{3}*), 135.3 (C*^{10}*), 135.0 (C*^{8}*), 134.7 (C*^{12}*), 130.7 (C*^{6}*), 130.5 (C*^{5}*), 129.4 (C*^{4}*), 128. (C*^{11}*), 124.8 (C*^{14}*), 119.9 (C*^{13}*), 115.8 (C*^{9}*), 81.4 (C*^{15}*), 63.8 (C*^{19}*), 52.7 (C*^{21}*), 52.4 (C*^{1}*), 51.9 (C*^{16}*), 30.7 (C*^{18}*), 23.5 (C*^{17}*). **^{19}F NMR** (282 MHz, Chloroform-*d*) δ -127.66 (q, *J*= 32.0 Hz), -128.06 (q, *J* = 32.1 Hz). **^{11}B NMR** (96 MHz, Chloroform-*d*) δ 0.85 (t, *J* = 34.0 Hz). **UV-Vis:** λ_{max} = 510 nm (DCM). **Molar extinction coefficient (ε)** = 36000 M^{-1} cm^{-1}.

6.2.4.7 Methyl (*S*)-4-(5,5-difluoro-3-iodo-7-((1-methoxy-4-methyl-1-oxopentan-2-yl)amino)-5*H*-5λ^4,6λ^4-dipyrrolo[1,2-c:2',1'-f][1,3,2]diazaborinin-10-yl)benzoate **4.12**

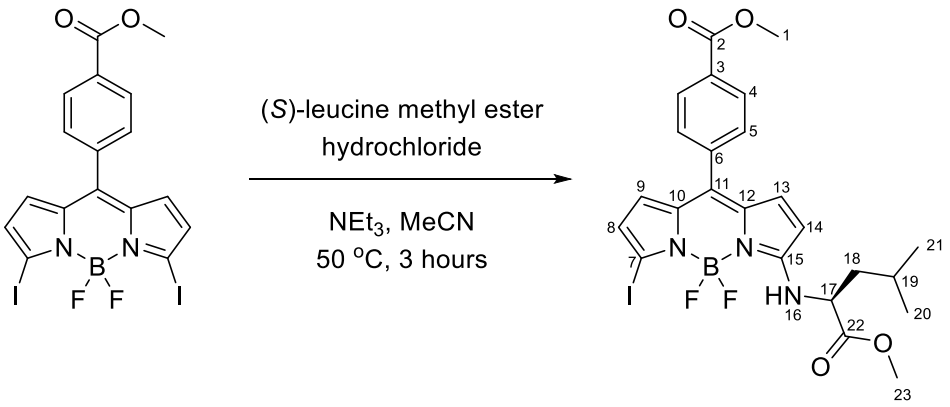

To a round bottom flask under nitrogen was added methyl 4-(5,5-difluoro-3,7-diiodo-5*H*-4λ^4,5λ^4-dipyrrolo[1,2-*c*:2',1'-*f*][1,3,2]diazaborinin-10-yl)benzoate (50 mg, 0.087 mmol), (*S*)-leucine methyl ester hydrochloride (31.4 mg, 0.173 mmol), NEt_3 (26.5 μL, 0.19 mmol) and MeCN (7 mL). The reaction was heated to 50°C, stirred for 3 hours, then allowed to cool to room temp. The reaction was diluted with DCM (20 mL) and was washed with water (3 x 20 mL). The organic layer was dried over $MgSO_4$, filtered and solvent removed under reduced pressure. The crude product was purified by silica gel column chromatography (DCM) to afford Methyl (*S*)-4-(5,5-difluoro-3-iodo-7-((1-methoxy-4-methyl-1-oxopentan-2-yl)amino)-5*H*-5λ^4,6λ^4-dipyrrolo[1,2-c:2',1'-f][1,3,2]diazaborinin-10-yl)benzoate (46.5 mg, 0.078 mmol, 90%) as an orange solid.

R_f: 0.59 (DCM). **IR** (neat): ν_{max}/cm^{-1} 3375 (N-H, w), 2955 (C-H, w), 1717 (C=O, m), 1601 (C=O, s). **^{1}H NMR** (300 MHz, Chloroform-*d*) δ 8.11 (d, *J* = 8.5 Hz, 2H, H*^{4}*), 7.50 (d, *J* = 8.5 Hz, 2H, H*^{5}*), 6.84 (d, *J* = 5.0 Hz, 1H, H*^{13}*), 6.58 (d, *J* = 8.9 Hz, 1H, H*^{16}*), 6.51 (d, *J* = 3.8 Hz, 1H, H*^{9}*), 6.22 (d, *J* = 3.8 Hz, 1H, H*^{8}*), 6.18 (d, *J* = 5.0 Hz, 1H, H*^{14}*), 4.28 – 4.16 (m, 1H, H*^{17}*), 3.95 (s, 3H, H*^{1}*), 3.78 (s, 3H, H*^{23}*), 1.88 – 1.75 (m, 3H, H*^{18,19}*), 0.97 (dd, *J* = 15.4, 6.3 Hz, 6H, H*^{20,21}*). **^{13}C NMR** (75 MHz, Chloroform-*d*) δ 171.30 (C*^{22}*), 166.54 (C*^{2}*), 161.43 (C*^{15}*), 138.40 (C*^{3}*), 135.91 (C*^{13}*), 135.81 (C*^{10}*) 133.46 (C*^{12}*), 131.09 (C*^{6}*), 130.82 (C*^{11}*), 130.38 (C*^{5}*), 129.60 (C*^{4}*), 125.09 (C*^{9}*), 122.16 (C*^{8}*) 111.23 (C*^{14}*), 83.39 (C*^{7}*), 56.38 (C*^{17}*), 53.01 (C*^{23}*), 52.48 (C*^{1}*), 41.71 (C*^{18}*), 24.65 (C*^{19}*), 22.82 (C*$^{20/21}$*), 21.83 (C*$^{20/21}$*). **^{11}B NMR** (96 MHz, Chloroform-*d*) δ 0.95 (t, *J* = 34.3 Hz). **^{19}F NMR** (282 MHz, Chloroform-*d*) δ -145.99 (d, *J* = 33.1 Hz).

UV-Vis: λ_{max} = 514 nm (DCM). **Molar extinction coefficient (ε)** = 38000 M^{-1} cm^{-1}. **ϕ_F:** 0.16.

6.2.4.8 Methyl 4-(5,5-difluoro-3-(((2S,3S)-3-hydroxy-1-methoxy-1-oxobutan-2-yl)amino)-7-iodo-5*H*-4λ^4,5λ^4-dipyrrolo[1,2-c:2',1'-f][1,3,2]diazaborinin-10-yl)benzoate **4.13**

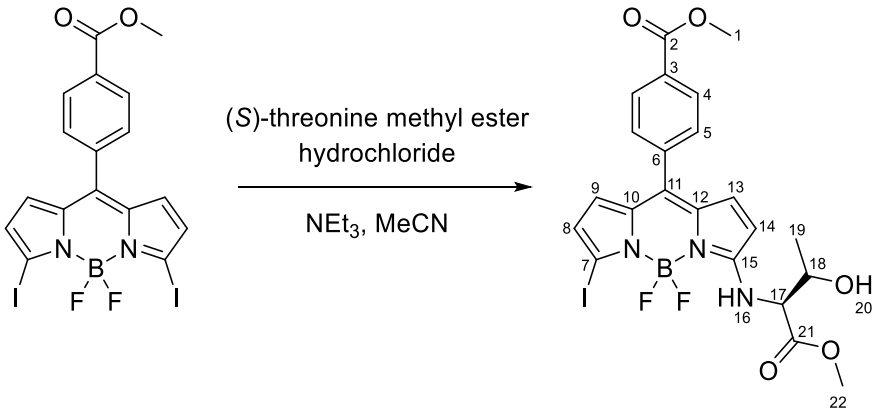

To a round bottom flask under nitrogen was added methyl 4-(5,5-difluoro-3,7-diiodo-5*H*-4λ^4,5λ^4-dipyrrolo[1,2-*c*:2',1'-*f*][1,3,2]diazaborinin-10-yl)benzoate (50 mg, 0.087 mmol), (*S*)-threonine methyl ester hydrochloride (29 mg, 0.173 mmol), NEt_3 (26.5 μL, 0.19 mmol) and MeCN (7 mL). The reaction was heated to 50°C, stirred for 3 hours, then allowed to cool to room temp. The reaction was diluted with DCM (20 mL) and was washed with water (3 x 20 mL). The organic layer was dried over $MgSO_4$, filtered and solvent removed under reduced pressure. The crude product was purified by silica plug (DCM – wash off impurities, ethyl acetate – flush out product) to afford methyl methyl 4-(5,5-difluoro-3-(((2S,3S)-3-hydroxy-1-methoxy-1-oxobutan-2-yl)amino)-7-iodo-5*H*-4λ^4,5λ^4-dipyrrolo[1,2-c:2',1'-f][1,3,2]diazaborinin-10-yl)benzoate (39.0 mg, 0.067 mmol, 77%) as an orange solid.

R_F: 0.81 (ethyl acetate). **IR** (neat): ν_{max}/cm^{-1} 3581 (O-H, w), 3379 (N-H, w), 2972 (C-H, w), 1717 (C=O, m), 1604 (C=O, s) 3610-3154 (O-H, N-H, br, w), 2953 (C-H, w). **^{1}H NMR** (300 MHz, Chloroform-*d*) δ 8.10 (d, *J* = 8.5 Hz, 2H, H^{4}), 7.50 (d, *J* = 8.5 Hz, 2H, H^{5}), 7.02 (d, *J* = 9.3 Hz, 1H, H^{16}), 6.84 (d, *J* = 5.0 Hz, 1H, H^{13}), 6.51 (d, *J* = 3.9 Hz, 1H, H^{8}), 6.22 (d, *J* = 3.9 Hz, 1H, H^{9}), 6.18 (d, *J* = 5.0 Hz, 1H, H^{14}), 4.43 (qd, *J* = 6.4, 3.2 Hz, 1H, J^{18}), 4.14 – 4.11 (m, 1H, H^{17}), 3.96 (s, 3H, H^{1}), 3.82 (s, 3H, H^{22}),

2.75 (s, 1H, H^{20}), 1.34 (d, *J* = 6.4 Hz, 3H, H^{19}). **^{13}C NMR** (75 MHz, Chloroform-*d*) δ 169.87 (C^{21}), 166.62 (C^{2}), 162.08 (C^{15}), 138.43 (C^{3}), 135.85 ($C^{11, 13}$), 133.51 (C^{12}), 131.09 (C^{6}), 130.84 (C^{10}), 130.41 (C^{5}), 129.63 (C^{4}), 125.14 (C^{8}), 122.18 (C^{9}), 111.64 (C^{14}), 83.49 (C^{7}), 68.11 (C^{18}), 62.86 (C^{17}), 53.32 (C^{22}), 52.53 (C^{1}), 19.94 (C^{19}). **^{11}B NMR** (96 MHz, Chloroform-*d*) δ 0.98 (t, *J* = 33.0 Hz). **^{19}F NMR** (282 MHz, Chloroform-*d*) δ -145.71 (q, *J* = 33.4 Hz).

6.2.4.9 Methyl (*R*)-4-(5,5-difluoro-3-((3-hydroxy-1-methoxy-1-oxopropan-2-yl)amino)-7-iodo-5*H*-4λ^4,5λ^4-dipyrrolo[1,2-c:2',1'-f][1,3,2]diazaborinin-10-yl)benzoate **4.16**

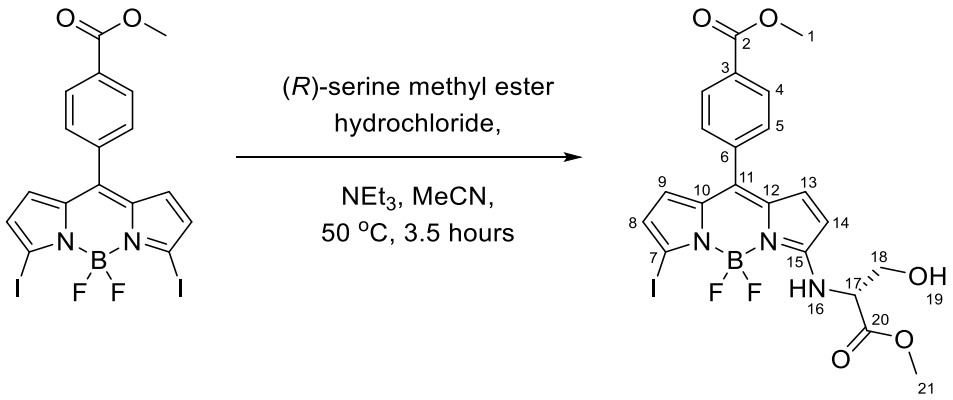

To a round bottom flask under nitrogen was added methyl 4-(3,7-diiodo-5,5-difluoro-5*H*-4λ^4,5λ^4-dipyrrolo[1,2-*c*:2',1'-*f*][1,3,2]diazaborinin-10-yl)benzoate (289 mg, 0.5 mmol), (*R*)-serine methyl ester hydrochloride (156 mg, 1.0 mmol), Et_3N (153 μL, 1.1 mmol) and MeCN (35 mL). The reaction was stirred at 50°C for 3.5 hours and then diluted with DCM (100 mL). The organic layer was washed with HCl (0.1 M, 50 mL) and water (2 x 50 mL). The organic layer was then dried over $MgSO_4$, filter and removed solvent under reduced pressure. This gave methyl (*R*)-4-(5,5-difluoro-3-((3-hydroxy-1-methoxy-1-oxopropan-2-yl)amino)-7-iodo-5*H*-4λ^4,5λ^4-dipyrrolo[1,2-c:2',1'-f][1,3,2]diazaborinin-10-yl)benzoate (281.4 mg, 0.49 mmol, 99%) as a red solid.

R_f: 0.81 (Ethyl acetate). **Mp:** 113-114°C. **IR** (neat): ν_{max}/cm^{-1} 3522 (O-H, w), 2981 (C-H, s), 1744 (C=O, s). **HRMS:** (ESI+) calcd for $C_{22}H_{22}BClF_2N_3O_5$ $[M+H]^+$: 492.1304, found 492.1295. **^{1}H NMR** (300 MHz, Chloroform-*d*) δ 8.08 (d, *J* = 8.4 Hz, 2H, H*^{4}*), 7.46 (d, *J* = 8.2 Hz, 2H, H*^{5}*), 7.07 (d, *J* = 8.2 Hz, 1H, H*^{16}*), 6.81 (d, *J* = 5.0 Hz, 1H, H*^{13}*), 6.49 (d, *J* = 3.8 Hz, 1H, H*^{9}*), 6.21 (d, J = 3.4 Hz, 1H, H*^{14}*), 6.20 (d, J = 2.3 Hz, 1H, H*^{8}*), 4.38 (dt, *J* = 8.4, 4.1 Hz, 1H, H*^{17}*), 4.10 (m, 2H, H*^{18}*), 3.95 (s, 3H, H*^{1}*), 3.82 (s, 3H, H*^{21}*), 3.08 (s, 1H, H*^{19}*). **^{13}C NMR** (75 MHz, Chloroform-*d*) δ 169.4, (C*^{20}*), 166.5 (C*^{2}*), 161.6 (C*^{15}*), 138.3 (C*^{3}*), 135.7 (C*^{13}*), 135.7 (C*^{10}*), 133.4 (C*^{12}*), 131.0 (C*^{6}*), 130.6 (C*^{11}*), 130.3 (C*^{5}*), 129.5 (C*^{4}*), 125.0 (C*^{9}*), 122.0 (C*^{8}*), 111.9 (C*^{14}*), 83.2 (C*^{7}*), 63.0 (C*^{18}*), 59.1 (C*^{17}*), 53.4 (C*^{21}*), 52.5 (C*^{1}*). **^{19}F NMR** (282 MHz, Chloroform-*d*) δ -144.92 (m), -146.17 (m). **^{11}B NMR** (96 MHz, Chloroform-*d*) δ 0.94 (t, *J* = 33.6 Hz). **UV-Vis:** λ_{max} = 515 nm (DCM). **Molar extinction coefficient** (ε) = 42000 M^{-1} cm^{-1}

6.2.4.10 Methyl (*S*)-4-(5,5-difluoro-3-iodo-7-((1-methoxy-1-oxopropan-2-yl)amino)-5*H*-5λ^4,6λ^4-dipyrrolo[1,2-*c*:2',1'-*f*][1,3,2]diazaborinin-10-yl)benzoate **4.17**

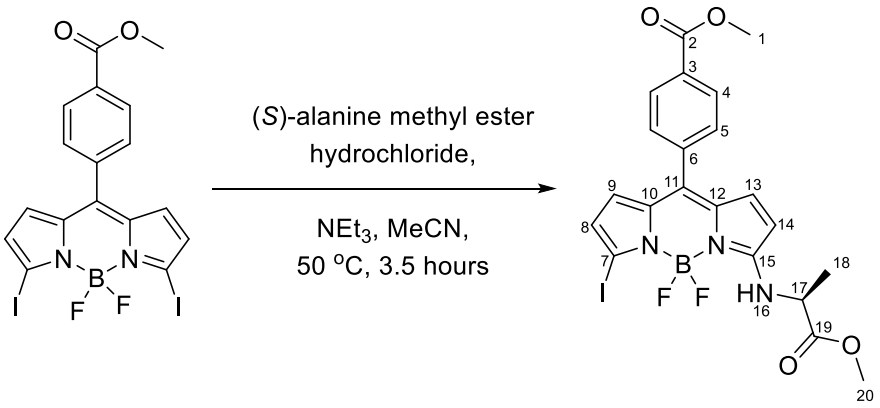

To a round bottom flask under nitrogen was added methyl 4-(5,5-difluoro-3,7-diiodo-5*H*-4λ^4,5λ^4-dipyrrolo[1,2-*c*:2',1'-*f*][1,3,2]diazaborinin-10-yl)benzoate (50 mg, 0.087 mmol), L-Alanine methyl ester hydrochloride (24.1 mg, 0.173 mmol), NEt_3 (26.5 μL, 0.19 mmol) and MeCN (7 mL). The reaction was heated to 50°C, stirred for 3.5 hours, then allowed to cool to room temp. The reaction was diluted with DCM (20 mL) and was washed with water (3 x 20 mL). The organic layer was dried over $MgSO_4$, filtered and solvent removed under reduced pressure. The crude product was purified by silica gel column chromatography (DCM) to afford methyl (S)-4-(5,5-difluoro-3-iodo-7-((1-methoxy-1-oxopropan-2-yl)amino)-5*H*-5λ^4,6λ^4-dipyrrolo[1,2-*c*:2',1'-*f*][1,3,2]diazaborinin-10-yl)benzoate (44.3 mg, 0.08 mmol, 92%) as an orange solid.

R_f: 0.62 (DCM) **Mp:** 172-174 °C. **^{1}H NMR (300 MHz, Chloroform-*d*)** δ 8.10 (d, *J* = 8.5 Hz, 2H, H^{4}), 7.50 (d, *J* = 8.5 Hz, 2H, H^{5}), 6.83 (d, *J* = 5.0 Hz, 1H, H^{13}), 6.75 (d, *J* = 8.5 Hz, 1H, H^{16}), 6.51 (d, *J* = 3.8 Hz, 1H, H^{8}), 6.22 (d, *J* = 3.9 Hz, 1H, H^{9}), 6.16 (d, *J* = 5.0 Hz, 1H, H^{14}), 4.37 – 4.24 (m, 1H, H^{17}), 3.95 (s, 3H, H^{1}), 3.80 (s, 3H, H^{20}), 1.62 (d, *J* = 7.1 Hz, 3H, H^{18}). **^{13}C NMR (75 MHz, Chloroform-*d*)** δ 171.30 (C^{19}), 166.54 (C^{2}), 161.13 (C^{15}), 138.40 (C^{3}), 135.85 (C^{13}), 135.79 (C^{10}), 133.46 (C^{12}), 131.09 (C^{11}), 130.86 (C^{6}), 130.39 (C^{5}), 129.60 (C^{4}), 125.09 (C^{8}), 122.16 (C^{9}), 111.35 (C^{14}), 83.44 (C^{7}), 53.19 (C^{17}), 53.15 (C^{20}), 52.49 (C^{1}), 19.18 (C^{18}). **^{11}B NMR** (96

MHz, Chloroform-*d*) δ 0.96 (t, *J* = 34.0 Hz). **^{19}F NMR** (282 MHz, Chloroform-*d*) δ -145.40 - -146.90 (m).

6.2.4.11 Methyl (*S*)-4-(3-bromo-5,5-difluoro-7-((3-hydroxy-1-methoxy-1-oxopropan-2-yl)amino)-5*H*-5λ^4,6λ^4-dipyrrolo[1,2-*c*:2',1'-*f*][1,3,2]diazaborinin-10-yl)benzoate **4.20**

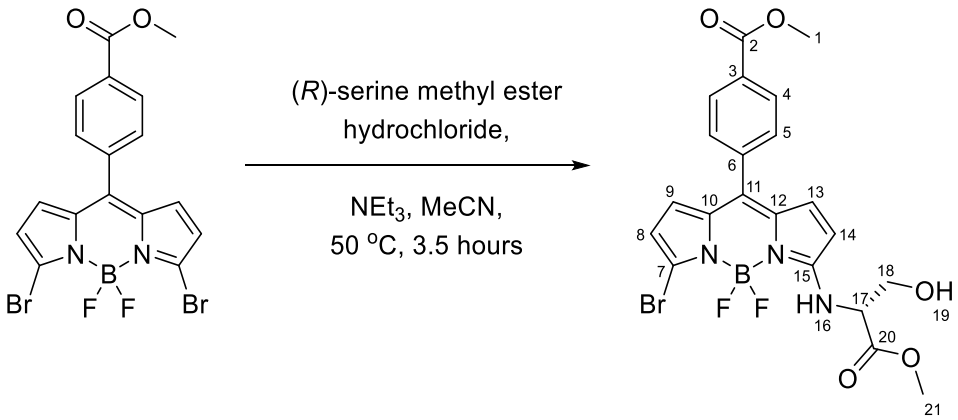

To a 100 mL round bottom flask was added methyl 4-(3,7-dibromo-5,5-difluoro-5*H*-4λ^4,5λ^4-dipyrrolo[1,2-*c*:2',1'-*f*][1,3,2]diazaborinin-10-yl)benzoate (77 mg, 0.207 mmol), D-Serine methyl ester hydrochloride (64.4 mg, 0.414 mmol), Et_3N (63.4 μL, 0.455 mmol) and MeCN (14 mL). The reaction was stirred at 40°C for 2 hours and then diluted with DCM (50 mL). The organic layer was washed with water (2 x 25 mL) and then dried over $MgSO_4$, filtered and solvent removed under reduced pressure to give an orange solid. The crude product was purified by silica plug (DCM:acetic acid 99:1, flush with ethyl acetate) to give methyl (*S*)-4-(3-bromo-5,5-difluoro-7-((3-hydroxy-1-methoxy-1-oxopropan-2-yl)amino)-5*H*-5λ^4,6λ^4-dipyrrolo[1,2-*c*:2',1'-*f*][1,3,2]diazaborinin-10-yl)benzoate (108 mg, 0.207 mmol, 100%) as an orange solid.

^{1}H NMR (300 MHz, Chloroform-*d*) δ 8.07 (d, *J* = 7.9 Hz, 2H, H^{4}), 7.45 (d, *J* = 7.9 Hz, 2H, H^{5}), 7.10 (d, *J* = 7.9 Hz, 1H, H^{16}), 6.80 (d, *J* = 5.0 Hz, 1H, H^{13}), 6.27 (d, *J* = 3.9 Hz, 1H, H^{9}), 6.24 (d, *J* = 3.9 Hz, 1H, H^{8}), 6.21 (d, *J* = 5.0 Hz, 1H, H^{14}), 4.38 (dt, *J* = 8.5, 4.1 Hz, 1H, H^{17}), 4.15 – 4.01 (m, 2H, H^{19}), 3.94 (s, 3H, H^{1}), 3.81 (s, 3H, H^{21}). **^{13}C NMR** (75 MHz, Chloroform-*d*) δ 169.4 (C^{20}), 166.6 (C^{2}), 161.6 (C^{15}), 138.3 (C^{3}), 135.8 (C^{13}), 133.3 (d, C^{10,12}), 131.5 (C^{11}), 131.1 (C^{6}), 130.5 (C^{5}), 129.6 (C^{4}), 121.5 (C^{8}), 117.4 (C^{9}), 116.9 (C^{7}), 111.7 (C^{14}), 63.1 (C^{19}), 59.2 (C^{17}), 53.4 (C^{21}), 52.5 (C^{1}).

^{19}F NMR (282 MHz, Chloroform-*d*) δ -144.15 – -149.97 (m). **^{11}B NMR** (96 MHz, Chloroform-*d*) δ 0.93 (t, *J* = 32.8 Hz).

6.2.4.12 Methyl (*S*)-4-(5,5-difluoro-3-((3-hydroxy-1-methoxy-1-oxopropan-2-yl)amino)-7-iodo-5*H*-4λ^4,5λ^4-dipyrrolo[1,2-c:2',1'-f][1,3,2]diazaborinin-10-yl)benzoate **4.21**

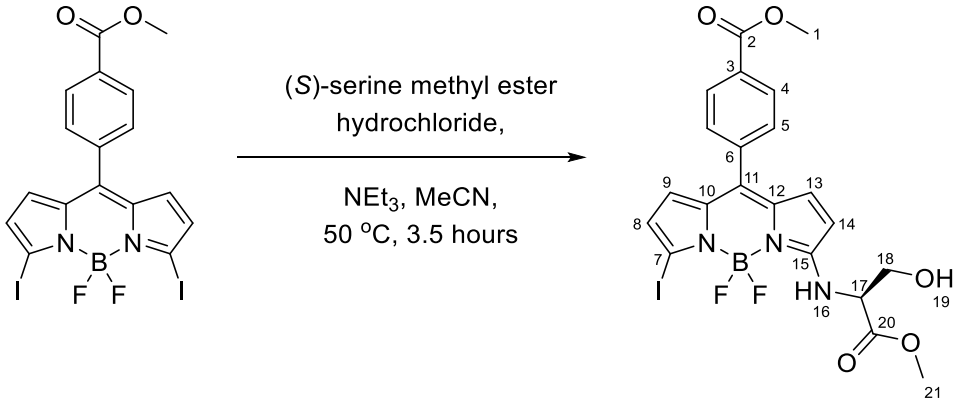

To a round bottom flask under nitrogen was added methyl 4-(5,5-difluoro-3,7-diiodo-5*H*-4λ^4,5λ^4-dipyrrolo[1,2-*c*:2',1'-*f*][1,3,2]diazaborinin-10-yl)benzoate (50 mg, 0.087 mmol), L-Serine methyl ester hydrochloride (26.9 mg, 0.173 mmol), NEt_3 (26.5 μL, 0.19 mmol) and MeCN (7 mL). The reaction was heated to 50°C, stirred for 3.5 hours, then allowed to cool to room temp. The reaction was diluted with DCM (20 mL) and was washed with water (3 x 20 mL). The organic layer was dried over $MgSO_4$, filtered and solvent removed under reduced pressure. The crude product was purified by silica gel column chromatography (1:1 petrol:ethyl acetate) to afford methyl (*S*)-4-(5,5-difluoro-3-((3-hydroxy-1-methoxy-1-oxopropan-2-yl)amino)-7-iodo-5*H*-4λ^4,5λ^4-dipyrrolo[1,2-*c*:2',1'-*f*][1,3,2]diazaborinin-10-yl)benzoate (49.5 mg, 0.087 mmol, 100%) as an orange solid.

R_f: 0.2 (1:1 petrol:ethyl acetate). **IR** (neat): ν_{max}/cm^{-1} 3610-3154 (O-H, N-H, br, w), 2953 (C-H, w). **^{1}H NMR** (300 MHz, Chloroform-*d*) δ 8.09 (d, *J* = 8.2 Hz, 2H, H*^{4}*), 7.48 (d, *J* = 8.2 Hz, 2H, H*^{5}*), 7.06 (d, *J* = 8.5 Hz, 1H, H*^{16}*), 6.82 (d, *J* = 5.0 Hz, 1H, H*^{13}*), 6.50 (d, *J* = 3.8 Hz, 1H, H*^{9}*), 6.22 (s, 1H, H*^{10}*), 6.20 (d, *J* = 2.1 Hz, 1H, H*^{14}*), 4.37 (dt, *J* = 8.7, 4.3 Hz, 1H, H*^{17}*), 4.17 – 4.01 (m, 2H, H*^{20}*), 3.95 (s, 3H, H*^{1}*), 3.83 (s, 3H, H*^{19}*), 3.08 (s, 1H, H*^{21}*). **^{13}C NMR** (75 MHz, Chloroform-*d*) δ 169.42 (C*^{18}*), 166.64 (C*^{2}*), 161.66 (C*^{15}*), 138.37 (C*^{3}*), 135.84 (C*^{13}*), 135.78 (C*^{11}*), 133.51 (C*^{12}*), 131.08 (C*^{6}*),

130.84 (C^{7}), 130.41 (C^{5}), 129.63 (C^{4}), 125.13 (C^{9}), 122.17 (C^{10}), 111.88 (C^{14}), 83.40 (C^{8}), 63.16 (C^{20}), 59.21 (C^{17}), 53.44 (C^{19}), 52.54 (C^{1}). **^{11}B NMR** (96 MHz, Chloroform-*d*) δ 0.98 (t, *J* = 33.1 Hz). **^{19}F NMR** (282 MHz, Chloroform-*d*) δ -144.69 - -145.65 (m).

6.2.4.13 Methyl (*R*)-4-(5,5-difluoro-3-((3-hydroxy-1-methoxy-1-oxopropan-2-yl)amino)-7-(2-hydroxyphenyl)-5*H*-4λ^4,5λ^4-dipyrrolo[1,2-*c*:2',1'-*f*][1,3,2]diazaborinin-10-yl)benzoate **4.22**

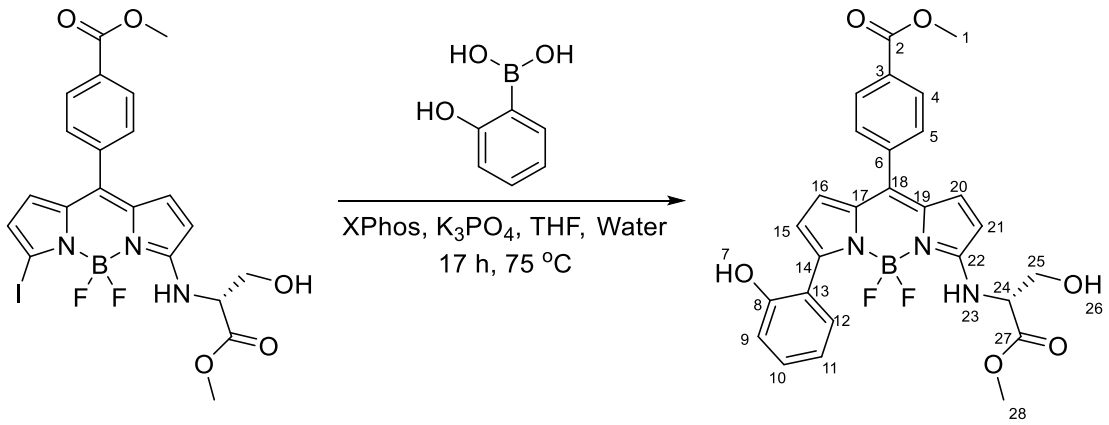

To a 50 mL Schlenk flask was added methyl 4-(5,5-difluoro-3-((3-hydroxy-1-methoxy-1-oxopropan-2-yl)amino)-7-iodo-5*H*-4λ^4,5λ^4-dipyrrolo[1,2-*c*:2',1'-*f*][1,3,2]diazaborinin-10-yl)benzoate (56.9 mg, 0.1 mmol), 2-hydroxyphenyl boronic acid (27.6 mg, 0.2 mmol), XPhos (5.1 m, 0.006 mmol, 6 mol%), K_3PO_4 (46 mg, 0.2 mmol) and subsequently degassed (x3). Dry THF (8 mL) and water (1.2 mL) were added to the Schlenk flask and degassed (x3). The reaction was heated to 75^{o}C and stirred, under a nitrogen atmosphere, for 1.1 hours. The reaction mixture was diluted with DCM (40 mL) and washed with water (3 x 25 mL), dried over $MgSO_4$, filtered and the solvent was removed under reduced pressure to give methyl (*R*)-4-(5,5-difluoro-3-((3-hydroxy-1-methoxy-1-oxopropan-2-yl)amino)-7-(2-hydroxyphenyl)-5*H*-4λ^4,5λ^4-dipyrrolo[1,2-*c*:2',1'-*f*][1,3,2]diazaborinin-10-yl)benzoate (crude yield: 43.9 mg, 0.08 mmol, 82%) as a red/pink solid.

Rf: 0.256 (2:3 petrol:ethyl acetate). **IR** (neat): ν_{max}/cm^{-1} 3658 (O-H, w), 3337 (N-H, m) 2971 (C-H, s), 1655 (C=O, w).**Mp:** 101-104^{o}C. **^{1}H NMR** (300 MHz, Chloroform-*d*) δ 8.15 (d, *J* = 8.3 Hz, 2H, H^{4}), 7.59 (d, *J* = 8.3 Hz, 2H, H^{5}), 7.49 (dd, *J* = 7.6, 1.6 Hz, 1H, H^{12}), 7.32 (ddd, *J* = 8.1, 7.4, 1.7 Hz, 1H, H^{10}), 7.04 – 6.95 (m, 2H, H^{9,12}), 6.90 – 6.83 (m, 2H, H^{20,23})*, 6.50 (d, *J* = 3.8 Hz, 1H, H^{16}), 6.37 (d, *J* = 3.8 Hz, 1H, H^{15}), 6.15 (d, *J* = 4.9 Hz, 1H, H^{21}), 5.74 (s, 1H, H^{7}), 4.27 (dt, *J* = 8.7, 4.4 Hz, 1H, H^{24}), 3.98 (s, 5H, H^{1,25}), 3.77 (s, 3H, H^{28}), 2.62 (s, 1H, H^{26}). **^{13}C NMR** (75 MHz, Chloroform-*d*) δ 169.4 (C^{27}), 166.7 (C^{2}), 161.4 (C^{22}), 154.0 (C^{8}), 142.1 (C^{14}), 138.9 (C^{3}), 135.7 (C^{20}),

133.9 (C^{17}), 133.4 (C^{19}), 132.8 (C^{18}), 131.6 (C^{12}), 131.2 (C^{6}), 130.5 (C^{5}), 130.4 (C^{10}), 129.7 (C^{4}), 121.8 (C^{16}), 121.4 (C^{13}), 120.2 (C^{11}), 116.5 (C^{15}), 116.2 (C^{9}), 111.4 (C^{21}), 63.0 (C^{25}), 59.1 (C^{24}), 53.4 (C^{28}), 52.6 (C^{1}). **^{19}F NMR** (282 MHz, Chloroform-*d*) δ -142.51 – -143.50 (m), -144.97 – -145.54 (m). **^{11}B NMR** (96 MHz, Chloroform-*d*) δ 1.19 (t, *J* = 35.3 Hz).

* 6.90 – 6.83 (m, 2H, $H^{20,23}$) = 6.88 (d, *J* = 4.9 Hz, 1H, H^{20}) with broad NH^{23} underneath.

6.2.4.14 Methyl (*R*)-4-(10b-(4-fluorophenyl)-10-((3-hydroxy-1-methoxy-1-oxopropan-2-yl)amino)-10b*H*-11-oxa-4b1,10aλ^4-diaza-10bλ^4-boracyclopenta[e]aceanthrylen-7-yl)benzoate **4.23a** and **4.23b**

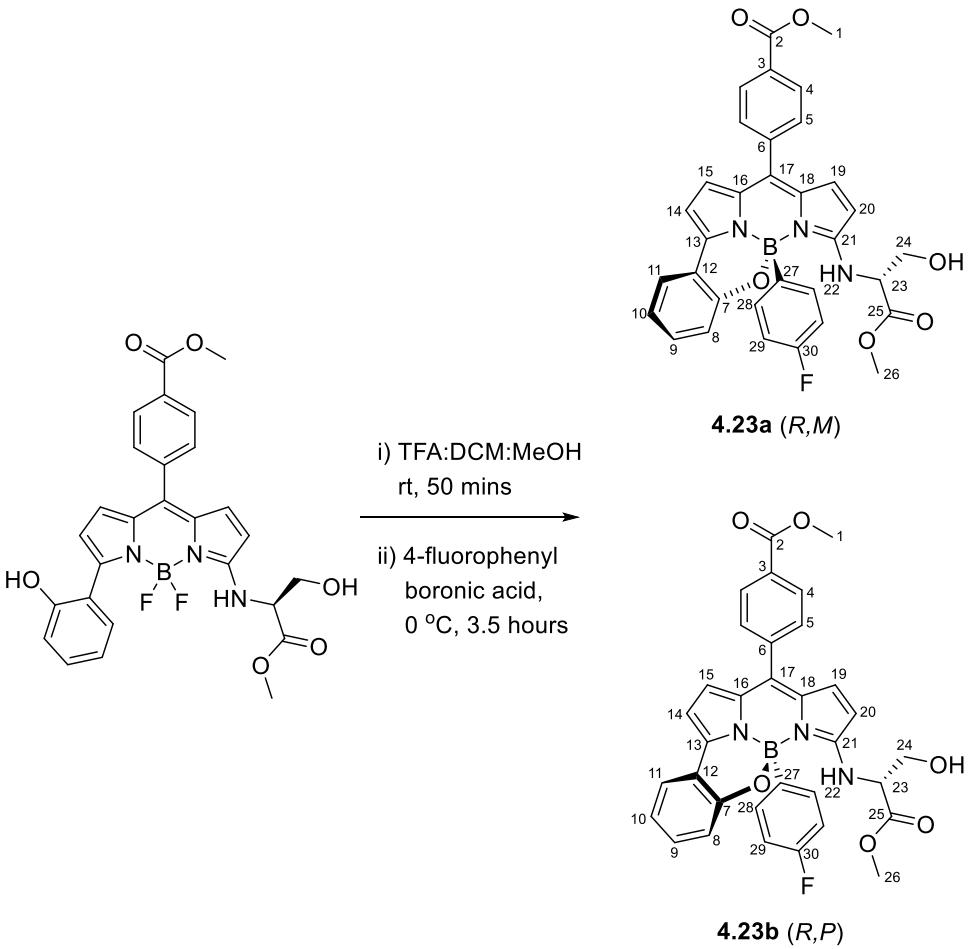

4.23a (*R,M*)

4.23b (*R,P*)

To a 25 mL round bottom flask was added methyl (*R*)-4-(5,5-difluoro-3-((3-hydroxy-1-methoxy-1-oxopropan-2-yl)amino)-7-(2-hydroxyphenyl)-5*H*-4λ^4,5λ^4-dipyrrolo[1,2-*c*:2',1'-*f*][1,3,2]diazaborinin-10-yl)benzoate (13 mg, 0.025 mmol), TFA, DCM, MeOH (90:5:5, 2.25 mL, 0.125 mL, 0.125 mL and was stirred at room temp for 50 mins. The solvent was then removed under reduced pressure, diluted with DCM (10 mL) and washed with water (3 x 25 mL). The organic layer was dried over $MgSO_4$, filtered and solvent was removed under reduced pressure to afford methyl (*Z*)-4-((5-((3-hydroxy-1-methoxy-1-oxopropan-2-yl)amino)-2*H*-pyrrol-2-ylidene)(5-(2-hydroxyphenyl)-1*H*-pyrrol-2-yl)methyl)benzoate as a purple solid. To the crude intermediate, under a nitrogen atmosphere, was added $CHCl_3$ (5 mL), cooled to 0^{o}C, subsequently added 4-fluorphenyl boronic acid (5.2 mg, 0.037 mmol) and stirred for 3.5 hours. The solvent was removed under reduced pressure and purified by silica

gel column chromatography (3:2 petrol:ethyl acetate) to give methyl (*R*)-4-(10b-(4-fluorophenyl)-10-((3-hydroxy-1-methoxy-1-oxopropan-2-yl)amino)-10b*H*-11-oxa-4b1,10aλ^4-diaza-10bλ^4-boracyclopenta[e]aceanthrylen-7-yl)benzoate as two diasteroisomers (A = 4.1 mg, 0.0063 mmol, 28%, B = 2.1 mg, 0.0035 mmol, 14% *de* = 33) as a blue solid.

4.23a:

R_f: 0.2 (3:2 petrol:ethyl acetate). **Mp**: 151-154°C. **IR** (neat): ν_{max}/cm^{-1} 3658 (O-H, m), 3524 (N-H, m), 2981 (C-H, s), 1718 (C=O, s). **HRMS:** (ASAP[SOLID]) calcd for $C_{33}H_{27}BFN_3O_6$ [M+H]$^-$: 592.2061, found 592.2071. **^{1}H NMR** (300 MHz, $CDCl_3$) δ 8.16 (d, *J* = 8.5 Hz, 2H, H*^{4}*), 7.67 (d, *J* = 8.5 Hz, 2H, H*^{5}*), 7.52 – 7.41 (m, 2H, H*^{11,22}*), 7.25 – 7.18 (m, 4H, H*^{9,10,28}*), 6.94 (d, *J* = 4.7 Hz, 1H, H*^{20}*), 6.88 (ddd, *J* = 8.1, 4.9, 3.5 Hz, 1H, H*^{8}*), 6.64 (d, *J* = 4.0 Hz, 1H, H*^{14}*), 6.62 (d, *J* = 4.0 Hz, 1H, H*^{15}*), 6.01 (d, *J* = 4.9 Hz, 1H, H*^{19}*), 4.23 (dt, *J* = 8.2, 4.0 Hz, 1H, H*^{23}*), 4.05 (dd, *J* = 4.8, 4.8 Hz, 2H, H*^{24}*), 3.98 (s, 3H, H*^{1}*), 3.73 (s, 3H, H*^{26}*).**^{13}C NMR** (75 MHz, $CDCl_3$) δ 169.8 (C*^{25}*), 166.7 (C*^{2}*), 162.3 (d, *J* = 243.5 Hz, C*^{30}*), 159.2 (C*^{21}*), 154.1 (C*^{7}*), 141.4 (C*^{13}*), 139.3 (C*^{3}*), 133.9 (C*^{20}*), 133.0 (d, *J* = 7.0 Hz, C*^{28}*), 132.7 (C*^{17}*), 131.1 (C*^{6}*), 130.4 (C*^{5}*), 130.3 (C*$^{9/10}$*), 129.8 (C*^{16}*), 129.8 (C*^{4}*), 125.1 (C*^{11}*), 122.6 (C*^{14}*), 120.3 (C*^{8}*), 119.8 (C*^{9}*), 119.7 (C*^{12}*), 114.1 (d, *J* = 19.2 Hz, C*^{28}*), 110.5 (C*^{15}*), 108.3 (C*^{19}*), 63.5 (C*^{24}*), 58.7 (C*^{23}*), 53.1 (C*^{1}*), 52.5 (C*^{26}*).**^{19}F NMR** (282 MHz, Chloroform-*d*) δ -116.41.**^{11}B NMR** (96 MHz, Chloroform-*d*) δ 2.28. **UV-Vis:** λ_{max} = 584 nm (DCM). Molar extinction coefficient (ε) = 35000 M^{-1} cm^{-1}. **ϕ_F:** 0.06

4.23b:

R_f: 0.2375 (3:2 petrol:ethyl acetate). **Mp**: 152-154°C **IR** (neat): ν_{max}/cm^{-1} 3658 (N-H, /w), 2981 (C-H, s), 1715 (C=O, m). **HRMS:** (ASAP[SOLID]) calcd for $C_{33}H_{27}BFN_3O_6$ [M+H]$^-$: 592.2061, found 592.2067. **^{1}H NMR** (700 MHz, $CDCl_3$) δ 8.18 (d, *J* = 8.5 Hz, 2H, H*^{4}*), 7.71 (d, *J* = 8.0 Hz, 2H, H*^{5}*), 7.51 (m, 1H, H*^{22}*), 7.50 (d, *J* = 8.4 Hz, 1H, H*^{11}*), 7.27 (d, *J* = 3.1 Hz, 2H, H*^{9,10}*), 7.21 (dd, *J* = 8.5, 6.3 Hz, 2H, H*^{28}*), 7.02 (d, *J* = 4.7 Hz, 1H, H*^{19}*), 6.90 (ddd, *J* = 8.2, 8.2, 4.7 Hz, 1H, H*^{8}*), 6.78 (dd, *J* = 8.9, 8.9 Hz, 2H, H*^{29}*), 6.66 (d, *J* = 4.0 Hz, 1H, H*^{15}*), 6.64 (d, *J* = 4.0 Hz, 1H, H*^{14}*), 6.04 (d, *J* = 4.8 Hz, 1H, H*^{20}*), 4.27 (dt, *J* = 7.8, 3.6 Hz, 1H, H*^{23}*), 3.99 (s, 3H, H*^{1}*), 3.90 (s, 3H, H*^{26}*), 3.86 (dd, *J* = 11.6, 3.7 Hz, 1H, H*^{24}*), 3.73 (dd, *J* = 12.3, 3.0 Hz, 1H, H*^{24}*). **^{13}C NMR** (176 MHz,

$CDCl_3$) δ 169.9 (C^{25}), 166.7 (C^{2}), 162.3 (d, *J* = 244.4 Hz, C^{30}), 159.0 (C^{21}), 154.6 (C^{7}), 142.6 (C^{27}), 141.9 (C^{13}), 139.3 (C^{3}), 134.1 (C^{17}), 133.7 (C^{19}), 132.9 (d, *J* = 7.0 Hz, H^{28}), 132.7 (C^{18}), 131.2 (C^{6}), 130.5 ($C^{9/10}$), 129.9 (C^{16}), 129.8 (C^{4}), 125.2 (C^{11}), 123.2 (C^{15}), 120.2 (C^{8}), 119.7 ($C^{9/10}$), 119.6 (C^{12}), 114.4 (d, *J* = 19.3 Hz, C^{29}), 110.8 (C^{14}), 108.0 (C^{20}), 63.5 (C^{24}), 58.6 (C^{23}), 53.4 (C^{26}), 52.6 (C^{1}). **^{19}F NMR** (282 MHz, Chloroform-*d*) δ -115.58. **^{11}B NMR** (96 MHz, Chloroform-*d*) δ 1.30. **UV-Vis:** λ_{max} = 584 nm (DCM). Molar extinction coefficient (ε) = 36000 M^{-1} cm^{-1}. **ϕ_F:** 0.04

6.2.4.15 Methyl (Z)-4-((5-bromo-1H-pyrrol-2-yl)(5-bromo-2H-pyrrol-2-ylidene)methyl)benzoate **2.18a**

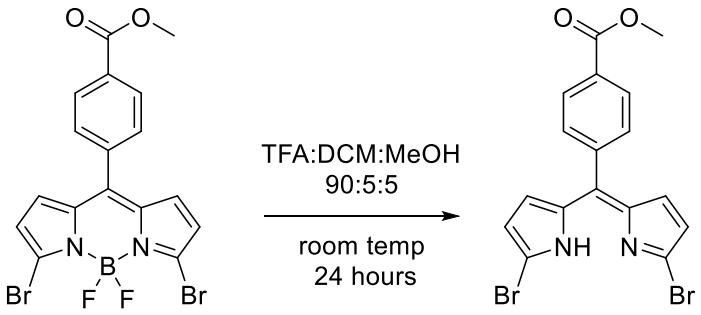

To a 25 mL round bottom flask was added methyl 4-(3,7-dibromo-5,5-difluoro-5H-4λ^4,5λ^4-dipyrrolo[1,2-c:2',1'-f][1,3,2]diazaborinin-10-yl)benzoate (50 mg, 0.103 mmol) and TFA, DCM, MeOH (90:5:5, 9 mL, 0.5 mL, 0.5 mL and was stirred at room temp for 24 hours.. The solvent was then removed under reduced pressure, diluted with DCM (10 mL) and washed with water (3 x 25 mL). The organic layer was dried over $MgSO_4$, filtered and solvent was removed under reduced pressure to afford a red product. The crude product was purified by silica gel column chromatography (DCM) to give methyl (Z)-4-((5-bromo-1*H*-pyrrol-2-yl)(5-bromo-2*H*-pyrrol-2-ylidene)methyl)benzoate (39.4 mg, 0.906 mmol, 88%) was a red solid.

Methyl (Z)-4-((5-bromo-1H-pyrrol-2-yl)(5-bromo-2H-pyrrol-2-ylidene)methyl)benzoate **2.18a**

Analytical data as reported above.

6.2.4.16 Methyl (Z)-4-((5-iodo-1H-pyrrol-2-yl)(5-iodo-2H-pyrrol-2-ylidene)methyl)benzoate **4.28**

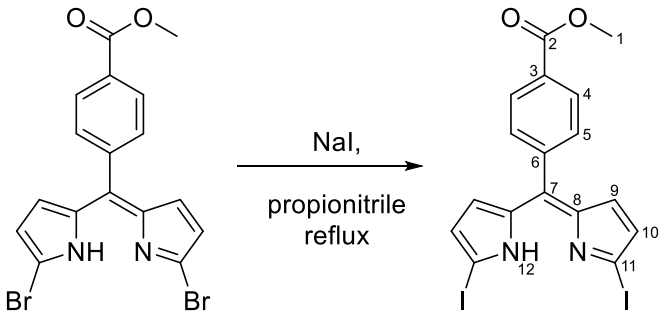

To a 250mL round bottom flask was added methyl (Z)-4-((5-bromo-1H-pyrrol-2-yl)(5-bromo-2H-pyrrol-2-ylidene)methyl)benzoate (4.08 g, 9.4 mmol) and saturated NaI solution (100 mL). The reaction mixture was refluxed for 24 hours then diluted with DCM (150 mL). The organic layer was washed with H_2O (2 x 150 mL), dried over Na_2SO_4, filtered and the solvent was removed under reduced pressure to give a dark red solid. The crude product was purified through silica gel column chromatography (DCM) to give methyl (Z)-4-((5-iodo-1H-pyrrol-2-yl)(5-iodo-2H-pyrrol-2-ylidene)methyl)benzoate (4.60 g, 0.12 mmol, 93%) as a red solid.

R_f: 0.73 (DCM). **Mp:** 123-125 ^oC. **^{1}H NMR** (300 MHz, $CDCl_3$) δ 8.10 (d, *J* = 8.6 Hz, 2H, H*4*), 7.51 (d, *J* = 8.6 Hz, 2H, H*5*), 6.49 (d, *J* = 4.2 Hz, 2H, H*10*), 6.29 (d, *J* = 4.2 Hz, 2H, H*9*), 3.97 (s, 3H). **^{13}C NMR** (75 MHz, $CDCl_3$) δ 166.7 (C*2*), 143.0 (C*8*), 140.2 (C*3*), 136.7 (C*6*), 131.1 (C*7*), 130.8 (C*5*), 123.0 (C*9*), 129.2 (C*4*), 127.5 (C*10*), 101.2 (C*11*), 52.5 (C*1*).

6.2.4.17 Methyl (*Z*)-4-((5-bromo-1H-pyrrol-2-yl)(5-((3-hydroxy-1-methoxy-1-oxopropan-2-yl)amino)-2H-pyrrol-2-ylidene)methyl)benzoate **4.30**

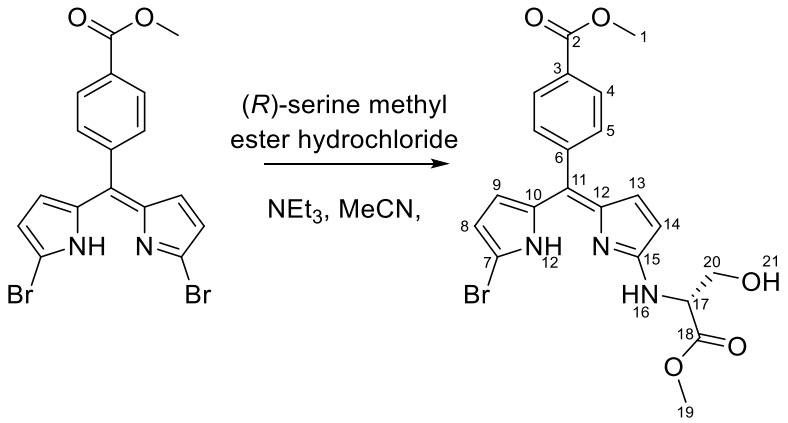

To a 150 mL round bottom flask was added methyl (Z)-4-((5-bromo-1*H*-pyrrol-2-yl)(5-bromo-2*H*-pyrrol-2-ylidene)methyl)benzoate (250 mg, 0.574 mmol), (*R*)-serine methyl ester hydrochloride (178 mg, 1.147 mmol), NEt_3 (176 μL, 1.26 mmol) and MeCN (42.5 mL). The reaction was heated to reflux, stirred for 24 hours and then washed with water (2 x 50 mL). The organic layer was dried over $MgSO_4$, filtered and solvent removed under reduced pressure to give a red/orange product. The crude product was purified by silica plug (flushed with ethyl acetate then collected product with DCM) to give methyl (Z)-4-((5-bromo-1*H*-pyrrol-2-yl)(5-((3-hydroxy-1-methoxy-1-oxopropan-2-yl)amino)-2*H*-pyrrol-2-ylidene)methyl)benzoate (272 mg, 0.574 mmol, 100%) as an red/orange solid.

R_f: 0.36 (Petrol:Ethyl acetate). **Mp:** 156-158 °C. **1H NMR** (300 MHz, CDCl3) δ 7.97 (d, *J* = 8.3 Hz, 2H, H^{4}), 7.38 (d, *J* = 8.2 Hz, 2H, H^{5}), 6.57 (dd, *J* = 4.7, 1.0 Hz, $H^{8/9/13/14}$), 6.14 (dd, *J* = 4.7, 2.4 Hz, $H^{8/9/13/14}$), 6.04 (d, *J* = 3.8 Hz, $H^{8/9/13/14}$), 5.94 (d, *J* = 3.9 Hz, $H^{8/9/13/14}$), 5.86 (t, *J* = 4.0 Hz, $H^{8/9/13/14}$), 4.71 – 4.57 (m, 1H, H^{17}), 4.20 – 3.99 (m, 2H, H^{20}), 3.87 (s, 3H, $H^{1/19}$), 3.80 (s, 3H, $H^{1/19}$).

6.2.4.18 Methyl (*S*)-4-(5,5-difluoro-3-((3-hydroxy-1-methoxy-1-oxopropan-2-yl)amino)-7-(2-hydroxyphenyl)-5*H*-4λ^4,5λ^4-dipyrrolo[1,2-*c*:2',1'-*f*][1,3,2]diazaborinin-10-yl)benzoate **4.35**

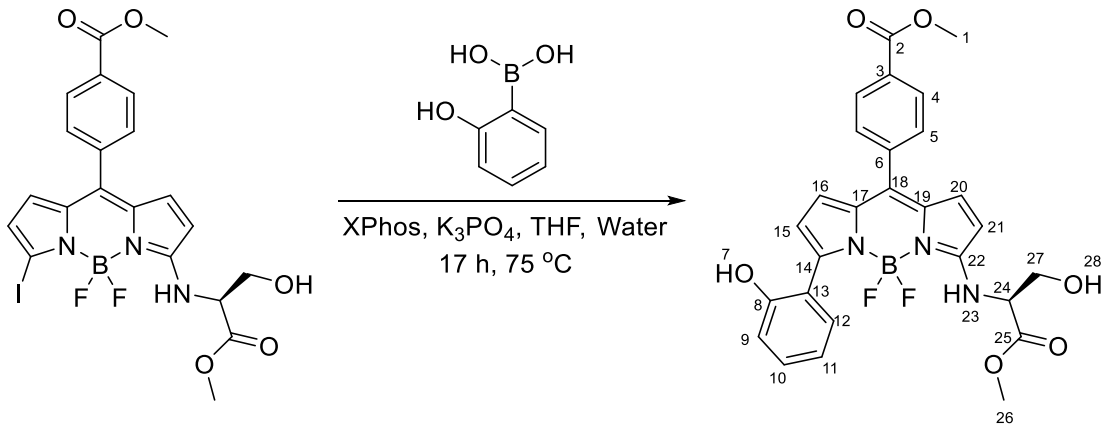

To a 50 mL Schlenk flask was added methyl (S)-4-(5,5-difluoro-3-((3-hydroxy-1-methoxy-1-oxopropan-2-yl)amino)-7-iodo-5*H*-4λ^4,5λ^4-dipyrrolo[1,2-*c*:2',1'-*f*][1,3,2]diazaborinin-10-yl)benzoate (947.1 mg, 1.66 mmol), 2-hydroxyphenyl boronic acid (459.3 mg, 3.33 mmol), XPhos (84.5 mg, 0.1 mmol, 6 mol%), K_3PO_4 (766 mg, 3.32 mmol) and subsequently degassed (x3). Dry THF (8 mL) and water (1.2 mL) were added to the Schlenk flask, degassed (x3) and freeze/thawed (x3). The reaction was heated to 75^{o}C and stirred, under a nitrogen atmosphere, for 1.1 hours. The reaction mixture was diluted with DCM (100 mL) and washed with water (3 x 100 mL), dried over $MgSO_4$, filtered and the solvent was removed under reduced pressure to give methyl (*R*)-4-(5,5-difluoro-3-((3-hydroxy-1-methoxy-1-oxopropan-2-yl)amino)-7-(2-hydroxyphenyl)-5*H*-4λ^4,5λ^4-dipyrrolo[1,2-*c*:2',1'-*f*][1,3,2]diazaborinin-10-yl)benzoate (crude yield: 712.0 mg, 1.33 mmol, 80%) as a red/pink solid.

R_f: 0.69 (Ethyl Acetate). **IR** (neat): ν_{max}/cm^{-1} 3393 (N-H, m, broad), 2961-2953 (C-H, m), 1604 (C=C, s). **Mp:** 106-109^{o}C. **^{1}H NMR** (300 MHz, $CDCl_3$) δ 8.13 (d, *J* = 8.5 Hz, 2H, H^{4}), 7.55 (d, *J* = 8.4 Hz, 2H, H^{5}), 7.48 (d, *J* = 7.6 Hz, 2H), 7.20 (dd, *J* = 8.5, 7.3 Hz, 1H), 6.99 (dd, *J* = 7.6, 2.3 Hz, 4H), 6.90 – 6.77 (m, 4H), 6.48 (d, *J* = 3.8 Hz, 1H), 6.36 (d, *J* = 3.8 Hz, 1H), 6.13 (d, *J* = 5.1 Hz, 1H), 4.33 – 4.00 (m, 2H, H^{27}) 3.97 (s, 3H, H^{1}), 3.74 (s, 3H, H^{26}). **^{13}C NMR** (75 MHz, $CDCl_3$) δ 170.0 (C^{25}), 166.8 (C^{2}), 159.48, 155.77, 152.89, 141.26, 139.06, 134.46, 131.06, 130.5 (C^{5}), 129.81 – 129.58 (m), (C^{4}), 115.38, 63.4 (C^{27}) 53.6 (C^{26}), 53.39, 52.6 (C^{1}), 31.08, 30.43. **^{11}B**

NMR: ^{11}B NMR (96 MHz, $CDCl_3$) δ 1.14 (t, *J* = 35.2 Hz). **^{19}F NMR:** ^{19}F NMR (282 MHz, $CDCl_3$) δ -62.69. **UV-Vis:** λ_{max} = 579 nm (DCM). **Molar extinction coefficient (ε)** = 23000 $M^{-1}\,cm^{-1}$.

6.2.4.19 Methyl (*S,Z*)-4-((5-((3-hydroxy-1-methoxy-1-oxopropan-2-yl)amino)-2*H*-pyrrol-2-ylidene)(5-(2-hydroxyphenyl)-*1H*-pyrrol-2-yl)methyl)benzoate **4.36**

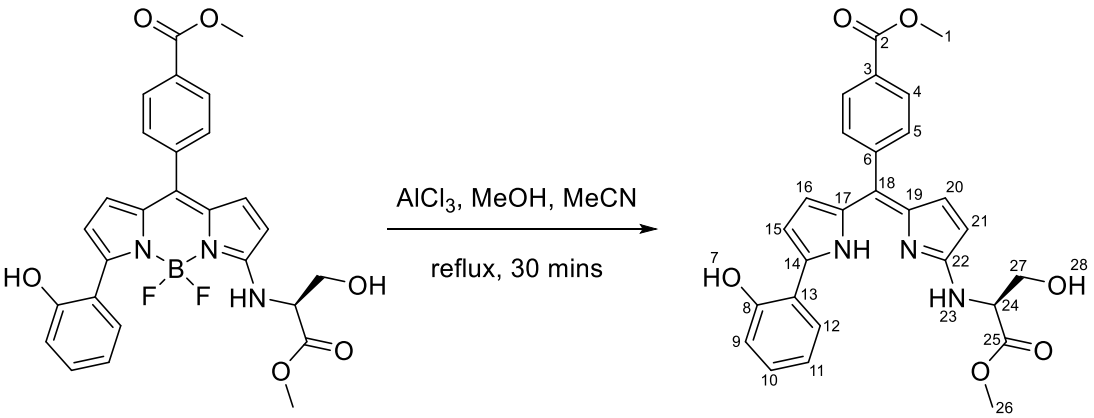

To a 500 mL round bottom flask was added methyl 4-(5,5-difluoro-3-((3-hydroxy-1-methoxy-1-oxopropan-2-yl)amino)-7-(2-hydroxyphenyl)-5*H*-4λ^4,5λ^4-dipyrrolo[1,2-*c*:2',1'-*f*][1,3,2]diazaborinin-10-yl)benzoate (1.4874 g, 2.8 mmol), MeCN (275 mL) and [108] (1.85 g, 13.89 mmol) dissolved in MeOH (55 mL). The reaction was heated to reflux, stirred for 30 mins, diluted with DCM and washed with water (3 x 200 mL). The organic layer was dried over $MgSO_4$, filtered and solvent was removed under reduced pressure to give a red/brown product. The crude product was purified by silica gel column chromatography (98:2, DCM:Methanol) to give methyl (Z)-4-((5-((3-hydroxy-1-methoxy-1-oxopropan-2-yl)amino)-2*H*-pyrrol-2-ylidene)(5-(2-hydroxyphenyl)-1*H*-pyrrol-2-yl)methyl)benzoate (678 mg, 1.39 mmol, 50%) as a red/brown solid.

R_f: 0.12 (98:2, DCM:Methanol). **Mp:** 99-102 ^oC. **IR** (neat): ν_{max}/cm^{-1} 3358 (O-H, m), 2981 (C-H, s), 1716 (C=O, w). **HRMS:** (ESI+) calcd for $C_{27}H_{25}N_3O_6$ $[M+H]^+$: 488.1816, found 488.1847. **^{1}H NMR** (300 MHz, Methanol-d_4) δ 8.07 (d, *J* = 8.3 Hz, 2H, H*[4]*), 7.61 (dd, *J* = 7.8, 1.6 Hz, 1H, H*[9]*), 7.52 (d, *J* = 8.3 Hz, 2H, H*[5]*), 7.09 (ddd, *J* = 8.7, 7.2, 1.6 Hz, 1H, H*[11]*), 6.94 (dd, *J* = 8.2, 1.2 Hz, 1H, H*[12]*), 6.89 (ddd, *J* = 8.3, 7.2, 1.3 Hz, 1H, H*[10]*), 6.61 (d, *J* = 3.0 Hz, 1H, H*[20]*), 6.59 (d, *J* = 2.3 Hz, 1H, H*[15]*), 6.33 (d, *J* = 4.6 Hz, 1H, H*[21]*), 5.97 (d, *J* = 3.9 Hz, 1H, H*[16]*), 5.02 (t, *J* = 4.4 Hz, 1H, H*[24]*), 4.08 (dd, *J* = 4.3, 3.0 Hz, 2H, H*[27]*), 3.94 (s, 3H, H*[1]*), 3.72 (s, 3H, H*[26]*). **^{13}C NMR** (75 MHz, Methanol-d_4) δ 173.7 (C*[25]*), 168.4 (C*[2]*), 168.2 (C*[22]*), 154.7 (C*[8]*), 148.5 (C*[19]*), 145.1 (C*[6]*), 137.7 (C*[20]*), 136.0 (C*[14]*), 133.5 (C*[18]*), 132.4 (C*[5]*), 130.6 (C*[3]*), 129.8 (C*[4]*), 128.6

(C[11]), 127.9 (C[9]), 127.7 (C[17]), 121.2 (C[10]), 120.3 (C[21]), 120.3 (C[13]) 117.5 (C[12]), 117.3 (C[16]), 109.3 (C[15]), 63.4 (C[27]), 58.8 (C[24]), 52.8 (C[26]), 52.7 (C[1]).

6.2.4.20 Methyl (*S*)-4-(10b-(4-fluorophenyl)-10-((3-hydroxy-1-methoxy-1-oxopropan-2-yl)amino)-10b*H*-11-oxa-4b1,10aλ^4-diaza-10bλ^4-boracyclopenta[e]aceanthrylen-7-yl)benzoate **4.37a** and **4.37b**

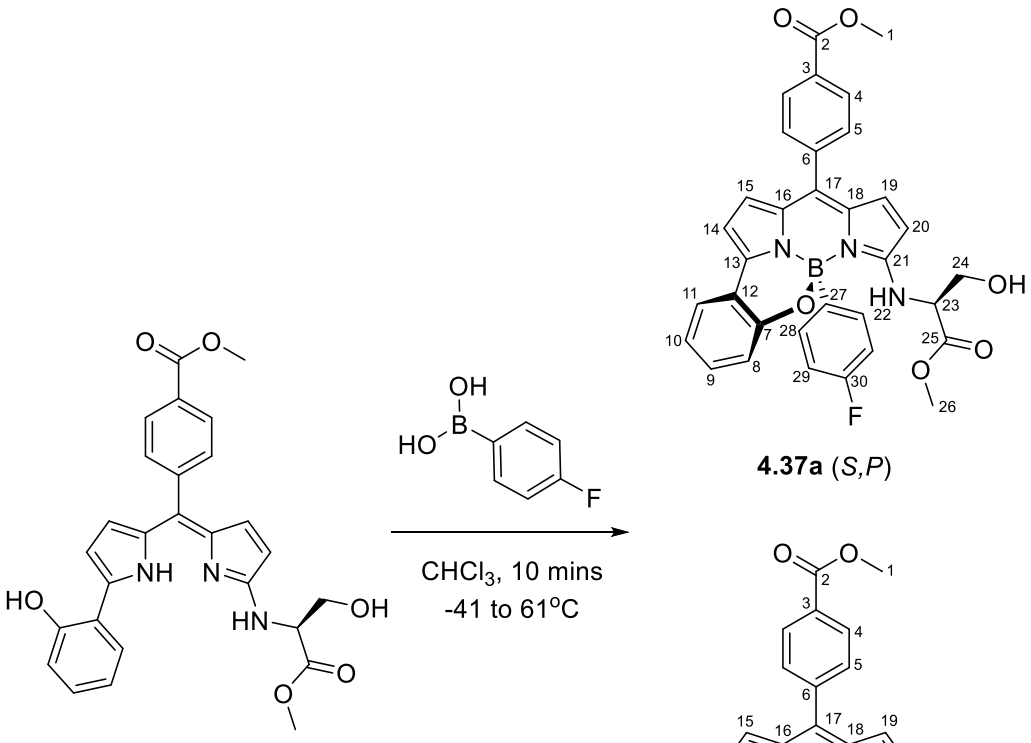

4.37a (*S,P*)

4.37b (*S,M*)

To a 50mL round bottom flask was added methyl (Z)-4-((5-((3-hydroxy-1-methoxy-1-oxopropan-2-yl)amino)-2*H*-pyrrol-2-ylidene)(5-(2-hydroxyphenyl)-1*H*-pyrrol-2-yl)methyl)benzoate (48.8 mg, 0.1 mmol) and $CHCl_3$ (20 mL). The reaction mixture was equilibrated at the desired reaction temperature, stirred for 30 mins and flushed with N_2 (see table X). 4-fluorphenyl boronic acid (21.0 mg, 0.15 mmol) was dissolved in $CHCl_3$ (5 mL) and was added dropwise to the reaction mixture over 5 mins. The crude mixture was washed with water (3 x 50 mL), dried over $MgSO_4$, filtered and the solvent was removed under reduced pressure to give a purple product. The crude product was purified by silica gel column chromatograpy (49:1, DCM:Methanol) to give:

4.37a:

Mp: 151-153°C. **Rf:** 0.39. **^{1}H NMR** (300 MHz, $CDCl_3$) δ 8.16 (d, *J* = 8.5 Hz, 2H, H^{4}), 7.67 (d, *J* = 8.5 Hz, 2H, H^{5}), 7.52 – 7.41 (m, 2H, $H^{11,22}$), 7.25 – 7.18 (m, 4H, $H^{9,10,28}$), 6.94 (d, *J* = 4.7 Hz, 1H, H^{20}), 6.88 (ddd, *J* = 8.1, 4.9, 3.5 Hz, 1H, H^{8}), 6.64 (d, *J* = 4.0 Hz, 1H, H^{14}), 6.62 (d, *J* = 4.0 Hz, 1H, H^{15}), 6.01 (d, *J* = 4.9 Hz, 1H, H^{19}), 4.23 (dt, *J* = 8.2, 4.0 Hz, 1H, H^{23}), 4.05 (dd, *J* = 4.8, 4.8 Hz, 2H, H^{24}), 3.98 (s, 3H, H^{1}), 3.73 (s, 3H, H^{26}).**^{13}C NMR** (75 MHz, $CDCl_3$) δ 169.8 (C^{25}), 166.7 (C^{2}), 162.3 (d, *J* = 243.5 Hz, C^{30}), 159.2 (C^{21}), 154.1 (C^{7}), 141.4 (C^{13}), 139.3 (C^{3}), 133.9 (C^{20}), 133.0 (d, *J* = 7.0 Hz, C^{28}), 132.7 (C^{17}), 131.1 (C^{6}), 130.4 (C^{5}), 130.3 ($C^{9/10}$), 129.8 (C^{16}), 129.8 (C^{4}), 125.1 (C^{11}), 122.6 (C^{14}), 120.3 (C^{8}), 119.8 (C^{9}), 119.7 (C^{12}), 114.1 (d, *J* = 19.2 Hz, C^{28}), 110.5 (C^{15}), 108.3 (C^{19}), 63.5 (C^{24}), 58.7 (C^{23}), 53.1 (C^{1}), 52.5 (C^{26}).**^{19}F NMR** (282 MHz, Chloroform-*d*) δ -116.41.**^{11}B NMR** (96 MHz, Chloroform-*d*) δ 2.05. **IR** (neat): ν_{max}/cm^{-1} 3658 (O-H, m), 3496 (N-H, w) 2980 (C-H, s), 1716 (C=O, w). **UV-Vis:** λ_{max} = 579 nm (DCM). Molar extinction coefficient (ε) = 19000 M^{-1} cm^{-1}. **ϕ_F:** 0.02 (EtOH).

4.37b:

Mp: 151-154°C. **Rf:** 0.40. **HRMS:** (ESI+) calcd for $C_{33}H_{27}BFN_3O_6$ $[M+H]^+$: 592.2050, found 592.2052. **^{1}H NMR** (700 MHz, $CDCl_3$) δ 8.18 (d, *J* = 8.5 Hz, 2H, H^{4}), 7.71 (d, *J* = 8.0 Hz, 2H, H^{5}), 7.51 (m, 1H, H^{22}), 7.50 (d, *J* = 8.4 Hz, 1H, H^{11}), 7.27 (d, *J* = 3.1 Hz, 2H, $H^{9,10}$), 7.21 (dd, *J* = 8.5, 6.3 Hz, 2H, H^{28}), 7.02 (d, *J* = 4.7 Hz, 1H, H^{19}), 6.90 (ddd, *J* = 8.2, 8.2, 4.7 Hz, 1H, H^{8}), 6.78 (dd, *J* = 8.9, 8.9 Hz, 2H, H^{29}), 6.66 (d, *J* = 4.0 Hz, 1H, H^{15}), 6.64 (d, *J* = 4.0 Hz, 1H, H^{14}), 6.04 (d, *J* = 4.8 Hz, 1H, H^{20}), 4.27 (dt, *J* = 7.8, 3.6 Hz, 1H, H^{23}), 3.99 (s, 3H, H^{1}), 3.90 (s, 3H, H^{26}), 3.86 (dd, *J* = 11.6, 3.7 Hz, 1H, H^{24}), 3.73 (dd, *J* = 12.3, 3.0 Hz, 1H, H^{24}). **^{13}C NMR** (176 MHz, $CDCl_3$) δ 169.9 (C^{25}), 166.7 (C^{2}), 162.3 (d, *J* = 244.4 Hz, C^{30}), 159.0 (C^{21}), 154.6 (C^{7}), 142.6 (C^{27}), 141.9 (C^{13}), 139.3 (C^{3}), 134.1 (C^{17}), 133.7 (C^{19}), 132.9 (d, *J* = 7.0 Hz, H^{28}), 132.7 (C^{18}), 131.2 (C^{6}), 130.5 ($C^{9/10}$), 129.9 (C^{16}), 129.8 (C^{4}), 125.2 (C^{11}), 123.2 (C^{15}), 120.2 (C^{8}), 119.7 ($C^{9/10}$), 119.6 (C^{12}), 114.4 (d, *J* = 19.3 Hz, C^{29}), 110.8 (C^{14}), 108.0 (C^{20}), 63.5 (C^{24}), 58.6 (C^{23}), 53.4 (C^{26}), 52.6 (C^{1}). **^{19}F NMR** (282 MHz, Chloroform-*d*) δ -115.58. **^{11}B NMR** (96 MHz, Chloroform-*d*) δ 1.30. **IR** (neat): ν_{max}/cm^{-1} 3658 (O-H, m), 3339 (N-H, w) 2981-2972 (C-H, s), 1722 (C=O, w). **UV-Vis:** λ_{max} = 579 nm (DCM). Molar extinction coefficient (ε) = 28000 M^{-1} cm^{-1}. **ϕ_F:** 0.03 (EtOH)

Temperature/^{oC}	Yield/%	*de* before column	*de* after purification
-41	92	57	49
0	87	70	55
RT (25)	75	84	81
35	73	83	84
45	78	82	77
55	72	77	69
reflux	79	66	57

6.3 Photophysical and Chiroptical Measurements

6.3.1 Normalised UV/Vis Absorption and Emission Spectra

6.3.1.1 Methyl 4-(3,7-dichloro-5,5-difluoro-5*H*-4λ^4,5λ^4-dipyrrolo[1,2-*c*:2',1'-*f*][1,3,2]diazaborinin-10-yl)benzoate **2.13a**

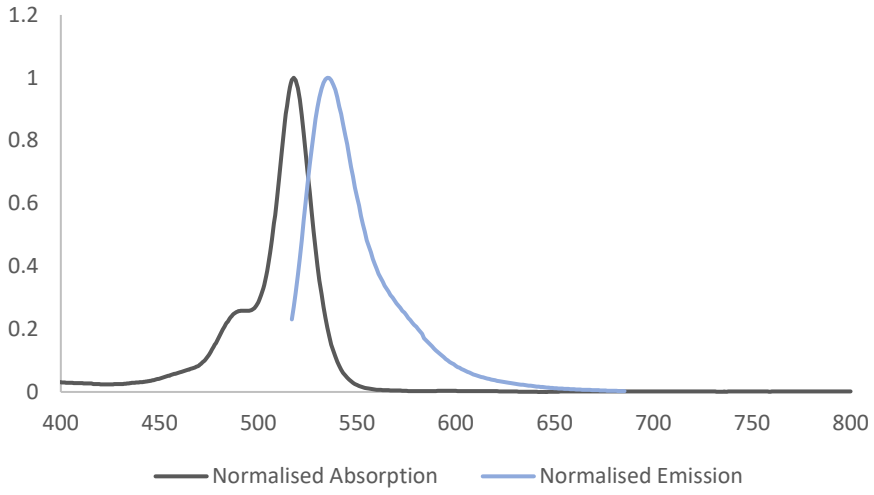

Figure 6.1. Normalised emission and absorption spectra of BODIPY **2.13a** from the fluorescence and UV-vis spectra respectively, run in DCM.

6.3.1.2 3,7-Dichloro-5,5-difluoro-10-(3-nitrophenyl)-5H-4λ^4,5λ^4-dipyrrolo[1,2-*c*:2',1'-f][1,3,2]diazaborinine **2.13b**

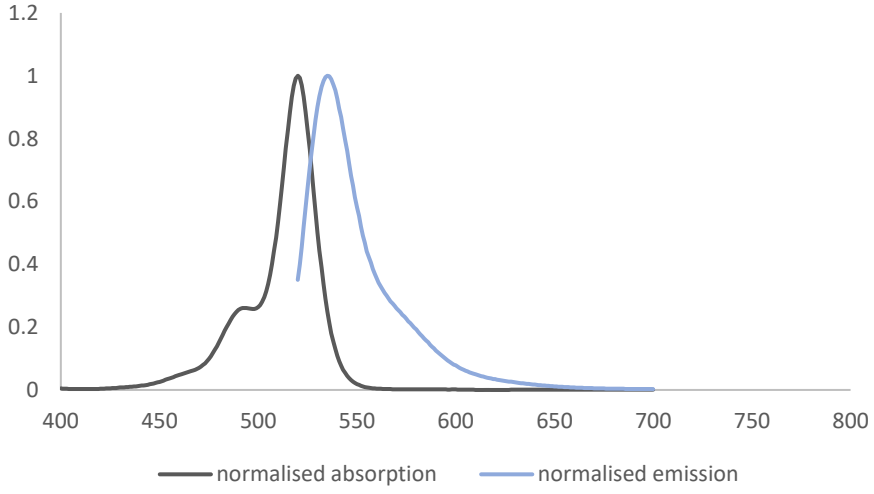

Figure 6.2. Normalised emission and absorption spectra of BODIPY **2.13b** from the fluorescence and UV-vis spectra respectively, run in DCM.

6.3.1.3 3,7-Dichloro-5,5-difluoro-10-(4-nitrophenyl)-5H-4λ^4,5λ^4-dipyrrolo[1,2-*c*:2',1'-*f*][1,3,2]diazaborinine **2.13e**

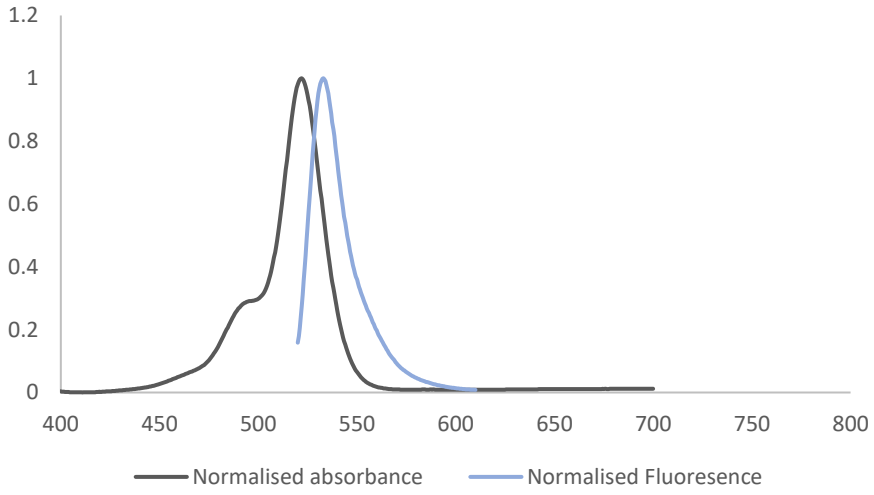

Figure 6.3. Normalised emission and absorption spectra of BODIPY **2.13e** from the fluorescence and UV-vis spectra respectively, run in DCM.

6.3.1.4 3,7-Dichloro-5,5-difluoro-10-(4-methoxyphenyl)-5H-4λ^4,5λ^4-dipyrrolo[1,2-*c*:2',1'-*f*][1,3,2]diazaborinine **2.13c**

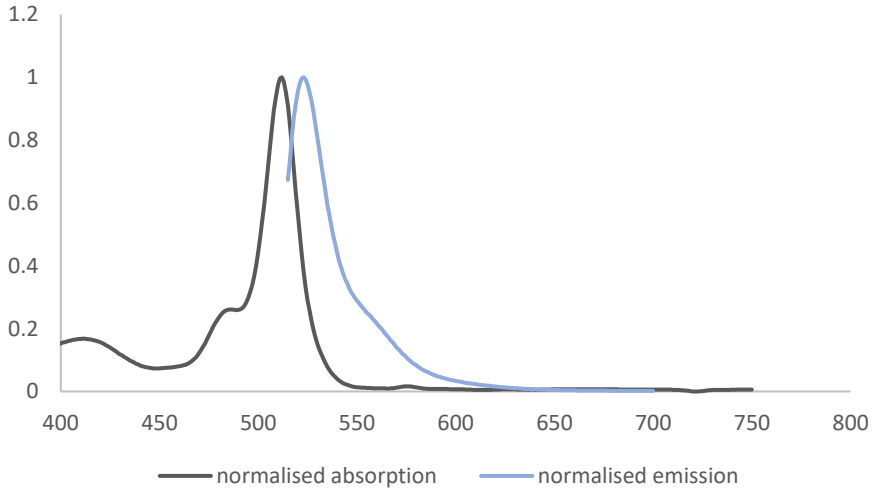

Figure 6.4. Normalised emission and absorption spectra of BODIPY **2.13c** from the fluorescence and UV-vis spectra respectively, run in DCM.

6.3.1.5 3,7-Dichloro-5,5-difluoro-10-(3-methoxyphenyl)-5H-4λ^4,5λ^4-dipyrrolo[1,2-*c*:2',1'-*f*][1,3,2]diazaborinine **2.13d**

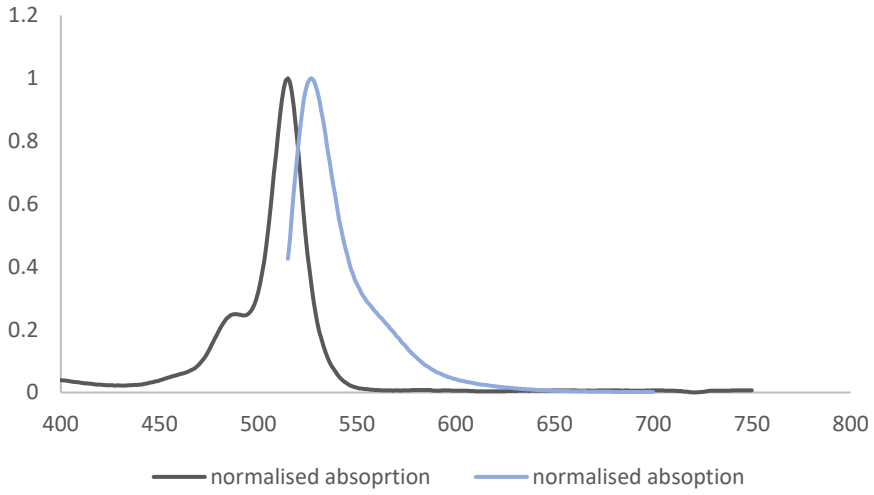

Figure 6.5. Normalised emission and absorption spectra of BODIPY **2.13d** from the fluorescence and UV-vis spectra respectively run in DCM.

6.3.1.6 3,7-Dichloro-5,5-difluoro-10-(*o*-tolyl)-5H-4λ^4,5λ^4-dipyrrolo[1,2-*c*:2',1'-*f*][1,3,2]diazaborinine **2.13f**

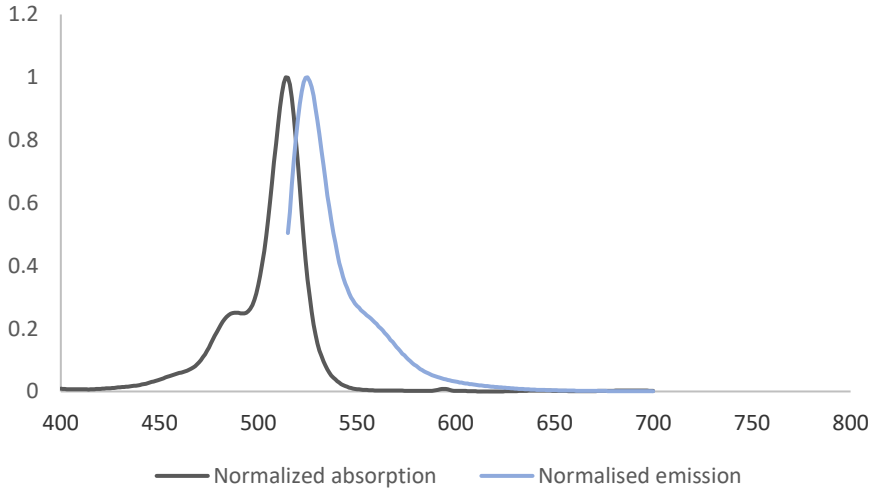

Figure 6.6. Normalised emission and absorption spectra of BODIPY **2.13f** from the fluorescence and UV-vis spectra respectively, run in DCM.

6.3.1.7 Methyl 4-(3,7-dibromo-5,5-difluoro-5*H*-4λ^4,5λ^4-dipyrrolo[1,2-c:2',1'-f][1,3,2]diazaborinin-10-yl)benzoate **2.14a**

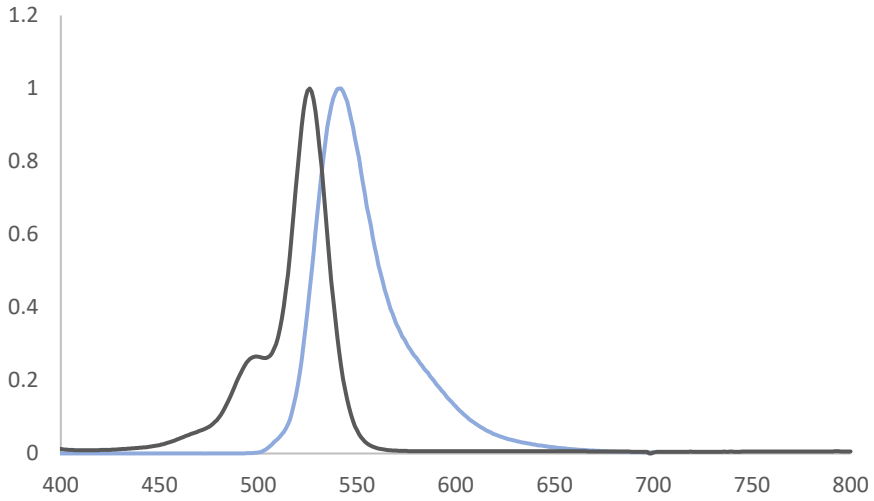

Figure 6.7. Normalised emission and absorption spectra of BODIPY **2.14a** from the fluorescence and UV-vis spectra respectively run in DCM.

6.3.1.8 3,7-Dibromo-5,5-difluoro-10-(4-methoxyphenyl)-5*H*-4λ^4,5λ^4-dipyrrolo[1,2-*c*:2',1'-*f*][1,3,2]diazaborinine **2.14c**

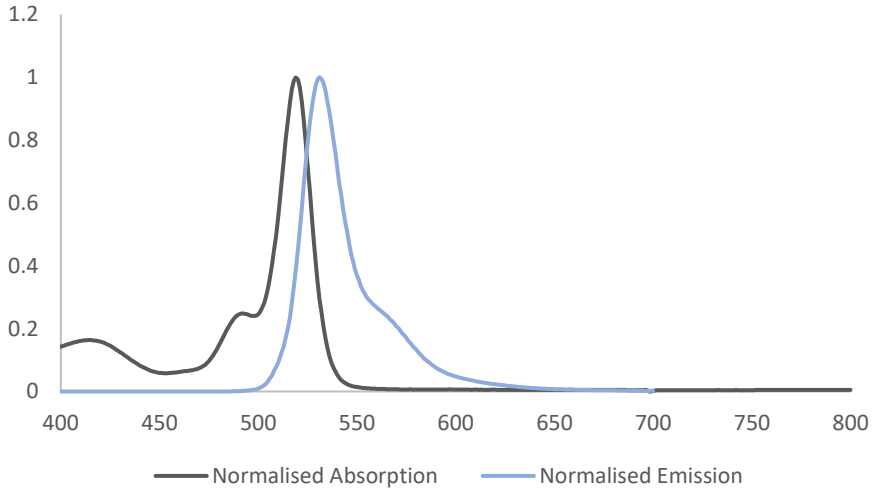

Figure 6.8. Normalised emission and absorption spectra of BODIPY **2.14c** from the fluorescence and UV-vis spectra respectively run in DCM.

6.3.1.9 Methyl 4-(5,5-difluoro-3,7-diiodo-5*H*-4λ^4,5λ^4-dipyrrolo[1,2-*c*:2',1'-*f*][1,3,2]diazaborinin-10-yl)benzoate **3.17a**

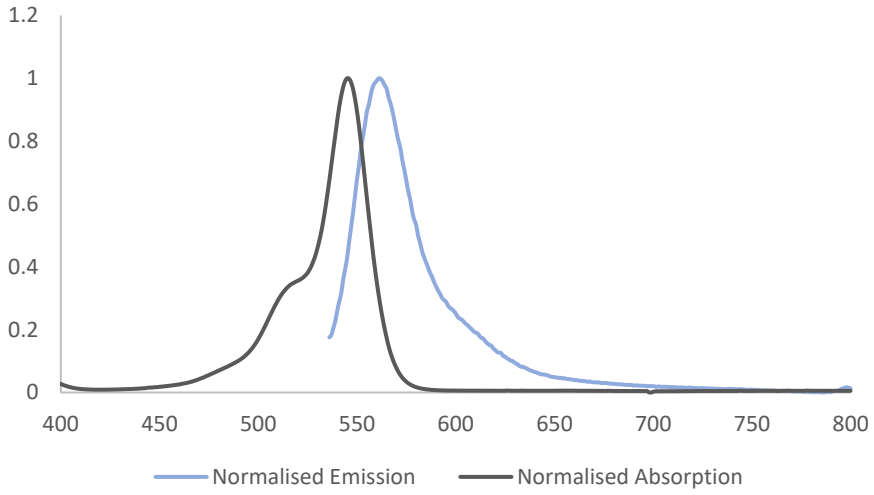

Figure 6.9. Normalised emission and absorption spectra of BODIPY **3.17a** from the fluorescence and UV-vis spectra respectively, run in DCM.

6.3.1.10 5,5-Difluoro-3,7-diiodo-10-(3-nitrophenyl)-5*H*-4λ^4,5λ^4-dipyrrolo[1,2-*c*:2',1'-*f*][1,3,2]diazaborinine **3.17b**

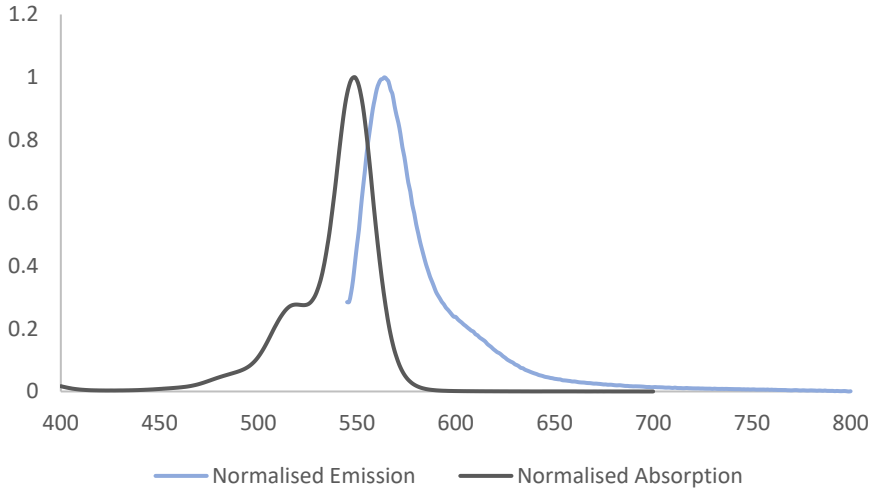

Figure 6.10. Normalised emission and absorption spectra of BODIPY **3.17b** from the fluorescence and UV-vis spectra respectively, run in DCM.

6.3.1.11 5,5-Difluoro-3,7-diiodo-10-(4-methoxyphenyl)-5*H*-4λ^4,5λ^4-dipyrrolo[1,2-*c*:2',1'-*f*][1,3,2]diazaborinine **3.17c**

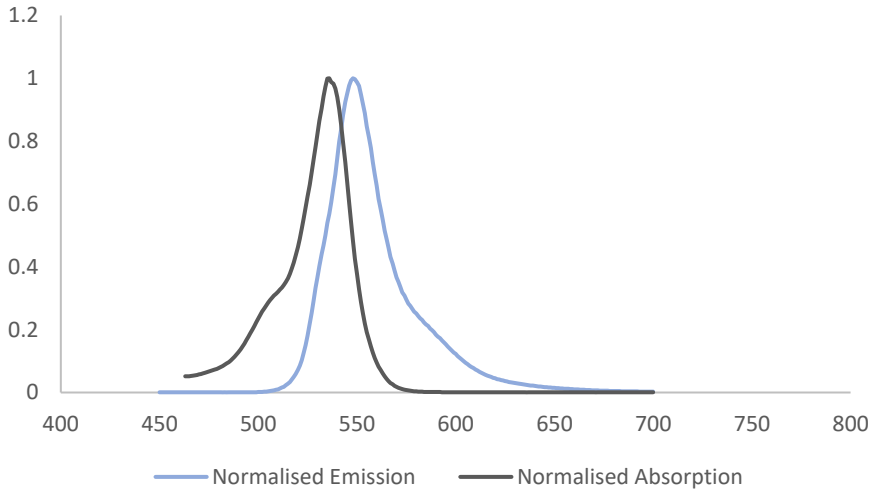

Figure 6.11. Normalised emission and absorption spectra of BODIPY **3.17c** from the fluorescence and UV-vis spectra respectively, run in DCM.

6.3.1.12 5,5-Difluoro-3,7-diiodo-10-(3-methoxyphenyl)-5*H*-4λ^4,5λ^4-dipyrrolo[1,2-*c*:2',1'-*f*][1,3,2]diazaborinine **3.17d**

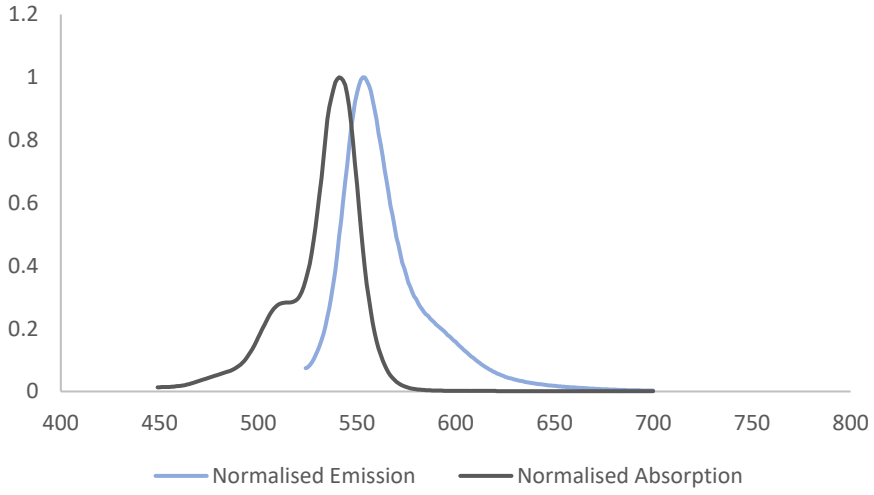

Figure 6.12. Normalised emission and absorption spectra of BODIPY **3.17d** from the fluorescence and UV-vis spectra respectively, run in DCM.

6.3.1.13 Methyl 4-(5,5-difluoro-3,7-diphenyl-5*H*-4λ^4,5λ^4-dipyrrolo[1,2-*c*:2',1'-*f*][1,3,2]diazaborinin-10-yl)benzoate **3.21**

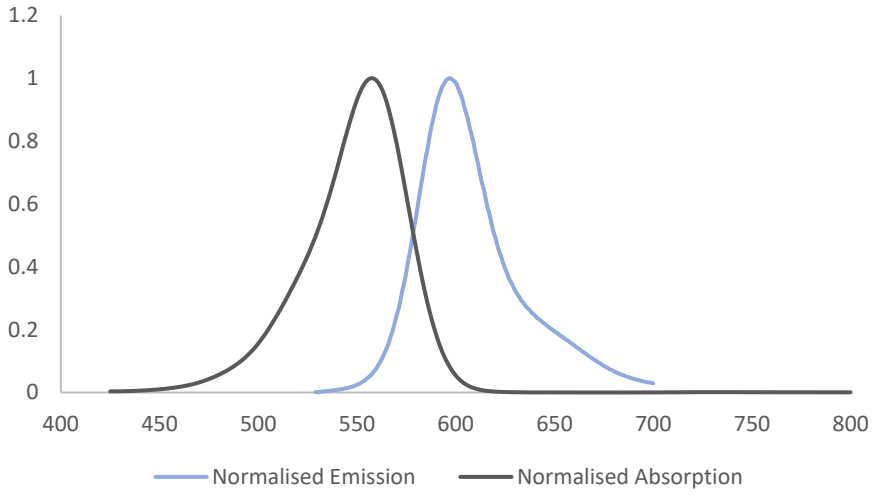

Figure 6.13. Normalised emission and absorption spectra of BODIPY **3.21** from the fluorescence and UV-vis spectra respectively, run in DCM.

6.3.1.14 Methyl 4-(3-butyl-5,5-difluoro-7-phenyl-5*H*-5λ4,6λ4-dipyrrolo[1,2-*c*:2',1'-*f*][1,3,2]diazaborinin-10-yl)benzoate **3.22**

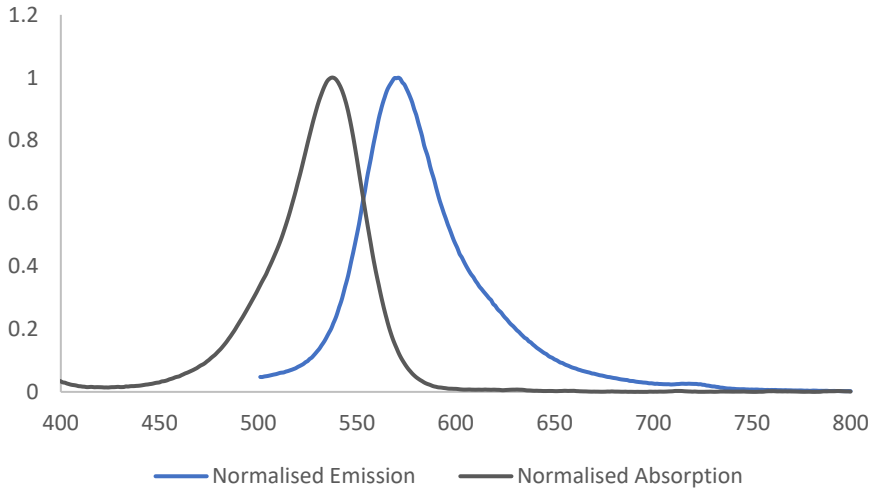

Figure 6.14. Normalised emission and absorption spectra of BODIPY **3.22** from the fluorescence and UV-vis spectra respectively, run in DCM.

6.3.1.15 Methyl 4-(5,5-difluoro-3,7-di((*E*)-styryl)-5H-4λ^4,5λ^4-dipyrrolo[1,2-*c*:2',1'-*f*][1,3,2]diazaborinin-10-yl)benzoate **3.25**

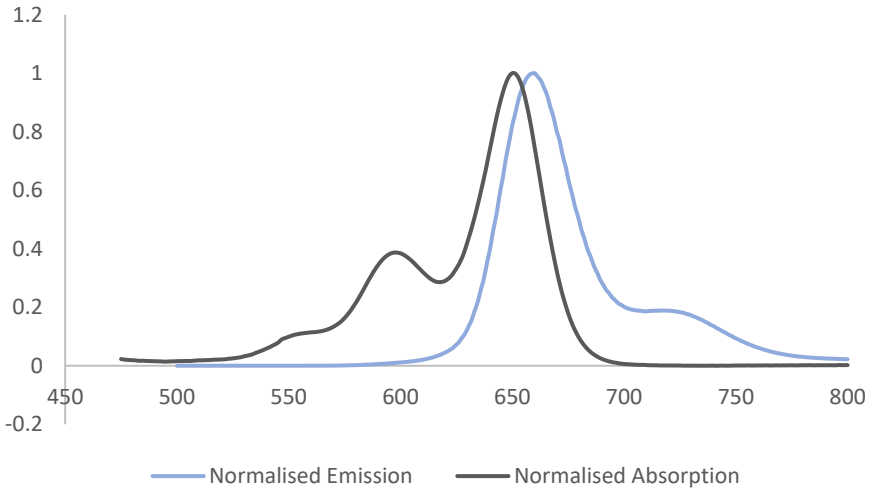

Figure 6.15. Normalised emission and absorption spectra of BODIPY **3.25** from the fluorescence and UV-vis spectra respectively, run in DCM.

6.3.1.16 Methyl 4-(5,5-difluoro-3,7-bis(phenylethynyl)-5*H*-4λ^4,5λ^4-dipyrrolo[1,2-*c*:2',1'-*f*][1,3,2]diazaborinin-10-yl)benzoate **3.28**

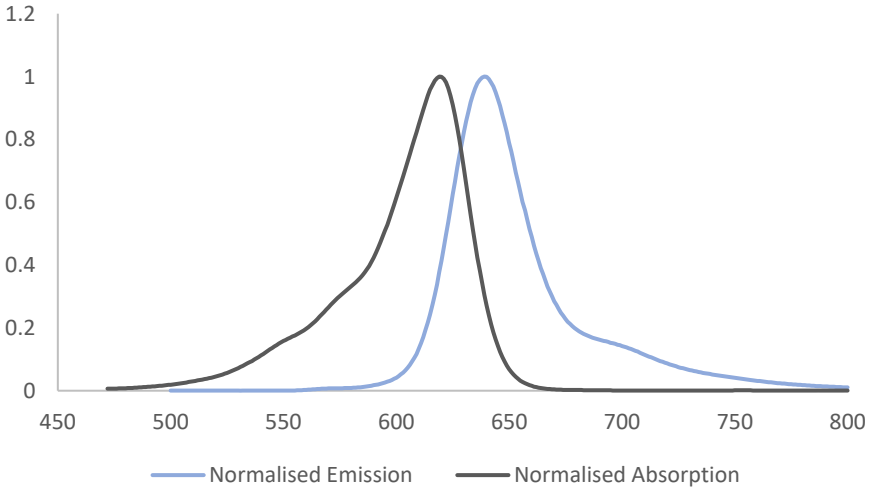

Figure 6.16. Normalised emission and absorption spectra of BODIPY **3.28** from the fluorescence and UV-vis spectra respectively, run in DCM.

6.3.1.17 Methyl 4-(3-chloro-5,5-difluoro-7-(phenylethynyl)-5*H*-4λ4,5λ4-dipyrrolo[1,2-*c*:2',1'-*f*][1,3,2]diazaborinin-10-yl)benzoate **3.29**

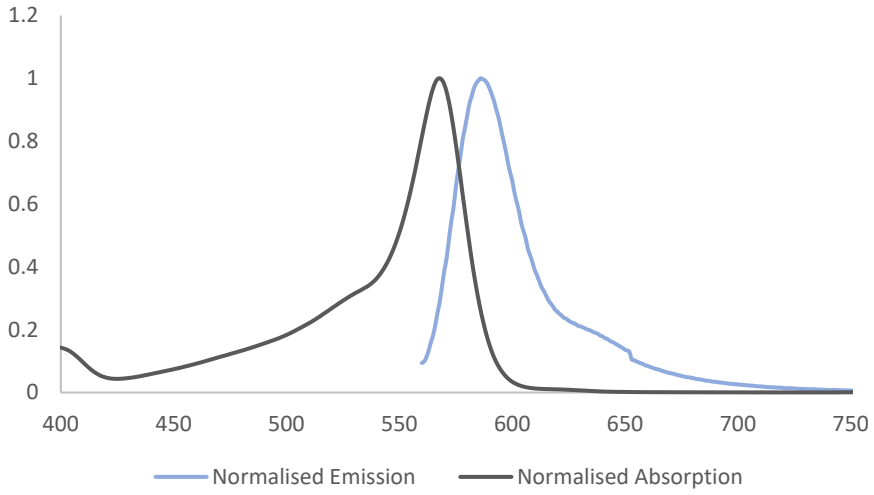

Figure 6.17. Normalised emission and absorption spectra of BODIPY **3.29** from the fluorescence and UV-vis spectra respectively, run in DCM.

6.3.1.18 Methyl 4-(3-chloro-5,5-difluoro-7-phenyl-5*H*-5λ^4,6λ^4-dipyrrolo[1,2-*c*:2',1'-*f*][1,3,2]diazaborinin-10-yl)benzoate **3.38**

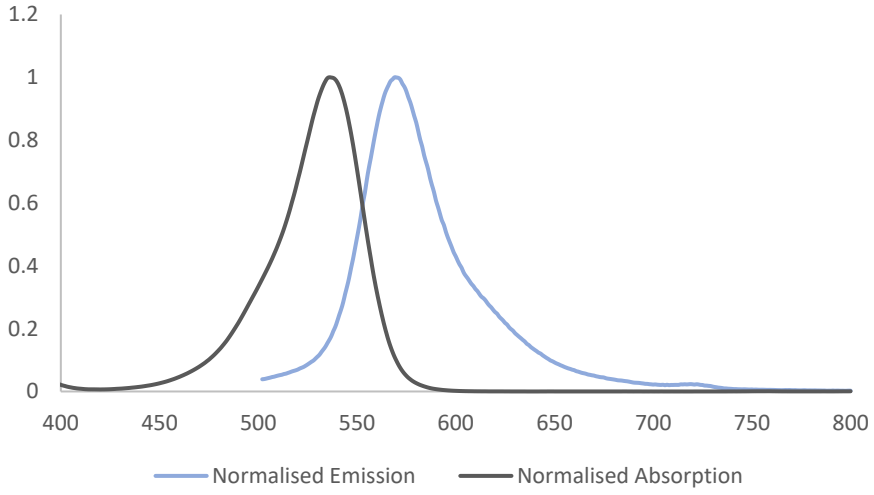

Figure 6.18. Normalised emission and absorption spectra of BODIPY 9 from the fluorescence and UV-vis spectra respectively, run in DCM.

6.3.1.19 Methyl 4-(10b-(4-fluorophenyl)-10-((3-hydroxy-1-methoxy-1-oxopropan-2-yl)amino)-10b*H*-11-oxa-4b1,10aλ^4-diaza-10bλ^4-boracyclopenta[e]aceanthrylen-7-yl)benzoate **4.23a**

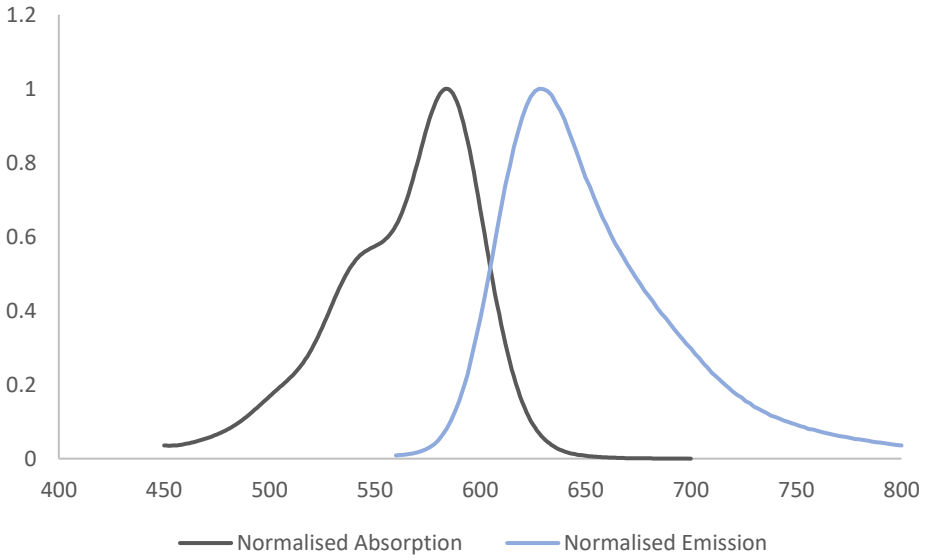

Figure 6.19. Normalised emission and absorption spectra of BODIPY **4.23a** from the fluorescence and UV-vis spectra respectively, run in DCM.

6.3.1.20 Methyl 4-(10b-(4-fluorophenyl)-10-((3-hydroxy-1-methoxy-1-oxopropan-2-yl)amino)-10b*H*-11-oxa-4b1,10aλ^4-diaza-10bλ^4-boracyclopenta[e]aceanthrylen-7-yl)benzoate **4.23b**

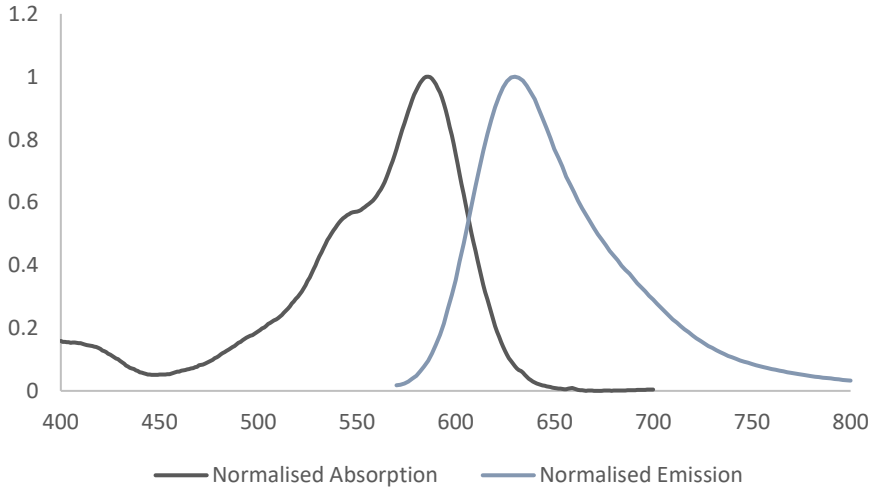

Figure 6.20. Normalised emission and absorption spectra of BODIPY **4.23b** from the fluorescence and UV-vis spectra respectively, run in DCM.

6.3.1.21 Methyl 4-(10b-(4-fluorophenyl)-10-((3-hydroxy-1-methoxy-1-oxopropan-2-yl)amino)-10b*H*-11-oxa-4b1,10aλ^4-diaza-10bλ^4-boracyclopenta[e]aceanthrylen-7-yl)benzoate **4.37a**

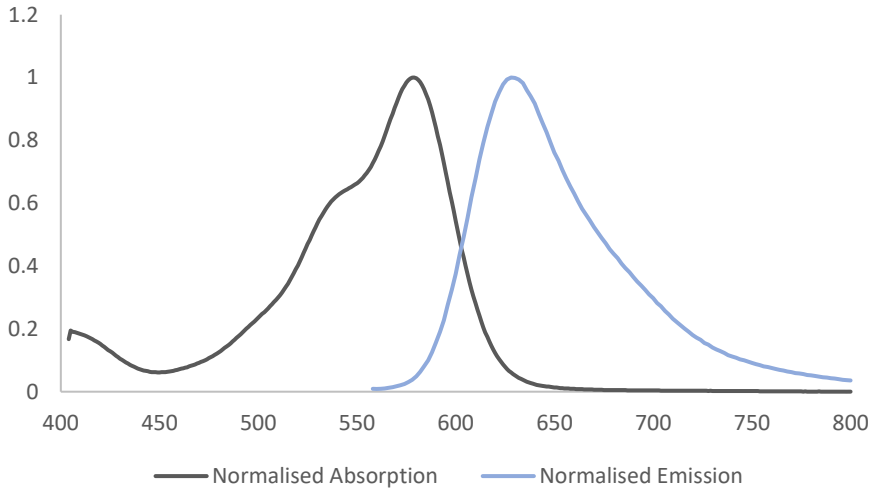

Figure 6.21. Normalised emission and absorption spectra of BODIPY **4.37a** from the fluorescence and UV-vis spectra respectively, run in DCM.

6.3.1.22 Methyl 4-(10b-(4-fluorophenyl)-10-((3-hydroxy-1-methoxy-1-oxopropan-2-yl)amino)-10b*H*-11-oxa-4b1,10aλ^4-diaza-10bλ^4-boracyclopenta[e]aceanthrylen-7-yl)benzoate **4.37b**

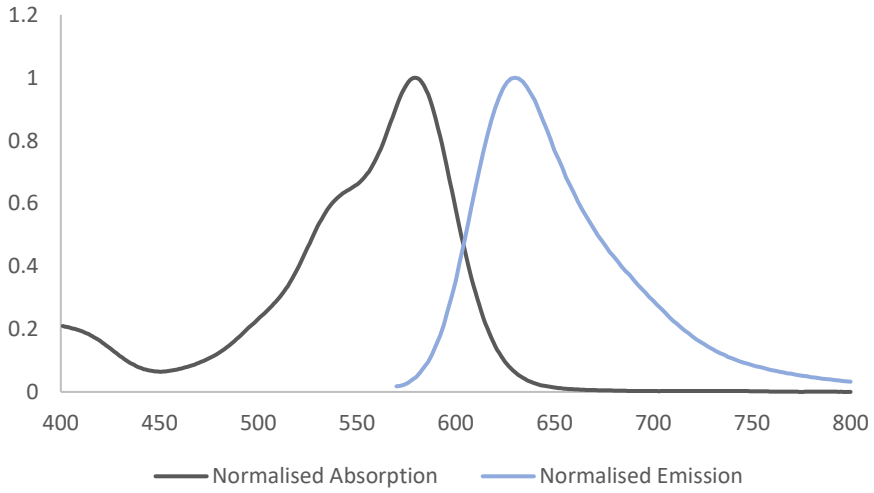

Figure 6.22. Normalised emission and absorption spectra of BODIPY **4.37b** from the fluorescence and UV-vis spectra respectively, run in DCM.

6.3.2 UV/Vis absorption spectra and extinction coefficient measurements

6.3.2.1 Methyl 4-(3,7-dichloro-5,5-difluoro-5*H*-4λ^4,5λ^4-dipyrrolo[1,2-*c*:2',1'-*f*][1,3,2]diazaborinin-10-yl)benzoate **2.13a**

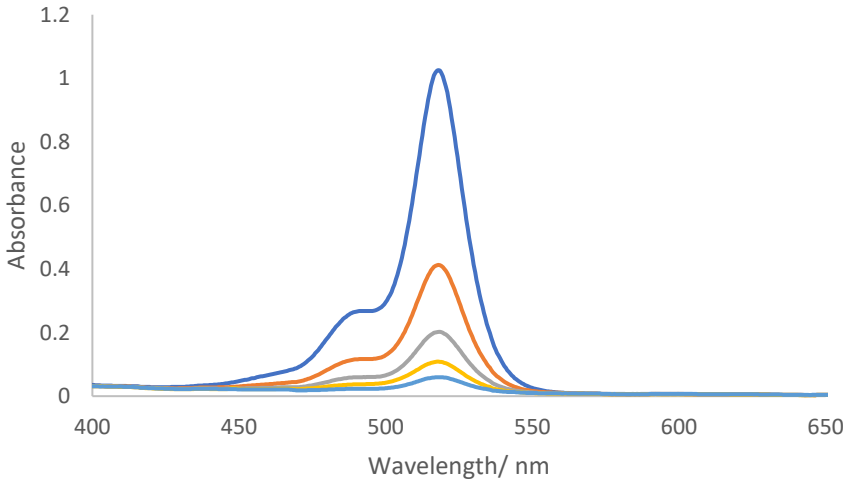

Figure 6.23. UV-Vis spectrum of BODIPY **2.13a**, concentrations (M): 2.53x10^{-5}, 7.60x10^{-6}, 3.80x10^{-6}, 1.90x10^{-6}, 9.50x10^{-7} respectively.

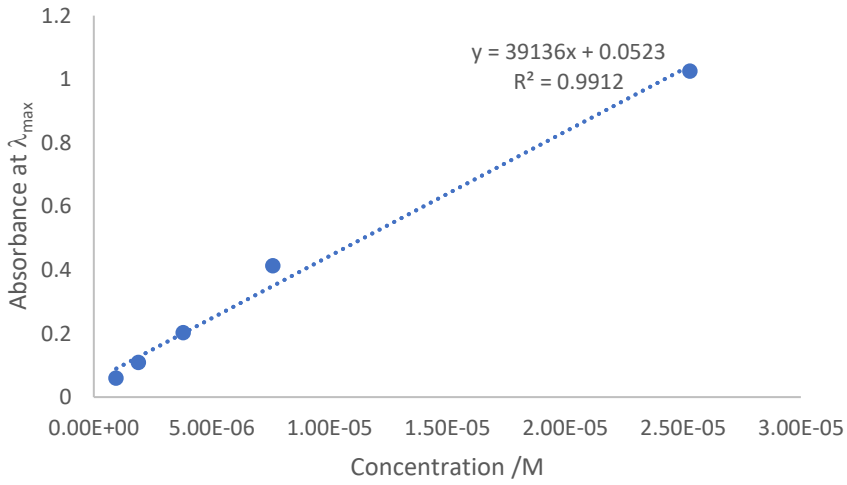

Figure 6.24. Absorbance of BODIPY **2.13a** at λ_{max} with respect to concentration, molar extinction coefficient (ε) = 39000 M^{-1} cm^{-1}.

6.3.2.2 3,7-Dichloro-5,5-difluoro-10-(3-nitrophenyl)-5H-4λ^4,5λ^4-dipyrrolo[1,2-*c*:2',1'-f][1,3,2]diazaborinine **2.13b**

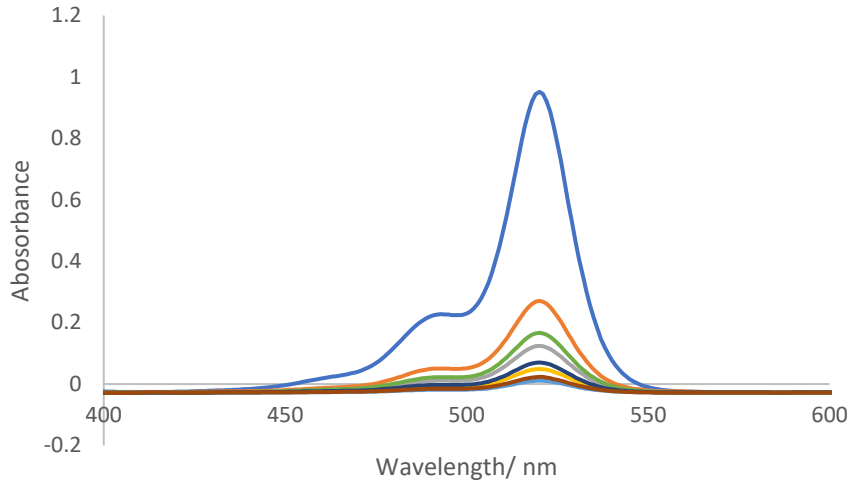

Figure 6.25. UV-vis spectrum of BODIPY **2.13b** in DCM, concentrations (M): 2.6x10^{-5}, 7.80x10^{-6}, 5.20x10^{-6}, 3.9x10^{-6}, 2.60x10^{-6}, 1.95x10^{-6}, 1.30x10^{-6}, 9.75x10^{-7} respectively.

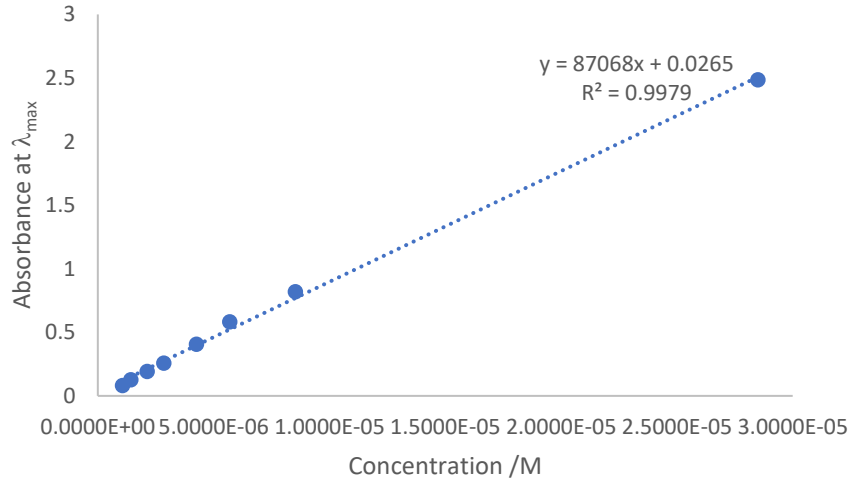

Figure 6.26. Absorbance of BODIPY **2.13b** at λ_{max} with respect to concentration, molar extinction coefficient (ε) = 87000 M^{-1} cm^{-1}.

6.3.2.3 3,7-Dichloro-5,5-difluoro-10-(4-nitrophenyl)-5H-4λ^4,5λ^4-dipyrrolo[1,2-*c*:2',1'-*f*][1,3,2]diazaborinine **2.13e**

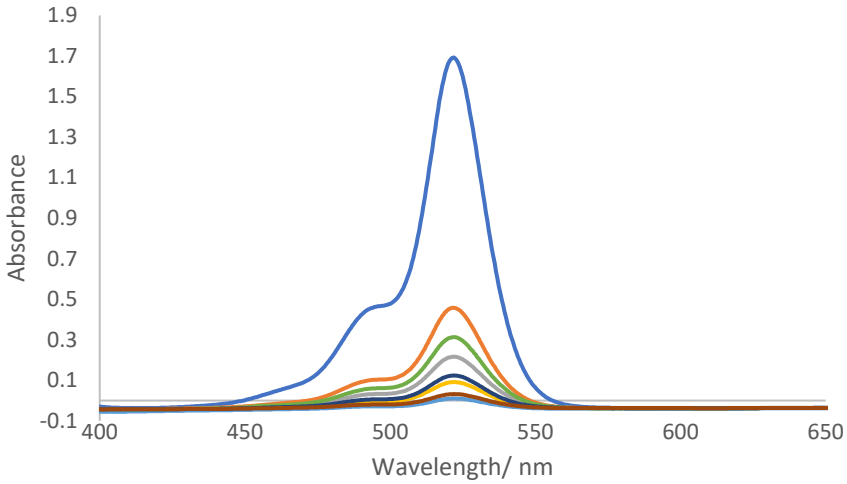

Figure 6.27. UV-vis spectrum of BODIPY **2.13e** in DCM, concentrations (M): 2.6x10^{-5}, 7.8x10^{-6}, 5.2x10^{-6}, 3.9x10^{-6}, 2.6x10^{-6}, 1.95x10^{-6}, 1.3x10^{-6}, 9.75x10^{-7} respectively.

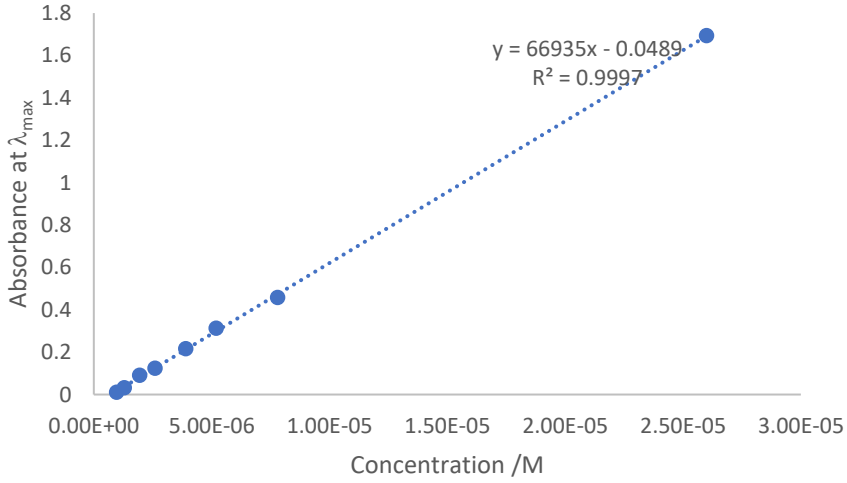

Figure 6.28. Absorbance of BODIPY **2.13e** at λ_{max} with respect to concentration, molar extinction coefficient (ε) = 67000 M^{-1} cm^{-1}.

6.3.2.4 3,7-Dichloro-5,5-difluoro-10-(4-methoxyphenyl)-5H-4λ^4,5λ^4-dipyrrolo[1,2-*c*:2',1'-*f*][1,3,2]diazaborinine **2.13c**

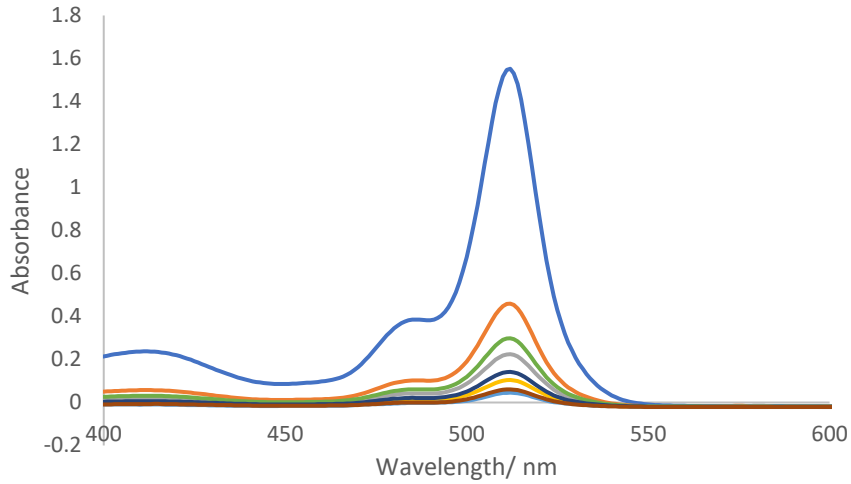

Figure 6.29. UV-Vis spectrum of BODIPY **2.13c** in DCM, concentrations (M): 2.72x10^{-5}, 8.17x10^{-6}, 5.44x10^{-6}, 4.09x10^{-6}, 2.72x10^{-6}, 2.04x10^{-6}, 1.36x10^{-6}, 1.02x10^{-6} respectively.

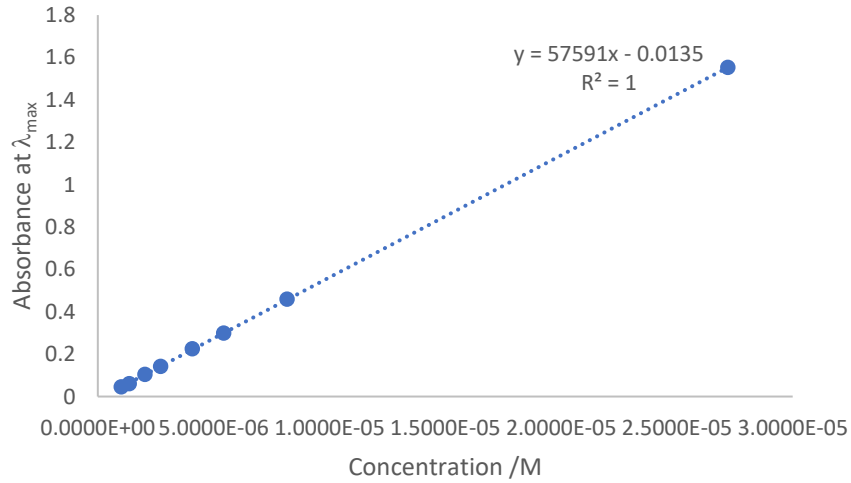

Figure 6.30. Absorbance of BODIPY **2.13c** at λ_{max} with respect to concentration, molar extinction coefficient (ε) = 58000 M^{-1} cm^{-1}.

6.3.2.5 3,7-Dichloro-5,5-difluoro-10-(3-methoxyphenyl)-5H-4λ^4,5λ^4-dipyrrolo[1,2-*c*:2',1'-*f*][1,3,2]diazaborinine **2.13d**

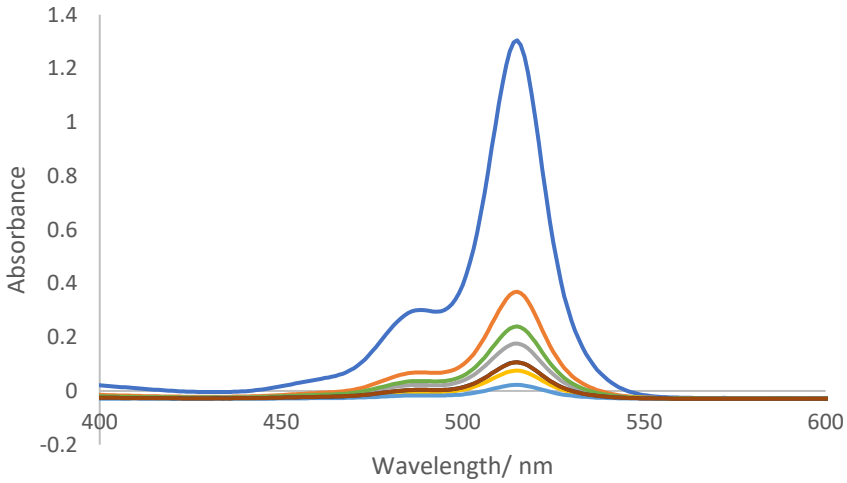

Figure 6.31. UV-Vis spectrum of BODIPY **2.13d** in DCM, concentrations (M): 2.72x10^{-5}, 8.17x10^{-6}, 5.44x10^{-6}, 4.09x10^{-6}, 2.72x10^{-6}, 2.04x10^{-6}, 1.36x10^{-6}, 1.02x10^{-6} respectively.

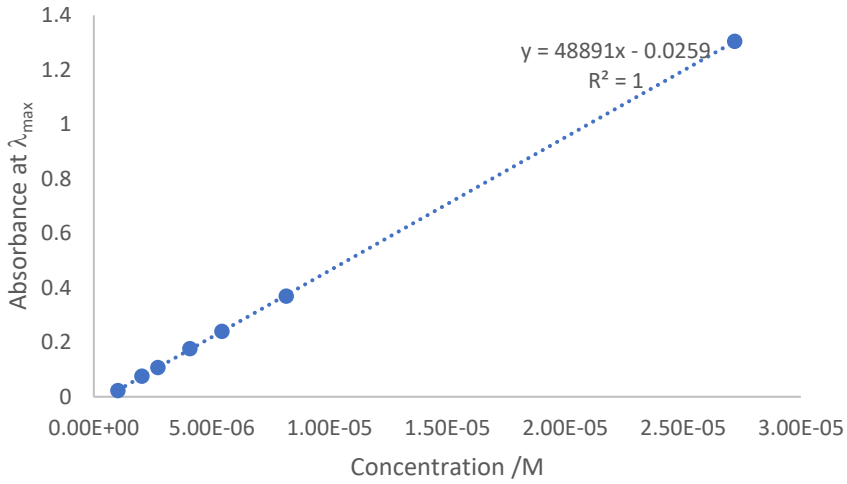

Figure 6.32. Absorbance of BODIPY **2.13d** at λ_{max} with respect to concentration, molar extinction coefficient (ε) = 49000 M^{-1} cm^{-1}.

6.3.2.6 3,7-Dichloro-5,5-difluoro-10-(*o*-tolyl)-5H-4λ^4,5λ^4-dipyrrolo[1,2-*c*:2',1'-*f*][1,3,2]diazaborinine **2.13f**

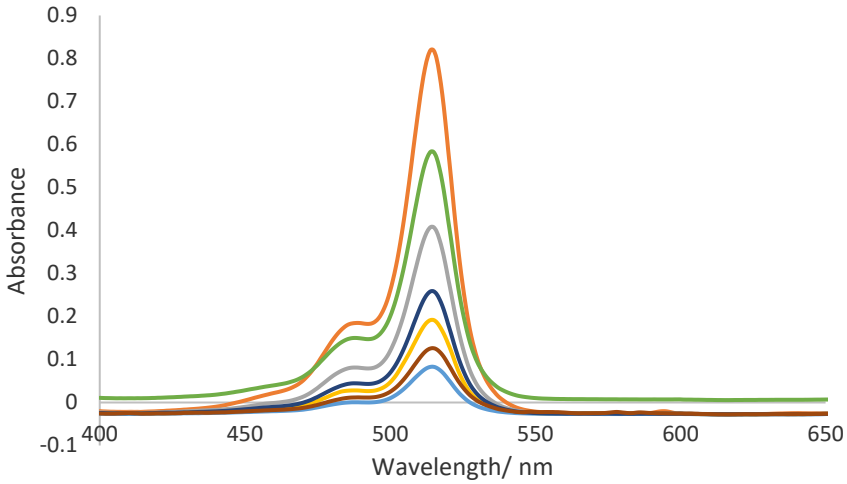

Figure 6.33. UV-Vis spectrum of BODIPY **2.13f** in DCM, concentrations (M): 2.85x10^{-5}. 8.54x10^{-6}, 4.27x10^{-6}, 2.14x10^{-6}, 1.07x10^{-6}, 5.70x10^{-6}, 2.84x10^{-6}, 1.42x10^{-6} respectively.

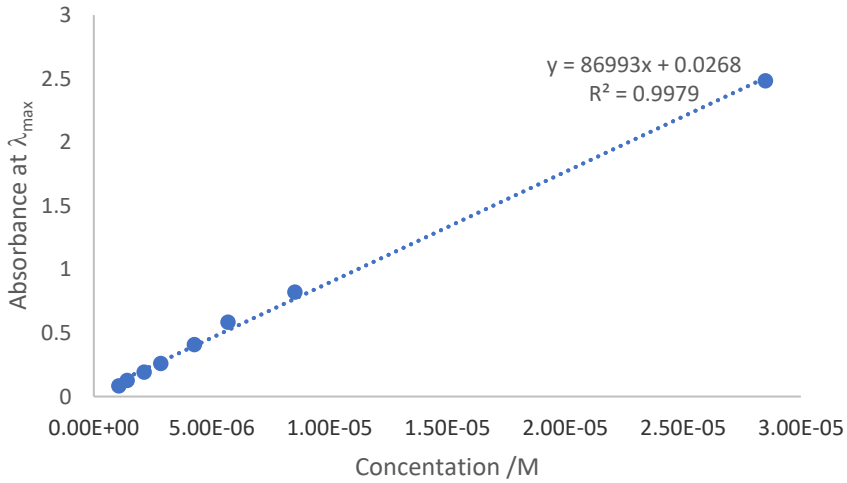

Figure 6.34. Absorbance of BODIPY **2.13f** at λ_{max} with respect to concentration, molar extinction coefficient (ε) = 87000 M^{-1} cm^{-1}.

6.3.2.7 Methyl 4-(3,7-dibromo-5,5-difluoro-5*H*-4λ^4,5λ^4-dipyrrolo[1,2-c:2',1'-f][1,3,2]diazaborinin-10-yl)benzoate **2.14a**

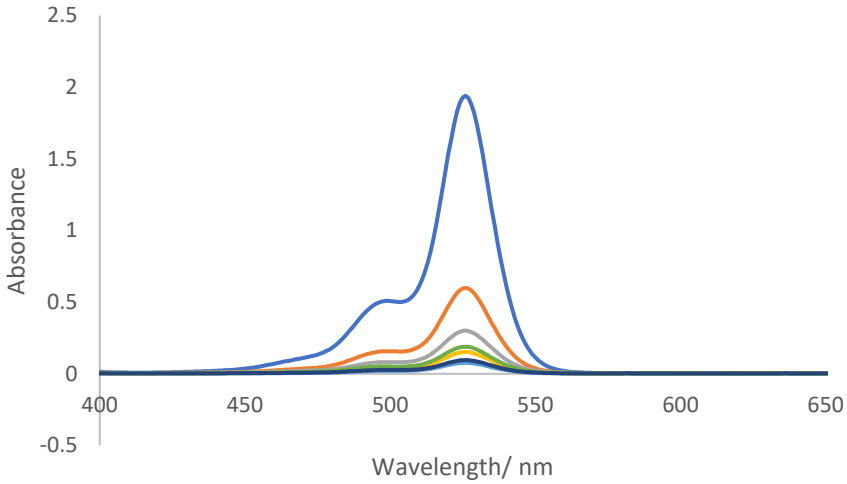

Figure 6.35. UV-Vis spectrum of BODIPY **2.14a** in DCM, concentrations (M): 2.07x10-5, 6.20x10-6, 4.13x10-6, 2.07x10-6, 1.55x10-6, 1.03x10-6, 7.79x10-7 respectively.

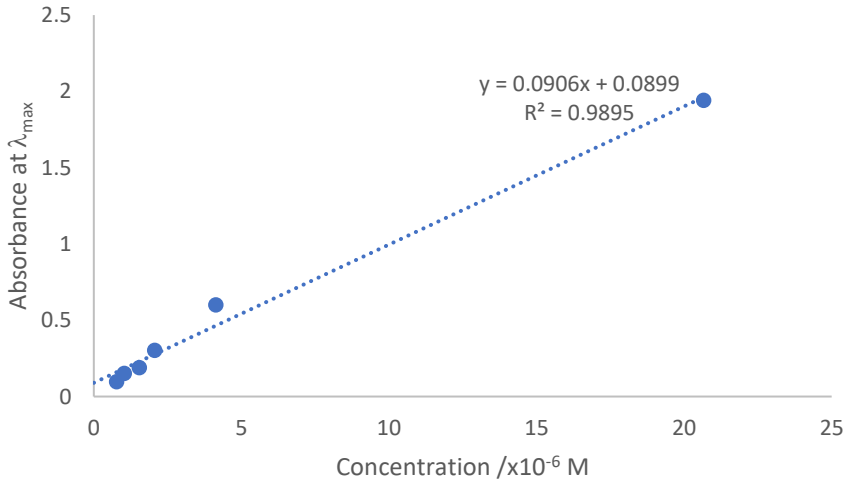

Figure 6.36. Absorbance of BODIPY **2.14a** at λ_{max} with respect to concentration, molar extinction coefficient (ε) = 91000 M^{-1} cm^{-1}.

6.3.2.8 3,7-Dibromo-5,5-difluoro-10-(4-methoxyphenyl)-5*H*-4λ^4,5λ^4-dipyrrolo[1,2-*c*:2',1'-*f*][1,3,2]diazaborinine **2.14c**

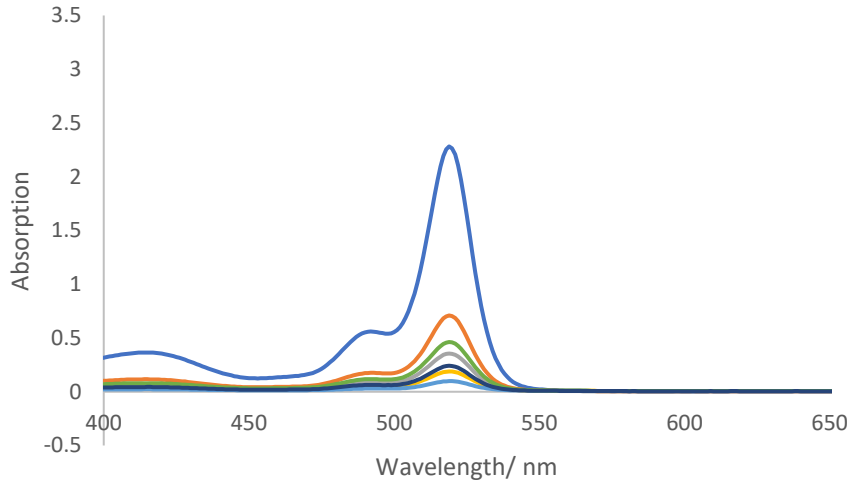

Figure 6.37. UV-Vis spectrum of BODIPY **2.14c** in DCM, concentrations (M): 2.19x10-5, 6.20x10-6, 4.39x10-6, 2.19x10-6, 1.10x10-6, 5.48x10-6, 3.29x-6, 1.65x-6 respectively.

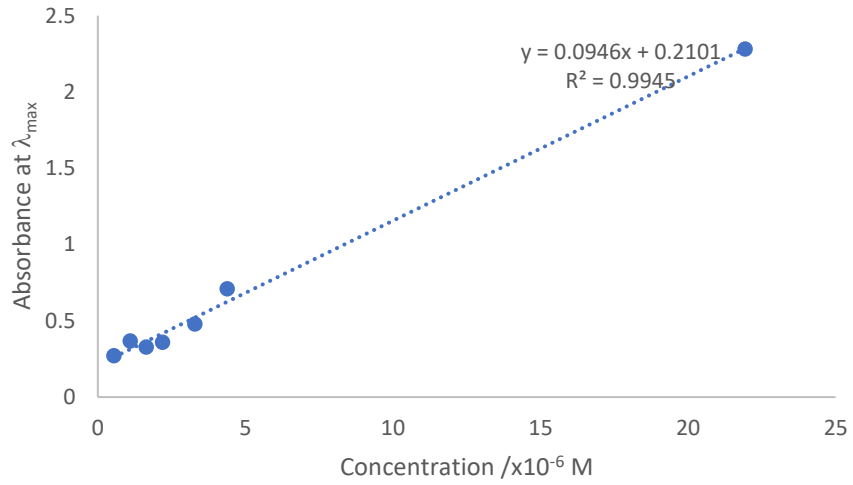

Figure 6.38. Absorbance of BODIPY **2.14c** at λ_{max} with respect to concentration, molar extinction coefficient (ε) = 95000 M^{-1} cm^{-1}.

6.3.2.9 Methyl 4-(5,5-difluoro-3,7-diiodo-5*H*-4λ^4,5λ^4-dipyrrolo[1,2-*c*:2',1'-*f*][1,3,2]diazaborinin-10-yl)benzoate **3.17a**

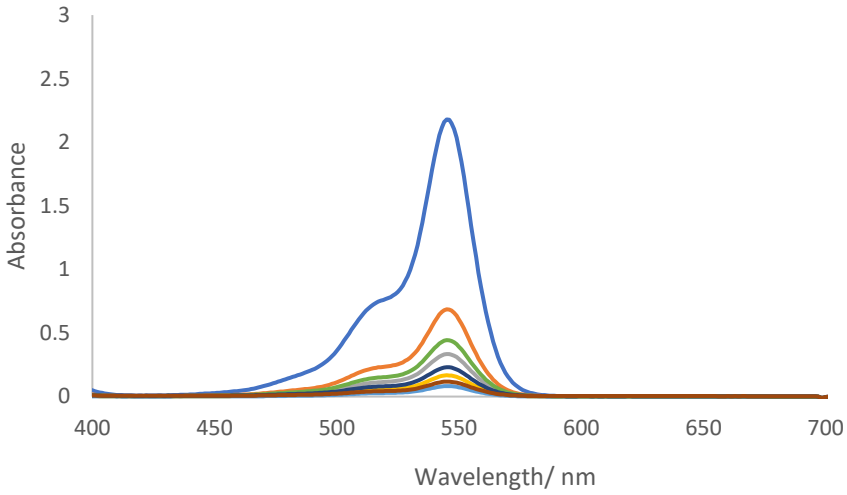

Figure 6.39. UV-Vis spectrum of BODIPY **3.17a**, concentrations (M): 3.46 x10^{-5}, 1.04 x10^{-5}, 6.92 x10^{-6}, 5.19 x10^{-6}, 3.46 x10^{-6}, 2.60 x10^{-6}, 1.73 x10^{-6}, 1.30 x10^{-6} respectively.

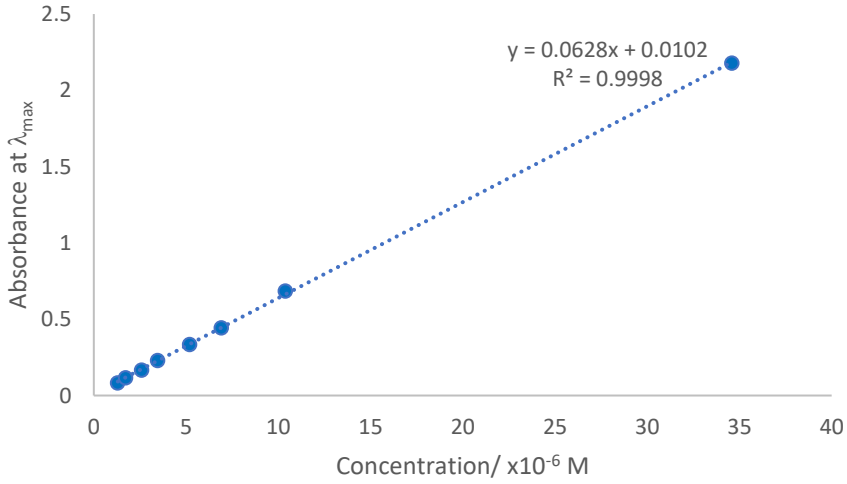

Figure 6.40. Absorbance of BODIPY **3.17a** at λ_{max} with respect to concentration, molar extinction coefficient (ε) = 63000 M^{-1} cm^{-1}.

6.3.2.10 5,5-Difluoro-3,7-diiodo-10-(3-nitrophenyl)-5*H*-4λ^4,5λ^4-dipyrrolo[1,2-*c*:2',1'-*f*][1,3,2]diazaborinine **3.17b**

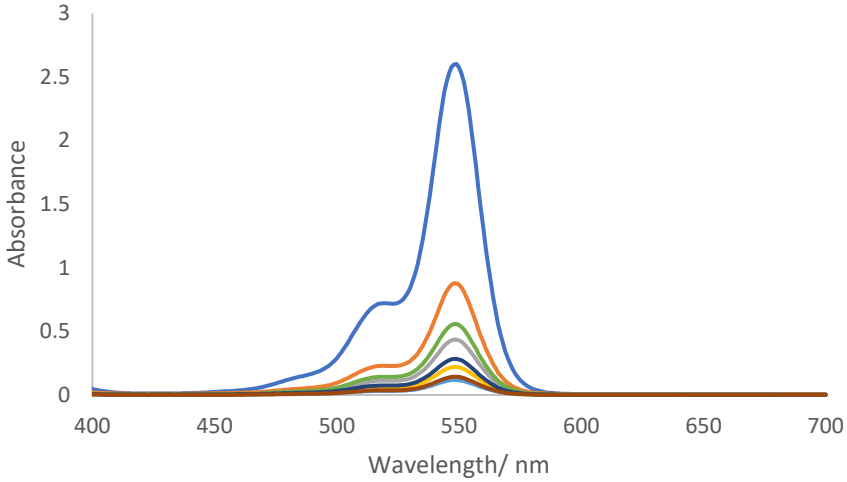

Figure 6.41. UV-Vis spectrum of BODIPY **3.17b**, concentrations (M): 3.54 x10^{-5}, 1.06 x10^{-5}, 7.08 x10^{-6}, 5.31 x10^{-6}, 3.54 x10^{-6}, 2.66 x10^{-6}, 1.77 x10^{-6}, 1.33 x10^{-6} respectively.

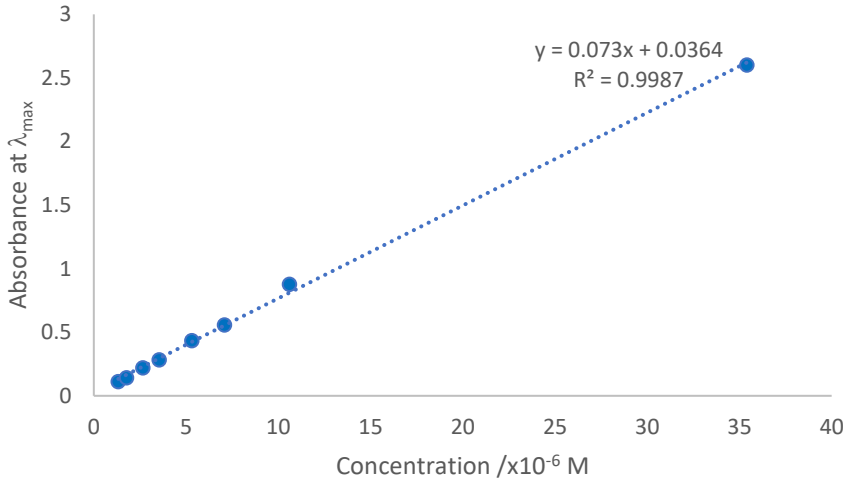

Figure 6.42. Absorbance of BODIPY **3.17b** at λ_{max} with respect to concentration, molar extinction coefficient (ε) = 73000 M^{-1} cm^{-1}.

6.3.2.11 5,5-Difluoro-3,7-diiodo-10-(4-methoxyphenyl)-5*H*-4λ^4,5λ^4-dipyrrolo[1,2-*c*:2',1'-*f*][1,3,2]diazaborinine **3.17c**

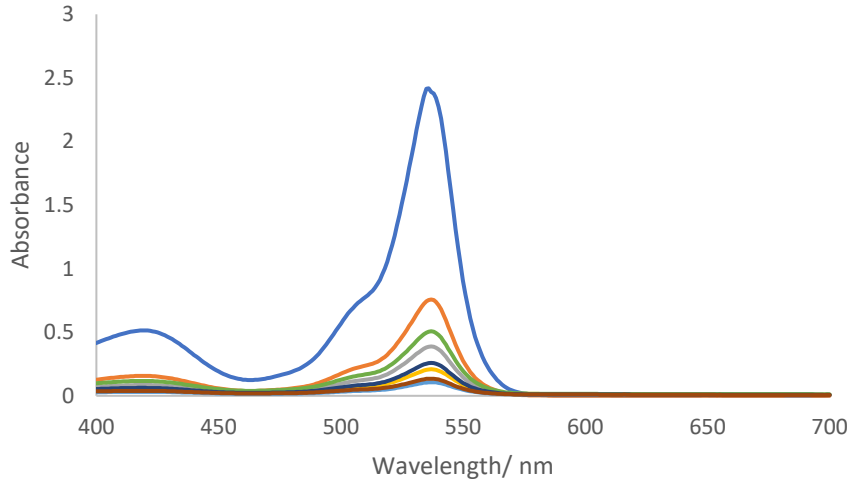

Figure 6.43. UV-Vis spectrum of BODIPY **3.17c**, concentrations (M): 3.64 x10^{-5}, 1.09 x10^{-5}, 7.27 x10^{-6}, 5.46 x10^{-6}, 3.64 x10^{-6}, 2.73 x10^{-6}, 1.82 x10^{-6}, 1.36 x10^{-6} respectively.

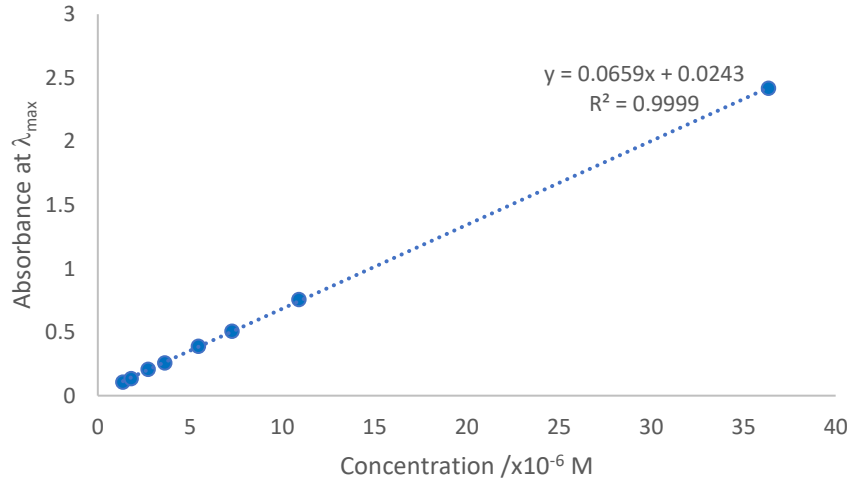

Figure 6.44. Absorbance of BODIPY **3.17c** at λ_{max} with respect to concentration, molar extinction coefficient (ε) = 66000 M^{-1} cm^{-1}.

6.3.2.12 5,5-Difluoro-3,7-diiodo-10-(3-methoxyphenyl)-5*H*-4λ^4,5λ^4-dipyrrolo[1,2-*c*:2',1'-*f*][1,3,2]diazaborinine **3.17d**

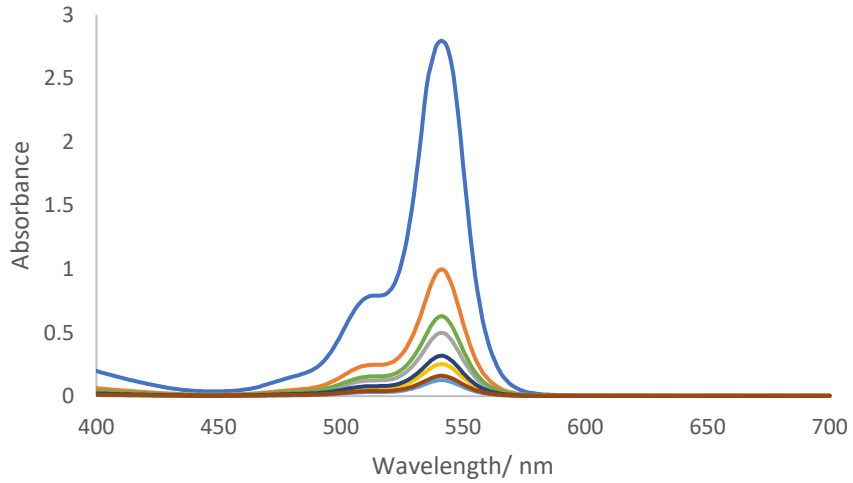

Figure 6.45. UV-Vis spectrum of BODIPY **3.17d**, concentrations (M): 3.64 x10^{-5}, 1.09 x10^{-5}, 7.27 x10^{-6}, 5.46 x10^{-6}, 3.64 x10^{-6}, 2.73 x10^{-6}, 1.82 x10^{-6}, 1.36 x10^{-6} respectively.

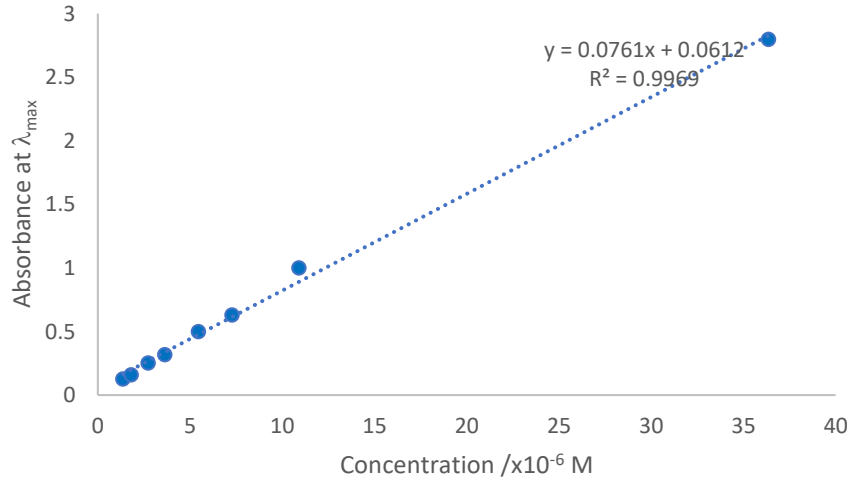

Figure 6.46. Absorbance of BODIPY **3.17d** at λ_{max} with respect to concentration, molar extinction coefficient (ε) = 76000 M^{-1} cm^{-1}.

6.3.2.13 Methyl 4-(5,5-difluoro-3,7-diphenyl-5*H*-4λ^4,5λ^4-dipyrrolo[1,2-*c*:2',1'-*f*][1,3,2]diazaborinin-10-yl)benzoate **3.21**

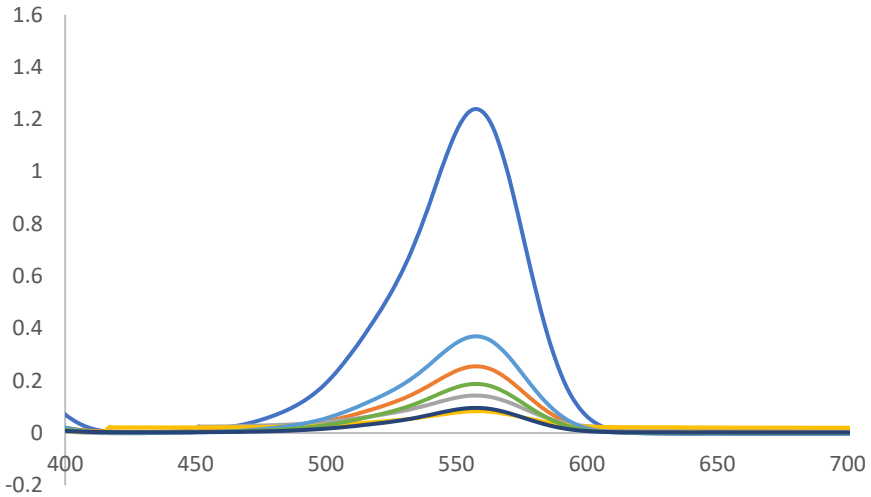

Figure 6.47. UV-Vis spectrum of BODIPY **3.21**, concentrations (M): 2.10 x10^{-5}, 6.30 x10^{-6}, 4.20 x10^{-6}, 3.15 x10^{-6}, 2.10 x10^{-6}, 1.58 x10^{-6}, 1.05 x10^{-6} respectively.

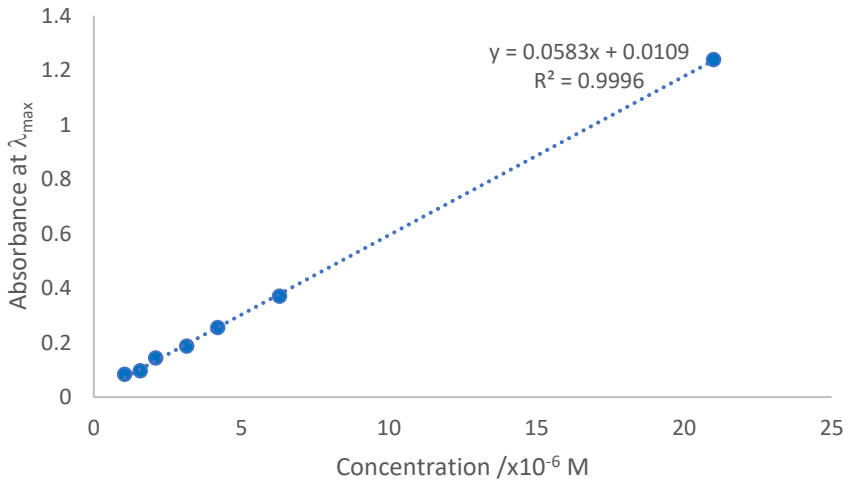

Figure 6.48. Absorbance of BODIPY **3.21** at λ_{max} with respect to concentration, molar extinction coefficient (ε) = 58000 M^{-1} cm^{-1}.

6.3.2.14 Methyl 4-(3-butyl-5,5-difluoro-7-phenyl-5*H*-5λ4,6λ4-dipyrrolo[1,2-*c*:2',1'-*f*][1,3,2]diazaborinin-10-yl)benzoate **3.22**

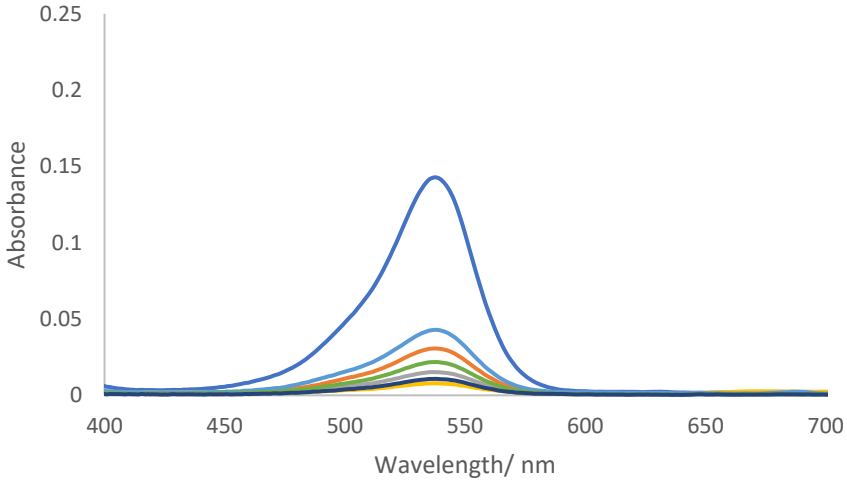

Figure 6.49. UV-Vis spectrum of BODIPY **3.22**, concentrations (M): 2.07 x10^{-6}, 6.21 x10^{-7}, 4.16 x 10^{-7}, 3.11 x10^{-7}, 2.08 x10^{-7}, 1.55 x10^{-7}, 1.04 x10^{-7} respectively.

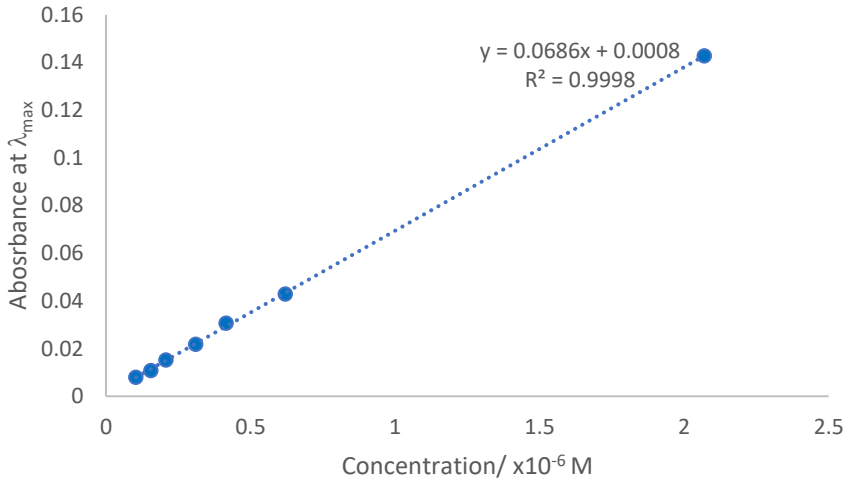

Figure 6.50. Absorbance of BODIPY **3.22** at λ_{max} with respect to concentration, molar extinction coefficient (ε) = 69000 M^{-1} cm^{-1}.

6.3.2.15 Methyl 4-(5,5-difluoro-3,7-di((*E*)-styryl)-5H-4λ^4,5λ^4-dipyrrolo[1,2-*c*:2',1'-*f*][1,3,2]diazaborinin-10-yl)benzoate **3.25**

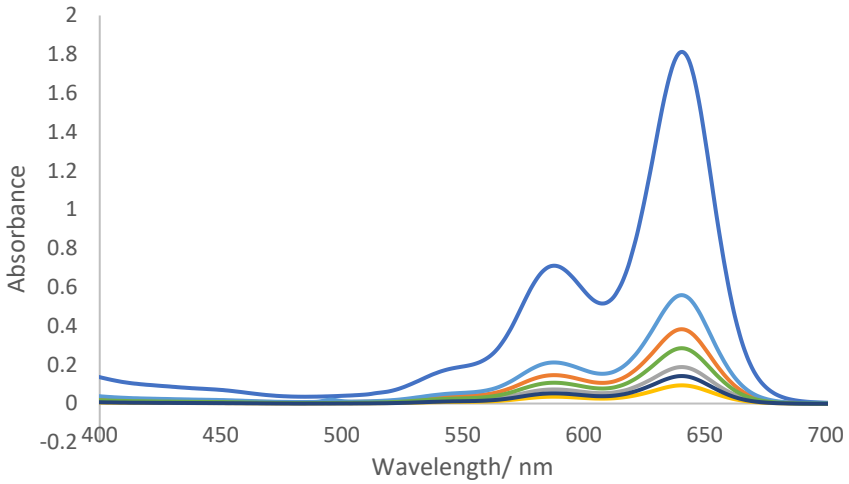

Figure 6.51. UV-Vis spectrum of BODIPY **3.25**, concentrations (M): 1.89 x10^{-5}, 5.66 x10^{-6}, 3.77 x10^{-6}, 2.83 x10^{-6}, 1.89 x10^{-6}, 1.41 x10^{-6}, 9.43 x10^{-7} respectively.

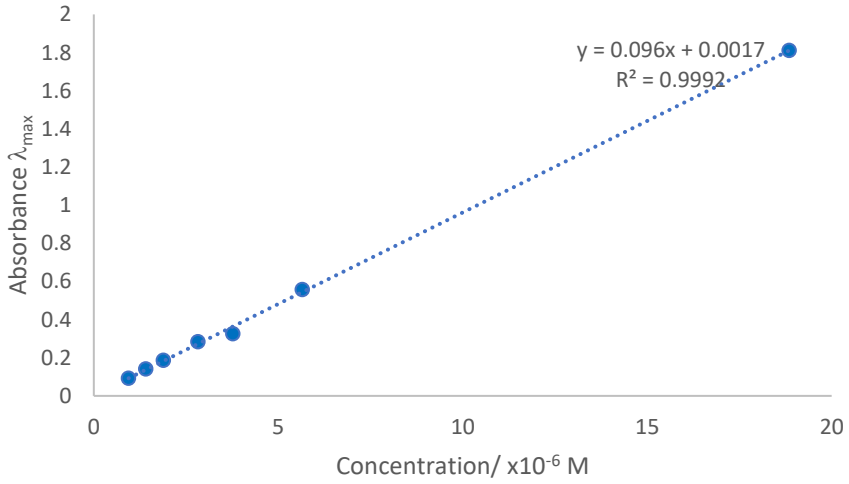

Figure 6.52. Absorbance of BODIPY **3.25** at λ_{max} with respect to concentration, molar extinction coefficient (ε) = 96000 M^{-1} cm^{-1}.

6.3.2.16 Methyl 4-(5,5-difluoro-3,7-bis(phenylethynyl)-5*H*-4λ^4,5λ^4-dipyrrolo[1,2-*c*:2',1'-*f*][1,3,2]diazaborinin-10-yl)benzoate **3.28**

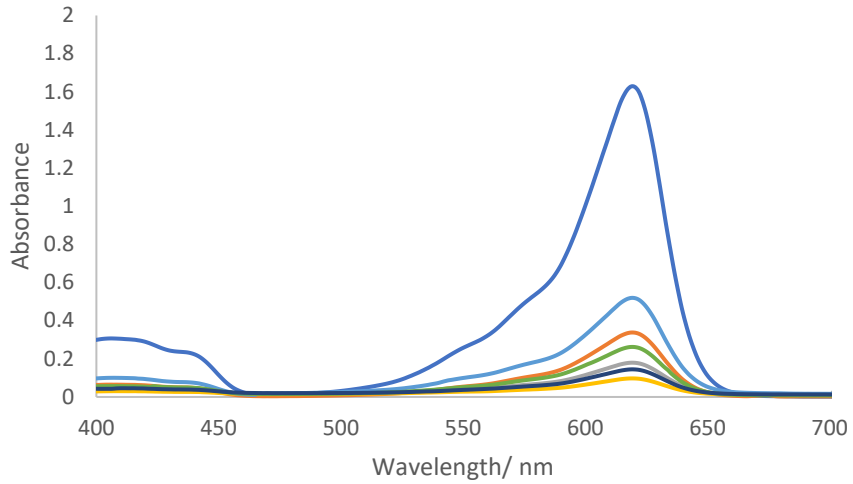

Figure 6.53. UV-Vis spectrum of BODIPY **3.28**, concentrations (M): 1.90 x10^{-5}, 5.70 x10^{-6}, 3.80 x10^{-6}, 2.85 x10^{-6}, 1.90 x10^{-6}, 1.43 x10^{-6}, 9.50 x10^{-7} respectively.

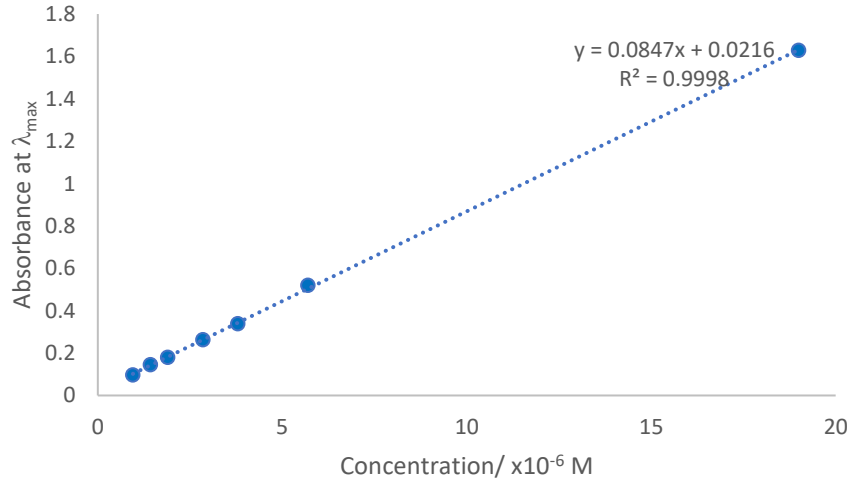

Figure 6.54. Absorbance of BODIPY **3.28** at λ_{max} with respect to concentration, molar extinction coefficient (ε) = 85000 M^{-1} cm^{-1}.

6.3.2.17 Methyl 4-(3-chloro-5,5-difluoro-7-(phenylethynyl)-5*H*-4λ4,5λ4-dipyrrolo[1,2-*c*:2',1'-*f*][1,3,2]diazaborinin-10-yl)benzoate **3.29**

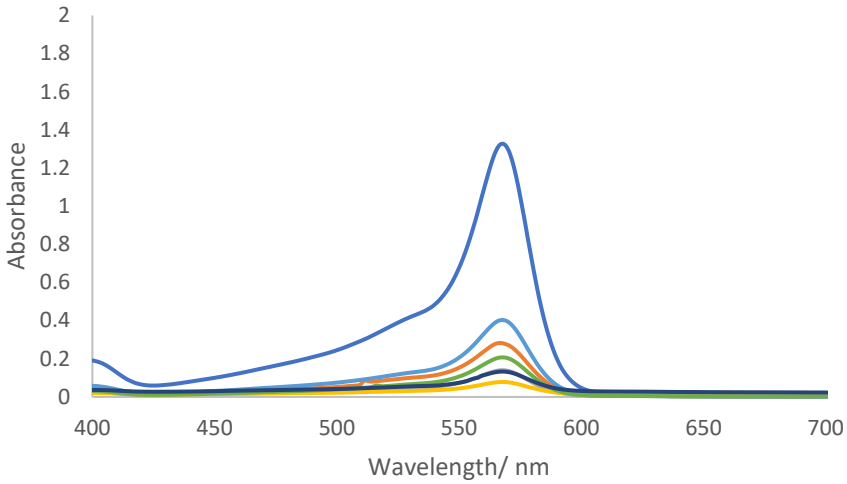

Figure 6.55. UV-Vis spectrum of BODIPY **3.29**, concentrations (M): 2.17 x10^{-5}, 6.51 x10^{-6}, 4.34 x10^{-6}, 3.26 x10^{-6}, 2.17 x10^{-6}, 1.62 x10^{-6}, 1.09 x10^{-6} respectively.

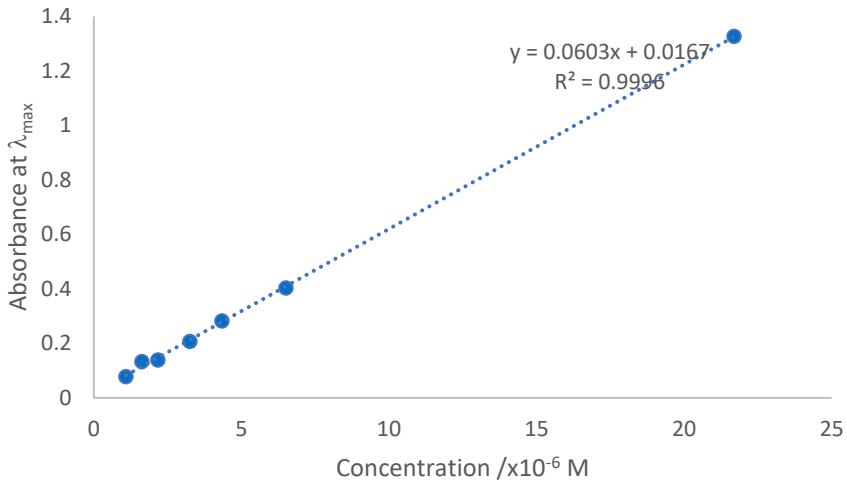

Figure 6.56. Absorbance of BODIPY **3.29** at λ_{max} with respect to concentration, molar extinction coefficient (ε) = 60000 M^{-1} cm^{-1}.

6.3.2.18 Methyl 4-(3-chloro-5,5-difluoro-7-phenyl-5*H*-5λ^4,6λ^4-dipyrrolo[1,2-*c*:2',1'-*f*][1,3,2]diazaborinin-10-yl)benzoate **3.38**

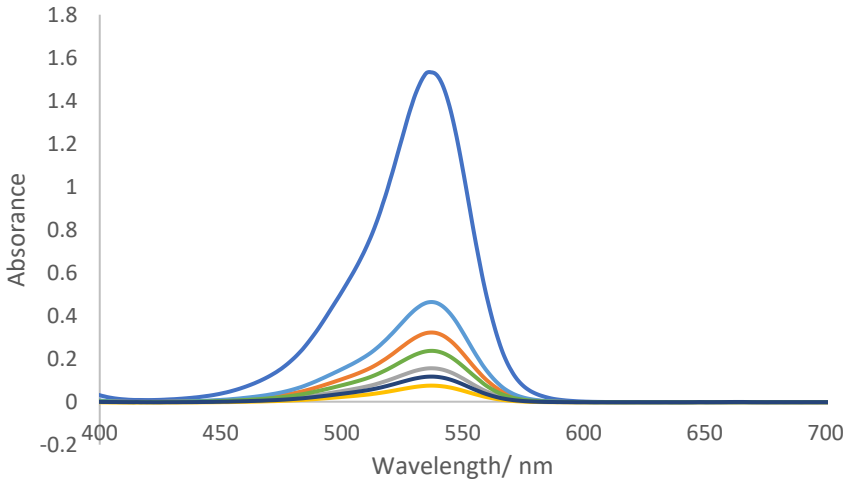

Figure 6.57. UV-Vis spectrum of BODIPY **3.38**, concentrations (M): 2.29 x10^{-5}, 6.87 x10^{-6}, 4.58 x10^{-6}, 3.44 x10^{-6}, 2.29 x10^{-6}, 1.72 x10^{-6}, 1.15 x10^{-6} respectively.

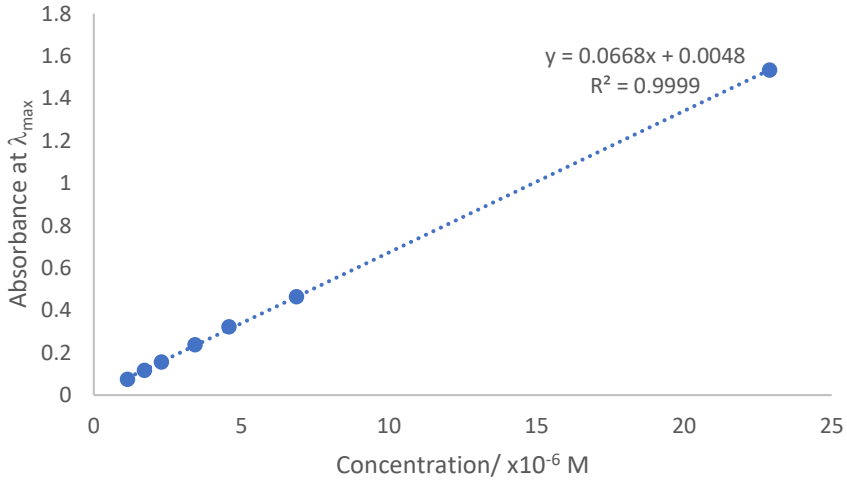

Figure 6.58. Absorbance of BODIPY **3.38** at λ_{max} with respect to concentration, molar extinction coefficient (ε) = 67000 M^{-1} cm^{-1}.

6.3.2.19 Methyl (*R*)-4-(10b-(4-fluorophenyl)-10-((3-hydroxy-1-methoxy-1-oxopropan-2-yl)amino)-10b*H*-11-oxa-4b1,10aλ^4-diaza-10bλ^4-boracyclopenta[e]aceanthrylen-7-yl)benzoate **4.23a**

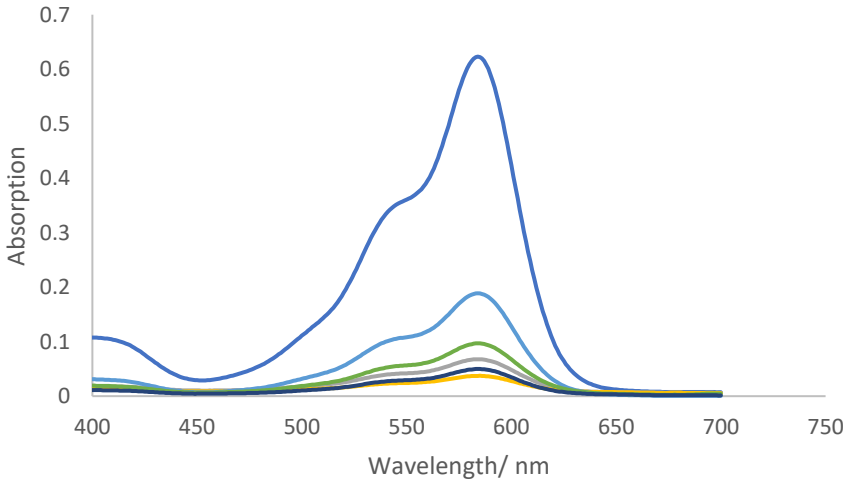

Figure 6.59. UV-Vis spectrum of BODIPY **4.23b**, concentrations (M): 2.29 x10-5, 6.87 x10-6, 4.58 x10-6, 3.44 x10-6, 2.29 x10-6, 1.72 x10-6, 1.15 x10-6 respectively.

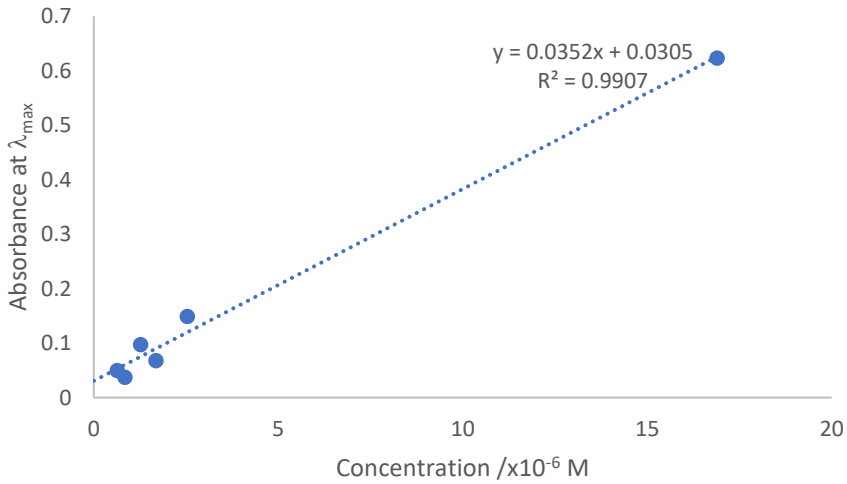

Figure 6.60. Absorbance of BODIPY **4.23b** at λ_{max} with respect to concentration, molar extinction coefficient (ε) = 35000 M^{-1} cm^{-1}.

6.3.2.20 Methyl (*R*)-4-(10b-(4-fluorophenyl)-10-((3-hydroxy-1-methoxy-1-oxopropan-2-yl)amino)-10b*H*-11-oxa-4b1,10aλ^4-diaza-10bλ^4-boracyclopenta[e]aceanthrylen-7-yl)benzoate **4.23b**

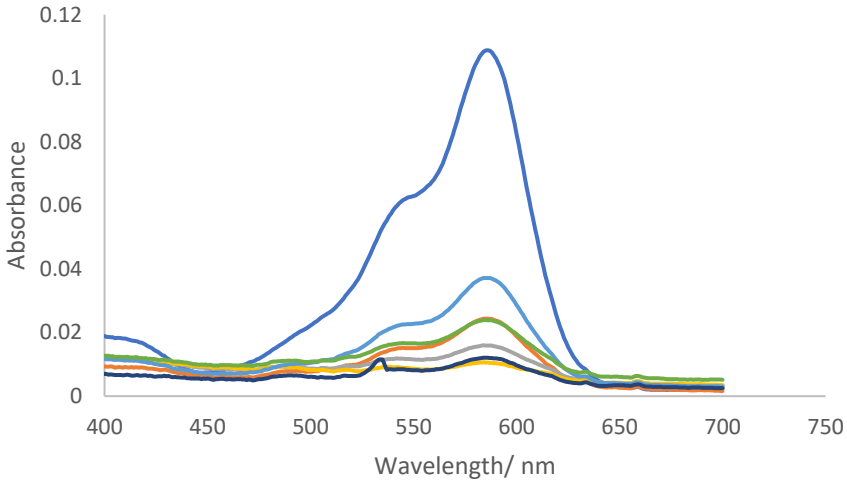

Figure 6.61. UV-Vis spectrum of BODIPY **4.23b**, concentrations (M): 2.29 x10-5, 6.87 x10-6, 4.58 x10-6, 3.44 x10-6, 2.29 x10-6, 1.72 x10-6, 1.15 x10-6 respectively.

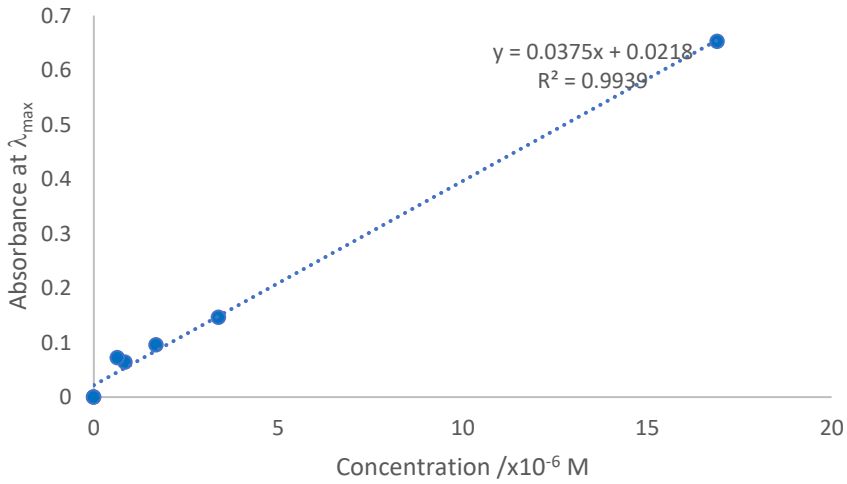

Figure 6.62. Absorbance of BODIPY **4.23b** at λ_{max} with respect to concentration, molar extinction coefficient (ε) = 38000 M^{-1} cm^{-1}.

6.3.2.21 Methyl (*S*)-4-(10b-(4-fluorophenyl)-10-((3-hydroxy-1-methoxy-1-oxopropan-2-yl)amino)-10b*H*-11-oxa-4b1,10aλ^4-diaza-10bλ^4-boracyclopenta[e]aceanthrylen-7-yl)benzoate **4.37a**

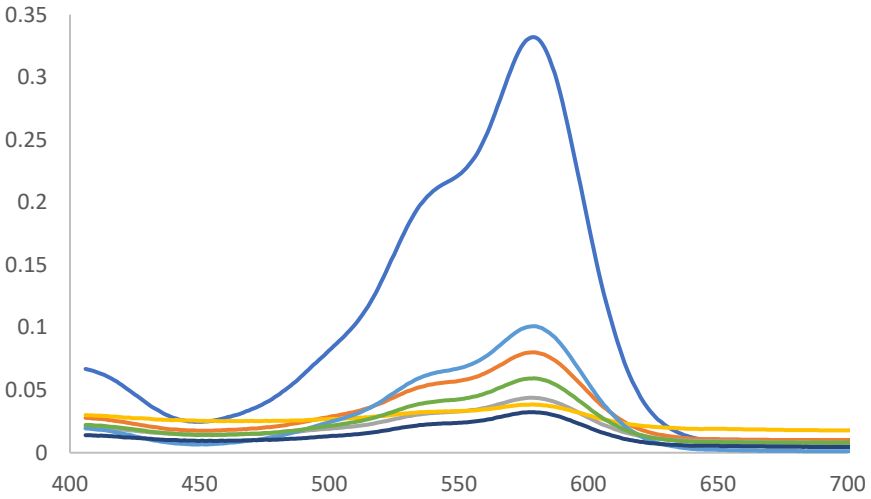

Figure 6.63. UV-Vis spectrum of BODIPY **4.37a**, concentrations (M): 1.69 x10-5, 5.07 x10-6, 3.38 x10-6, 2.54 x10-6, 1.69 x10-6, 1.27 x10-6, 1.8.45 x10-7 respectively.

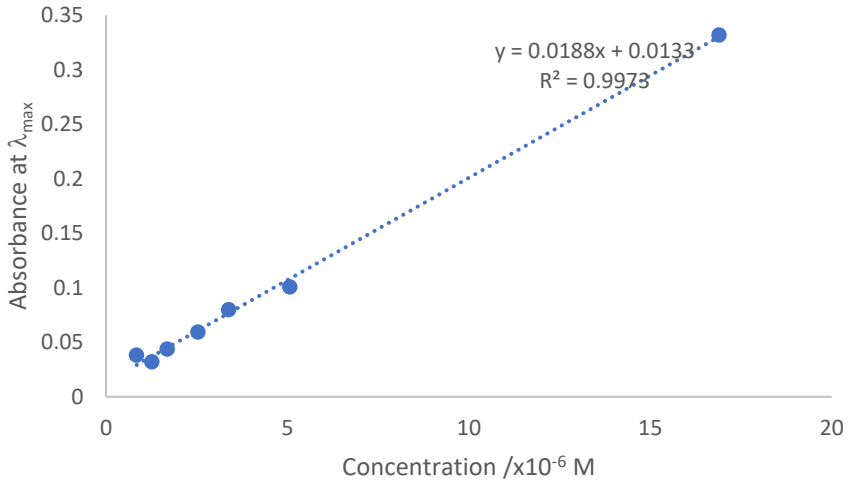

Figure 6.64. Absorbance of BODIPY **4.37a** at λ_{max} with respect to concentration, molar extinction coefficient (ε) = 19000 M^{-1} cm^{-1}.

6.3.2.22 Methyl (*S*)-4-(10b-(4-fluorophenyl)-10-((3-hydroxy-1-methoxy-1-oxopropan-2-yl)amino)-10b*H*-11-oxa-4b1,10aλ^4-diaza-10bλ^4-boracyclopenta[e]aceanthrylen-7-yl)benzoate **4.37b**

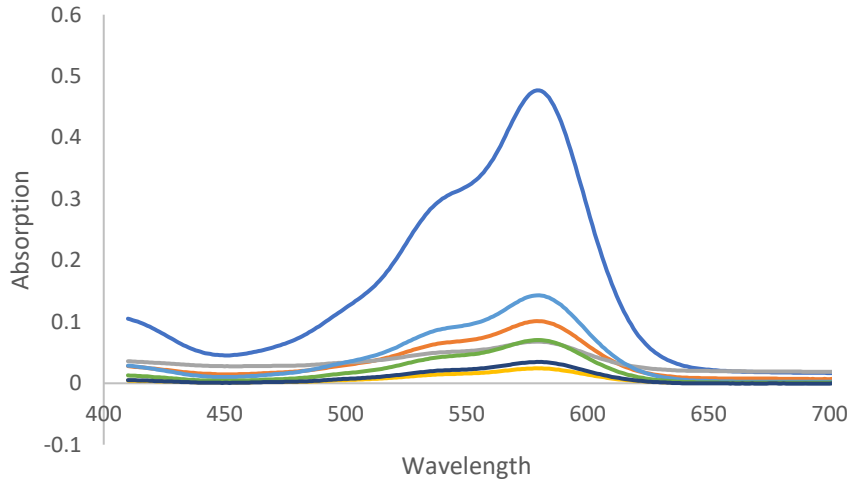

Figure 6.65. UV-Vis spectrum of BODIPY **4.37b**, concentrations (M): 21.69 x10-5, 5.07 x10-6, 3.38 x10-6, 2.54 x10-6, 1.69 x10-6, 1.27 x10-6, 1.8.45 x10-7 respectively.

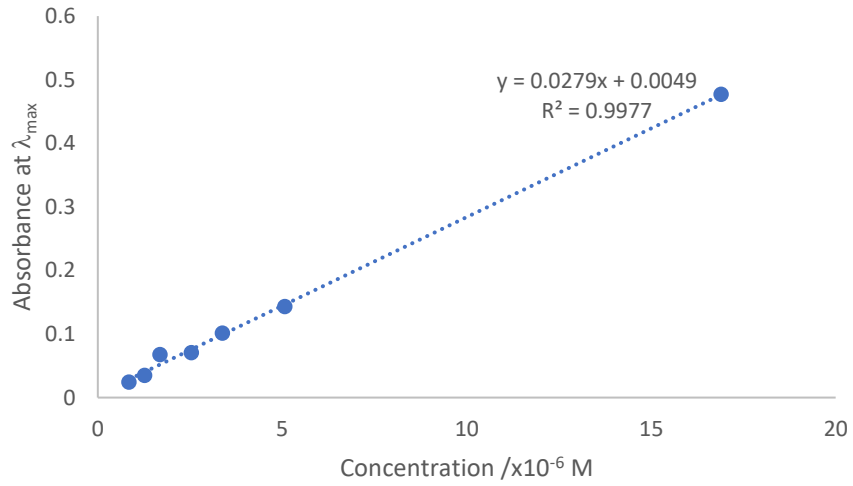

Figure 6.66. Absorbance of BODIPY **4.37b** at λ_{max} with respect to concentration, molar extinction coefficient (ε) = 28000 M^{-1} cm^{-1}.

6.4 Chiral HPLC Spectra

6.4.1 Methyl (*R*)-4-(10b-(4-fluorophenyl)-10-((3-hydroxy-1-methoxy-1-oxopropan-2-yl)amino)-10b*H*-11-oxa-4b1,10aλ^4-diaza-10bλ^4-boracyclopenta[e]aceanthrylen-7-yl)benzoate **4.23a** and methyl (*S*)-4-(10b-(4-fluorophenyl)-10-((3-hydroxy-1-methoxy-1-oxopropan-2-yl)amino)-10b*H*-11-oxa-4b1,10aλ^4-diaza-10bλ^4-boracyclopenta[e]aceanthrylen-7-yl)benzoate **4.37a.**

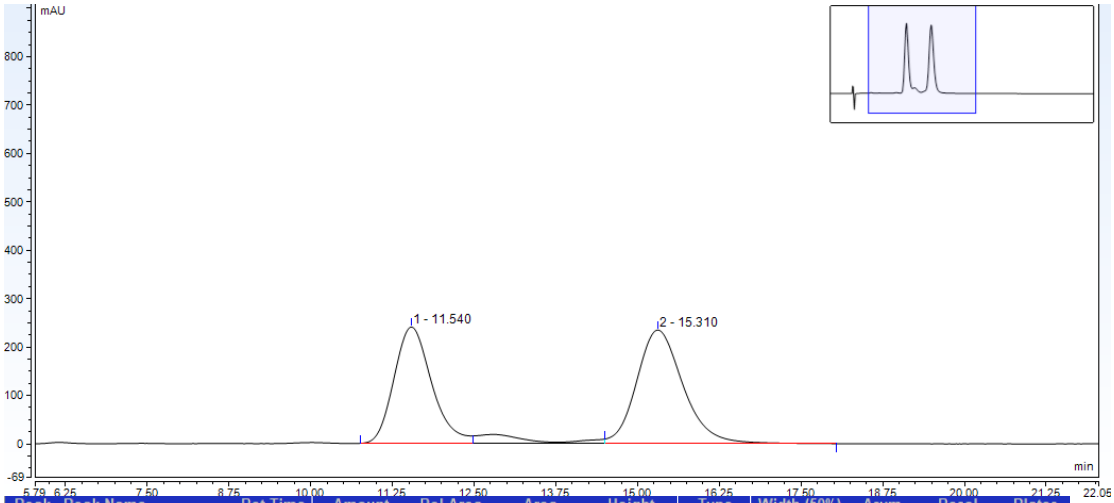

Peak No.	Peak Name	Ret.Time min	Amount n.a.	Rel.Area %	Area mAU*min	Height mAU	Type	Width (50%) min	Asym. EP	Resol. EP	Plates EP
1		11.540	n.a.	45.52	160.8486	240.49	BM *	0.610	n.a.	3.29	1983
2		15.310	n.a.	54.48	192.4951	234.49	MB*	0.741	1.17	n.a.	2364
Maximum			0.0000	54.48	192.4951	240.49		0.741	1.17	3.29	2364
Minimum			0.0000	45.52	160.8486	234.49		0.610	1.17	3.29	1983
Sum			0.0000	100.00	353.3437	474.98					

Figure 6.67. Chiral HPLC spectra of BODIPY **4.23a** and BODIPY **4.37a** using IC column.

6.4.2 Methyl (*R*)-4-(10b-(4-fluorophenyl)-10-((3-hydroxy-1-methoxy-1-oxopropan-2-yl)amino)-10b*H*-11-oxa-4b1,10aλ^4-diaza-10bλ^4-boracyclopenta[e]aceanthrylen-7-yl)benzoate **4.23a**

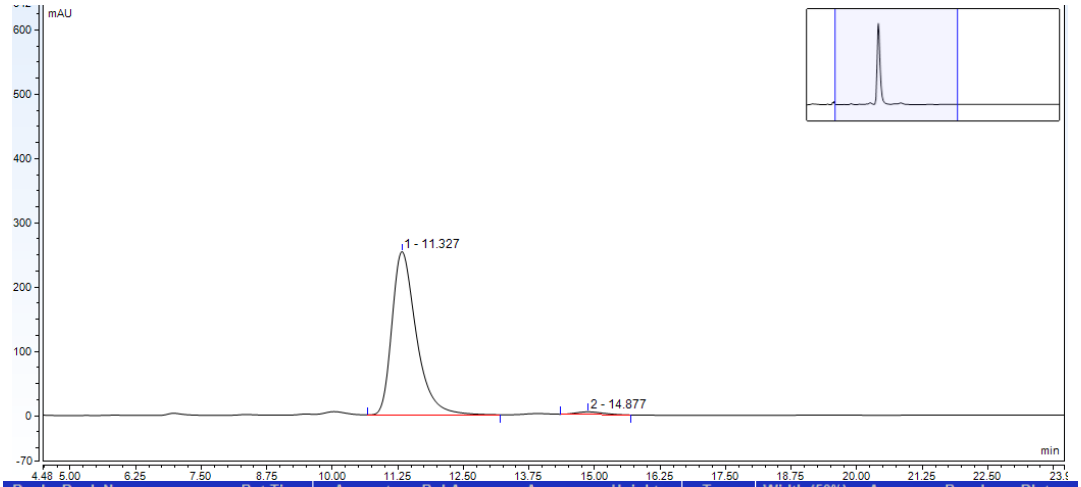

Peak No.	Peak Name	Ret.Time min	Amount n.a.	Rel.Area %	Area mAU*min	Height mAU	Type	Width (50%) min	Asym. EP	Resol. EP	Plates EP
1		11.327	n.a.	98.19	136.7641	254.06	BMB*	0.478	1.43	3.97	3111
2		14.877	n.a.	1.81	2.5191	4.17	BMB*	0.577	1.24	n.a.	3687
Maximum			0.0000	98.19	136.7641	254.06		0.577	1.43	3.97	3687
Minimum			0.0000	1.81	2.5191	4.17		0.478	1.24	3.97	3111
Sum			0.0000	100.00	139.2832	258.23					

Figure 6.68. Chiral HPLC spectra of BODIPY **4.23a** and using IC column.

6.4.3 Methyl (*S*)-4-(10b-(4-fluorophenyl)-10-((3-hydroxy-1-methoxy-1-oxopropan-2-yl)amino)-10b*H*-11-oxa-4b1,10aλ^4-diaza-10bλ^4-boracyclopenta[e]aceanthrylen-7-yl)benzoate **4.37a**

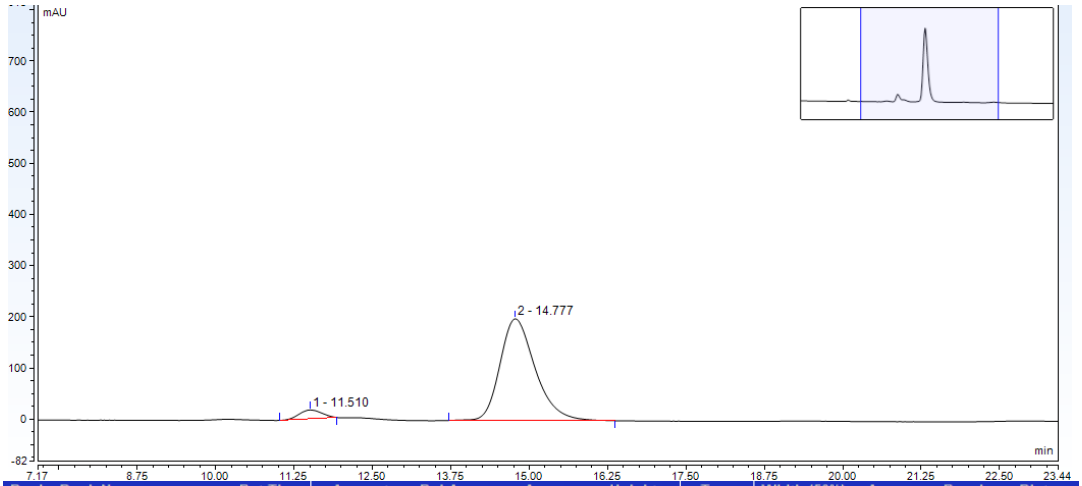

Peak No.	Peak Name	Ret.Time min	Amount n.a.	Rel.Area %	Area mAU*min	Height mAU	Type	Width (50%) min	Asym. EP	Resol. EP	Plates EP
1		11.510	n.a.	5.26	7.1845	17.26	BMB*	0.409	1.01	3.87	4385
2		14.777	n.a.	94.74	129.3074	198.84	BMB*	0.587	1.29	n.a.	3507
Maximum			0.0000	94.74	129.3074	198.84		0.587	1.29	3.87	4385
Minimum			0.0000	5.26	7.1845	17.26		0.409	1.01	3.87	3507
Sum			0.0000	100.00	136.4919	216.09					

Figure 6.69. Chiral HPLC spectra of BODIPY **4.37a** and using IC column.

6.4.4 Methyl (*R*)-4-(10b-(4-fluorophenyl)-10-((3-hydroxy-1-methoxy-1-oxopropan-2-yl)amino)-10b*H*-11-oxa-4b1,10aλ^4-diaza-10bλ^4-boracyclopenta[e]aceanthrylen-7-yl)benzoate **4.23b** and Methyl (*S*)-4-(10b-(4-fluorophenyl)-10-((3-hydroxy-1-methoxy-1-oxopropan-2-yl)amino)-10b*H*-11-oxa-4b1,10aλ^4-diaza-10bλ^4-boracyclopenta[e]aceanthrylen-7-yl)benzoate **4.37b**

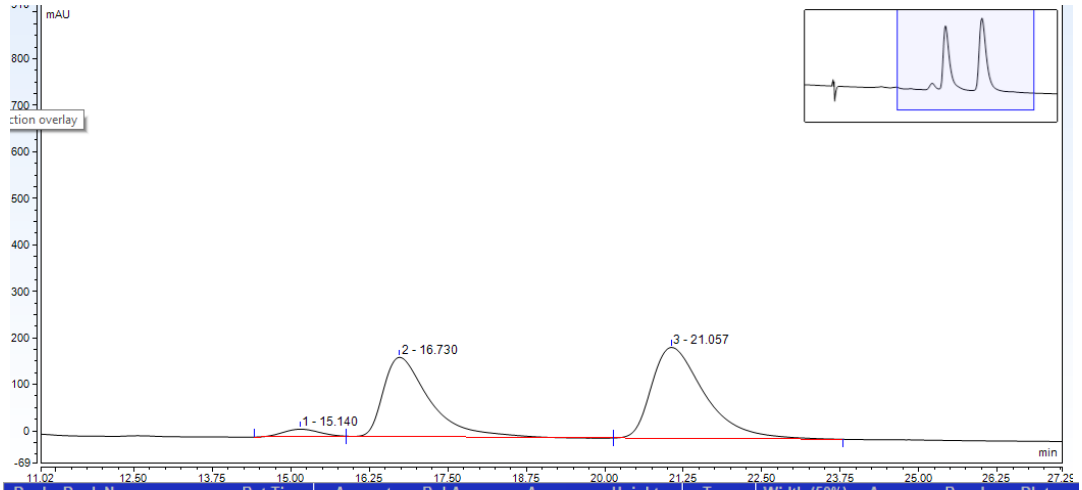

Peak No.	Peak Name	Ret.Time min	Amount n.a.	Rel.Area %	Area mAU*min	Height mAU	Type	Width (50%) min	Asym. EP	Resol. EP	Plates EP
1		15.140	n.a.	3.14	10.8778	16.24	BMB*	0.643	1.07	1.36	3067
2		16.730	n.a.	41.77	144.7653	170.26	BMB*	0.737	1.97	3.17	2857
3		21.057	n.a.	55.09	190.9377	195.43	BMB*	0.872	1.65	n.a.	3232
Maximum			0.0000	55.09	190.9377	195.43		0.872	1.97	3.17	3232
Minimum			0.0000	3.14	10.8778	16.24		0.643	1.07	1.36	2857
Sum			0.0000	100.00	346.5809	381.92					

Figure 6.70. Chiral HPLC spectra of BODIPY **4.23b** and **4.37b** and using IB column

6.4.5 Methyl (*R*)-4-(10b-(4-fluorophenyl)-10-((3-hydroxy-1-methoxy-1-oxopropan-2-yl)amino)-10b*H*-11-oxa-4b1,10aλ^4-diaza-10bλ^4-boracyclopenta[e]aceanthrylen-7-yl)benzoate **4.23b**

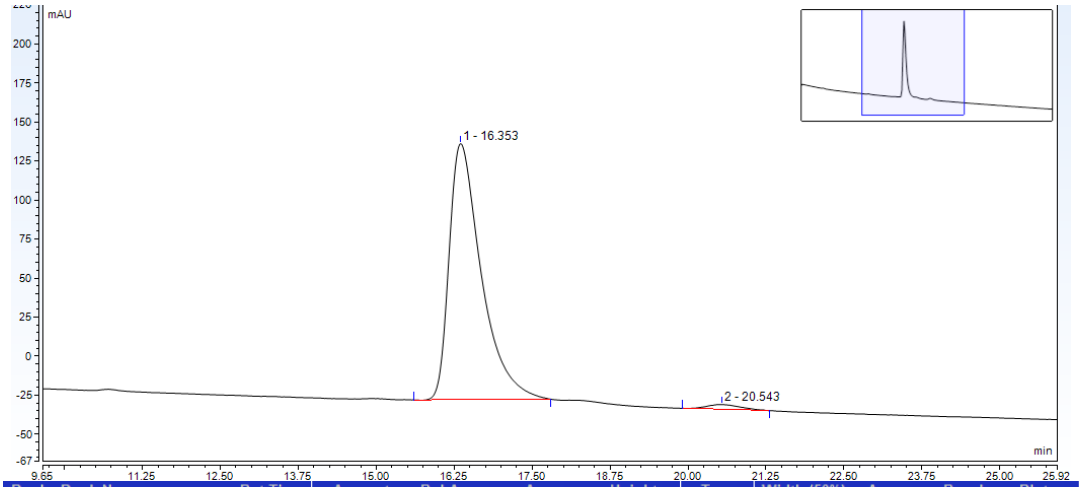

Peak No.	Peak Name	Ret.Time min	Amount n.a.	Rel.Area %	Area mAU*min	Height mAU	Type	Width (50%) min	Asym. EP	Resol. EP	Plates EP
1		16.353	n.a.	98.15	98.0402	163.97	BMB*	0.528	1.74	4.39	5322
2		20.543	n.a.	1.85	1.8464	3.03	BMB*	0.598	1.21	n.a.	6535
Maximum			0.0000	98.15	98.0402	163.97		0.598	1.74	4.39	6535
Minimum			0.0000	1.85	1.8464	3.03		0.528	1.21	4.39	5322
Sum			0.0000	100.00	99.8866	167.00					

Figure 6.71. Chiral HPLC spectra of BODIPY **4.23b** and using IB column.

6.4.6 Methyl (*S*)-4-(10b-(4-fluorophenyl)-10-((3-hydroxy-1-methoxy-1-oxopropan-2-yl)amino)-10b*H*-11-oxa-4b1,10aλ^4-diaza-10bλ^4-boracyclopenta[e]aceanthrylen-7-yl)benzoate **4.37b**

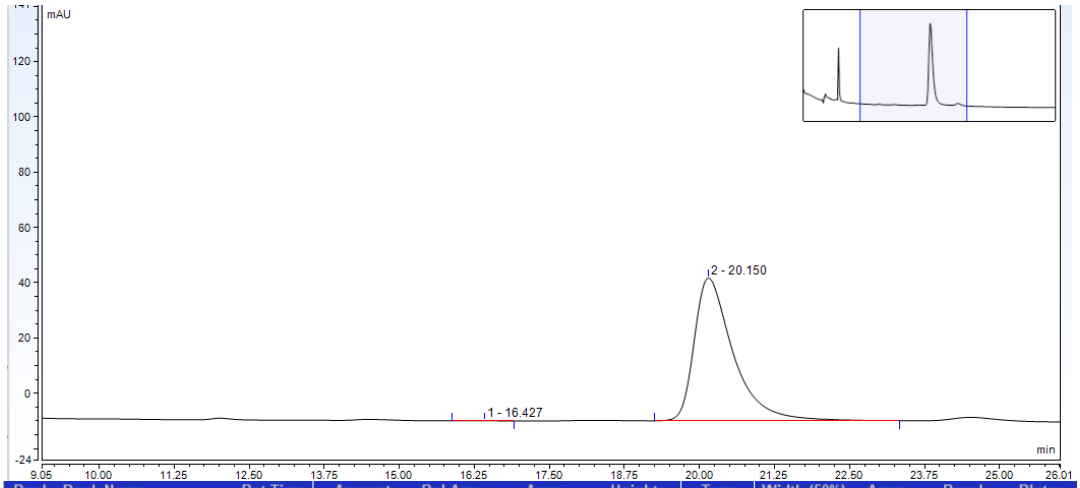

Peak No.	Peak Name	Ret.Time min	Amount n.a.	Rel.Area %	Area mAU*min	Height mAU	Type	Width (50%) min	Asym. EP	Resol. EP	Plates EP
1		16.427	n.a.	0.09	0.0335	0.07	BMB*	0.415	0.94	4.12	8670
2		20.150	n.a.	99.91	38.8207	51.64	BMB*	0.650	1.69	n.a.	5317
Maximum			0.0000	99.91	38.8207	51.64		0.650	1.69	4.12	8670
Minimum			0.0000	0.09	0.0335	0.07		0.415	0.94	4.12	5317
Sum			0.0000	100.00	38.8543	51.71					

Figure 6.72. Chiral HPLC spectra of BODIPY 4.37b and using IB column.

6.5 Crystal Structures

The following crystal structure data was collected on a Xcalibur, Atlas, Gemini ulter diffractormeter equipped with a fine-focus sealed X-ray tube (λ CuKα = 1.54184 Å) and an Oxford Cryosystems CryostreamPlus open-flow N2 cooling device. The analysis of the X-ray diffraction data of all the following compounds were performed by Dr Paul Waddell.

6.5.1 Methyl 4-(5,5-difluoro-5*H*-4λ^4,5λ^4-dipyrrolo[1,2-c:2',1'-*f*][1,3,2] diazaborinin-10-yl)benzoate **2.11a**

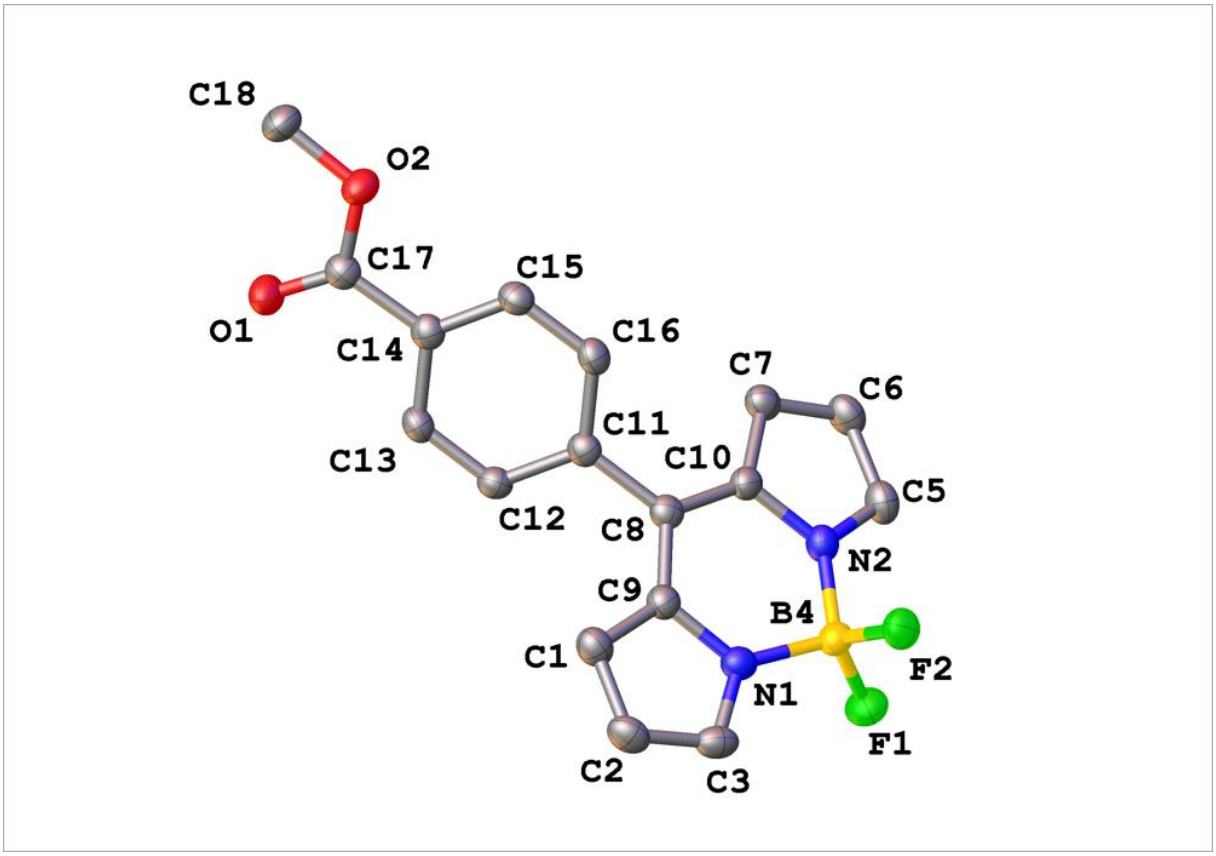

Identification code	mjh180029
Empirical formula	$C_{17}H_{13}BF_2N_2O_2$
Formula weight	326.10
Temperature/K	150.0(2)
Crystal system	triclinic

Space group	P-1
a/Å	7.5420(4)
b/Å	7.8420(5)
c/Å	13.3895(9)
α/°	79.522(6)
β/°	77.664(5)
γ/°	75.502(5)
Volume/$Å^3$	742.06(8)
Z	2
$\rho_{calc}g/cm^3$	1.459
μ/mm^{-1}	0.951
F(000)	336.0
Crystal size/mm^3	0.28 × 0.13 × 0.1
Radiation	CuKα (λ = 1.54184)
2Θ range for data collection/°	6.82 to 133.608
Index ranges	-8 ≤ h ≤ 8, -9 ≤ k ≤ 9, -15 ≤ l ≤ 15
Reflections collected	9230
Independent reflections	2613 [R_{int} = 0.0376, R_{sigma} = 0.0314]
Data/restraints/parameters	2613/0/218
Goodness-of-fit on F^2	1.035
Final R indexes [I>=2σ (I)]	R_1 = 0.0360, wR_2 = 0.0869
Final R indexes [all data]	R_1 = 0.0537, wR_2 = 0.0974
Largest diff. peak/hole / e $Å^{-3}$	0.14/-0.23

6.5.2 Methyl 4-(3,7-dichloro-5,5-difluoro-5*H*-4λ^4,5λ^4-dipyrrolo[1,2-*c*:2',1'-*f*][1,3,2]diazaborinin-10-yl)benzoate **2.13a**

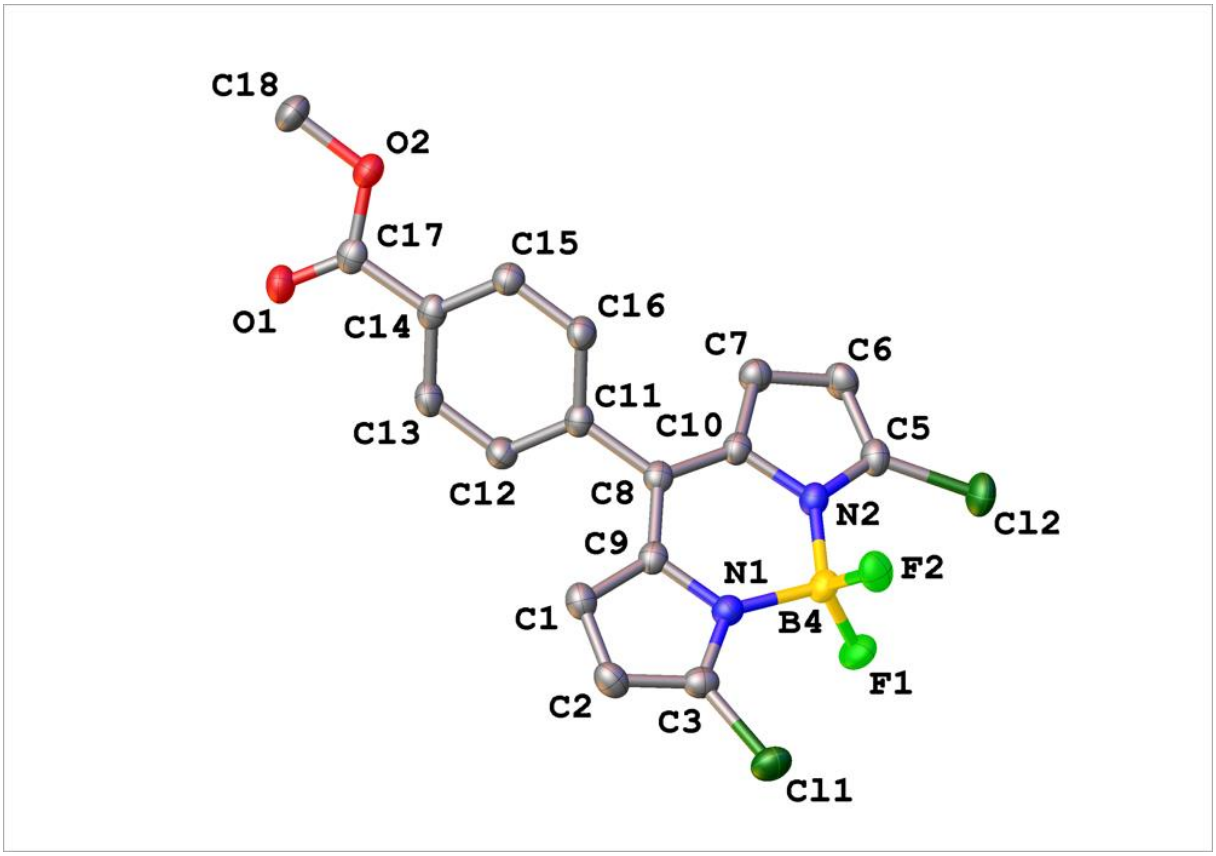

Identification code	mjh180027
Empirical formula	$C_{17}H_{11}BCl_2F_2N_2O_2$
Formula weight	394.99
Temperature/K	150.0(2)
Crystal system	monoclinic
Space group	C2/c
a/Å	19.6924(4)
b/Å	9.35108(15)
c/Å	18.0995(3)
α/°	90
β/°	100.0838(17)
γ/°	90
Volume/Å^3	3281.46(10)

Z	8
ρ_{calc}g/cm^3	1.599
μ/mm^{-1}	3.902
F(000)	1600.0
Crystal size/mm^3	0.3 × 0.14 × 0.13
Radiation	CuKα (λ = 1.54184)
2Θ range for data collection/°	9.122 to 133.932
Index ranges	-23 ≤ h ≤ 23, -11 ≤ k ≤ 9, -21 ≤ l ≤ 20
Reflections collected	11919
Independent reflections	2905 [R_{int} = 0.0267, R_{sigma} = 0.0213]
Data/restraints/parameters	2905/0/237
Goodness-of-fit on F^2	1.024
Final R indexes [I>=2σ (I)]	R_1 = 0.0290, wR_2 = 0.0732
Final R indexes [all data]	R_1 = 0.0329, wR_2 = 0.0766
Largest diff. peak/hole / e Å^{-3}	0.23/-0.28

6.5.3 Methyl 4-(2,3,7,8-tetrabromo-5,5-difluoro-5*H*-4λ4,5λ4-dipyrrolo[1,2-*c*:2',1'-*f*][1,3,2]diazaborinin-10-yl)benzoate **2.15**

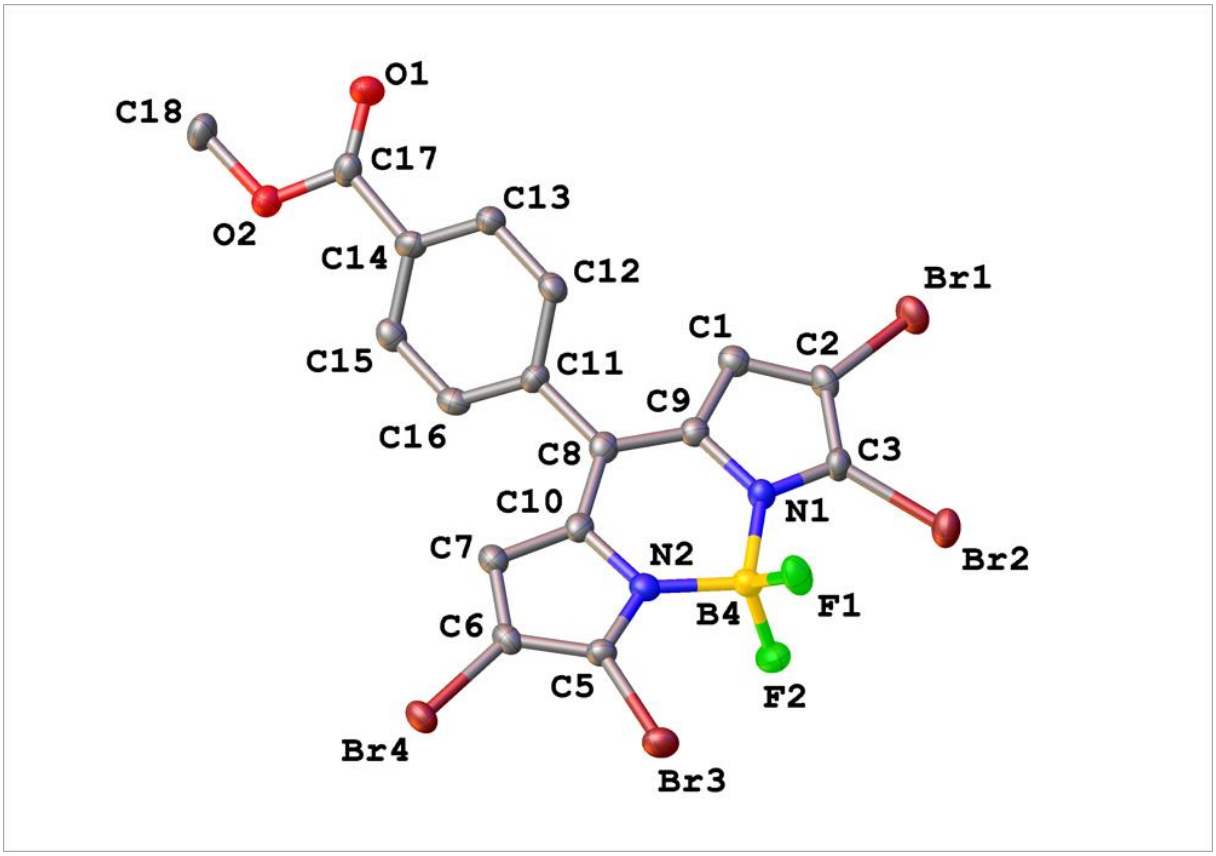

Identification code	mjh180025
Empirical formula	$C_{17}H_9BBr_4F_2N_2O_2$
Formula weight	641.71
Temperature/K	150.0(2)
Crystal system	monoclinic
Space group	$P2_1/c$
a/Å	7.6102(3)
b/Å	18.3734(6)
c/Å	13.8969(5)
α/°	90

β/°	103.937(3)
γ/°	90
Volume/Å^3	1885.93(12)
Z	4
ρ_{calc}g/cm^3	2.260
μ/mm^{-1}	10.759
F(000)	1216.0
Crystal size/mm^3	0.25 × 0.12 × 0.07
Radiation	CuKα (λ = 1.54184)
2Θ range for data collection/°	8.132 to 133.798
Index ranges	-9 ≤ h ≤ 9, -21 ≤ k ≤ 21, -16 ≤ l ≤ 16
Reflections collected	7353
Independent reflections	7353 [R_{int} = ?, R_{sigma} = 0.0128]
Data/restraints/parameters	7353/0/255
Goodness-of-fit on F^2	1.070
Final R indexes [I>=2σ (I)]	R_1 = 0.0490, wR_2 = 0.1416
Final R indexes [all data]	R_1 = 0.0518, wR_2 = 0.1438
Largest diff. peak/hole / e Å^{-3}	1.20/-0.67

6.5.4Methyl 4-(2,3,7,8-tetrabromo-5,5-difluoro-5*H*-4λ4,5λ4-dipyrrolo[1,2-*c*:2',1'-*f*][1,3,2]diazaborinin-10-yl)benzoate **2.15** and methyl 4-(2,3,8-tribromo-5,5-difluoro-5*H*-5λ^4,6λ^4-dipyrrolo[1,2-c:2',1'-f][1,3,2]diazaborinin-10-yl)benzoate **2.16**

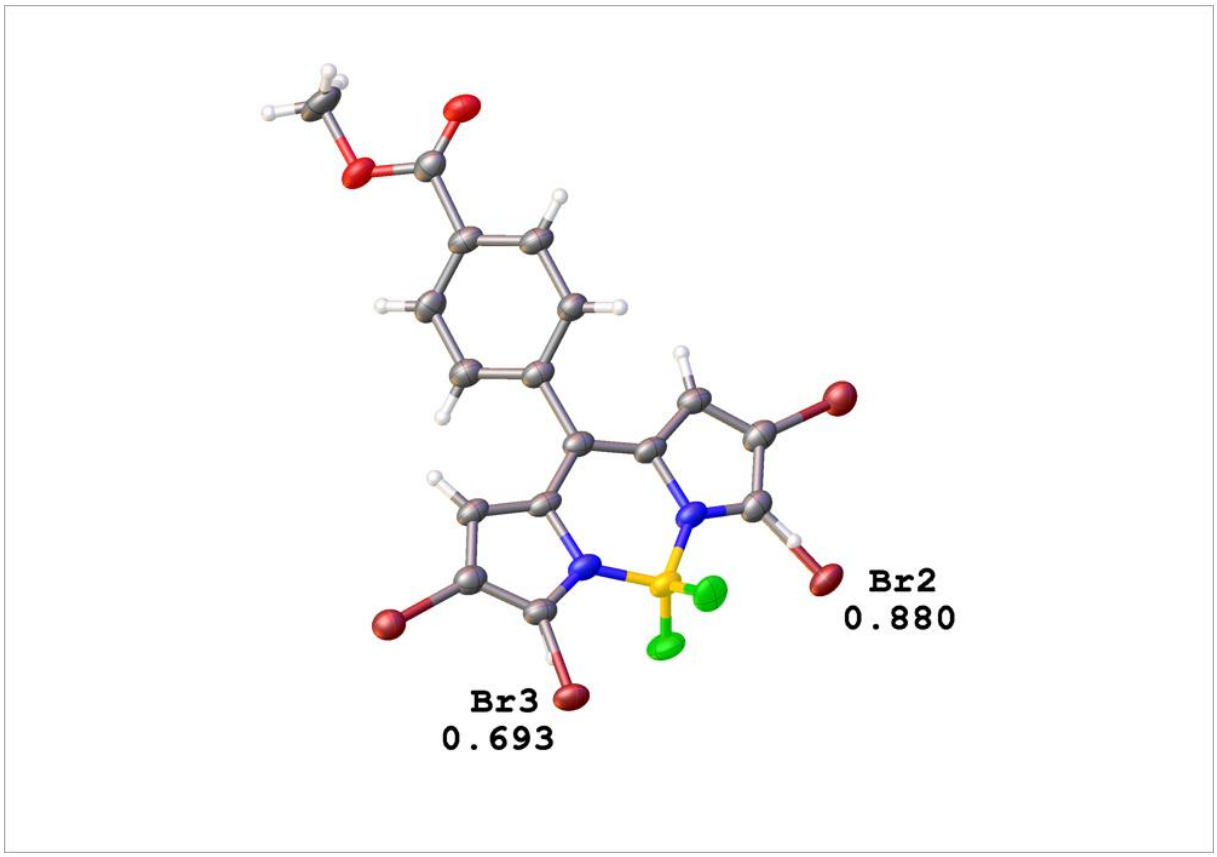

Identification code	mjh180026
Empirical formula	$C_{17}H_{9.43}BBr_{3.57}F_2N_2O_2$
Formula weight	607.98
Temperature/K	150.0(2)
Crystal system	monoclinic
Space group	$P2_1/c$
a/Å	7.6257(5)
b/Å	18.1556(12)
c/Å	13.9069(7)
α/°	90
β/°	104.315(6)
γ/°	90

Volume/Å^3	1865.6(2)
Z	4
ρ_{calc}g/cm^3	2.165
μ/mm^{-1}	9.794
F(000)	1158.0
Crystal size/mm^3	0.25 × 0.15 × 0.15
Radiation	CuKα (λ = 1.54184)
2Θ range for data collection/°	8.172 to 133.686
Index ranges	-9 ≤ h ≤ 8, -21 ≤ k ≤ 21, -16 ≤ l ≤ 16
Reflections collected	12969
Independent reflections	3280 [R_{int} = 0.0438, R_{sigma} = 0.0335]
Data/restraints/parameters	3280/0/254
Goodness-of-fit on F^2	1.120
Final R indexes [I>=2σ (I)]	R_1 = 0.0427, wR_2 = 0.0941
Final R indexes [all data]	R_1 = 0.0531, wR_2 = 0.0991
Largest diff. peak/hole / e Å^{-3}	0.51/-0.64

6.5.5 Methyl 4-(5,5-difluoro-3,7-di((*E*)-styryl)-5H-4λ^4,5λ^4-dipyrrolo[1,2-*c*:2',1'-*f*][1,3,2]diazaborinin-10-yl)benzoate **3.25**

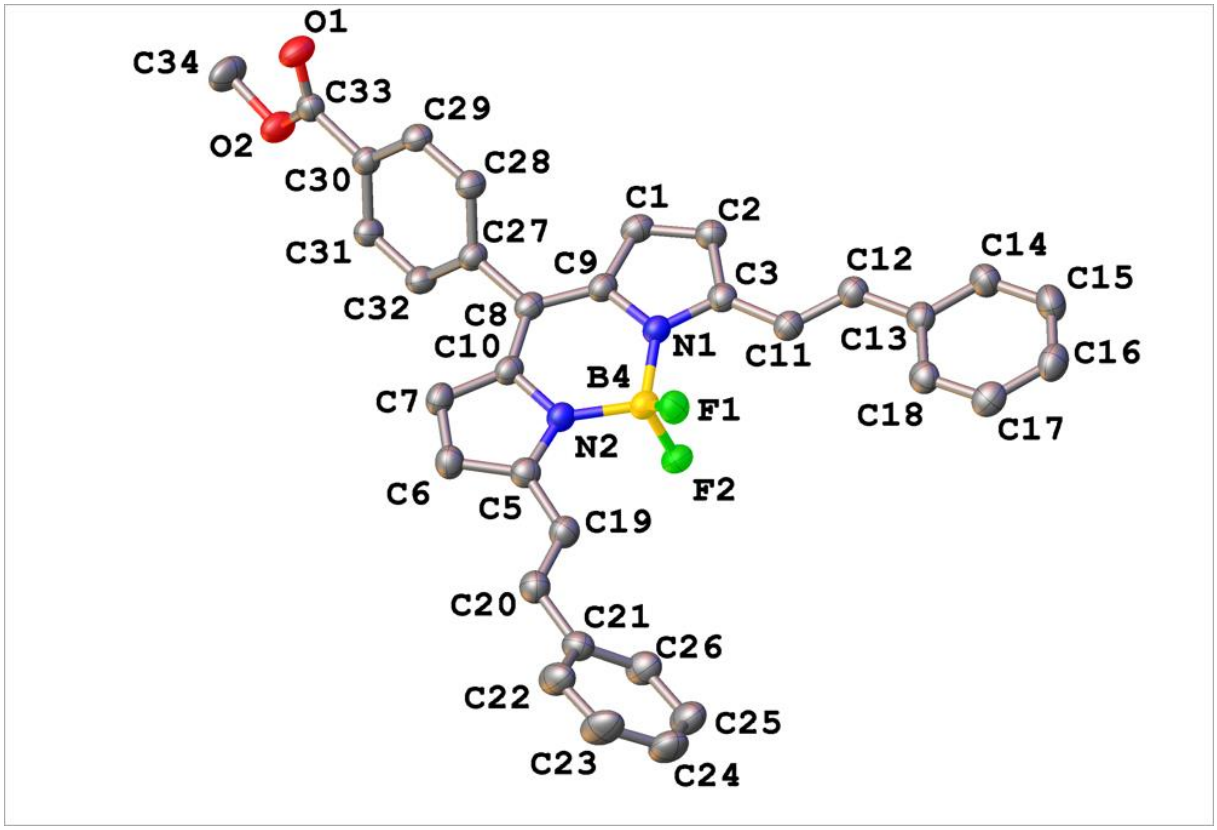

Identification code	mjh200073
Empirical formula	$C_{33}H_{25}BF_2N_2O_2$
Formula weight	530.36
Temperature/K	150.0(2)
Crystal system	monoclinic
Space group	$P2_1/n$
a/Å	7.8877(2)
b/Å	17.3177(3)
c/Å	19.2110(4)
α/°	90
β/°	97.202(2)
γ/°	90
Volume/Å^3	2603.46(10)
Z	4

ρ_{calc}g/cm^3	1.353
μ/mm^{-1}	0.764
F(000)	1104.0
Crystal size/mm^3	0.21 × 0.15 × 0.06
Radiation	Cu Kα (λ = 1.54184)
2Θ range for data collection/°	6.896 to 133.622
Index ranges	-9 ≤ h ≤ 7, -20 ≤ k ≤ 20, -22 ≤ l ≤ 22
Reflections collected	36358
Independent reflections	4602 [R_{int} = 0.0597, R_{sigma} = 0.0277]
Data/restraints/parameters	4602/0/362
Goodness-of-fit on F^2	1.048
Final R indexes [I>=2σ (I)]	R_1 = 0.0435, wR_2 = 0.1109
Final R indexes [all data]	R_1 = 0.0531, wR_2 = 0.1207
Largest diff. peak/hole / e Å^{-3}	0.30/-0.21

6.5.6 Methyl 4-(5,5-difluoro-3,7-diphenyl-5*H*-4λ^4,5λ^4-dipyrrolo[1,2-*c*:2',1'-*f*][1,3,2]diazaborinin-10-yl)benzoate **3.21**

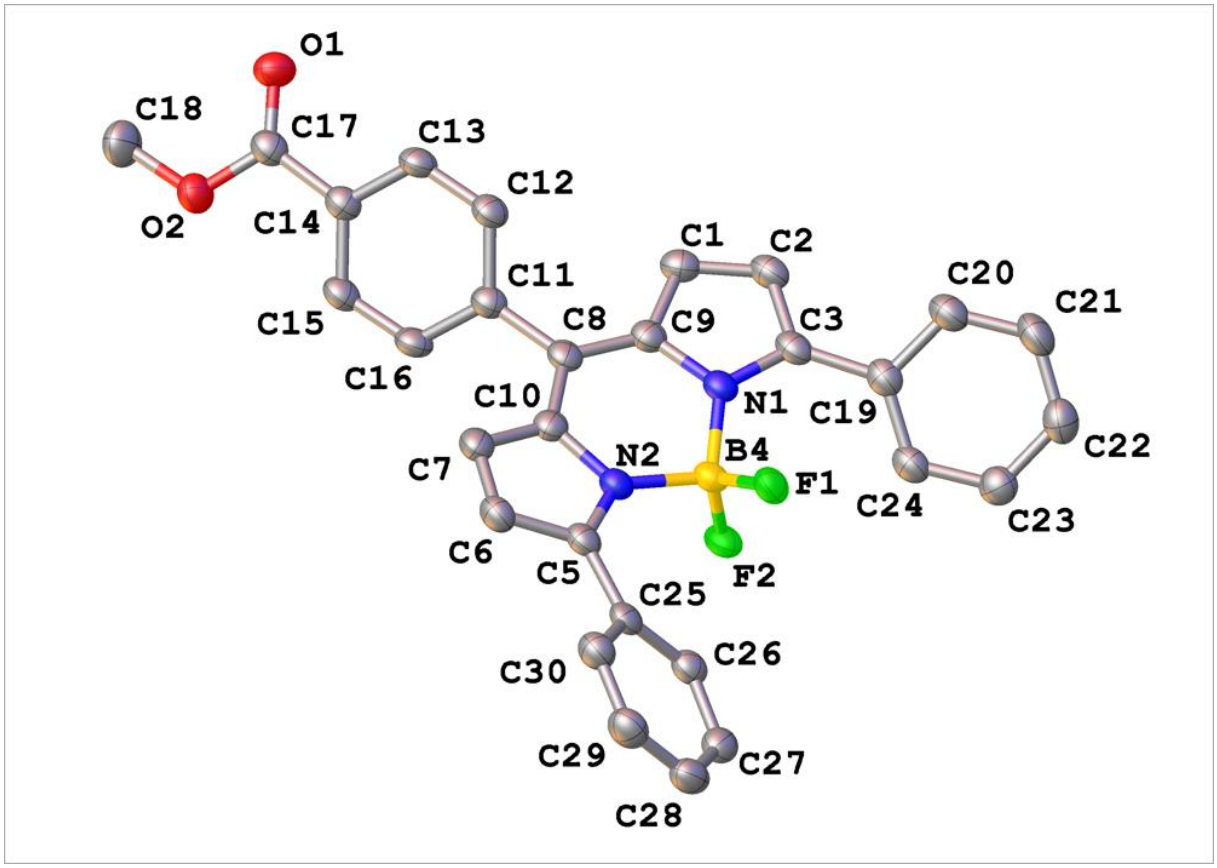

Identification code	mjh190055_fa
Empirical formula	$C_{29}H_{21}BF_2N_2O_2$
Formula weight	478.29
Temperature/K	150.0(2)
Crystal system	triclinic
Space group	P-1
a/Å	7.0294(4)
b/Å	12.3775(8)
c/Å	13.2399(8)
α/°	86.938(5)
β/°	86.908(5)
γ/°	88.030(5)
Volume/Å^3	1148.06(12)

Z	2
ρ_{calc}g/cm^3	1.384
μ/mm^{-1}	0.804
F(000)	496.0
Crystal size/mm^3	0.258 × 0.089 × 0.022
Radiation	CuKα (λ = 1.54184)
2Θ range for data collection/°	7.156 to 133.664
Index ranges	-8 ≤ h ≤ 8, -14 ≤ k ≤ 14, -15 ≤ l ≤ 15
Reflections collected	16406
Independent reflections	4059 [R_{int} = 0.0577, R_{sigma} = 0.0424]
Data/restraints/parameters	4059/0/326
Goodness-of-fit on F^2	1.028
Final R indexes [I>=2σ (I)]	R_1 = 0.0418, wR_2 = 0.1015
Final R indexes [all data]	R_1 = 0.0602, wR_2 = 0.1144
Largest diff. peak/hole / e Å^{-3}	0.18/-0.21

6.5.7 Methyl (Z)-4-((5-iodo-1H-pyrrol-2-yl)(5-iodo-2H-pyrrol-2-ylidene)methyl)benzoate **4.28**

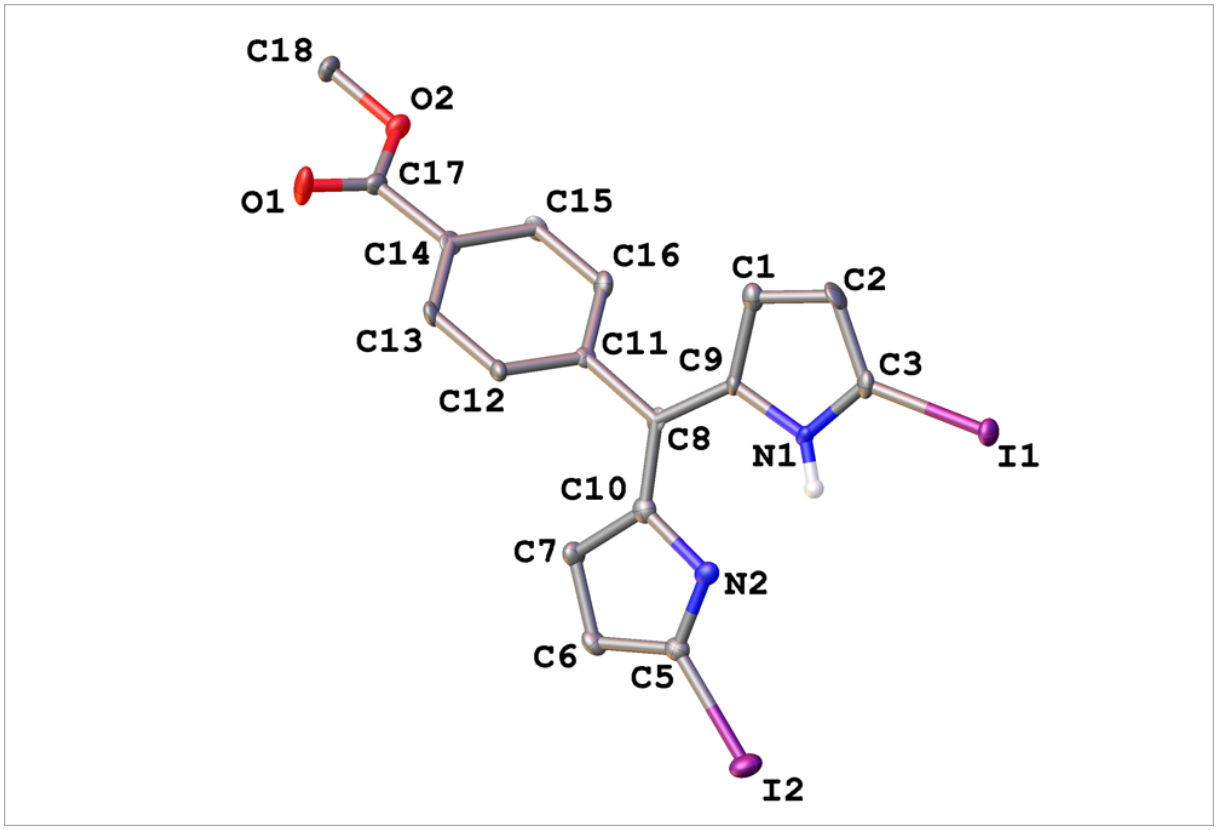

Identification code	mjh210026
Empirical formula	$C_{17}H_{12}I_2N_2O_2$
Formula weight	530.09
Temperature/K	150.0(2)
Crystal system	triclinic
Space group	P-1
a/Å	7.9582(4)
b/Å	9.9853(5)
c/Å	11.2481(5)
α/°	93.038(4)
β/°	98.075(4)
γ/°	105.382(4)
Volume/Å^3	849.44(7)
Z	2

ρ_{calc}g/cm^3	6.5.82.072
μ/mm^{-1}	29.170
F(000)	500.0
Crystal size/mm^3	0.28 × 0.21 × 0.14
Radiation	Cu Kα (λ = 1.54184)
2Θ range for data collection/°	7.974 to 133.716
Index ranges	-9 ≤ h ≤ 9, -9 ≤ k ≤ 11, -13 ≤ l ≤ 13
Reflections collected	12031
Independent reflections	2995 [R_{int} = 0.0630, R_{sigma} = 0.0507]
Data/restraints/parameters	2995/1/212
Goodness-of-fit on F^2	1.045
Final R indexes [I>=2σ (I)]	R_1 = 0.0390, wR_2 = 0.0936
Final R indexes [all data]	R_1 = 0.0480, wR_2 = 0.1007
Largest diff. peak/hole / e Å^{-3}	1.14/-1.35

6.5.9 Methyl (*R*)-4-(10b-(4-fluorophenyl)-10-((3-hydroxy-1-methoxy-1-oxopropan-2-yl)amino)-10b*H*-11-oxa-4b1,10aλ^4-diaza-10bλ^4-boracyclopenta[e]aceanthrylen-7-yl)benzoate **4.23a**

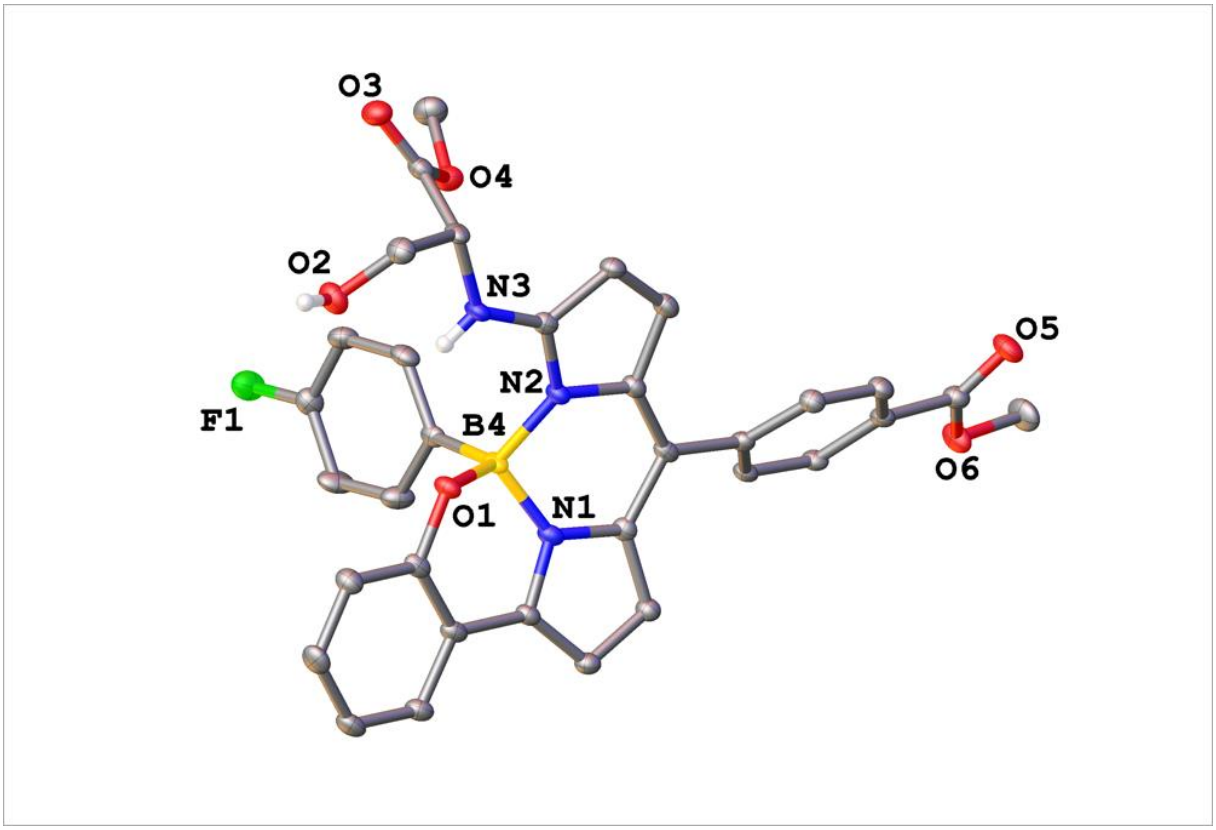

Identification code	mjh220011
Empirical formula	$C_{35}H_{33}BFN_3O_7S$
Formula weight	669.51
Temperature/K	100.0(2)
Crystal system	triclinic
Space group	P-1
a/Å	9.672(7)
b/Å	11.360(8)
c/Å	14.549(10)
α/°	91.756(18)
β/°	100.195(19)
γ/°	93.582(17)
Volume/Å^3	1568.9(19)

Z	2
ρ_{calc}g/cm^3	1.417
μ/mm^{-1}	0.154
F(000)	700.0
Crystal size/mm^3	0.088 × 0.077 × 0.017
Radiation	Synchrotron (λ = 0.6889)
2Θ range for data collection/°	2.76 to 53.144
Index ranges	-12 ≤ h ≤ 12, -14 ≤ k ≤ 14, -18 ≤ l ≤ 18
Reflections collected	17593
Independent reflections	7016 [R_{int} = 0.0678, R_{sigma} = 0.0897]
Data/restraints/parameters	7016/0/443
Goodness-of-fit on F^2	1.045
Final R indexes [I>=2σ (I)]	R_1 = 0.0737, wR_2 = 0.2069
Final R indexes [all data]	R_1 = 0.0898, wR_2 = 0.2177
Largest diff. peak/hole / e Å^{-3}	0.98/-0.75

References

1. W. T. Godbey, in *Biotechnology and its Applications (Second Edition)*, ed. W. T. Godbey, Academic Press, 2022, pp. 187-201.

2. J. Hu and C.-y. Zhang, *Anal. Chem*, 2013, **85**, 2000-2004.

3. R. M. Christie, in *Handbook of Textile and Industrial Dyeing*, ed. M. Clark, Woodhead Publishing, 2011, vol. 1, pp. 562-587.

4. E. S. Battistelli, *Journal*, 2021, 11-11-11-19.

5. E. Gussakovsky, 2010, pp. 425-459.

6. Y. Zhang, S. Yu, B. Han, Y. Zhou, X. Zhang, X. Gao and Z. Tang, *Matter*, 2022, **5**, 837-875.

7. L. Arrico, L. Di Bari and F. Zinna, *chem. Eur. J.*, 2021, **27**, 2920-2934.

8. R. Clarke, K. L. Ho, A. A. Alsimaree, O. J. Woodford, P. G. Waddell, J. Bogaerts, W. Herrebout, J. G. Knight, R. Pal, T. J. Penfold and M. J. Hall, *ChemPhotoChem*, 2017, **1**, 513-517.

9. V. Raghavan and P. L. Polavarapu, in *Chiral Analysis (Second Edition)*, ed. P. L. Polavarapu, Elsevier, 2018, pp. 153-200.

10. K. Staszak, K. Wieszczycka, V. Marturano and B. Tylkowski, *Coord. Chem. Rev.*, 2019, **397**, 76-90.

11. S. Chen, D. Yan, M. Xue, Y. Hong, Y. Yao and Q. Shen, *Org. Lett.*, 2017, **19**, 3382-3385.

12. V. L. Weidner, C. J. Barger, M. Delferro, T. L. Lohr and T. J. Marks, *ACS Catal.*, 2017, **7**, 1244-1247.

13. F. Zinna and L. Di Bari, *Chirality*, 2015, **27**, 1-13.

14. R. Carr, N. H. Evans and D. Parker, *Chem. Soc. Rev.*, 2012, **41**, 7673-7686.

15. J. W. Walton, L. D. Bari, D. Parker, G. Pescitelli, H. Puschmann and D. S. Yufit, *ChemComm*, 2011, **47**, 12289-12291.

16. E. M. Sánchez-Carnerero, A. R. Agarrabeitia, F. Moreno, B. L. Maroto, G. Muller, M. J. Ortiz and S. de la Moya, *chem.*, 2015, **21**, 13488-13500.

17. C. A. Emeis and L. J. Oosterhoff, *Chem. Phys. Lett.*, 1967, **1**, 129-132.

18. J. E. Field, G. Muller, J. P. Riehl and D. Venkataraman, *J. Am. Chem. Soc.*, 2003, **125**, 11808-11809.

19. Y. Chen, *Mater. Today Chem.*, 2022, **23**, 100651.

20. Y. Deng, M. Wang, Y. Zhuang, S. Liu, W. Huang and Q. Zhao, *Light Sci. Appl.*, 2021, **10**, 76.

21. M. Cei, L. Di Bari and F. Zinna, *Chirality*, 2023, **35**, 192-210.

22. K. Fujise, E. Tsurumaki, G. Fukuhara, N. Hara, Y. Imai and S. Toyota, *Chem. Asian J.*, 2020, **15**, 2456-2461.

23. Y. Inoue, D. Sakamaki, Y. Tsutsui, M. Gon, Y. Chujo and S. Seki, *J. Am. Chem. Soc.*, 2018, **140**, 7152-7158.

24. Y. Imai, Springer, 2020, ch. 2, pp. 11-30.

25. Y. Shen and C.-F. Chen, *Chem. Rev.*, 2012, **112**, 1463-1535.

26. L. Yang, Y. Liu, C. Ma, W. Liu, Y. Li and L. Li, *Dyes Pigm.*, 2015, **122**, 1-5.

27. S. Zhu, J. Zhang, G. Vegesna, F. T. Luo, S. A. Green and H. Liu, *Org. Lett.*, 2011, **13**, 438-441.

28. X.-F. Zhang and J. Zhu, *J. Lumin.*, 2019, **205**, 148-157.

29. P. Kaur and K. Singh, *J. Mater. Chem. C*, 2019, **7**, 11361-11405.

30. N. I. Georgiev, R. Bryaskova, R. Tzoneva, I. Ugrinova, C. Detrembleur, S. Miloshev, A. M. Asiri, A. H. Qusti and V. B. Bojinov, *Bioorg. Med. Chem.*, 2013, **21**, 6292-6302.

31. C. S. Kue, S. Y. Ng, S. H. Voon, A. Kamkaew, L. Y. Chung, L. V. Kiew and H. B. Lee, *Photochem. Photobiol. Sci.*, 2018, **17**, 1691-1708.

32. Y. Ni and J. Wu, *Org. Biomol. Chem.*, 2014, **12**, 3774-3791.

33. M. Poddar and R. Misra, *Coord. Chem. Rev.*, 2020, **421**, 213462.

34. B. M. Squeo, L. Ganzer, T. Virgili and M. Pasini, *Mol.*, 2020, **26**.

35. K. Krumova and G. Cosa, *JACS*, 2010, **132**, 17560-17569.

36. A. Treibs and F.-H. Kreuzer, *Justus Liebigs Ann. Chem.*, 1968, **718**, 208-223.

37. V. Leen, PhD, Katholieke Universiteit, Leuven, 2010.

38. P. D. Rao, S. Dhanalekshmi, B. J. Littler and J. S. Lindsey, *J. Org. Chem*, 2000, **65**, 7323-7344.

39. M. Ravikanth, L. Vellanki and R. Sharma, *Org. Chem. Res.*, 2016, DOI: 10.2147/ROC.S60504, 1.

40. N. Boens, B. Verbelen and W. Dehaen, *Eur. J. Chem.*, 2015, **2015**, 6577-6595.

41. L. Jiao, W. Pang, J. Zhou, Y. Wei, X. Mu, G. Bai and E. Hao, *J Org Chem*, 2011, **76**, 9988-9996.

42. M. R. Rao, S. M. Mobin and M. Ravikanth, *Tetrahedron*, 2010, **66**, 1728-1734.

43. A. Loudet and K. Burgess, *Chem. Rev.*, 2007, **107**, 4891-4932.

44. I. W. Badon, J. P. Jee, T. P. Vales, C. Kim, S. Lee, J. Yang, S. K. Yang and H. J. Kim, *Pharm.*, 2023, **15**.

45. X. Zhou, C. Yu, Z. Feng, Y. Yu, J. Wang, E. Hao, Y. Wei, X. Mu and L. Jiao, *Org. Lett.*, 2015, **17**, 4632-4635.

46. L. Li, B. Nguyen and K. Burgess, *Bioorganic Med. Chem. Lett.*, 2008, **18**, 3112-3116.

47. C. Zhao, X. Wang, J. Cao, P. Feng, J. Zhang, Y. Zhang, Y. Yang and Z. Yang, *Dyes Pigm.*, 2013, **96**, 328-332.

48. Z. Zhang, B. Wen, Y. Rao, L. Xu, A. Osuka and J. Song, *ChemistrySelect*, 2022, **7**, e202200619.

49. W. Miao, X. Guo, X. Yan, Y. Shang, C. Yu, E. Dai, T. Jiang, E. Hao and L. Jiao, *Chem. Eur. J.*, 2023, **29**, e202203832.

50. E. Fron, E. Coutiño-Gonzalez, L. Pandey, M. Sliwa, M. Van der Auweraer, F. C. De Schryver, J. Thomas, Z. Dong, V. Leen, M. Smet, W. Dehaen and T. Vosch, *NJC*, 2009, **33**, 1490-1496.

51. T. Rohand, M. Baruah, W. Qin, N. Boens and W. Dehaen, *ChemComm*, 2006, DOI: 10.1039/B512756D, 266-268.

52. H. Finkelstein, *Ber. Dtsch. Chem. Ges.*, 1910, **43**, 1528-1532.

53. G. Evano, A. Nitelet, P. Thilmany and D. F. Dewez, *Front. Chem.*, 2018, **6**.

54. A. Agafonova, I. Smetanin, N. Rostovskii, A. Khlebnikov and M. Novikov, *Synthesis*, 2019, **51**.

55. S. Rihn, P. Retailleau, N. Bugsaliewicz, A. D. Nicola and R. Ziessel, *Tetrahedron Lett.*, 2009, **50**, 7008-7013.

56. T. Rohand, W. Qin, N. Boens and W. Dehaen, *EurJOC*, 2006, **2006**, 4658-4663.

57. Z. Feng, L. Jiao, Y. Feng, C. Yu, N. Chen, Y. Wei, X. Mu and E. Hao, *J. Org. Chem.*, 2016, **81**, 6281-6291.

58. F. Zinna, T. Bruhn, C. A. Guido, J. Ahrens, M. Bröring, L. Di Bari and G. Pescitelli, *Chem.*, 2016, **22**, 16089-16098.

59. S. Kolemen, Y. Cakmak, Z. Kostereli and E. U. Akkaya, *Org. Lett.*, 2014, **16**, 660-663.

60. R. B. Alnoman, S. Rihn, D. C. O'Connor, F. A. Black, B. Costello, P. G. Waddell, W. Clegg, R. D. Peacock, W. Herrebout, J. G. Knight and M. J. Hall, *Chem. Eur. J.*, 2016, **22**, 93-96.

61. M. Saikawa, T. Nakamura, J. Uchida, M. Yamamura and T. Nabeshima, *Chem comm*, 2016, **52**, 10727-10730.

62. E. M. Sánchez-Carnerero, F. Moreno, B. L. Maroto, A. R. Agarrabeitia, M. J. Ortiz, B. G. Vo, G. Muller and S. d. l. Moya, *J. Am. Chem. Soc.*, 2014, **136**, 3346-3349.

63. G. Diaz-Muñoz, I. L. Miranda, S. K. Sartori, D. C. de Rezende and M. Alves Nogueira Diaz, *Chirality*, 2019, **31**, 776-812.

64. A. Nazari, M. M. Heravi and V. Zadsirjan, *J. Organomet. Chem.*, 2021, **932**, 121629.

65. M. M. Heravi, V. Zadsirjan and B. Farajpour, *RSC Adv.*, 2016, **6**, 30498-30551.

66. G. L. Beutner, B. M. Cohen, A. J. DelMonte, D. D. Dixon, K. J. Fraunhoffer, A. W. Glace, E. Lo, J. M. Stevens, D. Vanyo and C. Wilbert, *Org. Process Res. Dev.*, 2019, **23**, 1378-1385.

67. J. P. Reid, *Commun. Chem.*, 2021, **4**, 171.

68. R. J. Armstrong, M. Nandakumar, R. M. P. Dias, A. Noble, E. L. Myers and V. K. Aggarwal, *Angew Chem Int Ed Engl*, 2018, **57**, 8203-8208.

69. M. R. Crittall, N. W. G. Fairhurst and D. R. Carbery, *Chem. Commun.*, 2012, **48**, 11181-11183.

70. M. Baruah, W. Qin, N. Basarić, W. M. De Borggraeve and N. Boens, *J. Org. Chem.*, 2005, **70**, 4152-4157.

71. N. Boens, B. Verbelen and W. Dehaen, *Eur. J. Org. Chem.*, 2015, **2015**, 6577-6595.

72. R. W. Wagner and J. S. Lindsey, *Pure Appl. Chem.*, 1996, **68**, 1373-1380.

73. I. A. Cody, S. I. Woodburn, M. W. Blackmore and R. J. Magee, *J. Inorg. Nucl. Chem.*, 1970, **32**, 3263-3269.

74. F. Frank, L. M. Alice, P. Mauker, A. A. Alsimaree, P. G. Waddell, M. R. Probert, T. J. Penfold, J. G. Knight and M. J. Hall, *Tetrahedron*, 2020, **76**, 131113.

75. M. J. Ortiz, A. R. Agarrabeitia, G. Duran-Sampedro, J. Bañuelos Prieto, T. A. Lopez, W. A. Massad, H. A. Montejano, N. A. García and I. Lopez Arbeloa, *Tetrahedron*, 2012, **68**, 1153-1162.

76. *China Pat.,* CN107556333A, 2018.

77. *China Pat.,* CN108373478A, 2018.

78. Q. Meng, F. R. Fronczek and M. G. H. Vicente, *New Journal of Chemistry*, 2016, **40**, 5740-5751.

79. *Japan Pat.,* WO2023049828, 2021.

80. Z. Ruan, W. Miao, P. Yuan, L. Le, L. Jiao, E. Hao and L. Yan, *Bioconjugate Chem.*, 2018, **29**, 3441-3451.

81. Q. Meng, F. R. Fronczek and M. G. H. Vicente, *New J. Chem.*, 2016, **40**, 5740-5751.

82. Z. Wang, in *Comprehensive Organic Name Reactions and Reagents*, ed. Z. Wang, 2010, pp. 1060-1063.

83. T. Furuya, J. E. Klein and T. Ritter, *Synthesis (Stuttg)*, 2010, **2010**, 1804-1821.

84. S. Rohrbach, A. J. Smith, J. H. Pang, D. L. Poole, T. Tuttle, S. Chiba and J. A. Murphy, *Angew. Chem., Int. Ed. Engl.*, 2019, **58**, 16368-16388.

85. S. Xu, Q.-D. Wang, M.-M. Sun, G. Yin and J. Liang, *RSC Adv.*, 2021, **11**, 29690-29701.

86. L. Li, W. Liu, H. Zeng, X. Mu, G. Cosa, Z. Mi and C.-J. Li, *J. Am. Chem. Soc.*, 2015, **137**, 8328-8331.

87. F. J. Frank, P. G. Waddell, M. J. Hall and J. G. Knight, *Org. Lett.*, 2021, **23**, 8595-8599.

88. W. Sheng, X. Guo, B. Tang, W. Bu, F. Zhang, E. Hao and L. Jiao, *SAA*, 2023, **285**, 121902.

89. G. Kerric, E. Le Grognec, F. Zammattio, M. Paris and J.-P. Quintard, *J. Organomet. Chem*, 2010, **695**, 103-110.

90. A. F. Littke, L. Schwarz and G. C. Fu, *J. Am. Chem. Soc.*, 2002, **124**, 6343-6348.

91. M. Tichý, R. Pohl, E. Tloušťová, J. Weber, G. Bahador, Y.-J. Lee and M. Hocek, *Bioorg. Med. Chem.*, 2013, **21**, 5362-5372.

92. W.-J. Zhou, K.-H. Wang and J.-X. Wang, *J. Org. Chem.*, 2009, **74**, 5599-5602.

93. L. Gai, J. Mack, H. Lu, H. Yamada, D. Kuzuhara, G. Lai, Z. Li and Z. Shen, *Eur. J. Chem.*, 2014, **20**, 1091-1102.

94. W. Mao, L. Xia and H. Xie, *Angew. Chem., Int. Ed.*, 2017, **56**, 4468-4472.

95. L. Gai, J. Mack, H. Lu, H. Yamada, D. Kuzuhara, G. Lai, Z. Li and Z. Shen, *Chem. Eur. J.*, 2014, **20**, 1091-1102.

96. C. Bellomo, D. Zanetti, F. Cardano, S. Sinha, M. Chaari, A. Fin, A. Maranzana, R. Núñez, M. Blangetti and C. Prandi, *Dyes Pigm.*, 2021, **194**, 109644.

97. S. Osati, H. Ali, B. Guerin and J. E. van Lier, *Steroids*, 2017, **123**, 27-36.

98. N. Matouq, PhD Thesis PhD Thesis, Newcastle University, 2020.

99. N. C. Bruno, M. T. Tudge and S. L. Buchwald, *Chem. Sci.*, 2013, **4**, 916-920.

100. N. Algoazy, R. G. Clarke, T. J. Penfold, P. G. Waddell, M. R. Probert, R. Aerts, W. Herrebout, P. Stachelek, R. Pal, M. J. Hall and J. G. Knight, *ChemPhotoChem*, 2022, **6**, e202200090.

101. D. Sirbu, A. C. Benniston and A. Harriman, *Org. Lett.*, 2017, **19**, 1626-1629.

102. H. F.-J. A. N. v. Koeller, MPhil, Newcastle University, 2019.

103. M. Yu, J. K. H. Wong, C. Tang, P. Turner, M. H. Todd and P. J. Rutledge, *Beilstein J. Org. Chem.*, 2015, **11**, 37-41.

104. H. R. Snyder, J. A. Kuck and J. R. Johnson, *J. Am. Chem. Soc.*, 1938, **60**, 105-111.

105. K. L. Bhat, G. D. Markham, J. D. Larkin and C. W. Bock, *J. Phys. Chem. A.*, 2011, **115**, 7785-7793.

106. V. Lakshmi, T. Chatterjee and M. Ravikanth, *Eur. J. Chem.*, 2014, **2014**, 2105-2110.

107. J. P. Metherall, R. C. Carroll, S. J. Coles, M. J. Hall and M. R. Probert, *Chem. Soc. Rev.*, 2023, **52**, 1995-2010.

108. M. J. Maslow and C. Portal-Celhay, in *Mandell, Douglas, and Bennett's Principles and Practice of Infectious Diseases (Eighth Edition)*, eds. J. E. Bennett, R. Dolin and M. J. Blaser, W.B. Saunders, Philadelphia, 2015, pp. 339-349.e333.